

UNIVERSIDAD AUTÓNOMA DE MADRID
Facultad de Ciencias
Departamento de Física Teórica

Hunting a dynamical Higgs

Memoria de Tesis Doctoral realizada por

Ilaria Brivio

presentada ante el Departamento de Física Teórica
de la Universidad Autónoma de Madrid
para la obtención del Título de Doctora en Ciencias.

Tesis Doctoral dirigida por

Catedrática M. Belén Gavela-Legazpi

del Departamento de Física Teórica
de la Universidad Autónoma de Madrid

Madrid, 24 de Junio de 2016

Acknowledgments

This thesis is the result of several people's work and dedication.

In primis, Belén, who's the mother of this project and who guided its development with her unique wisdom. I am extremely thankful for her caring teachings, about physics and beyond, for disseminating my PhD with all kinds of opportunities and for encouraging my interaction with the international community.

A fundamental component of this work is Luca's contribution. I owe to him and to our daily discussions a large part of my understanding of theoretical physics, and he deserves a special thanks for having taken on the burden of introducing me to this world, computation by computation, without ever leaving me behind.

There would have been no pheno analysis in this thesis without Concha, Oscar, Juan and Tyler. I would like to express my gratitude to all of them, and in particular to Concha and Juan for their constant availability to clarify any doubt with detailed explanations and for going through every single formula and Feynman rule with endless patience and thoroughness.

I am also grateful for having had the chance to collaborate with Rodrigo and Stefano, who had a crucial role in this work too, and to learn a great deal about collider and Dark Matter physics working with Gino, Florian, Verónica, Ken, Josemi and Rocío.

I am indebted to Belén and Luca for revising patiently this manuscript and giving me precious suggestions, and to Rocío for polishing carefully (a.k.a. redoing) the translation into Spanish. Finally, Marino deserves tremendous credit for improving my English and my understanding of experimental results and, above all, for his unequalled support during every stage of this PhD.

Motivations and Purpose

Particle physics is at the dawn of a new era: the discovery in 2012 of a new scalar resonance at the LHC [1, 2], that has been subsequently established to be compatible with the Higgs boson [3–5], has marked a turning point. The mere existence of the Higgs is a milestone in the already long history of success of the Standard Model of particle physics (SM), as it ultimately confirms the set of particles included in the theory. Such a triumph is even reinforced by the fact that, so far, the couplings of the Higgs scalar measured by the ATLAS and CMS experiments are compatible with those predicted by the SM [6].

In this perspective, the years to come will necessarily push our knowledge into unexplored territory: the LHC at CERN will keep colliding protons at the unprecedented center-of-mass energy of 13 and 14 TeV and it will certainly provide new information about the nature of fundamental interactions. Would a new particle be discovered, it would be a revolutionary event that could pave the way to the formulation of a totally new “Standard Theory”. If such a new resonance will not appear, instead, the road of precision measurements will have to be further explored.

The body of experimental evidence for the existence of new physics beyond the Standard Model (BSM) is quite broad. To begin with, the cosmological models, based on the classical description of gravity, are confronted with the presence of “Dark Energy”, a popular name for the unknown mechanism behind the accelerated expansion of the Universe. While this puzzle does not necessarily seem to require an explanation in terms of particle physics, others definitely call for an extension of the SM: Dark Matter (DM) and the non-zero neutrino masses are among the most firmly established, but yet unexplained, phenomena. Another question, unexplained by SM physics and posed by cosmological results, concerns instead the origin of the disparity between the amount of matter and of antimatter present in the Universe. At the same time, the SM construction also raises some theoretical concerns, that mostly manifest themselves in the form of a fine-tuning to be imposed on some parameters appearing in the Lagrangian. For instance, a source of quandary is the so-called “strong CP problem”. The origin of this issue is a tension between the presence, a priori, of a CP-violating θ -term in the QCD Lagrangian and the experimental absence of a neutron’s electric dipole moment induced by it: the current experimental bounds on this quantity set the very strong limit $\bar{\theta} \lesssim 10^{-10}$. Although CP conservation could be imposed by hand in the strong sector, this would not solve the problem, as contributions from the electroweak sector (or from new physics in general) entering this term via the chiral anomaly, would tend to restore a non-zero value for $\bar{\theta}$.

Going further, a major lacuna of the Standard Model is certainly the lack of a rationale that could account for the peculiar flavor structure observed in Nature. The masses and mixings of the known fermions are merely described in the SM Lagrangian by arbitrary parameters, whose values are determined on an empirical basis, in contrast with particles’ interactions, whose assortment and strength are elegantly fixed by the gauge principle. Indeed, the latter principle is the only one imposing a significant constraint on the structure of the fermionic sector, requiring the presence of “complete” families for ensuring anomaly cancellation. The presence of exactly three families and the wide difference between the pattern of mass hierarchies and mixings for quarks and leptons are also unexplained.

The flavor puzzle may be connected - or not - to the mechanism of mass generation implemented in the SM, namely the electroweak symmetry breaking (EWSB) process. To elucidate the origin of the mass of visible matter is indeed a fundamental quest in itself, that may also have a bearing on other problems mentioned, such as those of strong CP or of DM. It is precisely on the mechanism of mass generation and on the unknowns concerning the Higgs sector that this thesis will focus. One of the main reasons why the SM Higgs mechanism is often considered not satisfactory, despite the compatibility with the Higgs data,

is represented by the hierarchy problem. The latter can be stated as the question of why the Higgs is so light if it can couple, a priori, to any larger new physics scale. The relevance of the hierarchy problem motivated the formulation of a wide variety of possible solutions to this issue. In this thesis we address it taking a well-known path, that historically proved effective in facing theoretical fine-tunings (a great example is the prediction of the existence of the charm quark and of its mass [7, 8]): we follow a symmetry principle. A guidance in this approach is provided by 't Hooft's naturalness criterion [9], according to which all dimensionless free parameters not constrained by a symmetry should be of order one, and all dimensionful ones should be of the order of the scale of the theory. In this perspective, the hierarchy problem should be addressed by tackling the question of what is the symmetry that stabilizes the Higgs mass m_h against large radiative corrections.

There are two widely explored applications of the symmetry principle to the Higgs' case. It's worth noting that, once a new symmetry is advocated, the Higgs is accompanied by new physical states, that complete its multiplet representation under the new group: precisely the presence of these Higgs partners allows, technically, to solve the hierarchy problem. The BSM theory may then be realized in a perturbative regime and with the Higgs being an elementary state that belongs to a $SU(2)$ doublet Φ , together with the three electroweak Goldstone bosons, *i.e.* the W^\pm and Z longitudinal components. This type of construction is often referred to as a *linear realization* of the electroweak symmetry. A paradigmatic example of this class of models is that of supersymmetry, where the protection ensured by the chiral symmetry on the Higgsino's mass term is transferred to the Higgs' one.

In another class of theories, the Higgs is assumed to be a pseudo-Goldstone boson of some spontaneously broken symmetry, so that its mass is protected by an approximate shift invariance. This option is most naturally associated to scenarios with new strong interactions, whose condensation would trigger the spontaneous symmetry breaking that delivers the electroweak scalars: this kind of construction implements a *non-linear realization* of the EWSB. Popular representatives of these theories are composite Higgs models and little Higgs models, that descend from Technicolor [10–12]. Other apparently quite distant constructions, such as theories with extra-dimensions, can also be reconducted to this paradigm. A characteristic feature of this framework is that, here, the properties of the Higgs particle detected at low energy can generically depart from those of an exact $SU(2)$ doublet. This hypothesis is indeed still viable, as the Higgs' couplings are known within an experimental accuracy of only 20% on average.

It is worth pointing out, for completeness, that, although solutions based on the direct application of symmetries remain most attractive, alternative possibilities have also been explored in the literature. A recent example is provided by the “cosmological relaxation” mechanism [13], which builds upon the ideas in Ref. [14]. In this work we will anyway stick to the guideline marked by symmetry explanations.

The road to precision

The main purpose of this thesis is that of exploring in depth the differences between the two main scenarios mentioned above - linear and non-linear EWSB -, searching for distinctive signatures that may allow to identify which is the solution adopted by Nature. We will do so exploring the corresponding electroweak-scale phenomenology and analyzing, in particular, signals that may be observed at the LHC. Specifically, if no new particle is discovered in the near future, the main way of gaining insight into BSM physics will be by searching for anomalies in the measurement of given observables. In particular, deviations from the SM values of the Higgs bosons' couplings would provide invaluable information for determining whether the Higgs is an exact $SU(2)$ doublet or not. This fundamental quest requires, at the same time, both an

increase in the measurements’ accuracy and the development of an adequate theoretical tool for interpreting the observations. This work is meant to contribute to the latter line of research, with the realization of a phenomenological study of Effective Field Theories (EFTs). The effective description has the advantage of being rather model-independent as it uses only the information relative to the symmetries and particle content of the system at a given energy. In practice, today the established, unquestionable low-energy symmetry is that of the SM gauge group $SU(3) \times SU(2) \times U(1)$. The EFT is written in terms of a complete set of independent operators invariant under the chosen symmetry and systematically organized in an expansion in which each operator is weighted down by an appropriate inverse power of the BSM scale. The model dependence is thus encoded in the arbitrary Wilson coefficients that parameterize the expansion.

There are two categories of EFTs pertinent in the low-energy description of the EWSB sector, that are in natural correspondence with the two scenarios described above: the most familiar is the *linear Lagrangian*, which contains a series of invariants constructed out of the SM fields and organized in an expansion in canonical dimensions (for this reason it is also dubbed SMEFT). In particular, the Higgs particle is contained in the $SU(2)$ doublet Φ and its interactions are consequently encoded in structures of the form $(v + h)^n$. The leading-order Lagrangian is thus that of the SM itself, while the first corrections are represented by a basis of effective operators of dimension $d = 6$ (plus one term with $d = 5$ that generates Majorana neutrino masses). With these choices, the effective description reproduces correctly the effects of new physics of the first class, where the EWSB is realized linearly.

On the other hand, scenarios in which the Higgs arises as a pseudo-Goldstone boson are customarily associated to a more general formalism, that of the *non-linear- or chiral- Lagrangian*. Here the physical Higgs field is treated independently of the electroweak Goldstone bosons: because of their shift symmetry, the latter only have derivative couplings and their interactions are consequently ordered in a momentum expansion. In the Goldstone sector, the leading order Lagrangian typically corresponds to the two-derivative level of a non-linear σ -model, while first order corrections are described by an independent basis of operators with four derivatives, that at this level coincides with the so-called Applequist-Longhitano-Feruglio (ALF) effective Lagrangian [15–19] constructed long ago without the inclusion of the Higgs particle. The latter can be introduced in the chiral Lagrangian as a generic singlet h [20–23] since, in this framework, the Higgs particle is not necessarily a component of an exact $SU(2)$ doublet. Moreover, being a *pseudo*-Goldstone boson with a mass of the same order as the EWSB scale, its interactions are not limited to derivative couplings: its dependence is rather encoded into generic functionals $\mathcal{F}(h)$ [23–25], that can be parameterized in the form

$$\mathcal{F}(h) = 1 + 2a\frac{h}{v} + b\frac{h^2}{v^2} + \dots$$

where the dots stand for higher powers of (h/v) and the series’ coefficients are model-dependent quantities. This replaces the polynomial dependence on the structure $(v + h)$ that characterizes the linear expansion. It is worth noting that, since the couplings of the Higgs are not fixed by the $SU(2) \times U(1)$ symmetry, this parameterization is actually more general than the linear one, and it can account for setups in which the Higgs boson is embedded in arbitrary representations of $SU(2)$; in particular, it includes the exact doublet case (and thus the linear SMEFT) as a specific limit in the parameter space. The resulting Lagrangian may also be used to describe scenarios other than those discussed above, for instance one in which the Higgs is an “impostor” not related to electroweak symmetry breaking, such as a dark sector scalar, or a dilaton.

The effective linear and chiral Lagrangians with a light Higgs particle are intrinsically different. As a general result, the leading corrections for the non-linear Lagrangian include a higher number of independent (uncorrelated) couplings. Although this apparently implies a reduced predictivity for the chiral EFT, we

will show that it is possible to identify a number of distinctive signatures of this framework. Specifically, there are two sources of disparity between the linear and the non-linear EFTs:

- (i) In the non-linear realization, the interactions of the Higgs particle are contained in generic functions $\mathcal{F}(h)$ rather than coming in the structure $(v + h)$, as mentioned above. Phenomenologically, this corresponds to decorrelation effects between couplings with different number of Higgs legs, to be observed in the non-linear case compared to the linear one.
- (ii) The two EFTs differ in the expansion parameters: while the linear Lagrangian orders the operators by canonical dimensions, the chiral one presents a more complex structure. In fact the simultaneous presence of the Higgs, Goldstone and transverse gauge bosons leads to a hybrid linear-nonlinear expansion. This implies that some couplings appear at a different order (typically lower) in the non-linear expansion compared to the linear case [25–27]. The extra structures appearing as lowest-order corrections, that do not have an equivalent in the $d = 6$ linear basis, would then produce distinctive signatures of non-linearity, that could indeed be detected at present or future collider experiments.

In this thesis¹ we construct/complete the non-linear electroweak effective Lagrangian with a light Higgs and we study it in detail devoting particular attention to its relation with the linear EFT. In particular, we carry out for the first time a phenomenological comparison between the two scenarios, considering both LEP and LHC data, identifying signals belonging to both categories indicated above. This analysis accounts only for tree-level insertions of Higgs BSM couplings, as justified by the current experimental accuracy on Higgs measurements, which ranges between 10 % and 30 % [6].

¹ This thesis contains the results of four papers produced during my PhD and listed in Refs. [28–31]. However, I also worked on other projects, two of which have already resulted into a publication: Ref. [32] contains the proposal of a new technique for measuring the charm Yukawa coupling at the LHC studying Higgs-charm associated production. In Ref. [33], instead, we considered the Higgs portal to scalar Dark Matter in the context of a non-linearly realized EWSB: we constructed a chiral basis describing the leading DM interactions and studied for the first time their phenomenological impact.

Motivaciones y Objetivos

La física de partículas se encuentra a las puertas de una nueva época: el descubrimiento en 2012 de una nueva resonancia escalar en el LHC [1, 2], posteriormente establecida como compatible con el bosón de Higgs [3–5], ha resultado ser un punto de inflexión en su desarrollo. La mera existencia del Higgs es un hito en la ya larga historia de éxito del Modelo Estándar (ME) de las interacciones fundamentales, ya que confirma finalmente el conjunto de partículas incluidas en la teoría. Un triunfo reforzado por el hecho de que, hasta el momento, los acoplos del escalar de Higgs medidos por los experimentos ATLAS y CMS son compatibles con los predichos por el ME [6].

Ante esta perspectiva, es de esperar que los próximos años lleven nuestro conocimiento a territorio desconocido: el LHC y el CERN continuarán colisionando protones a una energía de centro de masa de 13 y 14 TeV, que no conoce precedentes y que, sin duda, aportará información nueva sobre la naturaleza de las interacciones fundamentales. El descubrimiento de una partícula nueva sería sin duda un acontecimiento revolucionario que allanaría el camino hacia la formulación de un “Modelo Estándar” completamente nuevo. En caso contrario, el camino a seguir será aquel de las medidas de precisión.

El catálogo de indicios experimentales de la existencia de nueva física más allá del Modelo Estándar (MME) es bastante amplio. Para empezar, los modelos cosmológicos, basados en la descripción clásica de la gravedad, se enfrentan con la presencia de la “Energía Oscura”, el nombre popular para el mecanismo desconocido responsable de la expansión acelerada del Universo. Mientras este rompecabezas no parece necesitar forzosamente de una explicación en términos de física de partículas, otros requieren decididamente de una extensión del ME: la Materia Oscura (MO) y las masas no-nulas de los neutrinos están entre los fenómenos que se han establecido más robustamente, y que todavía no tienen explicación. Otra cuestión aún inexplicada por la física del ME y planteada por los resultados cosmológicos, es la del origen de la desigualdad entre la cantidad de materia y de antimateria presente en el Universo.

Al mismo tiempo, la construcción del ME levanta también cuestiones teóricas, que se manifiestan principalmente en forma de ajustes muy finos que deben imponerse sobre los parámetros que aparecen en el Lagrangiano. Por ejemplo, una fuente de dilemas es lo a que se llama “problema CP fuerte”. Este problema encuentra su origen en una tensión entre la presencia, a priori, del llamado término- θ que viola la simetría de CP en el Lagrangiano de QCD, y la ausencia experimental de un momento de dipolo eléctrico del neutrón, que sería inducido por este mismo término: los límites experimentales actuales sobre esta cantidad ponen una restricción muy fuerte de $\bar{\theta} \lesssim 10^{-10}$. Aunque sería posible imponer a mano la conservación de la simetría CP en el sector fuerte, esto no resolvería el problema, ya que las contribuciones a este término provenientes del sector electrodébil (o de nueva física en general), que entran a través de la anomalía quiral, tenderían a restablecer un valor no-nulo de $\bar{\theta}$.

Además, una laguna innegable del Modelo Estándar es la ausencia de una lógica que pueda dar cuenta de la peculiar estructura de sabor observada en la Naturaleza. Las masas y mezclas de los fermiones conocidos están meramente descritas en el Lagrangiano del ME por parámetros arbitrarios cuyos valores han sido determinados de modo empírico, en contraste con las interacciones entre las partículas cuyo surtido y fuerza están elegantemente fijados por el principio gauge. Efectivamente, sólo éste impone una restricción significativa sobre la estructura del sector fermiónico, requiriendo la presencia de familias “completas” para asegurar la cancelación de anomalías. La presencia de exactamente tres familias y la amplia diferencia entre los patrones de jerarquías de masas y mezclas entre quarks y leptones están aún sin explicar.

El puzle de sabor podría – o no – tener relación con el mecanismo de generación de masas implementado en el ME, es decir el proceso de ruptura espontánea de la simetría electrodébil (RESE). Dilucidar el origen

de la masa de la materia visible es, en sí, una cruzada fundamental que puede llegar a influir en otros de entre los problemas mencionados, como por ejemplo el problema CP-fuerte o la MO. Es precisamente el mecanismo de generación de masas, junto con los aspectos desconocidos del sector del Higgs aquello que se aborda en esta tesis. Una de las razones principales por las que a menudo se considera insatisfactorio el mecanismo de Higgs del ME, a pesar de la compatibilidad con los datos sobre el Higgs, es el denominado problema de la jerarquía. Éste último se puede enunciar como la cuestión de cómo puede el Higgs ser tan ligero si, a priori, se acopla con cualquier escala más pesada de nueva física. La relevancia del problema de la jerarquía motivó la formulación de una gran variedad de posibles soluciones. Hacemos frente al mismo en esta tesis utilizando un método bien conocido, que históricamente ha mostrado su eficacia a la hora de tratar ajustes teóricos (un gran ejemplo es la predicción de la existencia del quark charm y de su masa [7, 8]): seguimos un principio de simetría. A modo de guía para este tipo de acercamientos encontramos el criterio de naturalidad de 't Hooft [9], que asegura que todos los parámetros adimensionales que no están acotados por una simetría deberán ser de orden uno, y todos los que son dimensionales deberán ser del orden de la escala de la teoría. Bajo esta perspectiva, el problema de la jerarquía se puede abordar preguntando cuál es la simetría que estabiliza la masa del Higgs m_h frente a grandes correcciones radiativas.

Existen dos usos ampliamente explorados del principio de simetría en el caso del Higgs. Al propugnar una nueva simetría, el Higgs se encuentra acompañado por nuevos estados físicos, que completan la representación de multiplete bajo el nuevo grupo: precisamente la presencia de estos compañeros del Higgs es lo que permite, técnicamente, resolver el problema de la jerarquía. La teoría MME puede por tanto existir en un régimen perturbativo, y siendo el Higgs un estado elemental que pertenece a un doblete Φ de $SU(2)$, junto con los tres bosones de Goldstone electrodébiles, *i.e.* las componentes longitudinales de los bosones W^\pm y Z . Este tipo de construcciones se denominan comúnmente *realizaciones lineales* de la simetría electrodébil. El ejemplo paradigmático de esta clase de teorías es aquel de la supersimetría, en el que la protección proporcionada por la simetría quiral al termino de masa del Higgsino se transfiere a aquel del Higgs.

En otra clase de teorías se asume que el Higgs es un pseudo-bosón de Goldstone de una simetría rota espontáneamente, de manera que su masa queda protegida por una simetría de traslación aproximada. Esta opción se asocia de manera más natural a escenarios con nuevas interacciones fuertes, cuya condensación desencadenaría la ruptura espontánea de la simetría que produce los escalares electrodébiles: este tipo de construcciones conlleva una *realización no-lineal* de la RESE. Ejemplos típicos de estas teorías son los modelos de Higgs compuesto y modelos de “pequeño Higgs” que provienen de las teorías de Technicolor. Bajo este paradigma se pueden interpretar también otras construcciones aparentemente distantes de las anteriores, como las teorías con dimensiones extra. Una característica de este marco es que, bajo este tipo de esquemas, las propiedades del campo de Higgs detectadas a baja energía pueden alejarse genéricamente de aquellas de un doblete de $SU(2)$ exacto. Dado que los acoplos del Higgs se conocen, de media, con una precisión experimental del 20 %, esta hipótesis se encuentra todavía abierta.

Merece la pena señalar, por completitud, que, aunque las soluciones basadas en aplicaciones directas de las simetrías siguen siendo las más atractivas, se han explorado en la literatura otras alternativas. Un ejemplo reciente es el mecanismo conocido como “relajación cosmológica” [13], que se nutre de las ideas encontradas en Ref. [14]. En cualquier caso, a lo largo de este trabajo nos atenemos a las indicaciones dadas por las explicaciones en lo referente a la simetría.

El camino hacia la precisión

El objetivo principal de esta tesis es explorar a fondo las diferencias entre los dos escenarios mencionados arriba – RESE lineal y no-lineal –, buscando marcas distintivas que puedan permitir identificar cuál es la solución elegida por la Naturaleza. Lo haremos explorando la fenomenología correspondiente a la escala electrodébil y analizando, en particular, señales que se pueden observar en el LHC. Si no se llegase a descubrir ninguna partícula nueva en el futuro más cercano, la manera principal de llegar a una comprensión de la física MME será la búsqueda de anomalías en las medidas de determinados observables. En particular, desviaciones de los valores ME en los acoplos del bosón de Higgs proporcionarían información inestimable para determinar si el Higgs es, o no, un doblete de $SU(2)$ exacto. Esta misión fundamental requiere, al mismo tiempo, tanto de un aumento en la precisión de las medidas como del desarrollo de un instrumento teórico adecuado para interpretar las observaciones. Este trabajo quiere contribuir a esta última línea de investigación, con la realización de un estudio fenomenológico de Teorías Efectivas de Campos (TECs). La descripción efectiva tiene la ventaja de ser bastante independiente de los modelos, dado que usa solo informaciones relativas a las simetrías y al contenido en partículas del sistema a una energía dada. En la práctica, hoy las simetrías establecidas y incuestionables son las del grupo gauge del ME $SU(3) \times SU(2) \times U(1)$. La TEC se escribe en términos de un conjunto de operadores independientes, invariantes bajo la simetría elegida y sistemáticamente organizados en una expansión en la cual cada operador está suprimido por la potencia adecuada de la escala MME. De este modo la dependencia de un cierto modelo queda codificada dentro de los coeficientes de Wilson arbitrarios que parametrizan la expansión.

Hay dos categorías de TECs pertinentes en la descripción de baja energía del sector RESE, que se encuentran en una correspondencia natural con los dos escenarios descritos anteriormente: el más familiar es el *Lagrangiano lineal*, que contiene una serie de invariantes contruidos con campos del ME y organizados en una expansión en dimensiones canónicas. En particular, la partícula de Higgs está contenida en un doblete Φ de $SU(2)$ y sus interacciones están consiguientemente codificadas en estructuras de la forma $(v + h)^n$. El Lagrangiano al orden dominante es, entonces, el del mismo ME, mientras las primeras correcciones están representadas por una base de operadores efectivos de dimensión $d = 6$ (además de un término con $d = 5$ que genera masas de Majorana para los neutrinos). Con estas elecciones, la descripción efectiva reproduce correctamente los efectos de nueva física de la primera clase, donde la RESE se realiza linealmente.

Por otro lado, los escenarios en que el Higgs aparece como un pseudo-bosón de Goldstone están normalmente asociados a un formalismo más general, el del Lagrangiano *no-lineal* - o *quiral*. Aquí los campos del Higgs físico y de los bosones de Goldstone electrodébiles se tratan de manera independiente: a causa de su simetría de traslación, los Goldstone tienen solo acoplos derivativos y sus interacciones están consiguientemente ordenadas en una expansión en momentos. Para el sector de los bosones de Goldstone, el Lagrangiano de orden dominante corresponde típicamente al nivel de dos-derivadas de un modelo- σ no-lineal, mientras las correcciones de primer orden están descritas por una base independiente de operadores con hasta cuatro derivadas, que a este nivel coincide con el denominado Lagrangiano efectivo de Applequist-Longhitano-Feruglio (ALF) [15–19] construido tiempo atrás sin incluir a la partícula de Higgs. Esta última se puede introducir en el Lagrangiano como un singlete genérico [20–23] ya que, en este marco, la partícula de Higgs no es necesariamente una componente de un doblete $SU(2)$ exacto. Además, siendo un *pseudo*-bosón de Goldstone con una masa del mismo orden que la escala de RESE, sus interacciones no están limitadas a acoplos derivativos: su dependencia está más bien codificada dentro de funcionales genéricos $\mathcal{F}(h)$ [23–25],

que se pueden parametrizar de la forma

$$\mathcal{F}(h) = 1 + 2a \frac{h}{v} + b \frac{h^2}{v^2} + \dots$$

donde los puntos representan potencias más altas de (h/v) y los coeficientes de la serie son cantidades dependientes del modelo. Esto reemplaza la dependencia polinomial de la estructura $(v + h)$ que caracteriza la expansión lineal. Merece la pena notar que, como los acoplos del Higgs no están fijados por la simetría $SU(2) \times U(1)$, esta parameterización es de hecho más general que la lineal, y puede dar cuenta de configuraciones en las que el bosón de Higgs está incrustado en una representación arbitraria de $SU(2)$; en particular, esto incluye al caso de doblete exacto como un límite específico en el espacio de parámetros. El Lagrangiano resultante se puede utilizar, además, para describir escenarios distintos de los discutidos arriba, por ejemplo alguno en que el Higgs es un “impostor” que no está relacionado con la ruptura de la simetría electrodébil, como un escalar del sector oscuro, o un dilatón.

Los Lagrangianos efectivos lineal y quiral con un Higgs ligero son intrínsecamente distintos. Como resultado general, las correcciones dominantes para el Lagrangiano no-lineal incluyen un número de acoplos independientes (descorrelacionados) más alto. Aunque esto implica aparentemente una menor predictividad para la TEC quiral, mostraremos que es posible identificar varias señales características de esta construcción. En concreto, existen dos fuentes de disparidad entre las TECs lineal y no-lineal:

1. En la realización no-lineal, las interacciones de la partícula de Higgs están contenidas dentro de funciones genéricas $\mathcal{F}(h)$, en lugar de aparecer en la estructura $(v + h)$, como se ha descrito previamente. Fenomenológicamente, esto corresponde a efectos de descorrelación entre acoplos con distinto número de patas de Higgs, que se observarían en el caso no-lineal frente al caso lineal.
2. Las dos TECs difieren en los parámetros de expansión: mientras el Lagrangiano lineal ordena los operadores por dimensiones canónicas, el quiral presenta una estructura más compleja. De hecho la presencia simultánea de los bosones de Higgs, de Goldstone y de gauge lleva a una expansión híbrida lineal-nolineal. Esto implica que determinados acoplos aparecen a un orden distinto (típicamente inferior) en la expansión no-lineal comparado con el caso lineal [25–27]. Las estructuras adicionales que aparecen como correcciones de primer orden y que no tienen un equivalente en la base lineal a $d = 6$, producirán entonces señales distintivas de no-linealidad, que podrían ser detectadas en experimentos actuales o futuros.

En esta tesis² construimos/completamos el Lagrangiano electrodébil efectivo y lo estudiamos en detalle, dedicando especial atención a su relación con la TEC lineal. En concreto, se lleva a cabo un estudio detallado del Lagrangiano quiral con un Higgs ligero, prestando especial atención a su relación en la TEC lineal. En particular, realizamos por primera vez una comparación fenomenológica entre los dos escenarios, considerando datos tanto de LEP como de LHC e identificando señales pertenecientes a las dos categorías anteriormente descritas. Este análisis tiene en cuenta únicamente inserciones a nivel-árbol de los acoplos MME del Higgs, elección justificada por la precisión experimental actual de los datos de Higgs, que oscila entre el 10 y el 30 % [6].

² Esta tesis contiene los resultados de cuatro artículos producidos a lo largo de mi doctorado y listados en la Refs. [28–31]. Sin embargo, en este tiempo he trabajado también en otros proyectos, entre los cuales dos desembocaron en publicación: la Ref. [32] contiene la propuesta de una nueva técnica para medir el acoplo Yukawa del quark charm al LHC, estudiando la producción asociada de Higgs y charm. Por otro lado, en la Ref. [33] consideramos el portal de Higgs a la Materia Oscura escalar en el contexto de una RESE realizada no-linealmente: construimos una base quiral que describe las interacciones dominantes de la MO y estudiamos por primera vez su impacto fenomenológico.

Contents

Acknowledgments	i
Motivations and Purpose	iii
Motivaciones y Objetivos	vii
1 Introduction: the Standard Model Higgs boson	1
1.1 The Standard Model	1
1.1.1 Symmetries and particle content	1
1.1.2 Electroweak symmetry breaking and Higgs mechanism	3
1.1.3 Open problems	7
1.2 The current experimental portrait of the Higgs boson	10
1.2.1 Main properties of the h particle	10
1.2.2 Production and decay channels at the LHC	11
1.2.3 Couplings to SM particles	13
2 Dynamics of the electroweak symmetry breaking	17
2.1 Spontaneous symmetry breaking of continuous symmetries	18
2.1.1 Global symmetries: Goldstone's theorem	18
2.1.2 Local symmetries: Higgs mechanism	20
2.1.3 Goldstone boson equivalence theorem	23
2.2 Spontaneous EW symmetry breaking: linear realization	23
2.2.1 A preliminary example from QCD: linear σ -model	24
2.2.2 The EW case: Higgs mechanism	27
2.3 Spontaneous EW symmetry breaking: non-linear realization	29
2.3.1 A preliminary example from QCD: non-linear σ -model	30
2.3.2 The EW case: Higgs-less EWSB	33
2.3.3 Violation of perturbative unitarity	34
2.4 The Higgs as a pseudo-Goldstone boson	38
2.4.1 Composite Higgs models: general structure	38

CONTENTS

3	Effective field theories with a light Higgs	41
3.1	The linear Lagrangian (SMEFT)	42
3.2	The chiral Lagrangian: Appelquist-Longhitano-Feruglio basis	43
3.3	The chiral Lagrangian with a light Higgs (HEFT)	44
3.4	Linear <i>vs.</i> non-linear in a nutshell	47
3.4.1	Matching between both EFTs	48
4	Disentangling a dynamical Higgs	51
5	Higgs ultraviolet softening	115
6	Sigma decomposition	147
7	The complete HEFT Lagrangian after the LHC Run I	189
8	Summary and Conclusions	265
	Resumen y Conclusiones	269
	Bibliography	280

Introduction: the Standard Model Higgs boson

1.1 The Standard Model

The Standard Model (SM) encompasses our knowledge of the particles existing in nature and of the three fundamental forces that have been understood at the quantum level: electromagnetic, weak and strong interactions. This theory is the impressive result of more than half-a-century of efforts, and its solid success has been established by a very wide number of experimental tests. In its fundamental structure it is a very simple and elegant theory, described by the Lagrangian:

$$\begin{aligned}
\mathcal{L}_{\text{SM}} = & -\frac{1}{4}W_{\mu\nu}^a W^{a\mu\nu} - \frac{1}{4}B_{\mu\nu}B^{\mu\nu} + \\
& + i\bar{Q}_L \not{D} Q_L + i\bar{U}_R \not{D} U_R + i\bar{D}_R \not{D} D_R + i\bar{L}_L \not{D} L_L + i\bar{E}_R \not{D} E_R + \\
& + D_\mu \Phi^\dagger D^\mu \Phi - \frac{\mu^2}{2}\Phi^\dagger \Phi - \frac{\lambda}{4}(\Phi^\dagger \Phi)^2 + \\
& - \left[\bar{Q}_L \Phi \mathbf{y}_D D_R + \bar{Q}_L \tilde{\Phi} \mathbf{y}_U U_R + \bar{L}_L \Phi \mathbf{y}_E E_R + \text{h.c.} \right] + \\
& + \frac{g_s^2}{16\pi^2} \theta G_{\mu\nu}^A \tilde{G}^{A\mu\nu},
\end{aligned} \tag{1.1.1}$$

whose properties and motivations will be summarized in this section.

1.1.1 Symmetries and particle content

The SM is a Quantum Field Theory based on a principle of invariance under the local (gauge) symmetry group $SU(3)_c \times SU(2)_L \times U(1)_Y$, where the first term describes the strong interactions and the remaining account for the electric and weak ones. As a consequence of this group choice it contains twelve gauge bosons: eight gluons (G^A) and four mediators of the electroweak (EW) interactions (W^a, B). The first line

1. Introduction: the Standard Model Higgs boson

of Eq. (1.1.1) accounts for their kinetic terms, with the corresponding field strength defined as

$$\begin{aligned} G_{\mu\nu}^A &= \partial_\mu G_\nu^A - \partial_\nu G_\mu^A + g_s f^{ABC} G_\mu^B G_\nu^C, & \{A, B, C\} &\in [1, 8] \\ W_{\mu\nu}^a &= \partial_\mu W_\nu^a - \partial_\nu W_\mu^a - ig \varepsilon^{abc} W_\mu^b W_\nu^c, & \{a, b, c\} &\in [1, 3] \\ B_{\mu\nu} &= \partial_\mu B_\nu - \partial_\nu B_\mu. & & \end{aligned} \quad (1.1.2)$$

Here uppercase (lowercase) indices span the color (isospin) space, f^{ABC} are the structure constants of $SU(3)$, while ε^{abc} is the completely antisymmetric Levi-Civita tensor. The equation above also defines the color and isospin coupling constants g_s and g ; the one for hypercharge will be denoted by g' .

Twelve are also the fermions whose interactions are described by the SM: six quarks and six leptons that can be grouped in three generations (also *families* or *flavors*). The generations differ from one another in the particles' masses, while they are identical from the point of view of the gauge interactions. It is customary to define the fermion fields as flavor multiplets, that is, as weak interaction eigenstates, denoted simply by the names of the first generation:

$$U = (u, c, t), \quad D = (d, s, b), \quad E = (e, \mu, \tau), \quad \nu = (\nu_e, \nu_\mu, \nu_\tau). \quad (1.1.3)$$

Both the up- and down-type quarks are in turn triplets of the $SU(3)$ color group, while leptons do not participate in the strong interactions. It is well-established that the electroweak interactions are chiral, *i.e.* they act differently on the left- and right-handed components of the fermion fields, and have a $V - A$ Lorentz structure. In particular, right-handed quarks and charged leptons are singlet under the $SU(2)_L$ group, while their left-handed counterparts are embedded in complex doublet representations:

$$Q_L = (U_L, D_L)^T, \quad L_L = (\nu_L, E_L)^T. \quad (1.1.4)$$

The SM spectrum does not include right-handed neutrinos, as their existence has never been established. All fermions are assigned an hypercharge which, as will be justified below, is determined by the condition that the electric charge shall be obtained as $Q = T_3 + Y$, where T_3 is the third component of the isospin: $T_3 = \pm 1/2$ within left-handed doublets and $T_3 = 0$ for right-handed fields. The transformation properties of the SM fermions under the color ($SU(3)_c$), isospin ($SU(2)_L$) and hypercharge ($U(1)_Y$) groups are summarized in table 1.1. The last column indicates the explicit form of the corresponding covariant derivative, that appears in the kinetic terms in the second line of Eq. (1.1.1). It is worth pointing out that this particular set of fermions is not justified *a priori* by any guiding principle: the fermionic fields of the SM and their charge assignments were rather determined on an empirical basis, interpreting the experimental observations. The only significant constraint on the structure of the fermionic sector is again imposed by gauge invariance, which requires the presence of “complete” families for ensuring anomaly cancellation.

Indeed, the fact that electroweak interactions are chiral exposes the SM to the appearance of gauge anomalies: however, the charge assignments to the fermions are such that the gauge anomalies cancel in all sectors of the SM. Still, a global anomaly is present for the axial symmetry $U(1)_A$, under which the fermions transform as $\psi \mapsto e^{i\alpha\gamma_5} \psi$. The divergence of the associated axial current j_5^μ receives both a classical and a quantum contribution: the former is proportional to the quarks' masses, while the latter comes from the triangle diagram that couples j_5^μ to a gluon pair and it has the same structure as the QCD θ -term in the last line of Eq (1.1.1), that violates CP . Despite being a total divergence, this term cannot be removed from the Lagrangian as it can induce physical non-perturbative effects: in fact, there exist topologically non trivial configurations of the gauge fields, called instantons, for which this term is not irrelevant. The θ -term gives a non-negligible contribution to the neutron electric dipole moment, and the experimental upper bounds on this quantity allow to infer a strong limit $\theta \ll 10^{-9}$. The problem of why θ is so small is known as the *strong CP problem*. Notice that an analogous interaction with the structure $W_{\mu\nu} \tilde{W}^{\mu\nu}$ may be written *a priori* for the other non-abelian gauge group of the SM, $SU(2)_L$. However, this can be completely removed via a $B + L$ transformation, which is also anomalous in association with $SU(2)_L$, and is therefore non-physical.

field	$SU(3)_c$	$SU(2)_L$	$U(1)_Y$	covariant derivative D_μ
$Q_L = (U_L, D_L)^T$	3	2	1/6	$\partial_\mu + \frac{ig_s}{2} G_\mu^A \lambda^A + \frac{ig}{2} W_\mu^a \tau^a + \frac{ig'}{6} B_\mu$
U_R	3	1	2/3	$\partial_\mu + \frac{ig_s}{2} G_\mu^A \lambda^A + \frac{2ig'}{3} B_\mu$
D_R	3	1	-1/3	$\partial_\mu + \frac{ig_s}{2} G_\mu^A \lambda^A - \frac{ig'}{3} B_\mu$
$L_L = (\nu_L, E_L)^T$	1	2	-1/2	$\partial_\mu + \frac{ig}{2} W_\mu^a \tau^a - \frac{ig'}{2} B_\mu$
E_R	1	1	-1	$\partial_\mu - ig' B_\mu$

Table 1.1: Transformation properties of the fermions under the Standard Model gauge groups. The Pauli and Gell-Mann matrices are denoted by τ^a and λ^A respectively.

Finally, a very important piece in the Standard Model construction is represented by the Higgs field Φ , which is a complex scalar with the transformation properties $\Phi \sim (\mathbf{2}, 1/2)$ under the electroweak group. Being a complex doublet, Φ contains four elementary degrees of freedom, one of which is the physical Higgs boson h . The role of the Higgs doublet is that of triggering the spontaneous breaking of the electroweak symmetry $SU(2)_L \times U(1)_Y$ down into the residual $U(1)_{\text{em}}$ of electromagnetic interactions. This can be achieved for appropriate values of the parameters μ and λ in the scalar potential (the third line of Eq. (1.1.1)) and allows both the fermions and the mediators of the weak interactions (W^\pm, Z) to acquire a non-vanishing mass. The latter stem directly from the Higgs' kinetic term, while the former emerge from the Yukawa couplings in the second-to-last line of Eq. (1.1.1).

The phenomenon of spontaneous electroweak symmetry breaking (EWSB) is the central topic of this thesis: its Standard Model implementation will be briefly illustrated in this section, while a deeper and extended analysis of its dynamics will be presented in Chapter 2.

1.1.2 Electroweak symmetry breaking and Higgs mechanism

The gauge group $SU(2)_L \times U(1)_Y$ provides a unified description of the weak and electromagnetic interactions. It was suggested for the first time by Glashow in 1961 [34] and by Salam and Ward in 1964 and finally completed with the Higgs mechanism of spontaneous electroweak symmetry breaking (EWSB) by Weinberg (1967) [35] and Salam (1968).

The fact that this could not be an exact symmetry of Nature was clear from the observation that an exact gauge symmetry requires the corresponding gauge bosons to be massless, while the shortness of the weak interactions' range suggested that the mediators must be pretty heavy³. In addition, since the weak interactions are chiral, their exact conservation is not compatible with fermion masses either, which is a quite serious problem. On the other hand, the electromagnetic interactions were known to be described with thrilling accuracy by an exact $U(1)$ gauge symmetry in quantum electrodynamics (QED): this clearly had to be the residual group after the breaking. Figure 1.1 shows a pictorial representation of how the electromagnetic group has been eventually embedded in the EW one.

The issue of EWSB was a major challenge in the formulation of the Standard Model.

³ This issue was first studied in the context of strong interactions, that captured larger attention than the weak ones in the 1950s. Most of the work on spontaneous symmetry breaking was indeed carried out with the aim of obtaining massive gluons and thus a short-range strong force, and was applied to the electroweak sector only later, by Weinberg and Salam in 1967. A few years after, in 1979, it was understood that the color group is not broken, and that the extremely short range of strong interactions is due to confinement.

1. Introduction: the Standard Model Higgs boson

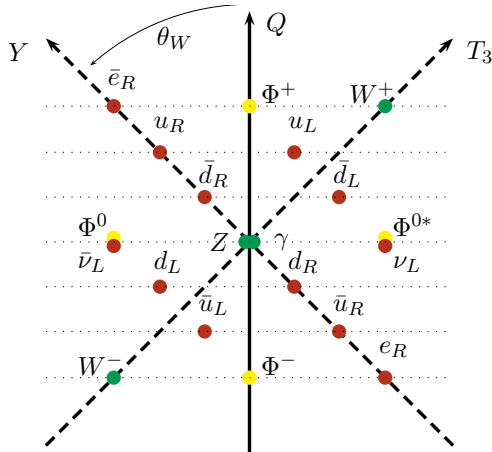


Figure 1.1: *A pictorial view of the charge assignment for the SM particles.*

In several papers, including those of Glashow and of Salam and Ward, the gauge bosons' and fermions' masses were simply added by hand to the Lagrangian. However, this was far from being a good solution, as it was well known that the insertion of explicit mass terms for the gauge bosons, breaking a gauge symmetry which in this case in non-abelian, makes the whole model non-renormalizable. This was a very serious issue for electroweak gauge theories, whose primary motivation was to supersede the old Fermi model, curing precisely its non-renormalizability. As an alternative to explicit violation, it was suggested that EWSB may rather take place spontaneously, which means that the Lagrangian could be invariant under the gauge symmetry, although the spectrum of physical particle does not form a representation of the local group.

The idea came from the recent discoveries on su-

perconductors and had been brought to particle physics by Nambu in 1960 [36]. It was known, in fact, that magnetic flux is excluded from these materials in the superconducting phase: the photon effectively behaves as if it acquired a mass inside the medium while the electric charge remains conserved. In the case of the electroweak model, this would have allowed the Lagrangian to remain invariant under the whole EW symmetry, thus ensuring renormalizability, while the vacuum state of the theory would have respected electromagnetic invariance only, allowing for massive gauge bosons.

Irrespective of how the EW symmetry was to be broken, though, a major obstacle to the formulation of the theory was represented by Goldstone’s theorem [37, 38] (1960, see Section 2.1.1) that stated that, whenever a symmetry gets broken, a bunch of massless particles necessarily appears in the spectrum. This conclusion was so discouraging that in a paper published in 1962 (in which they worked out the general proof of the theorem) Weinberg, Salam and Goldstone himself described this fact as an “intractable difficulty” [38]. The impasse was solved four years later, in 1964, when the work of three independent groups (Englert and Brout [3], Higgs [4, 5] and finally Guralnik, Hagen and Kibble [39]) demonstrated that Goldstone’s theorem is not valid for local symmetries. In fact, the degrees of freedom liberated by the spontaneous breaking of a gauge symmetry would not remain in the spectrum, but they rather emerge as the longitudinal components of the gauge bosons, that thus become massive.

As mentioned above, the idea of spontaneous EWSB was finally joined with that of electroweak unification based on $SU(2) \times U(1)$ invariance by Weinberg in 1967 [35] and Salam in 1968, establishing the core structure of the standard model. The EWSB was implemented with the addition of a single complex scalar field that transformed as a doublet under $SU(2)$ and with hypercharge 1/2, namely the Higgs doublet. This contains four real degrees of freedom:

$$\Phi = \begin{pmatrix} \Phi^+ \\ \Phi^0 \end{pmatrix} = \frac{1}{\sqrt{2}} \begin{pmatrix} i\phi_1 + \phi_2 \\ \phi_0 - i\phi_3 \end{pmatrix} \quad \text{and} \quad D_\mu \Phi = \partial_\mu \Phi + \frac{ig}{2} W_\mu^a \tau^a \Phi + \frac{ig'}{2} B_\mu \Phi. \quad (1.1.5)$$

The most general $SU(2) \times U(1)$ invariant Lagrangian for the Higgs sector that can be constructed at the renormalizable ($d \leq 4$) level is therefore

$$\begin{aligned} \mathcal{L}_\Phi = & D_\mu \Phi^\dagger D^\mu \Phi - \frac{\mu^2}{2} \Phi^\dagger \Phi - \frac{\lambda}{4} (\Phi^\dagger \Phi)^2 + \\ & - \left[\bar{Q}_L \Phi \mathbf{y}_D D_R + \bar{Q}_L \tilde{\Phi} \mathbf{y}_U U_R + \bar{L}_L \Phi \mathbf{y}_E E_R + \text{h.c.} \right]. \end{aligned} \quad (1.1.6)$$

Here the coupling constants \mathbf{y}_f are 3×3 hermitian matrices in flavor space. The coupling to right-handed up quarks has to be constructed with the conjugate Φ^* , in order to preserve hypercharge. Since this field transforms in a $\bar{\mathbf{2}}$ representation of $SU(2)$, however, it shall also be contracted with the $\bar{\mathbf{2}}$ of \bar{Q}_L through the antisymmetric tensor $\varepsilon_{ij} = (i\tau^2)_{ij}$. For this reason, it is usually written in terms of a “tilded” field, defined as

$$\tilde{\Phi} = i\tau^2 \Phi^* = \begin{pmatrix} \Phi^{0*} \\ -\Phi^- \end{pmatrix} = \frac{1}{\sqrt{2}} \begin{pmatrix} \phi_0 + i\phi_3 \\ i\phi_1 - \phi_2 \end{pmatrix}, \quad \tilde{\Phi} \sim (\mathbf{2}, -1/2). \quad (1.1.7)$$

The parameter λ in the scalar potential is necessarily positive in order for the potential to be bounded from below. If also $\mu^2 > 0$, the potential has a unique minimum in $|\Phi| = 0$, that leaves the EW symmetry intact. Requiring $\mu^2 < 0$, instead, the potential is minimized for $|\Phi| = \sqrt{-\mu^2/\lambda}$. In practice, the potential is shaped as a “mexican hat” and there is an infinite set of degenerate vacua laying on a ring of fixed radius, which defines the *EW vacuum expectation value* (vev) v :

$$v = \sqrt{2\langle \Phi^\dagger \Phi \rangle} = \sqrt{-\frac{2\mu^2}{\lambda}} \simeq 246 \text{ GeV}. \quad (1.1.8)$$

This is the characteristic scale of the EW theory: every physical parameter that appears in the EW observables and carries a mass dimension should be proportional to v . Experimentally, its value is inferred by that of the Fermi constant G_F via the relation $v = (\sqrt{2}G_F)^{-1/2}$, where the value of G_F is extracted from the muon decay rate [40].

Although the Lagrangian and the scalar potential are invariant under the full $SU(2)_L \times U(1)_Y$, each vacuum state only admits a residual $U(1)$ symmetry. Among the infinite ground states available, the alignment parallel to the neutral component of the doublet $\langle \Phi \rangle \sim v(0, 1)^T$ preserves the electromagnetic group identified as $U(1)_{\text{em.}} = U(1)_{T_3+Y}$. Excitations around this particular vacuum can be parameterized in polar coordinates as

$$\Phi(x) = \frac{v + h(x)}{\sqrt{2}} e^{i\pi_a(x)\tau^a/v} \begin{pmatrix} 0 \\ 1 \end{pmatrix} = \frac{1}{\sqrt{2}} \begin{pmatrix} i\pi_1(x) + \pi_2(x) \\ v + h(x) - i\pi_3(x) \end{pmatrix} + \mathcal{O}(\pi_i^2), \quad (1.1.9)$$

Here the radial excitation $h(x)$ is the physical Higgs boson [41], while the three phases $\pi_i(x)$ are the three Goldstone bosons of the EWSB that shall be “eaten” by the gauge fields of the weak interactions via the redefinition $(W_\mu^a)' = W_\mu^a + \partial_\mu \pi^a/(gv)$. At this point, it is possible to go to unitary gauge, where $\pi_i(x) \equiv 0$ and see that the scalar potential provides then the Higgs mass term and self-couplings

$$\frac{\mu^2}{2} \Phi^\dagger \Phi + \frac{\lambda}{4} (\Phi^\dagger \Phi)^2 = \frac{m_h^2}{2} h^2 + \frac{\lambda v}{4} h^3 + \frac{\lambda}{16} h^4, \quad m_h^2 = -\mu^2 = \frac{\lambda v^2}{2}, \quad (1.1.10)$$

while the Higgs’ kinetic term yields

$$D_\mu \Phi^\dagger D^\mu \Phi = \frac{\partial_\mu h \partial^\mu h}{2} + \frac{(v+h)^2}{4} g^2 W_\mu^+ W^{-\mu} + \frac{(v+h)^2}{8} (g^2 + g'^2) Z_\mu Z^\mu, \quad (1.1.11)$$

upon defining the physical fields

$$W_\mu^\pm = \frac{W_\mu^1 \mp iW_\mu^2}{\sqrt{2}}, \quad Z_\mu = \cos\theta W_\mu^3 - \sin\theta B_\mu, \quad A_\mu = \sin\theta W_\mu^3 + \cos\theta B_\mu, \quad (1.1.12)$$

where θ is the weak angle $\theta = \arctan(g'/g) \simeq 0.23$. Equation (1.1.11) provides masses for the W and Z bosons:

$$m_W = \frac{gv}{2}, \quad m_Z = \frac{gv}{2\cos\theta}, \quad (1.1.13)$$

1. Introduction: the Standard Model Higgs boson

while leaving a massless photon A_μ in the spectrum. The electromagnetic constant is then given by $e = g \sin \theta = g' \cos \theta$. Finally, the Yukawa interactions give to every fermion a mass $m_f = v y_f / \sqrt{2}$. In unitary gauge they read

$$-\bar{Q}_L \Phi \mathbf{y}_D D_R + \bar{Q}_L \tilde{\Phi} \mathbf{y}_U U_R + \bar{L}_L \Phi \mathbf{y}_E E_R + \text{h.c.} = -\frac{v+h}{\sqrt{2}} (\bar{D}_L \mathbf{y}_D D_R + \bar{U}_L \mathbf{y}_U U_R + \bar{E}_L \mathbf{y}_E E_R + \text{h.c.}). \quad (1.1.14)$$

Here the constants \mathbf{y}_f represent 3×3 matrices in flavor space, that are in general not diagonal. However, it is always possible to switch to the mass eigenbasis applying the redefinition

$$f_L \rightarrow V_L^f f'_L, \quad f_R \rightarrow V_R^f f'_R \quad (1.1.15)$$

where V_L^f and V_R^f are unitary matrices such that

$$(V_L^d)^\dagger \mathbf{y}_D V_R^d = \text{diag}(m_d, m_s, m_b), \quad (V_L^u)^\dagger \mathbf{y}_U V_R^u = \text{diag}(m_u, m_c, m_t), \quad (V_L^e)^\dagger \mathbf{y}_E V_R^e = \text{diag}(m_e, m_\mu, m_\tau). \quad (1.1.16)$$

This rotation has no impact on the electromagnetic and neutral currents, where the matrices V^f enter in the combination $V^{f\dagger} V^f = \mathbb{1}$. This means that flavor-changing neutral currents (FCNC) are absent at tree-level in the SM. However, the charged-current interactions now connect different generations read (primes on the fermion fields are dropped)

$$\mathcal{L}_{CC} = -\frac{g}{\sqrt{2}} W_\mu^+ (\bar{U}_L g^\mu (V_L^u)^\dagger V_L^d D_L + \bar{\nu}_L \gamma_\mu (V_L^\nu)^\dagger V_L^e E_L) + \text{h.c.} \quad (1.1.17)$$

In the quarks' sector, this determines the presence of flavor-changing charged currents, that are controlled by the Cabibbo-Kobayashi-Maskawa (CKM) matrix $V_{\text{CKM}} \equiv (V_L^u)^\dagger V_L^d$ [42, 43]. This matrix is unitary by definition and it contains four physical parameters that can be chosen to be three mixing angles plus one CP-violating phase [40]:

$$V_{\text{CKM}} \equiv (V_L^u)^\dagger V_L^d = \begin{pmatrix} c_{12}c_{13} & s_{12}c_{13} & s_{13}e^{-i\delta} \\ -s_{12}c_{23} - c_{12}s_{23}s_{13}e^{i\delta} & c_{12}c_{23} - s_{12}s_{23}s_{13}e^{i\delta} & s_{23}c_{13} \\ s_{12}s_{23} - c_{12}c_{23}s_{13}e^{i\delta} & -c_{12}s_{23} - s_{12}c_{23}s_{13}e^{i\delta} & c_{23}c_{13} \end{pmatrix}, \quad (1.1.18)$$

where $s_{ij} = \sin \theta_{ij}$, $c_{ij} = \cos \theta_{ij}$. The mixing angles are chosen to lie in the first quadrant $\theta_{ij} \in [0, \pi/2]$, while δ can vary in the range $[-\pi, \pi]$. The magnitudes of the different CKM entries are extracted from the semileptonic decay rates of the relevant quarks: for instance, $|V_{ud}|$ is determined from nuclear beta decays, while $|V_{us}|$ can be inferred from semileptonic decays of the K mesons, such as $K^0 \rightarrow \pi e \nu$. The experimental results reveal a hierarchy between the mixing angles $s_{13} \ll s_{23} \ll s_{12} \ll 1$.

Flavor-changing effects in the leptonic sector are absent if neutrinos are exactly massless: in this case, in fact, it is possible to choose $V_L^\nu \equiv V_L^e$ in order to compensate for the charged leptons' rotation in Eq. (1.1.17). Nonetheless, the phenomenon of neutrino oscillations has been firmly established experimentally, which implies the existence of a leptonic mixing matrix. The simplest and by now well-established explanation to this phenomenon is that neutrinos do have masses, which, additionally, are not equal for the three families. The leptonic mixing matrix is known as Pontecorvo-Maki-Nakagawa-Sakata (PMNS) matrix [44, 45] and it is customarily written

$$U_{\text{PMNS}} = V_{\text{PMNS}} U_P, \quad (1.1.19)$$

where V_{PMNS} is parameterized analogously to the CKM in Eq. (1.1.18) and $U_P = \text{diag}(1, e^{i\alpha}, e^{i\beta})$. The phases α, β contained in the latter matrix are physical if neutrinos are Majorana particles. The observed pattern of leptonic mixing angles is very different from that of the quarks sector: two angles, θ_{12} and θ_{23} are large (with θ_{23} nearly maximal) and the third is only one order of magnitude smaller, namely $\theta_{13} \simeq 0.15$. No significant constraint is currently available on the three complex phases.

When the Weinberg-Salam model was first proposed, there was no indication for the presence of the Z boson (while the W^\pm had been hypothesized as a weak mediator), nor the existence of quarks had been established. Nonetheless, the model predicted a number of peculiarities of the electroweak interactions that have gradually been observed, with amazing accuracy, by the experiments performed in the following decades. Among the first decisive discoveries we recall that of the existence of neutral currents due to Z mediation, discovered at CERN in 1973 and that of parity violation, observed in 1978. The success of the Standard Model exploded with the discovery of the charm quark to complete the second family and, subsequently, with that at LEP in 1983 of the W and Z bosons, whose masses were found to be 80.4 and 91.2 GeV respectively: these values are within the allowed window predicted by Weinberg in 1967 [35] from the values of the electromagnetic and Fermi constant. The last missing piece has remained for a very long time the Higgs boson, the scalar leftover of the EWSB. Searches were complicated by the fact that the Higgs mass is not predicted within the Standard Model, but a particle compatible with this state has been finally discovered by the ATLAS and CMS experiments at the LHC in 2012. Its properties are currently being measured and analyzed: the present knowledge about the new resonance is summarized in Section 1.2.

1.1.3 Open problems

Despite its long-standing success, the Standard Model could not be an exhaustive theory of nature as, on one hand, some open theoretical problems still need to be addressed and, on the other, the SM does not provide account for well-established experimental observations that call for an explanation in terms of particle physics. The most striking examples are the existence of Dark Matter (DM) and the fact that neutrinos are massive. None of the known particles appears to be a suitable Dark Matter candidate and we are completely ignorant about the interactions in which DM may participate, besides the gravitational one. In particular, there is no evidence that DM can communicate with the visible sector, although it is plausible that this may happen at some level. Because of the absence of right-handed neutrinos, the Standard formulation is also lacking a mechanism for the generation of neutrino masses. This issue is intimately connected to another important question, which is whether neutrinos are Dirac or Majorana particles: the latter option is viable for neutrinos as they are electrically neutral. In the Majorana case, the possibility of lepton number violation would be open and processes such as neutrino-less double beta decay may be observed. This kind of signal has been searched for by several dedicated experiments, but their results are still not conclusive; intensive searches are currently ongoing. On the other hand, restricting to the gauge symmetries and particle content of the SM, an effective mass term for neutrinos can be written in the form of the Weinberg operator $(\bar{L}_L \tilde{\Phi})(\tilde{\Phi}^T L_L^c)$, which is a $d = 5$ interaction. It is suggestive that this yields a Majorana mass term which, in fact, violates the lepton number by two units. Another (related?) unsolved issue which is worth mentioning, is the so-called *flavor puzzle*, namely the lack of an explanation for the existence of three copies of all fundamental fermions, with such hierarchical masses, and of a rationale that could justify the observed mixing pattern among the three families of quark and leptons.

There are good reasons to believe that some new physics should exist above the TeV scale: indications that it may not be too far from this energy either, come mainly from theoretical considerations that concern the scalar sector of the SM. In fact this sector, which is so important for the symmetry structure of the whole theory, is affected by a few theoretical weaknesses that basically reflect the lack of a deep understanding of the EWSB mechanism. The Higgs mechanism gives a correct description of this process, but it does not account for the underlying dynamics, which is still unknown.

The hierarchy problem

The main issue related to the Higgs sector is known as hierarchy (or naturalness) problem, which originates from the fact that radiative corrections to the mass of a fundamental scalar are quadratically sensitive to high energy thresholds. In other words, any particle X that couples to the Higgs induces a radiative

1. Introduction: the Standard Model Higgs boson

correction to its mass of the form

$$m_h^2(\mu) - m_h^2(\mu_0) \sim \pm m_X^2 \log \frac{\mu^2}{\mu_0^2}, \quad (1.1.20)$$

where bosons and fermions contribute with a positive and negative sign respectively, and μ_0 is a reference renormalization scale. This implies that the Higgs mass should be naturally pushed towards the highest scale that couples to the Standard Model fields. Although the existence of new physics with such destabilizing properties has never been established, it is possible, for instance, that the Higgs field couples at some level with quantum gravity, which is characterized by the Planck scale $M_P \sim 10^{19}$ GeV. In this hypothesis it would be quite difficult to keep the Higgs as light as we observed it to be. In fact, demanding that $m_h \ll M_P$ is satisfied at all orders is equivalent to requiring an extremely precise cancellation between the bare mass parameter and all the loop corrections, that should take place with an accuracy of one part in 10^{15} . In a slightly different formulation, the accent of the problem can be put on the *unnaturalness* of the fine-tuning that would be required for keeping the electroweak scale much lighter than any new physics able to communicate with the Higgs sector. The notion of “naturalness” in particle physics is often employed in the definition given by ‘t Hooft [9]

At any energy scale μ , a physical parameter or set of physical parameters $\alpha_i(\mu)$ is allowed to be very small only if the replacement $\alpha_i(\mu) = 0$ would increase the symmetry of the system.

While setting a fermion’s (or a gauge boson’s mass) to zero increases the symmetry of a system to include chiral invariance, the mass of a fundamental scalar is not “protected” by the appearance of any new invariance, which explains why the hierarchy problem is typical of the Higgs boson and it is not shared by other SM particles.

The hierarchy problem has been object of study for quite a long time, during which a wide variety of solutions has been formulated. The Higgs discovery lately generated renewed attention to this issue, impulsing new lines of research: a recent example is provided by the “cosmological relaxation” mechanism [13], which builds upon the ideas in Ref. [14]. However, among all solutions, the two most popular ones remain those that make a direct use of the symmetry principle: supersymmetry (SUSY) and composite Higgs models (CHM). Both these class of theories put ‘t Hooft’s statement into practice, albeit in two distinct ways: the latter is based on the idea that the Higgs may be a pseudo-Goldstone boson, so that its mass would be protected by an approximate shift symmetry, while the former introduces a symmetry (SUSY) under which the Higgs field transforms as a multiplet’s component. As explained below, the fields that complete the Higgs’ multiplet have a key role in stabilizing the electroweak scale. Here we review briefly the main features of these two frameworks.

Supersymmetry is a weakly coupled theory, in which the Higgs boson remains elementary, and it is based on the hypothesis of a symmetry that relates particles of different spin: every fermion must be combined with its bosonic superpartner, and vice versa, to form a superfield. Importantly, supersymmetric theories contain at least two complex scalar doublets in the scalar sector, and therefore predict the existence of at least one charged and three neutral particles. One of the neutral states is a pseudoscalar, while the other two are CP-even particles. The properties of the lightest among them are typically similar to those of the SM Higgs boson, meaning that its vacuum expectation value is predominantly responsible for EWSB, and that this particle has SM-like couplings to the W and Z gauge bosons. In the limit in which SUSY is exact, the mass of the would-be Higgs boson is identical to that of its fermion partner, the Higgsino. In this way, the chiral symmetry that protects the fermion’s mass is transmitted to the bosonic sector, thereby solving the hierarchy problem. However, since supersymmetric partners of the SM particles have never been identified, supersymmetry must be broken at some level; consequently, corrections to the Higgs mass should be proportional to the SUSY breaking scale. An attractive possibility would then be to have SUSY broken around the TeV, so as not to reintroduce the EW hierarchy problem. This choice is also supported by other fascinating considerations: besides providing interesting Dark Matter candidates, this

scenario could allow for the unification of the strong and electroweak forces in a consistent and impressive way. However, direct searches for supersymmetric particles in the TeV mass region have not been successful yet, implying increasingly stringent constraints on the SUSY parameter space. These bounds can be evaded, although losing somewhat of the original motivation, opting for example for a non-minimal particle content or assuming either a harder or a more compressed spectrum.

An alternative application of 't Hooft principle for stabilizing the electroweak scale is based on the idea the Higgs may arise as a pseudo-Goldstone boson, which builds on an analogy with QCD pions. The Higgs could still be an elementary state in this context, however, the most popular class of theories that implement this idea are composite Higgs models. These assume the existence of some strong interacting new physics that induces a strong breaking of the electroweak symmetry, producing, among others, four light bound states to be identified with the three EW Goldstone bosons plus the physical Higgs. The work of this thesis is mainly motivated by this kind of scenario, whose detailed description is deferred to Chapter 2.

Triviality and stability of the scalar potential

Finally, two further issues are worth mentioning, that have drawn much attention before the Higgs discovery, as they implied bounds on the Higgs mass, but that are not considered as actual problems in the light of the recently measured value for m_h . They are related to the running of the quartic coupling λ , which have raised *a priori* triviality and/or stability concerns. In practice, the former would have been relevant for a heavy Higgs ($m_h \gtrsim 400 - 500$ GeV) as, in this regime, the quartic constant $\lambda = 2m_h^2/v^2$ would have been relatively large and its RGE evolution would have been approximately proportional to its value at a fixed scale:

$$\lambda(\mu) \sim \frac{\lambda(\mu_0)}{1 - \frac{3\lambda(\mu_0)}{16\pi^2} \log\left(\frac{\mu^2}{\mu_0^2}\right)}$$

In this case the coupling would have been growing with the renormalization scale and ultimately hit a Landau pole at $\hat{\mu} = \mu_0 \exp(8\pi^2/3\lambda(\mu_0))$. Evidently, pushing $\hat{\mu} \rightarrow \infty$ is tantamount to taking the limit $\lambda(\mu_0) \rightarrow 0$, but this would imply a *trivial* theory, in which EWSB cannot occur. Instead, requiring that the Landau pole lays beyond some finite reference scale (*e.g.* the Planck scale) and fixing $\mu_0 = v$ leads to $\lambda(v) = 2m_h^2/v^2 < -8\pi^2 \log(v/M_P)/3$ which is an upper bound on the Higgs mass.

Since the Higgs has been found to be quite light, though, the triviality bound is automatically satisfied, while there are more serious reasons to worry about the stability of the EW vacuum, if the SM is the ultimate quantum field theory. In fact it turns out that, assuming only contributions of SM particles in the loops, $\lambda(\mu)$ is actually a decreasing function of the renormalization scale because the dominant contribution to the running comes from a fermion, the top quark. Requiring that the quartic couplings remains positive up to a fixed cutoff scale provides a lower bound on the Higgs mass. For the measured value, $m_h = 125$ GeV the sign flip is expected to happen around $10^{10} - 10^{12}$ GeV. Luckily it has been shown [46] that, even if there was nothing between the EW and the Planck scales, the EW vacuum would remain metastable with an estimated lifetime of at least 10^{150} years, much larger than the age of the Universe. Still, as briefly illustrated above, there are good reasons to believe that some new physics should intervene before reaching this energy, which may alter this behavior either alleviating or worsening the stability problem.

1.2 The current experimental portrait of the Higgs boson

The discovery of a neutral boson compatible with the Higgs boson of the Standard Model has been announced in July 2012 by the ATLAS [1] and CMS [2] experiments currently operating at CERN. ATLAS observed the largest excess with a local significance of 5.9σ at a mass $m_h = 126.5$ GeV, while CMS observed an excess with a local significance of 4.9σ at a mass of 125.5 GeV.

The analyses were subsequently updated and complemented by several tests of the resonance’s properties and couplings, mainly aimed at verifying whether these are entirely consistent with those of the Standard Model Higgs boson. This section summarizes the currently available information about the new particle, that has been extracted from the data recorded by the ATLAS and CMS experiments at the LHC Run 1, corresponding to an integrated luminosity of approximately 5 fb^{-1} at the pp center-of-mass energy of $\sqrt{s} = 7$ TeV (recorded during 2011) and 20 fb^{-1} at $\sqrt{s} = 8$ TeV (recorded during 2012). With a slight abuse of language, justified by the common usage and by the experimental status, we will refer to the new particle simply as the “Higgs boson”.

1.2.1 Main properties of the h particle

J^{PC} Some basic characteristics of the newly discovered particle follow immediately from the fact that it has been observed decaying into two photons: it must be electrically neutral, colorless and of integer spin. The Landau-Yang theorem [47, 48] additionally ensures that, due to conservation of angular momentum and to the Bose symmetry, a particle decaying into $\gamma\gamma$ cannot have spin $J = 1$. Finally, the study of the angular distribution of the four leptons in the $h \rightarrow ZZ^* \rightarrow 4\ell$ decay channel allowed to determine that the spin-parity of the Higgs boson is $J^P = 0^+$, excluding the hypothesis 0^- and 2^+ at confidence levels above 97.8% [49, 50].

Mass The mass of the Higgs boson is one of the most important parameters for understanding the electroweak symmetry breaking process. As mentioned in the previous section, depending on whether the Higgs is light or heavy, the scalar potential of the Standard Model may be exposed to triviality or stability problems. Furthermore, a large number of the beyond-Standard-Model theories that had been proposed before 2012 gave a prediction for m_h or at least indicated a range where this parameter should lie: for example, a light mass was preferred by minimal supersymmetric models and in scenarios that assumed no new physics up to the Planck scale.

The measurement of the Higgs boson’s mass has been obtained from the reconstructed invariant mass peaks in the two cleanest decay channels $h \rightarrow \gamma\gamma$ and $h \rightarrow ZZ^*$ (see Fig. 1.2). The combination of both channels for both the ATLAS and CMS experiments has been recently provided in [51]:

$$m_h = 125.09 \pm 0.21(\text{stat.}) \pm 0.11(\text{syst.}) \text{ GeV} = (125.09 \pm 0.24) \text{ GeV}. \quad (1.2.21)$$

This also determines the last unknown parameter of the Standard Model, *i.e.* the quartic coupling in the scalar potential. In the normalization of Eq. (1.1.1):

$$\lambda = \frac{2m_h^2}{v^2} = 0.52, \quad (1.2.22)$$

which is consistent with a perturbative regime when analyzed in the SM framework.

Width Measuring the width of the Higgs boson can provide valuable information about the observed resonance: for example, if the latter was found to be broader than expected, this would possibly indicate either that the couplings of the Higgs boson to visible particles are larger than in the SM, or even that what has been produced are actually two quasi-degenerate states.

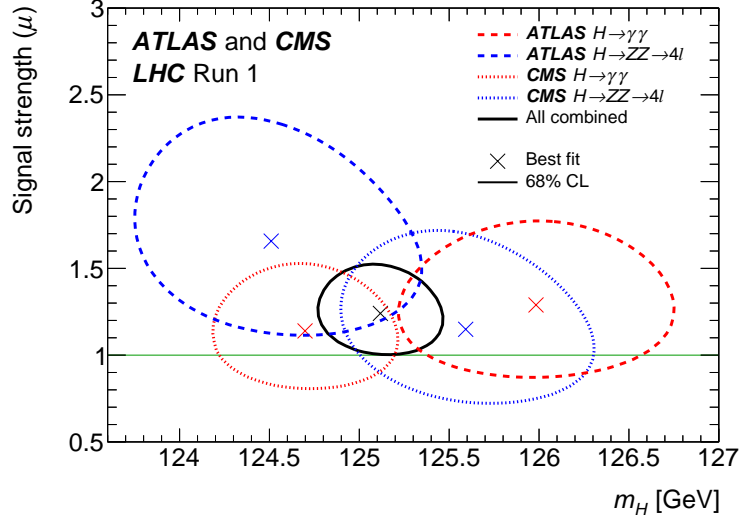


Figure 1.2: Likelihood summary in the plane of signal strength μ versus Higgs boson mass m_h for the $h \rightarrow \gamma\gamma$ and $h \rightarrow ZZ^*$ measured by the ATLAS and CMS experiments [51]. The curves delimit the 68% CL confidence regions of the individual (dashed) and combined (solid) measurements. The markers indicate the respective best-fit values. The SM signal strength is indicated by the horizontal line at $\mu = 1$.

In the Standard model the Higgs boson is predicted to be very narrow: $\Gamma_h^{\text{SM}} = 4.07 \pm 0.16 \text{ MeV}$. This value is well below the experimental resolution of the LHC experiments, which typically lays in the 1 to 3 GeV range, and therefore it has not been possible to measure directly the Higgs width with significant precision: at the moment, the best direct upper limit has been obtained via modeling of the Breit-Wigner distribution of the di-photon decay and gives $\Gamma_h < 2.4 \text{ GeV}$ at 95% CL [52]. More precise estimates can be obtained indirectly comparing the kinematic properties of the di-boson decay channel near and away from the resonance peak (on- vs. off-shell production) [53, 54]. The best indirect limit is

$$\Gamma_h \lesssim 22 \text{ MeV} \quad \text{at 95\% CL}, \quad (1.2.23)$$

which is still about 5.4 times larger than the SM expectation, but remarkably improves the direct constraints. It is important to remark that, unlike direct measurement, the indirect estimate relies on presuppositions on the underlying theory and, in particular, on the assumption that the couplings of the Higgs boson are the same on and above the resonance peak. This is tantamount to neglecting beyond-Standard-Model contributions both to Higgs production and decay.

Finally, recent analyses allow to constrain the Higgs invisible branching fraction. The best result has been obtained by the ATLAS experiment combining the searches performed with the Higgs produced in VBF, in association with a leptonically decaying Z boson and with an hadronically decaying gauge boson [55]. The result is

$$\text{Br}(h \rightarrow \text{invisible}) < 0.25 \quad \text{at 95\% CL}. \quad (1.2.24)$$

1.2.2 Production and decay channels at the LHC

The main modes through which the Higgs is produced at the LHC (and in general at a hadron collider) are gluon-gluon fusion (ggF), vector boson fusion (VBF) and associated production with vector bosons (VH) or a pair of top quarks (ttH).

1. Introduction: the Standard Model Higgs boson

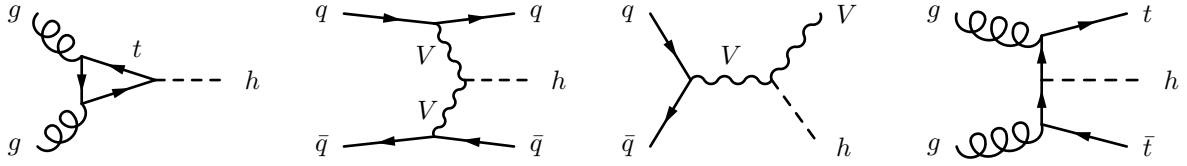


Figure 1.3: Sample Feynman diagrams for the main Higgs production modes at the LHC: gluon-gluon fusion (ggF), vector-boson fusion (VBF), associated production with a gauge boson (VH) and with a $t\bar{t}$ pair (ttH). In the two central diagrams, $V = \{Z, W^\pm\}$.

At high-energy hadron colliders, the dominating Higgs production channel is by far gluon-gluon fusion (see Fig. 1.3). Despite being radiatively induced, this process takes advantage of the absence of weak couplings (that suppress other tree-level channels) in the leading diagrams and, most importantly, of large corrections due to higher order QCD contributions, which increase significantly the cross-section. The comparison of the measured ggF cross-section with the one predicted by the SM tests both the size of the top-Yukawa coupling and the existence of new generations of heavy fermions that may run in the loop. The theoretical estimation is complicated by the relatively large size of the QCD radiative corrections, that need to be evaluated up to high orders. The cross-section for ggF Higgs production has been computed at 3-loops ($N^3\text{LO}$) in QCD [56], reaching a precision of order $\sim 10\%$. This result is very recent and has been obtained in the customary approximation of large top-mass $m_t \rightarrow \infty$ by matching the Higgs-gluon-gluon interaction to an effective local operator $hG_{\mu\nu}^A G^{A\mu\nu}$. Higgs production via VBF proceeds by the scattering of two quarks, mediated by t or u -channel exchange of a W or Z boson that radiates the Higgs. The characteristic signature of this process, that allows to distinguish it from the large QCD background, are the two hard jets in the forward and backward regions of the detector produced by the scattered quarks. Such peculiarity makes VBF a particularly clean environment also for the determination of the Higgs couplings to gauge bosons. A complementary context where the latter may be tested, is in VH associated production. This channel also turns out to be the most sensitive for the study of the coupling to the bottom quark. In fact, the process $pp \rightarrow hV$ with the V boson going into leptons is characterized by a particularly low QCD background, that allows the best observation of the decay $h \rightarrow b\bar{b}$. Finally, an alternative access to the top-Higgs interaction is provided in principle by the ttH production mode. Although its observation has not been significantly established at LHC Run 1 due to the large backgrounds and low statistics (see e.g. [57, 58]), there are promising prospects for isolating this process at LHC Run 2, profiting of an approximately 5-times larger cross-section and of improved jet substructure techniques.

According to the Standard Model prediction, the main decay channels for a Higgs boson with a mass $m_h = 125 \text{ GeV}$ are $h \rightarrow b\bar{b}$ and $h \rightarrow WW^*$, followed by $h \rightarrow gg$, $h \rightarrow \tau^+\tau^-$ and $h \rightarrow ZZ^*$. Smaller branching fractions are expected for the loop-induced channels, such as $h \rightarrow \gamma\gamma$ and $h \rightarrow Z\gamma$ and for the Yukawa-suppressed ones, e.g. $h \rightarrow \mu^+\mu^-$ (see Table 1.2). This sums up to a quite varied number of channels, that offer the opportunity to investigate the Higgs coupling to several SM particles, providing complementary information with respect to the production modes. Despite enjoying relatively low rates, the $h \rightarrow \gamma\gamma$ and $h \rightarrow ZZ^* \rightarrow 4\ell$ signatures are the cleanest ones at the LHC: they benefit of a high mass resolution and of low backgrounds. The former property is the main advantage with respect to the $WW^* \rightarrow \ell^+\nu\ell^-\bar{\nu}$ channel, where the presence of the neutrinos prevents the total invariant mass from being reconstructed precisely. The absence of hadrons in the final state, instead, allows to remove easily the overwhelming QCD background that plagues the $b\bar{b}$ and gg modes. Indeed, $h \rightarrow \gamma\gamma$ and $h \rightarrow 4\ell$ were the two “discovery channels” of 2012, namely those in which the Higgs was first detected with high significance. With the statistics collected in the whole Run 1 of the LHC by the ATLAS and CMS experiments it has been possible to observe the Higgs decaying into WW^* , $\tau^+\tau^-$ and $b\bar{b}$, in addition to the two main channels. Searches for decays into $Z\gamma$ [59, 60] and into muons and electrons [61, 62] have not been conclusive.

production	ggF	VBF	WH	ZW	ttH	tot
$\sqrt{s} = 7 \text{ TeV}$	$16.85^{+9\%}_{-12\%}$	$1.22^{+3\%}_{-2\%}$	$0.58 \pm 4\%$	$0.33 \pm 6\%$	$0.09^{+12\%}_{-18\%}$	19.07
$\sqrt{s} = 8 \text{ TeV}$	$21.42^{+9\%}_{-11\%}$	$1.58^{+3\%}_{-2\%}$	$0.70^{+4\%}_{-5\%}$	$0.41 \pm 6\%$	$0.13^{+12\%}_{-18\%}$	24.24
$\sqrt{s} = 14 \text{ TeV}$	$54.67^{+9\%}_{-11\%}$	$4.18 \pm 3\%$	$1.50 \pm 4\%$	$0.88^{+6\%}_{-5\%}$	$0.61^{+15\%}_{-28\%}$	61.84
decay	$h \rightarrow b\bar{b}$	$h \rightarrow WW^*$	$h \rightarrow \tau\tau$	$h \rightarrow ZZ^*$	$h \rightarrow \gamma\gamma$	
SM Br (%)	57.5 ± 1.9	21.6 ± 0.9	6.30 ± 0.36	2.67 ± 0.11	0.228 ± 0.011	

Table 1.2: Higgs boson production cross sections (pb) and branching fractions computed in the Standard Model with $m_h = 125 \text{ GeV}$ and for pp collisions with different center-of-mass energies \sqrt{s} . The calculation for ggF is done at NLO EW + $N^3\text{LO}$ QCD [56]. Those for VBF and VH are at NLO EW + NNLO QCD, while ttH has been computed at NLO QCD [63]. The list includes only the decay channels that have been observed with sufficient significance.

Signal strengths

Higgs boson data is usually expressed in terms of signal strengths. This parameter, denoted with μ , is defined as the ratio between the observed rate and the SM expectation. Since the Higgs is very narrow, the measured signal strength for a given production and decay channel $i \rightarrow h \rightarrow f$ can be expressed as

$$\mu_i^f \equiv \frac{\sigma(i \rightarrow h) \cdot \text{Br}(h \rightarrow f)}{\sigma_{\text{SM}}(i \rightarrow h) \cdot \text{Br}_{\text{SM}}(h \rightarrow f)} \quad (1.2.25)$$

which can be factorized in individual signal strengths for the production mode and for the decay channel $\mu_i^f = \mu_i \cdot \mu^f$ where

$$\mu_i \equiv \frac{\sigma(i \rightarrow h)}{\sigma_{\text{SM}}(i \rightarrow h)}, \quad \mu^f \equiv \frac{\text{Br}(h \rightarrow f)}{\text{Br}_{\text{SM}}(h \rightarrow f)}. \quad (1.2.26)$$

Although only the total signal strength μ_i^f can be directly measured at experiments, the value of each μ_i and μ^f can be extracted from a combined analysis of the data. The latest results have been published in Ref. [6] and are reported in Fig. 1.4 for the most relevant channels.

The last point of Figure 1.4a shows the result for the global signal strength μ , obtained fitting the whole dataset assuming a universal scaling for all the production and decay channels: $\mu_i \equiv \mu^f \equiv \mu$ for all i, f . This parameterization provides the simplest test of the compatibility of the experimental data with the SM predictions. The result reported by the collaborations is [6]

$$\mu = 1.09^{+0.11}_{-0.10} \quad (1.2.27)$$

which is consistent with the Standard Model within 1σ .

1.2.3 Couplings to SM particles

In order for the observed scalar resonance to be recognized as the “Standard Model Higgs boson”, it is necessary that all its couplings align with the Standard Model prediction. This implies, in particular, that *all* the leading-order (LO) couplings of the h particle to a pair of fermions have to be flavor diagonal and proportional to the fermion’s mass, with a proportionality constant equal to $v = 246 \text{ GeV} \equiv (\sqrt{2}G_F)^{-1/2}$. Analogously, pairs of gauge bosons’ should couple to the Higgs proportionally to the square of their masses. The effective couplings to gluons and photons, that arise only at next-to-leading order (NLO), can also be

1. Introduction: the Standard Model Higgs boson

sources of important information, as they are in principle sensitive to the presence of heavy BSM particles running inside the loop.

More in general, testing the Higgs couplings experimentally is extremely important in order to establish its nature and to gain an insight into the electroweak symmetry breaking process. Nonetheless, accessing some of the Higgs interactions can be very challenging: this is especially true for light fermions, whose Yukawas are very suppressed.

The experimental collaborations have been constraining the tree-level Higgs couplings within the so-called κ -framework [63, 64], that provides a set of scale factors κ_i defined in such a way that each of the relevant production cross-section and decay width of the h particle is formally rescaled by an associated factor κ_i^2 with respect to the SM prediction. For example, according to this prescription the process $gg \rightarrow h \rightarrow ZZ$ is parameterized as

$$\sigma(gg \rightarrow h) \cdot \text{Br}(h \rightarrow ZZ) = \sigma_{\text{SM}}(gg \rightarrow h) \cdot \text{Br}_{\text{SM}}(h \rightarrow ZZ) \frac{\kappa_g^2 \kappa_Z^2}{\kappa_h^2} \quad (1.2.28)$$

where κ_h rescales the total Higgs width. In practice, each κ_i parameterizes deviations from the SM of a specific Higgs coupling. Indeed, it is possible to write a phenomenological Lagrangian that in unitary gauge takes the form

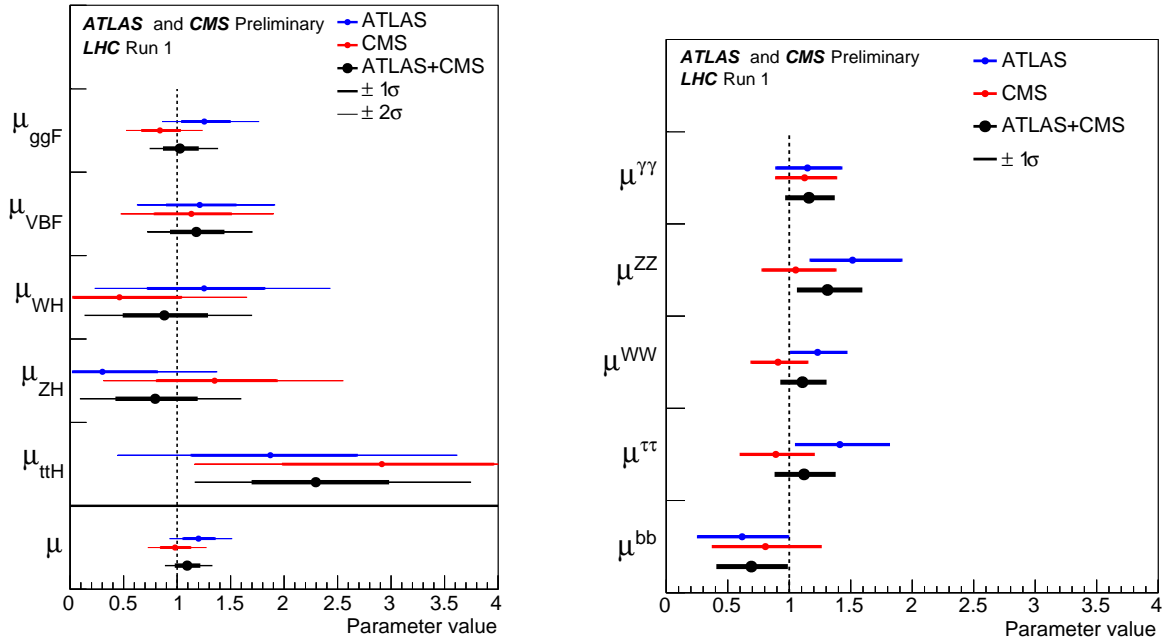
$$\begin{aligned} \mathcal{L}_{h,\kappa} = & - \sum_f \kappa_f \frac{m_f}{v} \bar{f} f h + \kappa_Z \frac{m_Z^2}{v} Z_\mu Z^\mu h + \kappa_W \frac{2m_W^2}{v} W^{+\mu} W_\mu^- h + \\ & + \kappa_g \frac{g_s^2}{48\pi^2 v} G_{\mu\nu}^A G^{A\mu\nu} h + \kappa_\gamma \frac{e^2}{16\pi^2 v} A_{\mu\nu} A^{\mu\nu} h + \kappa_{Z\gamma} \frac{e^2}{4\pi^2 v} A_{\mu\nu} Z^{\mu\nu} h. \end{aligned} \quad (1.2.29)$$

Notice that the second line of this Lagrangian contains effective interactions that are generated at the one-loop level in the Standard Model. The parameterization of Eq. (1.2.29) has some limitations: for example, it respects the Lorentz and the electromagnetic symmetries, but it is not explicitly invariant under the whole $SU(2) \times U(1)$, and it includes only the Lorentz structures expected within the SM. As a consequence it cannot be used for the analysis of kinematic distributions, nor it is adequate for beyond LO computations. Nonetheless, it is particularly simple and well-suited for constraining the size of the SM couplings via the analysis of total rates. Figure 1.5a shows the current constraints on these parameters, as provided by the most recent combined ATLAS-CMS analysis [6]. As shown in Eq. (1.2.28), Higgs data is sensitive to the total Higgs width, which is rescaled, compared to the SM, by the factor κ_h . This quantity depends in principle on the other κ 's that describe the Higgs decay into two SM particles, and is also sensitive to any BSM contributions to Γ_h . In order to fit the individual κ parameters it is then necessary to make an assumption about the Higgs width: for example, the combined ATLAS-CMS analysis in Ref. [6] considers two different setups, either assuming $\text{Br}(h \rightarrow \text{BSM}) = 0$, or allowing for BSM decays of the Higgs, but constraining the parameter space to $\kappa_V = \kappa_{Z,W} \leq 1$. Figure 1.5a shows that the current results are generically compatible with the SM expectations, although the error bars are still quite large. Indeed, the p -value of the compatibility with the SM for this particular fit is relatively low, around 11%.

The proportionality of the couplings to the other particles' masses also gives a quite SM-like picture of the Higgs boson: in figure 1.5b the best fit values for the reduced couplings $g_{hff} = \kappa_f m_f/v$ and $g_{VVh} = \sqrt{\kappa_V} m_V/v$, for fermions and gauge bosons respectively, are plotted against the corresponding masses. In this picture the Standard Model alignment is represented by the dashed line, whose slope is $1/v = (246 \text{ GeV})^{-1}$: values $\kappa_i < 1$ correspond to points below the line and vice versa. Notice that there is no perfect agreement between Figures 1.5a and 1.5b, as the latter has been derived with a more constraining setup, fixing $\text{Br}_{\text{BSM}} = 0$ and $\kappa_g = \kappa_\gamma = \kappa_{Z\gamma} = 1$, *i.e.* forbidding BSM contributions in the loops while allowing to include the $h \rightarrow \mu^+ \mu^-$ data.

The analyses presented in Figures 1.4 and 1.5 represent the most generic studies of compatibility of the observed resonance with the Standard Model Higgs boson. There are of course several other tests that can

be performed under more restrictive assumptions. Among these, two have particular relevance for this work: the test of violation of the custodial symmetry in the couplings of the Higgs to the Z and W bosons and the combined fit to the couplings κ_V *vs.* κ_F , obtained assuming a universal scaling for the Higgs couplings to vector bosons $\kappa_Z = \kappa_W \equiv \kappa_V$ and for the Higgs couplings to all fermions $\kappa_f \equiv \kappa_F \forall f$. The former test has been performed only by the CMS Collaboration [52], that used the combined data from $h \rightarrow ZZ \rightarrow 4\ell$ and $h \rightarrow WW \rightarrow \ell\nu\ell\nu$ decays to fit the parameter $\lambda_{WZ} = \kappa_W/\kappa_Z$ that is expected to be unity in the SM. Neglecting anomalous couplings of the Higgs to fermions, they obtain $\lambda_{WZ} = 0.94^{+0.22}_{-0.18}$ which is largely compatible with SM. The analysis of κ_V *vs.* κ_F has been presented in the combined analysis note: the best fit and 1σ regions obtained are indicated by the star and the black line in Fig. 1.6. Once again, the result is in very good agreement with the SM (p -value 59%). The colored areas show the contributions of the individual decay channels $h \rightarrow VV$ and $h \rightarrow f\bar{f}$. It is interesting to see that the fermionic decay channels are basically blind to the sign of the coupling, while the preference for the positive quadrant is determined by the bosonic decays.

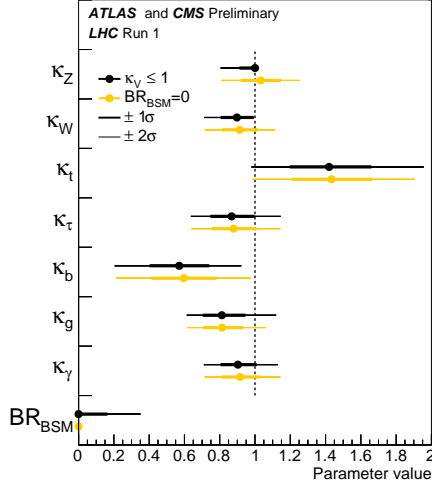


(a) Production signal strengths μ_i and global signal strength μ .

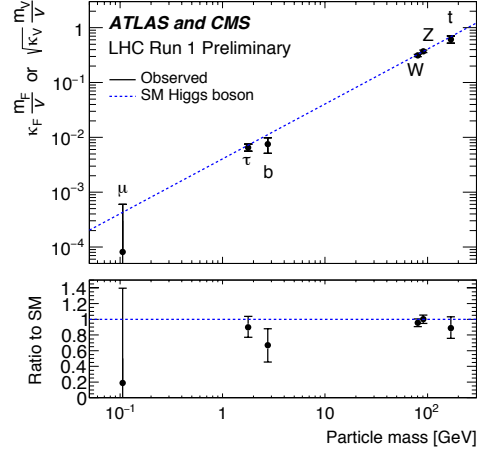
(b) Decay signal strengths μ^f .

Figure 1.4: Best-fit results for the production (left) and decay (right) signal strengths for the combination of the ATLAS and CMS results [6]. The last line of the left plot shows the global signal strength μ , obtained assuming the same scaling for all the production and decay channels.

1. Introduction: the Standard Model Higgs boson



(a) Fit of the κ_i parameters obtained either requiring $\kappa_V \leq 1$ (black) or imposing absence of BSM contributions to the Higgs boson width (yellow).



(b) Fit of the reduced couplings against the particle's mass. This analysis assumes no BSM contributions in the loops, i.e. $\kappa_g = \kappa_\gamma = 1$.

Figure 1.5: Combined measurement of the Higgs couplings [6]. The dashed line marks the Standard Model alignment.

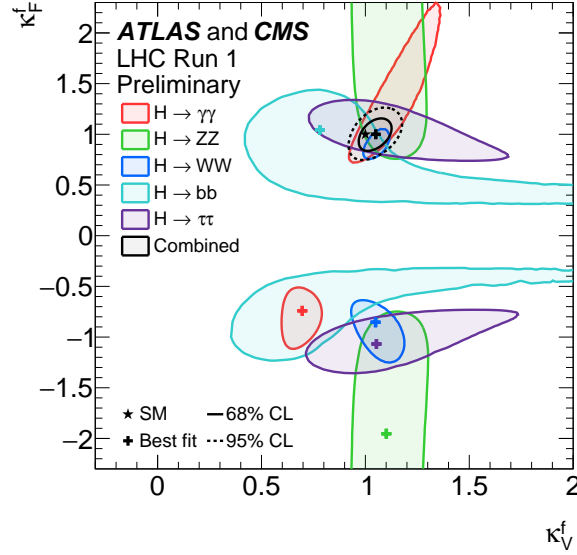


Figure 1.6: Negative log-likelihood contours of κ_F vs. κ_V for the combination of ATLAS and CMS and for the individual decay channels [6]. The black line shows their global combination, obtained assuming a universal κ_F for all the fermions and $\kappa_V = \kappa_Z = \kappa_W$.

Dynamics of the electroweak symmetry breaking

As already reviewed in Chapter 1, the theory of electroweak (EW) interactions requires the implementation of a mechanism of electroweak symmetry breaking (EWSB): the local symmetry $SU(2)_L \times U(1)_Y$ must be broken in order to allow the description of massive fermions and gauge bosons. Moreover, for the theory to be renormalizable the breaking must be spontaneous. In the Standard Model, this is implemented via the Higgs mechanism, which is a phenomenologically successful model: the recent discovery of the Higgs boson seems to confirm that this is a correct description of nature. Indeed, as was shown in Sec. 1.2, the measured properties of the Higgs are so strikingly compatible with the SM predictions, that we may be tempted to believe that the EWSB process has been mostly understood. However, most of the still unsolved mysteries of particle physics, including the hierarchy and stability problems and even the flavor puzzle, are definitely related to the scalar sector of the theory. This condition signals that a deep understanding of the EWSB is still lacking: although the Higgs mechanism gives a correct *description* of this process, it does not account for the underlying dynamics, which is still unknown.

For this reason, it is useful to take a step back and reexamine the structure of the EWSB sector. To begin with, in this chapter we present the main properties of spontaneous symmetry breaking, highlighting the differences between breakings that take place in global and in a local symmetry. Then, focusing on the case of the EW symmetry, we will show that its breaking can be realized in two ways: either linearly or non-linearly, discussed in Secs. 2.2 and 2.3 respectively. The former option can be generically implemented with a linear σ -model, which is equivalent to the Higgs mechanism described in Sec. 1.1.2, and it is characterized by the presence of a residual massive scalar in the spectrum: the Higgs boson. As will be shown, this particle has an important role in ensuring the unitarity of the S -matrices for scattering processes involving longitudinally polarized gauge bosons. This construction is typically the one embedded in models with weakly-interacting new physics, such as supersymmetric theories.

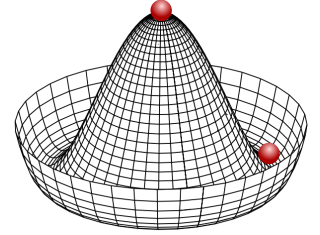
As an alternative, the EWSB can be realized non-linearly via a non-linear σ -model: in this case the Higgs boson is not indispensable for preserving gauge invariance, and it could even be removed from the spectrum. In this way one would obtain an effective Lagrangian that contains only the three degrees of freedom needed to give mass to the W^\pm and Z bosons (see Sec. 2.3.2). This theory, however, would violate unitarity and the interactions among the Goldstone bosons would ultimately become non-perturbative around the TeV scale. This paradigm for the realization of the EWSB is naturally associated with the idea of a new strong-

2. Dynamics of the electroweak symmetry breaking

interacting sector. In this case, the EW Goldstone bosons would correspond to composite states produced in the confinement of exotic heavy fermions. In analogy with QCD, the latter would also produce vector resonances that would cure the unitarity violation. The Higgs-less versions of these theories (that go under the name of Technicolor) are currently strongly disfavored, due both to incompatibilities with EW precision tests and flavor data, and of course to the fact that the Higgs has been discovered. However, the idea of strong-interacting new physics is easily reconcilable with the existence of the Higgs: indeed, this scalar boson may be composite. This scenario currently represents the most popular alternative to supersymmetry (which implements a linear realization of EWSB) as a plausible solution to the hierarchy problem. It will be discussed in Sec. 2.4.

2.1 Spontaneous symmetry breaking of continuous symmetries

Spontaneous symmetry breaking takes place in systems where the vacuum state does not exhibit the same symmetry as the Lagrangian. This is quite common in nature. The most classical example is that of a ball on the top of a dome: although the system is rotationally symmetric, the state of minimum energy, in which the ball sits at some point at the feet of the dome, is not. In fact, there is an infinite set of different ground states, all degenerate in energy and connected with each other via transformations of the broken symmetry.



In this chapter we focus on configurations similar to the ball-on-the-dome example, *i.e.* on systems exhibiting a spontaneously broken *continuous* symmetry: in a quantum system, it is easy to prove that this condition is always associated to the existence of a degenerate set of vacuum states. Consider a quantum system with n global continuous symmetries. By Noether's theorem, this corresponds to a set of n conserved charges Q_i that commute with the Hamiltonian of the system $[H, Q_a] = 0$ and the associated transformations are described by the action of the unitary operators $U_a = e^{i\alpha Q_a}$. The vacuum state $|\Omega\rangle$ of the system is the one with minimum energy: $H|\Omega\rangle = E_{\min}|\Omega\rangle$. Let us assume that this state is not invariant under all of the n symmetries, but only under a subset of k transformations. Indicating with hatted indices the $(n - k)$ broken generators, this corresponds to the condition

$$\begin{aligned} U_a|\Omega\rangle &= e^{i\alpha Q_a}|\Omega\rangle = |\Omega\rangle \Rightarrow Q_a|\Omega\rangle = 0 & a &= \{1, \dots, k\} \\ U_{\hat{a}}|\Omega\rangle &= e^{i\alpha Q_{\hat{a}}}|\Omega\rangle \neq |\Omega\rangle \Rightarrow Q_{\hat{a}}|\Omega\rangle \neq 0 & \hat{a} &= \{k+1, \dots, n\}. \end{aligned} \quad (2.1.1)$$

It's easy to show that the states $U_{\hat{a}}|\Omega\rangle$, that are connected by transformations of the broken symmetries, have the same energy as $|\Omega\rangle$ and therefore constitute a degenerate set of vacua:

$$HU_{\hat{a}}|\Omega\rangle = ([H, U_{\hat{a}}] + U_{\hat{a}}H)|\Omega\rangle = U_{\hat{a}}H|\Omega\rangle = E_{\min}U_{\hat{a}}|\Omega\rangle. \quad (2.1.2)$$

This result holds irrespectively of whether the broken symmetry is global or local. Nonetheless, the physical properties of the system are very different in the two cases: as shown in Sec. 2.1.1, Goldstone's theorem ensures that, in the global case, the spontaneous breaking leads to the appearance of a massless boson in the spectrum, called Goldstone boson (GB). On the other hand, this fundamental result does not apply if the symmetry is a local one: in this case, the main effect of the spontaneous breaking is that the associated gauge boson becomes massive. This is the essence of the Higgs mechanism, illustrated in Sec. 2.1.2. Finally, we will conclude enunciating the Goldstone bosons equivalence theorem in Sec. 2.1.3.

2.1.1 Global symmetries: Goldstone's theorem

One of the most important results on spontaneous symmetry breaking is Goldstone's theorem [36–38], that can be stated as follows:

Consider a system whose Lagrangian is invariant under an n -dimensional set of continuous, global transformations. If the vacuum of the theory is invariant under the action of only k among the n generators, then there must exist $n - k$ spinless particles of zero mass.

A simple proof⁴ can be given for a toy model involving an arbitrary number of scalar fields $\varphi_i(x)$. The Lagrangian would simply read

$$\mathcal{L} = \frac{1}{2} \partial_\mu \varphi_i \partial^\mu \varphi_i - V(\varphi). \quad (2.1.3)$$

The vacuum state of this system corresponds to a constant configuration $\langle \varphi_i \rangle$ that minimizes the scalar potential:

$$\left. \frac{\delta}{\delta \varphi_i} V(\varphi) \right|_{\varphi_i(x) \equiv \langle \varphi_i \rangle} = 0. \quad (2.1.4)$$

Let's assume that the Lagrangian \mathcal{L} is invariant under a *global* symmetry group \mathcal{G} , spanned by n generators T_{ij}^a , $a = \{1, \dots, n\}$. Under an infinitesimal transformation, parametrized by $\varepsilon \ll 1$, the fields are shifted according to $\varphi_i(x) \mapsto \varphi_i(x) + i\varepsilon T_{ij}^a \varphi_j(x)$. The invariance condition for the scalar potential can then be expressed as

$$\Delta V = V(\varphi + i\varepsilon T^a \varphi) - V(\varphi) = i\varepsilon \frac{\delta V}{\delta \varphi_i} T_{ij}^a \varphi_j = 0 \quad \forall \varepsilon. \quad (2.1.5)$$

Differentiating this equation with respect to φ_b gives

$$0 = \frac{\delta^2 V}{\delta \varphi_b \delta \varphi_i} T_{ij}^a \varphi_j + \frac{\delta V}{\delta \varphi_i} T_{ij}^a \frac{\delta \varphi_j}{\delta \varphi_b} = \frac{\delta^2 V}{\delta \varphi_b \delta \varphi_i} T_{ij}^a \varphi_j + \frac{\delta V}{\delta \varphi_i} T_{ib}^a. \quad (2.1.6)$$

In the vacuum state the last term vanishes due to (2.1.4), and therefore we conclude that

$$\left. \frac{\delta^2 V}{\delta \varphi_b \delta \varphi_i} \right|_{\varphi_i = \langle \varphi_i \rangle} T_{ij}^a \langle \varphi_j \rangle = 0. \quad (2.1.7)$$

We now make the hypothesis that the vacuum is not invariant under the whole group \mathcal{G} , but only under a subgroup \mathcal{H} , generated by k among the n generators. Indicating with hatted indices the $(n - k)$ broken generators, this corresponds to the condition

$$\begin{aligned} T_{ij}^a \langle \varphi_j \rangle &= 0 \quad \forall i, & a &= \{1, \dots, k\} \\ \exists i : T_{ij}^{\hat{a}} \langle \varphi_j \rangle &\neq 0 & \hat{a} &= \{k+1, \dots, n\}. \end{aligned} \quad (2.1.8)$$

With this assumption, Eq. (2.1.7) implies that the second derivative of the scalar potential, evaluated in the vacuum state, has exactly $n - k$ zero eigenvalues. Since the quantum excitations around the vacuum $\pi_i(x) = \varphi_i(x) - \langle \varphi_i \rangle$, satisfy the Klein Gordon equation

$$\left(\square \delta_{ij} + \left. \frac{\delta^2 V}{\delta \varphi_i \delta \varphi_j} \right|_{\varphi_i = \langle \varphi_i \rangle} \right) \pi_j(x) = 0 \quad (2.1.9)$$

we conclude that there must be $n - k$ massless physical fields, each corresponding to a broken generator. These are called Goldstone bosons (GBs) of the theory.

Finally, it is worth noticing that the invariance of the original Lagrangian $\mathcal{L}(\varphi)$ under transformations of the broken symmetry translates, in the Lagrangian written in terms of physical fields, into an invariance under shifts of the $(n - k)$ Goldstone fields. As a consequence, the latter can only have derivative couplings.

⁴ A most general proof, valid also for non-perturbative theories, can be found in the original paper [38].

2. Dynamics of the electroweak symmetry breaking

An example from QCD: chiral symmetry breaking

It is important to remark that the spontaneous breaking of a symmetry (either global or local) does not rely on the presence of fundamental scalars. In fact, although some scalar degrees of freedom are required (only spin-less fields can acquire non-zero vacuum expectation value), these do not need to be fundamental, but may as well be composite objects. A most famous example of this scenario is that of the spontaneous breaking of the chiral symmetry in QCD, that is briefly reviewed in this paragraph.

In the limit of vanishing quark masses, the Lagrangian of QCD with two flavors $\Psi = (U, D)$ is invariant under the global chirally symmetry $SU(2)_L \times SU(2)_R$, under which the quark fields of each chirality transform as doublets:

$$\begin{aligned} \Psi_L = \begin{pmatrix} U_L \\ D_L \end{pmatrix} &\mapsto U_L \Psi_L, & U_L = e^{i\alpha_L^i \tau^i / 2} \in SU(2)_L \\ \Psi_R = \begin{pmatrix} U_R \\ D_R \end{pmatrix} &\mapsto U_R \Psi_R & U_R = e^{i\alpha_R^i \tau^i / 2} \in SU(2)_R. \end{aligned} \quad (2.1.10)$$

However, quark-antiquark pairs form spinless condensates whose vacuum expectation value is not vanishing:

$$\langle \bar{\Psi} \Psi \rangle = \langle \bar{\Psi}_L \Psi_R + \bar{\Psi}_R \Psi_L \rangle \neq 0. \quad (2.1.11)$$

This vacuum configuration is not symmetric under the whole chiral group: instead, it is left invariant only by transformations with $U_L = U_R$, *i.e.* by the vectorial subgroup $SU(2)_V = SU(2)_{L+R}$. The Goldstone theorem implies then the existence of $\dim(SU(2) \times SU(2)) - \dim(SU(2)) = 3$ massless, spin-0 Goldstone bosons. It also ensures that these particles have the same quantum numbers as the associated broken currents, which in this case are the axial currents $i\bar{\Psi}\gamma^\mu\gamma_5\tau^i\Psi$: therefore they must be pseudoscalars. In fact, the GBs of the two-flavor chiral symmetry breaking are identified with the pions π^0, π^\pm : since the up and down quarks actually have a small but non-zero mass, the chiral symmetry of QCD is only approximate and this allows to have massive, albeit light, Goldstone bosons.

2.1.2 Local symmetries: Higgs mechanism

There are profound differences between the spontaneous breaking taking place in a global and in a local⁵ continuous symmetries: in the local case, in fact, the degrees of freedom corresponding to the Goldstone bosons do not show up as massless particles in the spectrum, but rather materialize as the longitudinally polarized states of the vector bosons associated to the broken generators. Consequently, these gauge bosons acquire a mass. This phenomenon is generally referred to as *Higgs mechanism*.

The inadequacy of Goldstone's theorem for the case of local symmetries was discovered in 1964 by three independent groups: Brout-Englert [3], Higgs [5] and Guralnik-Hagen-Kibble [39].

Consider a system analogous to the one presented in Sec. 2.1.1, containing a multiplet of real-valued scalar fields $\varphi_i(x)$ and invariant under the continuous group \mathcal{G} whose generators are in a real, antisymmetric representation defined by the matrices T_{ij}^a , $a = \{1, \dots, n\}$. This symmetry is promoted to a local invariance inserting an associated set of gauge bosons $A_\mu^a(x)$. The transformation rules and the covariant derivatives for the scalars read

$$\varphi_i(x) \mapsto \varphi_i(x) - \alpha^a(x) T_{ij}^a \varphi_j(x) \quad (2.1.12)$$

$$D_\mu \varphi_i = \partial_\mu \varphi_i + g A_\mu^a T_{ij}^a \varphi_j = \partial_\mu \varphi_i + g A_\mu^a (T^a \varphi)_i \quad (2.1.13)$$

⁵ Technically, the expression “spontaneously broken local symmetry” is not correct. As stated by Elitzur's theorem [65], in fact, such a breaking cannot possibly occur in quantum field theory. Indeed the condition of gauge-invariance is never dismissed. With a slight abuse of language, motivated by its widespread acceptance, this expression will be occasionally used here to indicate the condition in which the spectrum of physical particles do not form a representation of a local symmetry group.

where g is a coupling constant. The Lagrangian of this system is therefore

$$\begin{aligned}\mathcal{L} &= -\frac{1}{4}A_{\mu\nu}^a A^{a\mu\nu} + \frac{1}{2}D_\mu\varphi_i D^\mu\varphi_i - V(|\varphi|) = \\ &= \frac{1}{2}A_\mu^a (g^{\mu\nu}\square - \partial^\mu\partial^\nu)A_\nu^a - V(|\varphi|) + \\ &\quad + \frac{1}{2}\partial_\mu\varphi_i\partial^\mu\varphi_i + gA_\mu^a j^{a\mu} + \frac{1}{2}g^2 A_\mu^a A^{b\mu} (T^a\varphi)_i (T^b\varphi)_i\end{aligned}\tag{2.1.14}$$

where j_μ^a is the Noether's current associated to the generator T^a : $j^{a\mu} = \partial^\mu\varphi_i T_{ij}^a \varphi_j$.

Let us assume that the scalar fields acquire a vacuum expectation value $\langle\varphi_i\rangle$ that leaves the system invariant under a subgroup $\mathcal{H} \subset \mathcal{G}$ generated by k among the n generators, while the remaining $n - k$ symmetries are spontaneously broken. In this configuration, the last term of Eq. (2.1.14) yields a mass term for the gauge bosons

$$\frac{(m^2)_{ab}}{2}A_\mu^a A^{b\mu} \quad \text{with} \quad (m^2)_{ab} = g^2 \langle T^a\varphi \rangle_i \langle T^b\varphi \rangle_i\tag{2.1.15}$$

that is non-vanishing only for the gauge bosons associated to the broken generators, for which $(T^a\langle\varphi\rangle)_i \neq 0$, while those corresponding to the preserved transformations, defined by $(T^{\hat{a}}\langle\varphi\rangle)_i = 0$, remain massless. Still, the interaction in Eq. (2.1.15) alone cannot describe in a massive vector boson in a properly gauge-invariant way. In order to see this, it is instructive to compute the self-energies of the gauge bosons A_μ^a : prior to the spontaneous symmetry breaking, the latter are massless, and therefore their propagator is just

$$\Delta_{\mu\nu}(q^2) = \frac{-i}{q^2} g_{\mu\nu} .\tag{2.1.16}$$

Defining $(i\Pi_{\mu\nu}(q^2))$ to be the sum of all the one-particle-irreducible (1PI) insertions into the propagator, the exact gauge bosons two-point function is given by the infinite series

$$\begin{aligned}\text{Diagram} &= \text{Diagram} + \text{Diagram (1PI)} + \text{Diagram (1PI)} + \dots \\ &= \Delta_{\mu\nu} + \Delta_{\mu\rho}(i\Pi^{\rho\sigma})\Delta_{\sigma\nu} + \Delta_{\mu\rho}(i\Pi^{\rho\sigma})\Delta_{\sigma\lambda}(i\Pi^{\lambda\eta})\Delta_{\eta\nu} + \dots\end{aligned}\tag{2.1.17}$$

The Ward identity $iq_\mu\Pi^{\mu\nu}(q^2) = 0$ requires $i\Pi_{\mu\nu}(q^2)$ to be completely transverse, *i.e.* of the form

$$i\Pi_{\mu\nu}(q^2) = i(q^2 g_{\mu\nu} - q_\mu q_\nu)\Pi(q^2) .\tag{2.1.18}$$

The infinite geometric series of Eq. (2.1.17) can therefore be re-summed with the result

$$\text{Diagram} = \frac{-i}{q^2} \left[\frac{1}{(1 - \Pi(q^2))} \left(g_{\mu\nu} - \frac{q_\mu q_\nu}{q^2} \right) \right] ,\tag{2.1.19}$$

which represents the renormalized two-point function of a massive vector field *iff*⁶ the vacuum-polarization function $\Pi(q^2)$ has a pole in $q^2 \rightarrow 0$

$$\Pi(q^2) \Big|_{q^2 \rightarrow 0} \simeq \frac{m^2}{q^2}\tag{2.1.20}$$

that in fact would cause the renormalized propagator to have a pole in $q^2 = m^2$. It is shown in what follows that the presence of the Goldstone bosons is exactly what ensures that the vacuum polarization function has the appropriate momentum dependence.

⁶ This is strictly true in four space-time dimension, while a counterexample is known in $d = 2$.

2. Dynamics of the electroweak symmetry breaking

Once the fields acquire a vacuum expectation value, we can expand the fields around the vacuum. We adopt the notation

$$\begin{aligned}\varphi_i(x) &\equiv \langle \varphi \rangle_i + \chi_i(x), \\ T_{ij}^a \varphi_j(x) &= (T^a \langle \varphi \rangle)_i + T_{ij}^a \chi_j(x) \equiv F_i^a + T_{ij}^a \chi_j(x).\end{aligned}\quad (2.1.21)$$

The constant vectors F_i^a associated to the preserved generators are identically vanishing, while those associated to the broken ones are $F_i^{\hat{a}} = T_{ij}^{\hat{a}} \langle \varphi \rangle_j \neq 0$. The field fluctuations along the latter directions correspond to the Goldstone bosons. Eq. (2.1.14) now reads

$$\begin{aligned}\mathcal{L} &= \frac{1}{2} A_\mu^a (g^{\mu\nu} \square - \partial^\mu \partial^\nu) A_\nu^a - V(|\chi|) + \frac{1}{2} \partial_\mu \chi_i \partial^\mu \chi_i + \\ &+ g A_\mu^a \partial^\mu \chi_i (F_i^a + T_{ij}^a \chi_j) + \frac{1}{2} g^2 A_\mu^a A^{b\mu} (F_i^a + T_{ij}^a \chi_j) (F_i^b + T_{ik}^b \chi_k).\end{aligned}\quad (2.1.22)$$

The gauge bosons have an explicit mass term, now written as $(m^a)_{ab} = F_i^a F_i^b$, and the scalar potential contains a mass matrix for the scalar particles that, as in the global case, has $n - k$ vanishing eigenvalues, corresponding to the Goldstone bosons' excitation. All the states that are orthogonal to the latter are instead massive. It is also worth noticing that the term $g A_\mu^a \partial^\mu \chi_i F_i^a$ yields a very important kinetic mixing between the Goldstones and the associated gauge bosons. This does not come as a surprise, as the two associated fields have the same quantum numbers (they are both created by the broken symmetry current). Given the interactions in Eq. (2.1.22), the sum of 1PI insertions into the gauge bosons propagators is therefore

$$\begin{aligned}i\Pi_{\mu\nu}(q^2) &= \text{diagram with wavy line and cross} + \text{diagram with dashed line and cross} = \\ &= i(m_{ab})^2 g_{\mu\nu} + (m_{ai} q_\mu) \frac{-i\delta_{ij}}{q^2} (m_{jb} q_\nu) = \\ &= im_{ab}^2 \left(g_{\mu\nu} - \frac{q_\mu q_\nu}{q^2} \right)\end{aligned}\quad (2.1.23)$$

hence, equating to (2.1.18),

$$\Pi(q^2) = \frac{m_{ab}^2}{q^2}. \quad (2.1.24)$$

It is evident, at this point, that the explicit mass term of Eq. (2.1.15) alone cannot possibly provide a transverse $i\Pi_{\mu\nu}(q^2)$: since this condition is required by the Ward identity, the Goldstone bosons' contribution is strictly necessary in order to preserve gauge invariance.

Let us now get back to Eq. (2.1.22): the presence of the kinetic mixing $g A_\mu^a \partial^\mu \chi_i F_i^a$ signals that the excitations associated to the Goldstone bosons are not actually describing physical massless particles. This term must not appear in the Lagrangian, when the fields constitute a physical basis. In order not to spoil the gauge invariance it is necessary, at this point, to introduce explicitly the gauge fixing term required the Faddeev-Popov quantization procedure. In the well-known R_ξ gauges, it can be chosen of the form

$$\mathcal{L}_{\text{GF}} = \frac{1}{2\xi} [\partial_\mu A^{a\mu} - \xi g F_i^a \chi_i]^2 \quad (2.1.25)$$

so that

$$\begin{aligned}\mathcal{L} + \mathcal{L}_{\text{GF}} &= \frac{1}{2} \partial_\mu \chi_i \partial^\mu \chi_i - V(|\chi|) + \frac{1}{2} A_\mu^a \left[g^{\mu\nu} \square - \left(1 - \frac{1}{\xi} \right) \partial^\mu \partial^\nu \right] A_\nu^a + \\ &+ g A_\mu^a \partial^\mu \chi_i T_{ij}^a \chi_j + \frac{1}{2} g^2 A_\mu^a A^{b\mu} (F_i^a + T_{ij}^a \chi_j) (F_i^b + T_{ik}^b \chi_k) + \\ &- \frac{1}{2} \xi g^2 F_i^a F_j^b \chi_i \chi_j.\end{aligned}\quad (2.1.26)$$

We see that with the gauge fixing choice of Eq. (2.1.25) the kinetic mixing cancels automatically. At the same time, the Goldstone bosons acquire a mass proportional to the gauge fixing parameter itself. Since the physics of the system cannot depend on ξ , this is again a sign that the Goldstone bosons of this theory are unphysical particles: in fact, in the *unitary gauge* $\xi \rightarrow \infty$ the Goldstone fields become infinitely heavy and they can be integrated out of the Lagrangian. In this way they are completely removed from the spectrum, unlike the other massive scalars that in fact describe physical particles.

As a final remark, it is important to notice that in a system with spontaneous breaking of a local continuous symmetry both the number of degrees of freedom and the symmetries of the Lagrangian remain unvaried throughout the phase transition. The $(n - k)$ real fields describing the Goldstone excitations, that in the unbroken phase represent free scalars, become the longitudinal polarization states of the $(n - k)$ massive vector bosons in the broken phase. For this reason, it is customarily said that the Goldstones “get eaten” by the gauge bosons.

The most important example of spontaneous breaking of a local continuous symmetry is that of the Standard Model, described in Sec. 1.1.2. In that case, the initial symmetry is $SU(2) \times U(1)$ which gets broken down to the electromagnetic group $U(1)$ when an appropriate combination of the four real scalars contained in the Higgs doublet acquires a non-vanishing vev. This produces three Goldstone bosons: two charged ones, that are eaten by the W^\pm , and a neutral one, eaten by the Z . The photon, being aligned with the preserved generator, remains massless, while the fourth scalar remains in the spectrum as the massive Higgs boson.

2.1.3 Goldstone boson equivalence theorem

An important result related to the spontaneous breaking of a gauge symmetry is the Goldstone boson equivalence theorem, that ensures that the Goldstone bosons π^a , once they have been eaten, physically coincide with the longitudinal polarization states of the corresponding gauge bosons A_L^a . This must be so, on an intuitive basis, because massive and massless vector fields contain a different number of degrees of freedom: while the latter have only two possible polarization states (in the transverse plane), the former are also allowed to be longitudinally polarized. Since, in a gauge theory, this extra freedom can only be acquired by absorbing a Goldstone boson, physical processes involving A_L^a and π^a must be somehow related. It is also expected that the longitudinal polarization states reveal their origin as Goldstone bosons only at energies $E \gg m_A^2$, while in the limit in which the gauge boson is at rest they should be indistinguishable from the transverse states. Indeed, the Equivalence theorem is enunciated as follows: in any R_ξ gauge of a spontaneously broken gauge theory, the amplitude for emission or absorption of a longitudinally polarized gauge boson is equal, up to corrections of order $\mathcal{O}(m_A/\sqrt{s})$, to the amplitude for emission or absorption of the associated Goldstone boson. This statement, generalized to the scattering of N longitudinally polarized gauge bosons, is expressed by the equation:

$$\mathcal{A}\left(A_L(p_1) \dots A_L(p_n) + X \rightarrow A_L(q_1) \dots A_L(q_m) + Y\right) = (-i)^{n+m} \mathcal{A}\left(\pi(p_1) \dots \pi(p_n) + X \rightarrow \pi(q_1) \dots \pi(q_m) + Y\right) \left(1 + \mathcal{O}(m_A/\sqrt{s})\right) \quad (2.1.27)$$

The first proof of the theorem, valid at tree level, was given by Cornwall et al. and by Vayonakis in Refs. [66] and [67]. The complete proof at any order in perturbation theory was given by Chanowitz and Gaillard [68] and Gounaris et al. [69].

2.2 Spontaneous EW symmetry breaking: linear realization

After discussing the general properties of the spontaneous breaking of a continuous symmetry, we now focus on the specific case of the electroweak symmetry breaking (EWSB). It is particularly worth to differentiate

2. Dynamics of the electroweak symmetry breaking

between two different parameterizations of the EW symmetry breaking (EWSB): the *linear* and *non-linear* realizations. Here the nomenclature refers to the representation of the global chiral symmetry $SU(2)_L \times SU(2)_R$ to which the EW Goldstone bosons are assigned. It turns out that the two realizations provide equivalent descriptions of the EW Goldstone bosons, while they differ in the treatment of the physical Higgs boson.

In this section we focus on the linear case, that can be identified with the SM Higgs mechanism already introduced in Sec. 1.1.2. This formalism is also the one implemented in theories with weakly-coupled new physics, such as supersymmetric model. The main characteristics of this realization are the following:

- it is described by a renormalizable Lagrangian that respects a global chiral symmetry $SU(2)_L \times SU(2)_R$. The latter is spontaneously broken to the *custodial* subgroup $SU(2)_c \equiv SU(2)_{L+R}$. The EW gauge group $SU(2)_L \times U(1)_Y$ is embedded in the chiral group, as $U(1)_Y \subset SU(2)_R$.
- The scalar sector contains four fields: the three Goldstone bosons and the physical Higgs boson. These are embedded altogether in a bi-doublet of the chiral symmetry and transform linearly under the latter. The couplings of the four scalars (and in particular of the Higgs) are fixed by the symmetry.
- The chiral symmetry forbids to decouple the physical Higgs from the spectrum so that, in this formalism, it is not possible to construct an invariant effective theory for energies $E \ll m_h$ that contained only the three Goldstone bosons.

These properties are not peculiar of the EW case: indeed, they are most transparent in a simpler example, that represents a paradigm for the linear realization of spontaneous symmetry breaking: the *linear σ -model* of QCD. It is instructive, therefore, to illustrate the latter before moving to the more complex case of the EW interactions.

2.2.1 A preliminary example from QCD: linear σ -model

An instructive model of spontaneous symmetry breaking is the linear σ -model, first introduced by Gell-Mann and Lévy in 1960 [70]. This model is very general, but we first focus on its application to the spontaneous breaking of the chiral symmetry in QCD, an example very close to that considered in Sec. 2.1.1.

The fields involved are the following: a doublet of spin 1/2 nucleon fields

$$\psi = \begin{pmatrix} p \\ n \end{pmatrix} \quad (2.2.28)$$

and four real scalars: a set of three of fields $\vec{\pi} = (\pi^1, \pi^2, \pi^3)$ that transform as a triplet under the $SU(2)$ isospin group, plus a singlet σ . Notice that the fermion field has been chosen differently compared to the example of Sec. 2.1.1, as here the doublet embeds nucleons rather than quarks. The Lagrangian is

$$\mathcal{L} = i\bar{\psi}\not{\partial}\psi + \frac{1}{2}\partial_\mu\sigma\partial^\mu\sigma + \frac{1}{2}\partial_\mu\vec{\pi} \cdot \partial^\mu\vec{\pi} - g\bar{\psi}(\sigma - i\vec{\tau} \cdot \vec{\pi}\gamma_5)\psi - V(\sigma, \pi^i) \quad (2.2.29)$$

where $\vec{\tau}$ denotes the triplet of Pauli matrices and the scalar potential has the form

$$V(\sigma, \pi^i) = \frac{\mu^2}{2}(\sigma^2 + \vec{\pi} \cdot \vec{\pi}) + \frac{\lambda}{4}(\sigma^2 + \vec{\pi} \cdot \vec{\pi})^2. \quad (2.2.30)$$

The kinetic term of the fermionic fields is manifestly invariant under a global $U(2)_L \times U(2)_R$ symmetry, that can be decomposed into $U(1)_{L+R} \times U(1)_{L-R} \times SU(2)_L \times SU(2)_R$. The first two factors, that correspond respectively to the baryon number and to the anomalous chiral symmetry, will be neglected in this context. The initial isospin symmetry corresponds instead to the vector subgroup $SU(2)_{L+R}$.

Importantly, the scalar sector is also invariant under the chiral group $SU(2)_L \times SU(2)_R$, although the symmetry is somehow hidden in the parameterization of Eq. (2.2.29). Nonetheless, the scalar potential (2.2.30) depends only on the modulus of the multiplet $(\sigma, \vec{\pi})$ and therefore it is invariant under a $SO(4)$ symmetry. Since this group is isomorphic to $SU(2) \times SU(2)$, it must be possible to recast the scalars in a configuration that makes the chiral invariance manifest for the whole Lagrangian. In the *linear s -model*⁷, this is achieved defining the matrix field

$$\Sigma = \sigma \mathbb{1} + i \vec{\tau} \cdot \vec{\pi} = \begin{pmatrix} \sigma + i\pi^3 & i\pi^1 + \pi^2 \\ i\pi^1 - \pi^2 & \sigma - i\pi^3 \end{pmatrix}. \quad (2.2.31)$$

Given the structure of the interaction between nucleons and scalars, the field Σ shall be assigned to a bi-doublet representation of $SU(2)_L \times SU(2)_R$:

$$\Sigma(x) \mapsto U_L \Sigma(x) U_R^\dagger \quad (2.2.32)$$

with $U_{L,R}$ defined as in Eq. (2.1.10). The transformation properties of the single components consequently read

$$\begin{aligned} \sigma &\mapsto \sigma + (\alpha_L^i - \alpha_R^i) \frac{\pi^i}{2} \\ \pi^i &\mapsto \pi^i - (\alpha_L^i - \alpha_R^i) \frac{\sigma}{2} + \varepsilon^{ijk} (\alpha_L^j + \alpha_R^j) \frac{\pi^k}{2}. \end{aligned} \quad (2.2.33)$$

For $\alpha_L^i = \alpha_R^i$ one recovers transformation properties under the isospin group (singlet and triplet respectively), while for $\alpha_L^i = -\alpha_R^i$ the fields σ and $\vec{\pi}$ are interchanged.

By definition, Σ satisfies

$$\frac{1}{2} \text{Tr}(\Sigma^\dagger \Sigma) = \sigma^2 + \vec{\pi} \cdot \vec{\pi}. \quad (2.2.34)$$

As a consequence, the Lagrangian of Eq. (2.2.29) can be rewritten as

$$\mathcal{L} = i\bar{\psi}_L \not{\partial} \psi_L + i\bar{\psi}_R \not{\partial} \psi_R + \frac{1}{4} \text{Tr}(\partial_\mu \Sigma^\dagger \partial^\mu \Sigma) - g(\bar{\psi}_L \Sigma \psi_R + \bar{\psi}_R \Sigma^\dagger \psi_L) - V(\Sigma) \quad (2.2.35)$$

with

$$V(\Sigma) = \frac{\mu^2}{4} \text{Tr}(\Sigma^\dagger \Sigma) + \frac{\lambda}{16} \text{Tr}(\Sigma^\dagger \Sigma)^2. \quad (2.2.36)$$

The invariance under the global chiral group $SU(2)_L \times SU(2)_R$ is now completely manifest. Consider now the scalar potential: the parameter λ must be positive in order for the potential to be bounded from below, but the parameter μ is free. For $\mu^2 > 0$ the configuration of minimum energy for the scalar fields is $\langle \Sigma \rangle \equiv 0$ and the chiral symmetry is preserved. However, if $\mu^2 < 0$ the potential has a minimum in

$$\frac{\langle \text{Tr}(\Sigma^\dagger \Sigma) \rangle}{2} = \langle \sigma^2 + \vec{\pi} \cdot \vec{\pi} \rangle = \frac{-\mu^2}{\lambda} \equiv f^2, \quad (2.2.37)$$

which is not invariant under the whole $SU(2) \times SU(2)$. The global symmetry is spontaneously broken down to a single $SU(2)$ subgroup that, if the vacuum is aligned in the direction

$$\langle \sigma \rangle = f, \quad \langle \pi^i \rangle = 0 \quad \Leftrightarrow \quad \langle \Sigma \rangle = f \mathbb{1} \quad (2.2.38)$$

coincides with the isospin $SU(2)_{L+R}$. In fact, it can be immediately checked using the result in Eq. (2.2.33), that this vacuum is invariant only under transformations with $\alpha_L^i = \alpha_R^i$.

⁷ An alternative parameterization, that characterizes the *non-linear σ -model*, will be described in Sec. 2.3.1.

2. Dynamics of the electroweak symmetry breaking

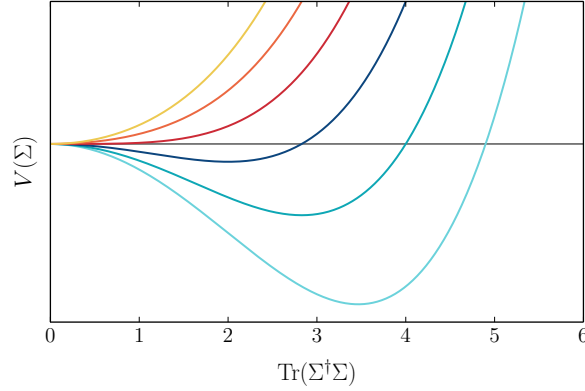


Figure 2.1: *Scalar potential for the linear σ -model, defined in Eq. (2.2.36), with different choices of μ^2/λ . The red/orange lines are drawn for $\mu^2 \geq 0$ and show a minimum in $\text{Tr}(\Sigma^\dagger \Sigma) = 0$, while the blue lines correspond to the case $\mu^2 < 0$, where the minimum is shifted to $\text{Tr}(\Sigma^\dagger \Sigma) = -2\mu^2/\lambda$.*

Expanding around the vacuum, the physical fields are $(\sigma' = \sigma - f, \vec{\pi})$ and, dropping the primes, the Lagrangian finally reads

$$\begin{aligned} \mathcal{L} = & i\bar{\psi}\not{\partial}\psi + \frac{1}{2}\partial_\mu \vec{\pi} \cdot \partial^\mu \vec{\pi} - m_\psi \bar{\psi}\psi + ig\bar{\psi}(\vec{\tau} \cdot \vec{\pi})\gamma_5\psi + \\ & + \frac{1}{2}\partial_\mu \sigma \partial^\mu \sigma - \frac{m_\sigma^2}{2}\sigma^2 - g\bar{\psi}\psi\sigma - \frac{\lambda}{4}(\sigma^2 + \vec{\pi} \cdot \vec{\pi})^2 - \lambda f\sigma(\sigma^2 + \vec{\pi} \cdot \vec{\pi}). \end{aligned} \quad (2.2.39)$$

This final result describes three massless pions (as in the example of Sec. 2.1.1), two massive nucleons with $m_p = m_n = gf$ and a massive σ meson, with mass $m_\sigma = 2\sqrt{\lambda}f$. A more realistic result can be obtained taking into account that the initial chiral symmetry is only approximate in nature and inserting in the initial Lagrangian a soft chiral breaking term, such as $\varepsilon \text{Tr}(\Sigma)$ with $\varepsilon \ll 1$. This would result in small pion masses and lift the degeneracy between m_p and m_n .

The physical interpretation of the scale f is clarified computing the matrix element for the destruction of a pion with four-momentum q via the action of the associated broken current:

$$\begin{aligned} \langle 0 | J_{L-R}^{i\mu}(x) | \pi^j(q) \rangle &= \langle 0 | \left[\bar{\psi} \gamma^\mu \gamma_5 \frac{\tau^i}{2} \psi + \pi^i \partial^\mu (\sigma + f) - (\sigma + f) \partial^\mu \pi^i \right] | \pi^j \rangle = \\ &= -f \langle 0 | \partial^\mu \pi^i(x) | \pi^j(q) \rangle = if \delta^{ij} q^\mu e^{-iqx} \end{aligned} \quad (2.2.40)$$

hence the scale f must coincide with the decay constant of the pions by $\langle \sigma \rangle = f = -f_\pi$, where f_π is defined as the scale that parameterizes the annihilation matrix element

$$\langle 0 | J^\mu(x) | \pi(q) \rangle = -if_\pi q^\mu e^{-iqx}. \quad (2.2.41)$$

Finally, it is worth to point out a few important properties of the linear σ -model just described: first, the model is renormalizable. Second, in this parameterization the presence of the σ field is indispensable for constructing a Lagrangian invariant under a global $SU(2) \times SU(2)$ symmetry. Indeed the couplings of the σ to the pions are totally determined by the symmetry and the σ cannot be possibly decoupled from the spectrum.

2.2.2 The EW case: Higgs mechanism

The Higgs mechanism of the Standard Model described in Sec. 1.1.2 can be formulated as a linear σ -model for the electroweak symmetry breaking, in which the role of the σ field is played by the Higgs boson, and the three massless pions are eventually eaten by the W^\pm and Z bosons, as the isospin and hypercharge symmetries are gauged.

Indeed, the Standard Model Lagrangian can be written in terms of the Σ field

$$\Sigma = \frac{1}{\sqrt{2}} (\phi_0 \mathbb{1} + i\vec{\tau} \cdot \vec{\pi}) = \frac{1}{\sqrt{2}} \begin{pmatrix} \phi_0 + i\pi_3 & i\pi_1 + \pi_2 \\ i\pi_1 - \pi_2 & \phi_0 - i\pi_3 \end{pmatrix} \equiv \begin{pmatrix} \tilde{\Phi} & \Phi \end{pmatrix} \quad (2.2.42)$$

where Φ is the Higgs doublet introduced in Eq. (1.1.5), while $\tilde{\Phi}$ was defined in Eq. (1.1.7). This matrix satisfies

$$\frac{1}{2} \text{Tr}(\Sigma^\dagger \Sigma) = \Phi^\dagger \Phi = \frac{1}{2} (\phi_0^2 + \vec{\pi} \cdot \vec{\pi}). \quad (2.2.43)$$

As in the QCD example, the field Σ transforms as a bi-doublet of a global $SU(2)_L \times SU(2)_R$. In the electroweak case, importantly, the $SU(2)_L$ isospin symmetry is gauged, while $SU(2)_R$ embeds the gauged hypercharge $U(1)_Y$ as a subgroup, generated by τ^3 . The associated covariant derivative is therefore

$$D_\mu \Sigma(x) = \partial_\mu \Sigma(x) + \frac{igW_\mu^i(x)}{2} \tau^i \Sigma(x) - \frac{ig'B_\mu(x)}{2} \Sigma(x) \tau^3 \quad (2.2.44)$$

which can be easily seen to match the covariant derivative for the Higgs doublet as in Eq. (1.1.5).

In the language of the linear σ -model, the Higgs Lagrangian of Eq. (1.1.6) reads

$$\begin{aligned} \mathcal{L}_\Phi \rightarrow \mathcal{L}_\Sigma = & \frac{1}{2} \text{Tr} (D_\mu \Sigma^\dagger D^\mu \Sigma) - \mu^2 \text{Tr}(\Sigma^\dagger \Sigma) - \frac{\lambda}{2} \text{Tr}(\Sigma^\dagger \Sigma)^2 + \\ & - \left[\bar{Q}_L \Sigma \begin{pmatrix} \mathbf{y}_U & \\ & \mathbf{y}_D \end{pmatrix} \begin{pmatrix} U_R \\ D_R \end{pmatrix} + \bar{L}_L \Sigma \begin{pmatrix} 0 & \\ & \mathbf{y}_E \end{pmatrix} \begin{pmatrix} 0 \\ E_R \end{pmatrix} + \text{h.c.} \right] \end{aligned} \quad (2.2.45)$$

where the right-handed fermions have been gathered in $SU(2)_R$ doublets. It is worth noticing that, unlike in the QCD example (Eq. (2.2.35)), this Lagrangian is not invariant under the full $SU(2)_R$ global symmetry, as the latter is explicitly broken by the heterogeneity of the Yukawa couplings ($\mathbf{y}_U \neq \mathbf{y}_D$ and $\mathbf{y}_E \neq 0$) and the fact only the hypercharge subgroup $U(1)_Y$ is gauged.

The spontaneous electroweak symmetry breaking takes place for $\mu^2 < 0$, so that the scalar potential has a minimum in

$$\frac{\langle \text{Tr}(\Sigma^\dagger \Sigma) \rangle}{2} = \langle \Phi^\dagger \Phi \rangle = \frac{-\mu^2}{\lambda} \equiv \frac{v^2}{2}. \quad (2.2.46)$$

Picking the alignment

$$\langle \phi_0 \rangle = v, \quad \langle \pi^i \rangle = 0 \quad (2.2.47)$$

and expanding around the vacuum with $\phi_0 = v + h$, h represents the physical Higgs boson. In this case, the gauge fixing term for a generic R_ξ gauge is

$$\mathcal{L}_{\text{G.F.}} = -\frac{1}{2\xi} \left(\partial_\mu W^{i\mu} + \xi g \frac{v}{\sqrt{2}} \pi^i \right)^2 - \frac{1}{2\xi} \left(\partial_\mu B^\mu + \xi g' \frac{v}{\sqrt{2}} \pi^3 \right)^2. \quad (2.2.48)$$

Going to the unitary gauge, that corresponds to $\xi \rightarrow \infty$, one recovers the results of the Higgs mechanism reported in Sec. 1.1.2.

2. Dynamics of the electroweak symmetry breaking

Custodial symmetry

The analogy between the Higgs mechanism of the Standard Model and the linear σ -model of the QCD example in Section 2.2.1 allows to highlight a very important feature of the SM, which is the presence of the so-called *custodial symmetry* [71].

As mentioned above, in the limit $g' = 0$ and $\mathbf{y}_U = \mathbf{y}_D, \mathbf{y}_E = 0$, the Higgs Lagrangian in Eq. (2.2.45) has a global $SU(2)_L \times SU(2)_R$ symmetry. However, as it was pointed out for the system of Sec. 2.2.1, the vacuum of Eq. (2.2.47) is only invariant under the vector subgroup $SU(2)_{L+R}$. The latter, in the EW context, is referred to as *custodial group* and often denoted by $SU(2)_c$.

In this limit, in which the hypercharge is not gauged, there are only three gauge bosons, and all of them are associated to broken generators. The weak angle is vanishing as $\tan \theta = g'/g = 0$ and, consequently, the W_μ^3 boson coincides with the physical Z . Indeed, there is no photon in the spectrum, because the residual $U(1)_{\text{em}}$ symmetry is not a local one. Furthermore, the masses of the W^\pm and the Z turn out to be identical: $m_W = m_Z = gv/\sqrt{2}$. This is consistent with the fact that the three massive vector bosons form a triplet of the unbroken custodial group.

In the real world the initial chiral invariance is violated by $g' \neq 0$ and therefore the custodial symmetry is not exact: the equality $m_W = m_Z$ is then replaced by the relation

$$\rho \equiv \frac{m_W^2}{m_Z^2 \cos^2 \theta} = 1, \quad (2.2.49)$$

which is exact at tree-level. In general, the parameter ρ will receive higher-order corrections that, in the context of the SM, must be proportional to g' or to $(\mathbf{y}_U - \mathbf{y}_D)$ and therefore are always small. The fact that the EW vacuum is approximately custodially symmetric is a very important property of the SM Higgs mechanism, which is easily spoiled in presence of new physics contributions. For this reason, custodial invariance has been tested experimentally to a high precision: the most significant constraints are derived from the electroweak precision measurements performed at LEP [72], that allow to bound the three Peskin-Takeuchi oblique parameters S, T, U [73]. The latter quantities parameterize new-physics contributions to the vacuum polarization functions of the EW gauge bosons. It is convenient to write the the sum of 1PI new-physics contributions to the propagator of the gauge bosons as⁸

$$i\bar{\Pi}_{ab}^{\mu\nu} = i\bar{\Pi}_{ab}(q^2)g^{\mu\nu} + (q^\mu q^\nu \text{ terms}) \quad (2.2.50)$$

and to parameterize the vacuum polarization by

$$\bar{\Pi}_{ab}(q^2) = A_{ab} + q^2 F_{ab} + \mathcal{O}(q^2/m^2). \quad (2.2.51)$$

Here the indices a, b take values from zero (corresponding to the field B) to three (fields $W^{1,2,3}$). The three oblique parameters are then defined as:

$$\alpha_{\text{em}} S = 2 \sin(2\theta) \frac{d}{dq^2} (\bar{\Pi}_{30}(q^2)) \Big|_{q^2=0} = 2 \sin(2\theta) F_{30} \quad (2.2.52a)$$

$$\alpha_{\text{em}} T = \frac{1}{m_W^2} (\bar{\Pi}_{11}(0) - \bar{\Pi}_{33}(0)) = \frac{1}{m_W^2} (A_{11} - A_{33}) \quad (2.2.52b)$$

$$\alpha_{\text{em}} U = 4 \sin^2 \theta \frac{d}{dq^2} (\bar{\Pi}_{11}(q^2) - \bar{\Pi}_{33}(q^2)) \Big|_{q^2=0} = 4 \sin^2 \theta (F_{11} - F_{33}). \quad (2.2.52c)$$

Among these, the parameter T is the most sensitive to effects of violation of the custodial symmetry. Indeed, imposing custodial invariance at all orders implies $T \equiv 0$. The T is also related to the ρ parameter defined

⁸ We use the notation $i\bar{\Pi}^{\mu\nu}$ in order to stress that this is not the complete two-point function for gauge bosons, but it contains only the sum of new physics contributions.

in Eq. (2.2.49): this can be easily understood noticing that the quantities A_{ab} contribute to the poles of the vacuum polarization functions for the gauge bosons and, therefore, they represent shifts to the W and Z masses. Going to the physical basis one has⁹

$$m_W^2 = m_{W0}^2 + A_{11}, \quad m_Z^2 = m_{Z0}^2 + A_{33} \cos^2 \theta \quad (2.2.53)$$

hence

$$\rho = \frac{m_W^2}{m_Z^2 \cos^2 \theta} = \left(1 + \frac{A_{11}}{m_{W0}^2}\right) \left(1 + \frac{A_{33} \cos^2 \theta}{m_{Z0}^2}\right)^{-1} \simeq 1 + \frac{A_{11}}{m_{W0}^2} - \frac{A_{33}}{m_{W0}^2} = 1 + \alpha_{\text{em}} T. \quad (2.2.54)$$

The current best-fit values for the oblique parameters, obtained from a global fit on electroweak precision data, are [74]:

$$S = 0.08 \pm 0.1, \quad T = -0.1 \pm 0.12, \quad U = 0.0 \pm 0.09, \quad (2.2.55)$$

hence we see that the invariance under the custodial symmetry has been established at the percent level. This is one of the strongest constraints on BSM models and it has particular relevance for all the theories that aim at explaining the dynamics of the electroweak symmetry breaking, providing a UV completion to the Higgs sector.

2.3 Spontaneous EW symmetry breaking: non-linear realization

The alternative to the Higgs mechanism description of the EWSB process is provided by the non-linear realization of the symmetry breaking. The main point of this parameterization is that it allows to disentangle the physical Higgs from the Goldstone bosons in a gauge invariant way, and to assign them to different representations of the SM symmetries. This appeared as a particularly attractive feature prior to the discovery of the Higgs boson, fostered by some skepticism about its existence. The non-linear parameterization is naturally associated to scenarios with strongly-interacting new physics: this is easily understood noticing that, in absence of the Higgs, the couplings of the Goldstone bosons grow with the energy until they become non-perturbative. Indeed, this scenario mirrors quite closely the behavior of the pions of QCD. Typical theories that implement a non-linear EWSB are the now disfavored Technicolor models and the still plausible composite Higgs models.

Here we summarize the properties of the non-linear EW symmetry breaking, to be compared with the characteristics of the linear scenario listed in Sec. 2.2:

- The scalar sector in principle contains four fields: the three Goldstone bosons and the physical Higgs boson. In this realization, the former are in a triplet of the chiral symmetry, while the latter is a singlet. This is achieved at the cost of assigning the Goldstone bosons to a non-linear representation, that allows them to compensate for the non-transformation of the Higgs.
- Being a singlet, the physical Higgs can be integrated out without spoiling the chiral (gauge) invariance. In this way one obtains an effective Lagrangian, often called *chiral Lagrangian* that correctly describes the Goldstone bosons in the low-energy regime. This represents the minimal parameterization of the EWSB sector, and in principle it can be UV-completed in an arbitrary way, that does not need to include the Higgs scalar.
- The effective theory is non-renormalizable and violates perturbative unitarity in the processes that contain the Goldstone bosons (or, equivalently, longitudinally polarized W^\pm and Z bosons).

⁹ The mass m_Z^2 does not receive contributions from A_{00} and A_{30} because these are identically zero by ward identities: the photon's self-energy cannot have a pole in $q^2 \rightarrow 0$. Analogously, the self-energy of the W in principle contains a term A_{22} , but this must be identical to A_{11} .

2. Dynamics of the electroweak symmetry breaking

In analogy with in the previous section, we begin with the preliminary example of the non-linear σ model for QCD. Importantly, the results obtained in this context are actually general: Callan, Coleman, Wess and Zumino developed the general theory of non-linear realization of a broken symmetry (hence known as CCWZ formalism) in Refs. [75, 76], proving that it is always possible to construct an effective theory containing only Goldstone bosons for any symmetry breaking scheme $\mathcal{G} \rightarrow \mathcal{H}$, provided that \mathcal{G} is a compact, connected, semi-simple Lie group and that it contains \mathcal{H} as a subgroup.

2.3.1 A preliminary example from QCD: non-linear σ -model

Section 2.2.1 contained the description of the linear σ -model for pions, nucleons and the (hypothetical) σ -meson. It was underlined that the linear σ -model is a renormalizable theory with a global chiral symmetry that requires all the four scalar fields to be in the spectrum. In particular, it is not possible to integrate out the σ field from the Lagrangian, not even at energies well below the symmetry breaking scale, because this would violate explicitly the global $SU(2)_L \times SU(2)_R$ invariance.

It turns out, however, that the σ is not a fundamental ingredient of the symmetry breaking description, and that it can actually be decoupled from the model. This can be done using another parameterization of the σ -model, called *non-linear realization*, without spoiling the chiral invariance but at the cost of giving up renormalizability. The Lagrangian constructed in this way defines the *non-linear σ -model* that was again introduced by Gell-Mann and Lévy in another section of their paper in 1960 [70]. The model contains only the three pions and therefore is an effective theory valid only at energies lower than the σ mass. Here we review its formulation.

The starting point is again the Lagrangian of Eq. (2.2.29): in the linear realization the scalar fields were embedded in the matrix Σ defined in Eq. (2.2.31). In the non-linear realization, instead, one introduces the scalar φ and the matrix \mathbf{U} , defined by

$$\Sigma = \varphi \mathbf{U}. \quad (2.3.56)$$

The scalar φ is not only a singlet of the $SU(2)_{L+R}$ group, as σ , but it is an invariant of the whole global symmetry $SU(2)_L \times SU(2)_R$. On the other hand, the matrix \mathbf{U} is a bi-doublet, and transforms as Σ : $\mathbf{U} \mapsto U_L \mathbf{U} U_R^\dagger$. Moreover, \mathbf{U} can be parameterized in terms of three real fields χ^i that must be in a triplet of the residual group $SU(2)_{L+R}$:

$$\mathbf{U} \equiv \exp \left(i \vec{\tau} \cdot \frac{\vec{\chi}}{f} \right) = \cos \frac{|\vec{\chi}|}{f} + i \frac{\vec{\tau} \cdot \vec{\chi}}{|\vec{\chi}|} \sin \frac{|\vec{\chi}|}{f}, \quad (2.3.57)$$

where f must coincide with the vev of the singlet: $f = \langle \varphi \rangle = \sqrt{-\mu^2/\lambda}$ (see Eq. (2.3.61)). The matching with the fields σ and $\vec{\pi}$ is therefore non-trivial:

$$\begin{aligned} \sigma &= \varphi \cos \frac{|\vec{\chi}|}{f} = \varphi \left(1 - \frac{1}{2} \frac{\vec{\chi} \cdot \vec{\chi}}{f^2} + \dots \right) \\ \pi_i &= \varphi \sin \frac{|\vec{\chi}|}{f} \frac{\chi_i}{|\vec{\chi}|} = \chi_i \left(\frac{\varphi}{f} - \frac{1}{6} \frac{\varphi}{f} \frac{\vec{\chi} \cdot \vec{\chi}}{f^2} + \dots \right). \end{aligned} \quad (2.3.58)$$

With the non-linear change of variables defined by these relations it has been possible to concentrate all the chiral information carried by the matrix Σ , that contains four degrees of freedom, into the matrix \mathbf{U} , that contains only three. The fourth scalar has been isolated and excluded from the chiral transformations, but this requires the fields χ_i to transform non-linearly under $SU(2)_L \times SU(2)_R$, in order to compensate for the missing bi-doublet component.

In this notation, the Lagrangian of the σ -model is written

$$\mathcal{L} = i \bar{\psi} \not{\partial} \psi + \frac{1}{2} \partial_\mu \varphi \partial^\mu \varphi + \frac{\varphi^2}{4} \text{Tr}(\partial_\mu \mathbf{U}^\dagger \partial^\mu \mathbf{U}) - g \varphi (\bar{\psi}_L \mathbf{U} \psi_R + \bar{\psi}_R \mathbf{U}^\dagger \psi_L) - V(\varphi). \quad (2.3.59)$$

Since $\text{Tr}(\Sigma^\dagger \Sigma) = 2\varphi^2$, the field \mathbf{U} does not participate in the scalar potential, that reads just:

$$V(\varphi) = \frac{\mu^2}{2}\varphi^2 + \frac{\lambda}{4}\varphi^4. \quad (2.3.60)$$

As in the linear σ -model, the spontaneous chiral symmetry breaking takes place for $\mu^2 < 0$. In this case, there is only one alignment allowed:

$$\langle \varphi \rangle = \frac{-\mu^2}{\lambda} = f^2. \quad (2.3.61)$$

The fields χ_i do not even participate in the minimization of the potential, as by construction they describe excitations exactly parallel to the broken generators. Indeed, they only appear in the Lagrangian with derivative couplings. In the broken phase, expanding $\varphi = f + \varphi'$ and dropping the primes, the Lagrangian is

$$\begin{aligned} \mathcal{L} = & i\bar{\psi}\not{\partial}\psi + \frac{(f + \varphi)^2}{4} \text{Tr}(\partial_\mu \mathbf{U}^\dagger \partial^\mu \mathbf{U}) - g(f + \varphi)(\bar{\psi}_L \mathbf{U} \psi_R + \bar{\psi}_R \mathbf{U}^\dagger \psi_L) + \\ & + \frac{1}{2} \partial_\mu \varphi \partial^\mu \varphi - \frac{m_\varphi^2}{2} \varphi^2 - \frac{\lambda}{4} \varphi^4 - \lambda f \varphi^3. \end{aligned} \quad (2.3.62)$$

As in the linear case, there is a massive singlet scalar with mass $m_\varphi^2 = 2\lambda f^2$ and a mass term for the nucleons is triggered by the first term in the expansion of the \mathbf{U} exponential, yielding $m_\psi = gf$. At this point, the scalar φ can be easily decoupled taking the limit $\lambda \rightarrow \infty$ while keeping $f^2 = -\mu^2/\lambda$ constant. Importantly, this means that the φ scalar can be integrated out only in the limit in which it is strongly interacting. In this way one is left with the Lagrangian

$$\mathcal{L} = i\bar{\psi}\not{\partial}\psi + \frac{f^2}{4} \text{Tr}(\partial_\mu \mathbf{U}^\dagger \partial^\mu \mathbf{U}) - gf(\bar{\psi}_L \mathbf{U} \psi_R + \bar{\psi}_R \mathbf{U}^\dagger \psi_L). \quad (2.3.63)$$

This represents an effective Lagrangian for the pions, which is only valid at energies considerably lower than the mass of the σ meson. It is often referred to as *effective chiral Lagrangian* for pions. That this is not a renormalizable theory is clear from the fact that the matrix \mathbf{U} contains couplings among an arbitrary number of pions: for example, expanding the kinetic term one obtains

$$\frac{f^2}{4} \text{Tr}(\partial_\mu \mathbf{U}^\dagger \partial^\mu \mathbf{U}) = \frac{1}{2} \partial_\mu \vec{\chi} \cdot \partial^\mu \vec{\chi} + \frac{1}{6f^2} ((\vec{\chi} \cdot \partial_\mu \vec{\chi})^2 - (\vec{\chi} \cdot \vec{\chi})(\partial_\mu \vec{\chi} \cdot \partial^\mu \vec{\chi})) + \dots \quad (2.3.64)$$

where the dots imply an infinite power series in $(\chi/f)^n$.

An alternative representation

The “exponential” parameterization chosen in Eq. (2.3.58) is not the only one that allows to disentangle the three Goldstone bosons from the massive scalar, assigning the latter to a singlet representation of the chiral symmetry. A well-known alternative is provided by the “square root” representation in which, after the spontaneous symmetry breaking, one defines the following fields φ and $\vec{\chi}$:

$$\begin{aligned} \varphi &= \sqrt{(\sigma + f)^2 + \vec{\pi} \cdot \vec{\pi}} - f = \sigma + \frac{\vec{\pi} \cdot \vec{\pi}}{2v} - \sigma \frac{\vec{\pi} \cdot \vec{\pi}}{2v^2} + \dots \\ \vec{\chi} &= \frac{\vec{\pi}}{\sqrt{(\sigma + f)^2 + \vec{\pi} \cdot \vec{\pi}}} = \frac{\vec{\pi}}{f} \left(1 - \frac{\varphi}{f} + \frac{\varphi^2}{f^2} - \frac{\vec{\pi} \cdot \vec{\pi}}{2v^2} + \dots \right). \end{aligned} \quad (2.3.65)$$

In this case, the Lagrangian of the non-linear σ -model is

$$\begin{aligned} \mathcal{L} = & i\bar{\psi}\not{\partial}\psi + \frac{1}{2} \left(1 + \frac{\varphi}{f} \right)^2 \left(\partial_\mu \vec{\chi} \cdot \partial^\mu \vec{\chi} + \frac{(\vec{\chi} \cdot \partial_\mu \vec{\chi})^2}{f^2 - \vec{\chi} \cdot \vec{\chi}} \right) - g \left(1 + \frac{\varphi}{f} \right) \bar{\psi} \left(\sqrt{f^2 - \vec{\chi} \cdot \vec{\chi}} - i\vec{\tau} \cdot \vec{\chi} \gamma_5 \right) \psi + \\ & + \frac{1}{2} \partial_\mu \varphi \partial^\mu \varphi - \frac{m_\varphi^2}{2} \varphi^2 - \frac{\lambda}{4} \varphi^4 - \lambda f \varphi^3 \end{aligned} \quad (2.3.66)$$

2. Dynamics of the electroweak symmetry breaking

with $m_\varphi^2 = 2\lambda f^2$. Although the Goldstone bosons are described in a different way with respect to the exponential parameterization, this Lagrangian shares some important features with that of Eq. (2.3.62): on one hand the Goldstones have only derivative couplings and do not occur in the potential, and on the other the φ scalar can be decoupled from the theory in the limit $\lambda \rightarrow 0$ with $f^2 = -\mu^2/\lambda$ constant. Once the φ is integrated out, the Lagrangian of the non-linear σ -model in this representation is just

$$\mathcal{L} = i\bar{\psi}\not{\partial}\psi + \frac{1}{2} \left(\partial_\mu \vec{\chi} \cdot \partial^\mu \vec{\chi} + \frac{(\vec{\chi} \cdot \partial_\mu \vec{\chi})^2}{f^2 - \vec{\chi} \cdot \vec{\chi}} \right) - g\bar{\psi} \left(\sqrt{f^2 - \vec{\chi} \cdot \vec{\chi}} - i\vec{\tau} \cdot \vec{\chi} \gamma_5 \right) \psi. \quad (2.3.67)$$

It should be stressed that the different representations of the σ -model do not imply different physical properties of the particles described: in fact, as long as two parameterizations are connected by a smooth change of variables, they are totally equivalent. This is a general result in field theory, first proved by Haag in 1958 [77]. The theorem basically states that if two fields are related by a (non-linear) functional dependence $\phi = \chi F(\chi)$ with $F(0) = 1$, the S-matrices calculated in terms of ϕ with the Lagrangian $\mathcal{L}(\phi)$ and in terms of χ with $\mathcal{L}(\chi F(\chi))$ are identical. This follows from the fact that two S-matrices are identical if they have the same single particle singularities, and the latter are preserved by a change of variables with $F(0) = 1$. In practice, Haag's theorem ensures that the Goldstone bosons can be described indifferently in the linear or non-linear representation. The physical differences between the linear and the non-linear σ -model appear only when the σ field is integrated out: it is at this stage that the non-linear theory becomes intrinsically non-renormalizable and that the validity of the Lagrangian gets restricted to low energies.

The non-linear σ model as an Effective Theory

The Lagrangian (2.3.63) could have been constructed directly using only the information that the theory has a global $\mathcal{G} = SU(2)_L \times SU(2)_R$ symmetry broken down to the diagonal subgroup $\mathcal{H} = SU(2)_{L+R}$: this is sufficient for knowing that at low energies there must be three Goldstone bosons, that transform linearly under \mathcal{H} (but non-linearly under \mathcal{G}) and that must be embedded in an object that transforms in a linear representation of \mathcal{G} . The information about the existence of a σ -meson is unnecessary at this level, although one must be aware that a theory that describes only the Goldstone bosons will lose its validity at the energy scale where σ resonance appears. Remarkably, the description provided by the effective chiral Lagrangian matches not only the low-energy limit of the σ -model, but that of any theory based on the symmetry breaking pattern $SU(2) \times SU(2)/SU(2)$. Therefore Eq. (2.3.63) represents the most general, model-independent Lagrangian for pions' physics at low energies.

As an effective theory, the chiral Lagrangian of Eq. (2.3.63) can be interpreted as the leading order (LO) of an infinite expansion in powers of some small parameter. In the specific case of the chiral expansion, the most natural expansion parameter is (p/Λ) , where p is the momentum of an interacting pion and Λ is the cutoff scale at which the Lagrangian loses its validity. This is a consequence of the fact that \mathbf{U} is a unitary matrix: since $\text{Tr}(\mathbf{U}^\dagger \mathbf{U}) = 1$, the only non trivial interaction terms are those involving derivatives. Moreover, the number of derivatives in a coupling (or, equivalently, of momenta in the vertices) obviously defines a hierarchy among the different operators, as the Lagrangian is only valid in the regime where $p/\Lambda \ll 1$. The leading order of the chiral expansion is therefore given by all the terms with two derivatives. As the energy considered grows, higher orders in the (p/Λ) expansion must be taken into account: the first corrections to the LO are provided by all terms with four derivatives and so on. This systematic organization of the effective operators goes under the name of Weinberg's counting rule [78], and it can be shown that it is consistent with the renormalization procedure for the chiral Lagrangian: although the latter is non-renormalizable in the classical sense, it is possible to make the theory finite order-by-order. For example, the divergences stemming from one-loop diagrams constructed with LO vertices can be reabsorbed adding the required counterterms, that consequently would constitute the NLO of the loop expansion. Since the Lagrangian is the most general one consistent with the chiral symmetry, it must be possible to construct a number of invariants sufficient for canceling all the divergences. Moreover, by a trivial power counting, these counterterms must be of

order $\mathcal{O}(E^4)$, *i.e.* they must contain four derivatives. Hence, in chiral perturbation theory, the expansion in derivatives basically coincides with the ordering defined by the renormalization procedure. It can be shown that, for this to be consistently realized in the theory, the f and Λ scales must satisfy the constraint $\Lambda \leq 4\pi f$ [79]. This is a typical condition for models that implement a non-linearly realized symmetry: for instance, in QCD the inequality can be replaced by the estimate $\Lambda_{\text{QCD}} \simeq 4\pi f_\pi \sim 1 \text{ GeV}$.

2.3.2 The EW case: Higgs-less EWSB

The non-linear σ -model for the pions of QCD discussed above is an interesting example of how a system with a spontaneously broken symmetry can be described using only the fields corresponding to the Goldstone bosons. As was mentioned above, in 1969 CCWZ proved that this can actually be done for any spontaneous symmetry breaking pattern \mathcal{G}/\mathcal{H} , as long as \mathcal{G} is a well-behaved group [75, 76].

Among all applications, we are particularly interested in using the non-linear formalism for describing the spontaneous breaking of the electroweak symmetry. Exploiting the correspondence between the Higgs mechanism of the Standard Model and the linear σ -model (see Sec. 2.2.2), it is easy to switch to a non-linear parameterization: defining

$$\phi_0 = v + h \quad \text{and} \quad \mathbf{U} = \exp \left(i \frac{\vec{\tau} \cdot \vec{\pi}}{v} \right) \quad (2.3.68)$$

such that

$$\frac{\phi_0}{\sqrt{2}} \mathbf{U} = \Sigma = \begin{pmatrix} \tilde{\Phi} \\ \Phi \end{pmatrix}, \quad (2.3.69)$$

with Σ defined in Eq. (2.2.42). The scalar ϕ_0 is an EW singlet, while the matrix \mathbf{U} is a bi-doublet of the chiral group: once the EW symmetries are gauged, its covariant derivative reads

$$D_\mu \mathbf{U} = \partial_\mu \mathbf{U} + ig W_\mu^a \frac{\tau^a}{2} \mathbf{U} - ig' B_\mu \mathbf{U} \frac{\tau^3}{2}. \quad (2.3.70)$$

The Higgs Lagrangian of Eq. (1.1.6) therefore becomes

$$\begin{aligned} \mathcal{L}_\Phi \rightarrow & \frac{(v+h)^2}{4} \text{Tr}(D_\mu \mathbf{U}^\dagger D^\mu \mathbf{U}) + \frac{1}{2} \partial_\mu h \partial^\mu h - \frac{m_h^2}{2} h^2 - \frac{\lambda v}{4} h^3 - \frac{\lambda}{16} h^4 + \\ & - \frac{(v+h)}{\sqrt{2}} [\bar{Q}_L \mathbf{U} \mathcal{Y}_Q Q_R + \bar{L}_L \mathbf{U} \mathcal{Y}_L L_R + \text{h.c.}] \end{aligned} \quad (2.3.71)$$

where

$$\mathcal{Y}_Q = \begin{pmatrix} \mathbf{y}_U & \\ & \mathbf{y}_D \end{pmatrix} \quad \mathcal{Y}_L = \begin{pmatrix} 0 & \\ & \mathbf{y}_E \end{pmatrix} \quad (2.3.72)$$

and the right-handed fermions have been grouped in $SU(2)_R$ doublets. The Higgs boson can be decoupled in the limit in which it is a strongly interacting particle $\lambda \rightarrow \infty$, leaving:

$$\mathcal{L}_0 = \frac{v^2}{4} \text{Tr}(D_\mu \mathbf{U}^\dagger D^\mu \mathbf{U}) - \frac{v}{\sqrt{2}} [\bar{Q}_L \mathbf{U} \mathcal{Y}_Q Q_R + \bar{L}_L \mathbf{U} \mathcal{Y}_L L_R + \text{h.c.}]. \quad (2.3.73)$$

This Lagrangian is extremely important as it provides the minimal description of the electroweak symmetry breaking. The gauge fixing term can be written as

$$\mathcal{L}_{\text{G.F.}} = -\frac{1}{\xi} \left(\partial_\mu W^\mu + \xi \frac{igv^2}{8} (\mathbf{U} - \mathbf{U}^\dagger) \right)^2 - \frac{1}{4\xi} \left(\partial_\mu B^\mu - \xi \frac{ig'v^2}{4} (\mathbf{U} \tau^3 - \tau^3 \mathbf{U}^\dagger) \right)^2 \quad (2.3.74)$$

2. Dynamics of the electroweak symmetry breaking

for a generic R_ξ gauge. The unitary gauge $\xi \rightarrow \infty$ corresponds to replacing $\mathbf{U} \equiv \mathbb{1}$ everywhere in the Lagrangian, and in this limit \mathcal{L}_0 yields the correct mass terms for the gauge bosons and the fermions:

$$\mathcal{L}_0 \xrightarrow{\mathbf{U} \equiv \mathbb{1}} \frac{v^2}{4} \left(2g^2 W_\mu^+ W^{-\mu} + \frac{g^2}{\cos^2 \theta} Z_\mu Z^\mu \right) - \frac{v}{\sqrt{2}} [\bar{U}_L \mathbf{Y}_U U_R + \bar{D}_L \mathbf{Y}_D D_R + \bar{E}_L \mathbf{Y}_E E_R + \text{h.c.}] . \quad (2.3.75)$$

The chiral Lagrangian \mathcal{L}_0 respects the same custodial symmetry as the Lagrangian for the Higgs mechanism (Eq. (2.2.45)). However, once the Higgs has been removed from the spectrum, it is possible to introduce a new source of custodial violation in the Lagrangian: for this purpose it is useful to define the following chiral objects

$$\mathbf{V}_\mu \equiv D_\mu \mathbf{U} \mathbf{U}^\dagger, \quad \mathbf{T} \equiv \mathbf{U} \tau^3 \mathbf{U}^\dagger . \quad (2.3.76)$$

Both these fields transform in the adjoint representation of $SU(2)_L$: $\mathbf{V}_\mu \mapsto U_L \mathbf{V}_\mu U_L^\dagger$ and $\mathbf{T} \mapsto U_L \mathbf{T} U_L^\dagger$. The vector \mathbf{V}_μ is also a singlet of $SU(2)_R$, so that insertions of \mathbf{V}_μ automatically preserve the custodial invariance. On the other hand, the scalar \mathbf{T} does not have well-defined transformation properties under $SU(2)_R$: it is invariant under the hypercharge but breaks explicitly the other two components of the $SU(2)_R$ symmetry. In this sense, \mathbf{T} is a spurion of the custodial symmetry. The LO of the chiral expansion for the EW Goldstone bosons is expected to contain all the possible interactions with two derivatives. If the custodial symmetry is not imposed by hand, the most general Lagrangian is then

$$\mathcal{L}_2 = -\frac{v^2}{4} \text{Tr}(\mathbf{V}_\mu \mathbf{V}^\mu) + c_T \frac{v^2}{4} \text{Tr}(\mathbf{T} \mathbf{V}_\mu) \text{Tr}(\mathbf{T} \mathbf{V}^\mu) - \frac{v}{\sqrt{2}} [\bar{Q}_L \mathbf{U} \mathbf{Y}_Q Q_R + \bar{L}_L \mathbf{U} \mathbf{Y}_L L_R + \text{h.c.}] , \quad (2.3.77)$$

where $\text{Tr}(\mathbf{V}_\mu \mathbf{V}^\mu) \equiv -\text{Tr}(D_\mu \mathbf{U}^\dagger D^\mu \mathbf{U})$. The second term, parameterized by an arbitrary coefficient c_T , breaks explicitly $SU(2)_c$. Indeed, in unitary gauge, it yields a contribution to the mass term for the Z boson but not to that of the W^\pm . As a consequence:

$$\rho = \frac{m_W^2}{m_Z^2 \cos^2 \theta} = \frac{1}{1 - 2c_T} \simeq 1 + 2c_T . \quad (2.3.78)$$

Applying the definitions in Eq. (2.2.52) it is also straightforward to see that this operators contributes to the T parameter giving $\alpha_{\text{em}} T = 2c_T$, as was expected from the relation (2.2.54). The experimental bounds on the oblique parameters imply, then, constraints of order 10^{-2} on the coefficient c_T , which *a posteriori* allows to consider the interaction $\text{Tr}(\mathbf{T} \mathbf{V}_\mu)^2$ as a NLO term. This is a relevant example of how the custodial symmetry, that arises accidentally in the SM Higgs mechanism, actually represents quite a strong constraint for alternative parameterizations of the EWSB.

2.3.3 Violation of perturbative unitarity

The electroweak chiral Lagrangian \mathcal{L}_0 given in Eq. (2.3.73) describes the masses of the gauge bosons and fermions of the Standard Model in a gauge invariant way and without the need of introducing the Higgs scalar. This remarkable result provides the minimal parameterization of the electroweak symmetry breaking at low energy and it can be interpreted as the most general starting point for the study of the EWSB sector. From this point of view, the Higgs mechanism of the Standard Model represents only one viable UV completion to the effective Lagrangian \mathcal{L}_0 among many. In particular, it would be even possible to formulate totally Higgs-less theories of EWSB, such as the Technicolor models first introduced by Weinberg [10] and Susskind [11] in the late 1970s.

The construction of viable UV completions for the effective chiral Lagrangian must keep into account an important constraint, that originates from an internal inconsistency of the effective theory. In fact, the latter predicts scattering amplitudes that violate perturbative unitarity; in particular, this happens for the S-matrices that contain longitudinally polarized gauge bosons. As a consequence, the heavier states added to the spectrum must be able to cure this problem.

A relevant example of unitarity violation is given by the cross-section for the elastic scattering of four longitudinal W bosons: for energies sufficiently larger than the W mass, this can be computed applying the Equivalence Theorem of Sec. 2.1.3. With the couplings contained in \mathcal{L}_0 , one obtains then

$$\mathcal{A}(W_L^+ W_L^- \rightarrow W_L^+ W_L^-) = \mathcal{A}(\pi^+ \pi^- \rightarrow \pi^+ \pi^-) \sim \frac{s+t}{v^2}, \quad (2.3.79)$$

where s and t stand for the Mandelstam variables. Since this amplitude grows quadratically with the energy, it violates the partial wave unitarity bound, or Froissart bound [80], which is a direct consequence of the unitarity of the S-matrix. This bound basically ensures that the total cross-section of a process cannot be arbitrarily large, and in particular it cannot grow faster than $\log^2 s$.

The same problem appears, for example, with the scattering into fermions, $W_L^+ W_L^- \rightarrow \bar{\psi}\psi$, that yields

$$\mathcal{A}(W_L^+ W_L^- \rightarrow \bar{\psi}\psi) = \mathcal{A}(\pi^+ \pi^- \rightarrow \bar{\psi}\psi) \sim \frac{m_\psi}{v^2} \sqrt{s}. \quad (2.3.80)$$

There are two main avenues for solving the unitarity problem, that eventually define two paradigms for the implementation of the electroweak symmetry breaking:

- (a) one possibility is that new particles come in to cancel the energy dependence in the cross-sections, thus restoring perturbativity. This is the case of the Higgs mechanism in its linear description where, as illustrated below, the Higgs boson plays a central role.
- (b) An alternative is that the interaction among the Goldstone bosons indeed increases with the energy up to the point at which the perturbative description breaks down. This scenario is naturally associated with a strong interacting EWSB sector, and its simplest interpretation is that the EW Goldstone bosons are composite states of heavier fundamental particles, pretty much like QCD pions.

Restoration of unitarity with a fundamental scalar: back to the Higgs mechanism

The first option for the restoration of unitarity is the addition of an extra particle to the chiral Lagrangian of Eq. (2.3.73). The most economical choice is the addition of a real scalar degree of freedom φ . The minimal requirement on this particle is that it must be a singlet under the custodial symmetry: the Lagrangian can therefore be parameterized as [81]

$$\begin{aligned} \mathcal{L}_{0\varphi} = & \frac{1}{2} \partial_\mu \varphi \partial^\mu \varphi - V(\varphi) + \frac{v^2}{4} \text{Tr}(D_\mu \mathbf{U}^\dagger D^\mu \mathbf{U}) \left(1 + 2a \frac{\varphi}{v} + b \frac{\varphi^2}{v^2} \right) + \\ & - \frac{v}{\sqrt{2}} [\bar{Q}_L \mathbf{U} \mathcal{Y}_Q Q_R + \bar{L}_L \mathbf{U} \mathcal{Y}_L L_R + \text{h.c.}] \left(1 + c \frac{\varphi}{v} \right), \end{aligned} \quad (2.3.81)$$

where the couplings a, b, c are in principle free. The scalar φ now enters the diagrams for the scattering of Goldstone bosons. Here we report the dominant terms of three sample amplitudes. The corresponding diagrams are drawn in Figure 2.2.

$$\mathcal{A}(\pi^+ \pi^- \rightarrow \pi^+ \pi^-) \sim \frac{1}{v^2} \left[s + t - a^2 \left(\frac{s^2}{s - m_\varphi^2} + \frac{t^2}{t - m_\varphi^2} \right) \right] = \frac{s+t}{v^2} (1 - a^2) + \mathcal{O}(m_\varphi^2/s) \quad (2.3.82a)$$

$$\mathcal{A}(\pi^+ \pi^- \rightarrow \varphi \varphi) \sim \frac{s}{v^2} (b - a^2) + \mathcal{O}(m_\varphi^2/s) \quad (2.3.82b)$$

$$\mathcal{A}(\pi^+ \pi^- \rightarrow \bar{\psi}\psi) \sim \frac{m_\psi}{v^2} \sqrt{s} (1 - ac) + \mathcal{O}(m_\varphi^2/s). \quad (2.3.82c)$$

Imposing that the scalar restores perturbative unitarity in all these processes fixes completely the three couplings to be

$$a = b = c = 1. \quad (2.3.83)$$

2. Dynamics of the electroweak symmetry breaking

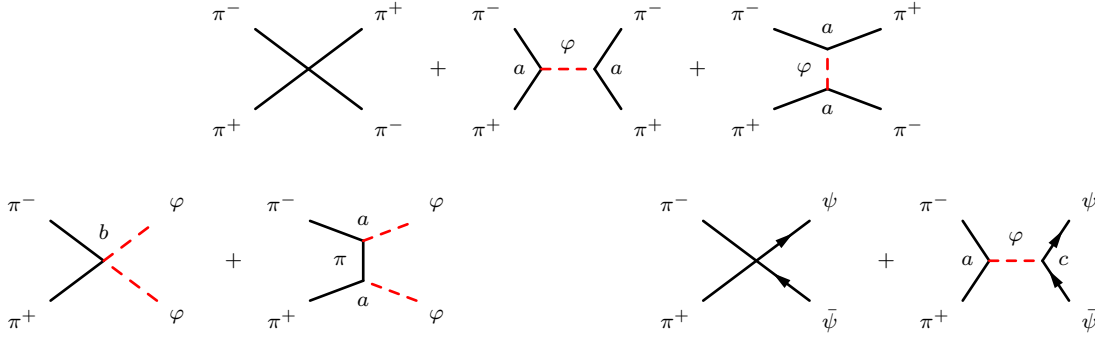


Figure 2.2: *Feynman diagrams for the three sample scattering processes of Eqs. (2.3.82). The scalar field φ , indicated with red dashed lines, eventually re-unitarizes the S -matrices of these processes. The parameters a, b, c , defined in Eq. (2.3.81), represent arbitrary couplings of φ to Goldstone boson and fermions.*

But this means that the scalar φ must have the same couplings as the Higgs field that was integrated out from Eq. (2.3.71) which, at that stage, simply described the Standard Model Higgs mechanism in a non-linear parameterization. Thus we must conclude that, by Haag’s theorem, the additional scalar must be the SM Higgs boson: evidently, its role is not only that of completing the $SU(2) \times SU(2)$ multiplet of scalars, but it also ensures the perturbative unitarity of the theory.

Despite being renormalizable and phenomenologically successful, it is well-known that the Higgs model does not provide a self-contained theory of EWSB (see Sec. 1.1.3), as it doesn’t provide any dynamical explanation of the symmetry breaking process and it is affected by the hierarchy problem. The idea of UV-completing the EW Goldstone bosons’ Lagrangian with the insertion of a weakly-interacting Higgs boson is then often embedded in larger constructions. In particular, this scenario matches particularly well to supersymmetric theories and, more in general, with theories of EWSB that are weakly-coupled at high energies.

Restoration of unitarity with strong resonances: Technicolor

The second option for addressing the unitarity problem is assuming that the EW Goldstone bosons really become strongly interacting in the high energy limit. This scenario resembles quite closely that of QCD, which can be used as a prototype for the construction of a strongly-coupled EWSB sector. In fact, the scattering amplitude of QCD pions, computed in the description of the chiral Lagrangian (2.3.63), is also proportional to the square of the momenta involved. However, the effective theory breaks down before the unitarity bound is violated, more precisely when the energy becomes high enough for some composite resonances to be produced. At this point, the pions can exchange a whole tower of heavier states that eventually restore unitarity. In absence of a bound state with the quantum numbers of the σ (analogous to the Higgs), the most relevant contribution comes from the ρ meson, which is the lightest vector resonance.

Models of EWSB based on the analogy with QCD began to be developed in the late 1970s [10–12] and go under the name of Technicolor theories. They are based on the idea of some strong-interacting sector, similar to ordinary QCD but living at a much higher scale. These interactions must have a global $SU(2)_L \times SU(2)_R$ chiral invariance and contain N fundamental, heavy “techniquarks”. In the assumption that Technicolor interactions confine, the formation of condensates triggers the breaking of the chiral symmetry down to the custodial group: the resulting Goldstone bosons serve as the scalar degrees of freedom required for EWSB.

In this sense, the EW Goldstone bosons, eaten by the W and the Z , are identified with the “technipions”¹⁰. In the simplest scenario, the EW vev $v = 246$ GeV must then coincide with the decay constant F_π of the technipions (see the discussion at the end of Sec. 2.2.1). In this sense, Technicolor immediately appears as an attractive solution to the hierarchy problem: in this kind of scenario the electroweak scale is generated dynamically and can be naturally much smaller than the energies at which the fundamental states live, in complete analogy with QCD.

An important aspect of Technicolor models is that they predict the appearance of a whole tower of resonances at a relatively low energy, as these must be able to restore perturbative unitarity in the scattering of longitudinal gauge bosons. Indeed, the mass of the lightest vector resonance (the techni- ρ) can be naively estimated with a rough rescaling

$$m_{\rho_{\text{TC}}} \simeq \frac{v}{f_\pi} m_\rho = 2.1 \text{ TeV}. \quad (2.3.84)$$

It turns out that the presence of resonances at the TeV scale is a characteristic feature of any BSM theory based on a strongly-interacting sector: in particular this is maintained in composite Higgs scenarios. These resonances have a relevant phenomenological impact: besides restoring perturbative unitarity, they contribute significantly to the oblique parameters S, T, U and, obviously, their observation at the LHC would represent the most spectacular signature of these models.

Despite their attractiveness as non-linear solutions to the hierarchy problem, pure Technicolor models present a whole list of serious problems that undermined their viability well before the discovery of the Higgs boson. The two main issues are a parametrically too large correction to the S parameter and too fast flavor-changing neutral currents (FCNC) processes. The former has been computed by Peskin and Takeuchi in the case of Technicolor interactions based on the group $SU(N_{\text{TC}})$ [82]. In the large- N_{TC} approximation they obtain the proportionality:

$$S \sim \frac{N_{\text{TC}} N_{\text{TF}}}{\pi} \quad (2.3.85)$$

where N_{TC} and N_{TF} are the number of techni-colors and techni-flavors respectively and the proportionality constant depends on the particular TC model considered. It is clear that this easily provides an order 1 contribution to the S parameter, even for small $N_{\text{TC}}, N_{\text{TF}}$.

The FCNC issue, on the other hand, is related to the implementation of quark masses in this class of models: in absence of a Higgs mechanism, the simplest solution is assuming that the Technicolor and QCD groups are embedded in a larger Extended Technicolor (ETC) symmetry

$$SU(N_{\text{ETC}}) \supseteq SU(N_{\text{TC}}) \times SU(3)_c. \quad (2.3.86)$$

Assuming that $SU(N_{\text{ETC}})$ is spontaneously broken at some scale Λ_{ETC} , the associated massive gauge bosons can mediate the interaction of two techniquarks with two ordinary quarks. After TC condensation, this yields a mass term for the light quarks [83, 84]. Schematically:

$$\mathcal{L} \supset \frac{g_{\text{ETC}}^2}{\Lambda_{\text{ETC}}^2} (\bar{\Psi}_{\text{TC}} \Psi_{\text{TC}}) (\bar{q} q) \xrightarrow{\text{cond.}} \frac{g_{\text{ETC}}^2}{\Lambda_{\text{ETC}}^2} \langle \bar{\Psi}_{\text{TC}} \Psi_{\text{TC}} \rangle (\bar{q} q) = m_q (\bar{q} q), \quad (2.3.87)$$

where eventually $m_q \sim \Lambda_{\text{TC}} (\Lambda_{\text{TC}} / \Lambda_{\text{ETC}})^2$. Since $\Lambda_{\text{TC}} \simeq v$, masses of the correct order of magnitude are obtained for Λ_{ETC} very roughly in the range $1 - 100$ TeV. This quite baroque procedure has two evident drawbacks: to begin with, in order to reproduce the mass hierarchies it is necessary to assume that the different quark families are embedded in a ETC multiplet and that $SU(N_{\text{ETC}})$ undergoes a cascade of breakings. In this way, every quark flavor q^α would be associated to a different breaking scale $\Lambda_{\text{ETC}}^\alpha$. More

¹⁰ More precisely, the EW Goldstones would be a linear combination of the QCD pions with the technipions, as these states have the same quantum numbers: $|W_L, Z_L\rangle = \sin \alpha |\pi_{\text{QCD}}\rangle + \cos \alpha |\pi_{\text{TC}}\rangle$. However, the mixing angle would be $\alpha = \arctan(f_\pi / F_\pi) \ll 1$, being $f_\pi \sim \text{MeV}$ and $F_\pi \sim \text{GeV}$ the decay constants of the QCD and techni-pions respectively. Therefore, the QCD component, which is already present in the Standard Model, can be neglected.

2. Dynamics of the electroweak symmetry breaking

importantly, the ETC gauge bosons must also mediate interactions of four light quarks with a coupling $\sim \Lambda_{\text{ETC}}^{-2}$. Since the light quarks belong to a same ETC multiplet, these interactions typically violate flavor (and CP). The bounds derived from $K\bar{K}$ and $B\bar{B}$ oscillations impose then limits on the ETC scale of order $\Lambda_{\text{ETC}} \gtrsim 10^3 - 10^5 \text{ TeV}$ (see *e.g.* [85]), which is totally not compatible with the value needed to get realistic quark masses. In practice there is a tension between the generation of large quark masses and the suppression of FCNC processes.

The inconsistencies discussed above highlight that Technicolor models could not represent a plausible theory of EWSB. This is even more clear after the discovery of the Higgs boson, whose existence is not explained in this context. Nonetheless, the idea of a strong-interacting EWSB sector has an interesting implementation in models with a composite Higgs, that will be illustrated in the next section.

2.4 The Higgs as a pseudo-Goldstone boson

There is a fascinating variation of the EWSB paradigm presented in the previous Section that interpolates between simple Technicolor and the SM with an elementary Higgs. In this class of theories the Higgs boson is one among the bound states produced in the spontaneous symmetry breaking that takes place in the strongly interacting sector: this is the basic idea of Composite Higgs (CH) models. The main advantage of Technicolor, namely the absence of fundamental scalars that removes the hierarchy problem, is thus retained, while the presence of a light Higgs in the spectrum ameliorates the phenomenological viability of the theory. In such a framework, the lightness of the Higgs boson compared to the other resonances could be naturally justified if it emerges as a pseudo-Goldstone boson, *i.e.* it originates from the spontaneous breaking of an approximate global symmetry [86–91]. In analogy with the QCD pions, the Higgs' mass would then be non-vanishing but protected by the approximate invariance. Technically, the main difference between CH models from the Technicolor construction, is the existence of two separate phase transitions, as will be underlined in the next section.

It is worth underlining that the (low-energy) properties of a particular CH model are completely defined by the choice of the groups \mathcal{G} and \mathcal{H} . For this reason, it is customary to name the models by the implemented symmetry breaking pattern: the first CH model to be formulated is $SU(5)/SO(5)$, proposed by Georgi and Kaplan in 1984 [90]. One of the most popular ones is instead the minimal custodially-symmetric model $SO(5)/SO(4)$ [92, 93], while the most minimal construction, based on the coset $SU(3)/(SU(2) \times U(1))$ is strongly disfavored due to the large custodial breaking effects induced. Details about the construction of these specific models are deferred to Chapter 6.

2.4.1 Composite Higgs models: general structure

As explained above, the structure of a generic composite Higgs model must account for a double phase transition. This is typically achieved as follows:

Stage 1 – As in Technicolor, one postulates the existence of a strong interacting sector with a global symmetry \mathcal{G} dynamically broken to a subgroup \mathcal{H} . This creates $n = \dim \mathcal{G} - \dim \mathcal{H}$ Goldstone bosons with a characteristic scale f that satisfies $4\pi f \geq \Lambda$, being Λ roughly the mass scale of the strong resonances. In order to obtain a composite Higgs with the correct quantum numbers, the chosen groups must satisfy the following conditions:

- (i) the SM gauge group $SU(2)_L \times U(1)_Y$ is embeddable into the group \mathcal{H}
- (ii) the coset \mathcal{G}/\mathcal{H} allows for the presence of at least one $SU(2)$ doublet among the Goldstone bosons, that will play the role of the Higgs doublet.
- (iii) Although it is not mandatory, it is desirable that \mathcal{H} embeds the custodial symmetry. This prevents large contributions to the ρ parameter.

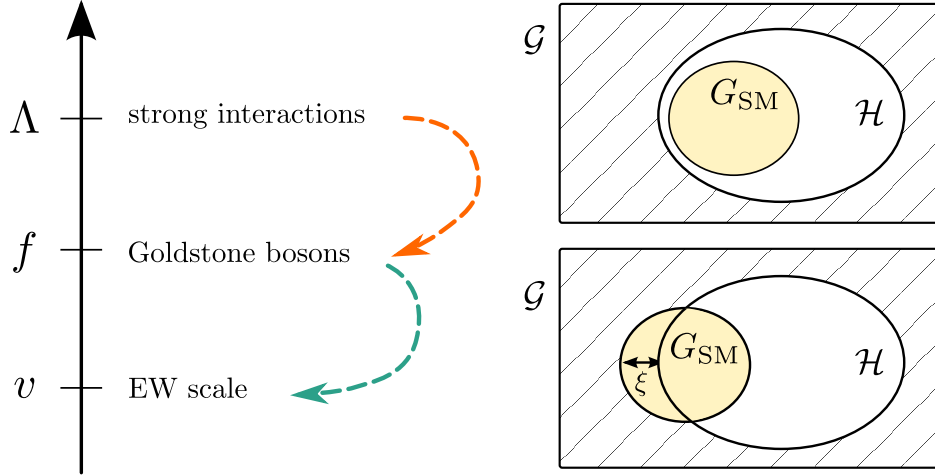


Figure 2.3: Pictorial view of the structure of a generic composite Higgs model. In a first stage the condensation of the strong interactions breaks the global symmetry \mathcal{G} down to the subgroup \mathcal{H} that contains the SM group $G_{\text{SM}} = SU(2) \times U(1)$, producing GBs with characteristic scale $f \geq \Lambda/4\pi$. In a second stage, radiative corrections due to the gauging of the SM group itself, that break explicitly \mathcal{G} , induce a vacuum misalignment that triggers the EWSB. This misalignment is quantified by the parameter $\xi = v^2/f^2$.

With this setup, at the energy scale f the EW symmetry is unbroken, the would-be Higgs doublet contains four massless GB, and its scalar potential is vanishing (at tree level).

Stage 2 – Let’s now assume that a subgroup $\mathcal{H}_g \subset \mathcal{G}$ is gauged. If the intersection with \mathcal{H} is non-trivial, *i.e.* $\mathcal{H}_0 = \mathcal{H} \cap \mathcal{H}_g \neq \emptyset$, $n_g = \dim \mathcal{H}_g - \dim \mathcal{H}_0$ among the Goldstones are eaten by as many gauge fields. The remaining $(n - n_g)$ states are either Goldstone bosons or pseudo-Goldstone bosons, depending on whether the associated symmetry was exact or approximate.

In our case, the mere gauging of the SM group represents an explicit breaking of the global symmetry \mathcal{G} , which makes the Higgs doublet a pseudo-Goldstone field. As a result, loops of SM fermions and gauge bosons generate an effective potential for the Higgs doublet. If this has the correct shape, with a negative mass squared, the breaking of the EW symmetry is triggered exactly as in the SM. Eventually, the Higgs boson emerges with a mass $m_h \sim gv$ where g is a generic SM coupling and v the EW scale.

In practice, radiative corrections induce a *misalignment* between the initial vacuum, invariant under \mathcal{H} , and the true vacuum.

The electroweak scale v is determined dynamically in this process and it is naturally smaller than f , as the two scales characterize two well-separated symmetry breakings. The distance between them, or equivalently the size of the vacuum misalignment, is customarily quantified by the ratio

$$\xi = \frac{v^2}{f^2} \in [0, 1]. \quad (2.4.88)$$

This parameter is phenomenologically relevant, as it fixes the parametric suppression of all the corrections to the precision observables. In particular, ξ enters the couplings of the physical Higgs boson, which therefore do not coincide with those fixed by the $SU(2)$ symmetry in the pure SM description. For example, in the model $SO(5)/SO(4)$ the Higgs couplings to gauge bosons, parameterized as in Eq. (2.3.81), are predicted to take the form [81]

$$a = \sqrt{1 - \xi}, \quad b = 1 - 2\xi, \quad (2.4.89)$$

2. Dynamics of the electroweak symmetry breaking

which in general deviates from unity. This is consistent with the fact that, in this hybrid theories, both the light h particle and the heavy resonances contribute to restoring the perturbative unitarity of the S-matrices. Remarkably, the parameter a is equivalent to the coupling modifier $\kappa_V \equiv \kappa_W = \kappa_Z$ defined in Sec. 1.2.2 and represented in Fig. 1.6. It is therefore possible to set a constraint on ξ , which currently reads $\xi \lesssim 0.1$ for this particular model. More details about the role of ξ in the low-energy description will be given in Sec. 3.4 and in Chapter 4.

It is also worth noticing that ξ parameterizes a smooth transition between the linear Higgs model and Technicolor: in the limit $\xi \rightarrow 0$ (*i.e.* $f \rightarrow \infty$) the Higgs remains light while the other resonances become infinitely heavy and ultimately decouple. This is equivalent to the SM description. On the other hand, when $\xi \rightarrow 1$ (*i.e.* $f \rightarrow v$) the two phase transitions exactly overlap, which means that the Technicolor picture has been recovered.

A final comment is in order about the generation of fermions' masses: the original model by Georgi and Kaplan implemented a mechanism similar to that of Extended Technicolor. In this case, the presence of two different phase transitions allows to disentangle the size of the quarks masses (proportional to $v(f/\Lambda_{\text{ETC}})^2$) from that of FCNC (proportional to $(v/\Lambda_{\text{ETC}})^2$). However, in order to obtain realistic results one needs to impose a very strong fine tuning on ξ , of the order $\xi \simeq 10^{-3} - 10^{-5}$. On top of this, this mechanism does not give a satisfactory solution for the hierarchies among fermions masses. An alternative and more attractive mechanism is rather that of *partial compositeness*, originally proposed by Kaplan [94]. The basic idea is the following: suppose to have linear (instead of bilinear) couplings between the light fermions and composite operators

$$\mathcal{L}_{\text{int.}} = \lambda \bar{q} O + \text{h.c.} \quad (2.4.90)$$

where O is a fermionic composite operator, made for example (but not necessarily) of three technifermions. At low energy the composite Higgs field is interpolated by pairs of composite operators $O_L O_R$. This generates effective Yukawa couplings and quark masses of the form

$$m_q \sim v \lambda_L \lambda_R. \quad (2.4.91)$$

Following an argument that we do not reproduce here, it can be shown that hierarchical mass terms can be generated inducing different RG evolution for the couplings λ . This can be done under quite generic assumptions and it ultimately boils down to assuming convenient anomalous dimensions of the corresponding composite operators [81].

This mechanism is combined with another important outcome of the construction of Eq. (2.4.90): once the strong interactions confine, the interaction term of Eq. (2.4.90) becomes a mass mixing term between the SM fermions and a tower of fermion resonances. In a similar way, the EW gauge fields turn out to mix with the tower of vector-like resonances. As a consequence, the SM particles are actually a superposition of elementary and composite states: this justifies the name “partial compositeness”. The mixing angles α can be naturally small because the RG evolution argument allows to have arbitrarily small mass mixing parameters.

An important result is that, since only the composite component of a given particle communicates with the strong sector, the degree of compositeness determines the strength with which a given particle feels the EWSB, which ultimately determines its mass. Indeed, the SM Yukawa matrices will have the structure

$$(\mathbf{y}^{\text{SM}})_{ij} = (\mathbf{y}^{\text{comp.}})_{ij} \sin \alpha_{Li} \sin \alpha_{Rj} \quad (2.4.92)$$

where $(\mathbf{y}^{\text{comp.}})_{ij}$ is the Yukawa of the composite state, which is determined by the strong dynamics, and $\alpha_{L,R}$ are the associated mixing angles. Finally, $\{i, j\}$ are flavor indices and no sum is intended in the RH side of the equation.

Effective field theories with a light Higgs

In the previous chapter we described the two main paradigms for the realization of the EWSB and we gave an overview of possible UV completions for the scalar sector of the EW theory. In particular, we underlined that a linear EWSB is typically realized in theories with weakly-interacting new physics (*e.g.* SUSY models) while a non-linearly realization of the EWSB is characteristic of theories based on strongly-interacting heavy sectors: the prototype is Technicolor, but this is also the case of composite Higgs models, which currently represent one of the most popular solutions to the hierarchy problem.

With these conclusions in mind, we now adopt a different point of view, that sets the approach of the work presented in the next Chapters: we choose to study the EWSB in a model-independent way and, to this aim, we make use of Effective Field Theories (EFTs). In this framework, the impact of any putative new physics on the low-energy (sub-TeV) observables is parameterized by an infinite expansion of operators built with a chosen set of degrees of freedom and preserving some given symmetries: in our case, Lorentz invariance, the SM gauge symmetry $SU(3)_c \times SU(2)_L \times U(1)_Y$ and both baryon and lepton number. The main advantage of employing an effective description resides in the universality of this parameterization, that relies only on the most fundamental assumptions: any model compatible with the chosen symmetries and particle content can be matched to the EFT, determining, in general, a set of specific constraints and relations among the parameters of the effective expansion.

In the case of Higgs physics, there are two categories of effective Lagrangians that are pertinent: the *linear* and the *non-linear* (or *chiral*) effective theories. As the names suggest, they are based on the two realizations of the EWSB presented in the previous chapter. In this sense, the linear Lagrangian is expected to capture the characteristic features of an elementary Higgs originating from some weakly-interacting new physics, while scenarios with a composite Higgs or, more in general, with a strongly-interacting EWSB sector are more properly described by the chiral Lagrangian. In practice, the distinction between the two formalisms is not dichotomous, as the non-linear parameterization is actually more general than the linear one, as already underlined in Sec. 2.3. Most importantly, the two EFT are intrinsically different and, as a consequence, they predict well-distinct patterns of signals around the TeV scale. The quest for these model-independent signatures of the EWSB nature is the main subject of this thesis, in which much attention will be devoted to studying the possibility of observing them at the LHC.

3. Effective field theories with a light Higgs

In this chapter we first consider the linear effective Lagrangian (Sec. 3.1), which is constructed adopting the particle content of the SM and, for this reason, is also often called *SM Effective Field Theory* (or SMEFT). We consider this expansion up to the first-order deviations from the SM, namely including operators with mass dimension up to 6. We then move to the non-linear framework, introducing first the so-called Appelquist-Longhitano-Feruglio (ALF) Lagrangian (Sec. 3.2), that was proposed in the 1980s as an effective description of the EW Goldstone bosons, in absence of a Higgs particle. At the leading order, this basically coincides with the EW chiral Lagrangian of Eq. (2.3.73), while the first corrections contain a set of operators with up to four derivatives. The ALF basis is subsequently extended with the insertion of an EW scalar singlet h (Sec. 3.3): the resulting Lagrangian provides the most general description of the EW interactions in presence of a light (Higgs) boson. To stress this property, it is often referred to as *Higgs Effective Field Theory* (HEFT, in contrast with SMEFT). Finally, we close this chapter with a schematic recapitulation of the main differences between the to EFTs (Sec. 3.4) and a comment on the connection between both descriptions (Sec. 3.4.1).

3.1 The linear Lagrangian (SMEFT)

The effective Lagrangian in the linear regime is constructed employing the relevant degrees of freedom and symmetries of the SM. In particular, in this case the Higgs boson is embedded in the Higgs doublet Φ , together with the three Goldstone bosons, that transform linearly under the gauge symmetry $SU(2)_L \times U(1)_Y$. The tower of invariant operators is canonically organized based on their mass dimension: the LO contains renormalizable terms with $d = 4$ and it coincides with the SM Lagrangian \mathcal{L}_{SM} (Eq. (1.1.1)). Higher order effects are instead described by operators with $d \geq 6$, that come suppressed by $(d - 4)$ powers of the cutoff Λ . Explicitly:

$$\mathcal{L}_{\text{linear}} = \mathcal{L}_{\text{SM}} + \Delta\mathcal{L}_{\text{linear}} = \mathcal{L}_{\text{SM}} + \sum_i \frac{f_i}{\Lambda^2} \mathcal{O}_i^{d=6} + \sum_i \frac{f_i}{\Lambda^4} \mathcal{O}_i^{d=8} + \dots \quad (3.1.1)$$

and cutting the expansion at NLO:

$$\Delta\mathcal{L}_{\text{linear}} \equiv \mathcal{L}_{d=6} = \sum_i \frac{f_i}{\Lambda^2} \mathcal{O}_i, \quad (3.1.2)$$

$\mathcal{O}_{GG} = -\frac{g_s^2}{4} \Phi^\dagger \Phi G_{\mu\nu} G^{\mu\nu}$	$\mathcal{O}_{WW} = -\frac{g^2}{4} \Phi^\dagger W_{\mu\nu} W^{\mu\nu} \Phi$
$\mathcal{O}_{BB} = -\frac{g'^2}{4} \Phi^\dagger B_{\mu\nu} B^{\mu\nu} \Phi$	$\mathcal{O}_{BW} = -\frac{gg'}{4} \Phi^\dagger B_{\mu\nu} W^{\mu\nu} \Phi$
$\mathcal{O}_W = \frac{ig}{2} (D_\mu \Phi)^\dagger W^{\mu\nu} (D_\nu \Phi)$	$\mathcal{O}_B = \frac{ig'}{2} (D_\mu \Phi)^\dagger B^{\mu\nu} (D_\nu \Phi)$
$\mathcal{O}_{\Phi 1} = (D_\mu \Phi)^\dagger \Phi \Phi^\dagger (D^\mu \Phi)$	$\mathcal{O}_{\Phi 2} = \frac{1}{2} \partial^\mu (\Phi^\dagger \Phi) \partial_\mu (\Phi^\dagger \Phi)$
$\mathcal{O}_{\Phi 3} = \frac{1}{3} (\Phi^\dagger \Phi)^3$	$\mathcal{O}_{\Phi 4} = (D_\mu \Phi)^\dagger (D^\mu \Phi) (\Phi^\dagger \Phi)$
$\mathcal{O}_{DW} = -\frac{g^2}{2} (D_\mu W_{\nu\rho}^i) (D^\mu W^{i\nu\rho})$	$\mathcal{O}_{DB} = -\frac{g'^2}{2} (\partial_\mu B_{\nu\rho}) (\partial^\mu B^{\nu\rho})$
$\mathcal{O}_{WWW} = -\frac{ig^3}{8} \text{Tr} (W_{\mu\nu} W^{\nu\rho} W_\rho^\mu)$	

Table 3.1: Linear EFT: basis of bosonic operators of dimension 6 that preserve both C and P [95, 96].

where the sum is extended over a non-redundant basis of operators with $d = 6$. The first complete classification of these invariants has been done in Ref. [97]. More recently, Ref. [98] corrected some inaccuracies of that work and proposed another basis of operators, which has been widely used in the literature. It contains a total number of 59 operators, assuming baryon number conservation and up to flavor indices.

An alternative choice, limited to the set of bosonic operators that preserve both C and P , is that of Refs [95, 96] (sometimes called HISZ basis). As this is the basis chosen for the phenomenological comparison worked out in the next chapters, we report it in Table 3.1.

Being based on the linear σ -model description of Sec. 2.2, the linear Lagrangian shares most of the features that were pointed out in that context. In particular, it has an approximate custodial invariance: for instance, in the Higgs sector, the custodial symmetry is violated only by one operator, which in the HISZ basis is identified with $\mathcal{O}_{\Phi,1}$. Another important property is that, in this language, insertions of the GBs are always accompanied by insertions of the physical Higgs h , because of the $SU(2)$ doublet structure. At the same time, the Higgs' couplings must always appear embedded in structures of the form $(v + h)^n$, due to the linear dynamics of the EWSB: here the scale v and the field h are respectively the vev and the residual physical excitation of the same scalar Φ_0 .

3.2 The chiral Lagrangian: Appelquist-Longhitano-Feruglio basis

When considering non-linearly realized EWSB, it is possible to decouple the Higgs particle from the theory and write a Lagrangian that describes only the low-energy interactions of the SM fermions, gauge bosons and Goldstones. As discussed in Sec. 2.3, this can be done constructing a non-linear σ model for the Goldstone bosons, obtaining a chiral Lagrangian:

$$\mathcal{L}_{\text{chiral}} = \mathcal{L}_0 + \Delta\mathcal{L}_{\text{chiral}} \quad (3.2.3)$$

which is organized as expansion in derivatives. At the leading order it reads

$$\begin{aligned} \mathcal{L}_0 = & -\frac{1}{4}W_{\mu\nu}W^{\mu\nu} - \frac{1}{4}B_{\mu\nu}B^{\mu\nu} - \frac{1}{4}G_{\mu\nu}^AG^{A\mu\nu} - \frac{v^2}{4}\text{Tr}[\mathbf{V}_\mu\mathbf{V}^\mu] + \\ & + i\bar{Q}\not{D}Q + i\bar{L}\not{D}L - \frac{v}{\sqrt{2}}[\bar{Q}_L\mathbf{U}\mathcal{Y}_Q Q_R + \bar{L}_L\mathbf{U}\mathcal{Y}_L L_R + \text{h.c.}] + \\ & + \frac{g_s^2}{16\pi^2}\theta G_{\mu\nu}^A\tilde{G}^{A\mu\nu}, \end{aligned} \quad (3.2.4)$$

where we have defined the chiral objects (see Sec. 2.3.2)

$$\mathbf{V}_\mu = D_\mu\mathbf{U}\mathbf{U}^\dagger = (\partial_\mu\mathbf{U})\mathbf{U}^\dagger + ig\frac{W_\mu^i}{2}\tau^i\mathbb{1} - ig'\frac{B_\mu}{2}\mathbf{T} \quad (3.2.5)$$

$$\mathbf{T} = \mathbf{U}\tau^3\mathbf{U}^\dagger \quad (3.2.6)$$

that transform in the adjoint of $SU(2)_L$. It is then immediate to see that the term $\text{Tr}(\mathbf{V}_\mu\mathbf{V}^\mu)$ yields the kinetic terms for the Goldstone bosons and the mass terms for the gauge fields. Moreover, the right-handed fermions have been grouped in $SU(2)_R$ doublets and the Yukawa matrices are therefore defined as

$$\mathcal{Y}_Q = \begin{pmatrix} \mathbf{y}_U & \\ & \mathbf{y}_D \end{pmatrix} \quad \mathcal{Y}_L = \begin{pmatrix} 0 & \\ & \mathbf{y}_E \end{pmatrix}. \quad (3.2.7)$$

Focusing on the bosonic sector, the first order corrections are described by a complete basis of independent operators with up to four derivatives. A customary choice is the so-called Appelquist-Longhitano-Feruglio (ALF) basis, introduced in Refs.[15–19] and reported Table 3.2. With the ALF notation:

$$\Delta\mathcal{L}_{\text{chiral}} = c_W\mathcal{L}_W + c_B\mathcal{L}_B + c_T\mathcal{L}_T + c_C\mathcal{L}_C + \sum_{i=1}^{14} c_i\mathcal{L}_i. \quad (3.2.8)$$

3. Effective field theories with a light Higgs

$\mathcal{L}_B = -\frac{g'^2}{4} B_{\mu\nu} B^{\mu\nu}$	$\mathcal{L}_6 = g^2 [\text{Tr}(\mathbf{T} W_{\mu\nu})]^2$
$\mathcal{L}_W = -\frac{g^2}{4} \text{Tr}(W_{\mu\nu} W^{\mu\nu})$	$\mathcal{L}_7 = ig \text{Tr}(\mathbf{T} W_{\mu\nu}) \text{Tr}(\mathbf{T}[\mathbf{V}^\mu, \mathbf{V}^\nu])$
$\mathcal{L}_T = \frac{v^2}{4} \text{Tr}(\mathbf{T} \mathbf{V}_\mu)^2$	$\mathcal{L}_8 = g \varepsilon^{\mu\nu\rho\sigma} \text{Tr}(\mathbf{T} \mathbf{V}_\mu) \text{Tr}(\mathbf{V}_\nu W_{\rho\sigma})$
$\mathcal{L}_C = -\frac{v^2}{4} \text{Tr}(\mathbf{V}_\mu \mathbf{V}^\mu)$	$\mathcal{L}_9 = \text{Tr}((\mathcal{D}_\mu \mathbf{V}^\mu)^2)$
$\mathcal{L}_1 = g^2 B_{\mu\nu} \text{Tr}(\mathbf{T} W^{\mu\nu})$	$\mathcal{L}_{10} = [\text{Tr}(\mathbf{T} \mathcal{D}_\mu \mathbf{V}^\mu)]^2$
$\mathcal{L}_2 = ig' B_{\mu\nu} \text{Tr}(\mathbf{T}[\mathbf{V}^\mu, \mathbf{V}^\nu])$	$\mathcal{L}_{11} = \text{Tr}([\mathbf{T}, \mathbf{V}_\mu] \mathcal{D}_\nu \mathbf{V}^\nu) \text{Tr}(\mathbf{T} \mathbf{V}^\nu)$
$\mathcal{L}_3 = ig \text{Tr}(W_{\mu\nu}[\mathbf{V}^\mu, \mathbf{V}^\nu])$	$\mathcal{L}_{12} = \text{Tr}(\mathbf{V}_\mu \mathbf{V}^\mu) [\text{Tr}(\mathbf{T} \mathbf{V}_\nu)]^2$
$\mathcal{L}_4 = [\text{Tr}(\mathbf{V}_\mu \mathbf{V}^\mu)]^2$	$\mathcal{L}_{13} = \text{Tr}(\mathbf{V}_\mu \mathbf{V}_\nu) \text{Tr}(\mathbf{T} \mathbf{V}^\mu) \text{Tr}(\mathbf{T} \mathbf{V}^\nu)$
$\mathcal{L}_5 = [\text{Tr}(\mathbf{V}_\mu \mathbf{V}_\nu)]^2$	$\mathcal{L}_{14} = [\text{Tr}(\mathbf{T} \mathbf{V}_\mu) \text{Tr}(\mathbf{T} \mathbf{V}_\nu)]^2$

Table 3.2: Chiral Lagrangian without Higgs scalar: complete basis of independent, CP-even bosonic operators with up to 4 derivatives. This is often referred to as Applegate-Longhitano-Feruglio (ALF) basis.

Unlike in the linear case, this Lagrangian contains several sources of custodial violation, which are easily recognized from the presence of the spurion \mathbf{T} . Depending on whether the latter is accompanied by the field B_μ or not, the breaking can be identified as having a SM-like origin or rather an external one: the custodial-violating terms of the first type are removed in the limit $g' \rightarrow 0$, while the others are retained. Unless specified, the attribute “custodial violating” will be implicitly referred to BSM custodial-breaking effects in what follows.

3.3 The chiral Lagrangian with a light Higgs (HEFT)

The ALF chiral Lagrangian presented in the previous section can be easily extended to account for the presence of a light scalar in the spectrum, namely the Higgs boson: the first attempts were made in Refs. [23, 24, 99]. In analogy with the procedure followed in Sec. 2.3.3, the physical Higgs h can be introduced as a gauge singlet: this choice is very general, as the resulting parameterization can indeed be used to describe a wide range of scenarios, including those in which the h field is embedded in a doublet or in another more exotic isospin representation, and even dilaton-like models. The chiral Lagrangian with a light Higgs is often referred to as Higgs EFT (HEFT) Lagrangian, to distinguish it from the linear one, called with the acronym SMEFT.

The dependence on the physical Higgs can then be expressed by generic functions [25]

$$\mathcal{F}_i(h) = 1 + 2a_i \frac{h}{v} + b_i \frac{h^2}{v^2} + \dots \quad (3.3.9)$$

which replace the polynomial dependence in $(1 + h/v)^n$ that characterizes the linear expansion. Notice that the h insertions are weighted by powers of v rather than of the cutoff Λ : in this sense, the Higgs field h is treated similarly to the Goldstone bosons, with the adimensional $\mathcal{F}(h)$ representing the counterpart of the \mathbf{U} matrix.

The Leading Order Lagrangian of Eq. (3.2.4) is consequently modified into

$$\begin{aligned} \mathcal{L}_0 = & -\frac{1}{4}W_{\mu\nu}^a W^{a\mu\nu} - \frac{1}{4}B_{\mu\nu}B^{\mu\nu} - \frac{1}{4}G_{\mu\nu}^A G^{A\mu\nu} - \frac{v^2}{4}\text{Tr}[\mathbf{V}_\mu \mathbf{V}^\mu]\mathcal{F}_C(h) + \\ & + i\bar{Q}\not{D}Q + i\bar{L}\not{D}L - \frac{v}{\sqrt{2}}(\bar{Q}_L \mathbf{U} \mathcal{Y}_Q(h) Q_R + \text{h.c.}) - \frac{v}{\sqrt{2}}(\bar{L}_L \mathbf{U} \mathcal{Y}_L(h) L_R + \text{h.c.}) + \\ & + \frac{1}{2}\partial_\mu h \partial^\mu h - V(h) + \frac{g_s^2}{16\pi^2} \theta G_{\mu\nu}^A \tilde{G}^{A\mu\nu}. \end{aligned} \quad (3.3.10)$$

Besides the appearance of a kinetic term and of a scalar potential for the h particle, the main change w.r.t Eq. (3.2.4) is the insertion of the function $\mathcal{F}_C(h)$, with the structure indicated in (3.3.9), and the promotion of the Yukawa matrices to h -dependent functionals: here

$$\mathcal{Y}_Q(h) = \text{diag} \left(\sum_n Y_U^{(n)} \frac{h^n}{v^n}, \sum_n Y_D^{(n)} \frac{h^n}{v^n} \right) \quad \mathcal{Y}_L(h) = \text{diag} \left(0, \sum_n Y_E^{(n)} \frac{h^n}{v^n} \right) \quad (3.3.11)$$

where the first terms $Y_\psi^{(0)} \equiv \mathbf{y}_\psi$ coincide with the SM Yukawas, while the higher orders describe the interaction with n insertions of the Higgs field, accounting in general for non-aligned contributions. Notice that none of the kinetic terms, besides the Goldstone bosons' one, has been multiplied by a $\mathcal{F}(h)$, although this would be allowed both by the gauge symmetry and by the adimensionality of the $\mathcal{F}(h)$ structure. The reason is the following: for the Higgs' and fermions' kinetic terms, the addition of extra h couplings is redundant, as it can be removed via a field redefinition and reabsorbed within the other arbitrary $\mathcal{F}(h)$ functions appearing in the Lagrangian. For the gauge bosons, the kinetic terms involve only the transverse components, that are assumed not to couple with the EWSB sector at LO. Indeed, operators with the structure $X_{\mu\nu} X^{\mu\nu} \mathcal{F}(h)$ are listed among the NLO terms (further details can be found in Chapter 7).

The Lagrangian \mathcal{L}_0 in Eq. (3.3.10) is totally equivalent to that of the Standard Model (Eq. (1.1.1)) in the limit

$$\mathcal{F}_C(h) \equiv (1 + h/v)^2, \quad \mathcal{Y}_\psi(h) \equiv \mathbf{y}_\psi(1 + h/v), \quad V(h) \equiv \frac{m_h^2}{2}h^2 + \frac{\lambda v}{4}h^3 + \frac{\lambda}{16}h^4. \quad (3.3.12)$$

The NLO Lagrangian contains a non-redundant basis of operators constructed with the same building blocks as those for the ALF Lagrangian, plus the adimensional structures $\mathcal{F}_i(h)$ and its derivatives. It is not so obvious, though, to establish where the boundary between NLO and NNLO lies exactly, *i.e.* to give a unique definition of the power counting for this EFT¹¹: this issue is currently object of debate in the literature [100–103]. The main source of confusion is the fact that the HEFT Lagrangian is de facto a merging of a non-linear σ -model for the scalar sector, that follows a derivative expansion, with a traditional, SM-like description for fermions and longitudinal gauge bosons, whose interactions are in principle organized according to their canonical dimension. This superposition spoils, for instance, the equivalence between derivative expansion and renormalization ordering that holds in pure chiral perturbation theory: while in the latter case the one-loop amplitudes constructed with two-derivative (LO) terms must be reabsorbed by four-derivative (NLO) operators, in the linear theory loop structures containing $d = 6$ operators give contributions at the same level ($d = 6$) in the expansion. The two countings, in derivatives and in canonical dimension, operate simultaneously in the EW chiral Lagrangian, and it is not possible to select either of the two as the dominating rationale, since this would lead to severe inconsistencies in at least one sector of the theory. On the other hand, comparing suppressions determined with two different criteria may become quite a delicate task.

Historically, the first attempt of constructing a unified counting rule was done in the 1980s, with the formulation of the Naive Dimensional Analysis (NDA) prescription [79], which is still the most widely used

¹¹ The power counting issue also affects the ALF chiral Lagrangian, that does not contain the Higgs field. We have deferred the topic to this section because its discussion is particularly relevant (and timely) in this context.

3. Effective field theories with a light Higgs

in the literature. The original version was subsequently generalized in [104] with the inclusion of weights for the coupling constants. In this latter version, the overall coefficient of a generic interaction with D derivatives, A gauge fields, F fermion insertions and S scalar fields, accompanied by N_g gauge coupling constants and N_y Yukawas, is estimated by the formula [103]

$$\frac{\Lambda^4}{16\pi^2} \left(\frac{p}{\Lambda}\right)^D \left(\frac{4\pi A_\mu}{\Lambda}\right)^A \left(\frac{4\pi\psi}{\Lambda^{3/2}}\right)^F \left(\frac{4\pi\phi}{\Lambda}\right)^S \left(\frac{g}{4\pi}\right)^{N_g} \left(\frac{y}{4\pi}\right)^{N_y}. \quad (3.3.13)$$

In the HEFT case, $\psi = \{Q, L\}$, $\phi = \{h, \pi^i\}$, $A_\mu = \{W_\mu^i, B_\mu\}$ and $g = \{g, g'\}$. It is easy to see that, for example, chiral operators with four derivatives, such as $\text{Tr}(\mathbf{V}_\mu \mathbf{V}^\mu)^2$, that are NLO in the purely chiral expansion, are assigned a NDA suppression $1/(4\pi)^2$ (notice that it coincides with the loop factor). On the other hand, four-fermion operators, that are NLO in the linear tower, come with a factor $(4\pi)^2/\Lambda^2$. Intuitively, both categories must belong to the NLO of the HEFT Lagrangian, although *a priori* the relative importance of their impact depends on Λ .

On practical grounds, the HEFT Lagrangian at NLO can be identified based on the following (intuitive) principles:

- the bosonic sector must include all the operators with up to four derivatives, that are required by the renormalization procedure of the LO chiral Lagrangian. A complete, non-redundant set of pure-gauge and gauge-Higgs interactions has been first proposed in Refs. [25, 105], where new physics effects in the fermionic sector were totally neglected. We do not report it here, as an equivalent basis is listed in Eqs (2.6)-(2.11) of Chapter 4.
- The fermionic sector must include at least four-fermion operators and dipole operators: these are naturally NLO in the dimensional counting that befits the fermionic fields, and encode interactions that receive one-loop contributions from \mathcal{L}_0 . Only a subset of these structures are required to reabsorb divergences, while others correspond to finite loops. However, generalizing, it is natural to assume that all the bilinears with up to two derivatives should belong to the basis.
- Redundancies across the two sectors can be eventually removed applying the Equations of Motion (EOMs) derived from the LO Lagrangian, that can be found in Appendix D of the publication in Chapter 7.

More details about the construction of the complete HEFT Lagrangian at NLO is provided in Chap. 7, where a non-redundant basis is also proposed. The latter contains 148 operators up to flavor indices. It should be stressed that, despite the ambivalence of the double expansion, the commonsense criteria indicated above allow for a safe and self-consistent identification of most of the operators that compose the NLO effective basis. Nonetheless, a limited number of invariants is affected by some residual ambiguities in the power counting. This is the source of a discrepancy between the bosonic bases presented in Chapters 4 and 7, that concerns operators with the structure $A_{\mu\nu} A^{\nu\rho} A_\rho^\mu$. According to the derivative expansion, in fact, these terms should represent NNLO effects. However, it may be argued that these interactions are unrelated to the strong EWSB sector, as they only involve transverse components of the gauge bosons. As such, they should rather follow a tower in canonical dimensions, which classifies them as NLO terms. The former option was chosen in the publication of Chap. 4, while the latter, which is somehow more conservative, was picked in Chap. 7. Neither of the two possibilities is clearly more rigorous than the other and indeed the NDA formula assigns to these invariants a weight $4\pi/\Lambda^2$, which in general is not smaller than that of four-fermion or four-derivative operators.

3.4 Linear *vs.* non-linear in a nutshell

We conclude this chapter with a compendium of the disparities between the linear and the non-linear effective Lagrangians, that is meant to be a handy reference for the works presented in the next pages. In Sec. 3.4.1 we briefly analyze the correspondence between the two EFTs, highlighting the role of the parameter $\xi = v^2/f^2$.

Higgs couplings

In the linear EFT, the Higgs couplings follow a polynomial dependence in $(v+h)^n$, determined by the $SU(2)$ doublet structure in which the h field is embedded. In the non-linear EFT, they are encoded in totally arbitrary functionals $\mathcal{F}(h)$. This marks a fundamental and intrinsic difference in the structure of the two theories, that has been recently interpreted in terms of the curvature of the manifold formed by the four scalar fields (the Higgs and the 3 GBs) [106].

Power counting

While the SMEFT (linear) Lagrangian is organized as an expansion in canonical mass dimensions, the HEFT (non-linear) Lagrangian is more complex. In particular, the Goldstone bosons' sector follows an expansion in derivatives, typical of the chiral expansion. Moreover, the physical Higgs h and the Goldstone bosons' matrix \mathbf{U} are independent objects in this framework. This causes a re-shuffling, compared to the linear setup, of the orders at which given interactions appear in the expansion. In particular, insertions of longitudinal gauge bosons are less suppressed in the chiral construction.

Number of invariants

All in all, the non-linear Lagrangian is more restrictive than the linear one, as it imposes less constraints on the scalar fields. As a result, it contains a larger number of parameters at any given order: the complete HEFT basis at NLO contains 148 independent operators [31], to be compared with the 59 of the SMEFT basis [98] (up to flavor indices in both cases).

Custodial symmetry

The SMEFT construction, based on a linear σ -model, shows an approximate custodial symmetry up to the NLO: in the Higgs sector, this invariance is broken only by one operator, $\mathcal{O}_{\Phi,1}$ in the basis of Tab. 3.1. By contrast, in the HEFT framework there is room for more custodial breaking effects, both of SM and BSM origin: the purely bosonic basis at the four-derivatives level contains 16 sources of custodial violation that survive even in the limit of massless fermions and $g' \rightarrow 0$ (see Sec. 2 of Chapter 4).

Physical scales involved

Only two explicit scales appear in the linear expansion: the electroweak vev v , defined by the mass of the W and Z gauge bosons, and the cutoff Λ . Strictly speaking, these are the only ones that have a well-defined physical meaning in the effective description. Nonetheless, in the non-linear scenario it makes sense to introduce explicitly another quantity: the characteristic scale f of the scalar fields, interpreted as Goldstone bosons of a larger symmetry breaking¹². This scale must satisfy the constraint $\Lambda \leq 4\pi f$ and in general it is $f \neq v$. Keeping the latter distinction, is tantamount to introducing a fine-tuning parameter in the effective Lagrangian, which is usually denoted by $\xi = v^2/f^2$. This quantity is reminiscent of the vacuum misalignment parameter that characterizes composite Higgs models (see Sec. 2.4) and it can be employed for keeping track of the correspondence between the linear and the non-linear expansions, as explained below.

¹² In complete generality, one may introduce different characteristic scales for the EW Goldstones and for the Higgs field: $f_\pi \neq f_h$. We do not consider this kind of scenario here, both for simplicity and because the condition $f_\pi = f_h = f$ is indeed fulfilled in most of the BSM theories we are interested in, such as composite Higgs models.

3. Effective field theories with a light Higgs

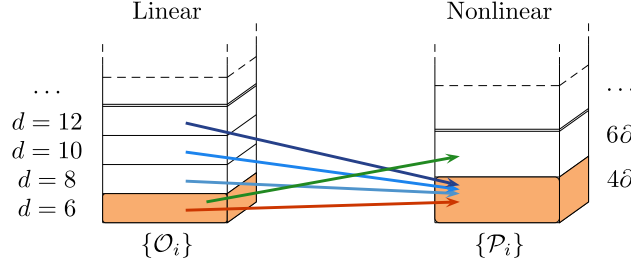


Figure 3.1: Schematic representation of the correspondence between the linear and non-linear EFTs. In both towers, the first order deviations from the SM are highlighted in color.

3.4.1 Matching between both EFTs

A correspondence between the two expansions can be defined as follows: every linear operator is uniquely associated to a particular combination of non-linear operators, that is easily identified with the replacement

$$\Phi \rightarrow \frac{v+h}{\sqrt{2}} \mathbf{U} \begin{pmatrix} 0 \\ 1 \end{pmatrix}. \quad (3.4.14)$$

Inverting this relation, each non-linear operator is associated to a *linear sibling* defined as the linear operator of the lowest possible dimension that contains its interactions. The sibling is not unique in general. As an example, for the operator \mathcal{O}_B of Table 3.1 one finds

$$\mathcal{O}_B = \frac{ig'}{2} D_\mu \Phi^\dagger B^{\mu\nu} D_\nu \Phi \rightarrow \frac{ig' B^{\mu\nu}}{4} \left(\text{Tr}(\mathbf{T}[\mathbf{V}_\mu, \mathbf{V}_\nu]) \frac{(v+h)^2}{2} + \text{Tr}(\mathbf{T}\mathbf{V}_\mu) \partial_\nu (v+h)^2 \right) \quad (3.4.15)$$

which, in the notation of Chapter 4, reads

$$\mathcal{O}_B \rightarrow \frac{v^2}{8} (\mathcal{P}_2 + 2\mathcal{P}_4) \Big|_{\mathcal{F}_2(h)=\mathcal{F}_4(h)\equiv(v+h)^2}. \quad (3.4.16)$$

Being the lowest dimensional operator that contains their interactions, \mathcal{O}_B is the *sibling* of both \mathcal{P}_2 and \mathcal{P}_4 . It is clear from this example that the correspondence between the two expansions is far from being bi-univocal at a given order: on the contrary, it looks rather intricate as indicated, schematically, in figure 3.1. Two effects are worth being underlined: i) the chiral EFT contains a larger number of invariants at any given order and ii) the correspondence defined above connects in general operators that belong to different orders in both expansions. As detailed in Chapter 4, these two facts are the key for identifying distinctive signals that may allow to disentangle the two scenarios experimentally. In particular, point i) translates into the presence of signals that are predicted to be correlated in the linear case but uncorrelated in general in the non-linear one. The example above already shows this feature: the couplings contained in the operators \mathcal{P}_2 and \mathcal{P}_4 are independent in the nonlinear parameterization, while in the linear setup they are described by the same object. On the other hand, point ii) implies that some effects are expected to be highly suppressed in one scenario but not necessarily in the other. An example are the C and P odd (but CP even) couplings of the operator \mathcal{P}_{14} , whose analysis is presented in Chapter 4.

The role of the ξ parameter in the HEFT

As shown in Sec. 2.4, realistic composite Higgs models typically require the Goldstone bosons' characteristic scale f to be well-separated from the EW scale v , defined by the masses of the EW gauge bosons. This is related to the fact that the spontaneous symmetry breaking takes place in two distinct stages, or, in other

words, that the vacuum of the first global breaking $\mathcal{G} \rightarrow \mathcal{H}$ is not aligned with the EW one. The parameter $\xi = v^2/f^2 \in [0, 1]$ quantifies such misalignment.

Intuitively, the limit $\xi \rightarrow 1$ ($f \rightarrow v$) represents the Technicolor limit, in which the gap between the two breakings is practically lifted. On the other hand, in the limit $\xi \ll 1$ ($v \ll f$), the strong sector can be decoupled and one recovers the weakly-interacting picture. In this sense, ξ can also be interpreted as a measure of the “non-linearity” of the EWSB dynamics. Based on this consideration, it is natural to expect ξ to appear in the HEFT Lagrangian that describes the low-energy effects of a concrete composite Higgs model. Moreover, the dependence on this parameter must be such that in the regime $\xi \ll 1$ the chiral series somehow aligns itself with the linear expansion. In practice, in this case ξ becomes an expansion parameter, and the hierarchy it induces among the effective interactions reproduces that determined by canonical dimensions.

This has been computed explicitly in the publication contained in Chapter 6, focusing on the bosonic sector, for three different composite Higgs models: the results obtained show that in all these frameworks the parameter ξ naturally appears both as an overall weight in front of each HEFT operator, and inside the functionals $\mathcal{F}(h)$ that encode the dependence on the physical Higgs. Although the exact numerical dependence varies depending on the chosen model, a universal feature is that chiral operators whose linear sibling have dimension d always appear weighted by a global factor $\xi^{(d-4)/2}$. At the same time, the form of the functionals $\mathcal{F}(h)$ is such that, at first order in ξ , it coincides with $(v+h)$ to some power n . As a result, the leading low-energy effects of a composite Higgs model are generally described by the non-linear Higgs EFT (with specific constraints imposed on the Wilson coefficients), but in the limit $\xi \ll 1$ one recovers the structure of the linear EFT.

It is worth stressing that, at the purely effective level, the parameter ξ is not physical, as it can always be reabsorbed within the Wilson coefficients. Nonetheless, it can be useful for keeping track of the correspondence with the linear expansion: in Chapter 4, the ξ weights of the chiral operators were assigned “by hand”, based on the dimensionality of the associated linear sibling. The results are however consistent with those derived in Chapter 6.

Disentangling a dynamical Higgs

This Chapter contains the publication in Ref. [28]. The main purpose of this work is the identification of a set of observables that may allow to discriminate between scenarios with linearly and non-linearly realized EWSB. The study is restricted to CP-even effects in the bosonic sector: the starting point is the complete basis of non-linear operators with up to four derivatives previously constructed in Ref. [25] and reported in Sec. 2 of this chapter. The set considered gives the most general description of first-order deviations from the Standard Model in a context of non-linear EWSB; its linear counterpart is a complete basis of bosonic operators of canonical dimension $d = 6$. As a reference, we chose the HISZ basis [95, 96]. The choice of neglecting the impact of new physics on the fermionic sector allows for a simpler analysis without weakening the results obtained. Indeed, the signatures identified in this context showcase all the salient phenomenological differences between the two EFT descriptions.

A theoretical comparison between the linear and the non-linear expansions is worked out in detail in Sec. 3. A correspondence between the two bases is established as follows: the leading effects of each linear operator are equivalent to those of a specific linear combination of chiral operators, with fixed $\mathcal{F}(h)$ functions, which is easily identified replacing Φ with $(v + h)/\sqrt{2} \mathbf{U}(1)$. Inverting this relation, we define the *sibling* of a non-linear operator as the linear invariant of the lowest possible dimension that contains its interactions. Not all the chiral operators have siblings at $d = 6$: to help tracking down the correspondence, the chiral operators are written multiplied with a power of $\xi = v^2/f^2$. A factor ξ^n indicates a sibling with $d = 2n + 4$.

The phenomenological study is contained in Sec. 4 of this chapter. A global fit is performed on a subset of relevant Wilson coefficients, employing electroweak precision data as well as the Higgs data available at the end of 2013. The most important result is the identification of a few sample observables that may serve as discriminators between the two EWSB realizations, once a greater accuracy in Higgs measurements will be achieved. There are two main sources of discriminating signatures: one is the presence of couplings that must be correlated in the linear case but are described by a larger set of parameters in the nonlinear setup. A promising example is that of triple gauge vertices (TGV) *vs.* couplings of the Higgs to two gauge bosons, illustrated in Fig. 2. Another type of signals originates from the mismatch in the tower of the operators: signals that are produced at the four-derivative level in the chiral expansion but only at $d > 6$ in the linear one may serve as smoking guns for the presence of non-linearity. An example is the anomalous TGV generated by \mathcal{P}_{14} , that has its linear sibling only at $d = 8$, whose impact has been analyzed in Sec. 4.3 of this chapter.

Disentangling a dynamical Higgs

**I. Brivio,^a T. Corbett,^b O.J.P. Éboli,^c M.B. Gavela,^a J. Gonzalez-Fraile,^d
M.C. Gonzalez-Garcia,^{e,d,b} L. Merlo^a and S. Rigolin^f**

^a*Departamento de Física Teórica and Instituto de Física Teórica, IFT-UAM/CSIC,
Universidad Autónoma de Madrid, Cantoblanco, 28049, Madrid, Spain*

^b*C.N. Yang Institute for Theoretical Physics and Department of Physics and Astronomy,
SUNY at Stony Brook, Stony Brook, NY 11794-3840, U.S.A.*

^c*Instituto de Física, Universidade de São Paulo,
C.P. 66318, 05315-970, São Paulo SP, Brazil*

^d*Departament d'Estructura i Constituents de la Matèria and ICC-UB, Universitat de Barcelona,
647 Diagonal, E-08028 Barcelona, Spain*

^e*Institució Catalana de Recerca i Estudis Avançats (ICREA),
Passeig Lluís Companys, 23, E-08010 Barcelona, Spain*

^f*Dipartimento di Fisica e Astronomia "G. Galilei", Università di Padova and
INFN, Sezione di Padova, Via Marzolo 8, I-35131 Padua, Italy*

E-mail: ilaria.brivio@uam.es, corbett.ts@gmail.com,
eboli@fma.if.usp.br, belen.gavela@uam.es, fraile@ecm.ub.edu,
concha@insti.physics.sunysb.edu, luca.merlo@uam.es,
stefano.rigolin@pd.infn.it

ABSTRACT: The pattern of deviations from Standard Model predictions and couplings is different for theories of new physics based on a non-linear realization of the $SU(2)_L \times U(1)_Y$ gauge symmetry breaking and those assuming a linear realization. We clarify this issue in a model-independent way via its effective Lagrangian formulation in the presence of a light Higgs particle, up to first order in the expansions: dimension-six operators for the linear expansion and four derivatives for the non-linear one. Complete sets of gauge and gauge-Higgs operators are considered, implementing the renormalization procedure and deriving the Feynman rules for the non-linear expansion. We establish the theoretical relation and the differences in physics impact between the two expansions. Promising discriminating signals include the decorrelation in the non-linear case of signals correlated in the linear one: some pure gauge versus gauge-Higgs couplings and also between couplings with the same number of Higgs legs. Furthermore, anomalous signals expected at first order in the non-linear realization may appear only at higher orders of the linear one, and vice versa. We analyze in detail the impact of both type of discriminating signals on LHC physics.

KEYWORDS: Higgs Physics, Chiral Lagrangians, Technicolor and Composite Models

ARXIV EPRINT: [1311.1823](https://arxiv.org/abs/1311.1823)

Contents

1	Introduction	1
2	The effective Lagrangian	5
3	Comparison with the linear regime	10
3.1	The effective Lagrangian in the linear regime	11
3.2	Decorrelation of signals with respect to the linear analysis	13
3.3	Signals specific to the linear expansion	15
3.4	New signals specific to the non-linear expansion	15
4	Phenomenology	16
4.1	Renormalization procedure	16
4.2	Present bounds on operators weighted by ξ	24
4.3	ξ^2 -weighted couplings: LHC potential to study g_5^Z	29
4.4	Anomalous quartic couplings	33
5	Conclusions	34
A	EOM and fermion operators	36
B	Equivalence of the $d = 6$ basis with the SILH Lagrangian	41
C	Relations between chiral and linear operators	42
D	Feynman rules	43

1 Introduction

The present ensemble of data does not show evidence for new exotic resonances and points to a scenario compatible with the Standard Model (SM) scalar boson (so-called “Higgs” for short) [1–3]. Either the SM is all there is even at energies well above the TeV scale, which would raise a number of questions about its theoretical consistency (electroweak hierarchy problem, triviality, stability), or new physics (NP) should still be expected around or not far from the TeV scale.

This putative NP could be either detected directly or studied indirectly, analysing the modifications of the SM couplings. To this aim, a rather model-independent approach is that of Lorentz and gauge-invariant effective Lagrangians, which respect a given set of symmetries including the low-energy established ones. These effective Lagrangians respect

symmetries in addition to $U(1)_{\text{em}}$ and Lorentz invariance and as a consequence they relate and constrain phenomenological couplings [4] based only on the latter symmetries.

With a light Higgs observed, two main classes of effective Lagrangians are pertinent, depending on how the electroweak (EW) symmetry breaking is assumed to be realized: linearly for elementary Higgs particles or non-linearly for “dynamical” -composite- ones. It is important to find signals which discriminate among those two categories and this will be one of the main focuses of this paper.

In elementary Higgs scenarios, the effective Lagrangian provides a basis for all possible Lorentz and $SU(3)_c \times SU(2)_L \times U(1)_Y$ gauge invariant operators built out of SM fields. The latter set includes a Higgs particle belonging to an $SU(2)_L$ doublet, and the operators are weighted by inverse powers of the unknown high-energy scale Λ characteristic of NP: the leading corrections to the SM Lagrangian have then canonical mass dimension (d) six [5, 6]. Many studies of the effective Lagrangian for the linear expansion have been carried out over the years, including its effects on Higgs production and decay [7, 8], with a revival of activity [9, 10] after the Higgs discovery [11, 12] (see also refs. [13–40] for studies of Higgs couplings in alternative and related frameworks). Supersymmetric models are a typical example of the possible underlying physics.

In dynamical Higgs scenarios, the Higgs particle is instead a composite field which happens to be a pseudo-goldstone boson (GB) of a global symmetry exact at scales Λ_s , corresponding to the masses of the lightest strong resonances. The Higgs mass is protected by the global symmetry, thus avoiding the electroweak hierarchy problem. Explicit realizations include the revived and now popular models usually dubbed “composite Higgs” scenarios [41–50], for various strong groups and symmetry breaking patterns.¹ To the extent that the light Higgs particle has a goldstone boson parenthood, the effective Lagrangian is non-linear [53] or “chiral”: a derivative expansion as befits goldstone boson dynamics. The explicit breaking of the strong group -necessary to allow a non-zero Higgs mass- introduces chiral-symmetry breaking terms. In this scenario, the characteristic scale f of the Goldstone bosons arising from the spontaneous breaking of the global symmetry at the scale Λ_s is different² from both the EW scale v defined by the EW gauge boson mass, e.g. the W mass $m_W = gv/2$, and the EW symmetry breaking (EWSB) scale $\langle h \rangle$, and respects $\Lambda_s < 4\pi f$. A model-dependent function g links the three scales, $v = g(f, \langle h \rangle)$, and a parameter measuring the degree of non-linearity of the Higgs dynamics is usually introduced:

$$\xi \equiv (v/f)^2. \quad (1.1)$$

The corresponding effective low-energy chiral Lagrangian is entirely written in terms of the SM fermions and gauge bosons and of the physical Higgs h . The longitudinal degrees of freedom of the EW gauge bosons can be effectively described at low energies by

¹Also “little Higgs” [51] (see ref. [52] for a review) models and some higher-dimensional scenarios can be cast in the category of constructions in which the Higgs is a goldstone boson.

²In the historical and simplest formulations of “technicolor” [54–56], the Higgs particle was completely removed from the low-energy spectrum, which only retained the three SM would-be-Goldstone bosons with a characteristic scale $f = v$.

a dimensionless unitary matrix transforming as a bi-doublet of the global symmetry:

$$\mathbf{U}(x) = e^{i\sigma_a \pi^a(x)/v}, \quad \mathbf{U}(x) \rightarrow L \mathbf{U}(x) R^\dagger, \quad (1.2)$$

where here the scale associated with the eaten GBs is v , and not f , in order to provide canonically normalized kinetic terms, and L, R denotes $SU(2)_{L,R}$ global transformations, respectively. Because of EWSB, the $SU(2)_{L,R}$ symmetries are broken down to the diagonal $SU(2)_C$, which in turn is explicitly broken by the gauged $U(1)_Y$ and by the heterogeneity of the fermion masses. On the other hand, while insertions of the Higgs particle are weighted down as h/f , as explained above, its couplings are now (model-dependent) general functions. In all generality, the $SU(2)_L$ structure is absent in them and, as often pointed out (e.g. refs. [57, 58]), the resulting effective Lagrangian can describe many setups including that for a light SM singlet isoscalar.

To our knowledge, the first attempts to formulate a non-linear effective Lagrangian in the presence of a “non standard/singlet light Higgs boson” go back to the 90’s [59, 60], and later works [57, 61]. More recently, ref. [62] introduced a relevant set of operators, while ref. [63] derived a complete effective Lagrangian basis for pure gauge and gauge- h operators up to four derivatives. Later on, ref. [64] added the pure Higgs operator in ref. [65] as well as fermionic couplings, proposing a complete basis for all SM fields up to four derivatives, and trading some of the operators in ref. [63] by fermionic ones.³

The effective linear and chiral Lagrangians with a light Higgs particle h are intrinsically different, in particular from the point of view of the transformation properties under the $SU(2)_L$ symmetry. There is not a one-to-one correspondence of the leading corrections of both expansions, and one expansion is not the limit of the other unless specific constraints are imposed by hand -as illustrated below- or follow from particular dynamics at high energies [68]. In the linear expansion, the physical Higgs h participates in the scalar $SU(2)_L$ doublet Φ ; having canonical mass dimension one, this field appears weighted by powers of the cut-off Λ in any non-renormalizable operator and, moreover, its presence in the Lagrangian must necessarily respect a pattern in powers of $(v + h)$. In the non-linear Lagrangian instead, the behaviour of the h particle does not abide any more to that of an $SU(2)_L$ doublet but h appears as a SM singlet. Less symmetry constraints means more possible invariant operators [69–71] at a given order, and in summary:

- In the non-linear realization, the chiral-symmetry breaking interactions of h are now generic/arbitrary functions $\mathcal{F}(h)$.
- Furthermore, a relative reshuffling of the order at which couplings appear in each expansion takes place [63, 72, 73]. As a consequence, a higher number of independent (uncorrelated) couplings are present in the leading corrections for a non-linear Lagrangian.

³The inferred criticisms in ref. [64] to the results in ref. [63] about missing and redundant operators are incorrect: ref. [63] concentrated by definition in pure gauge and gauge- h couplings and those criticized as “missing” are not in this category; a similar comment applies to the redundancy issue, explained by the choice mentioned above of trading some gauge operators by fermionic ones in ref. [64]. Finally, the ξ weights and the truncations defined for the first time in ref. [63] lead to rules for operator weights consistent with those defined long ago in the Georgi-Manohar counting [66], and more recently in ref. [67].

Both effects increase the relative freedom of the purely phenomenological Lorentz and $U(1)_{\text{em}}$ couplings required at a given order of the expansion, with respect to the linear analysis. Decorrelations induced by the first point have been recently stressed in ref. [74] (analysing form factors for Higgs decays), while those resulting from the second point above lead to further discriminating signals and should be taken into account as well. Both types of effects will be explored below.

In what respects the analysis of present LHC and electroweak data, a first step in the direction of using a non-linear realization was the substitution of the functional dependence on $(v + h)$ for a doublet Higgs in the linear expansion by a generic function $\mathcal{F}(h)$ for a generic SM scalar singlet h , mentioned in the first point above. This has already led to a rich phenomenology [26, 62, 74, 75]. Nevertheless, the scope of the decorrelations that a generic $\mathcal{F}(h)$ induces between the pure gauge and the gauge- h part of a given operator is limited: whenever data set a strong constraint on the pure gauge part of the coupling, that is on the global operator coefficient, this constraint also affects the gauge- h part as it is also proportional to the global coefficient; only in appealing to strong and, in general, unnatural fine-tunings of the constants inside $\mathcal{F}(h)$ could that constraint be overcome.

As for the second consequence mentioned above, the point is that if higher orders in both expansions are considered, all possible Lorentz and $U(1)_{\text{em}}$ couplings would appear in both towers (as it is easily seen in the unitary gauge), but not necessarily at the same leading or sub-leading order. One technical key to understand this difference is the adimensionality of the field $U(x)$. The induced tower of the leading low-energy operators is different for the linear and chiral regimes, a fact illustrated recently for the pure gauge and gauge- h effective non-linear Lagrangian [63, 72, 73]. More recently, and conversely, an example was pointed out [64] of a $d = 6$ operator of the linear expansion whose equivalent coupling does not appear among the leading derivative corrections in the non-linear expansion.

It will be shown below that, due to that reshuffling of the order at which certain leading corrections appear, correlations that are expected as leading corrections in one case may not hold in the other, unless specific constraints are imposed by hand or follow from high energy dynamics. Moreover, interactions that are strongly suppressed (subleading) in one regime may be leading order in the other.

In this paper we will first consider the basis of CP-even bosonic operators for the general non-linear effective Lagrangian and analyse in detail its complete and independent set of pure gauge and gauge-Higgs operators, implementing the tree-level renormalization procedure and deriving the corresponding Feynman rules. The similarities and differences with the couplings obtained in the linear regime will be carefully determined, considering in particular the Hagiwara-Ishihara-Szalapski-Zeppenfeld (HISZ) basis [76, 77]. Nevertheless, the physical results are checked to be independent of the specific linear basis used, as they should be. The comparison of the effects in both realizations will be performed in the context of complete bases of gauge and/or Higgs boson operators: all possible independent (and thus non-redundant) such operators will be contemplated for each expansion, and compared. For each non-linear operator we will identify linear ones which lead to the same gauge couplings, and it will be shown that up to $d = 12$ linear operators would be required to cover all the non-linear operators with at most four derivatives. We will then identify

some of the most promising signals to discriminate experimentally among both expansions in hypothetical departures from the size and Lorentz structure of couplings predicted by the SM. This task is facilitated by the partial use of results obtained earlier on the physics impact of the linear regime on LHC physics from $d = 6$ operators in refs. [9, 10, 78], and from previous analysis of 4-point phenomenological couplings carried out in refs. [79–83]. In this paper we concentrate on the tree-level effects of operators, as a necessary first step before loop effects are considered [84].

The structure of the paper can be easily inferred from the table of Contents.

2 The effective Lagrangian

We describe below the effective Lagrangian for a light dynamical Higgs [63] (see also ref. [64]), restricted to the bosonic operators, except for the Yukawa-like interactions, up to operators with four derivatives.⁴ Furthermore, only CP-even operators will be taken into account, under the assumption that h is a CP-even scalar.

The most up-to-date analysis to the Higgs results have established that the couplings of h to the gauge bosons and the absolute value of the couplings to fermions are compatible with the SM ones. On the contrary, the sign of the couplings between h and fermions is still to be measured, even if a slight preference for a positive value is indicated in some two parameter fits (see for example [16, 17, 26]) which take into account one-loop induced EW corrections. It is then justified to write the effective Lagrangian as a term \mathcal{L}_0 , which is in fact the SM Lagrangian except for the mentioned sign (would the latter be confirmed positive, \mathcal{L}_0 should be exactly identified with the SM Lagrangian $\mathcal{L}_0 = \mathcal{L}_{SM}$), and to consider as corrections the possible departures from it due to the unknown high-energy strong dynamics:

$$\mathcal{L}_{\text{chiral}} = \mathcal{L}_0 + \Delta\mathcal{L}. \quad (2.1)$$

This description is data-driven and, while being a consistent chiral expansion up to four derivatives, the particular division in eq. (2.1) does not match that in number of derivatives, usually adopted by chiral Lagrangian practitioners. For instance, the usual custodial breaking term $\text{Tr}(\mathbf{T}\mathbf{V}_\mu)\text{Tr}(\mathbf{T}\mathbf{V}^\mu)$ is a two derivative operator and is often listed among the leading order set in the chiral expansion; however, it is not present in the SM at tree level and thus here it belongs to $\Delta\mathcal{L}$ by definition. Moreover, data strongly constrain its coefficient so that it can be always considered [58] a subleading operator.

The first term in $\mathcal{L}_{\text{chiral}}$ reads then

$$\begin{aligned} \mathcal{L}_0 = & \frac{1}{2}(\partial_\mu h)(\partial^\mu h) - \frac{1}{4}W_{\mu\nu}^a W^{a\mu\nu} - \frac{1}{4}B_{\mu\nu}B^{\mu\nu} - \frac{1}{4}G_{\mu\nu}^a G^{a\mu\nu} - V(h) \\ & - \frac{(v+h)^2}{4}\text{Tr}[\mathbf{V}_\mu\mathbf{V}^\mu] + i\bar{Q}\not{D}Q + i\bar{L}\not{D}L \\ & - \frac{v+s_Y h}{\sqrt{2}}(\bar{Q}_L\mathbf{U}\mathbf{Y}_Q Q_R + \text{h.c.}) - \frac{v+s_Y h}{\sqrt{2}}(\bar{L}_L\mathbf{U}\mathbf{Y}_L L_R + \text{h.c.}), \end{aligned} \quad (2.2)$$

⁴As usual, derivative is understood in the sense of covariant derivative. That is, a gauge field and a momentum have both chiral dimension one and their inclusion in non-renormalizable operators is weighted down by the same high-scale Λ_s .

where $\mathbf{V}_\mu \equiv (\mathbf{D}_\mu \mathbf{U}) \mathbf{U}^\dagger$ ($\mathbf{T} \equiv \mathbf{U} \sigma_3 \mathbf{U}^\dagger$) is the vector (scalar) chiral field transforming in the adjoint of $\text{SU}(2)_L$. The covariant derivative reads

$$\mathbf{D}_\mu \mathbf{U}(x) \equiv \partial_\mu \mathbf{U}(x) + ig W_\mu(x) \mathbf{U}(x) - \frac{ig'}{2} B_\mu(x) \mathbf{U}(x) \sigma_3, \quad (2.3)$$

with $W_\mu \equiv W_\mu^a(x) \sigma_a/2$ and B_μ denoting the $\text{SU}(2)_L$ and $\text{U}(1)_Y$ gauge bosons, respectively. In eq. (2.2), the first line describes the h and gauge boson kinetic terms, and the effective scalar potential $V(h)$, accounting for the breaking of the electroweak symmetry. The second line describes the W and Z masses and their interactions with h , as well as the kinetic terms for GBs and fermions. Finally, the third line corresponds to the Yukawa-like interactions written in the fermionic mass eigenstate basis, where $s_Y \equiv \pm$ encodes the experimental uncertainty on the sign in the h -fermion couplings. A compact notation for the right-handed fields has been adopted, gathering them into doublets⁵ Q_R and L_R . \mathbf{Y}_Q and \mathbf{Y}_L are two 6×6 block-diagonal matrices containing the usual Yukawa couplings:

$$\mathbf{Y}_Q \equiv \text{diag}(Y_U, Y_D), \quad \mathbf{Y}_L \equiv \text{diag}(Y_\nu, Y_L). \quad (2.4)$$

$\Delta\mathcal{L}$ in eq. (2.1) includes all bosonic (that is, pure gauge and gauge- h operators plus pure Higgs ones) and Yukawa-like operators that describe deviations from the SM picture due to the strong interacting physics present at scales higher than the EW one, in an expansion up to four derivatives [63]:

$$\begin{aligned} \Delta\mathcal{L} = & \xi [c_B \mathcal{P}_B(h) + c_W \mathcal{P}_W(h) + c_G \mathcal{P}_G(h) + c_C \mathcal{P}_C(h) + c_T \mathcal{P}_T(h) + c_H \mathcal{P}_H(h) + c_{\square H} \mathcal{P}_{\square H}(h)] \\ & + \xi \sum_{i=1}^{10} c_i \mathcal{P}_i(h) + \xi^2 \sum_{i=11}^{25} c_i \mathcal{P}_i(h) + \xi^4 c_{26} \mathcal{P}_{26}(h) + \Sigma_i \xi^{n_i} c_{HH}^i \mathcal{P}_{HH}^i(h) \end{aligned} \quad (2.5)$$

where c_i are model-dependent constant coefficients, and the last term account for all possible pure Higgs operators weighted by ξ^{n_i} with $n_i \geq 2$. The set of pure-gauge and gauge- h operators are defined by [63].⁶

⁵The Cabibbo-Kobayashi-Maskawa mixing is understood to be encoded in the definition of Q_L .

⁶The set of pure gauge and gauge- h operators exactly matches that in ref. [63]; nevertheless, the labelling of some operators here and their ξ -weights are corrected with respect to those in ref. [63], see later.

Weighted by ξ :

$$\begin{aligned}
 \mathcal{P}_C(h) &= -\frac{v^2}{4} \text{Tr}(\mathbf{V}^\mu \mathbf{V}_\mu) \mathcal{F}_C(h) & \mathcal{P}_4(h) &= ig' B_{\mu\nu} \text{Tr}(\mathbf{T} \mathbf{V}^\mu) \partial^\nu \mathcal{F}_4(h) \\
 \mathcal{P}_T(h) &= \frac{v^2}{4} \text{Tr}(\mathbf{T} \mathbf{V}_\mu) \text{Tr}(\mathbf{T} \mathbf{V}^\mu) \mathcal{F}_T(h) & \mathcal{P}_5(h) &= ig \text{Tr}(W_{\mu\nu} \mathbf{V}^\mu) \partial^\nu \mathcal{F}_5(h) \\
 \mathcal{P}_B(h) &= -\frac{g'^2}{4} B_{\mu\nu} B^{\mu\nu} \mathcal{F}_B(h) & \mathcal{P}_6(h) &= (\text{Tr}(\mathbf{V}_\mu \mathbf{V}^\mu))^2 \mathcal{F}_6(h) \\
 \mathcal{P}_W(h) &= -\frac{g^2}{4} W_{\mu\nu}^a W^{a\mu\nu} \mathcal{F}_W(h) & \mathcal{P}_7(h) &= \text{Tr}(\mathbf{V}_\mu \mathbf{V}^\mu) \partial_\nu \partial^\nu \mathcal{F}_7(h) \\
 \mathcal{P}_G(h) &= -\frac{g_s^2}{4} G_{\mu\nu}^a G^{a\mu\nu} \mathcal{F}_G(h) & \mathcal{P}_8(h) &= \text{Tr}(\mathbf{V}_\mu \mathbf{V}_\nu) \partial^\mu \mathcal{F}_8(h) \partial^\nu \mathcal{F}'_8(h) \\
 \mathcal{P}_1(h) &= gg' B_{\mu\nu} \text{Tr}(\mathbf{T} W^{\mu\nu}) \mathcal{F}_1(h) & \mathcal{P}_9(h) &= \text{Tr}((\mathcal{D}_\mu \mathbf{V}^\mu)^2) \mathcal{F}_9(h) \\
 \mathcal{P}_2(h) &= ig' B_{\mu\nu} \text{Tr}(\mathbf{T} [\mathbf{V}^\mu, \mathbf{V}^\nu]) \mathcal{F}_2(h) & \mathcal{P}_{10}(h) &= \text{Tr}(\mathbf{V}_\nu \mathcal{D}_\mu \mathbf{V}^\mu) \partial^\nu \mathcal{F}_{10}(h) \\
 \mathcal{P}_3(h) &= ig \text{Tr}(W_{\mu\nu} [\mathbf{V}^\mu, \mathbf{V}^\nu]) \mathcal{F}_3(h)
 \end{aligned} \tag{2.6}$$

Weighted by ξ^2 :

$$\begin{aligned}
 \mathcal{P}_{11}(h) &= (\text{Tr}(\mathbf{V}_\mu \mathbf{V}_\nu))^2 \mathcal{F}_{11}(h) & \mathcal{P}_{19}(h) &= \text{Tr}(\mathbf{T} \mathcal{D}_\mu \mathbf{V}^\mu) \text{Tr}(\mathbf{T} \mathbf{V}_\nu) \partial^\nu \mathcal{F}_{19}(h) \\
 \mathcal{P}_{12}(h) &= g^2 (\text{Tr}(\mathbf{T} W_{\mu\nu}))^2 \mathcal{F}_{12}(h) & \mathcal{P}_{20}(h) &= \text{Tr}(\mathbf{V}_\mu \mathbf{V}^\mu) \partial_\nu \mathcal{F}_{20}(h) \partial^\nu \mathcal{F}'_{20}(h) \\
 \mathcal{P}_{13}(h) &= ig \text{Tr}(\mathbf{T} W_{\mu\nu}) \text{Tr}(\mathbf{T} [\mathbf{V}^\mu, \mathbf{V}^\nu]) \mathcal{F}_{13}(h) & \mathcal{P}_{21}(h) &= (\text{Tr}(\mathbf{T} \mathbf{V}_\mu))^2 \partial_\nu \mathcal{F}_{21}(h) \partial^\nu \mathcal{F}'_{21}(h) \\
 \mathcal{P}_{14}(h) &= g \varepsilon^{\mu\nu\rho\lambda} \text{Tr}(\mathbf{T} \mathbf{V}_\mu) \text{Tr}(\mathbf{V}_\nu W_{\rho\lambda}) \mathcal{F}_{14}(h) & \mathcal{P}_{22}(h) &= \text{Tr}(\mathbf{T} \mathbf{V}_\mu) \text{Tr}(\mathbf{T} \mathbf{V}_\nu) \partial^\mu \mathcal{F}_{22}(h) \partial^\nu \mathcal{F}'_{22}(h) \\
 \mathcal{P}_{15}(h) &= \text{Tr}(\mathbf{T} \mathcal{D}_\mu \mathbf{V}^\mu) \text{Tr}(\mathbf{T} \mathcal{D}_\nu \mathbf{V}^\nu) \mathcal{F}_{15}(h) & \mathcal{P}_{23}(h) &= \text{Tr}(\mathbf{V}_\mu \mathbf{V}^\mu) (\text{Tr}(\mathbf{T} \mathbf{V}_\nu))^2 \mathcal{F}_{23}(h) \\
 \mathcal{P}_{16}(h) &= \text{Tr}([\mathbf{T}, \mathbf{V}_\nu] \mathcal{D}_\mu \mathbf{V}^\mu) \text{Tr}(\mathbf{T} \mathbf{V}^\nu) \mathcal{F}_{16}(h) & \mathcal{P}_{24}(h) &= \text{Tr}(\mathbf{V}_\mu \mathbf{V}_\nu) \text{Tr}(\mathbf{T} \mathbf{V}^\mu) \text{Tr}(\mathbf{T} \mathbf{V}^\nu) \mathcal{F}_{24}(h) \\
 \mathcal{P}_{17}(h) &= ig \text{Tr}(\mathbf{T} W_{\mu\nu}) \text{Tr}(\mathbf{T} \mathbf{V}^\mu) \partial^\nu \mathcal{F}_{17}(h) & \mathcal{P}_{25}(h) &= (\text{Tr}(\mathbf{T} \mathbf{V}_\mu))^2 \partial_\nu \partial^\nu \mathcal{F}_{25}(h) \\
 \mathcal{P}_{18}(h) &= \text{Tr}(\mathbf{T} [\mathbf{V}_\mu, \mathbf{V}_\nu]) \text{Tr}(\mathbf{T} \mathbf{V}^\mu) \partial^\nu \mathcal{F}_{18}(h)
 \end{aligned} \tag{2.7}$$

Weighted by ξ^4 :

$$\mathcal{P}_{26}(h) = (\text{Tr}(\mathbf{T} \mathbf{V}_\mu) \text{Tr}(\mathbf{T} \mathbf{V}_\nu))^2 \mathcal{F}_{26}(h). \tag{2.8}$$

In eq. (2.7), \mathcal{D}_μ denotes the covariant derivative on a field transforming in the adjoint representation of $\text{SU}(2)_L$, i.e.

$$\mathcal{D}_\mu \mathbf{V}_\nu \equiv \partial_\mu \mathbf{V}_\nu + ig [W_\mu, \mathbf{V}_\nu]. \tag{2.9}$$

Finally, the pure Higgs operators are:

Weighted by ξ : this set includes two operators, one with two derivatives and one with four,

$$\mathcal{P}_H(h) = \frac{1}{2} (\partial_\mu h) (\partial^\mu h) \mathcal{F}_H(h), \quad \mathcal{P}_{\square H} = \frac{1}{v^2} (\partial_\mu \partial^\mu h)^2 \mathcal{F}_{\square H}(h). \tag{2.10}$$

In spite of not containing gauge interactions, they will be considered here as they affect the renormalization of SM parameters, and the propagator of the h field, respectively.

Weighted by $\xi^{\geq 2}$: this class consists of all possible pure Higgs operators with four derivatives weighted by $\xi^{\geq 2}$, $\mathcal{P}_{HH}^i(h)$. We refrain from listing them here, as pure- h operators are beyond the scope of this work and therefore they will not be taken into account in the phenomenological sections below. An example of ξ^2 -weighted operator would be [65, 85]

$$\mathcal{P}_{DH}(h) = \frac{1}{v^4} ((\partial_\mu h)(\partial^\mu h))^2 \mathcal{F}_{DH}(h). \quad (2.11)$$

In another realm, note that $\mathcal{P}_C(h)$, $\mathcal{P}_T(h)$ and $\mathcal{P}_H(h)$ are two-derivative operators and would be considered among the leading terms in any formal analysis of the non-linear expansion (as explained after eq. (2.1)), a fact of no consequence below.

The ξ weights within $\Delta\mathcal{L}$ do **not** reflect an expansion in ξ , but a reparametrisation that facilitates the tracking of the lowest dimension at which a “sibling” of a given operator appears in the linear expansion. To guarantee the procedure, such an analysis requires to compare with a specific linear basis; complete linear bases are only available up to $d = 6$ and here we use the completion of the original HISZ basis [6, 76], see section 3.1.

A sibling of a chiral operator $\mathcal{P}_i(h)$ is defined as the operator of the linear expansion whose pure gauge interactions coincide with those described by $\mathcal{P}_i(h)$. The canonical dimension d of the sibling, that is the power of ξ , is thus an indicator of at which order in the linear expansion it is necessary and sufficient to go to account for those gauge interactions: operators weighted by ξ^n require us to consider siblings of canonical dimension $d = 4 + 2n$. It may happen that an operator in eqs. (2.6)–(2.10) corresponds to a combination of linear operators with different canonical dimensions: the power of ξ refers then to the lowest dimension of such operators that leads to the same phenomenological gauge couplings. The lowest dimensional siblings of the operators in eqs. (2.6) and (2.10) have $d = 6$; those in eqs. (2.7) have $d = 8$; that of eq. (2.8) has $d = 12$. ξ is not a physical quantity *per se* in the framework of the effective Lagrangian. If preferred by the reader, the ξ weights can be reabsorbed in a redefinition of the coefficients c_i and be altogether forgotten; nevertheless, they allow a fast connection with the analyses performed in the linear expansion, as illustrated later on.

In the Lagrangian above, Eq. (2.5), we have chosen a definition of the operator coefficients which does not make explicit the weights expected from Naive Dimensional Analysis (NDA) [66, 67, 86]. While the NDA rules are known not to apply to the gauge and scalar kinetic and mass terms, for the higher-order corrections they would imply suppressions by factors of the goldstone boson scale f versus the high energy scale Λ_s . In particular, the coefficients of all operators in eq. (2.6) except $P_C(h)$, as well as all operators in eqs. (2.7), (2.8) and (2.10), would be suppressed by the factor $f^2/\Lambda_s^2 = 1/(16\pi^2)$. The coefficients can be easily redefined by the reader if wished.

The $\mathcal{F}(h)$ functions encode the chiral interactions of the light h , through the generic dependence on $(\langle h \rangle + h)$, and are model dependent. Each function can be defined by $\mathcal{F}(h) \equiv g_0(h, v) + \xi g_1(h, v) + \xi^2 g_2(h, v) + \dots$, where $g_i(h, v)$ are model-dependent functions of h and of v , once $\langle h \rangle$ is expressed in terms of ξ and v . Here we will assume that the $\mathcal{F}(h)$ functions are completely general polynomials of $\langle h \rangle$ and h (not including derivatives of h). Notice that when using the equations of motion (EOM) and integration by parts

to relate operators, $\mathcal{F}(h)$ would be assumed to be redefined when convenient, much as one customarily redefines the constant operator coefficients.

The insertions of the h field, explicit or through generic functions, deserve a separate comment: given their goldstonic origin, they are expected to be suppressed by the goldstone boson scale as h/f , as it has been already specified above. This is encoded in the present formalism by the combination of the $F_i(h)$ functions as defined in the text and the pertinent ξ -weights which have been explicitly extracted from them, as they constitute a useful tool to establish the relation with the linear expansions. Consider an initial generic dependence on the h field of the form $(h + \langle h \rangle)/f = \sqrt{\xi}(h + \langle h \rangle)/v$: for instance in the linear regime, in which $\langle h \rangle \sim v$, the $F_i(h)$ functions are defined in the text as leading to powers of $(1 + h/v)$, because the functional ξ -dependence has been made explicit in the Lagrangian.

Connection to fermionic operators. Several operators in the list in eqs. (2.6)–(2.8) are independent only in the presence of massive fermions: these are $\mathcal{P}_9(h)$, $\mathcal{P}_{10}(h)$, $\mathcal{P}_{15}(h)$, $\mathcal{P}_{16}(h)$, $\mathcal{P}_{19}(h)$, one out of $\mathcal{P}_6(h)$, $\mathcal{P}_7(h)$ and $\mathcal{P}_{20}(h)$, and one out of $\mathcal{P}_{21}(h)$, $\mathcal{P}_{23}(h)$ and $\mathcal{P}_{25}(h)$. Indeed, $\mathcal{P}_9(h)$, $\mathcal{P}_{10}(h)$, $\mathcal{P}_{15}(h)$, $\mathcal{P}_{16}(h)$, and $\mathcal{P}_{19}(h)$ contain the contraction $\mathcal{D}_\mu \mathbf{V}^\mu$ that is connected with the Yukawa couplings [63], through the manipulation of the gauge field EOM and the Dirac equations (see appendix A for details). When fermion masses are neglected, these five operators can be written in terms of the other operators in the basis (see eq. (A.16)). Furthermore, using the light h EOM (see eq. (A.3)), operator $\mathcal{P}_7(h)$ ($\mathcal{P}_{25}(h)$) can be reduced to a combination of $\mathcal{P}_6(h)$ and $\mathcal{P}_{20}(h)$ ($\mathcal{P}_{21}(h)$ and $\mathcal{P}_{23}(h)$), plus a term that can be absorbed in the redefinition of the h -gauge boson couplings, plus a term containing the Yukawa interactions (see appendix A for details). In summary, all those operators must be included to have a complete and independent bosonic basis; nevertheless, in the numerical analysis in section 4.2 their effect will be disregarded as the impact of fermion masses on data analysis will be negligible.

Other operators in the basis in eqs. (2.6)–(2.10) can be traded by fermionic ones independently of the size of fermion masses, applying the EOM for $\mathcal{D}_\mu W^{\mu\nu}$ and $\partial_\mu B^{\mu\nu}$, see eqs. (A.1), (A.2) and (A.11) in appendix A. The complete list of fermionic operators that are related to the pure gauge and gauge- h basis in eqs. (2.6)–(2.10) can also be found there.⁷ This trading procedure can turn out to be very useful [10, 35, 37, 38, 87] when analysing certain experimental data if deviations from the SM values for the h -fermion couplings were found. A basis including all possible fermionic couplings could be more useful in such a hypothetical situation. The bosonic basis defined above is instead “blind” [88] to some deviations in fermionic couplings. This should not come as a surprise: the choice of basis should be optimized with respect to the experimental data under analysis and the presence of blind directions is a common feature of any basis. In this work we are focused in exploring directly the experimental consequences of anomalous gauge and gauge- h couplings and eqs. (2.6)–(2.10) are the appropriate analysis tool.

⁷For completeness, the EOM of the gauge bosons, h and $\mathbf{U}(h)$, and the Dirac equations as well as the full list of fermionic operators that are related to the bosonic ones in eqs. (2.6)–(2.10) are presented in appendix A. In this paper, we will only rely on bosonic observables and therefore we will not consider any fermionic operators other than those mentioned.

Custodial symmetry. In the list in eqs. (2.6)–(2.10), the operators $\mathcal{P}_{\square H}(h)$, $\mathcal{P}_T(h)$, $\mathcal{P}_1(h)$, $\mathcal{P}_2(h)$, $\mathcal{P}_4(h)$, $\mathcal{P}_9(h)$, $\mathcal{P}_{10}(h)$ and $\mathcal{P}_{12-26}(h)$ are custodial symmetry breaking, as either they: i) are related to fermion masses; ii) are related to the hypercharge through $g'B_{\mu\nu}$; iii) they contain the scalar chiral operator \mathbf{T} but no $B_{\mu\nu}$. Among these, only $\mathcal{P}_T(h)$ and $\mathcal{P}_1(h)$ are strongly constrained from electroweak precision test, while the phenomenological impact of the remaining operators has never been studied and therefore they could lead to interesting effects.

If instead by “custodial breaking” operators one refers only to those in iii), a complete set of bosonic custodial preserving operators is given by the following eighteen operators:

$$\mathcal{P}_H(h), \quad \mathcal{P}_{\square H}(h), \quad \mathcal{P}_C(h), \quad \mathcal{P}_B(h), \quad \mathcal{P}_W(h), \quad \mathcal{P}_G(h), \quad \mathcal{P}_{1-11}(h), \quad \mathcal{P}_{20}(h). \quad (2.12)$$

Furthermore, if fermion masses are neglected, this ensemble is further reduced to a set of fourteen independent operators, given by

$$\mathcal{P}_H(h), \quad \mathcal{P}_C(h), \quad \mathcal{P}_B(h), \quad \mathcal{P}_W(h), \quad \mathcal{P}_G(h), \quad \mathcal{P}_{1-5}(h), \quad \mathcal{P}_8(h), \quad \mathcal{P}_{11}(h), \quad (2.13)$$

plus any two among the following three operators:

$$\mathcal{P}_6(h), \quad \mathcal{P}_7(h), \quad \mathcal{P}_{20}(h). \quad (2.14)$$

Under the same assumptions (no beyond SM sources of custodial breaking and massless fermions), a subset of only twelve operators has been previously proposed in ref. [62], as this reference in addition restricted to operators that lead to cubic and quartic vertices of GBs and gauge bosons and including one or two Higgs bosons.

The Lagrangian in eq. (2.1) is very general and can be used to describe an extended class of Higgs models, from the SM scenario with a linear Higgs sector (for $\langle h \rangle = v$, $\xi = 0$ and $s_Y = 1$), to the technicolor-like ansatz (for $f \sim v$ and omitting all terms in h) and intermediate situations with a light scalar h from composite/holographic Higgs models [41–49, 56] (in general for $f \neq v$) up to dilaton-like scalar frameworks [85, 89–94] (for $f \sim v$), where the dilaton participates in the electroweak symmetry breaking.

3 Comparison with the linear regime

The chiral and linear approaches are essentially different from each other, as explained in the introduction. The reshuffling with respect to the linear case of the order at which the leading operators appear plus the generic dependence on h imply that correlations among observables present in one scenario may not hold in the other and, moreover, interactions that are strongly suppressed in one case may be leading corrections in the other. As the symmetry respected by the non-linear Lagrangian is smaller, more freedom is generically expected for the latter. In this section, for the sake of comparison we will first present the effective Lagrangian in the linear regime, restricting to the HISZ basis [76, 77], and discuss then the coincidences and differences expected in observable predictions. The relation to another basis [87] can be found in appendix B.

3.1 The effective Lagrangian in the linear regime

Following the description pattern in eq. (2.1), the effective Lagrangian in the linear regime can be written accordingly as

$$\mathcal{L}_{\text{linear}} = \mathcal{L}_{SM} + \Delta\mathcal{L}_{\text{linear}}, \quad (3.1)$$

where the relation with the non-linear Lagrangian in eq. (2.2) is given by $\mathcal{L}_{SM} = \mathcal{L}_0|_{s_Y=1}$, and $\Delta\mathcal{L}_{\text{linear}}$ contains operators with canonical dimension $d > 4$, weighted down by suitable powers of the ultraviolet cut-off scale Λ . Restricting to CP -even and baryon and lepton number preserving operators, the leading $d = 6$ corrections

$$\Delta\mathcal{L}_{\text{linear}}^{d=6} = \sum_i \frac{f_i}{\Lambda^2} \mathcal{O}_i, \quad (3.2)$$

may be parametrized via a complete basis of operators [5, 6]. Only a small subset of those modify the Higgs couplings to gauge bosons. Consider the HISZ basis [76, 77]:

$$\begin{aligned} \mathcal{O}_{GG} &= \Phi^\dagger \Phi G_{\mu\nu}^a G^{a\mu\nu}, & \mathcal{O}_{WW} &= \Phi^\dagger \hat{W}_{\mu\nu} \hat{W}^{\mu\nu} \Phi, \\ \mathcal{O}_{BB} &= \Phi^\dagger \hat{B}_{\mu\nu} \hat{B}^{\mu\nu} \Phi, & \mathcal{O}_{BW} &= \Phi^\dagger \hat{B}_{\mu\nu} \hat{W}^{\mu\nu} \Phi, \\ \mathcal{O}_W &= (D_\mu \Phi)^\dagger \hat{W}^{\mu\nu} (D_\nu \Phi), & \mathcal{O}_B &= (D_\mu \Phi)^\dagger \hat{B}^{\mu\nu} (D_\nu \Phi), \\ \mathcal{O}_{\Phi,1} &= (D_\mu \Phi)^\dagger \Phi \Phi^\dagger (D^\mu \Phi), & \mathcal{O}_{\Phi,2} &= \frac{1}{2} \partial^\mu (\Phi^\dagger \Phi) \partial_\mu (\Phi^\dagger \Phi), \\ \mathcal{O}_{\Phi,4} &= (D_\mu \Phi)^\dagger (D^\mu \Phi) (\Phi^\dagger \Phi), \end{aligned} \quad (3.3)$$

where $D_\mu \Phi = (\partial_\mu + \frac{i}{2}g'B_\mu + \frac{i}{2}g\sigma_i W_\mu^i) \Phi$ and $\hat{B}_{\mu\nu} \equiv \frac{i}{2}g'B_{\mu\nu}$ and $\hat{W}_{\mu\nu} \equiv \frac{i}{2}g\sigma_i W_{\mu\nu}^i$. An additional operator is commonly added in phenomenological analysis,

$$\mathcal{O}_{\Phi,3} = \frac{1}{3} (\Phi^\dagger \Phi)^3, \quad (3.4)$$

which is a pure Higgs operator. An equivalent basis of ten operators in the linear expansion is often used nowadays instead of the previous set of ten linear operators: the so-called SILH [87] Lagrangian, in which four of the operators above are traded by combinations of them and/or by a fermionic one via EOM (the exact relation with the SILH basis can be found in appendix B).

The pure Higgs interactions described by the ξ -weighted operator $\mathcal{P}_{\square H}$ of the chiral expansion, eq. (2.10), are contained in the linear operator,

$$\mathcal{O}_{\square H} = (D_\mu D^\mu \Phi)^\dagger (D_\nu D^\nu \Phi). \quad (3.5)$$

Let us now explore the relation between the linear and non-linear analyses. Beyond the different h -dependence of the operators, that is (in the unitary gauge):

$$\Phi = \frac{1}{\sqrt{2}} \begin{pmatrix} 0 \\ v + h(x) \end{pmatrix} \quad \text{vs.} \quad \mathcal{F}(h), \quad (3.6)$$

it is interesting to explore the relation among the linear operators in eqs. (3.3) and those in the chiral expansion. A striking distinct feature when comparing both basis is the different number of independent couplings they span. This is best illustrated for instance truncating the non-linear expansion at order ξ -which may be specially relevant for small ξ - and comparing the result with the $d = 6$ linear basis that contributes to gauge-Higgs couplings: while the latter basis exhibits ten independent couplings, the former depends on sixteen. A more precise illustration follows when taking momentarily $\mathcal{F}_i(h) = (1 + h/v)^2$, with $n = 2$ in general, in all $\mathcal{P}_i(h)$ under discussion, which would lead to:

$$\begin{aligned}
 \mathcal{O}_{BB} &= \frac{v^2}{2} \mathcal{P}_B(h), & \mathcal{O}_{WW} &= \frac{v^2}{2} \mathcal{P}_W(h), \\
 \mathcal{O}_{GG} &= -\frac{2v^2}{g_s^2} \mathcal{P}_G(h), & \mathcal{O}_{BW} &= \frac{v^2}{8} \mathcal{P}_1(h), \\
 \mathcal{O}_B &= \frac{v^2}{16} \mathcal{P}_2(h) + \frac{v^2}{8} \mathcal{P}_4(h), & \mathcal{O}_W &= \frac{v^2}{8} \mathcal{P}_3(h) - \frac{v^2}{4} \mathcal{P}_5(h), \\
 \mathcal{O}_{\Phi,1} &= \frac{v^2}{2} \mathcal{P}_H(h) - \frac{v^2}{4} \mathcal{F}(h) \mathcal{P}_T(h), & \mathcal{O}_{\Phi,2} &= v^2 \mathcal{P}_H(h), \\
 \mathcal{O}_{\Phi,4} &= \frac{v^2}{2} \mathcal{P}_H(h) + \frac{v^2}{2} \mathcal{F}(h) \mathcal{P}_C(h), \\
 \mathcal{O}_{\square\Phi} &= \frac{v^2}{2} \mathcal{P}_{\square H}(h) + \frac{v^2}{8} \mathcal{P}_6(h) + \frac{v^2}{4} \mathcal{P}_7(h) - v^2 \mathcal{P}_8(h) - \frac{v^2}{4} \mathcal{P}_9(h) - \frac{v^2}{2} \mathcal{P}_{10}(h).
 \end{aligned} \tag{3.7}$$

These relations show that five chiral operators, $\mathcal{P}_B(h)$, $\mathcal{P}_W(h)$, $\mathcal{P}_G(h)$, $\mathcal{P}_1(h)$ and $\mathcal{P}_H(h)$ are then in a one-to-one correspondence with the linear operators \mathcal{O}_{BB} , \mathcal{O}_{WW} , \mathcal{O}_{GG} , \mathcal{O}_{BW} and $\mathcal{O}_{\Phi,2}$, respectively. Also the operator $\mathcal{P}_T(h)$ ($\mathcal{P}_C(h)$) corresponds to a combination of the linear operators $\mathcal{O}_{\Phi,1}$ and $\mathcal{O}_{\Phi,2}$ ($\mathcal{O}_{\Phi,4}$ and $\mathcal{O}_{\Phi,2}$). In contrast, it follows from eq. (3.7) above that:

- Only a specific combination of the non-linear operators $\mathcal{P}_2(h)$ and $\mathcal{P}_4(h)$ corresponds to the linear operator \mathcal{O}_B .
- Similarly, a specific combination of the non-linear operators $\mathcal{P}_3(h)$ and $\mathcal{P}_5(h)$ corresponds to the linear operator \mathcal{O}_W .
- Only a specific combination of the non-linear operators $\mathcal{P}_{\square H}(h)$, $\mathcal{P}_6(h)$, $\mathcal{P}_7(h)$, $\mathcal{P}_8(h)$, $\mathcal{P}_9(h)$ and $\mathcal{P}_{10}(h)$ corresponds to the linear operator $\mathcal{O}_{\square\Phi}$.

It is necessary to go to the next order in the linear basis, $d = 8$, to identify the operators which break these correlations (see eq. (C.2)). It can be checked that, for example for the first two correlations, the linear $d = 8$ operators

$$\left((D_\mu \Phi)^\dagger \Phi \right) \hat{B}^{\mu\nu} \left(\Phi^\dagger D_\nu \Phi \right) \quad \text{and} \quad \left((D_\mu \Phi)^\dagger \Phi \right) \hat{W}^{\mu\nu} \left(\Phi^\dagger D_\nu \Phi \right) \tag{3.8}$$

correspond separately to $\mathcal{P}_4(h)$ and $\mathcal{P}_5(h)$, respectively.

A comment is pertinent when considering the ξ truncation. In the $\xi \rightarrow 0$ limit, in which $\mathcal{F}(h) \rightarrow (1 + h/v)^2$, if the underlying theory is expected to account for EWSB, the ensemble of the non-linear Lagrangian should converge to a linear-like pattern. Nevertheless, the

size of ξ is not known in a model-independent way; starting an analysis by formulating the problem (only) in the linear expansion is somehow assuming an answer from the start: that ξ is necessarily small in any possible BSM construction. Furthermore, the non-linear Lagrangian accounts for more exotic singlet scalars, and that convergence is not granted in general.

The maximal set of CP-even independent operators involving gauge and/or the Higgs boson in any $d = 6$ linear basis is made out of 16 operators: the ten [76, 77] in eqs. (3.3) and (3.4), plus the operator [6] $\mathcal{O}_{\Box\Phi}$ defined in eq. (3.5), and another five which only modify the gauge boson couplings and do not involve the Higgs field⁸ [76, 77]:

$$\begin{aligned}\mathcal{O}_{WWW} &= i\epsilon_{ijk}\hat{W}_\mu^{i\nu}\hat{W}_\nu^{j\rho}\hat{W}_\rho^{k\mu}, & \mathcal{O}_{GGG} &= if_{abc}G_\mu^{a\nu}G_\nu^{b\rho}G_\rho^{c\mu}, \\ \mathcal{O}_{DW} &= \left(\mathcal{D}^\mu\hat{W}_{\mu\nu}\right)^i\left(\mathcal{D}_\rho\hat{W}^{\rho\nu}\right)^i, & \mathcal{O}_{DB} &= \left(\partial^\mu\hat{B}_{\mu\nu}\right)\left(\partial_\rho\hat{B}^{\rho\nu}\right), \\ \mathcal{O}_{DG} &= (\mathcal{D}^\mu G_{\mu\nu})^a(\mathcal{D}_\rho G^{\rho\nu})^a.\end{aligned}\quad (3.9)$$

The Lorentz structures contained in these five operators are *not* present in the non-linear Lagrangian expanded up to four derivatives: they would appear only at higher order in that expansion, i.e. six derivatives. They are not the siblings of any of the chiral operators discussed in this work, eqs. (2.6)–(2.10).

The rest of this paper will focus on how the present and future LHC gauge and gauge- h data, as well as other data, may generically shed light on the (non-)linearity of the underlying physics. In particular exploiting the decorrelations implied by the discussion above as well as via new anomalous discriminating signals.

Disregarding fine tunings, that is, assuming in general all dimensionless operator coefficients of $\mathcal{O}(1)$, the pattern of dominant signals expected from each expansion varies because the nature of some leading corrections is different, or because the expected relation between some couplings varies. In the next subsections we analyze first how some correlations among couplings expected in the linear regime are broken in the non-linear one. Next, it is pointed out that some couplings expected if the EWSB is linearly realized are instead expected to appear only as higher order corrections in the non-linear case. Conversely and finally, attention is paid to new anomalous couplings expected as leading corrections in the non-linear regime which appear only at $d \geq 8$ of the linear expansion.

3.2 Decorrelation of signals with respect to the linear analysis

The parameter ξ is a free parameter in the effective approach. Nevertheless, in concrete composite Higgs models electroweak corrections imply $\xi \lesssim 0.2 - 0.4$ [95] (more constraining bounds $\xi \lesssim 0.1 - 0.2$ have been advocated in older analyses [29, 96, 97]), and it is therefore interesting for the sake of comparison to consider the truncation of $\Delta\mathcal{L}$ which keeps only the terms weighted by ξ and disregard first those weighted by higher ξ powers. We will thus

⁸The Operators \mathcal{O}_{DW} , \mathcal{O}_{DB} and \mathcal{O}_{DG} are usually traded by \mathcal{O}_{WWW} and \mathcal{O}_{GGG} plus fermionic operators. As in this paper we focus on bosonic observables, such translation is not pertinent. Taken by themselves, the ensembles discussed constitute a non-redundant and complete set of gauge and/or Higgs operators. In \mathcal{O}_{DG} , \mathcal{D}^μ denotes the covariant derivative acting on a field transforming in the adjoint of $SU(3)_C$.

analyze first only those operators in eqs. (2.6) and (2.10). We will refer to this truncation as $\Delta\mathcal{L}^\xi$ and define $\mathcal{L}_{\text{chiral}}^\xi \equiv \mathcal{L}_0 + \Delta\mathcal{L}^\xi$.

All operators in $\Delta\mathcal{L}^\xi$ have by definition lowest dimensional linear siblings of $d = 6$. We will thus compare first $\mathcal{L}_{\text{chiral}}^\xi$ with the $d = 6$ linear expansion [5, 6, 87]. For low enough values of ξ , that is when the new physics scale $\Lambda_s \gg v$, $\mathcal{L}_{\text{chiral}}^\xi$ is expected to collapse into the $d = 6$ linear Lagrangian if it should account correctly for EW symmetry breaking via an $\text{SU}(2)_L$ doublet scalar, but the non-linear Lagrangian encodes more general scenarios (for instance that for a SM singlet) as well.

The comparison of the effects in the non-linear versus the linear expansion is illuminating when done in the context of the maximal set of independent (and thus non-redundant) operators on the gauge-boson/Higgs sector for each expansion: comparing complete bases of those characteristics. The number of independent bosonic operators that induce leading deviations in gauge- h couplings turns out to be then different for both expansions: ten $d = 6$ operators in the linear expansion, see eq. (3.3) and eq. (3.5), for sixteen ξ -weighted operators⁹ in the chiral one, see eq. (2.6) and (2.10). For illustration, further details are given here on one example pointed out in section 3.1: $\mathcal{P}_2(h)$ and $\mathcal{P}_4(h)$ versus the $d = 6$ operator \mathcal{O}_B . From eq. (3.7) it followed that only the combinations $\mathcal{P}_2(h) + 2\mathcal{P}_4(h)$ have a $d = 6$ linear equivalent (with $\mathcal{F}_i(h)$ substituted by $(1 + h/v)^2$). In the unitary gauge $\mathcal{P}_2(h)$ and $\mathcal{P}_4(h)$ read:

$$\mathcal{P}_2(h) = 2ieg^2 A_{\mu\nu} W^{-\mu} W^{+\nu} \mathcal{F}_2(h) - 2 \frac{ie^2 g}{\cos \theta_W} Z_{\mu\nu} W^{-\mu} W^{+\nu} \mathcal{F}_2(h), \quad (3.10)$$

$$\mathcal{P}_4(h) = -\frac{eg}{\cos \theta_W} A_{\mu\nu} Z^\mu \partial^\nu \mathcal{F}_4(h) + \frac{e^2}{\cos^2 \theta_W} Z_{\mu\nu} Z^\mu \partial^\nu \mathcal{F}_4(h), \quad (3.11)$$

with their coefficients c_2 and c_4 taking arbitrary (model-dependent) values. In contrast, their $d = 6$ sibling \mathcal{O}_B results in the combination:

$$\begin{aligned} \mathcal{O}_B = & \frac{ieg^2}{8} A_{\mu\nu} W^{-\mu} W^{+\nu} (v + h)^2 - \frac{ie^2 g}{8 \cos \theta_W} Z_{\mu\nu} W^{-\mu} W^{+\nu} (v + h)^2 \\ & - \frac{eg}{4 \cos \theta_W} A_{\mu\nu} Z^\mu \partial^\nu h (v + h) + \frac{e^2}{4 \cos^2 \theta_W} Z_{\mu\nu} Z^\mu \partial^\nu h (v + h). \end{aligned} \quad (3.12)$$

In consequence, the following interactions encoded in \mathcal{O}_B -and for the precise Lorentz structures shown above- get decorrelated in a general non-linear analysis:

- $\gamma - W - W$ from $\gamma - Z - h$, and $Z - W - W$ from $Z - Z - h$; these are examples of interactions involving different number of external h legs.
- $\gamma - W - W - h$ from $\gamma - Z - h$, and $Z - W - W - h$ from $Z - Z - h$, which are interactions involving the same number of external h legs.

While such decorrelations are expected among the leading SM deviations in a generic non-linear approach, they require us to consider $d = 8$ operators in scenarios with linearly realized EW symmetry breaking. This statement is a physical effect, which means that it holds

⁹Note that the first operator in eq. (2.10) impacts on the gauge- h couplings via the renormalization of the h field.

irrespective of the linear basis used, for instance it also holds in the bases in refs. [97, 98]. The study of the correlations/decorrelations described represents an interesting method to investigate the intimate nature of the light Higgs h .

The argument developed above focused on just one operator, for illustration. A parallel analysis on correlations/decorrelations also applies in other case, i.e. the interactions described by $\mathcal{P}_3(h)$ and $\mathcal{P}_5(h)$ versus those in the $d = 6$ linear operator \mathcal{O}_W . Obviously, in order to firmly establish the pattern of deviations expected, all possible operators at a given order of an expansion should be considered together, and this will be done in the phenomenological section 4 below.

3.3 Signals specific to the linear expansion

The $d = 6$ operators in eq. (3.9) have no equivalent among the dominant corrections of the non-linear expansion, eqs. (2.6)–(2.10), all ξ weights considered. This fact results in an interesting method to test the nature of the Higgs. Considering for example the operator \mathcal{O}_{WWW} in eq. (3.9), the couplings

$$\begin{aligned}
 & \begin{array}{c} W_\mu^+ \\ \text{---} \\ A_\rho \text{ ---} \\ \text{---} \\ W_\nu^- \end{array} \quad f_{WWW} \frac{3ie g^2}{4} \left[g_{\rho\mu} ((p_+ \cdot p_-) p_{A\nu} - (p_A \cdot p_-) p_{+\nu}) \right. \\
 & \quad + g_{\mu\nu} ((p_A \cdot p_-) p_{+\rho} - (p_A \cdot p_+) p_{-\rho}) \\
 & \quad \left. + g_{\rho\nu} ((p_A \cdot p_+) p_{-\mu} - (p_+ \cdot p_-) p_{A\mu}) + p_{A\mu} p_{+\nu} p_{-\rho} - p_{A\nu} p_{+\rho} p_{-\mu} \right], \\
 & \hspace{15em} (3.13) \\
 & \begin{array}{c} W_\mu^+ \\ \text{---} \\ Z_\rho \text{ ---} \\ \text{---} \\ W_\nu^- \end{array} \quad f_{WWW} \frac{3ig^3 \cos \theta_W}{4} \left[g_{\rho\mu} ((p_+ \cdot p_-) p_{Z\nu} - (p_Z \cdot p_-) p_{+\nu}) \right. \\
 & \quad + g_{\mu\nu} ((p_Z \cdot p_-) p_{+\rho} - (p_Z \cdot p_+) p_{-\rho}) \\
 & \quad \left. + g_{\rho\nu} ((p_Z \cdot p_+) p_{-\mu} - (p_+ \cdot p_-) p_{Z\mu}) + p_{Z\mu} p_{+\nu} p_{-\rho} - p_{Z\nu} p_{+\rho} p_{-\mu} \right],
 \end{aligned}$$

should be observable with a strength similar to that of other couplings described by $d = 6$ operators, if the EW breaking is linearly realized by the underlying physics. On the contrary, for a subadjacent non-linear dynamics their strength is expected to be suppressed (i.e. be of higher order) [64].¹⁰ A similar discussion holds for the other operators in eq. (3.9).

3.4 New signals specific to the non-linear expansion

For large ξ , all chiral operators weighted by ξ^n with $n \geq 2$, eqs. (2.7)–(2.10), are equally relevant to the ξ -weighted ones in eq. (2.6), and therefore their siblings require operators of dimension $d \geq 8$. Of special interest is $\mathcal{P}_{14}(h)$ which belongs to the former class, as some of the couplings encoded in it are absent from the SM Lagrangian. This fact provides a viable strategy to test the nature of the physical Higgs.

In appendix D, the Feynman rules for all couplings appearing in the non-linear Lagrangian for gauge and gauge- h operators can be found. A special column indicates directly the non-standard structures and it is easy to identify among those entries the couplings

¹⁰This coupling is usually referred to in the literature as λ_V [4].

weighted only by ξ^n with $n \geq 2$. Here, we report explicitly only the example of the anomalous $Z - W - W$ and $\gamma - Z - W - W$ vertices, assuming for simplicity that the $\mathcal{F}_{14}(h)$ function admits a polynomial expansion in h/v . The operator $\mathcal{P}_{14}(h)$ contains the couplings

$$\varepsilon^{\mu\nu\rho\lambda} \partial_\mu W_\nu^+ W_\rho^- Z_\lambda \mathcal{F}_{14}(h), \quad \varepsilon^{\mu\nu\rho\lambda} Z_\mu A_\nu W_\rho^- W_\lambda^+ \mathcal{F}_{14}(h), \quad (3.14)$$

which correspond to an anomalous $Z - W - W$ triple vertex and to an anomalous $\gamma - Z - W - W$ quartic vertex, respectively. The corresponding Feynman diagrams and rules read

$$- \xi^2 \frac{g^3}{\cos \theta_W} \varepsilon^{\mu\nu\rho\lambda} [p_{+\lambda} - p_{-\lambda}],$$

$$- 2 \xi^2 \frac{eg^3}{\cos \theta_W} \varepsilon^{\mu\nu\rho\lambda}.$$

(3.15)

These couplings are present neither in the SM nor in the $d = 6$ linear Lagrangian and are anomalous couplings due to their Lorentz nature. A signal of these type of interactions at colliders with a strength comparable with that expected for the couplings in the $d = 6$ linear Lagrangian would be a clear hint of a strong dynamics in the EWSB sector. More details are given in the phenomenological sections below.

4 Phenomenology

Prior to developing the strategies suggested above to investigate the nature of the Higgs particle, the renormalization procedure is illustrated next.

4.1 Renormalization procedure

Five electroweak parameters of the SM-like Lagrangian \mathcal{L}_0 are relevant in our analysis, when neglecting fermion masses: g_s , g , g' , v and the h self-coupling λ . The first four can be optimally constrained by four observables that are extremely well determined nowadays, while as a fifth one the Higgs mass m_h can be used; in summary:

$$\begin{aligned}
 \alpha_s & \text{ world average [99],} \\
 G_F & \text{ extracted from the muon decay rate [99],} \\
 \alpha_{\text{em}} & \text{ extracted from Thomson scattering [99],} \\
 m_Z & \text{ extracted from the } Z \text{ lineshape at LEP I [99],} \\
 m_h & \text{ now measured at LHC [11, 12].}
 \end{aligned} \tag{4.1}$$

This ensemble of observables defines the so-called Z-scheme: they will be kept as input parameters, and all predictions will be expressed as functions of them. Accordingly, whenever a dependence on the parameters g , g' , v (and e) or the weak mixing angle θ_W may appear

in the expressions below, it should be interpreted as corresponding to the combinations of experimental inputs as follows:

$$\begin{aligned} e^2 &= 4\pi\alpha_{\text{em}}, & \sin^2\theta_W &= \frac{1}{2} \left(1 - \sqrt{1 - \frac{4\pi\alpha_{\text{em}}}{\sqrt{2}G_F m_Z^2}} \right), \\ v^2 &= \frac{1}{\sqrt{2}G_F}, & \left(g = \frac{e}{\sin\theta_W}, \quad g' = \frac{e}{\cos\theta_W} \right) &\Big|_{\theta_W, e \text{ as above}}. \end{aligned} \quad (4.2)$$

The abbreviations s_θ ($s_{2\theta}$) and c_θ ($c_{2\theta}$) will stand below for $\sin\theta_W$ ($\sin 2\theta_W$) and $\cos\theta_W$ ($\cos 2\theta_W$), respectively. Furthermore, for concreteness, we assume a specific parametrization for the $\mathcal{F}_i(h)$ functions:

$$\mathcal{F}_i(h) \equiv 1 + 2\tilde{a}_i \frac{h}{v} + \tilde{b}_i \frac{h^2}{v^2} + \dots \quad (4.3)$$

where the dots stand for higher powers of h/v that will not be considered in what follows; to further simplify the notation a_i and b_i will indicate below the products $a_i \equiv c_i \tilde{a}_i$ and $b_i \equiv c_i \tilde{b}_i$, respectively, where c_i are the global operator coefficients.

Working in the unitary gauge to analyze the impact that the couplings in $\Delta\mathcal{L}$ in eq. (2.5) have on \mathcal{L}_0 , it is straightforward to show that $\mathcal{P}_B(h)$, $\mathcal{P}_W(h)$, $\mathcal{P}_G(h)$, $\mathcal{P}_H(h)$, $\mathcal{P}_1(h)$ and $\mathcal{P}_{12}(h)$ introduce corrections to the SM kinetic terms, and in consequence field redefinitions are necessary to obtain canonical kinetic terms. Among these operators, $\mathcal{P}_B(h)$, $\mathcal{P}_W(h)$ and $\mathcal{P}_G(h)$ can be considered innocuous operators with respect to \mathcal{L}_0 , as the impact on the latter of c_B , c_W and c_G can be totally eliminated from the Lagrangian by ineffectual field and coupling constant redefinitions; they do have a physical impact though on certain BSM couplings in $\Delta\mathcal{L}$ involving external scalar fields.

With canonical kinetic terms, it is then easy to identify the contribution of $\Delta\mathcal{L}$ to the input parameters:¹¹

$$\begin{aligned} \frac{\delta\alpha_{\text{em}}}{\alpha_{\text{em}}} &\simeq 4e^2 c_1 \xi + 4e^2 c_{12} \xi^2, & \frac{\delta G_F}{G_F} &\simeq 0, \\ \frac{\delta m_Z}{m_Z} &\simeq -c_T \xi - 2e^2 c_1 \xi + 2e^2 \cot^2\theta_W c_{12} \xi^2, & \frac{\delta m_h}{m_h} &\simeq 0, \end{aligned} \quad (4.4)$$

keeping only terms linear in the coefficients c_i . Expressing all other SM parameters in $\mathcal{L}_{\text{chiral}}$ in terms of the four input parameters leads to the predictions to be described next.

W mass. The prediction for the W mass departs from the SM expectation by

$$\begin{aligned} \frac{\Delta m_W^2}{m_W^2} &= \frac{4e^2}{c_{2\theta}} c_1 \xi + \frac{2c_\theta^2}{c_{2\theta}} c_T \xi - \frac{4e^2}{s_\theta^2} c_{12} \xi^2 \\ &\equiv \frac{e^2}{2c_{2\theta}} f_{BW} \frac{v^2}{\Lambda^2} - \frac{c_\theta^2}{2c_{2\theta}} f_{\Phi,1} \frac{v^2}{\Lambda^2}, \end{aligned} \quad (4.5)$$

where the second line shows for comparison the corresponding expression in the linear expansion at order $d = 6$.

¹¹The BSM corrections that enter into the definition of the input parameters will be generically denoted by the sign “ δ ”, while the predicted measurable departures from SM expectations will be indicated below by “ Δ ”.

S and T parameters. $\mathcal{P}_1(h)$ and $\mathcal{P}_T(h)$ generate tree-level contributions to the oblique parameters S and T [100], which read

$$\alpha_{\text{em}}\Delta S = -8e^2c_1\xi \quad \text{and} \quad \alpha_{\text{em}}\Delta T = 2c_T\xi. \quad (4.6)$$

Triple gauge-boson couplings. The effective operators described in the non-linear Lagrangian, eqs. (2.6)–(2.8), give rise to triple gauge-boson couplings γW^+W^- and ZW^+W^- . Following ref. [4], the CP-even sector of the Lagrangian that describes trilinear gauge boson vertices (TGV) can be parametrized as:

$$\begin{aligned} \mathcal{L}_{WWV} = & -ig_{WWV} \left\{ g_1^V \left(W_{\mu\nu}^+ W^{-\mu} V^\nu - W_\mu^+ V_\nu W^{-\mu\nu} \right) + \kappa_V W_\mu^+ W_\nu^- V^{\mu\nu} \right. \\ & \left. - ig_5^V \epsilon^{\mu\nu\rho\sigma} \left(W_\mu^+ \partial_\rho W_\nu^- - W_\nu^- \partial_\rho W_\mu^+ \right) V_\sigma + g_6^V \left(\partial_\mu W^{+\mu} W^{-\nu} - \partial_\mu W^{-\mu} W^{+\nu} \right) V_\nu \right\}, \end{aligned} \quad (4.7)$$

where $V \equiv \{\gamma, Z\}$ and $g_{WW\gamma} \equiv e = g \sin \theta_W$, $g_{WWZ} = g \cos \theta_W$ (see eq. (4.2) for their relation to observables). In this equation $W_{\mu\nu}^\pm$ and $V_{\mu\nu}$ stand exclusively for the kinetic part of the gauge field strengths. In contrast with the usual parameterization proposed in ref. [4], the coefficient λ_V (associated with a linear $d = 6$ operator) is omitted here as this coupling does not receive contributions from the non-linear effective chiral Lagrangian expanded up to four derivatives. Conversely, we have introduced the coefficients g_6^V associated to operators that contain the contraction $\mathcal{D}_\mu \mathbf{V}^\mu$; its $\partial_\mu \mathbf{V}^\mu$ part vanishes only for on-shell gauge bosons; in all generality $\mathcal{D}_\mu \mathbf{V}^\mu$ insertions could only be disregarded¹² in the present context when fermion masses are neglected, as explained in section 2 and appendix A.

Electromagnetic gauge invariance requires $g_1^\gamma = 1$ and $g_5^\gamma = 0$, and in consequence the TGV CP-even sector described in eq. (4.7) depends in all generality on six dimensionless couplings g_1^Z , g_5^Z , $g_6^{Z,Z}$ and $\kappa_{\gamma,Z}$. Their SM values are $g_1^Z = \kappa_\gamma = \kappa_Z = 1$ and $g_5^Z = g_6^{Z,Z} = g_6^Z = 0$. Table 1 shows the departures from those SM values due to the effective couplings in eq. (2.5); it illustrates the ξ and ξ^2 -weighted chiral operator contributions. For the sake of comparison, the corresponding expressions in terms of the coefficients of $d = 6$ operators in the linear expansion are shown as well. A special case is that of the linear operator $\mathcal{O}_{\square\Phi}$, whose physical interpretation is not straightforward [137–139] and will be analyzed in detail in ref. [140]; the corresponding coefficient $f_{\square\Phi}$ does not appear in table 1 as contributing to the measurable couplings, while nevertheless the symbol (*) recalls the theoretical link between some chiral operators and their sibling $\mathcal{O}_{\square\Phi}$. The analysis of table 1 leads as well to relations between measurable quantities, which are collected later on in eq. (4.14) and subsequent ones.

h couplings to SM gauge-boson pairs. The effective operators described in eqs. (2.6)–(2.8) also give rise to interactions involving the Higgs and two gauge bosons, to which we

¹²See for example ref. [101] for a general discussion on possible “off-shell” vertices associated to $d = 4$ and $d = 6$ operators.

	Coeff. $\times e^2/s_\theta^2$	Chiral		Linear $\times v^2/\Lambda^2$
		$\times \xi$	$\times \xi^2$	
$\Delta\kappa_\gamma$	1	$-2c_1+2c_2+c_3$	$-4c_{12}+2c_{13}$	$\frac{1}{8}(f_W+f_B-2f_{BW})$
Δg_6^γ	1	$-c_9$	—	(*)
Δg_1^Z	$\frac{1}{c_\theta^2}$	$\frac{s_\theta^2}{4e^2c_{2\theta}}c_T+\frac{2s_\theta^2}{c_{2\theta}}c_1+c_3$	—	$\frac{1}{8}f_W+\frac{s_\theta^2}{4c_{2\theta}}f_{BW}-\frac{s_\theta^2}{16e^2c_{2\theta}}f_{\Phi,1}$
$\Delta\kappa_Z$	1	$\frac{s_\theta^2}{e^2c_{2\theta}}c_T+\frac{4s_\theta^2}{c_{2\theta}}c_1-\frac{2s_\theta^2}{c_\theta^2}c_2+c_3$	$-4c_{12}+2c_{13}$	$\frac{1}{8}f_W-\frac{s_\theta^2}{8c_\theta^2}f_B+\frac{s_\theta^2}{2c_{2\theta}}f_{BW}-\frac{s_\theta^2}{4e^2c_{2\theta}}f_{\Phi,1}$
Δg_5^Z	$\frac{1}{c_\theta^2}$	—	c_{14}	—
Δg_6^Z	$\frac{1}{c_\theta^2}$	$s_\theta^2c_9$	$-c_{16}$	(*)

Table 1. Effective couplings parametrizing the VW^+W^- vertices defined in eq. (4.7). The coefficients in the second column are common to both the chiral and linear expansions. In the third and fourth columns the specific contributions from the operators in the chiral Lagrangian are shown. For comparison, the last column exhibits the corresponding contributions from the linear $d=6$ operators. The star (*) in the last column indicates the link between the chiral operator $\mathcal{P}_9(h)$ and its linear sibling $\mathcal{O}_{\square\Phi}$, without implying a physical impact of the latter on the VW^+W^- observables, as explained in the text and in ref. [140].

will refer as HVV couplings. The latter can be phenomenologically parametrized as

$$\begin{aligned}
 \mathcal{L}_{\text{HVV}} \equiv & g_{Hgg} G_{\mu\nu}^a G^{a\mu\nu} h + g_{H\gamma\gamma} A_{\mu\nu} A^{\mu\nu} h + g_{HZZ}^{(1)} A_{\mu\nu} Z^\mu \partial^\nu h + g_{HZZ}^{(2)} A_{\mu\nu} Z^{\mu\nu} h \\
 & + g_{HZZ}^{(1)} Z_{\mu\nu} Z^\mu \partial^\nu h + g_{HZZ}^{(2)} Z_{\mu\nu} Z^{\mu\nu} h + g_{HZZ}^{(3)} Z_\mu Z^\mu h + g_{HZZ}^{(4)} Z_\mu Z^\mu \square h \\
 & + g_{HZZ}^{(5)} \partial_\mu Z^\mu Z_\nu \partial^\nu h + g_{HZZ}^{(6)} \partial_\mu Z^\mu \partial_\nu Z^\nu h \\
 & + g_{HWW}^{(1)} (W_\mu^+ W^{-\mu} \partial^\nu h + \text{h.c.}) + g_{HWW}^{(2)} W_\mu^+ W^{-\mu\nu} h + g_{HWW}^{(3)} W_\mu^+ W^{-\mu} h \\
 & + g_{HWW}^{(4)} W_\mu^+ W^{-\mu} \square h + g_{HWW}^{(5)} (\partial_\mu W^{+\mu} W_\nu^- \partial^\nu h + \text{h.c.}) + g_{HWW}^{(6)} \partial_\mu W^{+\mu} \partial_\nu W^{-\nu} h,
 \end{aligned} \tag{4.8}$$

where $V_{\mu\nu} = \partial_\mu V_\nu - \partial_\nu V_\mu$ with $V = \{A, Z, W, G\}$. Separating the contributions into SM ones plus corrections,

$$g_i^{(j)} \simeq g_i^{(j)SM} + \Delta g_i^{(j)}, \tag{4.9}$$

it turns out that

$$g_{HZZ}^{(3)SM} = \frac{m_Z^2}{v}, \quad g_{HWW}^{(3)SM} = \frac{2m_Z^2 c_\theta^2}{v}, \tag{4.10}$$

while the tree-level SM value for all other couplings in eq. (4.8) vanishes (the SM loop-induced value for g_{Hgg} , $g_{H\gamma\gamma}$ and $g_{HZZ}^{(2)}$ will be taken into account in our numerical analysis, though); in these expressions, v is as defined in eq. (4.2). Table 2 shows the expressions for the corrections Δg_{Hgg} , $\Delta g_{H\gamma\gamma}$, $\Delta g_{HZZ}^{(1,2)}$, $\Delta g_{HWW}^{(1,2,3,4,5,6)}$, and $\Delta g_{HZZ}^{(1,2,3,4,5,6)}$ induced at tree-level by the effective non-linear couplings under discussion. In writing eq. (4.8) we have introduced the coefficients $\Delta g_{HZZ}^{(4,5,6)}$ and $\Delta g_{HWW}^{(4,5,6)}$: $\Delta g_{HVV}^{(4)}$ become redundant for on-shell h ; $\Delta g_{HVV}^{(5,6)}$ vanish for on-shell W_μ and Z_μ or massless fermions. Notice also that the leading chiral corrections include operators weighted by ξ powers up to ξ^2 . For the sake of

	Coeff. $\times e^2/4v$	Chiral $\times \xi$	$\times \xi^2$	Linear $\times v^2/\Lambda^2$
Δg_{Hgg}	$\frac{g^2}{e^2}$	$-2a_G$	—	$-4f_{GG}$
$\Delta g_{H\gamma\gamma}$	1	$-2(a_B + a_W) + 8a_1$	$8a_{12}$	$-(f_{BB} + f_{WW}) + f_{BW}$
$\Delta g_{HZZ}^{(1)}$	$\frac{1}{s_{2\theta}}$	$-8(a_5 + 2a_4)$	$-16a_{17}$	$2(f_W - f_B)$
$\Delta g_{HZZ}^{(2)}$	$\frac{c_\theta}{s_\theta}$	$4\frac{s_\theta^2}{c_\theta^2}a_B - 4a_W + 8\frac{c_{2\theta}}{c_\theta^2}a_1$	$16a_{12}$	$2\frac{s_\theta^2}{c_\theta^2}f_{BB} - 2f_{WW} + \frac{c_{2\theta}}{c_\theta^2}f_{BW}$
$\Delta g_{HZZ}^{(1)}$	$\frac{1}{c_\theta^2}$	$-4\frac{c_\theta^2}{s_\theta^2}a_5 + 8a_4$	$-8\frac{c_\theta^2}{s_\theta^2}a_{17}$	$\frac{c_\theta^2}{s_\theta^2}f_W + f_B$
$\Delta g_{HZZ}^{(2)}$	$-\frac{c_\theta^2}{s_\theta^2}$	$2\frac{s_\theta^4}{c_\theta^4}a_B + 2a_W + 8\frac{s_\theta^2}{c_\theta^2}a_1$	$-8a_{12}$	$\frac{s_\theta^4}{c_\theta^4}f_{BB} + f_{WW} + \frac{s_\theta^2}{c_\theta^2}f_{BW}$
$\Delta g_{HZZ}^{(3)}$	$\frac{m_Z^2}{e^2}$	$-2c_H + 2(2a_C - c_C) - 8(a_T - c_T)$	—	$f_{\Phi,1} + 2f_{\Phi,4} - 2f_{\Phi,2}$
$\Delta g_{HZZ}^{(4)}$	$-\frac{1}{s_{2\theta}^2}$	$16a_7$	$32a_{25}$	(*)
$\Delta g_{HZZ}^{(5)}$	$-\frac{1}{s_{2\theta}^2}$	$16a_{10}$	$32a_{19}$	(*)
$\Delta g_{HZZ}^{(6)}$	$-\frac{1}{s_{2\theta}^2}$	$16a_9$	$32a_{15}$	(*)
$\Delta g_{HWW}^{(1)}$	$\frac{1}{s_\theta^2}$	$-4a_5$	—	f_W
$\Delta g_{HWW}^{(2)}$	$\frac{1}{s_\theta^2}$	$-4a_W$	—	$-2f_{WW}$
$\Delta g_{HWW}^{(3)}$	$\frac{m_Z^2 c_\theta^2}{e^2}$	$-4c_H + 4(2a_C - c_C) + \frac{32e^2}{c_{2\theta}}c_1 + \frac{16c_\theta^2}{c_{2\theta}}c_T$	$-\frac{32e^2}{s_\theta^2}c_{12}$	$\frac{-2(3c_\theta^2 - s_\theta^2)}{c_{2\theta}}f_{\Phi,1} + 4f_{\Phi,4} - 4f_{\Phi,2} + \frac{4e^2}{c_{2\theta}}f_{BW}$
$\Delta g_{HWW}^{(4)}$	$-\frac{1}{s_\theta^2}$	$8a_7$	—	(*)
$\Delta g_{HWW}^{(5)}$	$-\frac{1}{s_\theta^2}$	$4a_{10}$	—	(*)
$\Delta g_{HWW}^{(6)}$	$-\frac{1}{s_\theta^2}$	$8a_9$	—	(*)

Table 2. The trilinear Higgs-gauge bosons couplings defined in eq. (4.8). The coefficients in the second column are common to both the chiral and linear expansions. The contributions from the operators weighted by ξ and $\xi^{\geq 2}$ are listed in the third and fourth columns, respectively. For comparison, the last column exhibits the corresponding expressions for the linear expansion at order $d = 6$. The star (*) in the last column indicates the link between the chiral operators $\mathcal{P}_7(h)$, $\mathcal{P}_9(h)$ and $\mathcal{P}_{10}(h)$, and their linear sibling $\mathcal{O}_{\square\Phi}$, without implying a physical impact of the latter on the observables considered, as explained in the text and in ref. [140].

comparison, the corresponding expressions in terms of the coefficients of the linear $d = 6$ operators in eq. (3.7) are also shown.¹³

Notice that the bosonic operators $\mathcal{P}_H(h)$ and $\mathcal{P}_C(h)$ induce universal shifts to the SM-like couplings of the Higgs to weak gauge bosons. Similarly $\mathcal{P}_H(h)$, induces universal shifts to the Yukawa couplings to fermions, see eq. (FR.32) in appendix D. It is straightforward to identify the link between the coefficients of these operators and the parameters a and c defined in refs. [17, 26, 62] assuming custodial invariance, which reads¹⁴

$$a = 1 - \frac{\xi c_H}{2} + \frac{\xi(2a_C - c_C)}{2}, \quad c = s_Y \left(1 - \frac{\xi c_H}{2} \right). \quad (4.11)$$

¹³Alternatively the coefficient of $\Delta g_{HWW}^{(3)}$ can be defined in terms of the *measured* value of M_W as M_W^2/e^2 . In this case the entries in columns 3–5 read $-4c_H + 4(2a_C - c_C)$, $-32\frac{e^2}{s_\theta^2}$, and $-2f_{\Phi,1} + 4f_{\Phi,4} - 4f_{\Phi,2}$ respectively.

¹⁴Supplementary terms are present when taking into account the custodial breaking couplings considered in this paper.

	Coeff.	Chiral		Linear
	$\times e^2/4s_\theta^2$	$\times \xi$	$\times \xi^2$	$\times v^2/\Lambda^2$
$\Delta g_{WW}^{(1)}$	1	$\frac{s_\theta^2}{e^2 c_{2\theta}} c_T + \frac{8s_\theta^2}{c_{2\theta}} c_1 + 4c_3$	$2c_{11} - 16c_{12} + 8c_{13}$	$\frac{f_W}{2} + \frac{s_\theta^2}{c_{2\theta}} f_{BW} - \frac{s_\theta^2}{4c_{2\theta} e^2} f_{\Phi 1}$
$\Delta g_{WW}^{(2)}$	1	$\frac{s_\theta^2}{e^2 c_{2\theta}} c_T + \frac{8s_\theta^2}{c_{2\theta}} c_1 + 4c_3 - 4c_6$	$-2c_{11} - 16c_{12} + 8c_{13}$	$\frac{f_W}{2} + \frac{s_\theta^2}{c_{2\theta}} f_{BW} - \frac{s_\theta^2}{4c_{2\theta} e^2} f_{\Phi 1} + (*)$
$\Delta g_{ZZ}^{(1)}$	$\frac{1}{c_\theta^4}$	c_6	$c_{11} + 2c_{23} + 2c_{24} + 4c_{26} \xi^2$	$(*)$
$\Delta g_{ZZ}^{(3)}$	$\frac{1}{c_\theta^2}$	$\frac{s_\theta^2 c_\theta^2}{e^2 c_{2\theta}} c_T + \frac{2s_\theta^2}{c_{2\theta}} c_1 + 4c_\theta^2 c_3 - 2s_\theta^4 c_9$	$2c_{11} + 4s_\theta^2 c_{16} + 2c_{24}$	$\frac{f_W c_\theta^2}{2} + \frac{s_\theta^2}{4c_{2\theta}} f_{BW} - \frac{s_\theta^2 c_\theta^2}{4e^2 c_{2\theta}} f_{\Phi 1} + (*)$
$\Delta g_{ZZ}^{(4)}$	$\frac{1}{c_\theta^2}$	$\frac{2s_\theta^2 c_\theta^2}{e^2 c_{2\theta}} c_T + \frac{4s_\theta^2}{c_{2\theta}} c_1 + 8c_\theta^2 c_3 - 4c_6$	$-4c_{23}$	$f_W c_\theta^2 + 2 \frac{s_\theta^2}{4c_{2\theta}} f_{BW} - \frac{s_\theta^2 c_\theta^2}{2e^2 c_{2\theta}} f_{\Phi 1} + (*)$
$\Delta g_{\gamma\gamma}^{(3)}$	s_θ^2	$-2c_9$	—	$(*)$
$\Delta g_{\gamma Z}^{(3)}$	$\frac{s_\theta}{c_\theta}$	$\frac{s_\theta^2}{e^2 c_{2\theta}} c_T + \frac{8s_\theta^2}{c_{2\theta}} c_1 + 4c_3 + 4s_\theta^2 c_9$	$-4c_{16}$	$\frac{f_W}{2} + \frac{s_\theta^2}{c_{2\theta}} f_{BW} - \frac{s_\theta^2}{4c_{2\theta} e^2} f_{\Phi 1} + (*)$
$\Delta g_{\gamma Z}^{(4)}$	$\frac{s_\theta}{c_\theta}$	$\frac{2s_\theta^2}{e^2 c_{2\theta}} c_T + \frac{16s_\theta^2}{c_{2\theta}} c_1 + 8c_3$	—	$f_W + 2 \frac{s_\theta^2}{c_{2\theta}} f_{BW} - \frac{s_\theta^2}{2c_{2\theta} e^2} f_{\Phi 1}$
$\Delta g_{\gamma Z}^{(5)}$	$\frac{s_\theta}{c_\theta}$	—	$8c_{14}$	—

Table 3. Effective couplings parametrizing the vertices of four gauge bosons defined in eq. (4.12). The contributions from the operators weighted by ξ and $\xi^{\geq 2}$ are listed in the third and fourth columns, respectively. For comparison, the last column exhibits the corresponding expressions for the linear expansion at order $d = 6$. The star (*) in the last column indicates the link between the chiral operators $\mathcal{P}_6(h)$ and $\mathcal{P}_9(h)$, and their linear sibling $\mathcal{O}_{\square\Phi}$, without implying a physical impact of the latter on the observables considered, as explained in the text and in ref. [140].

Quartic gauge-boson couplings. The quartic gauge boson couplings also receive contributions from the operators in eqs. (2.6)–(2.8). The corresponding effective Lagrangian reads

$$\begin{aligned}
 \mathcal{L}_{4X} \equiv g^2 \Big\{ & g_{ZZ}^{(1)} (Z_\mu Z^\mu)^2 + g_{WW}^{(1)} W_\mu^+ W^{+\mu} W_\nu^- W^{-\nu} - g_{WW}^{(2)} (W_\mu^+ W^{-\mu})^2 \\
 & + g_{VV'}^{(3)} W^{+\mu} W^{-\nu} (V_\mu V'_\nu + V'_\mu V_\nu) - g_{VV'}^{(4)} W_\nu^+ W^{-\nu} V^\mu V'_\mu \\
 & + i g_{VV'}^{(5)} \varepsilon^{\mu\nu\rho\sigma} W_\mu^+ W_\nu^- V_\rho V'_\sigma \Big\}, \quad (4.12)
 \end{aligned}$$

where $VV' = \{\gamma\gamma, \gamma Z, ZZ\}$. Notice that all these couplings are C and P even, except for $g_{VV'}^{(5)}$, that is CP even but both C and P odd. Some of these couplings are nonvanishing at tree-level in the SM:

$$\begin{aligned}
 g_{WW}^{(1)SM} &= \frac{1}{2}, & g_{WW}^{(2)SM} &= \frac{1}{2}, & g_{ZZ}^{(3)SM} &= \frac{c_\theta^2}{2}, & g_{\gamma\gamma}^{(3)SM} &= \frac{s_\theta^2}{2}, \\
 g_{Z\gamma}^{(3)SM} &= \frac{s_{2\theta}}{2}, & g_{ZZ}^{(4)SM} &= c_\theta^2, & g_{\gamma\gamma}^{(4)SM} &= s_\theta^2, & g_{Z\gamma}^{(4)SM} &= s_{2\theta},
 \end{aligned} \quad (4.13)$$

where the notation defined in eq. (4.9) has been used and the expression for the weak mixing angle can be found in eq. (4.2). Table 3 shows the contributions to the effective quartic couplings from the chiral operators in eqs. (2.6)–(2.8) and from the linear operator in eq. (3.3).

(De)correlation formulae. Some operators of the non-linear Lagrangian in section 2 participate in more than one of the couplings in tables 1 and 2. This fact leads to interesting series of relations that relate different couplings. First, simple relations on the TGV sector results:

$$\Delta\kappa_Z + \frac{s_\theta^2}{c_\theta^2}\Delta\kappa_\gamma - \Delta g_1^Z = \frac{16e^2}{s_\theta^2}(2c_{12} - c_{13})\xi^2, \quad (4.14)$$

$$\Delta g_6^\gamma + \frac{c_\theta^2}{s_\theta^2}\Delta g_6^Z = -\frac{e^2}{s_\theta^4}c_{16}\xi^2, \quad (4.15)$$

while other examples of relations involving HVV couplings are:

$$g_{HWW}^{(1)} - c_\theta^2 g_{HZZ}^{(1)} - c_\theta s_\theta g_{HZ\gamma}^{(1)} = \frac{2e^2}{vs_\theta^2}a_{17}\xi^2, \quad (4.16)$$

$$2c_\theta^2 g_{HZZ}^{(2)} + 2s_\theta c_\theta g_{HZ\gamma}^{(2)} + 2s_\theta^2 g_{H\gamma\gamma} - g_{HWW}^{(2)} = \frac{4e^2}{vs_\theta^2}a_{12}\xi^2, \quad (4.17)$$

$$\Delta g_{HZZ}^{(4)} - \frac{1}{2c_\theta^2}\Delta g_{HWW}^{(4)} = -\frac{8e^2}{vs_\theta^2}a_{25}\xi^2, \quad (4.18)$$

$$\Delta g_{HZZ}^{(5)} - \frac{1}{c_\theta^2}\Delta g_{HWW}^{(5)} = -\frac{8e^2}{vs_\theta^2}a_{19}\xi^2, \quad (4.19)$$

$$\Delta g_{HZZ}^{(6)} - \frac{1}{2c_\theta^2}\Delta g_{HWW}^{(6)} = -\frac{8e^2}{vs_\theta^2}a_{15}\xi^2 \quad (4.20)$$

The non-vanishing terms on the right-hand side of eqs. (4.14)–(4.17) stem from ξ^2 -weighted terms in the non-linear Lagrangian. It is interesting to note that they would vanish in the following cases: i) the $d = 6$ linear limit;¹⁵ ii) in the ξ -truncated non-linear Lagrangian; iii) in the custodial preserving limit. The first two relations with a vanishing right-hand side were already found in ref. [33]. Any hypothetical deviation from zero in the data combinations indicated by the left-hand side of those equations would thus be consistent with either $d = 8$ corrections of the linear expansion or a non-linear realisation of the underlying dynamics.

Furthermore, we found an interesting correlation which only holds in the linear regime at order $d = 6$, it mixes TGV and HVV couplings and stems from comparing tables 1 and 2:

$$\Delta\kappa_Z - \Delta g_1^Z = \frac{vs_\theta}{2c_\theta} \left[(c_\theta^2 - s_\theta^2) \left(g_{HZ\gamma}^{(1)} + 2g_{HZ\gamma}^{(2)} \right) + 2s_\theta c_\theta \left(2g_{H\gamma\gamma} - g_{HZZ}^{(1)} - 2g_{HZZ}^{(2)} \right) \right]. \quad (4.21)$$

This relation does not hold in the non-linear regime, not even when only ξ -weighted operators are considered. Its verification from experimental data would be an excellent test of BSM physics in which the EWSB is linearly realized and dominated by $d = 6$ corrections.

The above general (de)correlations are a few examples among many [68].

¹⁵Eq. (4.14) with vanishing right-hand side was already known [76, 102] to hold in the linear regime at order $d = 6$.

When in addition the strong experimental constraints on the S and T parameters are applied, disregarding thus c_T and c_1 (equivalently, $f_{\phi 1}$ and f_{BW} for the linear case), supplementary constraints follow, e.g.:

$$\begin{aligned}
 \frac{2}{m_Z^2} g_{HZZ}^{(3)} - \frac{1}{m_W^2 + \delta m_W^2} g_{HWW}^{(3)} &= \frac{16e^2}{v s_\theta^2} a_{12} \xi^2, \\
 2g_{H\gamma\gamma} + \frac{c_\theta}{s_\theta} g_{HZZ\gamma}^{(2)} - g_{HWW}^{(2)} &= -\frac{4e^2}{v s_\theta^2} a_{12} \xi^2, \\
 2g_{HZZ}^{(2)} + \frac{s_\theta}{c_\theta} g_{HZZ\gamma}^{(2)} - g_{HWW}^{(2)} &= -\frac{4e^2}{v s_\theta^2} a_{12} \xi^2, \\
 \frac{-2s_\theta^2}{c_\theta^2 - s_\theta^2} g_{H\gamma\gamma} + \frac{2c_\theta^2}{c_\theta^2 - s_\theta^2} g_{HZZ}^{(2)} - g_{HWW}^{(2)} &= -\frac{4e^2}{v s_\theta^2} a_{12} \xi^2,
 \end{aligned} \tag{4.22}$$

where again the non-zero entries on the right-hand sides vanish in either the $d = 6$ linear or the ξ -truncated non-linear limits.

Counting of degrees of freedom for the HVV Lagrangian. Given the present interest in the gauge- h sector, we analyze here the number of degrees of freedom involved in the HVV Lagrangian, eq. (4.8), for on-shell and off-shell gauge and Higgs bosons, with massive and massless fermions.

This can be schematically resumed as follows: for the massive fermion case,

$$\begin{array}{ll}
 \text{phen. couplings: } 16 \xrightarrow{\text{i)}} 12 \ (\Delta g_{HVV}^{5,6} = 0) & \xrightarrow{\text{ii)}} 10 \ (\Delta g_{HVV}^4 \text{ redundant}) \\
 \text{op. coefficients: } 17 \xrightarrow{\text{i)}} 13 \ (\mathcal{P}_{11}, \mathcal{P}_{12}, \mathcal{P}_{16}, \mathcal{P}_{17} \text{ irrelevant}) & \xrightarrow{\text{ii)}} 11 \ (\mathcal{P}_7, \mathcal{P}_{25} \text{ redundant})
 \end{array}$$

where the first line refers to the phenomenological couplings appearing in eq. (4.8), while the second one to the operator coefficients of the non-linear basis in eq. (2.5). Moreover, i) denotes the limit of on-shell gauge bosons, i.e. $\partial^\mu Z_\mu = 0$ and $\partial^\mu W_\mu^\pm = 0$, while ii) refers to the limit of, in addition, on-shell h . In brackets we indicate the couplings and the operator coefficients that are irrelevant or redundant under the conditions i) or ii).

If fermion masses are set to zero, the conditions $\partial^\mu Z_\mu = 0$ and $\partial^\mu W_\mu^\pm = 0$ hold also for off-shell gauge bosons, and therefore the counting starts with 12 phenomenological couplings and 13 operator coefficients.

This analysis for the number of operator coefficients refers to the full non-linear Lagrangian in eq. (2.5), which includes the custodial breaking operators.

Up to this point, as well as in appendices A, C and D for the EOM, $d = 6$ siblings and Feynman rules, respectively, all non-linear pure gauge and gauge- h operators of the chiral Lagrangian eq. (2.1) have been taken into account. The next subsection describes the results of the numerical analysis, and there instead the value of fermion masses on external legs will be neglected. This means that operators $\mathcal{P}_9(h)$, $\mathcal{P}_{10}(h)$, $\mathcal{P}_{15}(h)$, $\mathcal{P}_{16}(h)$, and $\mathcal{P}_{19-21}(h)$ become redundant then, and will not be analyzed.

4.2 Present bounds on operators weighted by ξ

At present, the most precise determination of S , T , U from a global fit to electroweak precision data (EWPd) yields the following values and correlation matrix [99]

$$\Delta S = 0.00 \pm 0.10 \quad \Delta T = 0.02 \pm 0.11 \quad \Delta U = 0.03 \pm 0.09 \quad (4.23)$$

$$\rho = \begin{pmatrix} 1 & 0.89 & -0.55 \\ 0.89 & 1 & -0.8 \\ -0.55 & -0.8 & 1 \end{pmatrix}. \quad (4.24)$$

Operators $\mathcal{P}_1(h)$ and $\mathcal{P}_T(h)$ contribute at tree-level to these observables, see eq. (4.6) and consequently they are severely constrained. The corresponding 95% CL allowed ranges for their coefficients read

$$-4.7 \times 10^{-3} \leq \xi_{c_1} \leq 4 \times 10^{-3} \quad \text{and} \quad -2 \times 10^{-3} \leq \xi_{c_T} \leq 1.7 \times 10^{-3}. \quad (4.25)$$

These constraints render the contribution of $\mathcal{P}_1(h)$ and $\mathcal{P}_T(h)$ to the gauge-boson self-couplings and to the present Higgs data too small to give any observable effect. Consequently we will not include them in the following discussion.

As for the ξ -weighted TGV contributions from $\mathcal{P}_2(h)$ and $\mathcal{P}_3(h)$, their impact on the coefficients $\Delta\kappa_\gamma$, Δg_1^Z and $\Delta\kappa_Z$ was described in table 1. At present, the most precise determination of TGV in this scenario results from the two-dimensional analysis in ref. [103] which was performed in terms of $\Delta\kappa_\gamma$ and Δg_1^Z with $\Delta\kappa_Z$ determined by the relation eq. (4.14) with the right-handed side set to zero:

$$\kappa_\gamma = 0.984_{-0.049}^{+0.049} \quad \text{and} \quad g_1^Z = 1.004_{-0.025}^{+0.024}, \quad (4.26)$$

with a correlation factor $\rho = 0.11$. In table 4 we list the corresponding 90% CL allowed ranges on the coefficients c_2 and c_3 from the analysis of the TGV data.

Now, let us focus on the constraints on ξ -weighted operators stemming from the presently available Higgs data on HVV couplings. There are seven bosonic operators in this category¹⁶

$$\mathcal{P}_G(h), \mathcal{P}_4(h), \mathcal{P}_5(h), \mathcal{P}_B(h), \mathcal{P}_W(h), \mathcal{P}_H(h), \mathcal{P}_C(h). \quad (4.27)$$

To perform a seven-parameter fit to the present Higgs data is technically beyond the scope of this paper and we will consider sets of “only” six of them simultaneously. We are presenting below two such analysis. Leaving out a different coupling in each set. In the first one, **A**, we will neglect $\mathcal{P}_C(h)$ and in the second one, **B**, we will link its contribution to that of $\mathcal{P}_H(h)$, so the 6 parameters in each set read:

$$\textbf{Set A :} \quad a_G, a_4, a_5, a_B, a_W, c_H, 2a_C - c_C = 0, \quad (4.28)$$

$$\textbf{Set B :} \quad a_G, a_4, a_5, a_B, a_W, c_H = 2a_C - c_C. \quad (4.29)$$

¹⁶In present Higgs data analysis, the Higgs state is on-shell and in this case $\Delta g_{HVV}^{(4)}$ can be recasted as a m_H^2 correction to $\Delta g_{HVV}^{(3)}$. Thus the contribution from c_7 , i.e. the coefficient of $\mathcal{P}_7(h)$ to the Higgs observables, can be reabsorbed in a redefinition of $2a_C - c_C$.

For both sets we will explore the sensitivity of the results to the sign of the h -fermion couplings by performing analysis with both values of the discrete parameter $s_Y = \pm$.

As mentioned above, $\mathcal{P}_H(h)$ and $\mathcal{P}_C(h)$ induce a universal shift to the SM-like HVV couplings involving electroweak gauge bosons, see eq. (FR.15) and (FR.17), while $\mathcal{P}_H(h)$ also induces a universal shift to the Yukawa Higgs-fermion couplings, see eq. (FR.32). In consequence, the two sets above correspond to the case in which the shift of the Yukawa Higgs-fermion couplings is totally unrelated to the modification of the HVV couplings involving electroweak bosons (**set B**), and to the case in which the shift of SM-like HVV couplings involving electroweak bosons and to the Yukawa Higgs-fermion couplings are the same (**set A**). In both sets we keep all other five operators which induce modifications of the HVV couplings with different Lorentz structures than those of the SM as well as tree-level contributions to the loop-induced vertices $h\gamma\gamma$, $h\gamma Z$ and hgg .

Notice also that a combination of $\mathcal{P}_H(h)$ and $\mathcal{P}_C(h)$ can be traded via the EOM (see third line in eq. (A.11)) by that of fermion-Higgs couplings $\mathcal{P}_{f,\alpha\beta}(h)$ plus that of other operators already present in the six-dimensional gauge- h set analyzed. So our choice allows us to stay close to the spirit of this work (past and future data confronting directly the gauge and gauge- h sector), while performing a powerful six-dimensional exploration of possible correlations.

Technically, in order to obtain the present constraints on the coefficients of the bosonic operators listed in eqs. (4.28) and (4.29) we perform a chi-square test using the available data on the signal strengths (μ). We took into account data from Tevatron D0 and CDF Collaborations and from LHC, CMS, and ATLAS Collaborations at 7 TeV and 8 TeV for final states $\gamma\gamma$, W^+W^- , ZZ , $Z\gamma$, $b\bar{b}$, and $\tau\bar{\tau}$ [104–117]. For CMS and ATLAS data, the included results on W^+W^- , ZZ and $Z\gamma$ correspond to leptonic final states, while for $\gamma\gamma$ all the different categories are included which in total accounts for 56 data points. We refer the reader to refs. [9, 78] for details of the Higgs data analysis.

The results of the analysis are presented in figure 1 which displays the chi-square ($\Delta\chi_{\text{Higgs}}^2$) dependence from the analysis of the Higgs data on the six bosonic couplings for the two sets **A** and **B** of operators and for the two values of the discrete parameter $s_Y = \pm$. In each panel $\Delta\chi_{\text{Higgs}}^2$ is shown after marginalizing over the other five parameters. As seen in this figure, there are no substantial difference between both sets in the determination of the five common parameters with only slight differences in a_G (more below). The quality of the fit is equally good for both sets ($|\chi_{\text{min,A}}^2 - \chi_{\text{min,B}}^2| < 0.5$). The SM lays at $\chi_{SM}^2 = 68.1$ within the 4% CL region in the six dimensional parameter space of either set.

In figure 1, for each set, the two curves of $\Delta\chi_{\text{Higgs}}^2$ for $s_Y = \pm$ are defined with respect to the same χ_{min}^2 corresponding to the minimum value of the two signs. However, as seen in the figure, the difference is inappreciable. In other words, we find that in both six-parameter analysis the quality of the description of the data is equally good for both signs of the h -fermion couplings. Quantitatively for either set $|\chi_{\text{min,+}}^2 - \chi_{\text{min,-}}^2|$ is compatible with zero within numerical accuracy. If all the anomalous couplings are set to zero the quality of the fit is dramatically different for both signs with $\chi_-^2 - \chi_+^2 = 26$. This arises from the different sign of the interference between the W - and top-loop contributions to $h\gamma\gamma$ which is negative for the SM value $s_Y = +$ and positive for $s_Y = -$ which increases

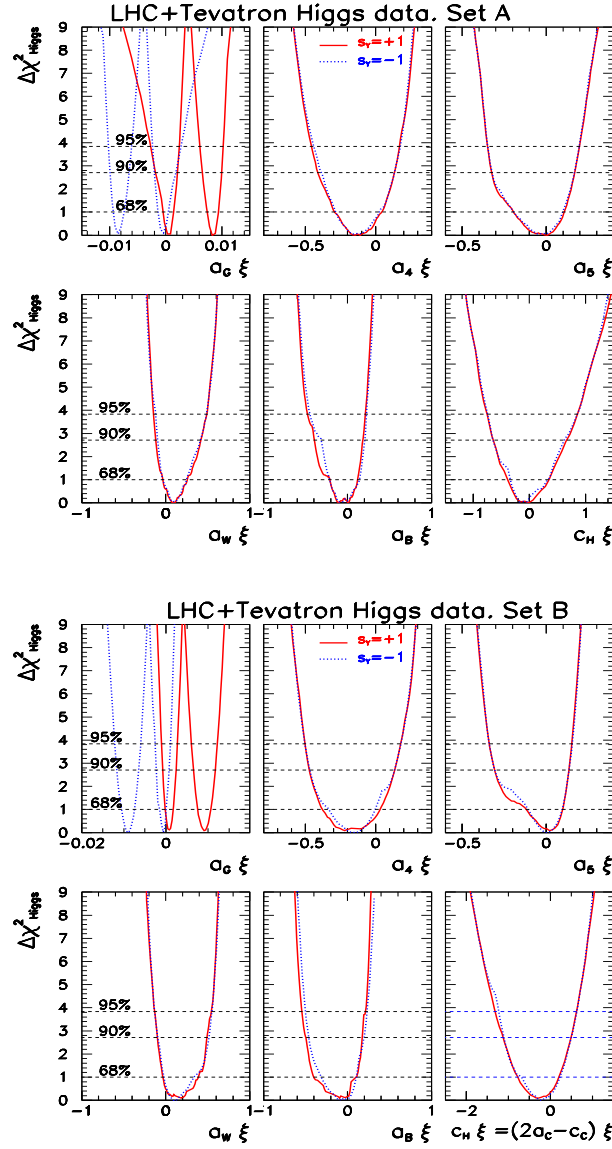


Figure 1. $\Delta\chi_{\text{Higgs}}^2$ dependence on the coefficients of the seven bosonic operators in eq. (4.27) from the analysis of all Higgs collider (ATLAS, CMS and Tevatron) data. In each panel, we marginalized over the five undisplayed variables. The six upper (lower) panels corresponds to analysis with set **A** (**B**). In each panel the red solid (blue dotted) line stands for the analysis with the discrete parameter $s_Y = +(-)$.

$BR_-(h \rightarrow \gamma\gamma)/BR_{SM}(h \rightarrow \gamma\gamma) \sim 2.5$, a value strongly disfavoured by data. However, once the effect of the 6 bosonic operators is included — in particular that of $\mathcal{P}_B(h)$ and $\mathcal{P}_W(h)$ which give a tree-level contribution to the $h\gamma\gamma$ vertex — we find that both signs of the h -fermion couplings are equally probable.

In the figure we also see that in all cases $\Delta\chi_{\text{Higgs}}^2$ as a function of a_G exhibits two degenerate minima. They are due to the interference between SM and anomalous contributions

	90% CL allowed range	
	Set A	Set B
$a_G \xi (\cdot 10^{-3})$	$s_Y = +1: [-1.8, 2.1] \cup [6.5, 10]$	$s_Y = +1: [-0.78, 2.4] \cup [6.5, 12]$
	$s_Y = -1: [-9.9, -6.5] \cup [-2.1, 1.8]$	$s_Y = -1: [-12, -6.5] \cup [-2.3, 0.75]$
$a_4 \xi$	[-0.47, 0.14]	
$a_5 \xi$	[-0.33, 0.17]	
$a_W \xi$	[-0.12, 0.51]	
$a_B \xi$	[-0.50, 0.21]	
$c_H \xi$	[-0.66, 0.66]	[-1.1, 0.49]
$c_2 \xi$	[-0.12, 0.076]	
$c_3 \xi$	[-0.064, 0.079]	

Table 4. 90% CL allowed ranges of the coefficients of the operators contributing to Higgs data (a_G , a_4 , a_5 , a_W , a_B , and c_H) and to TGV (c_2 and c_3). For the coefficients a_4 , a_5 , a_W , and a_B , for which the range is almost the same for analysis with both sets and both values of s_Y we show the inclusive range of the four analysis. For c_H the allowed range is the same for both signs of s_Y .

possessing exactly the same momentum dependence. Around the secondary minimum the anomalous contribution is approximately twice the one due to the top-loop but with an opposite sign. The gluon fusion Higgs production cross section is too depleted for a_G values between the minima, giving rise to the intermediate barrier. Obviously the allowed values of a_G around both minima are different for $s_Y = +$ and $s_Y = -$ as a consequence of the different relative sign of the a_G and the top-loop contributions to the hgg vertex. In the convention chosen for the chiral Lagrangian, the relative sign of both contributions is negative (positive) for $s_Y = +$, ($s_Y = -$) so that the non-zero minimum occurs for a_G around 0.01 (-0.01). The precise value of the a_G coupling at the minima is slightly different for the analysis with set **A** and **B** due to the effect of the coefficient c_H near the minima, which shifts the contribution of the top-loop by a slightly different quantity in both analysis.

Figure 1 also shows that in all cases the curves for a_4 and a_5 are almost “mirror symmetric”. This is due to the strong anticorrelation between those two coefficients, because they are the dominant contributions to the Higgs branching ratio into two photons, which is proportional to $a_4 + a_5$. In table 4 we list the corresponding 90% CL allowed ranges for the six coefficients, for the different variants of the analysis. With the expected uncertainties attainable in the Higgs signal strengths in CMS and ATLAS at 14 TeV with an integrated luminosity of 300 fb^{-1} [118, 119], we estimate that the sensitivity to those couplings can improve by a factor $\mathcal{O}(3 - 5)$ with a similar analysis.

We finish by stressing that in the context of ξ -weighted operators in the chiral expansion the results from TGV analysis and those from the HVV analysis apply to two independent sets of operators as discussed in section 3.2. This is unlike the case of the linear expansion

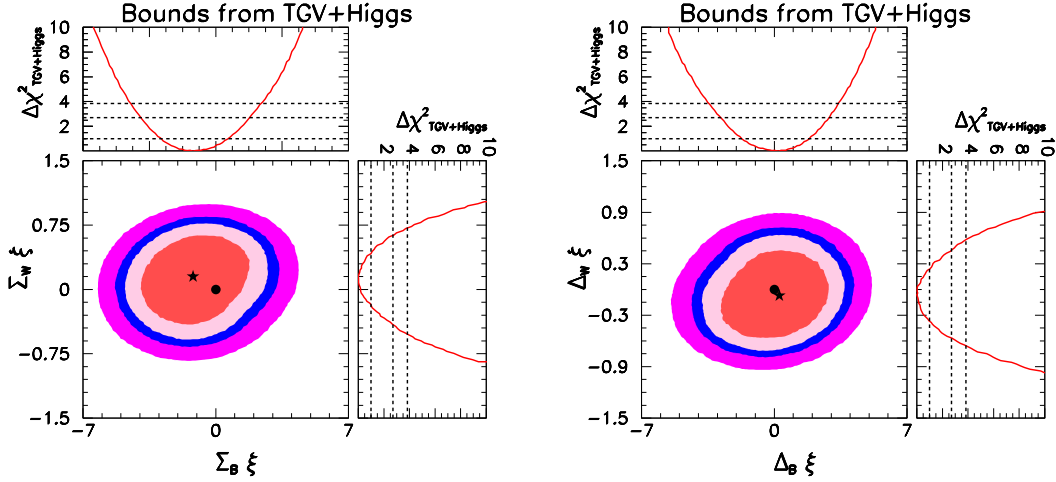


Figure 2. *Left:* A BSM sensor irrespective of the type of expansion: constraints from TGV and Higgs data on the combinations $\Sigma_B = 4(2c_2 + a_4)$ and $\Sigma_W = 2(2c_3 - a_5)$, which converge to f_B and f_W in the linear $d = 6$ limit. The dot at $(0, 0)$ signals the SM expectation. *Right:* A non-linear versus linear discriminator: constraints on the combinations $\Delta_B = 4(2c_2 - a_4)$ and $\Delta_W = 2(2c_3 + a_5)$, which would take zero values in the linear (order $d = 6$) limit (as well as in the SM), indicated by the dot at $(0, 0)$. For both figures the lower left panels shows the 2-dimensional allowed regions at 68%, 90%, 95%, and 99% CL after marginalization with respect to the other six parameters ($a_G, a_W, a_B, c_H, \Delta_B$, and Δ_W) and ($a_G, a_W, a_B, c_H, \Sigma_B$, and Σ_W) respectively. The star corresponds to the best fit point of the analysis. The upper left and lower right panels give the corresponding 1-dimensional projections over each of the two combinations.

for which $2c_2 = a_4$ and $2c_3 = -a_5$, which establishes an interesting complementarity in the experimental searches for new signals in TGV and HVV couplings in the linear regime [78]. Conversely, in the event of some anomalous observation in either of these two sectors, the presence of this (de)correlation would allow for direct testing of the nature of the Higgs boson. This is illustrated in figure 2, where the results of the combined analysis of the TGV and HVV data are projected into combinations of the coefficients of the operators $\mathcal{P}_2(h)$, $\mathcal{P}_3(h)$, $\mathcal{P}_4(h)$ and $\mathcal{P}_5(h)$:

$$\begin{aligned} \Sigma_B &\equiv 4(2c_2 + a_4), & \Sigma_W &\equiv 2(2c_3 - a_5), \\ \Delta_B &\equiv 4(2c_2 - a_4), & \Delta_W &\equiv 2(2c_3 + a_5), \end{aligned} \quad (4.30)$$

defined such that at order $d = 6$ of the linear regime $\Sigma_B = c_B$, $\Sigma_W = c_W$, while $\Delta_B = \Delta_W = 0$. With these variables, the $(0, 0)$ coordinate corresponds to the SM in figure 2 left panel, while in figure 2 right panel it corresponds to the linear regime (at order $d = 6$). Would future data point to a departure from $(0, 0)$ in the variables of the first figure it would indicate BSM physics irrespective of the linear or non-linear character of the underlying dynamics; while such a departure in the second figure would be consistent with a non-linear realization of EWSB. For concreteness the figures are shown for the $s_Y = +$ analysis with set **A**, but very similar results hold for the other variants of the analysis.

	Measurement ($\pm 68\%$ CL region)	95% CL region	
Experiment	g_5^Z	g_5^Z	$c_{14}\xi^2$
OPAL [120]	$-0.04^{+0.13}_{-0.12}$	$[-0.28, 0.21]$	$[-0.16, 0.12]$
L3 [121]	$0.00^{+0.13}_{-0.13}$	$[-0.21, 0.20]$	$[-0.12, 0.11]$
ALEPH [122]	$-0.064^{+0.13}_{-0.13}$	$[-0.317, 0.19]$	$[-0.18, 0.11]$
90% CL region from indirect bounds [123–125]		$g_5^Z: [-0.08, 0.04]$	$c_{14}\xi^2: [-0.04, 0.02]$

Table 5. Existing direct measurements of g_5^Z coming from LEP analyses [120–122] as well as the strongest constraints from the existing indirect bounds on g_5^Z in the literature [123–125]. In the last column we show the translated bounds on $c_{14}\xi^2$. These bounds were obtained assuming only g_5^Z different from zero while the rest of anomalous TGV were set to the SM values.

4.3 ξ^2 -weighted couplings: LHC potential to study g_5^Z

One interesting property of the ξ^2 -chiral Lagrangian is the presence of operator $\mathcal{P}_{14}(h)$ that generates a non-vanishing g_5^Z TGV, which is a C and P odd, but CP even operator; see eq. (4.7). Presently, the best direct limits on this anomalous coupling come from the study of W^+W^- pairs and single W production at LEP II energies [120–122]. Moreover, the strongest bounds on g_5^Z originate from its impact on radiative corrections to Z physics [123–125]; see table 5 for the available direct and indirect limits on g_5^Z .

We can use the relation in table 1 to translate the existing bounds on g_5^Z into limits on $\mathcal{P}_{14}(h)$. The corresponding limits can be seen in the last column of table 5. We note here that these limits were obtained assuming only a non-vanishing g_5^Z while the rest of anomalous TGV were set to their corresponding SM value.

At present, the LHC collaborations have presented some data analyses of anomalous TGV [126–130] but in none of them have they included the effects of g_5^Z . A preliminary study on the potential of LHC 7 to constrain this coupling was presented in ref. [131] where it was shown that the LHC 7 with a very modest luminosity had the potential of probing g_5^Z at the level of the present indirect bounds. In ref. [131] it was also discussed the use of some kinematic distributions to characterize the presence of a non-vanishing g_5^Z . So far the LHC has already collected almost 25 times more data than the luminosity considered in this preliminary study which we update here. Furthermore, in this update we take advantage of a more realistic background evaluation, by using the results of the experimental LHC analysis on other anomalous TGV couplings [126].

At the LHC, the anomalous coupling g_5^Z contributes to WW and WZ pair production, with the strongest limits originating from the last reaction [131]. Hence, the present study is focused on the WZ production channel, where we consider only the leptonic decays of the gauge bosons for a better background suppression, i.e., we analyze the reaction

$$pp \rightarrow \ell'^{\pm} \ell^+ \ell^- E_T^{miss}, \quad (4.31)$$

where $\ell^{(\prime)} = e$ or μ . The main background for the g_5^Z analysis is the irreducible SM production of WZ pairs. There are further reducible backgrounds like W or Z production with jets, ZZ production followed by the leptonic decay of the Z 's with one charged lepton escaping detection and $t\bar{t}$ pair production.

We simulated the signal and the SM irreducible background using an implementation of the anomalous operator g_5^Z in FeynRules [132] interfaced with MadGraph 5 [133] for event generation. We account for the different detection efficiencies by rescaling our simulation to the one done by ATLAS [126] for the study of $\Delta\kappa_Z$, g_1^Z and λ_Z . However, we also cross checked the results using a setup where the signal simulation is based on the same FeynRules [132] and MadGraph5 [133] implementation, interfaced then with PYTHIA [134] for parton shower and hadronization and with PGS 4 [135] for detector simulation. Finally, the reducible backgrounds for the 7 TeV analysis were obtained from the simulations presented in the ATLAS search [126], and they were properly rescaled for the 8 TeV and 14 TeV runs.

In order to make our simulations more realistic, we closely follow the TGV analysis performed by ATLAS [126]. Thus, the kinematic study of the WZ production starts with the usual detection and isolation cuts on the final state leptons. Muons are considered if their transverse momentum with respect to the collision axis z , $p_T \equiv \sqrt{p_x^2 + p_y^2}$, and pseudorapidity $\eta \equiv \frac{1}{2} \ln \frac{|\vec{p}| + p_z}{|\vec{p}| - p_z}$, satisfy

$$p_T^\ell > 15 \text{ GeV} , \quad |\eta^\mu| < 2.5 . \quad (4.32)$$

Electrons must comply with the same transverse momentum requirement than that applied to muons; however, the electron pseudo-rapidity cut is

$$|\eta^e| < 1.37 \text{ or } 1.52 < |\eta^e| < 2.47 . \quad (4.33)$$

To guarantee the isolation of muons (electrons), we required that the scalar sum of the p_T of the particles within $\Delta R \equiv \sqrt{\Delta\eta^2 + \Delta\phi^2} = 0.3$ of the muon (electron), excluding the muon (electron) track, is smaller than 15% (13%) of the charged lepton p_T . In the case where the final state contains both muons and electrons, a further isolation requirement has been imposed:

$$\Delta R_{e\mu} > 0.1 . \quad (4.34)$$

It was also required that at least two leptons with the same flavour and opposite charge are present in the event and that their invariant mass is compatible with the Z mass, i.e.

$$M_{\ell^+\ell^-} \in [M_Z - 10, \quad M_Z + 10] \text{ GeV} . \quad (4.35)$$

A further constraint imposed is that a third lepton is present which passes the above detection requirements and whose transverse momentum satisfies

$$p_T^\ell > 20 \text{ GeV} . \quad (4.36)$$

Moreover, with the purpose of suppressing most of the Z +jets and other diboson production background, we required

$$E_T^{\text{miss}} > 25 \text{ GeV and } M_T^W > 20 \text{ GeV} , \quad (4.37)$$

where E_T^{miss} is the missing transverse energy and the transverse mass is defined as

$$M_T^W = \sqrt{2p_T^\ell E_T^{\text{miss}} (1 - \cos(\Delta\phi))} , \quad (4.38)$$

with p_T^ℓ being the transverse momentum of the third lepton, and where $\Delta\phi$ is the azimuthal angle between the missing transverse momentum and the third lepton. Finally, it was required that at least one electron or one muon has a transverse momentum complying with

$$p_T^{e(\mu)} > 25 \text{ (20) GeV} . \quad (4.39)$$

Our Monte Carlo simulations have been tuned to the ATLAS ones [126], so as to incorporate more realistic detection efficiencies. Initially, a global k -factor was introduced to account for the higher order corrections to the process in eq. (4.31) by comparing our leading order prediction to the NLO one used in the ATLAS search [126], leading to $k \sim 1.7$. Next, we compared our results after cuts with the ones quoted by ATLAS in table 1 of ref. [126]. We tuned our simulation by applying a correction factor per flavour channel (eee , $ee\mu$, $e\mu\mu$ and $\mu\mu\mu$) that is equivalent to introducing a detection efficiency of $\epsilon^e = 0.8$ for electrons and $\epsilon^\mu = 0.95$ for muons. These efficiencies have been employed in our simulations for signal and backgrounds.

After applying all the above cuts and efficiencies, the cross section for the process (4.31) in the presence of a non-vanishing g_5^Z can be written as¹⁷

$$\sigma = \sigma_{\text{bck}} + \sigma_{SM} + \sigma_{\text{int}} g_5^Z + \sigma_{\text{ano}} (g_5^Z)^2 , \quad (4.40)$$

where σ_{SM} denotes the SM contribution to $W^\pm Z$ production, σ_{int} stands for the interference between this SM process and the anomalous g_5^Z contribution and σ_{ano} is the pure anomalous contribution. Furthermore, σ_{bck} corresponds to all background sources except for the SM EW $W^\pm Z$ production. We present in table 6 the values of σ_{SM} , σ_{int} and σ_{ano} for center-of-mass energies of 7, 8 and 14 TeV, as well as the cross section for the reducible backgrounds.

In order to quantify the expected limits on g_5^Z , advantage has been taken in this analysis of the fact that anomalous TGVs enhance the cross sections at high energies. Ref. [131] shows that the variables M_{WZ}^{rec} (the reconstructed $W-Z$ invariant mass), $p_T^{\ell \text{ max}}$ and p_T^Z are able to trace well this energy dependence, leading to similar sensitivities to the anomalous TGV. Here, we chose p_T^Z to study g_5^Z because this variable is strongly correlated with the subprocess center-of-mass energy (\hat{s}), and, furthermore, it can be directly reconstructed with good precision from the measured lepton momenta. The left (right) panel of figure 3 depicts the number of expected events with respect to the Z transverse momentum for the

¹⁷We assumed in this study that all anomalous TGV vanish except for g_5^Z .

COM Energy	σ_{bck} (fb)	σ_{SM} (fb)	σ_{int} (fb)	σ_{ano} (fb)
7 TeV	14.3	47.7	6.5	304
8 TeV	16.8	55.3	6.6	363
14 TeV	29.0	97.0	9.1	707

Table 6. Values of the cross section predictions for the process $pp \rightarrow \ell'^{\pm} \ell^{+} \ell^{-} E_T^{\text{miss}}$ after applying all the cuts described in the text. σ_{SM} is the SM contribution coming from EW $W^{\pm}Z$ production, σ_{int} is the interference between this SM process and the anomalous g_5^Z contribution, σ_{ano} is the pure anomalous contribution and σ_{bck} corresponds to all background sources except for the SM EW $W^{\pm}Z$ production.

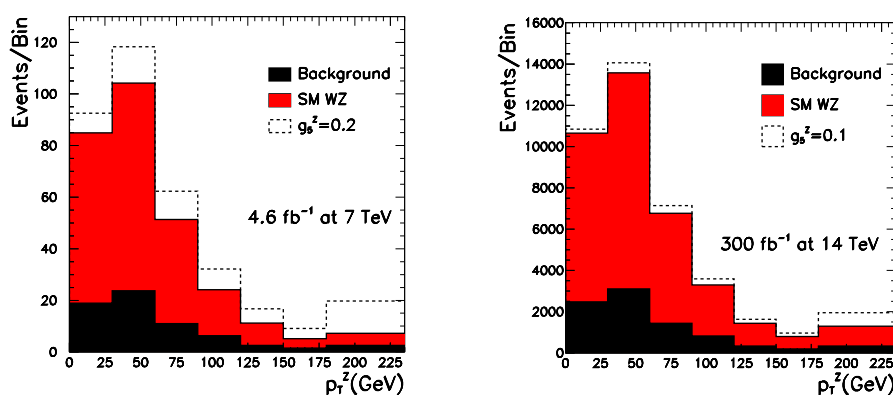


Figure 3. The left (right) panel displays the number of expected events as a function of the Z transverse momentum for a center-of-mass energy of 7 (14) TeV, assuming an integrated luminosity of 4.64 (300) fb^{-1} . The black histogram corresponds to the sum of all background sources except for the SM electroweak $pp \rightarrow W^{\pm}Z$ process, while the red histogram corresponds to the sum of all SM backgrounds, and the dashed distribution corresponds to the addition of the anomalous signal for $g_5^Z = 0.2$ ($g_5^Z = 0.1$). The last bin contains all the events with $p_T^Z > 180$ GeV.

7 (14) TeV run and an integrated luminosity of 4.64 (300) fb^{-1} . As illustrated by this figure, the existence of an anomalous g_5^Z contribution enhances the tail of the p_T^Z spectrum, signaling the existence of new physics.

Two procedures have been used to estimate the LHC potential to probe anomalous g_5^Z couplings. In the first approach, we performed a simple event counting analysis assuming that the number of observed events correspond to the SM prediction ($g_5^Z = 0$) and we look for the values of g_5^Z which are inside the 68% and 95% CL allowed regions. As suggested by ref. [131], the following additional cut was applied in this analysis to enhance the sensitivity to g_5^Z :

$$p_T^Z > 90 \text{ GeV}. \quad (4.41)$$

On a second analysis, a simple χ^2 was built based on the contents of the different bins of

Data sets used	68% CL range		95% CL range	
	Counting $p_T^Z > 90$ GeV	p_T^Z binned analysis	Counting $p_T^Z > 90$ GeV	p_T^Z binned analysis
7+8 TeV (4.64+19.6 fb ⁻¹)	(−0.066, 0.058)	(−0.057, 0.050)	(−0.091, 0.083)	(−0.080, 0.072)
7+8+14 TeV (4.64+19.6+300 fb ⁻¹)	(−0.030, 0.022)	(−0.024, 0.019)	(−0.040, 0.032)	(−0.033, 0.028)

Table 7. Expected sensitivity on g_5^Z at the LHC for the two different procedures described in the text.

the p_T^Z distribution, in order to obtain more stringent bounds. The binning used is shown in figure 3. Once again, it was assumed that the observed p_T^Z spectrum corresponds to the SM expectations and we sought for the values of g_5^Z that are inside the 68% and 95% allowed regions. The results of both analyses are presented in table 7.

We present in the first row of table 7 the expected LHC limits for the combination of the 7 TeV and 8 TeV existing data sets, where we considered an integrated luminosity of 4.64 fb⁻¹ for the 7 TeV run and 19.6 fb⁻¹ for the 8 TeV one. Therefore, the attainable precision on g_5^Z at the LHC 7 and 8 TeV runs is already higher than the present direct bounds stemming from LEP and it is also approaching the present indirect limits. Finally, the last row of table 7 displays the expected precision on g_5^Z when the 14 TeV run with an integrated luminosity of 300 fb⁻¹ is included in the combination. Here, once more, it was assumed that the observed number of events is the SM expected one. The LHC precision on g_5^Z will approach the per cent level, clearly improving the present both direct and indirect bounds.

4.4 Anomalous quartic couplings

As shown in section 3.4, in the chiral expansion several operators weighted by ξ or higher powers contribute to quartic gauge boson vertices without inducing any modification to TGVs. Therefore, their coefficients are much less constrained at present, and one can expect still larger deviations on future studies of quartic vertices at LHC for large values of ξ . This is unlike in the linear expansion, in which the modifications of quartic gauge couplings that do not induce changes to TGVs appear only when the $d = 8$ operators are considered [83]. For instance, the linear operators similar to $\mathcal{P}_6(h)$ and $\mathcal{P}_{11}(h)$ are $\mathcal{L}_{S,0}$ and $\mathcal{L}_{S,1}$ in ref. [83].

Of the five operators giving rise to purely quartic gauge boson vertices ($\mathcal{P}_6(h)$, $\mathcal{P}_{11}(h)$, $\mathcal{P}_{23}(h)$, $\mathcal{P}_{24}(h)$, $\mathcal{P}_{26}(h)$), none modifies quartic vertices including photons while all generate the anomalous quartic vertex $ZZZZ$ that is not present in the SM. Moreover, all these operators but $\mathcal{P}_{26}(h)$ modify the ZZW^+W^- vertex, while only $\mathcal{P}_6(h)$ and $\mathcal{P}_{11}(h)$ also induce anomalous contributions to $W^+W^-W^+W^-$.

Presently, the most stringent bounds on the coefficients of these operators are indirect, from their one-loop contribution to the EWPD derived in ref. [79] where it was shown that

coupling	90% CL allowed region
$c_6 \xi$	$[-0.23, 0.26]$
$c_{11} \xi^2$	$[-0.094, 0.10]$
$c_{23} \xi^2$	$[-0.092, 0.10]$
$c_{24} \xi^2$	$[-0.012, 0.013]$
$c_{26} \xi^4$	$[-0.0061, 0.0068]$

Table 8. 90% CL limits on the anomalous quartic couplings from their one-loop contribution to the EWPD. The bounds were obtained assuming only one operator different from zero at a time and for a cutoff scale $\Lambda_s = 2 \text{ TeV}$.

the five operators correct $\alpha\Delta T$ while render $\alpha\Delta S = \alpha\Delta U = 0$. In table 8 we give the updated indirect bounds using the determination of the oblique parameters in eq. (4.24).

At the LHC these anomalous quartic couplings can be directly tested in the production of three vector bosons (VVV) or in vector boson fusion (VBF) production of two gauge bosons [81]. At lower center-of-mass energies the best limits originate from the VVV processes, while the VBF channel dominates for the 14 TeV run [80–83, 136].

At the LHC with 14 TeV center-of-mass energy, the couplings c_6 and c_{11} can be constrained by combining their impact on the VBF channels

$$pp \rightarrow jjW^+W^- \quad \text{and} \quad pp \rightarrow jj(W^+W^+ + W^-W^-), \quad (4.42)$$

where j stands for a tagging jet and the final state W 's decay into electron or muon plus neutrino. It was shown in ref. [83] that the attainable 99% CL limits on these couplings are

$$-12 \times 10^{-3} < c_6 \xi < 10 \times 10^{-3} \quad , \quad -7.7 \times 10^{-3} < c_{11} \xi^2 < 14 \times 10^{-3} \quad (4.43)$$

for an integrated luminosity of 100 fb^{-1} . Notice that the addition of the channel $pp \rightarrow jjZZ$ does not improve significantly the above limits [80].

5 Conclusions

In this paper we have made a comparative study of the departures from the Standard Model predictions in theories based on linear and non-linear realizations of $\text{SU}(2)_L \times \text{U}(1)_Y$ gauge symmetry breaking. To address this question in a model-independent way, we have considered effective Lagrangians containing either a light fundamental Higgs in the linear realization or a light dynamical Higgs in the non-linear one. We have exploited the fact that these two expansions are intrinsically different from the point of view of the presence or absence, respectively, of a global $\text{SU}(2)_L$ symmetry in the effective Lagrangian, with the light Higgs scalar behaving as a singlet in the chiral case. Less symmetry means more possible invariant operators at a given order, and the result is that the non-linear realization for a light dynamical Higgs particle is expected to exhibit a larger number of

independent couplings than linear ones. This has been explored here concentrating on the CP-even operators involving pure gauge and gauge- h couplings. First, in section 2 we have presented the maximal set of independent (and thus non-redundant) operators of that type contained in the effective chiral Lagrangian for a light dynamical Higgs, up to operators with four derivatives. In section 3.1 the analogous complete basis of independent operators up to dimension six in the linear expansion is presented. Comparing both sets of operators, we have established the relations and differences between the chiral and the linear bases.

In particular, in sections 3.2 and 3.4 we have identified two sources of discriminating signatures. For small values of the ξ parameter the counting of operators is not the same in both sets, being larger by six for the chiral expansion. This implies that, even keeping only operators weighted by ξ , the expected deviations from the SM predictions in the Higgs couplings to gauge bosons and that of the triple gauge boson self-couplings are independent in the chiral expansion, unlike in the linear expansion at dimension six; one interesting set of (de)correlated couplings is explored in details as indicators of a non-linear character. Conversely, when considering operators weighted by ξ^n with $n \geq 2$ in the chiral expansion, we find anomalous signals which appear only at dimension eight of the linear Lagrangian; they may thus be detected with larger (leading) strength for a non-linear realization of EWSB than for a linear one, for sizeable values of ξ .

In order to quantify the observability of the above effects we have implemented the renormalization procedure as described in section 4.1 and derived the corresponding Feynman rules for the non-linear expansion (which we present in the detail in appendix D, for the complete set of independent operators under discussion). Neglecting external fermion masses only in the numerical analysis, the results of our simulations for some of the discriminating signatures at LHC are presented in sections 4.2–4.4. To our knowledge, this is the first six-parameter analysis in the context of the non-linear expansion, focusing on the ξ -weighted pure gauge and gauge- h effective couplings. In particular we have derived the present bounds on the coefficients of the latter from the analysis of electroweak precision physics, triple gauge boson coupling studies and Higgs data. The results are summarized in figure 1 and table 4 and the corresponding level of decorrelation between the triple gauge couplings and Higgs effects is illustrated in figure 2: the presently allowed values for the parameters $c_i\xi$ and $a_i\xi$ turn out to be of order 1, with only few exceptions bounded to the per cent level. With the expected uncertainties attainable in CMS and ATLAS at 14 TeV, that sensitivity can be improved by a factor $\mathcal{O}(3-5)$. Furthermore, our study of the present sensitivity to the C and P odd operator in the analysis of WWZ vertex, with the accumulated luminosity of LHC7+8 and with LHC14 in the future, show that per cent precision on the coupling of the operator $\mathcal{P}_{14}(h)$ is foreseeable. Similar precision should be attainable for the coefficients of the operators leading to generic quartic gauge couplings $\mathcal{P}_6(h)$ and $\mathcal{P}_{11}(h)$.

Acknowledgments

We acknowledge illuminating conversations with Rodrigo Alonso, Gino Isidori, Aneesh Manohar, Michael Trott, and Juan Yepes. We also acknowledge partial support of the Euro-

pean Union network FP7 ITN INVISIBLES (Marie Curie Actions, PITN-GA-2011-289442), of CiCYT through the project FPA2009-09017, of CAM through the project HEPHACOS P-ESP-00346, of the European Union FP7 ITN UNILHC (Marie Curie Actions, PITN-GA-2009-237920), of MICINN through the grant BES-2010-037869, of the Spanish MINECO's "Centro de Excelencia Severo Ochoa" Programme under grant SEV-2012-0249, and of the Italian Ministero dell'Università e della Ricerca Scientifica through the COFIN program (PRIN 2008) and the contract MRTN-CT-2006-035505. The work of I.B. is supported by an ESR contract of the European Union network FP7 ITN INVISIBLES mentioned above. The work of L.M. is supported by the Juan de la Cierva programme (JCI-2011-09244). The work of O.J.P.E. is supported in part by Conselho Nacional de Desenvolvimento Científico e Tecnológico (CNPq) and by Fundação de Amparo à Pesquisa do Estado de São Paulo (FAPESP), M.C.G-G and T.C are supported by USA-NSF grant PHY-09-6739, M.C.G-G is also supported by CUR Generalitat de Catalunya grant 2009SGR502 and together with J.G-F by MICINN FPA2010-20807 and consolider-ingenio 2010 program CSD-2008-0037. J.G-F is further supported by ME FPU grant AP2009-2546. I.B., J.G-F., M.C.G-G., B.G., L.M, and S.R. acknowledge CERN TH department and J.G-F. also acknowledges ITP Heidelberg for hospitality during part of this work.

A EOM and fermion operators

The EOM can be extracted from the \mathcal{L}_0 part of the chiral Lagrangian, eq. (2.2); as we will work at first order in $\Delta\mathcal{L}$ they read:¹⁸

$$(\mathcal{D}^\mu W_{\mu\nu})^a = \frac{g}{2} \bar{Q}_L \sigma^a \gamma_\nu Q_L + \frac{g}{2} \bar{L}_L \sigma^a \gamma_\nu L_L + \frac{igv^2}{4} \text{Tr}[\mathbf{V}_\nu \sigma^a] \left(1 + \frac{h}{v}\right)^2 \quad (\text{A.1})$$

$$\partial^\mu B_{\mu\nu} = -\frac{ig'v^2}{4} \text{Tr}[\mathbf{T}\mathbf{V}_\mu] \left(1 + \frac{h}{v}\right)^2 + g' \sum_{i=L,R} \left(\bar{Q}_i \mathbf{h}_i \gamma_\nu Q_i + \frac{1}{6} \bar{L}_L \gamma_\nu L_L \right) \quad (\text{A.2})$$

$$\square h = -\frac{\delta V(h)}{\delta h} - \frac{v+h}{2} \text{Tr}[\mathbf{V}_\mu \mathbf{V}^\mu] - \frac{s_Y}{\sqrt{2}} (\bar{Q}_L \mathbf{U} \mathbf{Y}_Q Q_R + \bar{L}_L \mathbf{U} \mathbf{Y}_L L_R + \text{h.c.}) \quad (\text{A.3})$$

$$\left[\mathbf{D}_\mu \left(\frac{(v+h)^2}{2\sqrt{2}} \mathbf{U}^\dagger \mathbf{D}^\mu \mathbf{U} \right) \right]_{ij} = \begin{cases} -(v + s_Y h) \left[(\bar{Q}_R \mathbf{Y}_Q^\dagger)_j (\mathbf{U}^\dagger Q_L)_i + (\bar{L}_R \mathbf{Y}_L^\dagger)_j (\mathbf{U}^\dagger L_L)_i \right] & \text{for } i \neq j \\ 0 & \text{for } i = j \end{cases} \quad (\text{A.4})$$

$$i\not{D} Q_L = \frac{v + s_Y h}{\sqrt{2}} \mathbf{U} \mathbf{Y}_Q Q_R \quad i\not{D} Q_R = \frac{v + s_Y h}{\sqrt{2}} \mathbf{Y}_Q^\dagger \mathbf{U}^\dagger Q_L \quad (\text{A.5})$$

$$i\not{D} L_L = \frac{v + s_Y h}{\sqrt{2}} \mathbf{U} \mathbf{Y}_L L_R \quad i\not{D} L_R = \frac{v + s_Y h}{\sqrt{2}} \mathbf{Y}_L^\dagger \mathbf{U}^\dagger L_L, \quad (\text{A.6})$$

where $\mathbf{h}_{L,R}$ are the 2×2 matrices of hypercharge for the left- and right-handed quarks.

¹⁸With alternative choices for the separation \mathcal{L}_0 versus $\Delta\mathcal{L}$ the EOM are correspondingly modified [63, 64, 73]: this is of no relevance to the focus of this paper, which explores the tree-level impact of effective operators.

By using these EOM, it is possible to identify relations between some bosonic operators listed in eqs. (2.6)–(2.8) and specific fermion operators. This allows us to trade those bosonic operators by the corresponding fermionic ones: this procedure can turn out to be very useful when analysing specific experimental data. For instance, if deviations from the SM values of the h -fermion couplings were found, then the following three operators,

$$\begin{aligned}\mathcal{P}_{U,\alpha\beta}(h) &= -\frac{v}{\sqrt{2}}\bar{Q}_{L\alpha}\mathbf{U}(\mathcal{F}_U(h)P_{\uparrow}Q_R)_{\beta} + \text{h.c.}, \\ \mathcal{P}_{D,\alpha\beta}(h) &= -\frac{v}{\sqrt{2}}\bar{Q}_{L\alpha}\mathbf{U}(\mathcal{F}_D(h)P_{\downarrow}Q_R)_{\beta} + \text{h.c.}, \\ \mathcal{P}_{E,\alpha\beta}(h) &= -\frac{v}{\sqrt{2}}\bar{L}_{L\alpha}\mathbf{U}(\mathcal{F}_E(h)P_{\downarrow}L_R)_{\beta} + \text{h.c.},\end{aligned}\tag{A.7}$$

would be a good choice for an operator basis. In the previous equations the two projectors

$$P_{\uparrow} = \begin{pmatrix} 1 & \\ & 0 \end{pmatrix} \quad P_{\downarrow} = \begin{pmatrix} 0 & \\ & 1 \end{pmatrix},\tag{A.8}$$

have been introduced.

On the contrary, without including the operators in eqs. (A.7), the bosonic basis defined in eqs. (2.6)–(2.10) is blind to these directions. The fermionic operators that arise applying the EOM to bosonic operators in the basis above is presented in the following list:

Weighted by ξ :

$$\begin{aligned}\mathcal{P}_{U,\alpha\beta}(h) &= -\frac{v}{\sqrt{2}}\bar{Q}_{L\alpha}\mathbf{U}(\mathcal{F}_U(h)P_{\uparrow}Q_R)_{\beta} + \text{h.c.} \\ \mathcal{P}_{D,\alpha\beta}(h) &= -\frac{v}{\sqrt{2}}\bar{Q}_{L\alpha}\mathbf{U}(\mathcal{F}_D(h)P_{\downarrow}Q_R)_{\beta} + \text{h.c.} \\ \mathcal{P}_{E,\alpha\beta}(h) &= -\frac{v}{\sqrt{2}}\bar{L}_{L\alpha}\mathbf{U}(\mathcal{F}_E(h)P_{\downarrow}L_R)_{\beta} + \text{h.c.} \\ \mathcal{P}_{1Q,\alpha\beta}(h) &= \frac{\alpha}{2}\bar{Q}_{L\alpha}\gamma^{\mu}\{\mathbf{T}, \mathbf{V}_{\mu}\}(\mathcal{F}_{1Q}(h)Q_L)_{\beta} \\ \mathcal{P}_{1L,\alpha\beta}(h) &= \frac{\alpha}{2}\bar{L}_{L\alpha}\gamma^{\mu}\{\mathbf{T}, \mathbf{V}_{\mu}\}(\mathcal{F}_{1L}(h)L_L)_{\beta} \\ \mathcal{P}_{1U,\alpha\beta}(h) &= \frac{\alpha}{2}\bar{Q}_{R\alpha}\gamma^{\mu}\left\{\sigma^3, \tilde{\mathbf{V}}_{\mu}\right\}(\mathcal{F}_{1U}(h)P_{\uparrow}Q_R)_{\beta} \\ \mathcal{P}_{1D,\alpha\beta}(h) &= \frac{\alpha}{2}\bar{Q}_{R\alpha}\gamma^{\mu}\left\{\sigma^3, \tilde{\mathbf{V}}_{\mu}\right\}(\mathcal{F}_{1D}(h)P_{\downarrow}Q_R)_{\beta} \\ \mathcal{P}_{1N,\alpha\beta}(h) &= \frac{\alpha}{2}\bar{L}_{R\alpha}\gamma^{\mu}\left\{\sigma^3, \tilde{\mathbf{V}}_{\mu}\right\}(\mathcal{F}_{1N}(h)P_{\uparrow}L_R)_{\beta} \\ \mathcal{P}_{1E,\alpha\beta}(h) &= \frac{\alpha}{2}\bar{L}_{R\alpha}\gamma^{\mu}\left\{\sigma^3, \tilde{\mathbf{V}}_{\mu}\right\}(\mathcal{F}_{1E}(h)P_{\downarrow}L_R)_{\beta} \\ \mathcal{P}_{2Q,\alpha\beta}(h) &= i\bar{Q}_{L\alpha}\gamma^{\mu}\mathbf{V}_{\mu}(\mathcal{F}_{2Q}(h)Q_L)_{\beta} \\ \mathcal{P}_{2L,\alpha\beta}(h) &= i\bar{L}_{L\alpha}\gamma^{\mu}\mathbf{V}_{\mu}(\mathcal{F}_{2L}(h)L_L)_{\beta} \\ \mathcal{P}_{3Q,\alpha\beta}(h) &= i\bar{Q}_{L\alpha}\gamma^{\mu}\mathbf{T}\mathbf{V}_{\mu}\mathbf{T}(\mathcal{F}_{3Q}(h)Q_L)_{\beta} \\ \mathcal{P}_{3L,\alpha\beta}(h) &= i\bar{L}_{L\alpha}\gamma^{\mu}\mathbf{T}\mathbf{V}_{\mu}\mathbf{T}(\mathcal{F}_{3L}(h)L_L)_{\beta}\end{aligned}\tag{A.9}$$

$$\begin{aligned}
 \mathcal{P}_{7E,\alpha\beta}(h) &= \text{Tr}[\mathbf{T}\mathbf{V}^\mu] \bar{L}_{L\alpha} \mathbf{T}\mathbf{U} (\partial^\mu \mathcal{F}_{7E}(h) P_\downarrow L_R)_\beta \\
 \mathcal{P}_{8U,\alpha\beta}(h) &= \text{Tr}[\mathbf{T}\mathbf{V}^\mu] \bar{Q}_{L\alpha} [\mathbf{T}, \mathbf{V}_\mu] \mathbf{U} (\mathcal{F}_{8U}(h) P_\uparrow Q_R)_\beta \\
 \mathcal{P}_{8D,\alpha\beta}(h) &= \text{Tr}[\mathbf{T}\mathbf{V}^\mu] \bar{Q}_{L\alpha} [\mathbf{T}, \mathbf{V}_\mu] \mathbf{U} (\mathcal{F}_{8D}(h) P_\downarrow Q_R)_\beta \\
 \mathcal{P}_{8N,\alpha\beta}(h) &= \text{Tr}[\mathbf{T}\mathbf{V}^\mu] \bar{L}_{L\alpha} [\mathbf{T}, \mathbf{V}_\mu] \mathbf{U} (\mathcal{F}_{8N}(h) P_\uparrow L_R)_\beta \\
 \mathcal{P}_{8E,\alpha\beta}(h) &= \text{Tr}[\mathbf{T}\mathbf{V}^\mu] \bar{L}_{L\alpha} [\mathbf{T}, \mathbf{V}_\mu] \mathbf{U} (\mathcal{F}_{8E}(h) P_\downarrow L_R)_\beta .
 \end{aligned}$$

Rearranging eqs. (A.1)–(A.4), one can derive the following relations between bosonic and fermionic operators:

$$\begin{aligned}
 2\mathcal{P}_B(h) + \frac{1}{2}\mathcal{P}_1(h) + \frac{1}{2}\mathcal{P}_2(h) + \mathcal{P}_4(h) - g'^2\mathcal{P}_T(h) \left(1 + \frac{h}{v}\right)^2 &= \\
 = \sum_\alpha \left\{ \frac{1}{3}g'^2\mathcal{P}_{1Q,\alpha\alpha}(h) + \frac{4}{3}g'^2\mathcal{P}_{1U,\alpha\alpha}(h) - \frac{2}{3}g'^2\mathcal{P}_{1D,\alpha\alpha}(h) - g'^2\mathcal{P}_{1L,\alpha\alpha}(h) - 2g'^2\mathcal{P}_{1E,\alpha\alpha}(h) \right\}, \\
 -\mathcal{P}_W(h) - g^2\mathcal{P}_C(h) \left(1 + \frac{h}{v}\right)^2 - \frac{1}{4}\mathcal{P}_1(h) - \frac{1}{2}\mathcal{P}_3(h) + \mathcal{P}_5(h) &= \frac{g^2}{2} \sum_\alpha \left\{ \mathcal{P}_{2Q,\alpha\alpha}(h) + \mathcal{P}_{2L,\alpha\alpha}(h) \right\}, \\
 \mathcal{P}_H(h) + 2\mathcal{P}_C(h) \left(1 + \frac{h}{v}\right)^2 + (v+h)\mathcal{F}(h) \frac{\delta V}{\delta h} &= s_Y \frac{v+h}{\sqrt{2}} \sum_{f=U,D,E} \sum_{\alpha\beta} \left\{ Y_{f,\alpha\beta} \mathcal{P}_{f,\alpha\beta}(h) + \text{h.c.} \right\}, \\
 g^2\mathcal{P}_T(h) \left(1 + \frac{h}{v}\right)^2 - \frac{1}{2}\mathcal{P}_1(h) - \mathcal{P}_3(h) + \frac{1}{2}\mathcal{P}_{12}(h) + \mathcal{P}_{13}(h) + \mathcal{P}_{17}(h) &= \\
 = \frac{g^2}{2} \sum_\alpha \left\{ (\mathcal{P}_{3Q,\alpha\alpha}(h) + \mathcal{P}_{2Q,\alpha\alpha}(h)) + (\mathcal{P}_{3L,\alpha\alpha}(h) + \mathcal{P}_{2L,\alpha\alpha}(h)) \right\}.
 \end{aligned} \tag{A.11}$$

The $\mathcal{F}_i(h)$ functions in all operators in these relations are the same, except for \mathcal{P}_H in the third line of eq. (A.11), which is related to it by

$$\mathcal{F}_H(h) = \mathcal{F}_C(h) + \left(1 + \frac{h}{v}\right) \frac{\delta \mathcal{F}_C(h)}{\delta h}. \tag{A.12}$$

Applying the EOM in eq. (A.3) to the operators $\mathcal{P}_{20}(h)$ and $\mathcal{P}_{21}(h)$ allows us to express them in terms of other operators in the basis, h -gauge boson couplings and Yukawa-like interactions:

$$\begin{aligned}
 \mathcal{P}_{20}(h) &= 2\mathcal{F}(h)\mathcal{P}_6(h) + 2\mathcal{F}(h)\mathcal{P}_7(h) - \frac{16}{v^3} \sqrt{\mathcal{F}(h)} \mathcal{P}_C(h) \frac{\delta V}{\delta h} \\
 &\quad - \frac{8\sqrt{2}s_Y}{v^3} \sqrt{\mathcal{F}(h)} \mathcal{P}_C(h) (\bar{Q}_L \mathbf{U} \mathbf{Y}_Q Q_R + \bar{L}_L \mathbf{U} \mathbf{Y}_L L_R + \text{h.c.}) , \\
 \mathcal{P}_{21}(h) &= 2\mathcal{F}(h)\mathcal{P}_{23}(h) + 2\mathcal{F}(h)\mathcal{P}_{25}(h) + \frac{16}{v^3} \sqrt{\mathcal{F}(h)} \mathcal{P}_T(h) \frac{\delta V}{\delta h} \\
 &\quad + \frac{8\sqrt{2}s_Y}{v^3} \sqrt{\mathcal{F}(h)} \mathcal{P}_T(h) (\bar{Q}_L \mathbf{U} \mathbf{Y}_Q Q_R + \bar{L}_L \mathbf{U} \mathbf{Y}_L L_R + \text{h.c.}) ,
 \end{aligned} \tag{A.13}$$

where all $\mathcal{F}_i(h)$ appearing explicitly in these expressions and included in the definition of the operators $\mathcal{P}_i(h)$ are the same and defined by

$$\mathcal{F}(h) = \left(1 + \frac{h}{v}\right)^2. \tag{A.14}$$

From eqs. (A.1), (A.2) and (A.5), it follows that

$$\begin{aligned}
 \frac{iv}{\sqrt{2}} \text{Tr}(\sigma^j \mathcal{D}_\mu \mathbf{V}^\mu) \left(1 + \frac{h}{v}\right)^2 &= \frac{v + s_Y h}{v} (i\bar{Q}_L \sigma^j \mathbf{U} \mathbf{Y}_Q Q_R + i\bar{L}_L \sigma^j \mathbf{U} \mathbf{Y}_L L_R + \text{h.c.}) \\
 &\quad - \frac{iv}{\sqrt{2}} \text{Tr}(\sigma^j \mathbf{V}_\mu) \partial^\mu \left(1 + \frac{h}{v}\right)^2, \\
 \frac{iv}{\sqrt{2}} \text{Tr}(\mathbf{T} \mathcal{D}_\mu \mathbf{V}^\mu) \left(1 + \frac{h}{v}\right)^2 &= \frac{v + s_Y h}{v} (i\bar{Q}_L \mathbf{T} \mathbf{U} \mathbf{Y}_Q Q_R + i\bar{L}_L \mathbf{T} \mathbf{U} \mathbf{Y}_L L_R + \text{h.c.}) \\
 &\quad - \frac{iv}{\sqrt{2}} \text{Tr}(\mathbf{T} \mathbf{V}_\mu) \partial^\mu \left(1 + \frac{h}{v}\right)^2,
 \end{aligned} \tag{A.15}$$

which allows us to rewrite the pure bosonic operators $\mathcal{P}_{11-13}(h)$, $\mathcal{P}_{10}(h)$ and $\mathcal{P}_{19}(h)$ as combination of other pure bosonic ones in eqs. (2.6)–(2.8) plus fermionic operators in eqs. (A.9) and (A.10):

$$\begin{aligned}
 \mathcal{P}_9(h) - \mathcal{P}_8(h) &= \frac{1}{v^2} \sum_{f_1, f_2=U,D,E} \sum_{\alpha\beta\gamma\delta} Y_{f_1, \alpha\beta} Y_{f_2, \gamma\delta} \mathcal{P}_{4f_1 f_2, \alpha\beta\gamma\delta}(h) \\
 &\quad - \frac{2\sqrt{2}}{v} \sum_{f=U,D,N,E} \sum_{\alpha\beta} (Y_{f, \alpha\beta} \mathcal{P}_{6f, \alpha\beta}(h) - \text{h.c.}), \\
 \mathcal{P}_{15}(h) - \mathcal{P}_{22}(h) &= \frac{2}{v^2} \sum_{f_1, f_2=U,D,E} \sum_{\alpha\beta\gamma\delta} Y_{f_1, \alpha\beta\gamma\delta} Y_{f_2, \gamma\delta} \mathcal{P}_{5f_1 f_2, \alpha\beta\gamma\delta}(h) \\
 &\quad - \frac{2\sqrt{2}}{v \cos \theta_W} \sum_{f=U,D,N,E} \sum_{\alpha\beta} (Y_{f, \alpha\beta} \mathcal{P}_{7f, \alpha\beta}(h) - \text{h.c.}), \\
 \mathcal{P}_{16}(h) + \mathcal{P}_{18}(h) &= \sum_{f=U,D,N,E} \sum_{\alpha\beta} \frac{\sqrt{2}}{v} (Y_{f, \alpha\beta} \mathcal{P}_{8f, \alpha\beta}(h) - \text{h.c.}), \\
 \mathcal{P}_{10}(h) + \mathcal{P}_8(h) &= \sum_{f=U,D,N,E} \sum_{\alpha\beta} \frac{\sqrt{2}}{v} (Y_{f, \alpha\beta} \mathcal{P}_{6f, \alpha\beta}(h) - \text{h.c.}), \\
 \mathcal{P}_{19}(h) + \mathcal{P}_{22}(h) &= \sum_{f=U,D,N,E} \sum_{\alpha\beta} \frac{\sqrt{2}}{v} (Y_{f, \alpha\beta} \mathcal{P}_{7f, \alpha\beta}(h) - \text{h.c.}).
 \end{aligned} \tag{A.16}$$

A straightforward consequence is that once the $\mathcal{F}_i(h)$ functions in the operators on the left-hand side of eq. (A.16) are specified, then the $\mathcal{F}_i(h)$ functions in the operators on the right-hand side are no longer general, but take the form of specific expressions.

B Equivalence of the $d = 6$ basis with the SILH Lagrangian

The SILH Lagrangian [87] is defined by the following 10 $d = 6$ linear operators:

$$\begin{aligned}
 \mathcal{O}_g^{\text{SILH}} &= \Phi^\dagger \Phi G_{\mu\nu}^a G^{a\mu\nu}, & \mathcal{O}_\gamma^{\text{SILH}} &= \Phi^\dagger \hat{B}_{\mu\nu} \hat{B}^{\mu\nu} \Phi, \\
 \mathcal{O}_W^{\text{SILH}} &= \frac{ig}{2} \left(\Phi^\dagger \sigma^i \overleftrightarrow{D}_\mu \Phi \right) D_\nu W_i^{\mu\nu}, & \mathcal{O}_B^{\text{SILH}} &= \left(\Phi^\dagger \overleftrightarrow{D}_\mu \Phi \right) \partial_\nu \hat{B}^{\mu\nu}, \\
 \mathcal{O}_{HW}^{\text{SILH}} &= (D_\mu \Phi)^\dagger \hat{W}^{\mu\nu} (D_\nu \Phi), & \mathcal{O}_{HB}^{\text{SILH}} &= (D_\mu \Phi)^\dagger (D_\nu \Phi) \hat{B}^{\mu\nu}, \\
 \mathcal{O}_T^{\text{SILH}} &= \frac{1}{2} \left(\Phi^\dagger \overleftrightarrow{D}_\mu \Phi \right) \left(\Phi^\dagger \overleftrightarrow{D}^\mu \Phi \right), & \mathcal{O}_H^{\text{SILH}} &= \frac{1}{2} \partial^\mu \left(\Phi^\dagger \Phi \right) \partial_\mu \left(\Phi^\dagger \Phi \right), \\
 \mathcal{O}_6^{\text{SILH}} &= \frac{1}{3} \left(\Phi^\dagger \Phi \right)^3, & \mathcal{O}_y^{\text{SILH}} &= \left(\Phi^\dagger \Phi \right) f_L \Phi \mathbf{Y} f_R + \text{h.c.},
 \end{aligned} \tag{B.1}$$

where $\Phi^\dagger \overleftrightarrow{D}_\mu \Phi \equiv \Phi^\dagger D_\mu \Phi - D_\mu \Phi^\dagger \Phi$ and $\Phi^\dagger \sigma^i \overleftrightarrow{D}_\mu \Phi \equiv \Phi^\dagger \sigma^i D_\mu \Phi - D_\mu \Phi^\dagger \sigma^i \Phi$. They can be related directly to the operators in eqs. (3.3) and (3.4):

$$\begin{aligned}
 \mathcal{O}_g^{\text{SILH}} &\equiv \mathcal{O}_{GG}, & \mathcal{O}_\gamma^{\text{SILH}} &\equiv \mathcal{O}_{BB}, \\
 \mathcal{O}_B^{\text{SILH}} &\equiv 2\mathcal{O}_B + \mathcal{O}_{BW} + \mathcal{O}_{BB}, & \mathcal{O}_W^{\text{SILH}} &\equiv 2\mathcal{O}_W + \mathcal{O}_{BW} + \mathcal{O}_{WW}, \\
 \mathcal{O}_{HW}^{\text{SILH}} &\equiv \mathcal{O}_W, & \mathcal{O}_{HB}^{\text{SILH}} &\equiv \mathcal{O}_B, \\
 \mathcal{O}_T^{\text{SILH}} &\equiv \mathcal{O}_{\Phi,2} - 2\mathcal{O}_{\Phi,1}, & \mathcal{O}_H^{\text{SILH}} &\equiv \mathcal{O}_{\Phi,2}, \\
 \mathcal{O}_6^{\text{SILH}} &\equiv \mathcal{O}_{\Phi,3}, & \mathcal{O}_y^{\text{SILH}} &\equiv 2\mathcal{O}_{\Phi,2} + 2\mathcal{O}_{\Phi,4} - \left(\Phi^\dagger \Phi \right) \Phi^\dagger \frac{\delta V(h)}{\delta \Phi^\dagger}.
 \end{aligned} \tag{B.2}$$

This shows the equivalence of the two linear expansions.

It can also be interesting to show explicitly the connection between the SILH operators and those of the chiral basis in eqs. (2.6)–(2.8), which is as follows:

$$\begin{aligned}
 \mathcal{O}_g^{\text{SILH}} &= \frac{v^2}{2g_s^2} \mathcal{P}_G, & \mathcal{O}_\gamma^{\text{SILH}} &= \frac{v^2}{2} \mathcal{P}_B, \\
 \mathcal{O}_B^{\text{SILH}} &= \frac{v^2}{8} (\mathcal{P}_2 + 2\mathcal{P}_4) + \frac{v^2}{8} \mathcal{P}_1 + \frac{v^2}{2} \mathcal{P}_B, & \mathcal{O}_{HB}^{\text{SILH}} &= \frac{v^2}{16} (\mathcal{P}_2 + 2\mathcal{P}_4) + \frac{v^2}{2} \mathcal{P}_W, \\
 \mathcal{O}_W^{\text{SILH}} &= \frac{v^2}{4} (\mathcal{P}_3 - 2\mathcal{P}_5) + \frac{v^2}{8} \mathcal{P}_1, & \mathcal{O}_{HW}^{\text{SILH}} &= \frac{v^2}{8} (\mathcal{P}_3 - 2\mathcal{P}_5), \\
 \mathcal{O}_T^{\text{SILH}} &= \frac{v^2}{2} \mathcal{F}(h) \mathcal{P}_T, & \mathcal{O}_H^{\text{SILH}} &= v^2 \mathcal{P}_H, \\
 \mathcal{O}_y^{\text{SILH}} &= 3v^2 \mathcal{P}_H + v^2 \mathcal{F}(h) \mathcal{P}_C - \frac{(v+h)^3}{2} \frac{\delta V(h)}{\delta h},
 \end{aligned} \tag{B.3}$$

where the $\mathcal{F}_i(h)$ appearing in these relations and inside the individual $\mathcal{P}_i(h)$ operators are all defined by

$$\mathcal{F}(h) = \left(1 + \frac{h}{v} \right)^2. \tag{B.4}$$

C Relations between chiral and linear operators

In this appendix, the connections between the operators of the chiral and linear bases is discussed. As the number and nature of the leading order operators in the chiral and linear expansion are not the same, there are pairs of chiral operators that correspond to the same lowest dimensional linear one: in order to get then a one-to-one correspondence between these chiral operators and (combinations of) linear ones, operators of higher dimension should be taken into consideration. For those weighted by a single power of ξ , the list of the siblings can be read from eq. (3.7). Below, we also indicate which chiral operators, weighted by higher powers of ξ , should be combined in order to generate the gauge interactions contained in specific linear ones.

For operators weighted by ξ :

$$\begin{aligned}
 \mathcal{P}_B(h) &\rightarrow \mathcal{O}_{BB} & \mathcal{P}_W(h) &\rightarrow \mathcal{O}_{WW} & \mathcal{P}_G(h) &\rightarrow \mathcal{O}_{GG} \\
 \mathcal{P}_C(h) &\rightarrow \mathcal{O}_{\Phi,4} & \mathcal{P}_T(h) &\rightarrow \mathcal{O}_{\Phi,1} & \mathcal{P}_H(h) &\rightarrow \mathcal{O}_{\Phi,2} \\
 \mathcal{P}_1(h) &\rightarrow \mathcal{O}_{BW} & \mathcal{P}_2(h), \mathcal{P}_4(h) &\rightarrow \mathcal{O}_B & \mathcal{P}_3(h), \mathcal{P}_5(h) &\rightarrow \mathcal{O}_W \\
 & & \mathcal{P}_6(h), \mathcal{P}_7(h), \mathcal{P}_8(h), \mathcal{P}_9(h), \mathcal{P}_{10}(h), \mathcal{P}_{\square H}(h) &\rightarrow \mathcal{O}_{\square\Phi}
 \end{aligned} \tag{C.1}$$

For operators weighted by ξ^2 :

$$\begin{aligned}
 \mathcal{P}_{DH}(h), \mathcal{P}_{20}(h) &\rightarrow \left[D_\mu \Phi^\dagger D^\mu \Phi \right]^2 \\
 \mathcal{P}_{11}(h), \mathcal{P}_{18}(h), \mathcal{P}_{21}(h), \mathcal{P}_{22}(h), \mathcal{P}_{23}(h), \mathcal{P}_{24}(h) &\rightarrow \left[D^\mu \Phi^\dagger D^\nu \Phi \right]^2 \\
 \mathcal{P}_{12}(h) &\rightarrow \left(\Phi^\dagger W^{\mu\nu} \Phi \right)^2 \\
 \mathcal{P}_{13}(h), \mathcal{P}_{17}(h) &\rightarrow \left(\Phi^\dagger W^{\mu\nu} \Phi \right) D_\mu \Phi^\dagger D_\nu \Phi \\
 \mathcal{P}_{14}(h) &\rightarrow \epsilon^{\mu\nu\rho\lambda} \left(\Phi^\dagger \overleftrightarrow{D}_\rho \Phi \right) \left(\Phi^\dagger \sigma_i \overleftrightarrow{D}_\lambda \Phi \right) W_{\mu\nu}^i \\
 \mathcal{P}_{15}(h), \mathcal{P}_{19}(h) &\rightarrow \left[\Phi^\dagger D_\mu D^\mu \Phi - D_\mu D^\mu \Phi^\dagger \Phi \right]^2 \\
 \mathcal{P}_{16}(h), \mathcal{P}_{25}(h) &\rightarrow \left(D^\nu \Phi^\dagger D_\mu D^\mu \Phi - D_\mu D^\mu \Phi^\dagger D^\nu \Phi \right) \left(\Phi^\dagger \overleftrightarrow{D}_\nu \Phi \right)
 \end{aligned} \tag{C.2}$$

For operators weighted by ξ^4 :

$$\mathcal{P}_{26}(h) \rightarrow \left[\left(\Phi^\dagger \overleftrightarrow{D}_\mu \Phi \right) \left(\Phi^\dagger \overleftrightarrow{D}_\nu \Phi \right) \right]^2. \tag{C.3}$$

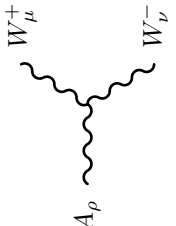
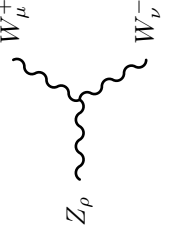
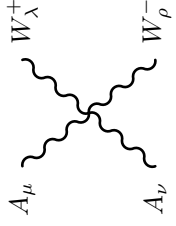
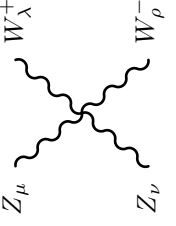
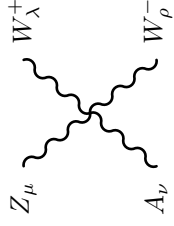
D Feynman rules


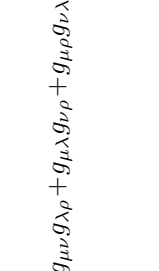
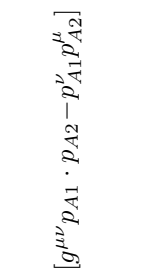
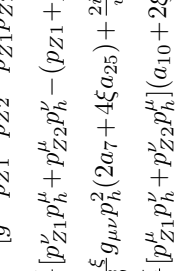
This appendix provides a complete list of all the Feynman rules resulting from the operators discussed here in the Lagrangian $\mathcal{L}_{\text{chiral}}$ of eq. (2.1) (except for the pure Higgs ones weighted by powers of ξ higher than one). Only diagrams with up to four legs are shown and the notation $\mathcal{F}_i(h) = 1 + 2\tilde{a}_i h/v + \tilde{b}_i h^2/v^2 + \dots$ has been adopted. Moreover, for brevity, the products $c_i \tilde{a}_i$ and $c_i \tilde{b}_i$ have been redefined as a_i and b_i , respectively. For the operators \mathcal{P}_8 , and \mathcal{P}_{20-22} , that contain two functions $\mathcal{F}_X(h)$ and $\mathcal{F}'_X(h)$ we redefine $c_X \tilde{a}_X \tilde{a}'_X \rightarrow a_X$. In all Feynman diagrams the momenta are chosen to be flowing inwards in the vertices and are computed in the unitary gauge, with the exception of the propagator of the photon which is written in a generic gauge.

Finally, the standard (that is SM-like) and non-standard Lorentz structures are reported in two distinct columns, on the left and on the right, respectively. Greek indices indicate flavour and are assumed to be summed over when repeated; whenever they do not appear, it should be understood that the vertex is flavour diagonal. All the quantities entering the Feynman diagrams can be expressed in terms of the parameters of the Z -renormalization scheme, as shown in eq. (4.2).

	standard structure	non-standard structure
(FR.1)	$\mu \quad \text{---}\gamma\text{---} \quad \nu$	$\frac{-i}{p^2} \left[g^{\mu\nu} - (1-\eta) \frac{p^\mu p^\nu}{p^2} \right] \quad (\eta \text{ is the gauge fixing parameter})$
(FR.2)	$\mu \quad \text{---}Z\text{---} \quad \nu$	$\frac{-i}{p^2 - m_Z^2} \left[g^{\mu\nu} - \frac{p^\mu p^\nu}{p^2 - m_Z^2 / X} \left(1 - \frac{1}{X} \right) \right]; \quad X = \frac{g^2 \xi (c_9 + 2\xi c_{15})}{2c_\theta^2}$
(FR.3)	$\mu \quad \text{---}W\text{---} \quad \nu$	$\frac{-i}{p^2 - m_W^2} \left[g^{\mu\nu} - \frac{p^\mu p^\nu}{p^2 - m_W^2 / X} \left(1 - \frac{1}{X} \right) \right]; \quad \begin{aligned} X &= g^2 \xi c_9 \\ m_W^2 &= m_Z^2 c_\theta^2 \left(1 + \frac{4e^2 \xi c_1}{c_\theta^2 - s_\theta^2} + \frac{2\xi c_T c_\theta^2}{c_\theta^2 - s_\theta^2} - 4g^2 \xi^2 c_{12} \right) \end{aligned}$
(FR.4)	$\mu \quad \text{---}^G\text{---} \quad \nu$	$\frac{-i g^{\mu\nu}}{p^2} \left[g^{\mu\nu} - (1-\eta) \frac{p^\mu p^\nu}{p^2} \right]$
(FR.5)	$\text{---}h\text{---}$	$(*)^{19}$
(FR.6)	$\text{---}\xrightarrow{f}\text{---}$	$\frac{i(\not{p} + m_f)}{p^2 - m_f^2}; \quad m_f = -\frac{vy_f}{\sqrt{2}}, \quad f = U, D, E$

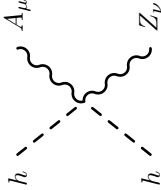
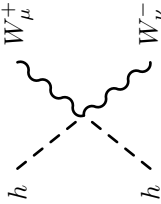
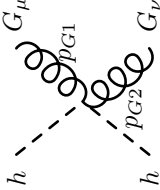
¹⁹ When considering the operator $\mathcal{P}_{\Box H}(h)$, a p^4 contribution to the h propagator arises and it can be written as $-i(p^2 - m_h^2 - p^4 c_{\Box H}/v^2)^{-1}$. However, the physical interpretation of this contribution is not straightforward [137–139] and will not be developed here, but in ref. [140].

standard structure	non-standard structure
<p>(FR.7)</p> 	$-ieg^2\xi(p_+^\mu g_{\nu\rho} - p_-^\nu g_{\mu\rho})c_9$
<p>(FR.8)</p> 	$- \varepsilon^{\mu\nu\rho\lambda} [p_+^\lambda - p_-^\lambda] \frac{g^3 \xi^2 c_{14}}{c_\theta}$ $+ \frac{ig_\theta^3 \xi}{c_\theta^2} [p_+^\mu g_{\nu\rho} - p_-^\nu g_{\mu\rho}] (s_\theta^2 c_9 - \xi c_{16})$
<p>(FR.9)</p> 	$-ie^2[2g_{\mu\nu}g_{\lambda\rho} - (g_{\lambda\mu}g_{\rho\nu} + g_{\lambda\nu}g_{\rho\mu})](1 - g^2\xi c_9)]$
<p>(FR.10)</p> 	$-ig^2c_\theta^2 \left(1 + \frac{2\xi c_T}{c_\theta^2 - s_\theta^2} + \frac{4e^2\xi c_1}{c_\theta^2(c_\theta^2 - s_\theta^2)} + \frac{2g^2\xi c_3}{c_\theta^2} \right) \left[2g_{\mu\nu}g_{\lambda\rho} \left(1 - \frac{g^2\xi c_6}{c_\theta^4} - \frac{g^2\xi^2 c_{23}}{c_\theta^4} \right) \right. \\ \left. - (g_{\lambda\mu}g_{\rho\nu} + g_{\lambda\nu}g_{\rho\mu}) \left(1 + \frac{\xi(-e^2s_\theta^2 c_9 + g^2\xi c_{11} + 2e^2\xi c_{16})}{c_\theta^4} + \frac{g^2\xi^2 c_{24}}{c_\theta^4} \right) \right]$
<p>(FR.11)</p> 	$-iegc_\theta \left(1 + \frac{\xi c_T}{c_\theta^2 - s_\theta^2} + \frac{2\xi e^2 c_1}{c_\theta^2(c_\theta^2 - s_\theta^2)} + \frac{g^2\xi c_3}{c_\theta^2} \right) \cdot \left[2g_{\mu\nu}g_{\lambda\rho} - (g_{\lambda\mu}g_{\rho\nu} + g_{\lambda\nu}g_{\rho\mu}) \left(1 + \frac{\xi(e^2 c_9 - g^2\xi c_{16})}{c_\theta^2} \right) \right]$ $- \varepsilon^{\mu\nu\rho\lambda} \frac{2eg^3\xi^2 c_{14}}{c_\theta}$

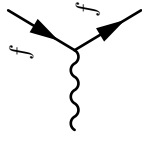
standard structure	non-standard structure
<div style="display: flex; align-items: center; justify-content: center;">  </div> <p style="text-align: center;">(FR.12)</p>	$ig^2 \left(1 + \frac{2\xi(c_T c_\theta^2 + 2e^2 c_1)}{c_\theta^2 - s_\theta^2} + 2g^2 \xi c_3 \right) \cdot \left[-(g_{\mu\nu} g_{\lambda\rho} + g_{\lambda\nu} g_{\mu\rho}) (1 + g^2 \xi (-2c_6 - \xi c_{11} - 8\xi c_{12} + 4\xi c_{13})) + 2g_{\lambda\mu} g_{\nu\rho} (1 + g^2 \xi^2 (c_{11} - 8c_{12} + 4c_{13})) \right]$
<div style="display: flex; align-items: center; justify-content: center;">  </div> <p style="text-align: center;">(FR.13)</p>	$\frac{ig^4 \xi}{c_\theta^4} [g_{\mu\nu} g_{\lambda\rho} + g_{\mu\lambda} g_{\nu\rho} + g_{\mu\rho} g_{\nu\lambda}] (c_6 + \xi (c_{11} + 2c_{23} + 2c_{24}) + 4\xi^3 c_{26})$
<div style="display: flex; align-items: center; justify-content: center;">  </div> <p style="text-align: center;">(FR.14)</p>	$i \frac{8e^2 \xi}{v} [g^{\mu\nu} p_{A1} \cdot p_{A2} - p_{A1}^\nu p_{A2}^\mu] \left(\frac{a_B + a_W}{4} - a_1 - \xi a_{12} \right)$
<div style="display: flex; align-items: center; justify-content: center;">  </div> <p style="text-align: center;">(FR.15)</p>	$i \frac{2g^2 c_\theta^2 \xi}{v} [g^{\mu\nu} p_{Z1} \cdot p_{Z2} - p_{Z1}^\nu p_{Z2}^\mu] \left(a_B \frac{s_\theta^4}{c_\theta^4} + a_W + 4 \frac{s_\theta^2}{c_\theta^2} a_1 - 4\xi a_{12} \right) - \frac{ie^2 \xi}{v} [p_{Z1}^\nu p_h^\mu + p_{Z2}^\mu p_h^\nu - (p_{Z1} + p_{Z2}) \cdot p_h g^{\mu\nu}] \left(\frac{2a_4}{c_\theta^2} - \frac{a_5 + 2\xi a_{17}}{s_\theta^2} \right) + \frac{2ig_\theta^2 \xi}{v c_\theta^2} g_{\mu\nu} p_h^2 (2a_7 + 4\xi a_{25}) + \frac{2ig_\theta^2 \xi}{v c_\theta^2} p_{Z1}^\mu p_{Z2}^\nu (a_9 + 2\xi a_{15}) + \frac{ig_\theta^2 \xi}{v c_\theta^2} [p_{Z1}^\mu p_h^\nu + p_{Z2}^\nu p_h^\mu] (a_{10} + 2\xi a_{19})$

	standard structure	non-standard structure
(FR.16)		$\begin{aligned} & -\frac{2ig^2c_\theta s_\theta\xi}{v}[g^{\mu\nu}(p_A \cdot p_Z) - p_A^\nu p_Z^\mu] \cdot \\ & \cdot \left(a_B \frac{s_\theta^2}{c_\theta^2} - a_W + 2a_1 \frac{c_\theta^2 - s_\theta^2}{c_\theta^2} + 4\xi a_{12} \right) \\ & + \frac{ieg\xi}{vc_\theta}[p_A^\nu p_h^\mu - p_A \cdot p_h g^{\mu\nu}](2a_4 + a_5 + 2\xi a_{17}) \end{aligned}$
(FR.17)		$\begin{aligned} & \frac{ig^2\xi}{v}[2g^{\mu\nu}(p_+ \cdot p_-) - 2p_+^\nu p_-^\mu]a_W \\ & - \frac{ig^2\xi}{v}[(p_+^\nu p_h^\mu + p_-^\mu p_h^\nu) - (p_+ + p_-) \cdot p_h g^{\mu\nu}]a_5 \\ & + \frac{2ig^2\xi}{v}g_{\mu\nu}p_h^2a_7 + \frac{2ig^2\xi}{v}p_+^\mu p_-^\nu a_9 + \frac{ig^2\xi}{v}(p_+^\mu p_h^\nu + p_-^\nu p_h^\mu)c_{10} \end{aligned}$
(FR.18)		$i\frac{2g_s^2\xi}{v}[g^{\mu\nu}p_{G1} \cdot p_{G2} - p_{G1}^\nu p_{G2}^\mu]a_G$
(FR.19)		$\begin{aligned} & -\frac{2ieg^2\xi}{v}[g_{\mu\nu}(p_+ - p_-)_\rho + g_{\mu\rho}p_{-\nu} + g_{\nu\rho}p_{+\mu}]a_W \\ & - \frac{2ieg^2\xi}{v}[-g_{\mu\rho}p_{A\nu} + g_{\nu\rho}p_{A\mu}](a_W - 2a_1 + 2a_2 + a_3 + 2\xi(a_{13} - 2a_{12})) \\ & - \frac{ieg^2\xi}{v}[g_{\mu\rho}p_{h\nu} - g_{\nu\rho}p_{h\mu}](a_5 - a_{10}) - \frac{2ieg^2\xi}{v}(p_+^\mu p_{-\nu} - p_-^\nu p_{+\mu})a_9 \end{aligned}$

standard structure	non-standard structure
<div data-bbox="510 172 686 627" data-label="Diagram"> </div> <div data-bbox="550 772 598 862">(FR.20)</div>	$ \begin{aligned} & -\frac{2ig^3c_\theta\xi}{v}[g_{\mu\nu}(p_+-p_-)_\rho+g_{\mu\rho}p_{-\nu}+g_{\nu\rho}p_{+\mu}]\left(a_W+\frac{a_3}{c_\theta}\right) \\ & -\frac{2ig^3c_\theta\xi}{v}[-g_{\mu\rho}p_{Z\nu}+g_{\nu\rho}p_{Z\mu}]\left(a_W+a_3+2\frac{s_\theta^2}{c_\theta^2}(a_1-a_2)+2\xi(a_{13}-2a_{12})\right) \\ & +\frac{ige^2\xi}{vc_\theta}[g_{\mu\rho}p_{h\nu}-g_{\nu\rho}p_{h\mu}]\left(a_5-a_{10}+\frac{2\xi(a_{17}+a_{18})}{s_\theta^2}\right) \\ & +\frac{i2g^3\xi}{vc_\theta^2}[p_+^\mu g_{\nu\rho}-p_-^\nu g_{\mu\rho}](s_\theta^2a_9-\xi a_{16})-\frac{2g^3\xi^2}{vc_\theta}\varepsilon^{\mu\nu\rho\lambda}[p_{+\lambda}-p_{-\lambda}]a_{14} \end{aligned} $
<div data-bbox="734 172 893 627" data-label="Diagram"> </div> <div data-bbox="774 772 821 862">(FR.21)</div>	$i\frac{8e^2\xi}{v^2}[g^{\mu\nu}p_{A1}\cdot p_{A2}-p_{A1}^\nu p_{A2}^\mu]\left(\frac{b_B+b_W}{4}-b_1-\xi b_{12}\right)$
<div data-bbox="941 172 1101 627" data-label="Diagram"> </div> <div data-bbox="1013 772 1061 862">(FR.22)</div>	$ \begin{aligned} & i\frac{2g^2c_\theta^2\xi}{v^2}[g^{\mu\nu}p_{Z1}\cdot p_{Z2}-p_{Z1}^\nu p_{Z2}^\mu]\left(b_B\frac{s_\theta^4}{c_\theta^2}+b_W+4\frac{s_\theta^2}{c_\theta^2}b_1-\xi b_{12}\right) \\ & -\frac{ie^2\xi}{v^2}[p_{Z1}^\nu(p_{h1}+p_{h2})^\mu+p_{Z2}^\mu(p_{h1}+p_{h2})^\nu-(p_{Z1}+p_{Z2})\cdot(p_{h1}+p_{h2})g^{\mu\nu}]\left(\frac{2b_4}{c_\theta^2}-\frac{b_7+2\xi b_{17}}{s_\theta^2}\right) \\ & +\frac{2ig^2\xi}{v^2c_\theta^2}g_{\mu\nu}\left[2p_{h1}\cdot p_{h2}(b_7+2\xi a_{20}+4\xi a_{21}+2\xi b_{25})+(p_{h1}^2+p_{h2}^2)(b_7+2\xi b_{25})\right] \\ & +\frac{2ig^2\xi}{v^2c_\theta^2}p_{Z1}^\mu p_{Z2}^\nu(b_9+2\xi b_{15})+\frac{4ig^2\xi}{v^2c_\theta^2}[p_{h1}^\mu p_{h2}^\nu+p_{h1}^\nu p_{h2}^\mu](a_8+2\xi a_{22}) \\ & +\frac{ig^2\xi}{v^2c_\theta^2}[p_{Z1}^\mu(p_{h1}+p_{h2})^\nu+p_{Z2}^\nu(p_{h1}+p_{h2})^\mu](b_{10}+2\xi b_{19}) \end{aligned} $

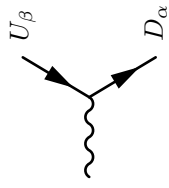
standard structure	non-standard structure
 <p>(FR.23)</p>	$ \begin{aligned} & \frac{-2ig^2 c_\theta s_\theta \xi}{v^2} [g^{\mu\nu} (p_A \cdot p_Z) - p_A^\nu p_Z^\mu] \cdot \\ & \cdot \left(b_B \frac{s_\theta^2}{c_\theta^2} - b_W + 2b_1 \frac{c_\theta^2 - s_\theta^2}{c_\theta^2} + 4\xi b_{12} \right) \\ & + \frac{ie g \xi}{v^2 c_\theta} [p_A^\nu (p_{h1} + p_{h2})^\mu - p_A \cdot (p_{h1} + p_{h2}) g^{\mu\nu}] (2b_4 + b_5 + 2\xi b_{17}) \end{aligned} $
 <p>(FR.24)</p>	$ \begin{aligned} & i \frac{2m_Z^2 c_\theta^2}{v^2} g_{\mu\nu} \left(1 - \xi c_H + \xi b_C + \frac{4e^2 \xi c_1}{(c_\theta^2 - s_\theta^2)} \right. \\ & \left. + \frac{2c_\theta^2 \xi c_T}{(c_\theta^2 - s_\theta^2)} - 4g^2 \xi^2 c_{12} \right) \\ & + \frac{ig^2 \xi}{v^2} [2g^{\mu\nu} (p_+ \cdot p_-) - 2p_+^\nu p_-^\mu] g^2 b_W + \frac{2ig^2 \xi}{v^2} p_+^\mu p_-^\nu b_9 \\ & + \frac{ig^2 \xi}{v^2} [p_+^\nu (p_{h1} + p_{h2})^\mu + p_-^\mu (p_{h1} + p_{h2})^\nu - (p_+ + p_-) \cdot (p_{h1} + p_{h2}) g^{\mu\nu}] b_5 \\ & + \frac{2ig^2 \xi}{v^2} g_{\mu\nu} [2p_{h1} \cdot p_{h2} (b_7 + 2\xi a_{20}) + (p_{h1}^2 + p_{h2}^2) b_7] \\ & + \frac{4ig^2 \xi}{v^2} [p_{h1}^\mu p_{h2}^\nu + p_{h1}^\nu p_{h2}^\mu] a_8 \\ & + \frac{ig^2 \xi}{v^2} [p_+^\mu (p_{h1} + p_{h2})^\nu + p_-^\nu (p_{h1} + p_{h2})^\mu] b_{10} \end{aligned} $
 <p>(FR.25)</p>	$i \frac{2g_\xi^2}{v^2} [g^{\mu\nu} p_{G1} \cdot p_{G2} - p_{G1}^\nu p_{G2}^\mu] b_G$

standard structure	non-standard structure
--------------------	------------------------



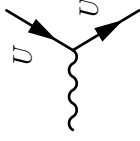
(FR.26) A_μ

$$-ieq_f \gamma_\mu; \quad q_U = \frac{2}{3}, q_D = -\frac{1}{3}, q_N = 0, q_E = -1$$



(FR.27) W_μ^-

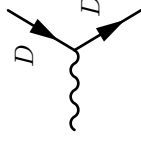
$$\frac{ig}{\sqrt{2}} \frac{\gamma_\mu (1-\gamma_5)}{2} (V^\dagger)_{\alpha\beta} \left(1 + \frac{\xi(c_T c_\theta^2 + 2e^2 c_1)}{c_\theta^2 - s_\theta^2} - 2g^2 \xi^2 c_{12} \right)$$



(FR.28) Z_μ

$$\frac{igc_\theta}{2} \left(\frac{s_\theta^2}{3c_\theta^2} - 1 \right) \frac{\gamma_\mu (1-\gamma_5)}{2} \left[1 + \frac{8\xi e^2 c_1}{(c_\theta^2 - s_\theta^2)(1+2(c_\theta^2 - s_\theta^2))} + \frac{\xi c_T}{c_\theta^2 - s_\theta^2} \frac{1+2c_\theta^2}{1+2(c_\theta^2 - s_\theta^2)} \right]$$

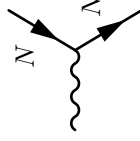
$$\frac{2}{3} i e \frac{s_\theta}{c_\theta} \frac{\gamma_\mu (1+\gamma_5)}{2} \left[1 - \frac{\xi(c_T + 2g^2 c_1)}{c_\theta^2 - s_\theta^2} \right]$$



(FR.29) Z_μ

$$\frac{igc_\theta}{2} \left(\frac{s_\theta^2}{3c_\theta^2} + 1 \right) \frac{\gamma_\mu (1-\gamma_5)}{2} \left[1 + \frac{\xi 4e^2 c_1}{(c_\theta^2 - s_\theta^2)(2+(c_\theta^2 - s_\theta^2))} + \frac{\xi c_T}{c_\theta^2 - s_\theta^2} \frac{4c_\theta^2 - 1}{2+(c_\theta^2 - s_\theta^2)} \right]$$

$$-\frac{1}{3} i e \frac{s_\theta}{c_\theta} \frac{\gamma_\mu (1+\gamma_5)}{2} \left[1 - \frac{\xi(c_T + 2g^2 c_1)}{c_\theta^2 - s_\theta^2} \right]$$

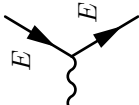


(FR.30) Z_μ

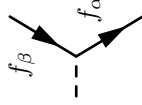
$$-\frac{ig}{2c_\theta} \frac{\gamma_\mu (1-\gamma_5)}{2} \left[1 + \frac{\xi 4e^2 c_1}{(c_\theta^2 - s_\theta^2)(2+(c_\theta^2 - s_\theta^2))} + \frac{\xi c_T}{c_\theta^2 - s_\theta^2} \frac{4c_\theta^2 - 1}{2+(c_\theta^2 - s_\theta^2)} \right]$$

standard structure

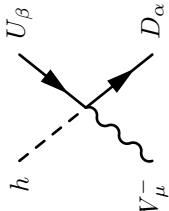
non-standard structure

(FR.31) 

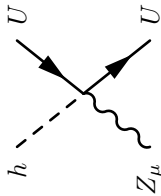
$$\frac{ig(c_\theta^2-s_\theta^2)}{2c_\theta} \frac{\gamma_\mu(1-\gamma_5)}{2} \left[1 + \frac{\xi 4e^2 c_1}{(c_\theta^2-s_\theta^2)(2+(c_\theta^2-s_\theta^2))} + \frac{\xi c_T}{c_\theta^2-s_\theta^2} \frac{4c_\theta^2-1}{2+(c_\theta^2-s_\theta^2)} \right] - ie \frac{s_\theta}{c_\theta} \frac{\gamma_\mu(1+\gamma_5)}{2} \left[1 - \frac{\xi(c_T+2g^2 c_1)}{c_\theta^2-s_\theta^2} \right]$$

(FR.32) 

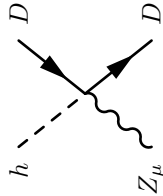
$$-i \frac{s_Y}{\sqrt{2}} Y_{f,\alpha\beta} \left(1 - \frac{\xi c_H}{2} \right), \quad f = U, D, E$$

(FR.33) 

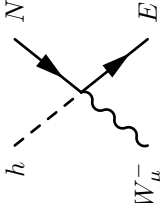
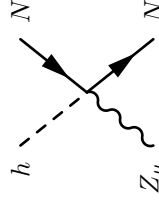
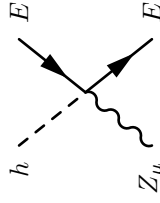
$$\frac{\sqrt{2}ig\xi}{v} \frac{\gamma_\mu(1-\gamma_5)}{2} (V^\dagger)_{\alpha\beta} \left(\frac{a_T c_\theta^2 + 2e^2 a_1}{c_\theta^2 - s_\theta^2} - 2g^2 \xi a_{12} \right)$$

(FR.34) 

$$\frac{ig\xi c_\theta}{v} \left(\frac{s_\theta^2}{3c_\theta^2} - 1 \right) \frac{\gamma_\mu(1-\gamma_5)}{2} \left[\frac{8e^2 a_1}{(c_\theta^2-s_\theta^2)(1+2(c_\theta^2-s_\theta^2))} + \frac{a_T}{c_\theta^2-s_\theta^2} \frac{1+2c_\theta^2}{1+2(c_\theta^2-s_\theta^2)} \right] + \frac{4}{3} \frac{ie\xi}{v} \frac{s_\theta}{c_\theta} \frac{\gamma_\mu(1+\gamma_5)}{2} \left[\frac{a_T+2g^2 a_1}{c_\theta^2-s_\theta^2} \right]$$

(FR.35) 

$$\frac{i\xi g c_\theta}{v} \left(\frac{s_\theta^2}{3c_\theta^2} + 1 \right) \frac{\gamma_\mu(1-\gamma_5)}{2} \left[\frac{4e^2 a_1}{(c_\theta^2-s_\theta^2)(2+(c_\theta^2-s_\theta^2))} + \frac{a_T}{c_\theta^2-s_\theta^2} \frac{4c_\theta^2-1}{2+(c_\theta^2-s_\theta^2)} \right] - \frac{2}{3} \frac{ie\xi s_\theta}{v} \frac{\gamma_\mu(1+\gamma_5)}{c_\theta} \left[\frac{a_T+2g^2 a_1}{c_\theta^2-s_\theta^2} \right]$$

standard structure	non-standard structure
 <p>(FR.36)</p>	$\frac{\sqrt{2}ig\xi}{v}\frac{\gamma_\mu(1-\gamma_5)}{2}\left(\frac{a_Tc_\theta^2+2e^2a_1}{c_\theta^2-s_\theta^2}-2g^2\xi a_{12}\right)$
 <p>(FR.37)</p>	$-\frac{ig\xi}{vc_\theta}\frac{\gamma_\mu(1-\gamma_5)}{2}\left[\frac{8e^2a_1}{(c_\theta^2-s_\theta^2)(1+2(c_\theta^2-s_\theta^2))}+\frac{a_T}{c_\theta^2-s_\theta^2}\frac{1+2c_\theta^2}{1+2(c_\theta^2-s_\theta^2)}\right]$
 <p>(FR.38)</p>	$\frac{ig\xi(c_\theta^2-s_\theta^2)}{vc_\theta}\frac{\gamma_\mu(1-\gamma_5)}{2}\left[\frac{4e^2a_1}{(c_\theta^2-s_\theta^2)(2+(c_\theta^2-s_\theta^2))}+\frac{a_T}{c_\theta^2-s_\theta^2}\frac{4c_\theta^2-1}{2+(c_\theta^2-s_\theta^2)}\right]$ $-\frac{ig\xi e s_\theta}{v}\frac{\gamma_\mu(1+\gamma_5)}{2}\left[\frac{a_T+2g^2a_1}{c_\theta^2-s_\theta^2}\right]$

Open Access. This article is distributed under the terms of the Creative Commons Attribution License ([CC-BY 4.0](https://creativecommons.org/licenses/by/4.0/)), which permits any use, distribution and reproduction in any medium, provided the original author(s) and source are credited.

References

- [1] F. Englert and R. Brout, *Broken Symmetry and the Mass of Gauge Vector Mesons*, *Phys. Rev. Lett.* **13** (1964) 321 [[INSPIRE](#)].
- [2] P.W. Higgs, *Broken symmetries, massless particles and gauge fields*, *Phys. Lett.* **12** (1964) 132 [[INSPIRE](#)].
- [3] P.W. Higgs, *Broken Symmetries and the Masses of Gauge Bosons*, *Phys. Rev. Lett.* **13** (1964) 508 [[INSPIRE](#)].
- [4] K. Hagiwara, R. Peccei, D. Zeppenfeld and K. Hikasa, *Probing the Weak Boson Sector in $e^+e^- \rightarrow W^+W^-$* , *Nucl. Phys. B* **282** (1987) 253 [[INSPIRE](#)].
- [5] W. Buchmüller and D. Wyler, *Effective Lagrangian Analysis of New Interactions and Flavor Conservation*, *Nucl. Phys. B* **268** (1986) 621 [[INSPIRE](#)].
- [6] B. Grzadkowski, M. Iskrzynski, M. Misiak and J. Rosiek, *Dimension-Six Terms in the Standard Model Lagrangian*, *JHEP* **10** (2010) 085 [[arXiv:1008.4884](#)] [[INSPIRE](#)].
- [7] K. Hagiwara, R. Szalapski and D. Zeppenfeld, *Anomalous Higgs boson production and decay*, *Phys. Lett. B* **318** (1993) 155 [[hep-ph/9308347](#)] [[INSPIRE](#)].
- [8] M. Gonzalez-Garcia, *Anomalous Higgs couplings*, *Int. J. Mod. Phys. A* **14** (1999) 3121 [[hep-ph/9902321](#)] [[INSPIRE](#)].
- [9] T. Corbett, O. Eboli, J. Gonzalez-Fraile and M. Gonzalez-Garcia, *Constraining anomalous Higgs interactions*, *Phys. Rev. D* **86** (2012) 075013 [[arXiv:1207.1344](#)] [[INSPIRE](#)].
- [10] T. Corbett, O. Eboli, J. Gonzalez-Fraile and M. Gonzalez-Garcia, *Robust Determination of the Higgs Couplings: Power to the Data*, *Phys. Rev. D* **87** (2013) 015022 [[arXiv:1211.4580](#)] [[INSPIRE](#)].
- [11] ATLAS collaboration, *Observation of a new particle in the search for the Standard Model Higgs boson with the ATLAS detector at the LHC*, *Phys. Lett. B* **716** (2012) 1 [[arXiv:1207.7214](#)] [[INSPIRE](#)].
- [12] CMS collaboration, *Observation of a new boson at a mass of 125 GeV with the CMS experiment at the LHC*, *Phys. Lett. B* **716** (2012) 30 [[arXiv:1207.7235](#)] [[INSPIRE](#)].
- [13] I. Low, J. Lykken and G. Shaughnessy, *Have We Observed the Higgs (Imposter)?*, *Phys. Rev. D* **86** (2012) 093012 [[arXiv:1207.1093](#)] [[INSPIRE](#)].
- [14] J. Ellis and T. You, *Global Analysis of the Higgs Candidate with Mass 125 GeV*, *JHEP* **09** (2012) 123 [[arXiv:1207.1693](#)] [[INSPIRE](#)].
- [15] P.P. Giardino, K. Kannike, M. Raidal and A. Strumia, *Is the resonance at 125 GeV the Higgs boson?*, *Phys. Lett. B* **718** (2012) 469 [[arXiv:1207.1347](#)] [[INSPIRE](#)].
- [16] M. Montull and F. Riva, *Higgs discovery: the beginning or the end of natural EWSB?*, *JHEP* **11** (2012) 018 [[arXiv:1207.1716](#)] [[INSPIRE](#)].
- [17] J. Espinosa, C. Grojean, M. Muhlleitner and M. Trott, *First Glimpses at Higgs' face*, *JHEP* **12** (2012) 045 [[arXiv:1207.1717](#)] [[INSPIRE](#)].

- [18] D. Carmi, A. Falkowski, E. Kuflik, T. Volansky and J. Zupan, *Higgs After the Discovery: A Status Report*, *JHEP* **10** (2012) 196 [[arXiv:1207.1718](#)] [[INSPIRE](#)].
- [19] S. Banerjee, S. Mukhopadhyay and B. Mukhopadhyaya, *New Higgs interactions and recent data from the LHC and the Tevatron*, *JHEP* **10** (2012) 062 [[arXiv:1207.3588](#)] [[INSPIRE](#)].
- [20] F. Bonnet, T. Ota, M. Rauch and W. Winter, *Interpretation of precision tests in the Higgs sector in terms of physics beyond the Standard Model*, *Phys. Rev. D* **86** (2012) 093014 [[arXiv:1207.4599](#)] [[INSPIRE](#)].
- [21] T. Plehn and M. Rauch, *Higgs Couplings after the Discovery*, *Europhys. Lett.* **100** (2012) 11002 [[arXiv:1207.6108](#)] [[INSPIRE](#)].
- [22] A. Djouadi, *Precision Higgs coupling measurements at the LHC through ratios of production cross sections*, *Eur. Phys. J. C* **73** (2013) 2498 [[arXiv:1208.3436](#)] [[INSPIRE](#)].
- [23] B. Batell, S. Gori and L.-T. Wang, *Higgs Couplings and Precision Electroweak Data*, *JHEP* **01** (2013) 139 [[arXiv:1209.6382](#)] [[INSPIRE](#)].
- [24] G. Moreau, *Constraining extra-fermion(s) from the Higgs boson data*, *Phys. Rev. D* **87** (2013) 015027 [[arXiv:1210.3977](#)] [[INSPIRE](#)].
- [25] G. Cacciapaglia, A. Deandrea, G.D. La Rochelle and J.-B. Flament, *Higgs couplings beyond the Standard Model*, *JHEP* **03** (2013) 029 [[arXiv:1210.8120](#)] [[INSPIRE](#)].
- [26] A. Azatov and J. Galloway, *Electroweak Symmetry Breaking and the Higgs Boson: Confronting Theories at Colliders*, *Int. J. Mod. Phys. A* **28** (2013) 1330004 [[arXiv:1212.1380](#)] [[INSPIRE](#)].
- [27] E. Masso and V. Sanz, *Limits on Anomalous Couplings of the Higgs to Electroweak Gauge Bosons from LEP and LHC*, *Phys. Rev. D* **87** (2013) 033001 [[arXiv:1211.1320](#)] [[INSPIRE](#)].
- [28] G. Passarino, *NLO Inspired Effective Lagrangians for Higgs Physics*, *Nucl. Phys. B* **868** (2013) 416 [[arXiv:1209.5538](#)] [[INSPIRE](#)].
- [29] A. Falkowski, F. Riva and A. Urbano, *Higgs at last*, *JHEP* **11** (2013) 111 [[arXiv:1303.1812](#)] [[INSPIRE](#)].
- [30] P.P. Giardino, K. Kannike, I. Masina, M. Raidal and A. Strumia, *The universal Higgs fit*, [arXiv:1303.3570](#) [[INSPIRE](#)].
- [31] J. Ellis and T. You, *Updated Global Analysis of Higgs Couplings*, *JHEP* **06** (2013) 103 [[arXiv:1303.3879](#)] [[INSPIRE](#)].
- [32] A. Djouadi and G. Moreau, *The couplings of the Higgs boson and its CP properties from fits of the signal strengths and their ratios at the 7+8 TeV LHC*, [arXiv:1303.6591](#) [[INSPIRE](#)].
- [33] R. Contino, M. Ghezzi, C. Grojean, M. Muhlleitner and M. Spira, *Effective Lagrangian for a light Higgs-like scalar*, *JHEP* **07** (2013) 035 [[arXiv:1303.3876](#)] [[INSPIRE](#)].
- [34] B. Dumont, S. Fichet and G. von Gersdorff, *A Bayesian view of the Higgs sector with higher dimensional operators*, *JHEP* **07** (2013) 065 [[arXiv:1304.3369](#)] [[INSPIRE](#)].
- [35] J. Elias-Miro, J. Espinosa, E. Masso and A. Pomarol, *Higgs windows to new physics through $D = 6$ operators: constraints and one-loop anomalous dimensions*, *JHEP* **11** (2013) 066 [[arXiv:1308.1879](#)] [[INSPIRE](#)].
- [36] D. López-Val, T. Plehn and M. Rauch, *Measuring extended Higgs sectors as a consistent free couplings model*, *JHEP* **10** (2013) 134 [[arXiv:1308.1979](#)] [[INSPIRE](#)].

- [37] E.E. Jenkins, A.V. Manohar and M. Trott, *Renormalization Group Evolution of the Standard Model Dimension Six Operators I: Formalism and λ Dependence*, *JHEP* **10** (2013) 087 [[arXiv:1308.2627](#)] [[INSPIRE](#)].
- [38] A. Pomarol and F. Riva, *Towards the Ultimate SM Fit to Close in on Higgs Physics*, *JHEP* **01** (2014) 151 [[arXiv:1308.2803](#)] [[INSPIRE](#)].
- [39] S. Banerjee, S. Mukhopadhyay and B. Mukhopadhyaya, *Higher dimensional operators and LHC Higgs data: the role of modified kinematics*, [arXiv:1308.4860](#) [[INSPIRE](#)].
- [40] A. Alloul, B. Fuks and V. Sanz, *Phenomenology of the Higgs Effective Lagrangian via FeynRules*, [arXiv:1310.5150](#) [[INSPIRE](#)].
- [41] D.B. Kaplan and H. Georgi, *SU(2) \times U(1) Breaking by Vacuum Misalignment*, *Phys. Lett. B* **136** (1984) 183 [[INSPIRE](#)].
- [42] D.B. Kaplan, H. Georgi and S. Dimopoulos, *Composite Higgs Scalars*, *Phys. Lett. B* **136** (1984) 187 [[INSPIRE](#)].
- [43] T. Banks, *Constraints on SU(2) \times U(1) breaking by vacuum misalignment*, *Nucl. Phys. B* **243** (1984) 125 [[INSPIRE](#)].
- [44] H. Georgi, D.B. Kaplan and P. Galison, *Calculation of the Composite Higgs Mass*, *Phys. Lett. B* **143** (1984) 152 [[INSPIRE](#)].
- [45] H. Georgi and D.B. Kaplan, *Composite Higgs and Custodial SU(2)*, *Phys. Lett. B* **145** (1984) 216 [[INSPIRE](#)].
- [46] M.J. Dugan, H. Georgi and D.B. Kaplan, *Anatomy of a Composite Higgs Model*, *Nucl. Phys. B* **254** (1985) 299 [[INSPIRE](#)].
- [47] K. Agashe, R. Contino and A. Pomarol, *The Minimal composite Higgs model*, *Nucl. Phys. B* **719** (2005) 165 [[hep-ph/0412089](#)] [[INSPIRE](#)].
- [48] R. Contino, L. Da Rold and A. Pomarol, *Light custodians in natural composite Higgs models*, *Phys. Rev. D* **75** (2007) 055014 [[hep-ph/0612048](#)] [[INSPIRE](#)].
- [49] B. Gripaios, A. Pomarol, F. Riva and J. Serra, *Beyond the Minimal Composite Higgs Model*, *JHEP* **04** (2009) 070 [[arXiv:0902.1483](#)] [[INSPIRE](#)].
- [50] D. Marzocca, M. Serone and J. Shu, *General Composite Higgs Models*, *JHEP* **08** (2012) 013 [[arXiv:1205.0770](#)] [[INSPIRE](#)].
- [51] N. Arkani-Hamed, A.G. Cohen and H. Georgi, *Electroweak symmetry breaking from dimensional deconstruction*, *Phys. Lett. B* **513** (2001) 232 [[hep-ph/0105239](#)] [[INSPIRE](#)].
- [52] M. Schmaltz and D. Tucker-Smith, *Little Higgs review*, *Ann. Rev. Nucl. Part. Sci.* **55** (2005) 229 [[hep-ph/0502182](#)] [[INSPIRE](#)].
- [53] C.G. Callan Jr., S.R. Coleman, J. Wess and B. Zumino, *Structure of phenomenological Lagrangians. 2.*, *Phys. Rev.* **177** (1969) 2247 [[INSPIRE](#)].
- [54] L. Susskind, *Dynamics of Spontaneous Symmetry Breaking in the Weinberg-Salam Theory*, *Phys. Rev. D* **20** (1979) 2619 [[INSPIRE](#)].
- [55] S. Dimopoulos and L. Susskind, *Mass Without Scalars*, *Nucl. Phys. B* **155** (1979) 237 [[INSPIRE](#)].
- [56] S. Dimopoulos and J. Preskill, *Massless Composites With Massive Constituents*, *Nucl. Phys. B* **199** (1982) 206 [[INSPIRE](#)].

- [57] B. Grinstein and M. Trott, *A Higgs-Higgs bound state due to new physics at a TeV*, *Phys. Rev. D* **76** (2007) 073002 [[arXiv:0704.1505](#)] [[INSPIRE](#)].
- [58] R. Contino, C. Grojean, M. Moretti, F. Piccinini and R. Rattazzi, *Strong Double Higgs Production at the LHC*, *JHEP* **05** (2010) 089 [[arXiv:1002.1011](#)] [[INSPIRE](#)].
- [59] J. Bagger et al., *The Strongly interacting $W W$ system: Gold plated modes*, *Phys. Rev. D* **49** (1994) 1246 [[hep-ph/9306256](#)] [[INSPIRE](#)].
- [60] V. Koulovassilopoulos and R.S. Chivukula, *The Phenomenology of a nonstandard Higgs boson in $W(L) W(L)$ scattering*, *Phys. Rev. D* **50** (1994) 3218 [[hep-ph/9312317](#)] [[INSPIRE](#)].
- [61] C. Burgess, J. Matias and M. Pospelov, *A Higgs or not a Higgs? What to do if you discover a new scalar particle*, *Int. J. Mod. Phys. A* **17** (2002) 1841 [[hep-ph/9912459](#)] [[INSPIRE](#)].
- [62] A. Azatov, R. Contino and J. Galloway, *Model-Independent Bounds on a Light Higgs*, *JHEP* **04** (2012) 127 [Erratum *ibid.* **1304** (2013) 140] [[arXiv:1202.3415](#)] [[INSPIRE](#)].
- [63] R. Alonso, M. Gavela, L. Merlo, S. Rigolin and J. Yepes, *The Effective Chiral Lagrangian for a Light Dynamical “Higgs Particle”*, *Phys. Lett. B* **722** (2013) 330 [Erratum *ibid.* **B 726** (2013) 926] [[arXiv:1212.3305](#)] [[INSPIRE](#)].
- [64] G. Buchalla, O. Catà and C. Krause, *Complete Electroweak Chiral Lagrangian with a Light Higgs at NLO*, [arXiv:1307.5017](#) [[INSPIRE](#)].
- [65] R. Contino, D. Marzocca, D. Pappadopulo and R. Rattazzi, *On the effect of resonances in composite Higgs phenomenology*, *JHEP* **10** (2011) 081 [[arXiv:1109.1570](#)] [[INSPIRE](#)].
- [66] A. Manohar and H. Georgi, *Chiral Quarks and the Nonrelativistic Quark Model*, *Nucl. Phys. B* **234** (1984) 189 [[INSPIRE](#)].
- [67] E.E. Jenkins, A.V. Manohar and M. Trott, *Naive Dimensional Analysis Counting of Gauge Theory Amplitudes and Anomalous Dimensions*, *Phys. Lett. B* **726** (2013) 697 [[arXiv:1309.0819](#)] [[INSPIRE](#)].
- [68] I. Brivio et al., *$SU(N)$ Composite-Higgs Models and Dynamical Higgs Effective Lagrangian*, in preparation.
- [69] M.S. Chanowitz, M. Golden and H. Georgi, *Low-Energy Theorems for Strongly Interacting W 's and Z 's*, *Phys. Rev. D* **36** (1987) 1490 [[INSPIRE](#)].
- [70] C. Burgess and D. London, *On anomalous gauge boson couplings and loop calculations*, *Phys. Rev. Lett.* **69** (1992) 3428 [[INSPIRE](#)].
- [71] C. Burgess and D. London, *Uses and abuses of effective Lagrangians*, *Phys. Rev. D* **48** (1993) 4337 [[hep-ph/9203216](#)] [[INSPIRE](#)].
- [72] R. Alonso, M. Gavela, L. Merlo, S. Rigolin and J. Yepes, *Minimal Flavour Violation with Strong Higgs Dynamics*, *JHEP* **06** (2012) 076 [[arXiv:1201.1511](#)] [[INSPIRE](#)].
- [73] R. Alonso, M. Gavela, L. Merlo, S. Rigolin and J. Yepes, *Flavor with a light dynamical “Higgs particle”*, *Phys. Rev. D* **87** (2013) 055019 [[arXiv:1212.3307](#)] [[INSPIRE](#)].
- [74] G. Isidori and M. Trott, *Higgs form factors in Associated Production*, [arXiv:1307.4051](#) [[INSPIRE](#)].
- [75] G. Isidori, A.V. Manohar and M. Trott, *Probing the nature of the Higgs-like Boson via $h \rightarrow V F$ decays*, *Phys. Lett. B* **728** (2014) 131 [[arXiv:1305.0663](#)] [[INSPIRE](#)].

- [76] K. Hagiwara, S. Ishihara, R. Szalapski and D. Zeppenfeld, *Low-energy effects of new interactions in the electroweak boson sector*, *Phys. Rev. D* **48** (1993) 2182 [[INSPIRE](#)].
- [77] K. Hagiwara, T. Hatsukano, S. Ishihara and R. Szalapski, *Probing nonstandard bosonic interactions via W boson pair production at lepton colliders*, *Nucl. Phys. B* **496** (1997) 66 [[hep-ph/9612268](#)] [[INSPIRE](#)].
- [78] T. Corbett, O. Eboli, J. Gonzalez-Fraile and M. Gonzalez-Garcia, *Determining Triple Gauge Boson Couplings from Higgs Data*, *Phys. Rev. Lett.* **111** (2013) 011801 [[arXiv:1304.1151](#)] [[INSPIRE](#)].
- [79] A. Brunstein, O.J. Eboli and M. Gonzalez-Garcia, *Constraints on quartic vector boson interactions from Z physics*, *Phys. Lett. B* **375** (1996) 233 [[hep-ph/9602264](#)] [[INSPIRE](#)].
- [80] A. Belyaev et al., *Strongly interacting vector bosons at the CERN LHC: Quartic anomalous couplings*, *Phys. Rev. D* **59** (1999) 015022 [[hep-ph/9805229](#)] [[INSPIRE](#)].
- [81] O.J. Eboli, M. Gonzalez-Garcia, S. Lietti and S. Novaes, *Anomalous quartic gauge boson couplings at hadron colliders*, *Phys. Rev. D* **63** (2001) 075008 [[hep-ph/0009262](#)] [[INSPIRE](#)].
- [82] O. Eboli, M. Gonzalez-Garcia and S. Lietti, *Bosonic quartic couplings at CERN LHC*, *Phys. Rev. D* **69** (2004) 095005 [[hep-ph/0310141](#)] [[INSPIRE](#)].
- [83] O. Eboli, M. Gonzalez-Garcia and J. Mizukoshi, *$pp \rightarrow jje^\pm\mu^\pm\nu\nu$ and $jje^\pm\mu^\pm\nu\nu$ at $\mathcal{O}(\alpha_{em}^6)$ and $\mathcal{O}(\alpha_{em}^4\alpha_s^2)$ for the study of the quartic electroweak gauge boson vertex at CERN LHC*, *Phys. Rev. D* **74** (2006) 073005 [[hep-ph/0606118](#)] [[INSPIRE](#)].
- [84] M. B. Gavela et al., *Bosonic Chiral Lagrangian for a light dynamical Higgs at next-to-leading order*, in preparation.
- [85] W.D. Goldberger, B. Grinstein and W. Skiba, *Distinguishing the Higgs boson from the dilaton at the Large Hadron Collider*, *Phys. Rev. Lett.* **100** (2008) 111802 [[arXiv:0708.1463](#)] [[INSPIRE](#)].
- [86] G. Buchalla, O. Catà and C. Krause, *On the Power Counting in Effective Field Theories*, [arXiv:1312.5624](#) [[INSPIRE](#)].
- [87] G. Giudice, C. Grojean, A. Pomarol and R. Rattazzi, *The Strongly-Interacting Light Higgs*, *JHEP* **06** (2007) 045 [[hep-ph/0703164](#)] [[INSPIRE](#)].
- [88] A. De Rujula, M. Gavela, P. Hernández and E. Masso, *The Selfcouplings of vector bosons: Does LEP-1 obviate LEP-2?*, *Nucl. Phys. B* **384** (1992) 3 [[INSPIRE](#)].
- [89] E. Halyo, *Technidilaton or Higgs?*, *Mod. Phys. Lett. A* **8** (1993) 275 [[INSPIRE](#)].
- [90] L. Vecchi, *Phenomenology of a light scalar: the dilaton*, *Phys. Rev. D* **82** (2010) 076009 [[arXiv:1002.1721](#)] [[INSPIRE](#)].
- [91] B.A. Campbell, J. Ellis and K.A. Olive, *Phenomenology and Cosmology of an Electroweak Pseudo-Dilaton and Electroweak Baryons*, *JHEP* **03** (2012) 026 [[arXiv:1111.4495](#)] [[INSPIRE](#)].
- [92] S. Matsuzaki and K. Yamawaki, *Is 125 GeV techni-dilaton found at LHC?*, *Phys. Lett. B* **719** (2013) 378 [[arXiv:1207.5911](#)] [[INSPIRE](#)].
- [93] Z. Chacko, R. Franceschini and R.K. Mishra, *Resonance at 125 GeV: Higgs or Dilaton/Radion?*, *JHEP* **04** (2013) 015 [[arXiv:1209.3259](#)] [[INSPIRE](#)].
- [94] B. Bellazzini, C. Csáki, J. Hubisz, J. Serra and J. Terning, *A Higgslike Dilaton*, *Eur. Phys. J. C* **73** (2013) 2333 [[arXiv:1209.3299](#)] [[INSPIRE](#)].

- [95] C. Grojean, O. Matsedonskyi and G. Panico, *Light top partners and precision physics*, *JHEP* **10** (2013) 160 [[arXiv:1306.4655](#)] [[INSPIRE](#)].
- [96] D. Barducci et al., *The 4-Dimensional Composite Higgs Model (4DCHM) and the 125 GeV Higgs-like signals at the LHC*, *JHEP* **09** (2013) 047 [[arXiv:1302.2371](#)] [[INSPIRE](#)].
- [97] J. Elias-Miró, J. Espinosa, E. Masso and A. Pomarol, *Renormalization of dimension-six operators relevant for the Higgs decays $h \rightarrow \gamma\gamma, \gamma Z$* , *JHEP* **08** (2013) 033 [[arXiv:1302.5661](#)] [[INSPIRE](#)].
- [98] C. Grojean, E.E. Jenkins, A.V. Manohar and M. Trott, *Renormalization Group Scaling of Higgs Operators and $\Gamma(H \rightarrow \gamma\gamma)$* , *JHEP* **04** (2013) 016 [[arXiv:1301.2588](#)] [[INSPIRE](#)].
- [99] PARTICLE DATA GROUP collaboration, J. Beringer et al., *Review of Particle Physics (RPP)*, *Phys. Rev. D* **86** (2012) 010001 [[INSPIRE](#)].
- [100] M.E. Peskin and T. Takeuchi, *A New constraint on a strongly interacting Higgs sector*, *Phys. Rev. Lett.* **65** (1990) 964 [[INSPIRE](#)].
- [101] F. Feruglio and S. Rigolin, *Sum rules for asymptotic form-factors in $e^+e^- \rightarrow W^+W^-$ scattering*, *Phys. Lett. B* **397** (1997) 245 [[hep-ph/9611414](#)] [[INSPIRE](#)].
- [102] K. Hagiwara, S. Matsumoto and R. Szalapski, *Constraints on new physics in the electroweak bosonic sector from current data and future experiments*, *Phys. Lett. B* **357** (1995) 411 [[hep-ph/9505322](#)] [[INSPIRE](#)].
- [103] LEP collaborations and the LEP TGC working group, *A combination of preliminary results on gauge boson couplings measured by the LEP experiments*, Tech. Rep. LEPEWWG/TGC/2003-01 (2003).
- [104] D0, CDF collaborations, B. Tuchming, *Tevatron Higgs results*, *EPJ Web Conf.* **60** (2013) 02003 [[arXiv:1307.4873](#)] [[INSPIRE](#)].
- [105] ATLAS collaboration, *Search for the Standard Model Higgs boson in $H \rightarrow \tau\tau$ decays in proton-proton collisions with the ATLAS detector*, *ATLAS-CONF-2012-160* (2012).
- [106] ATLAS collaboration, *Search for the bb decay of the Standard Model Higgs boson in associated W/ZH production with the ATLAS detector*, *ATLAS-CONF-2013-079* (2013).
- [107] ATLAS collaboration, *Measurements of the properties of the Higgs-like boson in the four lepton decay channel with the ATLAS detector using 25fb^{-1} of proton-proton collision data*, *ATLAS-CONF-2013-013* (2013).
- [108] ATLAS collaboration, *Determination of the Top Quark Mass with a Template Method in the All Hadronic Decay Channel using $2.04/\text{fb}$ of ATLAS DATA*, *ATLAS-CONF-2012-030* (2012).
- [109] ATLAS collaboration, *Observation of an excess of events in the search for the Standard Model Higgs boson in the gamma-gamma channel with the ATLAS detector*, *ATLAS-CONF-2012-091* (2012).
- [110] ATLAS collaboration, *Measurements of the properties of the Higgs-like boson in the two photon decay channel with the ATLAS detector using 25fb^{-1} of proton-proton collision data*, *ATLAS-CONF-2013-012* (2013).
- [111] CMS collaboration, *Search for the Standard-Model Higgs boson decaying to tau pairs in proton-proton collisions at $\sqrt{s} = 7$ and 8 TeV* , *CMS-PAS-HIG-13-004*.

- [112] CMS collaboration, *Search for the standard model Higgs boson produced in association with W or Z bosons, and decaying to bottom quarks for LHCp 2013*, [CMS-PAS-HIG-13-012](#) (2013).
- [113] CMS collaboration, *Higgs to bb in the VBF channel*, [CMS-PAS-HIG-13-011](#).
- [114] CMS collaboration, *Properties of the Higgs-like boson in the decay H to ZZ to $4l$ in pp collisions at $\sqrt{s} = 7$ and 8 TeV*, [CMS-PAS-HIG-13-002](#).
- [115] CMS collaboration, *Evidence for a particle decaying to W^+W^- in the fully leptonic final state in a standard model Higgs boson search in pp collisions at the LHC*, [CMS-PAS-HIG-13-003](#).
- [116] CMS collaboration, *Updated measurements of the Higgs boson at 125 GeV in the two photon decay channel*, [CMS-PAS-HIG-13-001](#).
- [117] CMS collaboration, *Search for a Higgs boson decaying into a Z and a photon in pp collisions at $\sqrt{s} = 7$ and 8 TeV*, *Phys. Lett. B* **726** (2013) 587 [[arXiv:1307.5515](#)] [[INSPIRE](#)].
- [118] CMS collaboration, *Projected Performance of an Upgraded CMS Detector at the LHC and HL-LHC: Contribution to the Snowmass Process*, [arXiv:1307.7135](#) [[INSPIRE](#)].
- [119] ATLAS collaboration, *Physics at a High-Luminosity LHC with ATLAS*, [arXiv:1307.7292](#) [[INSPIRE](#)].
- [120] OPAL collaboration, G. Abbiendi et al., *Measurement of charged current triple gauge boson couplings using W pairs at LEP*, *Eur. Phys. J. C* **33** (2004) 463 [[hep-ex/0308067](#)] [[INSPIRE](#)].
- [121] L3 collaboration, P. Achard et al., *Measurement of triple gauge boson couplings of the W boson at LEP*, *Phys. Lett. B* **586** (2004) 151 [[hep-ex/0402036](#)] [[INSPIRE](#)].
- [122] ALEPH collaboration, S. Schael et al., *Improved measurement of the triple gauge-boson couplings γWW and ZWW in e^+e^- collisions*, *Phys. Lett. B* **614** (2005) 7 [[INSPIRE](#)].
- [123] O.J. Eboli, S. Lietti, M. Gonzalez-Garcia and S. Novaes, *ϵ_b constraints on selfcouplings of vector bosons*, *Phys. Lett. B* **339** (1994) 119 [[hep-ph/9406316](#)] [[INSPIRE](#)].
- [124] S. Dawson and G. Valencia, *Bounds on $g_5(Z)$ from precision LEP measurements*, *Phys. Lett. B* **333** (1994) 207 [[hep-ph/9406324](#)] [[INSPIRE](#)].
- [125] O.J. Eboli, M. Gonzalez-Garcia and S. Novaes, *Indirect constraints on the triple gauge boson couplings from $Z \rightarrow b\bar{b}$ partial width: An Update*, *Mod. Phys. Lett. A* **15** (2000) 1 [[hep-ph/9811388](#)] [[INSPIRE](#)].
- [126] ATLAS collaboration, *Measurement of WZ production in proton-proton collisions at $\sqrt{s} = 7$ TeV with the ATLAS detector*, *Eur. Phys. J. C* **72** (2012) 2173 [[arXiv:1208.1390](#)] [[INSPIRE](#)].
- [127] ATLAS collaboration, *Measurement of the WW cross section in $\sqrt{s} = 7$ TeV pp collisions with the ATLAS detector and limits on anomalous gauge couplings*, *Phys. Lett. B* **712** (2012) 289 [[arXiv:1203.6232](#)] [[INSPIRE](#)].
- [128] ATLAS, CMS collaborations, V. Lombardo, *Diboson production cross section at LHC*, [arXiv:1305.3773](#) [[INSPIRE](#)].
- [129] CMS collaboration, *Measurement of the $W\gamma$ and $Z\gamma$ inclusive cross sections in pp collisions at $\sqrt{s} = 7$ TeV and limits on anomalous triple gauge boson couplings*, [arXiv:1308.6832](#) [[INSPIRE](#)].

- [130] CMS collaboration, *Measurement of the sum of WW and WZ production with W +dijet events in pp collisions at $\sqrt{s} = 7$ TeV*, *Eur. Phys. J. C* **73** (2013) 2283 [[arXiv:1210.7544](#)] [[INSPIRE](#)].
- [131] O. Eboli, J. Gonzalez-Fraile and M. Gonzalez-Garcia, *Scrutinizing the ZW^+W^- vertex at the Large Hadron Collider at 7 TeV*, *Phys. Lett. B* **692** (2010) 20 [[arXiv:1006.3562](#)] [[INSPIRE](#)].
- [132] N.D. Christensen and C. Duhr, *FeynRules — Feynman rules made easy*, *Comput. Phys. Commun.* **180** (2009) 1614 [[arXiv:0806.4194](#)] [[INSPIRE](#)].
- [133] J. Alwall, M. Herquet, F. Maltoni, O. Mattelaer and T. Stelzer, *MadGraph 5: Going Beyond*, *JHEP* **06** (2011) 128 [[arXiv:1106.0522](#)] [[INSPIRE](#)].
- [134] T. Sjöstrand, S. Mrenna and P.Z. Skands, *PYTHIA 6.4 Physics and Manual*, *JHEP* **05** (2006) 026 [[hep-ph/0603175](#)] [[INSPIRE](#)].
- [135] J. Conway, *PGS 4*,
<http://physics.ucdavis.edu/~conway/research/software/pgs/pgs4-support.htm>.
- [136] C. Degrande et al., *Studies of Vector Boson Scattering And Triboson Production with DELPHES Parametrized Fast Simulation for Snowmass 2013*, [arXiv:1309.7452](#) [[INSPIRE](#)].
- [137] K. Jansen, J. Kuti and C. Liu, *The Higgs model with a complex ghost pair*, *Phys. Lett. B* **309** (1993) 119 [[hep-lat/9305003](#)] [[INSPIRE](#)].
- [138] K. Jansen, J. Kuti and C. Liu, *Strongly interacting Higgs sector in the minimal Standard Model?*, *Phys. Lett. B* **309** (1993) 127 [[hep-lat/9305004](#)] [[INSPIRE](#)].
- [139] B. Grinstein, D. O’Connell and M.B. Wise, *The Lee-Wick standard model*, *Phys. Rev. D* **77** (2008) 025012 [[arXiv:0704.1845](#)] [[INSPIRE](#)].
- [140] I. Brivio et al., *Impact of higher derivative operators on Higgs effective Lagrangians*, in preparation.

Higgs ultraviolet softening

This Chapter contains the publication in Ref. [29]. Here the focus is on the operators that induce a quartic momentum dependence in the Higgs propagator: $\mathcal{O}_{\Box\Phi} = (D_\mu D^\mu \Phi)^\dagger (D_\nu D^\nu \Phi)$ in the linear case and $\mathcal{P}_{\Box h} = \frac{1}{2}(\Box h)(\Box h)$ in the non-linear one. The relevance of this peculiar momentum structure resides in that it allows to soften the sensitivity of the Higgs mass to UV scales, as quadratic divergences are removed by the fast fall of the momentum dependence of the propagator. This can be interpreted as an alternative solution to the hierarchy problem [107, 108]. The treatment of these operators is quite delicate, as their presence induces a second pole in the Higgs propagator with a “wrong-sign” residue: in general, theories with higher derivative kinetic terms (also known as Lee-Wick theories [109, 110]) violate both unitarity and causality.

A safe and manageable way of handling these couplings is to trade them for the presence of a “ghost” state with negative norm: a field with the same quantum numbers as h but with a “wrong-sign” mass and kinetic term. As an alternative, the operators $\mathcal{O}_{\Box\Phi}$ and $\mathcal{P}_{\Box h}$ can be removed from the Lagrangian by applying the equations of motion for the Higgs. It is shown in Secs. 2 and 3 of this chapter that both approaches lead to the same result once the Lee-Wick ghost is integrated out of the spectrum.

Remarkably, there are significant differences between the results obtained in the linear *vs.* the non-linear case. In fact, the chiral operator $\mathcal{P}_{\Box h}$ is traded for a large amount of anomalous couplings listed in Tables 1-4, inducing both modifications of the SM vertices and the insertion of exotic Lorentz structures. In particular, this affects triple and quartic gauge couplings, gauge-Higgs and gauge-fermion interactions. On the other hand, the impact of the linear $\mathcal{O}_{\Box\Phi}$ is limited to the presence of anomalous Yukawa couplings and to the introduction of some four-fermion vertices. In practice, the gauge structure of the operator $\mathcal{O}_{\Box\Phi}$ determines a series of cancellations that do not take place in general in the non-linear case. In fact, in this framework, such a cancellation would only be recovered imposing a (quite unnatural) relation among the Wilson coefficients of 6 independent operators: $v^2 c_{\Box h} = 8c_6 = 4c_7 = -c_8 = -4c_9 = -2c_{10}$.

The presence of a larger number of vertices clearly offers an inviting window into chiral Higgs dynamics: a few examples of how this fact can be exploited in future experiments are given in Sec. 5 of this chapter. It turns out that a subset of the relevant Wilson coefficients ($c_{\Box h}$, c_6) can already be constrained combining electroweak precision data with measurements of HVV, Hff and quartic gauge couplings. An interesting signature, albeit quite challenging to observe at the LHC, is provided by the operator \mathcal{P}_7 , that induces ZZ and W^+W^- production mediated by an off-shell Higgs boson (see Sec. 5.2).

Higgs ultraviolet softening

I. Brivio^a O.J.P. Éboli^b M.B. Gavela^a M.C. Gonzalez-García^{c,d,e} L. Merlo^a
and S. Rigolin^f

^a*Departamento de Física Teórica and Instituto de Física Teórica, IFT-UAM/CSIC,
Universidad Autónoma de Madrid, Cantoblanco, 28049, Madrid, Spain*

^b*Instituto de Física, Universidade de São Paulo,
São Paulo — SP, Brazil*

^c*C.N. Yang Institute for Theoretical Physics and Department of Physics and Astronomy,
SUNY at Stony Brook, Stony Brook, NY 11794-3840, U.S.A.*

^d*Departament d'Estructura i Constituents de la Matèria and ICC-UB,
Universitat de Barcelona, 647 Diagonal, E-08028 Barcelona, Spain*

^e*Institució Catalana de Recerca i Estudis Avançats (ICREA),
Barcelona, Spain*

^f*Dipartimento di Fisica e Astronomia “G. Galilei”, Università di Padova
and INFN — Sezione di Padova,
Via Marzolo 8, I-35131 Padua, Italy*

E-mail: ilaria.brivio@uam.es, eboli@fma.if.usp.br,
belen.gavela@uam.es, concha@insti.physics.sunysb.edu,
luca.merlo@uam.es, stefano.rigolin@pd.infn.it

ABSTRACT: We analyze the leading effective operators which induce a quartic momentum dependence in the Higgs propagator, for a linear and for a non-linear realization of electroweak symmetry breaking. Their specific study is relevant for the understanding of the ultraviolet sensitivity to new physics. Two methods of analysis are applied, trading the Lagrangian coupling by: i) a “ghost” scalar, after the Lee-Wick procedure; ii) other effective operators via the equations of motion. The two paths are shown to lead to the same effective Lagrangian at first order in the operator coefficients. It follows a modification of the Higgs potential and of the fermionic couplings in the linear realization, while in the non-linear one anomalous quartic gauge couplings, Higgs-gauge couplings and gauge-fermion interactions are induced in addition. Finally, all LHC Higgs and other data presently available are used to constrain the operator coefficients; the future impact of $pp \rightarrow 4$ leptons data via off-shell Higgs exchange and of vector boson fusion data is considered as well. For completeness, a summary of pure-gauge and gauge-Higgs signals exclusive to non-linear dynamics at leading-order is included.

KEYWORDS: Higgs Physics, Chiral Lagrangians, Technicolor and Composite Models

ARXIV EPRINT: [1405.5412](https://arxiv.org/abs/1405.5412)

Contents

1	Introduction	1
2	Elementary Higgs: $\mathcal{O}_{\Box\Phi}$	4
2.1	Analysis in terms of the LW ghost	4
2.2	Analysis via EOM	6
3	Light dynamical Higgs: $\mathcal{P}_{\Box h}$	7
3.1	Analysis in terms of the LW ghost	8
3.2	Analysis via EOM	10
4	Chiral versus linear effective operators	11
5	Signatures and constraints	12
5.1	Effects from $\mathcal{O}_{\Box\Phi}$	12
5.2	Effects from $\mathcal{P}_{\Box h}$ and \mathcal{P}_{6-10}	13
6	Conclusions	18
A	Analysis with a generic chiral potential $V(h)$	20
B	Impact of $\mathcal{O}_{\Box\Phi}$ versus $\mathcal{P}_{\Box h}$ on $ZZ \rightarrow ZZ$ scattering	22
C	Chiral versus linear couplings	23
C.1	TGV couplings	23
C.2	HVV couplings	24
C.3	VVVV couplings	25

1 Introduction

A revival of interest in theories with higher derivative kinetic terms [1, 2] is taking place, as the increased momentum dependence of propagators softens the sensitivity to ultraviolet scales. Quadratic divergences are absent due to the faster fall-off of the momentum dependence of the propagators. For instance this avenue has been recently explored in view of an alternative solution to the electroweak hierarchy problem [3, 4].

Originally proposed by Lee and Wick [1, 2], a large literature followed to ascertain the field theoretical consistency of this type of theories, in particular from the point of view of unitarity and causality. The issue is delicate as a second pole appears in the field propagators, and this pole has a wrong-sign residue. Naively such theories are unstable and not unitary. The present understanding is that the S matrix for asymptotically free

states may remain unitary, though, and acausality only occurs at the microscopic level while macroscopically and/or in any measurable quantity causality holds as it should.

For the computation of physical amplitudes, a modification of the usual rules to compute perturbative amplitudes was proposed [5–8] respecting the aforementioned desired properties. A more user-friendly field-theory tool [3] to approach these theories consists in trading the higher derivative kinetic term by the presence of a new state with the same quantum numbers of the standard field and quadratic kinetic energy, albeit with a “wrong” sign for both quadratic terms (kinetic energy and mass), i.e. a state of negative norm: a Lee-Wick (LW) partner or “ghost”. It corresponds to the second pole in the propagator, describing an unstable state that would thus not threaten the unitarity of the S matrix, as only the asymptotically free states participating in a scattering process are relevant for the latter.

In this paper, we focus on the study of a higher derivative kinetic term for the Higgs particle, in a model independent way. Although present Higgs data are fully consistent with the Higgs particle being part of a gauge SU(2) scalar doublet, the issue is widely open and all efforts should be done to settle it. Two main classes of effective Lagrangians are pertinent, depending on how the Standard Model (SM) electroweak symmetry breaking (EWSB) is assumed to be realized in the presence of a light Higgs particle: linearly for an elementary Higgs particle [9–11] or non-linearly for a “dynamical” -composite- light one [12–19]. The relevant couplings to be added to the SM Lagrangian will be denoted by

$$\mathcal{O}_{\square\Phi} = (D_\mu D^\mu \Phi)^\dagger (D_\nu D^\nu \Phi) \quad (1.1)$$

for linearly realized electroweak symmetry breaking (EWSB) scenarios, and

$$\mathcal{P}_{\square h} = \frac{1}{2} \square h \square h = \frac{1}{2} (\partial_\mu \partial^\mu h) (\partial_\nu \partial^\nu h) \quad (1.2)$$

if the light Higgs stems from non-linearly realized EWSB. In eq. (1.1) Φ denotes the gauge SU(2) scalar doublet, which in the unitary gauge reads $\Phi = (0, (v+h)/\sqrt{2})$ with $v/\sqrt{2}$ being the Φ vacuum expectation value (vev) and h the Higgs excitation. D_μ stands for the covariant derivative

$$D_\mu \Phi \equiv \left(\partial_\mu + igW_\mu + \frac{ig'}{2} B_\mu \right) \Phi \quad (1.3)$$

with $W_\mu \equiv W_\mu^a(x)\sigma_a/2$ and B_μ denoting the SU(2)_L and U(1)_Y gauge bosons, respectively.

In equation (1.2), h denotes instead a generic scalar singlet, whose couplings are described by a non-linear Lagrangian (often dubbed chiral Lagrangian) and do not need to match those of a SU(2) doublet component.

Note that the operators $\mathcal{O}_{\square\Phi}$ and $\mathcal{P}_{\square\Phi}$ are but rarely [10] considered by practitioners of effective Lagrangian analyses, and almost never selected as one of the elements of the operator bases. They tend to be substituted instead by (a combination of) other operators –which include fermionic ones– because the bounds on exotic fermionic couplings are often more stringent in constraining BSM theories than those from bosonic interactions. Nevertheless, the new data and the special and profound theoretical impact of higher derivative kinetic terms deserve focalised studies, to which this paper intends to contribute.

In this context it is important to notice that, in order to have any impact on the hierarchy problem, the validity of the operators under study should be extrapolated into the regime $E \gg \Lambda$, which is beyond the usual regime where EFT description is valid. In this sense, the SM Lagrangian with the addition of these operators can be treated as the complete Lagrangian in the ultraviolet.

Either in the linear or the non-linear realizations, the contribution to the Lagrangian of the effective operators in eqs. (1.1) and (1.2) can be parametrised as

$$\delta\mathcal{L} = c_i \mathcal{O}_i, \quad (1.4)$$

with $\mathcal{O}_i \equiv \{\mathcal{O}_{\square\Phi}, \mathcal{P}_{\square h}\}$ respectively, with the parameters c_i having mass dimension -2 .¹ The impact of $\mathcal{O}_{\square\Phi}$ and $\mathcal{P}_{\square h}$ appears as a correction in the propagator of the h scalar which is quartic in four-momentum:

$$\frac{i}{p^2 - m_h^2 + c_i p^4}. \quad (1.5)$$

This propagator has now two poles and describes thus two degrees of freedom. For instance for $1/c_i \gg m_h^2$ they are approximately located at [3]

$$p^2 = m_h^2 \quad \text{and} \quad p^2 = -1/c_i, \quad (1.6)$$

which implies that the sign of the operator coefficient needs to obey $c_i < 0$ in order to avoid tachyonic instabilities.

It is important to find signals which discriminate among those two categories –linear versus non-linear EWSB– and this will be one of the main focuses of this paper for the higher derivative scalar kinetic terms considered. It will be shown that the effects of the couplings in eqs. (1.1) and (1.2) differ on their implications for the gauge and gauge-Higgs sectors. The phenomenological analysis will be restricted to tree-level effects and consistently to first order in c_i , and we will use two independent and alternative techniques, showing that they lead to the same results:

- To trade the higher-derivative coupling by a LW “ghost” heavy particle, which is subsequently integrated out.
- To apply first the Lagrangian equations of motion (EOM) to the operator, trading the coupling by other standard higher-dimension effective operators, which only require traditional fields and field-theory methods.

Together with exploring the different physical effects expected from the Higgs linear higher-derivative term $\mathcal{O}_{\square\Phi}$ and the non-linear one $\mathcal{P}_{\square h}$, we will clarify their exact theoretical relation, determining which specific combination of non-linear operators would result in the same physics impact than the linear operator $\mathcal{O}_{\square\Phi}$.

¹From the point of view of the chiral expansion, $\mathcal{P}_{\square\Phi}$ is a four-derivative coupling, and a slightly different normalization (by a v^2 factor) was adopted in ref. [20], using a dimensionless coefficient; the choice here allows to use the same notation for both expansions.

The phenomenological analysis below includes as well a study of the impact of both operators in present and future LHC data. In the case of the LW version of the SM, it has been shown [21] that the measurements of the S and T parameters set very strong constraints on the gauge and fermionic LW partner masses, which need to exceed several TeV; this implies a sizeable tension with the issue of the electroweak hierarchy problem, as the LW partners induce a finite shift in the Higgs mass proportional to their own masses. On the contrary, the EW constraints are mild for the Higgs doublet LW partners, whose impact may be within LHC reach [22]. We explore the experimental prospects for $\mathcal{O}_{\square\Phi}$ and $\mathcal{P}_{\square h}$ at first order in the effective operator coefficients, focusing only on the quark sector for simplicity as the extension to the lepton sector is straightforward.

The structure of the manuscript can be easily inferred from the table of Contents.

2 Elementary Higgs: $\mathcal{O}_{\square\Phi}$

The quark-Higgs sector of the SM Lagrangian supplemented by $\mathcal{O}_{\square\Phi}$ will be considered in this section:

$$\mathcal{L} = (D_\mu \Phi)^\dagger D^\mu \Phi - \left(\bar{q}_L \tilde{\Phi} Y_U u_R + \bar{q}_L \Phi Y_D d_R + \text{h.c.} \right) + c_{\square\Phi} \mathcal{O}_{\square\Phi} - V(\Phi^\dagger \Phi), \quad (2.1)$$

where $\tilde{\Phi} \equiv i\sigma_2 \Phi$, and the Standard Model potential,

$$V(\Phi^\dagger \Phi) = \lambda \left[\Phi^\dagger \Phi - \frac{v^2}{2} \right]^2, \quad (2.2)$$

can be rewritten for future convenience in the unitary gauge in terms of the Higgs particle mass, $m_h^2 = 2\lambda v^2$ and the Higgs doublet vev $\langle \Phi \rangle = v/\sqrt{2}$ as

$$V(h) = \frac{m_h^2}{2} h^2 + \frac{m_h^2}{2v} h^3 + \frac{m_h^2}{8v^2} h^4. \quad (2.3)$$

2.1 Analysis in terms of the LW ghost

The Lee-Wick method for the case of a complex scalar doublet is applied next to the analysis of the operator $\mathcal{O}_{\square\Phi}$ in eqs. (1.1) and (1.4), following ref. [3]. Defining an auxiliary complex SU(2) doublet φ , eq. (2.1) can be rewritten as a two-scalar-field Lagrangian:

$$\begin{aligned} \mathcal{L} = & (D_\mu \Phi)^\dagger D^\mu \Phi + (D_\mu \varphi)^\dagger D^\mu \Phi + (D_\mu \Phi)^\dagger D^\mu \varphi \\ & - \left(\bar{q}_L \tilde{\Phi} Y_U u_R + \bar{q}_L \Phi Y_D d_R + \text{h.c.} \right) - \frac{1}{c_{\square\Phi}} \varphi^\dagger \varphi - V(\Phi^\dagger \Phi). \end{aligned} \quad (2.4)$$

The mass squared term for the auxiliary field is given by $-1/c_{\square\Phi}$, which requires $c_{\square\Phi} < 0$ to avoid a tachyonic resonance. The kinetic energy terms can now be diagonalised via the simple field redefinitions $\Phi \rightarrow \Phi' - \varphi'$, $\varphi \rightarrow \varphi'$, and the mass terms can be diagonalised by a subsequent symplectic rotation given by:

$$\begin{pmatrix} \Phi' \\ \varphi' \end{pmatrix} = \begin{pmatrix} \cosh \alpha & \sinh \alpha \\ \sinh \alpha & \cosh \alpha \end{pmatrix} \begin{pmatrix} \Phi'' \\ \varphi'' \end{pmatrix}, \quad (2.5)$$

where

$$\tanh 2\alpha = \frac{2x}{1+2x}, \quad \text{with} \quad x \equiv -c_{\square\Phi} m_h^2/2. \quad (2.6)$$

Finally, dropping the primes on the field notation, the scalar Lagrangian in eq. (2.4) can be rewritten as

$$\mathcal{L}^{\varphi,\Phi} = (D_\mu \Phi)^\dagger D^\mu \Phi - (D_\mu \varphi)^\dagger D^\mu \varphi + \mathcal{L}_Y^\varphi - V(\Phi, \varphi) \quad (2.7)$$

with

$$\mathcal{L}_Y^\varphi = -(1+x) \left(\bar{q}_L (\tilde{\Phi} - \tilde{\varphi}) Y_U u_R + \bar{q}_L (\Phi - \varphi) Y_D d_R + \text{h.c.} \right), \quad (2.8)$$

$$\begin{aligned} V(\Phi, \varphi) = & -\frac{m_h^2}{2} \left(1 - x + \frac{1}{x} \right) \varphi^\dagger \varphi - \frac{m_h^2}{2} (1-x) \Phi^\dagger \Phi \\ & + \frac{m_h^2}{2v^2} (1-4x) \left((\Phi - \varphi)^\dagger (\Phi - \varphi) \right)^2, \end{aligned} \quad (2.9)$$

expanded at order x , assuming small x values. The location of the minimum of the Higgs potential gets $c_{\square\Phi}$ corrections. For instance, for a BSM scale large compared with the Higgs mass (i.e. $x \rightarrow 0$), the approximate location of the vacuum corresponds to:

$$\Phi \rightarrow \langle \Phi \rangle + \frac{h}{\sqrt{2}}, \quad \langle \Phi \rangle = \frac{v}{\sqrt{2}} \left(1 + \frac{15}{2} x^2 \right) + \mathcal{O}(x^3), \quad (2.10)$$

$$\varphi \rightarrow \langle \varphi \rangle + \frac{\chi}{\sqrt{2}}, \quad \langle \varphi \rangle = -x \frac{v}{\sqrt{2}} (1 - 2x) + \mathcal{O}(x^3), \quad (2.11)$$

where h and χ are the field excitation over the potential minima, and the exact potential has been retaken and terms up to x^2 considered. In consequence, at leading order in $c_{\square\Phi}$ the minimum of the Higgs potential remains unchanged. For the sake of comparison with the non-linear case in the next section, it is useful to write explicitly the potential restricted to the h and χ fields. After a further necessary diagonalization of the h and χ dependence, their scalar potential reads at first order in x :

$$\begin{aligned} V(h, \chi) = & \frac{m_h^2}{2} (1+2x) h^2 + \frac{m_h^2}{2} \left(1 + 2x - \frac{1}{2x} \right) \chi^2 + \frac{m_h^2}{2v} (1+6x) (h - \chi)^3 \\ & + \frac{m_h^2}{8v^2} (1+8x) (h - \chi)^4. \end{aligned} \quad (2.12)$$

Eqs. (2.7) and (2.12) illustrate that for small x the χ state exhibits a “wrong” sign in both the kinetic energy and the mass terms.

Integrating out the heavy scalar. At first order in the operator coefficient $c_{\square\Phi}$, the mixing in eq. (2.6) may be approximated by $\tanh \alpha \sim 2x = -c_{\square\Phi} m_h^2$, and the effect of the negative-norm heavy field described by φ with absolute mass $\sim |c_{\square\Phi}^{-1}|$ can be integrated out via its EOM:

$$\bar{\varphi}_i = c_{\square\Phi} \left(\bar{d}_R Y_D^\dagger q_{L,i} + \bar{q}_{L,j} \varepsilon_{ji} Y_U u_R + \frac{m_h^2}{v^2} (\Phi^\dagger \Phi) \Phi_i \right) + \mathcal{O}(c_{\square\Phi}^2), \quad (2.13)$$

Throughout the paper we will work on the so-called Z-scheme of renormalization, in which the five relevant electroweak parameters of the SM Lagrangian (neglecting fermion masses), g_s, g, g', v and the h self-coupling, are fixed from the following five observables: the world average value of α_s [23], the Fermi constant G_F as extracted from muon decay [23], α_{em} extracted from Thomson scattering [23], m_Z as determined from the Z lineshape at LEP I [23], and m_h from the present LHC measurement [24, 25]. Eq. (2.13) above indicates that $O_{\square\Phi}$ will impact the renormalised fermion masses and the Higgs sector parameters. Specifically for the latter, while the electroweak vev $v \equiv (\sqrt{2}G_F)^{-1/2}$ is not corrected, the Higgs mass renormalization must absorb a correction

$$\frac{\delta m_h^2}{m_h^2} = 2x. \quad (2.14)$$

The resulting renormalized effective Lagrangian reads (omitting again fermionic and gauge kinetic terms):

$$\mathcal{L}_{\square\Phi} = (D_\mu \Phi)^\dagger D^\mu \Phi + \mathcal{L}_{\square\Phi}^Y + \mathcal{L}_{\square\Phi}^{4F} - V_{\square\Phi}, \quad (2.15)$$

where

$$\begin{aligned} \mathcal{L}_{\square\Phi}^Y = & - \left[\bar{q}_L \tilde{\Phi} Y_U u_R + \bar{q}_L \Phi Y_D d_R + \text{h.c.} \right] \left(1 - x \left(1 - 2 \frac{\Phi^\dagger \Phi}{v^2} \right) \right) \xrightarrow{\text{unitary gauge}} \\ & - \frac{v+h}{\sqrt{2}} \left[\bar{u}_L Y_U u_R + \bar{d}_L Y_D d_R + \text{h.c.} \right] \left(1 + \frac{x}{v^2} (h^2 + 2hv) \right), \end{aligned} \quad (2.16)$$

$$\begin{aligned} \mathcal{L}_{\square\Phi}^{4F} = & -x \frac{2}{m_h^2} \left[(\bar{u}_R Y_U^\dagger d_L)(\bar{d}_L Y_U u_R) + (\bar{u}_R Y_U^\dagger u_L)(\bar{u}_L Y_U u_R) \right. \\ & + (\bar{u}_L Y_D d_R)(\bar{d}_R Y_D^\dagger u_L) + (\bar{d}_L Y_D d_R)(\bar{d}_R Y_D^\dagger d_L) \\ & \left. + \left\{ (\bar{u}_L Y_U u_R)(\bar{d}_L Y_D d_R) - (\bar{d}_L Y_U u_R)(\bar{u}_L Y_D d_R) + \text{h.c.} \right\} \right], \end{aligned} \quad (2.17)$$

$$\begin{aligned} V_{\square\Phi} = & -\frac{m_h^2}{2} (1-3x) \Phi^\dagger \Phi + \frac{m_h^2}{2v^2} (1-6x) (\Phi^\dagger \Phi)^2 + 2x \frac{m_h^2}{v^4} (\Phi^\dagger \Phi)^3 \xrightarrow{\text{unitary gauge}} \\ & \frac{m_h^2}{2} h^2 + \frac{m_h^2}{2v} (1+4x) h^3 + \frac{m_h^2}{8v^2} (1+24x) h^4 + x \frac{m_h^2}{2v^3} \left(3h^5 + \frac{1}{2v} h^6 \right). \end{aligned} \quad (2.18)$$

It follow deviations from SM expectations in fermion-Higgs couplings, four-fermion interactions and scalar properties; in particular, the relation between the Higgs self-couplings and its mass is different from the SM one; this fact can be directly probed at the LHC and ILC [26]. Moreover, the Higgs potential exhibits now h^5 and h^6 terms not present in the SM, which require $c_{\square\Phi} < 0$ for stability, consistently with the arguments given in the Introduction. Note as well that, *for the linear realization of EWSB under discussion, the couplings involving gauge particles are not modified with respect to their SM values.*

2.2 Analysis via EOM

An avenue alternative to the LW method when working at first order in the operator coefficient, and one which involves only standard fields and standard field theory rules, is

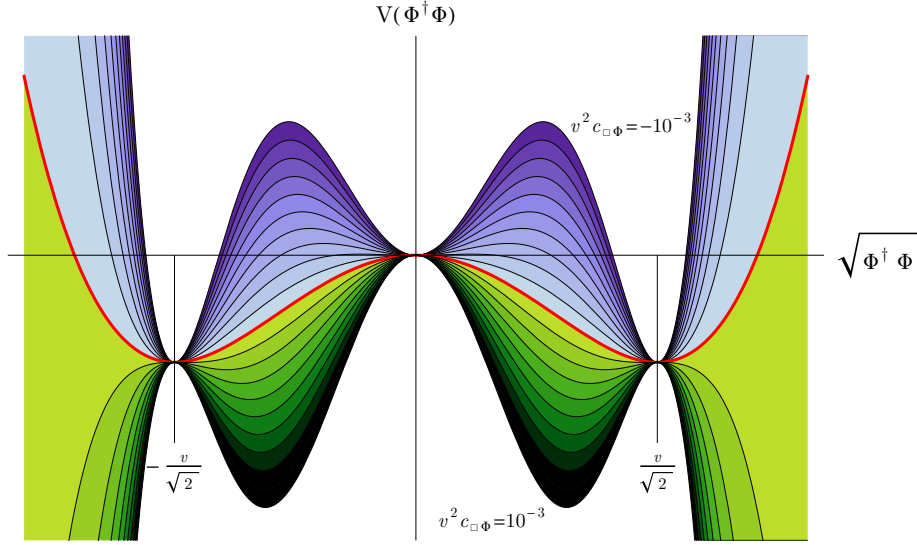


Figure 1. The scalar potential in the linear Lagrangian for different values of the coefficient $c_{\square\Phi}v^2$. The solid red line denotes the SM and the interline spacing is $\Delta(v^2c_{\square\Phi}) = 7.5 \cdot 10^{-5}$.

to apply directly the EOM for the Φ field to the operator $\mathcal{O}_{\square\Phi}$ in eq. (2.1):

$$\square\Phi_i = -\frac{\delta V}{\delta(\Phi^\dagger\Phi)}\Phi_i - \left(\bar{d}_R Y_D^\dagger q_{L,i} + \bar{q}_{L,j} \varepsilon_{ji} Y_U u_R\right), \quad (2.19)$$

$$\square\Phi_i^\dagger = -\Phi_i^\dagger \frac{\delta V}{\delta(\Phi^\dagger\Phi)} - \left(-\bar{u}_R Y_U^\dagger \varepsilon_{ij} q_{L,j} + \bar{q}_{L,i} Y_D d_R\right). \quad (2.20)$$

We have checked that this method leads to the same low-energy renormalized effective Lagrangian than that in eqs. (2.15)–(2.18), obtained via the Lee-Wick procedure involving a “ghost” field.

Higgs potential. Figure 1 shows the dependence of the scalar potential on $c_{\square\Phi}$: the points $|\Phi| = \pm v/\sqrt{2}$, corresponding to the SM vacuum, switch from stable minima to maxima as $c_{\square\Phi}$ runs from negative to positive values. The location of Higgs vev for negative $c_{\square\Phi}$ is not modified at this order, see eq. (2.10).

3 Light dynamical Higgs: $\mathcal{P}_{\square h}$

This section deals with the alternative scenario of a light dynamical Higgs, whose CP-even bosonic effective Lagrangian has been discussed in refs. [17, 20]. For simplicity and focus, the leading-order Lagrangian will be taken to be that of the SM modified only by the action of the operator $\mathcal{P}_{\square h}$ in eq. (1.2). The scalar potential will thus be assumed as well to take the SM form for h , to facilitate comparison with the linear case; nevertheless, in appendix A we discuss the extension to the case of a completely general potential for a singlet scalar field h , showing that the conclusions obtained below are maintained.

The quark-Higgs sector of the Lagrangian reads then

$$\mathcal{L} = \frac{1}{2} \partial_\mu h \partial^\mu h - \frac{(v+h)^2}{4} \text{Tr}[\mathbf{V}_\mu \mathbf{V}^\mu] - \frac{v+h}{\sqrt{2}} (\bar{Q}_L \mathbf{U} \mathbf{Y} Q_R + \text{h.c.}) + c_{\square h} \mathcal{P}_{\square h} - V(h), \quad (3.1)$$

where $V(h)$ takes the functional form in eq. (2.3). $\mathbf{V}_\mu \equiv (\mathbf{D}_\mu \mathbf{U}) \mathbf{U}^\dagger$, where $\mathbf{U}(x)$ is a dimensionless unitary matrix describing the longitudinal degrees of freedom of the EW gauge bosons:

$$\mathbf{U}(x) = e^{i\sigma_a \pi^a(x)/v}, \quad \mathbf{U}(x) \rightarrow L \mathbf{U}(x) R^\dagger, \quad (3.2)$$

where L, R denotes $\text{SU}(2)_{L,R}$ global transformations, respectively. \mathbf{V}_μ is thus a vector chiral field belonging to the adjoint of the global $\text{SU}(2)_L$ symmetry, and the covariant derivative reads

$$\mathbf{D}_\mu \mathbf{U}(x) \equiv \partial_\mu \mathbf{U}(x) + ig W_\mu(x) \mathbf{U}(x) - \frac{ig'}{2} B_\mu(x) \mathbf{U}(x) \sigma_3. \quad (3.3)$$

Note that eq. (3.1) is simply the SM Lagrangian written in chiral notation, but for the additional presence of the $\mathcal{P}_{\square h}$ coupling.

3.1 Analysis in terms of the LW ghost

In parallel to the analysis in section (2.1), for $c_{\square h} < 0$ the action of the operator $\mathcal{P}_{\square h}$ in the Lagrangian eq. (3.1) can be traded for that of an auxiliary SM singlet scalar field χ , and the Lagrangian in eq. (3.1) reads then

$$\mathcal{L} = \frac{1}{2} \partial_\mu h \partial^\mu h + \partial_\mu h \partial^\mu \chi - \frac{(v+h)^2}{4} \text{Tr}[\mathbf{V}_\mu \mathbf{V}^\mu] - \frac{v+h}{\sqrt{2}} (\bar{Q}_L \mathbf{U} \mathbf{Y} Q_R + \text{h.c.}) - V(h, \chi), \quad (3.4)$$

where the non-scalar kinetic terms were omitted and (see appendix A)

$$V(h, \chi) = \frac{m_h^2}{2} h^2 + \frac{m_h^2}{2v} h^3 + \frac{m_h^2}{8v^2} h^4 + \frac{1}{2c_{\square h}} \chi^2. \quad (3.5)$$

The kinetic energy terms are diagonalised via the field redefinitions $h \rightarrow h' - \chi'$, $\chi \rightarrow \chi'$, and the mass terms can be then diagonalised by a subsequent symplectic rotation analogous to that in eq. (2.5) (with Φ and φ replaced by h and χ , respectively), with a mixing angle given by

$$\tanh 2\alpha = \frac{-4x}{1-4x}, \quad \text{with} \quad x \equiv -c_{\square h} m_h^2/2. \quad (3.6)$$

Finally, dropping the primes on the field notation and omitting again fermionic and gauge kinetic terms, the Lagrangian reads:

$$\mathcal{L}^{h,\chi} = \frac{1}{2} \partial_\mu h \partial^\mu h - \frac{1}{2} \partial_\mu \chi \partial^\mu \chi + \mathcal{L}_Y^\chi + \mathcal{L}_{\text{gauge}}^\chi - V(h, \chi), \quad (3.7)$$

where, at first order in x ,

$$\mathcal{L}_Y^\chi = -\frac{1}{\sqrt{2}} (\bar{Q}_L \mathbf{U} \mathbf{Y} Q_R + \text{h.c.}) [v + (h - \chi)(1 + 2x)], \quad (3.8)$$

$$\mathcal{L}_{\text{gauge}}^\chi = -\frac{1}{4} \text{Tr}[\mathbf{V}_\mu \mathbf{V}^\mu] [v^2 + 2v(1 + 2x)(h - \chi) + (1 + 4x)(h - \chi)^2], \quad (3.9)$$

while the scalar potential $V(h, \chi)$ coincides with that given in eq. (2.12).

Integrating out the heavy scalar. For small x (that is, χ mass large compared to the Higgs mass), the first order EOM can be used to integrate out the LW partner,

$$\bar{\chi} = \frac{c_{\square h}}{2} \left[\sqrt{2}(\bar{Q}_L \mathbf{U} \mathbf{Y} Q_R + \text{h.c.}) + \text{Tr}[\mathbf{V}_\mu \mathbf{V}^\mu](v+h) + \frac{m_h^2}{v^2} h^2 (h+3v) \right] + \mathcal{O}(c_{\square h}^2). \quad (3.10)$$

While the masses of the gauge and fermion fields are unaffected by the presence of $\mathcal{P}_{\square h}$, the Higgs mass renormalization absorbs the correction

$$\frac{\delta m_h^2}{m_h^2} = 2x. \quad (3.11)$$

The resulting effective Lagrangian for the h field is given by (omitting kinetic terms other than the Higgs one)

$$\mathcal{L}_{\square h} = \frac{1}{2} \partial_\mu h \partial^\mu h + \mathcal{L}_{\square h}^Y + \mathcal{L}_{\square h}^{4F} + \mathcal{L}_{\square h}^{\text{gauge}} - V_{\square h}(h), \quad (3.12)$$

with

$$\begin{aligned} \mathcal{L}_{\square h}^Y = & -\frac{v+h}{\sqrt{2}} (\bar{Q}_L \mathbf{U} \mathbf{Y} Q_R + \text{h.c.}) \left(1 + \frac{x}{v^2} (h^2 + 2vh) \right) \\ & - \frac{x}{m_h^2} \frac{(v+h)}{\sqrt{2}} \text{Tr}[\mathbf{V}_\mu \mathbf{V}^\mu] (\bar{Q}_L \mathbf{U} \mathbf{Y} Q_R + \text{h.c.}), \end{aligned} \quad (3.13)$$

$$\mathcal{L}_{\square h}^{4F} = -\frac{x}{2m_h^2} (\bar{Q}_L \mathbf{U} \mathbf{Y} Q_R + \text{h.c.})^2, \quad (3.14)$$

$$\mathcal{L}_{\square h}^{\text{gauge}} = -\frac{(v+h)^2}{4} \text{Tr}[\mathbf{V}_\mu \mathbf{V}^\mu] \left(1 + 2\frac{x}{v^2} (h^2 + 2vh) \right) - \frac{x}{4m_h^2} \text{Tr}[\mathbf{V}_\mu \mathbf{V}^\mu]^2 (v+h)^2, \quad (3.15)$$

$$V_{\square h}(h) = \frac{m_h^2}{2} h^2 + \frac{m_h^2}{2v} (1+4x) h^3 + \frac{m_h^2}{8v^2} (1+24x) h^4 + x \frac{m_h^2}{2v^3} \left(3h^5 + \frac{1}{2v} h^6 \right). \quad (3.16)$$

$\mathcal{L}_{\square h}^Y$ above shows that anomalous gauge-fermion interactions weighted by Yukawas are expected in the non-linear realization, in addition to the pure Yukawa-like corrections present in the linear expansion, see eq. (2.16). Furthermore, the potential $V_{\square h}(h)$ in eq. (3.16) matches exactly the potential in eq. (2.18) for the linear case, as it should, exhibiting higher than quartic Higgs couplings that requires $c_{\square h} < 0$ (i.e., $x > 0$) for the stability of the potential.

In summary, the resulting effective Lagrangian for the non-linear case in eqs. (3.12)–(3.16) shows deviations from SM expectations in fermion-Higgs couplings, four-fermion interactions and scalar properties, a pattern already found in the previous section for an elementary Higgs. Nevertheless, important distinctive features appear with respect to the case of a higher derivative kinetic term for a Higgs particle in linearly realised EWSB:

- The number of effective couplings modified is larger than in the linear case in eqs. (2.15)–(2.18), a characteristic feature already explored previously in other settings [20].

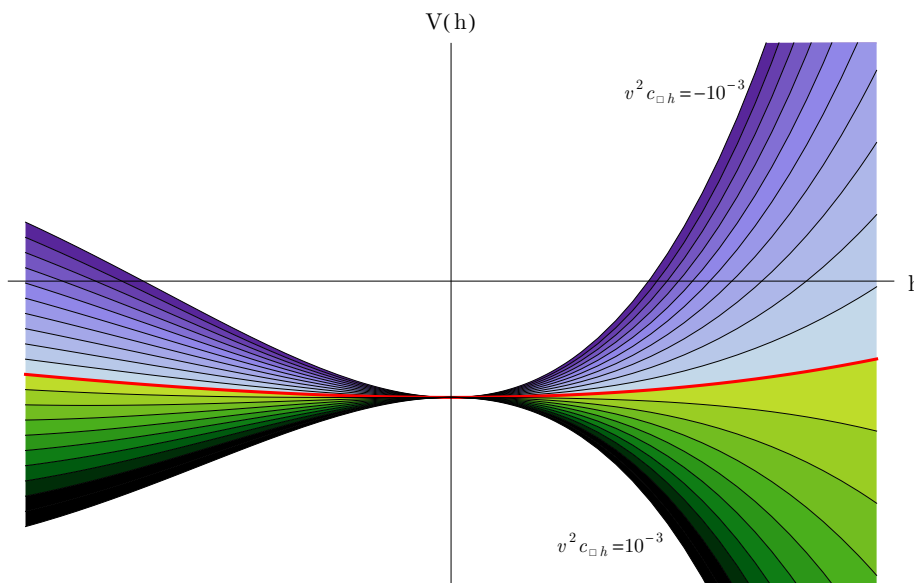


Figure 2. The scalar potential in the chiral Lagrangian for different values of the coefficient $v^2 c_{\Box h}$. The solid red line denotes the SM and the interline spacing is $\Delta(v^2 c_{\Box h}) = 7.5 \cdot 10^{-5}$.

- Specifically, *couplings involving gauge particles are now modified with respect to their SM values*; in addition to anomalous gauge-fermion interactions, particularly interesting anomalous Higgs couplings to two (HVV) and three gauge bosons (HVVV), two Higgs-two gauge bosons (HHVV) and quartic gauge couplings (VVVV) are expected. The pure-gauge and gauge-Higgs anomalous couplings will be analyzed in detail in the next sections; they constitute a new tool to disentangle experimentally an elementary versus a dynamical nature of the Higgs particle, in the presence of higher-derivative kinetic terms.

3.2 Analysis via EOM

The alternative method of applying directly to the operator $\mathcal{P}_{\Box h}$ in the original non-linear Lagrangian eq. (3.1) the standard field theory EOM for the h field,

$$\Box h = -\frac{\delta V(h)}{\delta h} - \frac{v+h}{2} \text{Tr}[\mathbf{V}_\mu \mathbf{V}^\mu] - \frac{1}{\sqrt{2}} (\bar{Q}_L \mathbf{U} \mathbf{Y} Q_R + \text{h.c.}), \quad (3.17)$$

leads to the same effective low-energy Lagrangian at first order on $c_{\Box h}$ than that in eqs. (3.12)–(3.16), obtained above via the LW procedure, as it can be easily checked. Again, the correction to the scalar potential requires to impose $c_{\Box h} < 0$ to ensure that the potential remains bounded from below.

Higgs potential. Figure 2 shows the dependence of the shape of the scalar potential on the perturbative parameter $c_{\Box h}$: for negative values the SM vacuum $\langle h \rangle = 0$ is still a minimum, while for positive values the potential is not bounded from below and moreover the SM vacuum is turned into a maximum.

4 Chiral versus linear effective operators

The linear operator $\mathcal{O}_{\square\Phi}$ involves gauge fields in its structure - see eq. (1.1), contrary to the chiral effective operator $\mathcal{P}_{\square h}$ defined in eq. (1.2). Nevertheless, the addition of the former operator to the SM Lagrangian turned out to give *no contribution* to couplings involving gauge fields, while the chiral operator $\mathcal{P}_{\square h}$ does. This seemingly paradoxical state of affairs and the consistency of the results can be ascertained by establishing the exact correspondence between both operators, which we find to be given by:

$$\begin{aligned}\mathcal{O}_{\square\Phi} &= \frac{1}{2}(\square h)^2 + \frac{(v+h)^2}{8} (\text{Tr}[\mathbf{V}_\mu \mathbf{V}^\mu])^2 + \frac{v+h}{2} \text{Tr}[\mathbf{V}_\mu \mathbf{V}^\mu] \partial_\nu \partial^\nu h - \text{Tr}[\mathbf{V}_\mu \mathbf{V}_\nu] \partial^\mu h \partial^\nu h \\ &\quad - \frac{(v+h)^2}{4} \text{Tr}[(D_\mu \mathbf{V}^\mu)^2] - (v+h) \text{Tr}[\mathbf{V}_\nu D_\mu \mathbf{V}^\mu] \partial^\nu h \\ &= \mathcal{P}_{\square h} + v^2 \left(\frac{1}{8} \mathcal{P}_6 + \frac{1}{4} \mathcal{P}_7 - \mathcal{P}_8 - \frac{1}{4} \mathcal{P}_9 - \frac{1}{2} \mathcal{P}_{10} \right)_{linear \mathcal{F}}.\end{aligned}\quad (4.1)$$

The right hand-side of eq. (4.1) describes a combination of the non-linear operator $\mathcal{P}_{\square h}$ and a particular set of independent effective operators of the non-linear basis as determined in ref. [20], defined by

$$\begin{aligned}\mathcal{P}_6 &= (\text{Tr}[\mathbf{V}_\mu \mathbf{V}^\mu])^2 \mathcal{F}_6(h), & \mathcal{P}_7 &= \text{Tr}[\mathbf{V}_\mu \mathbf{V}^\mu] \square \mathcal{F}_7(h), \\ \mathcal{P}_8 &= \text{Tr}[\mathbf{V}_\mu \mathbf{V}_\nu] \partial^\mu \mathcal{F}_8(h) \partial^\nu \mathcal{F}'_8(h), & \mathcal{P}_9 &= \text{Tr}[(D_\mu \mathbf{V}^\mu)^2] \mathcal{F}_9(h), \\ \mathcal{P}_{10} &= \text{Tr}[\mathbf{V}_\nu D_\mu \mathbf{V}^\mu] \partial^\nu \mathcal{F}_{10}(h),\end{aligned}\quad (4.2)$$

where the generic -model dependent- $\mathcal{F}_i(h)$ functions are often parametrised as [17, 20]

$$\mathcal{F}_i(h) = 1 + 2a_i \frac{h}{v} + b_i \frac{h^2}{v^2} \dots \quad (4.3)$$

The subscript “*linear \mathcal{F}* ” in the right-hand side of eq. (4.1) indicates that the equality holds when the arbitrary functions $\mathcal{F}_i(h)$ take the specific linear-like dependence — see ref. [20]²

$$\mathcal{F}_6(h) = \mathcal{F}_7(h) = \mathcal{F}_9(h) = \mathcal{F}_{10}(h) \stackrel{linear \mathcal{F}}{=} (1 + h/v)^2, \quad \mathcal{F}_8(h) = \mathcal{F}'_8(h) \stackrel{linear \mathcal{F}}{=} (1 + h/v). \quad (4.4)$$

Strictly speaking, in a general chiral Lagrangian the definition of $\mathcal{P}_{\square h}$ should also contain a $\mathcal{F}_{\square h}(h)$ factor on the right hand side of eq. (1.2) [19, 20]; it would be superfluous to keep track of $\mathcal{F}_{\square h}(h)$ here, though, as we will restrain the analysis to couplings involving at most two Higgs particles, which is tantamount to setting $\mathcal{F}_{\square h}(h) = 1$ in the phenomenological analysis.

Taken separately, $\mathcal{P}_{\square h}$ as well as each of the five operators in eq. (4.2) do induce deviations on the SM expectations for couplings involving gauge bosons. Eq. (4.1) implies

²In that reference, powers of the ξ parameter — which refers to ratios of scales involved — were extracted from the definition of the operator coefficients; we will refrain here from doing so, and adopt the simple notation in eq. (1.4).

nevertheless that the gauge contributions of these six operators will exactly cancel in any physical observable when their relative weights are given by

$$v^2 c_{\square h} = 8c_6 = 4c_7 = -c_8 = -4c_9 = -2c_{10}. \quad (4.5)$$

We have explicitly checked such cancellations in several examples of physical transitions; appendix B describes the particular case of $ZZ \rightarrow ZZ$ scattering, for illustration.

5 Signatures and constraints

Tables 1, 2, 3, and 4 list all couplings involving up to four particles that receive contributions from the effective linear operator $\mathcal{O}_{\square\Phi}$ or any of its chiral siblings $\mathcal{P}_{\square h}$ and \mathcal{P}_{6-10} . We work at first order in the operator coefficients, which are left arbitrary in those tables; the $\mathcal{F}_i(h)$ functionals are also assumed generic as defined in eq. (4.3). For the sake of comparison, a SM-like potential is taken for both the linear and chiral operators; the extension to a general scalar potential for the chiral expansion can be found in appendix A and has no significant impact.

It turns out that $\mathcal{O}_{\square\Phi}$ gives no tree-level contribution to couplings involving gauge particles as argued earlier, while instead $\mathcal{P}_{\square h}$ and \mathcal{P}_{6-10} are shown to have a strong impact on a large number of gauge couplings. On the other side, anomalous four-fermion interactions are induced by both $\mathcal{O}_{\square\Phi}$ and $\mathcal{P}_{\square h}$, even if with distinct patterns.

5.1 Effects from $\mathcal{O}_{\square\Phi}$

The only impact of $\mathcal{O}_{\square\Phi}$ on present Higgs and gauge boson observables is to generate the universal shift in the Higgs coupling to fermions shown in the first line of table 1. Equivalently, in the notation in refs. [16, 24, 25, 27, 28], in which the deviations of the Yukawa couplings and the gauge kinetic terms from SM predictions were parametrised as

$$\mathcal{L}_{Yukawa} \equiv -\frac{v}{\sqrt{2}} (\bar{Q}_L \mathbf{U} \mathbf{Y} Q_R + \text{h.c.}) \left(1 + c \frac{h}{v} + \dots \right), \quad (5.1)$$

$$\mathcal{L}_{gauge-kinetic} \equiv -\frac{v^2}{4} \text{Tr}(\mathbf{V}_\mu \mathbf{V}^\mu) \left(1 + 2a \frac{h}{v} + b \frac{h^2}{v^2} + \dots \right), \quad (5.2)$$

the shift induced by the operator $\mathcal{O}_{\square\Phi}$ reads

$$c \equiv \kappa_f \equiv 1 + \Delta_f = 1 - m_h^2 c_{\square\Phi}. \quad (5.3)$$

while

$$a \equiv \kappa_V \equiv 1 + \Delta_V = 1, \quad b = 1. \quad (5.4)$$

In refs. [20, 29], a general analysis of the constraints on departures of the Higgs couplings strength from SM expectations used all available collider and EW precision data, and it was found that

$$-0.55 \leq \Delta_f \leq 0.25, \quad (5.5)$$

Fermionic couplings	Coeff.	SM value	Chiral	Linear: $\mathcal{O}_{\square\Phi}$
$h (\bar{u}_L Y_U u_R + \bar{d}_L Y_D d_R + \text{h.c.})$	$-\frac{1}{\sqrt{2}}$	1	$-m_h^2 c_{\square h}$	$-m_h^2 c_{\square\Phi}$
$h^2 (\bar{u}_L Y_U u_R + \bar{d}_L Y_D d_R + \text{h.c.})$	$-\frac{1}{v\sqrt{2}}$	—	$-\frac{3m_h^2}{2} c_{\square h}$	$-\frac{3m_h^2}{2} c_{\square\Phi}$
$Z_\mu Z^\mu (\bar{u}_L Y_U u_R + \bar{d}_L Y_D d_R + \text{h.c.})$	$-\frac{g^2 v}{4\sqrt{2}c_\theta^2}$	—	$c_{\square h}$	—
$W_\mu^+ W^{-\mu} (\bar{u}_L Y_U u_R + \bar{d}_L Y_D d_R + \text{h.c.})$	$-\frac{g^2 v}{2\sqrt{2}}$	—	$c_{\square h}$	—
$(\bar{u}_L Y_U u_R)^2 + (\bar{u}_R Y_U^\dagger u_L)^2$	$\frac{1}{4}$	—	$c_{\square h}$	—
$(\bar{u}_L Y_U u_R) (\bar{u}_R Y_U^\dagger u_L)$	$\frac{1}{2}$	—	$c_{\square h}$	$2c_{\square\Phi}$
$(\bar{d}_L Y_D d_R)^2 + (\bar{d}_R Y_D^\dagger d_L)^2$	$\frac{1}{4}$	—	$c_{\square h}$	—
$(\bar{d}_L Y_D d_R) (\bar{d}_R Y_D^\dagger d_L)$	$\frac{1}{2}$	—	$c_{\square h}$	$2c_{\square\Phi}$
$(\bar{u}_L Y_U u_R) (\bar{d}_R Y_D^\dagger d_L) + \text{h.c.}$	$\frac{1}{2}$	—	$c_{\square h}$	—
$(\bar{u}_L Y_U u_R) (\bar{d}_L Y_D d_R) + \text{h.c.}$	$\frac{1}{2}$	—	$c_{\square h}$	$2c_{\square\Phi}$
$(\bar{u}_L Y_D d_R) (\bar{d}_L Y_U u_R) + \text{h.c.}$	−1	—	—	$c_{\square\Phi}$
$(\bar{u}_L Y_D d_R) (\bar{d}_R Y_D^\dagger u_L) + (\bar{d}_L Y_U u_R) (\bar{u}_R Y_U^\dagger d_L)$	1	—	—	$c_{\square\Phi}$

Table 1. Effective couplings involving fermions generated by the linear operator $\mathcal{O}_{\square\Phi}$ and its chiral siblings $\mathcal{P}_{\square h}$ and \mathcal{P}_{6-10} . For illustration only the couplings involving quark pairs are listed, although similar interactions involving lepton pairs are induced.

at 90% CL after marginalizing over all other effective couplings. Eq. (5.5) constrains $m_h^2 c_{\square\Phi}$, in addition to any combination of coefficients of other dimension-six operators which may also modify universally the Higgs couplings to fermions, see for instance ref. [20].

When only $\mathcal{O}_{\square\Phi}$ is added to the SM Lagrangian, eq. (5.5) translates into the bound $c_{\square\Phi} \lesssim 1.6 \cdot 10^{-5} \text{ GeV}^{-2}$. This constraint is quantitatively quite weak, a fact due to present sensitivity. For illustration, it could be rephrased as a lower limit of 250 GeV on the Higgs doublet LW partner mass. It shows that the bound obtained is of the order of magnitude of the constraints established by previous analyses, which considered direct production in colliders and/or indirect contributions to EW precision data and flavour data [21, 30–36], setting a lower bound for the LW scalar partner mass of 445 GeV.

5.2 Effects from $\mathcal{P}_{\square h}$ and \mathcal{P}_{6-10}

Tables 2, 3 and 4 illustrate that $\mathcal{P}_{\square h}$ generates tree-level corrections to the gauge boson self-couplings, as well as to gauge-Higgs couplings. Note that some of these interactions would not be induced by *any* $d = 6$ operator of a linear expansion, an example being the $ZZZZ$ interactions in table 2; other signals absent in both the SM and $d = 6$ linear expansions, and thus unique to the leading order chiral expansion, can be found in appendix C. They constitute a strong tool to disentangle a strong underlying EW dynamics from a linear one.

VV, TGV and VVVV	Coeff.	SM value	Chiral	Linear: $\mathcal{O}_{\square\Phi}$
$(\partial_\mu Z^\mu)(\partial_\nu Z^\nu)$	$-\frac{g^2}{2c_\theta^2}$	—	c_9	—
$(\partial_\mu W^{+\mu})(\partial_\nu W^{-\nu})$	$-g^2$	—	c_9	—
$i(\partial_\mu W^{-\mu})(Z_\nu W^{+\nu}) + \text{h.c.}$	$\frac{e^2 g}{c_\theta^2}$	—	c_9	—
$i(\partial_\mu W^{-\mu})(A_\nu W^{+\nu}) + \text{h.c.}$	$-eg^2$	—	c_9	—
$(Z_\mu Z^\mu)^2$	$\frac{g^4}{32c_\theta^4}$	—	$v^2 c_{\square h} + 8c_6$	—
$(W_\mu^+ W^{-\mu})^2$	$-\frac{g^2}{2}$	1	$-m_W^2 c_{\square h} - 2g^2 c_6$	—
$(W_\mu^+ W^{-\mu})(Z_\nu Z^\nu)$	$-g^2 c_\theta^2$	1	$-\frac{m_Z^2}{2} c_{\square h} - \frac{g^2}{c_\theta^4} c_6$	—
$(W_\mu^+ Z^\mu)(W_\nu^- Z^\nu)$	$g^2 c_\theta^2$	1	$-\frac{e^2 s_\theta^2}{c_\theta^4} c_9$	—
$(W_\mu^+ A^\mu)(W_\nu^- A^\nu)$	$e^2 g^2$	1	$-c_9$	—
$(W_\mu^+ A^\mu)(W_\nu^- Z^\nu) + \text{h.c.}$	egc_θ	1	$\frac{e^2}{c_\theta^2} c_9$	—

Table 2. Anomalous pure-gauge couplings involving two, three and four gauge bosons, induced by the chiral operators $\mathcal{P}_{\square h}$ and \mathcal{P}_{6-10} , in contrast with the non-impact of their linear sibling $\mathcal{O}_{\square\Phi}$.

The effects stemming from the operators \mathcal{P}_{6-10} , which are also siblings of the linear operator $\mathcal{O}_{\square\Phi}$, are displayed in these tables for gauge two-point functions (VV), triple gauge vertices (TGV) and VVVV couplings. As previously discussed, the tree-level contributions to physical amplitudes induced by that set of chiral operators cancel if the conditions in eqs. (4.4) and (4.5) are satisfied. Notwithstanding, for generic values of the coefficients of $\mathcal{P}_{\square h}$ and \mathcal{P}_{6-10} , some signatures characteristic of a non-linearly realised electroweak symmetry breaking are expected, as those discussed next.

From tables 3 and 1 it follows that $\mathcal{P}_{\square h}$ yields a universal correction to the SM Higgs couplings to gauge bosons and fermions. Furthermore, in present Higgs data the Higgs state is on-shell and, in this case, \mathcal{P}_7 gives also a correction to the SM-like HVV couplings, while the modifications generated by \mathcal{P}_9 and \mathcal{P}_{10} vanish for on-shell W and Z gauge bosons or massless fermions. Thus these corrections can be cast as, in the notation of eqs. (5.1) and (5.2),

$$a \equiv \kappa_V \equiv 1 + \Delta_V = 1 - \frac{m_h^2}{v^2} (v^2 c_{\square h} + 4c_7 a_7), \quad c \equiv \kappa_f \equiv 1 + \Delta_f = 1 - m_h^2 c_{\square h}, \quad (5.6)$$

with $b_7 = 0$. The general constraints resulting from present Higgs and other data [20, 29]

HVV and HVVV	Coeff.	SM value	Chiral	Linear: $\mathcal{O}_{\square\Phi}$
$Z_\mu Z^\mu h$	$\frac{vg^2}{4c_\theta^2}$	1	$-m_h^2 c_{\square h}$	—
$Z_\mu Z^\mu \square h$	$-\frac{g^2}{2c_\theta^2}$	—	$\frac{2c_7 a_7}{v}$	—
$(\partial_\mu Z^\mu)(\partial_\nu Z^\nu)h$	$-\frac{g^2}{2c_\theta^2}$	—	$\frac{2c_9 a_9}{v}$	—
$(\partial_\mu Z^\mu)(Z_\nu \partial^\nu h)$	$-\frac{g^2}{2c_\theta^2}$	—	$\frac{2c_{10} a_{10}}{v}$	—
$W_\mu^+ W^{-\mu} h$	$\frac{vg^2}{2}$	1	$-m_h^2 c_{\square h}$	—
$W_\mu^+ W^{-\mu} \square h$	$-g^2$	—	$\frac{2c_7 a_7}{v}$	—
$(\partial_\mu W^{+\mu})(\partial_\nu W^{-\nu})h$	$-g^2$	—	$\frac{2c_9 a_9}{v}$	—
$(\partial_\mu W^{+\mu})(W_\nu^- \partial^\nu h) + \text{h.c.}$	$-\frac{g^2}{2}$	—	$\frac{2c_{10} a_{10}}{v}$	—
$i(\partial_\mu W^{-\mu})(Z_\nu W^{+\nu})h + \text{h.c.}$	$\frac{e^2 g}{c_\theta^2}$	—	$\frac{2c_9 a_9}{v}$	—
$i(\partial_\mu W^{-\mu})(A_\nu W^{+\nu})h + \text{h.c.}$	$-eg^2$	—	$\frac{2c_9 a_9}{v}$	—
$i(Z_\mu W^{+\mu})(W_\nu^- \partial^\nu h) + \text{h.c.}$	$-\frac{e^2 g}{2c_\theta}$	—	$\frac{2c_{10} a_{10}}{v}$	—
$i(A_\mu W^{+\mu})(W_\nu^- \partial^\nu h) + \text{h.c.}$	$\frac{eg^2}{2}$	—	$\frac{2c_{10} a_{10}}{v}$	—

Table 3. Anomalous effective couplings of the Higgs particle to two or three gauge bosons, induced by the chiral operators $\mathcal{P}_{\square h}$ and \mathcal{P}_{6-10} , in contrast with the non-impact of their linear sibling $\mathcal{O}_{\square\Phi}$.

apply as well here. For instance, if the coefficients of operators contributing only to the SM-like HVV coupling — such as $c_7 a_7$ above — cancel, the bound on Δ_V and Δ_f becomes, at 90% CL,

$$-0.33 \leq \Delta_f = \Delta_V \leq 0.33, \quad (5.7)$$

which translates into a bound $c_{\square h} \lesssim 2.1 \cdot 10^{-5} \text{ GeV}^{-2}$.

Off-shell Higgs mediated gauge boson pair production. Potentially more interesting, \mathcal{P}_7 leads to a new contribution to the production of electroweak gauge-boson pairs ZZ and W^+W^- through

$$gg \rightarrow h^* \rightarrow ZZ \text{ or } W^+W^-, \quad (5.8)$$

where the Higgs boson is off-shell [37, 38]. For the sake of illustration, we consider the ZZ pair production with one Z decaying into e^+e^- while the other into $\mu^+\mu^-$. The left panel

H ² VV couplings	Coeff.	SM value	Chiral	Linear: $\mathcal{O}_{\Box\Phi}$
$Z_\mu Z^\mu h^2$	$\frac{g^2}{8c_\theta^2}$	1	$-5m_h^2 c_{\Box h}$	—
$Z_\mu Z^\mu \Box(h^2)$	$-\frac{g^2}{2c_\theta^2}$	—	$\frac{c_7 b_7}{v^2}$	—
$Z_\mu Z_\nu \partial^\mu h \partial^\nu h$	$-\frac{g^2}{2c_\theta^2}$	—	$\frac{4c_8 a_8 a'_8}{v^2}$	—
$(\partial_\mu Z^\mu)(\partial_\nu Z^\nu)h^2$	$-\frac{g^2}{2c_\theta^2}$	—	$\frac{c_9 b_9}{v^2}$	—
$(\partial_\mu Z^\mu)(Z_\nu \partial^\nu h)h$	$-\frac{g^2}{2c_\theta^2}$	—	$\frac{2c_{10} b_{10}}{v^2}$	—
$W_\mu^+ W^{-\mu} h^2$	$\frac{g^2}{4}$	1	$-5m_h^2 c_{\Box h}$	—
$W_\mu^+ W^{-\mu} \Box(h^2)$	$-g^2$	—	$\frac{c_7 b_7}{v^2}$	—
$W_\mu^+ W_\nu^- \partial^\mu h \partial^\nu h$	$-g^2$	—	$\frac{4c_8 a_8 a'_8}{v^2}$	—
$(\partial_\mu W^{+\mu})(\partial_\nu W^{-\nu})h^2$	$-g^2$	—	$\frac{c_9 b_9}{v^2}$	—
$(\partial_\mu W^{+\mu})(W_\nu^- \partial^\nu h)h + \text{h.c.}$	$-\frac{g^2}{2}$	—	$\frac{2c_{10} b_{10}}{v^2}$	—

Table 4. Anomalous effective couplings involving two Higgs particles and two gauge bosons, induced by the chiral operators $\mathcal{P}_{\Box h}$ and \mathcal{P}_{6-10} , in contrast with the non-impact of their linear sibling $\mathcal{O}_{\Box\Phi}$.

of figure 3 depicts the leading-order SM contribution to

$$pp \rightarrow e^+ e^- \mu^+ \mu^- ,$$

together with the SM higher-order and \mathcal{P}_7 contributions through the ZZ channel in eq. (5.8). The results presented in this figure were obtained assuming a center-of-mass energy at the LHC of 13 TeV, and requiring that all leptons have transverse momenta in excess of 10 GeV, that they are central ($|\eta| < 2.5$) and that the same-flavour opposite-charge lepton pairs reconstruct the Z mass ($|M_{\ell^+ \ell^-} - M_Z| < 5$ GeV). In presenting the \mathcal{P}_7 effects a coupling $c_7 a_7 = 0.5$ was assumed, which is compatible with the presently available Higgs data. Also, since the goal here is to illustrate the effects of \mathcal{P}_7 , we did not take into account the SM higher-order contribution to $gg \rightarrow e^+ e^- \mu^+ \mu^-$ which interferes with the off-shell Higgs one; for further details see ref. [39] and references therein.

The results in the left panel of the figure 3 show that \mathcal{P}_7 leads to an enhancement of the off-shell Higgs cross section with respect to the SM expectations at high four-lepton invariant masses. In fact, the scattering amplitude grows so fast that at some point unitarity is violated [37], and the introduction of some unitarization procedure will tend to

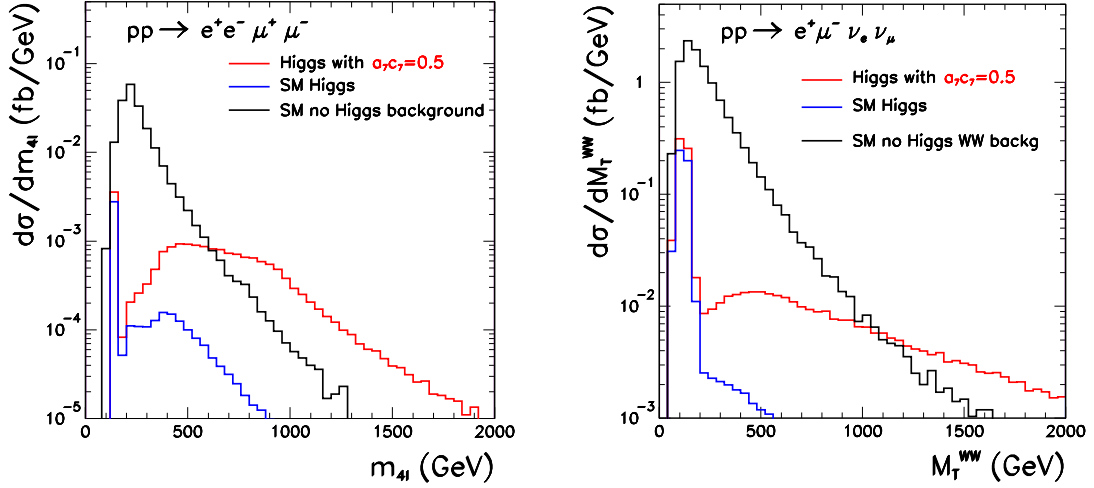


Figure 3. The left panel presents the four lepton invariant mass spectrum for the process $pp \rightarrow e^+e^-\mu^+\mu^-$. The right panel contains the WW transverse mass distribution of the process $pp \rightarrow e^+\nu_e\mu^-\nu_\mu$. In both panels the black line stands for the SM leading-order contribution while the blue (red) one represents the SM (\mathcal{P}_7) higher-order contribution given by eq. (5.8). In this figure we assumed a center-of-mass energy of 13 TeV and $c_7a_7 = 0.5$.

diminish the excess. Nevertheless, even without an unitarization procedure, the expected number of events above the leading order SM background induced by \mathcal{P}_7 is shown to be very small, meaning that unraveling the \mathcal{P}_7 contribution will be challenging.

We have analyzed as well the process

$$pp \rightarrow e^+\nu_e\mu^-\nu_\mu,$$

that can proceed via the W^+W^- channel in eq. (5.8). In the right panel of figure 3 the corresponding cross section is depicted as a function of the WW transverse mass

$$M_T^{WW} = \left[\left(\sqrt{(p_T^{\ell^+\ell'^-})^2 + m_{\ell^+\ell'^-}^2} + \sqrt{\vec{p}_T^2 + m_{\ell^+\ell'^-}^2} \right)^2 - (\vec{p}_T^{\ell^+\ell'^-} + \vec{p}_T)^2 \right]^{1/2}, \quad (5.9)$$

where \vec{p}_T stands for the missing transverse momentum vector, $\vec{p}_T^{\ell^+\ell'^-}$ is the transverse momentum of the pair $\ell^+\ell'^-$ and $m_{\ell^+\ell'^-}$ is the $\ell^+\ell'^-$ invariant mass. Here $\ell = e$ or μ . The transverse momentum and rapidity cuts used were the same than those for the left panel. As expected, an enhancement of the $gg \rightarrow e^+\nu_e\mu^-\nu_\mu$ cross section is induced by the operator \mathcal{P}_7 . Analogously to the case of ZZ production, the SM leading-order contribution dominates but for large M_T^{WW} ; the expected signals from the excess due to \mathcal{P}_7 will be thus very difficult to observe.

Corrections to four gauge boson scattering. As can be seen in tables 2 and 3 the combination $v^2c_{\square h} + 8c_6$ generates the anomalous quartic vertex $ZZZZ$ that is not present in the SM. Moreover, the same combination gives anomalous contributions to the ZZW^+W^- and $W^+W^-W^+W^-$. These are genuinely four gauge boson effects which do not induce any modification to triple gauge boson couplings and, therefore, these coefficients are much less constrained at present.

Nowadays the most stringent bounds on the coefficients of these operators are indirect, from their one-loop contribution to the electroweak precision data [40], in particular to $\alpha\Delta T$ which at 90% CL imply

$$-0.23 \leq \frac{1}{8}v^2 c_{\Box h} + c_6 \leq 0.26. \quad (5.10)$$

At the LHC with 13-14 TeV center-of-mass energy, they can be detected or constrained by combining their impact on the VBF channels

$$pp \rightarrow jjW^+W^- \quad \text{and} \quad pp \rightarrow jj(W^+W^+ + W^-W^-), \quad (5.11)$$

where j stands for a tagging jet and the final state W 's decay into electron or muon plus neutrino [41]; the attainable 99% CL limits on these couplings are

$$-1.2 \cdot 10^{-2} \leq \frac{1}{8}v^2 c_{\Box h} + c_6 < 10^{-2}. \quad (5.12)$$

Disregarding the contribution from c_6 , this would translate into $c_{\Box h} \lesssim 1.3 \cdot 10^{-6} \text{ GeV}^{-2}$, which would suggest a sensitivity to the mass of the LW partner for the singlet Higgs in the chiral EWSB realization up to $\sim 887 \text{ GeV}$.

Strictly speaking, the relevant four gauge boson cross-section also receives modifications induced by those operators which correct the HVV and TGV vertices when the Higgs boson or a gauge boson is exchanged in the s , t or u channels. In principle, these “triple vertex” effects can be discriminated from the purely VVVV effects by their different dependence on the scattering angle of the final state gauge bosons. In practice, a detailed simulation will be required to establish the final sensitivity to all relevant coefficients.

6 Conclusions

An effective coupling for bosons which is tantamount to a quartic kinetic energy is a full-rights member of the tower of leading effective operators accounting for BSM physics in a model-independent way. This is so in both the linear and non-linear realizations of electroweak symmetry breaking, or in other words irrespective of whether the light Higgs particle corresponds to an elementary or a composite (dynamical) Higgs. The corresponding higher derivative kinetic couplings, denoted here $\mathcal{O}_{\Box\Phi}$ and $\mathcal{P}_{\Box h}$, respectively, eqs. (1.1) and (1.2), are customarily not considered but traded by others (e.g. fermionic ones) instead of being kept as independent elements of a given basis.

It is most pertinent to analyze those couplings directly, though, as they are related to intriguing and potentially very important solutions to ultraviolet issues, such as the electroweak gauge hierarchy problem. The field theory challenges they rise constitute as well a fascinating theoretical conundrum. Their theoretical impact is “diluted” and hard to track, though, when they are traded by combinations of other operators. On top of which, the present LHC data offer increasingly rich and precise constraints on gauge and gauge-Higgs couplings, up to the point of becoming competitive with fermionic bounds in constraining BSM theories; this trend may be further strengthened with the post-LHC facilities presently under discussion.

We have analyzed and compared in this paper $\mathcal{O}_{\square\Phi}$ and $\mathcal{P}_{\square h}$, unravelling theoretical and experimental distinctive features.

On the theoretical side, two analyses have been carried in parallel and compared: i) the Lee-Wick procedure of trading the second pole in the propagator by a “ghost” scalar partner; ii) the application of the EOM to the operator, trading it by other effective operators and resulting in an analysis which only requires standard field-theory tools. Both paths have been shown to be consistent, producing the same effective Lagrangian at leading order in the operator coefficient dependence.

A most interesting property is that the physical impact differs for linearly versus non-linear EWSB realizations: departures from SM values for quartic-gauge boson, Higgs-gauge boson and fermion-gauge boson couplings are expected only for the case of a dynamical Higgs, i.e. only from $\mathcal{P}_{\square h}$ while not from $\mathcal{O}_{\square\Phi}$; in addition, they induce a different pattern of deviations on Yukawa-like fermionic couplings and on the Higgs potential.

Note that these distinctive signals of a dynamical origin of the Higgs particle would be altogether missed if a $d = 6$ linear effective Lagrangian was used to evaluate the possible impact of an underlying strong dynamics, showing that in general a linear approach is not an appropriate tool to the task. Indeed, for completeness we identified all TGV, HVV and VVVV experimental signals which are unique in resulting from the leading chiral expansion, while they cannot be induced neither by SM couplings at tree-level *nor* by $d = 6$ operators of the linear expansion: the TGV couplings Δg_6^γ , Δg_5^Z and Δg_6^Z , the HVV couplings $\Delta g_{HVV}^{(4)}$, $\Delta g_{HVV}^{(5)}$ and $\Delta g_{HVV}^{(6)}$ and the VVVV couplings $\Delta g_{ZZ}^{(1)}$ and $\Delta g_{\gamma Z}^{(5)}$, with the quartic kinetic energy coupling for non-linear EWSB scenarios $\mathcal{P}_{\square h}$ contributing only to $\Delta g_{ZZ}^{(1)}$ among the above. The experimental search of that ensemble of couplings and their correlations (see tables 5, 6 and 7 in appendix C), constitute a superb window into chiral dynamics associated to the Higgs particle.

To tackle the origin of the different physical impact of quartic derivative Higgs kinetic terms depending on the type of EWSB, we have explored and established the precise relation between the two couplings: it was shown that $\mathcal{O}_{\square\Phi}$ corresponds to a specific combination of $\mathcal{P}_{\square h}$ with five other non-linear operators.

On the phenomenological analysis, the impact of $\mathcal{O}_{\square\Phi}$, $\mathcal{P}_{\square h}$ and \mathcal{P}_{6-10} has been scrutinised. All LHC Higgs and other data presently available were used to constrain the $\mathcal{O}_{\square\Phi}$ and $\mathcal{P}_{\square h}$ coupling strengths. Moreover, the impact of future 14 TeV LHC data on $pp \rightarrow 4$ leptons has been explored; the operators under scrutiny intervene in the process via off-shell Higgs mediation in gluon-gluon fusion, $gg \rightarrow h^* \rightarrow ZZ$ or W^+W^- , inducing excesses at high four-lepton invariant masses via the ZZ channel, and at high values of the WW invariant mass in the WW channel. The corrections expected at LHC through their impact on four gauge boson scattering, extracted combining information from vector boson fusion channels, $pp \rightarrow jjW^+W^-$ and $pp \rightarrow jj(W^+W^+ + W^-W^-)$, has been also discussed. The possibility that LHC may shed light on Lee-Wick theories through the type of analysis and signals discussed here is a fascinating perspective.

Acknowledgments

We thank especially J. Gonzalez-Fraile for early discussions about the presence of new off-shell Higgs effects. We acknowledge partial support of the European Union network FP7 ITN INVISIBLES (Marie Curie Actions, PITN-GA-2011-289442), of CiCYT through the project FPA2009-09017, of CAM through the project HEPHACOS P-ESP-00346, of the European Union FP7 ITN UNILHC (Marie Curie Actions, PITN-GA-2009-237920), of MICINN through the grant BES-2010-037869, of the Spanish MINECO Centro de Excelencia Severo Ochoa Programme under grant SEV-2012-0249, and of the Italian Ministero dell'Università e della Ricerca Scientifica through the COFIN program (PRIN 2008) and the contract MRTN-CT-2006-035505. The work of I.B. is supported by an ESR contract of the European Union network FP7 ITN INVISIBLES mentioned above. The work of L.M. is supported by the Juan de la Cierva programme (JCI-2011-09244). The work of O.J.P.E. is supported in part by Conselho Nacional de Desenvolvimento Científico e Tecnológico (CNPq) and by Fundação de Amparo à Pesquisa do Estado de São Paulo (FAPESP). The work of M.C.G-G is supported by USA-NSF grant PHY-09-6739, by CUR Generalitat de Catalunya grant 2009SGR502, by MICINN FPA2010-20807 and by consolidator-ingenio 2010 program CSD-2008-0037.

A Analysis with a generic chiral potential $V(h)$

In the analysis performed in this paper the effective operators $\mathcal{P}_{\Box h}$ and $\mathcal{O}_{\Box \Phi}$ are assumed to be the only departures from the Standard Model present in the chiral and linear Lagrangians, respectively. However, the choice of a SM-like scalar potential might not appear satisfactory for the chiral case: *a priori* $V(h)$ is a completely generic polynomial in the singlet field h , and the current lack of direct measurements of the triple and quartic self-couplings of the Higgs boson leaves room for a less constrained parametrization.

Therefore, it can be interesting to test the stability of our results against deviations of the scalar potential from the SM pattern. To do this, we apply the Lee-Wick method to the Lagrangian in eq. (3.1) although with the SM-like potential in eq. (2.3) replaced by a generic one,

$$V(h) = a_1 h + \frac{m_h^2}{2} a_2 h^2 + \frac{m_h^2}{2v} a_3 h^3 + \frac{m_h^2}{8v^2} a_4 h^4, \quad (\text{A.1})$$

where we choose to omit higher h -dependent terms, as the analysis remains at tree level and limited to interactions involving at most two Higgs particles. The correction factor a_2 can always be reabsorbed in the definition of m_h , and will thus be fixed from the start to

$$a_2 = 1.$$

The comparison with the case described in section 3 is straightforward choosing, in addition, $a_3 = a_4 = 1$ and $a_1 = 0$. The resulting mass-diagonal Lagrangian containing the LW field χ is:

$$\mathcal{L}^\chi = (\text{kin. terms}) + \mathcal{L}_Y^\chi + \mathcal{L}_{\text{gauge}}^\chi - V(h, \chi), \quad (\text{A.2})$$

with

$$\mathcal{L}_Y^\chi = -\frac{1}{\sqrt{2}}(\bar{Q}_L \mathbf{U} \mathbf{Y} Q_R + \text{h.c.}) [1 + (1 + 2x)(h - \chi)] , \quad (\text{A.3})$$

$$\mathcal{L}_{\text{gauge}}^\chi = -\frac{1}{4} \text{Tr}[\mathbf{V}_\mu \mathbf{V}^\mu] [v^2 + 2v(1 + 2x)(h - \chi) + (1 + 4x)(h - \chi)^2] , \quad (\text{A.4})$$

$$\begin{aligned} V(h, \chi) = & a_1(1 + 2x)(h - \chi) + \frac{m_h^2}{2}(1 + 2x)h^2 + \frac{m_h^2}{2} \left(1 - \frac{1}{2x} + 2x\right) \chi^2 \\ & + \frac{m_h^2}{2v} a_3(1 + 6x)(h - \chi)^3 + \frac{m_h^2}{8v^2} a_4(1 + 8x)(h - \chi)^4 , \end{aligned} \quad (\text{A.5})$$

where $x = -c_{\square h} m_h^2/2 > 0$.

Upon integrating out the heavy LW ghost, the following renormalized Lagrangian results:

$$\mathcal{L}_{\square h} = \frac{1}{2} \partial_\mu h \partial^\mu h - \frac{1}{4} Z_{\mu\nu} Z^{\mu\nu} - \frac{1}{2} W_{\mu\nu}^+ W^{-\mu\nu} + i \bar{Q} \not{D} Q + \mathcal{L}_{\square h}^{\text{fer.}} + \mathcal{L}_{\square h}^{\text{gauge}} - V_{\square h}(h) , \quad (\text{A.6})$$

where

$$\mathcal{L}_{\square h}^{\text{fer.}} = -\frac{1}{\sqrt{2}} (\bar{Q}_L \mathbf{U} \mathbf{Y} Q_R + \text{h.c.}) \left[v + (1 + 2x)h + 3a_3 x \frac{h^2}{v} + a_4 x \frac{h^3}{v^2} \right] \quad (\text{A.7})$$

$$- \frac{x}{2m^2} (\bar{Q}_L \mathbf{U} \mathbf{Y} Q_R + \text{h.c.})^2 - \frac{x}{m_h^2} \frac{v + h}{\sqrt{2}} \text{Tr}[\mathbf{V}_\mu \mathbf{V}^\mu] (\bar{Q}_L \mathbf{U} \mathbf{Y} Q_R + \text{h.c.}) ,$$

$$\begin{aligned} \mathcal{L}_{\square h}^{\text{gauge}} = & -\frac{1}{4} \text{Tr}[\mathbf{V}_\mu \mathbf{V}^\mu] \left[(v + h)^2 \left(1 + 4x \frac{h}{v} + 2xh^2\right) \right. \\ & \left. + 2x(v + h) \frac{h^2}{v^2} (3v(a_3 - 1) + h(a_4 - 1)) \right] - \frac{x}{4m_h^2} (v + h)^2 \text{Tr}[\mathbf{V}_\mu \mathbf{V}^\mu]^2 , \end{aligned} \quad (\text{A.8})$$

$$\begin{aligned} V_{\square h}(h) = & \frac{m_h^2}{2} h^2 + a_1(1 + 2x)h + \frac{m_h^2}{2v} \left[a_3(1 + 4x) + \frac{2a_1 x}{m_h^2 v} (a_4 + a_3 - 3a_3^2) \right] h^3 \\ & + \frac{m_h^2}{8v^2} \left[a_4(1 + 6x) + 2x \left(9a_3^2 + \frac{a_1 a_4}{m_h^2 v} (2 - 3a_3) \right) \right] h^4 + \frac{3a_3 a_4 m_h^2 x}{2v^3} h^5 + \frac{a_4^2 m_h^2 x}{4v^4} h^6 . \end{aligned} \quad (\text{A.9})$$

Phenomenological impact. Assuming that the departures from unity of the a_i parameters are small (of order $c_{\square h}$ at most), we can replace

$$a_1 \rightarrow \Delta a_1 , \quad a_i \rightarrow 1 + \Delta a_i , \quad i = 3, 4 \quad (\text{A.10})$$

and expand the renormalized Lagrangian (A.6) up to first order in x and in the Δ_i 's. Restricting for practical reasons to vertices with up to four legs, the list of couplings that are modified is very reduced and only includes terms in the scalar potential:

$$\begin{aligned} & -\frac{m_h^2}{2v} (1 + 4x + \Delta a_3) h^3 , \\ & -\frac{m_h^2}{8v^2} (1 + 24x + \Delta a_4) h^4 , \\ & -\Delta a_1 h . \end{aligned} \quad (\text{A.11})$$

In consequence, upon the assumption that possible departures of the scalar potential from a SM-like form are quantitatively at most of the same order as $c_{\square h}$, those contributions would not affect the numerical analysis presented in the text.

B Impact of $\mathcal{O}_{\square\Phi}$ versus $\mathcal{P}_{\square h}$ on $ZZ \rightarrow ZZ$ scattering

This appendix provides an illustrative example of how the contributions of the chiral operators $\mathcal{P}_{\square h}, \mathcal{P}_{6-10}$ to physical amplitudes combine to reproduce those of the linear operator $\mathcal{O}_{\square\Phi}$, once the conditions (4.5) and (4.4) are imposed.

Let us consider the elastic scattering of two Z gauge bosons. This process is not affected by $\mathcal{O}_{\square\Phi}$, therefore the corrections induced by the six chiral operators are expected to cancel exactly, upon assuming (4.5) and (4.4).

Assuming the external Z bosons are on-shell, the only Feynman diagrams containing deviations from the Standard Model are the following

$$\mathcal{A}_s + \mathcal{A}_t + \mathcal{A}_u = \begin{array}{c} \begin{array}{ccc} Z_1 & & Z_3 \\ & \text{---} h \text{---} & \\ Z_2 & & Z_4 \end{array} + \begin{array}{ccc} Z_1 & & Z_3 \\ & \text{---} h \text{---} & \\ Z_2 & & Z_4 \end{array} + \begin{array}{ccc} Z_1 & & Z_4 \\ & \text{---} h \text{---} & \\ Z_2 & & Z_3 \end{array} \end{array} \quad (\text{B.1})$$

$$\mathcal{A}_{4Z} = \begin{array}{ccc} Z_2 & & Z_4 \\ & \text{---} & \\ Z_1 & & Z_3 \end{array} \quad (\text{B.2})$$

For the amplitudes depicted in (B.1), the relevant couplings are ZZh and $ZZ\square h$ (see table 3), and the contributions from each channel turn out to be

$$\mathcal{A}_s = -(\varepsilon_1 \cdot \varepsilon_2)(\varepsilon_3^* \cdot \varepsilon_4^*) \frac{i}{s - m_h^2} \frac{4m_Z^4}{v^2} \left(1 - 2m_h^2 c_{\square h} + \frac{8s}{v^2} c_7 a_7 \right), \quad (\text{B.3})$$

$$\mathcal{A}_t = -(\varepsilon_1 \cdot \varepsilon_3^*)(\varepsilon_2 \cdot \varepsilon_4^*) \frac{i}{t - m_h^2} \frac{4m_Z^4}{v^2} \left(1 - 2m_h^2 c_{\square h} + \frac{8s}{v^2} c_7 a_7 \right), \quad (\text{B.4})$$

$$\mathcal{A}_u = -(\varepsilon_1 \cdot \varepsilon_4^*)(\varepsilon_3^* \cdot \varepsilon_2) \frac{i}{u - m_h^2} \frac{4m_Z^4}{v^2} \left(1 - 2m_h^2 c_{\square h} + \frac{8s}{v^2} c_7 a_7 \right), \quad (\text{B.5})$$

where $\varepsilon_1, \varepsilon_2$ denote the polarizations of the incoming Z bosons, and $\varepsilon_3^*, \varepsilon_4^*$ those of the outgoing ones.

Imposing the constraints $c_7 = v^2 c_{\square h}/4$, from eq. (4.5) and $a_7 = 1$ from eq. (4.4), the dependence on the exchanged momentum drops from the non-standard part of the amplitudes:

$$\begin{aligned} \mathcal{A}_h = \mathcal{A}_s + \mathcal{A}_t + \mathcal{A}_u = & -\frac{4im_Z^4}{v^2} \left[\frac{(\varepsilon_1 \cdot \varepsilon_2)(\varepsilon_3^* \cdot \varepsilon_4^*)}{s - m_h^2} + \frac{(\varepsilon_1 \cdot \varepsilon_3^*)(\varepsilon_2 \cdot \varepsilon_4^*)}{t - m_h^2} + \frac{(\varepsilon_1 \cdot \varepsilon_4^*)(\varepsilon_2 \cdot \varepsilon_3^*)}{u - m_h^2} \right] \\ & - \frac{8im_Z^4}{v^2} c_{\square h} \left[(\varepsilon_1 \cdot \varepsilon_2)(\varepsilon_3^* \cdot \varepsilon_4^*) + (\varepsilon_1 \cdot \varepsilon_3^*)(\varepsilon_2 \cdot \varepsilon_4^*) + (\varepsilon_1 \cdot \varepsilon_4^*)(\varepsilon_2 \cdot \varepsilon_3^*) \right]. \end{aligned} \quad (\text{B.6})$$

The diagram (B.2) contains only the four-point vertex $ZZZZ$ (see table 2), and gives

$$\begin{aligned} \mathcal{A}_{4Z} = & \frac{32im_Z^4}{v^4} \left(c_6 + \frac{v^2}{8} c_{\square h} \right) \left[(\varepsilon_1 \cdot \varepsilon_2)(\varepsilon_3^* \cdot \varepsilon_4^*) + (\varepsilon_1 \cdot \varepsilon_3^*)(\varepsilon_2 \cdot \varepsilon_4^*) + (\varepsilon_1 \cdot \varepsilon_4^*)(\varepsilon_2 \cdot \varepsilon_3^*) \right] \\ = & \frac{8im_Z^4}{v^2} c_{\square h} \left[(\varepsilon_1 \cdot \varepsilon_2)(\varepsilon_3^* \cdot \varepsilon_4^*) + (\varepsilon_1 \cdot \varepsilon_3^*)(\varepsilon_2 \cdot \varepsilon_4^*) + (\varepsilon_1 \cdot \varepsilon_4^*)(\varepsilon_2 \cdot \varepsilon_3^*) \right]. \end{aligned} \quad (\text{B.7})$$

In the second line the condition (4.5) has been assumed, which imposes $v^2 c_{\square h} = 8c_6$.

The neat correction to the Standard Model amplitude for ZZ scattering induced by the chiral operators $\mathcal{P}_{\square h}, \mathcal{P}_{6-10}$ is finally proved to vanish, as

$$\Delta\mathcal{A} = \Delta\mathcal{A}_h + \mathcal{A}_{4Z} = 0. \quad (\text{B.8})$$

C Chiral versus linear couplings

In this appendix, we gather the departures from SM couplings in TGV, HVV and VVVV vertices, which are expected from the leading order tower of chiral scalar and/or gauge operators (which includes $\mathcal{P}_{\square h}$ and \mathcal{P}_{6-10} discussed in this manuscript), as well as from any possible chiral or $d = 6$ linear coupling which may affect those same vertices at leading order of the respective effective expansions. Their comparison allows a straightforward identification of which signals may point to a strong dynamics underlying EWSB, being free from SM or $d = 6$ linear operators contamination. In tables 5, 6 and 7 below:

- The $\mathcal{O}_{\square\Phi}$, $\mathcal{P}_{\square h}$ and \mathcal{P}_{6-10} operators are defined as in eqs. (1.1), (1.2) and (4.2), while for all other couplings mentioned — linear or chiral — the naming follows that in ref. [20], to which we refer the reader.
- All operator coefficients appearing in the tables below are defined as in eq. (1.4). In comparison with the definitions in ref. [20] this means that: i) the coefficient of the chiral operator $\mathcal{P}_{\square h}$ has been rescaled, see footnotes 1 and 2; ii) the $d = 6$ linear operator coefficients f_i in refs. [20, 29] are related to those in the tables below as follows:

$$c_i = f_i/\Lambda^2. \quad (\text{C.1})$$

As discussed in the text, new anomalous vertices related to a quartic kinetic energy for the Higgs particle include as well HHVV couplings and new corrections to fermionic vertices. We leave for a future publication the corresponding comparison between the complete linear and chiral bases. When referring below to the SM, only tree-level contributions are considered.

C.1 TGV couplings

The CP-even sector of the Lagrangian that describes TGV couplings can be parametrized as

$$\begin{aligned} \mathcal{L}_{WWV} = & -ig_{WWV} \left\{ g_1^V \left(W_{\mu\nu}^+ W^{-\mu} V^\nu - W_\mu^+ V_\nu W^{-\mu\nu} \right) + \kappa_V W_\mu^+ W_\nu^- V^{\mu\nu} \right. \\ & \left. - ig_5^V \epsilon^{\mu\nu\rho\sigma} \left(W_\mu^+ \partial_\rho W_\nu^- - W_\nu^- \partial_\rho W_\mu^+ \right) V_\sigma + g_6^V \left(\partial_\mu W^{+\mu} W^{-\nu} - \partial_\mu W^{-\mu} W^{+\nu} \right) V_\nu \right\}, \end{aligned} \quad (\text{C.2})$$

where $V \equiv \{\gamma, Z\}$ and $g_{WW\gamma} \equiv e = g \sin \theta_W$, $g_{WWZ} = g \cos \theta_W$. The SM values for the phenomenological parameters defined in this expression are $g_1^{Z,\gamma} = \kappa_{Z,\gamma} = 1$ and $g_5^{Z,\gamma} = g_6^{Z,\gamma} = 0$. The resulting TGV corrections are gathered in table 5. For instance, while Δg_6^γ and Δg_6^Z cannot be induced by any linear $d = 6$ operators, they receive contributions from the operators \mathcal{P}_{6-10} discussed in this manuscript. Barring fine-tunings and one-loop effects, a detection of such couplings with sizeable strength would point to a non-linear realization of EWSB.

	Coeff. $\times e^2/s_\theta^2$	Chiral	Linear $\times v^2$
$\Delta\kappa_\gamma$	1	$-2c_1 + 2c_2 + c_3 - 4c_{12} + 2c_{13}$	$\frac{1}{8}(c_W + c_B - 2c_{BW})$
Δg_6^γ	1	$-c_9$	—
Δg_1^Z	$\frac{1}{c_\theta^2}$	$\frac{s_\theta^2}{4e^2 c_{2\theta}} c_T + \frac{2s_\theta^2}{c_{2\theta}} c_1 + c_3$	$\frac{1}{8}c_W + \frac{s_\theta^2}{4c_{2\theta}} c_{BW} - \frac{s_\theta^2}{16e^2 c_{2\theta}} c_{\Phi,1}$
$\Delta\kappa_Z$	1	$\frac{s_\theta^2}{e^2 c_{2\theta}} c_T + \frac{4s_\theta^2}{c_{2\theta}} c_1 - \frac{2s_\theta^2}{ct^2} c_2 + c_3 - 4c_{12} + 2c_{13}$	$\frac{1}{8}c_W - \frac{s_\theta^2}{8ct^2} c_B + \frac{s_\theta^2}{2c_{2\theta}} c_{BW} - \frac{s_\theta^2}{4e^2 c_{2\theta}} c_{\Phi,1}$
Δg_5^Z	$\frac{1}{c_\theta^2}$	c_{14}	—
Δg_6^Z	$\frac{1}{c_\theta^2}$	$s_\theta^2 c_9 - c_{16}$	—

Table 5. Effective couplings parametrizing the VW^+W^- vertices defined in eq. (C.2). The coefficients in the second column are common to both the chiral and linear expansions. The third column lists the specific contributions from the operators in the chiral basis. For comparison, the last column exhibits the corresponding contributions from linear $d = 6$ operators.

C.2 HVV couplings

The Higgs to two gauge bosons couplings can be phenomenologically parametrized as

$$\begin{aligned}
 \mathcal{L}_{\text{HVV}} \equiv & g_{Hgg} G_{\mu\nu}^a G^{a\mu\nu} h + g_{H\gamma\gamma} A_{\mu\nu} A^{\mu\nu} h + g_{HZZ\gamma}^{(1)} A_{\mu\nu} Z^\mu \partial^\nu h + g_{HZZ\gamma}^{(2)} A_{\mu\nu} Z^{\mu\nu} h \\
 & + g_{HZZ}^{(1)} Z_{\mu\nu} Z^\mu \partial^\nu h + g_{HZZ}^{(2)} Z_{\mu\nu} Z^{\mu\nu} h + g_{HZZ}^{(3)} Z_\mu Z^\mu h + g_{HZZ}^{(4)} Z_\mu Z^\mu \Box h \\
 & + g_{HZZ}^{(5)} \partial_\mu Z^\mu Z_\nu \partial^\nu h + g_{HZZ}^{(6)} \partial_\mu Z^\mu \partial_\nu Z^\nu h \\
 & + g_{HWW}^{(1)} (W_\mu^+ W^{-\mu} \partial^\nu h + \text{h.c.}) + g_{HWW}^{(2)} W_\mu^+ W^{-\mu\nu} h + g_{HWW}^{(3)} W_\mu^+ W^{-\mu} h \\
 & + g_{HWW}^{(4)} W_\mu^+ W^{-\mu} \Box h + g_{HWW}^{(5)} (\partial_\mu W^{+\mu} W_\nu^- \partial^\nu h + \text{h.c.}) \\
 & + g_{HWW}^{(6)} \partial_\mu W^{+\mu} \partial_\nu W^{-\nu} h,
 \end{aligned} \tag{C.3}$$

where $V_{\mu\nu} = \partial_\mu V_\nu - \partial_\nu V_\mu$ with $V = \{A, Z, W, G\}$. Separating the contributions into SM ones plus corrections, $g_i^{(j)} \simeq g_i^{(j)SM} + \Delta g_i^{(j)}$, it turns out that

$$g_{HZZ}^{(3)SM} = \frac{m_Z^2}{v}, \quad g_{HWW}^{(3)SM} = \frac{2m_Z^2 c_\theta^2}{v}, \tag{C.4}$$

while the tree-level SM value for all other couplings in eq. (C.3) vanishes.

While $\mathcal{P}_{\Box h}$ may induce a departure from SM expectations in two HVV couplings, $\Delta g_{HZZ}^{(3)}$ and $\Delta g_{HWW}^{(3)}$, table 6 shows that those signals could be mimicked by some $d = 6$ linear operators. On the contrary, a putative detection of $\Delta g_{HVV}^{(4)}$ couplings may arise from the \mathcal{P}_7 operator discussed in this manuscript while neither from the SM nor any linear $d = 6$ couplings, and would thus be a smoking gun for a non-linear nature of EWSB realization; the same applies to $\Delta g_{HVV}^{(5)}$ from \mathcal{P}_{10} , and to $\Delta g_{HVV}^{(6)}$ from \mathcal{P}_9 .

	Coeff. $\times e^2/4v$	Chiral	Linear $\times v^2$
Δg_{Hgg}	$\frac{g_s^2}{e^2}$	$-2c_G a_G$	$-4c_{GG}$
$\Delta g_{H\gamma\gamma}$	1	$-2(c_B a_B + c_W a_W) + 8c_1 a_1 + 8c_{12} a_{12}$	$-(c_{BB} + c_{WW}) + c_{BW}$
$\Delta g_{HZZ}^{(1)}$	$\frac{1}{s_{2\theta}}$	$-8(c_5 a_5 + 2c_4 a_4) - 16c_{17} a_{17}$	$2(c_W - c_B)$
$\Delta g_{HZZ}^{(2)}$	$\frac{c_\theta}{s_\theta}$	$4\frac{s_\theta^2}{c_\theta^2} c_B a_B - 4c_W a_W + 8\frac{c_{2\theta}}{c_\theta^2} c_1 a_1 + 16c_{12} a_{12}$	$2\frac{s_\theta^2}{c_\theta^2} c_{BB} - 2c_{WW} + \frac{c_{2\theta}}{c_\theta^2} c_{BW}$
$\Delta g_{HZZ}^{(1)}$	$\frac{1}{c_\theta}$	$-4\frac{c_\theta^2}{s_\theta^2} c_5 a_5 + 8c_4 a_4 - 8\frac{c_\theta^2}{s_\theta^2} c_{17} a_{17}$	$\frac{c_\theta^2}{s_\theta^2} c_W + c_B$
$\Delta g_{HZZ}^{(2)}$	$-\frac{c_\theta^2}{s_\theta^2}$	$2\frac{s_\theta^4}{c_\theta^2} c_B a_B + 2c_W a_W + 8\frac{s_\theta^2}{c_\theta^2} c_1 a_1 - 8c_{12} a_{12}$	$\frac{s_\theta^4}{c_\theta^2} c_{BB} + c_{WW} + \frac{s_\theta^2}{c_\theta^2} c_{BW}$
$\Delta g_{HZZ}^{(3)}$	$\frac{m_h^2}{e^2}$	$-2c_H + 2c_C(2a_C - 1) - 8c_T(a_T - 1) - 4m_h^2 c_{\Box h}$	$c_{\Phi,1} + 2c_{\Phi,4} - 2c_{\Phi,2}$
$\Delta g_{HZZ}^{(4)}$	$-\frac{1}{s_{2\theta}^2}$	$16c_7 a_7 + 32c_{25} a_{25}$	—
$\Delta g_{HZZ}^{(5)}$	$-\frac{1}{s_{2\theta}^2}$	$16c_{10} a_{10} + 32c_{19} a_{19}$	—
$\Delta g_{HZZ}^{(6)}$	$-\frac{1}{s_{2\theta}^2}$	$16c_9 a_9 + 32c_{15} a_{15}$	—
$\Delta g_{HWW}^{(1)}$	$\frac{1}{s_\theta^2}$	$-4c_5 a_5$	c_W
$\Delta g_{HWW}^{(2)}$	$\frac{1}{s_\theta^2}$	$-4c_W a_W$	$-2c_{WW}$
$\Delta g_{HWW}^{(3)}$	$\frac{m_h^2 c_\theta^2}{e^2}$	$-4c_H + 4c_C(2a_C - 1) + \frac{32e^2}{c_{2\theta}} c_1 + \frac{16c_\theta^2}{c_{2\theta}} c_T - 8m_h^2 c_{\Box h} - \frac{32e^2}{s_\theta^2} c_{12}$	$\frac{-2(3c_\theta^2 - s_\theta^2)}{c_{2\theta}} c_{\Phi,1} + 4c_{\Phi,4} - 4c_{\Phi,2} + \frac{4e^2}{c_{2\theta}} c_{BW}$
$\Delta g_{HWW}^{(4)}$	$-\frac{1}{s_\theta^2}$	$8c_7 a_7$	—
$\Delta g_{HWW}^{(5)}$	$-\frac{1}{s_\theta^2}$	$4c_{10} a_{10}$	—
$\Delta g_{HWW}^{(6)}$	$-\frac{1}{s_\theta^2}$	$8c_9 a_9$	—

Table 6. Higgs-gauge bosons couplings as defined in eq. (C.3). The coefficients in the second column are common to both the chiral and linear expansions. The third column lists the specific contributions from the operators in the chiral basis. For comparison, the last column exhibits the corresponding contributions from linear $d = 6$ operators.

C.3 VVVV couplings

The effective Lagrangian for VVVV couplings reads

$$\begin{aligned}
 \mathcal{L}_{4X} \equiv & g^2 \left\{ g_{ZZ}^{(1)} (Z_\mu Z^\mu)^2 + g_{WW}^{(1)} W_\mu^+ W^{+\mu} W_\nu^- W^{-\nu} - g_{WW}^{(2)} (W_\mu^+ W^{-\mu})^2 \right. \\
 & + g_{VV'}^{(3)} W^{+\mu} W^{-\nu} (V_\mu V'_\nu + V'_\mu V_\nu) - g_{VV'}^{(4)} W_\nu^+ W^{-\nu} V^\mu V'_\mu \\
 & \left. + i g_{VV'}^{(5)} e^{\mu\nu\rho\sigma} W_\mu^+ W_\nu^- V_\rho V'_\sigma \right\}, \tag{C.5}
 \end{aligned}$$

where $VV' = \{\gamma\gamma, \gamma Z, ZZ\}$. At tree-level in the SM, the following couplings are non-vanishing:

$$\begin{aligned}
 g_{WW}^{(1)SM} &= \frac{1}{2}, & g_{WW}^{(2)SM} &= \frac{1}{2}, & g_{ZZ}^{(3)SM} &= \frac{c_\theta^2}{2}, & g_{\gamma\gamma}^{(3)SM} &= \frac{s_\theta^2}{2}, \\
 g_{Z\gamma}^{(3)SM} &= \frac{s_{2\theta}}{2}, & g_{ZZ}^{(4)SM} &= c_\theta^2, & g_{\gamma\gamma}^{(4)SM} &= s_\theta^2, & g_{Z\gamma}^{(4)SM} &= s_{2\theta}, \tag{C.6}
 \end{aligned}$$

table 7 shows the impact on the couplings in eq. (C.5) of the leading non-linear versus linear operators. While $\mathcal{P}_{\Box h}$ and \mathcal{P}_6 may induce $\Delta g_{WW}^{(2)}$ and $\Delta g_{ZZ}^{(4)}$ couplings, the table shows

	Coeff. $\times e^2/4s_\theta^2$	Chiral	Linear $\times v^2$
$\Delta g_{WW}^{(1)}$	1	$\frac{s_{2\theta}^2}{e^2 c_{2\theta}} c_T + \frac{8s_\theta^2}{c_{2\theta}} c_1 + 4c_3 + 2c_{11} - 16c_{12} + 8c_{13}$	$\frac{c_W}{2} + \frac{s_\theta^2}{c_{2\theta}} c_{BW} - \frac{s_{2\theta}^2}{4c_{2\theta}e^2} c_{\Phi 1}$
$\Delta g_{WW}^{(2)}$	1	$\frac{s_{2\theta}^2}{e^2 c_{2\theta}} c_T + \frac{8s_\theta^2}{c_{2\theta}} c_1 + 4c_3 - 4c_6 - \frac{v^2}{2} c_{\square h} - 2c_{11} - 16c_{12} + 8c_{13}$	$\frac{c_W}{2} + \frac{s_\theta^2}{c_{2\theta}} c_{BW} - \frac{s_{2\theta}^2}{4c_{2\theta}e^2} c_{\Phi 1}$
$\Delta g_{ZZ}^{(1)}$	$\frac{1}{c_\theta^4}$	$c_6 + \frac{v^2}{8} c_{\square h} + c_{11} + 2c_{23} + 2c_{24} + 4c_{26}$	—
$\Delta g_{ZZ}^{(3)}$	$\frac{1}{c_\theta^2}$	$\frac{s_{2\theta}^2 c_\theta^2}{e^2 c_{2\theta}} c_T + \frac{2s_{2\theta}^2}{c_{2\theta}} c_1 + 4c_\theta^2 c_3 - 2s_\theta^4 c_9 + 2c_{11} + 4s_\theta^2 c_{16} + 2c_{24}$	$\frac{c_W c_\theta^2}{2} + \frac{s_\theta^2}{4c_{2\theta}} c_{BW} - \frac{s_{2\theta}^2 c_\theta^2}{4e^2 c_{2\theta}} c_{\Phi 1}$
$\Delta g_{ZZ}^{(4)}$	$\frac{1}{c_\theta^2}$	$\frac{2s_{2\theta}^2 c_\theta^2}{e^2 c_{2\theta}} c_T + \frac{4s_{2\theta}^2}{c_{2\theta}} c_1 + 8c_\theta^2 c_3 - 4c_6 - \frac{v^2}{2} c_{\square h} - 4c_{23}$	$c_W c_\theta^2 + 2\frac{s_{2\theta}^2}{4c_{2\theta}} c_{BW} - \frac{s_{2\theta}^2 c_\theta^2}{2e^2 c_{2\theta}} c_{\Phi 1}$
$\Delta g_{\gamma\gamma}^{(3)}$	s_θ^2	$-2c_9$	—
$\Delta g_{\gamma Z}^{(3)}$	$\frac{s_\theta}{c_\theta}$	$\frac{s_{2\theta}^2}{e^2 c_{2\theta}} c_T + \frac{8s_\theta^2}{c_{2\theta}} c_1 + 4c_3 + 4s_\theta^2 c_9 - 4c_{16}$	$\frac{c_W}{2} + \frac{s_\theta^2}{c_{2\theta}} c_{BW} - \frac{s_{2\theta}^2}{4c_{2\theta}e^2} c_{\Phi 1}$
$\Delta g_{\gamma Z}^{(4)}$	$\frac{s_\theta}{c_\theta}$	$\frac{2s_{2\theta}^2}{e^2 c_{2\theta}} c_T + \frac{16s_\theta^2}{c_{2\theta}} c_1 + 8c_3$	$c_W + 2\frac{s_\theta^2}{c_{2\theta}} c_{BW} - \frac{s_{2\theta}^2}{2c_{2\theta}e^2} c_{\Phi 1}$
$\Delta g_{\gamma Z}^{(5)}$	$\frac{s_\theta}{c_\theta}$	$8c_{14}$	—

Table 7. Effective couplings parametrizing the vertices of four gauge bosons defined in eq. (C.5). The third column lists the specific contributions from the operators in the chiral basis. For comparison, the last column exhibits the corresponding contributions from linear $d = 6$ operators.

that those signals could be mimicked by some $d = 6$ linear operators. On the contrary, the $4Z$ coupling $\Delta g_{ZZ}^{(1)}$ is induced by $\mathcal{P}_{\square h}$, while it vanishes in the SM and in any linear $d = 6$ expansion. A detection of $\Delta g_{ZZ}^{(1)}$ would thus be a beautiful smoking gun of a non-linear nature of EWSB realization, which may simultaneously indicate a quartic kinetic energy for the Higgs scalar of LW theories (although $\Delta g_{ZZ}^{(1)}$ may also be induced by other chiral operators, including \mathcal{P}_6 as discussed towards the end of section 5).

Summarising this appendix, some experimental signals are unique in resulting from the leading chiral expansion, while they cannot be induced neither by the SM at tree-level *nor* by $d = 6$ operators of the linear expansion; among those analyzed here they are

- the TGV couplings Δg_6^γ , Δg_5^Z , and Δg_6^Z ,
- the HVV couplings $\Delta g_{HVV}^{(4)}$, $\Delta g_{HVV}^{(5)}$, and $\Delta g_{HVV}^{(6)}$,
- the VVVV couplings $\Delta g_{ZZ}^{(1)}$, and $\Delta g_{\gamma Z}^{(5)}$,

with the quartic kinetic energy coupling for non-linear EWSB scenarios $\mathcal{P}_{\square h}$ contributing only to $\Delta g_{ZZ}^{(1)}$ among the above. $\Delta g_{\gamma\gamma}^{(3)}$ does not receive contributions from $d = 6$ linear operators, but it is induced by three-level SM effects. The experimental search of that ensemble of couplings, with the correlations among them following from tables 5, 6 and 7, constitute a fascinating window into chiral dynamics associated to the Higgs particle.

Open Access. This article is distributed under the terms of the Creative Commons Attribution License ([CC-BY 4.0](https://creativecommons.org/licenses/by/4.0/)), which permits any use, distribution and reproduction in any medium, provided the original author(s) and source are credited.

References

- [1] T.D. Lee and G.C. Wick, *Finite theory of quantum electrodynamics*, *Phys. Rev. D* **2** (1970) 1033 [[INSPIRE](#)].
- [2] T.D. Lee and G.C. Wick, *Negative metric and the unitarity of the S matrix*, *Nucl. Phys. B* **9** (1969) 209 [[INSPIRE](#)].
- [3] B. Grinstein, D. O’Connell and M.B. Wise, *The Lee-Wick standard model*, *Phys. Rev. D* **77** (2008) 025012 [[arXiv:0704.1845](#)] [[INSPIRE](#)].
- [4] J.R. Espinosa and B. Grinstein, *Ultraviolet properties of the Higgs sector in the Lee-Wick standard model*, *Phys. Rev. D* **83** (2011) 075019 [[arXiv:1101.5538](#)] [[INSPIRE](#)].
- [5] R.E. Cutkosky, P.V. Landshoff, D.I. Olive and J.C. Polkinghorne, *A non-analytic S matrix*, *Nucl. Phys. B* **12** (1969) 281 [[INSPIRE](#)].
- [6] S. Coleman, *Acausality*, in *Erice 1969, Ettore Majorana school on subnuclear phenomena*, A. Zichichi ed., Academic Press, New York U.S.A. (1970).
- [7] T.D. Lee and G.C. Wick, *Questions of Lorentz invariance in field theories with indefinite metric*, *Phys. Rev. D* **3** (1971) 1046 [[INSPIRE](#)].
- [8] N. Nakanishi, *Lorentz noninvariance of the complex-ghost relativistic field theory*, *Phys. Rev. D* **3** (1971) 811 [[INSPIRE](#)].
- [9] W. Buchmüller and D. Wyler, *Effective Lagrangian analysis of new interactions and flavor conservation*, *Nucl. Phys. B* **268** (1986) 621 [[INSPIRE](#)].
- [10] B. Grzadkowski, M. Iskrzynski, M. Misiak and J. Rosiek, *Dimension-six terms in the standard model lagrangian*, *JHEP* **10** (2010) 085 [[arXiv:1008.4884](#)] [[INSPIRE](#)].
- [11] K. Hagiwara, S. Ishihara, R. Szalapski and D. Zeppenfeld, *Low-energy effects of new interactions in the electroweak boson sector*, *Phys. Rev. D* **48** (1993) 2182 [[INSPIRE](#)].
- [12] J. Bagger et al., *The strongly interacting W W system: gold plated modes*, *Phys. Rev. D* **49** (1994) 1246 [[hep-ph/9306256](#)] [[INSPIRE](#)].
- [13] V. Koulovassilopoulos and R.S. Chivukula, *The phenomenology of a nonstandard Higgs boson in $W_L W_L$ scattering*, *Phys. Rev. D* **50** (1994) 3218 [[hep-ph/9312317](#)] [[INSPIRE](#)].
- [14] C.P. Burgess, J. Matias and M. Pospelov, *A Higgs or not a Higgs? What to do if you discover a new scalar particle*, *Int. J. Mod. Phys. A* **17** (2002) 1841 [[hep-ph/9912459](#)] [[INSPIRE](#)].
- [15] B. Grinstein and M. Trott, *A Higgs-Higgs bound state due to new physics at a TeV*, *Phys. Rev. D* **76** (2007) 073002 [[arXiv:0704.1505](#)] [[INSPIRE](#)].
- [16] A. Azatov, R. Contino and J. Galloway, *Model-independent bounds on a light Higgs*, *JHEP* **04** (2012) 127 [Erratum *ibid.* **1304** (2013) 140] [[arXiv:1202.3415](#)] [[INSPIRE](#)].
- [17] R. Alonso, M.B. Gavela, L. Merlo, S. Rigolin and J. Yepes, *The effective chiral lagrangian for a light dynamical “Higgs particle”*, *Phys. Lett. B* **722** (2013) 330 [Erratum *ibid.* **B 726** (2013) 926] [[arXiv:1212.3305](#)] [[INSPIRE](#)].
- [18] R. Alonso, M.B. Gavela, L. Merlo, S. Rigolin and J. Yepes, *Flavor with a light dynamical “Higgs particle”*, *Phys. Rev. D* **87** (2013) 055019 [[arXiv:1212.3307](#)] [[INSPIRE](#)].

- [19] G. Buchalla, O. Catà and C. Krause, *Complete electroweak chiral lagrangian with a light Higgs at NLO*, *Nucl. Phys. B* **880** (2014) 552 [[arXiv:1307.5017](#)] [[INSPIRE](#)].
- [20] I. Brivio et al., *Disentangling a dynamical Higgs*, *JHEP* **03** (2014) 024 [[arXiv:1311.1823](#)] [[INSPIRE](#)].
- [21] E. Alvarez, L. Da Rold, C. Schat and A. Szyrkman, *Electroweak precision constraints on the Lee-Wick standard model*, *JHEP* **04** (2008) 026 [[arXiv:0802.1061](#)] [[INSPIRE](#)].
- [22] C.D. Carone, R. Ramos and M. Sher, *LHC constraints on the Lee-Wick Higgs sector*, *Phys. Lett. B* **732** (2014) 122 [[arXiv:1403.0011](#)] [[INSPIRE](#)].
- [23] PARTICLE DATA GROUP collaboration, J. Beringer et al., *Review of particle physics*, *Phys. Rev. D* **86** (2012) 010001 [[INSPIRE](#)].
- [24] ATLAS collaboration, *Measurements of Higgs boson production and couplings in diboson final states with the ATLAS detector at the LHC*, *Phys. Lett. B* **726** (2013) 88 [[arXiv:1307.1427](#)] [[INSPIRE](#)].
- [25] CMS collaboration, *Observation of a new boson with mass near 125 GeV in pp collisions at $\sqrt{s} = 7$ and 8 TeV*, *JHEP* **06** (2013) 081 [[arXiv:1303.4571](#)] [[INSPIRE](#)].
- [26] A. Efrati and Y. Nir, *What if $\lambda_{hhh} \neq 3m_h^2/v$* , [arXiv:1401.0935](#) [[INSPIRE](#)].
- [27] J.R. Espinosa, C. Grojean, M. Muhlleitner and M. Trott, *First glimpses at Higgs' face*, *JHEP* **12** (2012) 045 [[arXiv:1207.1717](#)] [[INSPIRE](#)].
- [28] T. Plehn and M. Rauch, *Higgs couplings after the discovery*, *Europhys. Lett.* **100** (2012) 11002 [[arXiv:1207.6108](#)] [[INSPIRE](#)].
- [29] T. Corbett, O.J.P. Éboli, J. Gonzalez-Fraile and M.C. Gonzalez-García, *Robust determination of the Higgs couplings: power to the data*, *Phys. Rev. D* **87** (2013) 015022 [[arXiv:1211.4580](#)] [[INSPIRE](#)].
- [30] T.G. Rizzo, *Searching for Lee-Wick gauge bosons at the LHC*, *JHEP* **06** (2007) 070 [[arXiv:0704.3458](#)] [[INSPIRE](#)].
- [31] T.G. Rizzo, *Unique identification of Lee-Wick gauge bosons at linear colliders*, *JHEP* **01** (2008) 042 [[arXiv:0712.1791](#)] [[INSPIRE](#)].
- [32] T.R. Dulaney and M.B. Wise, *Flavor changing neutral currents in the Lee-Wick standard model*, *Phys. Lett. B* **658** (2008) 230 [[arXiv:0708.0567](#)] [[INSPIRE](#)].
- [33] E. Alvarez, C. Schat, L. Da Rold and A. Szyrkman, *Electroweak precision constraints on the Lee-Wick standard model*, [arXiv:0810.3463](#) [[INSPIRE](#)].
- [34] T.E.J. Underwood and R. Zwicky, *Electroweak precision data and the Lee-Wick standard model*, *Phys. Rev. D* **79** (2009) 035016 [[arXiv:0805.3296](#)] [[INSPIRE](#)].
- [35] C.D. Carone and R.F. Lebed, *Minimal Lee-Wick extension of the standard model*, *Phys. Lett. B* **668** (2008) 221 [[arXiv:0806.4555](#)] [[INSPIRE](#)].
- [36] C.D. Carone and R. Primulando, *Constraints on the Lee-Wick Higgs sector*, *Phys. Rev. D* **80** (2009) 055020 [[arXiv:0908.0342](#)] [[INSPIRE](#)].
- [37] J.S. Gainer, J. Lykken, K.T. Matchev, S. Mrenna and M. Park, *Beyond geolocating: constraining higher dimensional operators in $H \rightarrow 4\ell$ with off-shell production and more*, [arXiv:1403.4951](#) [[INSPIRE](#)].
- [38] C. Englert and M. Spannowsky, *Limitations and opportunities of off-shell coupling measurements*, *Phys. Rev. D* **90** (2014) 053003 [[arXiv:1405.0285](#)] [[INSPIRE](#)].

- [39] J.M. Campbell, R.K. Ellis and C. Williams, *Bounding the Higgs width at the LHC using full analytic results for $gg \rightarrow e^-e^+\mu^-\mu^+$* , *JHEP* **04** (2014) 060 [[arXiv:1311.3589](#)] [[INSPIRE](#)].
- [40] A. Brunstein, O.J.P. Éboli and M.C. Gonzalez-García, *Constraints on quartic vector boson interactions from Z physics*, *Phys. Lett. B* **375** (1996) 233 [[hep-ph/9602264](#)] [[INSPIRE](#)].
- [41] O.J.P. Éboli, M.C. Gonzalez-García and J.K. Mizukoshi, *$pp \rightarrow jje^\pm\mu^\pm\nu\nu$ and $jje^\pm\mu^\pm\nu\nu$ at $O(\alpha_{\text{em}}^6)$ and $O(\alpha_{\text{em}}^4\alpha_s^2)$ for the study of the quartic electroweak gauge boson vertex at CERN LHC*, *Phys. Rev. D* **74** (2006) 073005 [[hep-ph/0606118](#)] [[INSPIRE](#)].

Sigma decomposition

This Chapter contains the publication in Ref. [30] This is a purely theoretical work that aims at clarifying the low energy impact of specific composite Higgs models: the original $SU(5)/SO(5)$ Georgi-Kaplan model [90], the minimal custodial-preserving $SO(5)/SO(4)$ [92] model and the minimal $SU(3)/(SU(2) \times U(1))$ model, which intrinsically breaks custodial symmetry.

To this aim, the general CCWZ description of non-linearly realized symmetries is employed for constructing the most general chiral effective Lagrangian for a symmetric coset \mathcal{G}/\mathcal{H} , which in the energy regime between the breaking of the global symmetry \mathcal{G} into the subgroup $\mathcal{H} \supseteq SU(2) \times U(1)$ and the EW symmetry breaking (*i.e.* roughly at $\Lambda_s \geq E \geq f$). It turns out, that, restricting to the bosonic CP-even sector, this Lagrangian contains only up to 10 free operators, listed in Sec. 3.3 of this chapter. This number may even be reduced for specific choices of the groups \mathcal{G} and \mathcal{H} due to relations among the generators. For example, in the models $SU(5)/SO(5)$ and $SU(5)/SO(4)$ only 8 among the 10 invariants constructed are independent, while in the case $SU(3)/(SU(2) \times U(1))$ there are 9 free parameters.

At low energy, *i.e.* after EWSB, the impact of any of the considered composite Higgs models, irrespective of the chosen symmetric coset \mathcal{G}/\mathcal{H} , can always be described in terms of the 33 effective operators of Refs. [25, 28], whose couplings shall have strong model-dependent constraints, as they are written in terms of only 8 or 9 free parameters. In Sec. 7 of this chapter the high-energy electroweak effective theory is explicitly projected onto the low-energy Lagrangian: this analysis allows to confirm the completeness of the low-energy basis of Refs. [25, 28] and to verify that the weights in powers of ξ that had been assigned artificially to each operator indeed match the dependence that arises naturally in composite Higgs models.

It is worth pointing out that, in all the models considered, the Higgs boson is part of a high-energy $SU(2)$ doublet embedded in a representation of the larger group \mathcal{G} . This ensures that, for vertices with a fixed number of external Higgs legs, the gauge couplings combine with the same relative weights as in the case of the $d = 6$ linear effective Lagrangian. Moreover, the low-energy projection is such that it reproduces exactly the linear expansion in the limit $\xi \rightarrow 0$. On the other hand, the couplings of the physical Higgs result encoded in structures $\mathcal{F}(h)$ that have trigonometric structures, rather than reproducing the $(v + h)$ dependence typical of the linear scenarios. The latter is recovered only in the limit $\xi \rightarrow 0$. A most striking result obtained in this work is the universality of the functions $\mathcal{F}(h)$, that turn out to be basically identical for the three models considered. As can be seen from Tables 1 and 2, they differ at most by a rescaling of f .

Sigma decomposition

R. Alonso,^a I. Brivio,^b M.B. Gavela,^b L. Merlo^b and S. Rigolin^c

^a*Department of Physics, University of California at San Diego,
9500 Gilman Drive, La Jolla, CA 92093-0319, U.S.A.*

^b*Departamento de Física Teórica and Instituto de Física Teórica, IFT-UAM/CSIC,
Universidad Autónoma de Madrid,
Cantoblanco, 28049, Madrid, Spain*

^c*Dipartimento di Fisica “G. Galilei”, Università di Padova and INFN, Sezione di Padova,
Via Marzolo 8, I-35131 Padua, Italy*

E-mail: ralonsod@ucsd.edu, ilaria.brivio@uam.es, belen.gavela@uam.es,
luca.merlo@uam.es, stefano.rigolin@pd.infn.it

ABSTRACT: In composite Higgs models the Higgs is a pseudo-Goldstone boson of a high-energy strong dynamics. We have constructed the effective chiral Lagrangian for a generic symmetric coset, restricting to CP-even bosonic operators up to four momenta which turn out to depend on seven parameters, aside from kinetic terms. Once the same sources of custodial symmetry breaking as in the Standard Model are considered, the total number of operators in the basis increases up to ten, again aside from kinetic terms. Under these assumptions, we have then particularised the discussion to three distinct frameworks: the original $SU(5)/SO(5)$ Georgi-Kaplan model, the minimal custodial-preserving $SO(5)/SO(4)$ model and the minimal $SU(3)/(SU(2) \times U(1))$ model, which intrinsically breaks custodial symmetry. The projection of the high-energy electroweak effective theory into the bosonic sector of the Standard Model is shown to match the low-energy chiral effective Lagrangian for a dynamical Higgs, and it uncovers strong relations between the operator coefficients. Finally, the relation with the bosonic basis of operators describing linear realisations of electroweak symmetry breaking is clarified.

KEYWORDS: Higgs Physics, Chiral Lagrangians, Technicolor and Composite Models

ARXIV EPRINT: [1409.1589](https://arxiv.org/abs/1409.1589)

Contents

1	Introduction	2
2	Electroweak low-energy effective chiral Lagrangian	4
3	Effective chiral Lagrangian for symmetric cosets	7
3.1	Non-linear realisations of the \mathcal{G}/\mathcal{H} symmetry breaking	7
3.2	Basis of independent operators	9
3.3	General EW effective Lagrangian for a symmetric \mathcal{G}/\mathcal{H} coset	10
4	The $SU(5)/SO(5)$ composite Higgs model	12
4.1	Spontaneous $SU(5)/SO(5)$ symmetry breaking setup	12
4.2	The low-energy effective EW chiral Lagrangian	14
4.2.1	The two-derivative low-energy projection	14
4.2.2	The four-derivative low-energy projection	15
5	The minimal $SO(5)/SO(4)$ composite Higgs model	16
5.1	Spontaneous $SO(5)/SO(4)$ symmetry breaking setup	16
5.2	The low-energy effective EW chiral Lagrangian	18
6	The $SU(3)/(SU(2) \times U(1))$ composite Higgs model	18
6.1	Spontaneous $SU(3)/(SU(2) \times U(1))$ symmetry breaking setup	18
6.2	The low-energy effective EW chiral Lagrangian	19
6.2.1	The two-derivative low-energy projection	19
6.2.2	The four-derivative low-energy projection	20
7	Matching the high- and the low-energy Lagrangians	21
7.1	The $SU(5)/SO(5)$ and $SO(5)/SO(4)$ models	21
7.2	The $SU(3)/(SU(2) \times U(1))$ model	23
7.3	The $\xi \ll 1$ limit and the linear effective Lagrangian	24
8	Conclusions	26
A	The Ω-representation	29
A.1	The high-energy effective chiral Lagrangian	29
A.2	$SO(5)/SO(4)$ model in the Ω -representation by refs. [49,57]	31
A.3	Comparison with the basis in ref. [49]	34

1 Introduction

A new resonance with mass around 125 GeV has been firmly established at LHC [1, 2]. Current data do not indicate deviations from the hypothesis of the Standard Model (SM) Higgs particle [3–5] being a component of the $SU(2)_L$ scalar boson doublet of the electroweak (EW) gauge symmetry. Moreover, even after the LHC 14 TeV upgrade, in the absence of exotic resonances it will not be possible to convincingly establish neither the nature of electroweak symmetry breaking (EWSB), nor the mechanism that protects the Higgs mass from large quadratic corrections.

To stabilise the Higgs mass and cure the electroweak hierarchy problem, two main frameworks for beyond the Standard Model (BSM) physics are commonly considered and still viable with the present data: the underlying high-energy dynamics could be either weakly or strongly interacting. In the first case, the EWSB mechanism is linearly realised, as in the SM, with the physical Higgs being an elementary particle. Even if this possibility is more familiar, the existence of an elementary scalar state would represent a surprising exception, as all known examples of scalar states in nature are understood as being composite. This is indeed the philosophy of the second scenario, in which the EWSB is non-linearly realised and the Higgs arises as a composite particle from the strong dynamics sector.

The idea of a light composite Higgs originating in the context of a strongly interacting dynamics was first developed in the 1980s [6–11] and underwent a recent revival of interest either in strong interacting 4D models [12, 13] or in 5D Ads/CFT versions [14–17]. In this framework, a global symmetry group \mathcal{G} is postulated at high energies and broken spontaneously by some strong dynamics mechanism to a subgroup \mathcal{H} at a scale Λ_s . The characteristic scale of the corresponding Goldstone boson (GB) sector is usually denoted by f and satisfies the relation $\Lambda_s \leq 4\pi f$ [18]. Among this set of GBs, three are usually identified with the would-be-longitudinal components of the SM gauge bosons and one with the Higgs field, φ . Subsequently, a scalar potential for the Higgs field is dynamically generated, inducing EWSB and providing a (light) mass to the Higgs particle. Being the Higgs a pseudo-GB arising from the global symmetry breaking, its mass is protected against quantum corrections of the high-energy symmetric theory, providing an elegant solution to the EW hierarchy problem (see for example ref. [19] for a recent review). The EWSB scale, identified with the vacuum expectation value (vev) of the Higgs field $\langle\varphi\rangle$ does not need to coincide with the EW scale v defined by the EW gauge boson masses, i.e. the W mass $m_W = gv/2$. On the other side, $\langle\varphi\rangle$ is typically predicted in any specific composite Higgs (CH) model to obey a constraint linking it to the EW scale v and to the GB scale f . A model-dependent coefficient for the ratio between the strong dynamics scale and the EW sector scale is usually introduced,

$$\xi \equiv (v/f)^2, \quad (1.1)$$

and it quantifies the degree of non-linearity of the theory. If the Higgs particle is embedded as an EW doublet in a representation of the high-energy group, in the limit $\xi \ll 1$ the construction converges to the corresponding linear realisations of EWSB for most of the operators, except for few structures connected to the Goldstone boson nature of h .

A general feature of these CH scenarios is the presence of exotic resonances lighter than about 1.5 TeV that mainly interact with the third family of quarks [20–27]. At present, however, direct searches at collider of these states are inconclusive. On the other side, indirect studies are viable strategies to shed some light on BSM physics. Low-energy effects of new physics (NP) can be described in a model-independent way via an effective field theory approach, with effective operators written in terms of SM fields and invariant under the SM symmetries. When considering non-linearly realised EWSB and restricting only to the pure gauge sector, i.e. decoupling the Higgs particle from the theory, the most general effective Lagrangian, describing gauge and GB interactions and with an expansion up to four momenta, is the so-called Appelquist-Longhitano-Feruglio (ALF) basis, introduced in refs. [28–32]. The first attempts of embedding a light Higgs particle in this context have been proposed in refs. [33–35]. Subsequently, the complete basis of pure-gauge and gauge-Higgs interactions, that extends the ALF basis including a light Higgs particle, has been presented in refs. [36, 37].¹

The effective chiral Lagrangian described in refs. [36, 37] represents a fundamental tool for Higgs analyses at colliders and the related phenomenology has been studied in refs. [37, 42, 43], mainly focusing on disentangling a composite Higgs from an elementary one, via the analysis of its couplings. Promising discriminating signals include the decorrelation, in the case of non-linear EWSB, of signals expected to be correlated within a given pattern in the linearly realised one, i.e. between some pure-gauge couplings versus gauge-Higgs ones and also between specific couplings with the same number of external Higgs legs (see also refs. [35, 44] for the latter type of decorrelations); furthermore, anomalous signals expected at first order in the non-linear realisation may appear only at higher orders of the linear one, and vice versa.

In this paper, the focus is on the connection between the high-energy (i.e. above the GB scale f) effective chiral Lagrangian of specific CH realisations and the low-energy (i.e. below f) effective chiral Lagrangian for a dynamical Higgs derived in ref. [36], restricting to the CP-even bosonic sector. Because of predictivity, an important issue on the analysis of generic symmetric cosets \mathcal{G}/\mathcal{H} will be the determination of the number of free parameters in the high-energy theory, which may constrain the freedom of the low-energy one. In particular, three explicit CH realisations will be considered in the following: the original $SU(5)/SO(5)$ Georgi-Kaplan model [10], the minimal intrinsically custodial-preserving $SO(5)/SO(4)$ model [15] and the minimal intrinsically custodial-breaking $SU(3)/(SU(2) \times U(1))$ model. By custodial breaking we mean here sources of breaking other than those resulting from gauging the SM subgroup.

The three models considered exhibit typical features of CH models present in the literature and therefore the results obtained here can be straightforwardly generalised to

¹The fermion sector has been discussed at different levels and with different aims in refs. [38–41]. Moreover, ref. [41] contains some inferred criticisms to the results presented in ref. [36], pointing to some allegedly missing and redundant operators. Nevertheless, one of the authors in ref. [41] agreed in a private communication on the correctness of ref. [36] under the specific assumptions considered there: the list of operators in ref. [36] is a complete basis when only effects that can be described by pure-gauge and gauge- h chiral operators up to four derivatives are considered.

other contractions. It will be shown that the low-energy effects of any of the considered CH models, irrespective of the chosen symmetric coset \mathcal{G}/\mathcal{H} , can always be described in terms of effective operators invariant under the SM symmetry and written in terms of SM gauge bosons and a scalar singlet h , whose couplings have model-dependent constraints. The existence of peculiar patterns in the coefficients of the low-energy effective chiral operators should indeed provide very valuable information when trying to unveil the nature of the EWSB mechanism.

The paper has been organised as follows. Section 2 is devoted to recalling the low-energy effective chiral Lagrangian introduced in ref. [36]. Section 3 contains the high-energy effective chiral Lagrangian, describing the CP-even interactions among SM gauge bosons and the GBs associated to the symmetric coset \mathcal{G}/\mathcal{H} . Only operators with at most four derivatives are retained in the Lagrangian. Furthermore, no source of custodial breaking besides the SM ones is considered. In sections 4, 5 and 6, the low-energy effective EW chiral Lagrangian is then derived from the high-energy one for the $SU(5)/SO(5)$, $SO(5)/SO(4)$ and $SU(3)/(SU(2) \times U(1))$ composite Higgs models. Finally in section 7, the connection with the EW effective linear Lagrangian is also discussed. Conclusions are presented in section 8. Technical details on the construction of the models and on the comparison with the literature are deferred to the appendix.

2 Electroweak low-energy effective chiral Lagrangian

The scalar sector of the SM is gifted with an accidental $SU(2)_L \times SU(2)_R$ global symmetry spontaneously broken to the diagonal component $SU(2)_C$ after the Higgs field gets a non-vanishing vev. The three $SU(2)_L \times SU(2)_R/SU(2)_C$ GBs, can be described at low-energies by a non-linear σ -model using a dimensionless unitary field $\mathbf{U}(x)$. The latter transforms in the bi-doublet representation of the $SU(2)_L \times SU(2)_R$ global group and is defined by

$$\mathbf{U}(x) = e^{i\boldsymbol{\pi}(x)/v}, \quad \mathbf{U}(x) \rightarrow L \mathbf{U}(x) R^\dagger, \quad (2.1)$$

where $\boldsymbol{\pi}(x) = \pi^a(x)\sigma_a$ (with σ_a the usual Pauli matrices) and L, R denoting respectively $SU(2)_{L,R}$ global transformations. Moreover, the covariant derivative of the non-linear field $\mathbf{U}(x)$ can be written as,

$$\mathbf{D}_\mu \mathbf{U}(x) \equiv \partial_\mu \mathbf{U}(x) + ig \mathbf{W}_\mu(x) \mathbf{U}(x) - \frac{ig'}{2} B_\mu(x) \mathbf{U}(x) \sigma_3, \quad (2.2)$$

where $\mathbf{W}_\mu(x) \equiv W_\mu^a(x)\sigma_a/2$. From the non-linear field $\mathbf{U}(x)$ and its covariant derivative $\mathbf{D}_\mu \mathbf{U}(x)$, it is possible to define (pseudo-)scalar and vector chiral fields transforming in the adjoint of $SU(2)_L$ as follows:

$$\begin{aligned} \mathbf{T}(x) &\equiv \mathbf{U}(x) \sigma_3 \mathbf{U}^\dagger(x), & \mathbf{T}(x) &\rightarrow L \mathbf{T}(x) L^\dagger, \\ \mathbf{V}_\mu(x) &\equiv (\mathbf{D}_\mu \mathbf{U}(x)) \mathbf{U}^\dagger(x), & \mathbf{V}_\mu(x) &\rightarrow L \mathbf{V}_\mu(x) L^\dagger. \end{aligned} \quad (2.3)$$

These two fields \mathbf{T} and \mathbf{V}_μ , together with the SM gauge fields W_μ^a and B_μ and their derivatives, would suffice as building blocks to construct the EW effective chiral Lagrangian [28–32], in the absence of a light Higgs in the low-energy spectrum. Performing

an expansion up to four momenta, a complete basis of $SU(2)_L \times U(1)_Y$ invariant CP-even operators — the ALF basis — is composed of eighteen independent operators.

The discovery of a light scalar degree of freedom, corresponding to the SM Higgs particle, implies the necessity of extending the ALF basis. The electroweak chiral effective Lagrangian should now describe also other interactions with a CP-even scalar singlet field h that may (or may not) participate in the EWSB mechanism. The extension of the ALF basis to include a new light scalar degree of freedom in the low-energy chiral Lagrangian (which we will denote by \mathcal{L}_{low} in what follows), has been derived in ref. [36], where the complete set of independent CP-even operators describing pure-gauge and gauge-Higgs interactions, up to four derivatives, has been listed.² For definiteness and later comparison, we report here the full set of operators, organised by their number of derivatives and their custodial character:³

Operators with two derivatives

Custodial preserving	Custodial breaking	
$\mathcal{P}_C = -\frac{v^2}{4} \text{Tr}(\mathbf{V}^\mu \mathbf{V}_\mu)$	$\mathcal{P}_T = \frac{v^2}{4} \text{Tr}(\mathbf{T} \mathbf{V}_\mu) \text{Tr}(\mathbf{T} \mathbf{V}^\mu)$	(2.4)

Operators with four derivatives

Custodial preserving	Custodial breaking	
$\mathcal{P}_B = -\frac{1}{4} B_{\mu\nu} B^{\mu\nu}$	$\mathcal{P}_{12} = g^2 (\text{Tr}(\mathbf{T} \mathbf{W}_{\mu\nu}))^2$	
$\mathcal{P}_W = -\frac{1}{2} \text{Tr}(\mathbf{W}_{\mu\nu} \mathbf{W}^{\mu\nu})$	$\mathcal{P}_{13} = ig \text{Tr}(\mathbf{T} \mathbf{W}_{\mu\nu}) \text{Tr}(\mathbf{T} [\mathbf{V}^\mu, \mathbf{V}^\nu])$	
$\mathcal{P}_1 = gg' B_{\mu\nu} \text{Tr}(\mathbf{T} \mathbf{W}^{\mu\nu})$	$\mathcal{P}_{14} = g \epsilon_{\mu\nu\rho\lambda} \text{Tr}(\mathbf{T} \mathbf{V}^\mu) \text{Tr}(\mathbf{V}^\nu \mathbf{W}^{\rho\lambda})$	
$\mathcal{P}_2 = ig' B_{\mu\nu} \text{Tr}(\mathbf{T} [\mathbf{V}^\mu, \mathbf{V}^\nu])$	$\mathcal{P}_{15} = \text{Tr}(\mathbf{T} \mathcal{D}_\mu \mathbf{V}^\mu) \text{Tr}(\mathbf{T} \mathcal{D}_\nu \mathbf{V}^\nu)$	
$\mathcal{P}_3 = ig \text{Tr}(\mathbf{W}_{\mu\nu} [\mathbf{V}^\mu, \mathbf{V}^\nu])$	$\mathcal{P}_{16} = \text{Tr}([\mathbf{T}, \mathbf{V}_\nu] \mathcal{D}_\mu \mathbf{V}^\mu) \text{Tr}(\mathbf{T} \mathbf{V}^\nu)$	
$\mathcal{P}_4 = ig' B_{\mu\nu} \text{Tr}(\mathbf{T} \mathbf{V}^\mu) \partial^\nu (h/v)$	$\mathcal{P}_{17} = ig \text{Tr}(\mathbf{T} \mathbf{W}_{\mu\nu}) \text{Tr}(\mathbf{T} \mathbf{V}^\mu) \partial^\nu (h/v)$	
$\mathcal{P}_5 = ig \text{Tr}(\mathbf{W}_{\mu\nu} \mathbf{V}^\mu) \partial^\nu (h/v)$	$\mathcal{P}_{18} = \text{Tr}(\mathbf{T} [\mathbf{V}_\mu, \mathbf{V}_\nu]) \text{Tr}(\mathbf{T} \mathbf{V}^\mu) \partial^\nu (h/v)$	
$\mathcal{P}_6 = (\text{Tr}(\mathbf{V}_\mu \mathbf{V}^\mu))^2$	$\mathcal{P}_{19} = \text{Tr}(\mathbf{T} \mathcal{D}_\mu \mathbf{V}^\mu) \text{Tr}(\mathbf{T} \mathbf{V}_\nu) \partial^\nu (h/v)$	
$\mathcal{P}_7 = \text{Tr}(\mathbf{V}_\mu \mathbf{V}^\mu) \partial_\nu \partial^\nu (h/v)$	$\mathcal{P}_{21} = (\text{Tr}(\mathbf{T} \mathbf{V}_\mu))^2 \partial_\nu (h/v) \partial^\nu (h/v)$	
$\mathcal{P}_8 = \text{Tr}(\mathbf{V}_\mu \mathbf{V}_\nu) \partial^\mu (h/v) \partial^\nu (h/v)$	$\mathcal{P}_{22} = \text{Tr}(\mathbf{T} \mathbf{V}_\mu) \text{Tr}(\mathbf{T} \mathbf{V}_\nu) \partial^\mu (h/v) \partial^\nu (h/v)$	
$\mathcal{P}_9 = \text{Tr}((\mathcal{D}_\mu \mathbf{V}^\mu)^2)$	$\mathcal{P}_{23} = \text{Tr}(\mathbf{V}_\mu \mathbf{V}^\mu) (\text{Tr}(\mathbf{T} \mathbf{V}_\nu))^2$	
$\mathcal{P}_{10} = \text{Tr}(\mathbf{V}_\nu \mathcal{D}_\mu \mathbf{V}^\mu) \partial^\nu (h/v)$	$\mathcal{P}_{24} = \text{Tr}(\mathbf{V}_\mu \mathbf{V}_\nu) \text{Tr}(\mathbf{T} \mathbf{V}^\mu) \text{Tr}(\mathbf{T} \mathbf{V}^\nu)$	
$\mathcal{P}_{11} = (\text{Tr}(\mathbf{V}_\mu \mathbf{V}_\nu))^2$	$\mathcal{P}_{25} = (\text{Tr}(\mathbf{T} \mathbf{V}_\mu))^2 \partial_\nu \partial^\nu (h/v)$	
$\mathcal{P}_{20} = \text{Tr}(\mathbf{V}_\mu \mathbf{V}^\mu) \partial_\nu (h/v) \partial^\nu (h/v)$	$\mathcal{P}_{26} = (\text{Tr}(\mathbf{T} \mathbf{V}_\mu) \text{Tr}(\mathbf{T} \mathbf{V}_\nu))^2$	(2.5)

²The complete set of CP-odd operators describing pure-gauge and gauge-Higgs interactions has been presented in ref. [37]. Chiral interactions including fermions have been considered in [39–41, 45].

³The set of pure-gauge and gauge-Higgs operators in eqs. (2.4) and (2.5) exactly matches that in ref. [36]; nevertheless, the labelling of some operators here is different with respect to that in ref. [36] and matches that in ref. [42] instead.

In eqs. (2.4) and (2.5), the operators have been classified according to their custodial character: those on the right column, indicated as “custodial breaking”, describe tree-level effects of custodial breaking sources beyond the SM (gauge) ones. All these operators are easily identified by the presence of the scalar chiral field $\mathbf{T}(x)$ not in association with the $B_{\mu\nu}$ field strength. The ALF basis can simply be obtained from eqs. (2.4) and (2.5), disregarding all the operators containing derivatives of h . In eq. (2.5), \mathcal{D}_μ denotes the covariant derivative in the adjoint representation of $SU(2)_L$, i.e.

$$\mathcal{D}_\mu \mathbf{V}_\nu \equiv \partial_\mu \mathbf{V}_\nu + i g [\mathbf{W}_\mu, \mathbf{V}_\nu] . \quad (2.6)$$

To fully encompass the h sector, this list should be extended by a set of four pure- h operators:

Operators with two derivatives

$$\mathcal{P}_H = \frac{1}{2} (\partial_\mu h)^2 . \quad (2.7)$$

Operators with four derivatives

$$\begin{aligned} \mathcal{P}_{\square H} &= \frac{1}{v^2} (\partial_\mu \partial^\mu h)^2 , & \mathcal{P}_{\Delta H} &= \frac{1}{v^3} (\partial_\mu h)^2 \square h , \\ \mathcal{P}_{DH} &= \frac{1}{v^4} ((\partial_\mu h)(\partial^\mu h))^2 . \end{aligned} \quad (2.8)$$

In summary, the low-energy electroweak chiral Lagrangian describing the CP-even gauge-Goldstone and the gauge-scalar interactions can thus be written as

$$\mathcal{L}_{\text{low}} = \mathcal{L}_{\text{low}}^{p^2} + \mathcal{L}_{\text{low}}^{p^4} , \quad (2.9)$$

where $\mathcal{L}_{\text{low}}^{p^2}$ and $\mathcal{L}_{\text{low}}^{p^4}$ contain two and four-derivative operators,

$$\begin{aligned} \mathcal{L}_{\text{low}}^{p^2} &= \mathcal{P}_C \mathcal{F}_C(h) + c_T \mathcal{P}_T \mathcal{F}_T(h) + \mathcal{P}_H \mathcal{F}_H(h) , \\ \mathcal{L}_{\text{low}}^{p^4} &= \mathcal{P}_B \mathcal{F}_B(h) + \mathcal{P}_W \mathcal{F}_W(h) + \sum_{i=1}^{26} c_i \mathcal{P}_i \mathcal{F}_i(h) + \\ &\quad + c_{\square H} \mathcal{P}_{\square H} \mathcal{F}_{\square H}(h) + c_{\Delta H} \mathcal{P}_{\Delta H} \mathcal{F}_{\Delta H}(h) + c_{DH} \mathcal{P}_{DH} \mathcal{F}_{DH}(h) , \end{aligned} \quad (2.10)$$

with the functions $\mathcal{F}_i(h)$ encoding a generic dependence on h (in particular, no derivatives of h are included in $\mathcal{F}_i(h)$).

The effective Lagrangian in eq. (2.9) describes at low-energy (EW scale v) any model with a light CP-even Higgs, focusing only on the bosonic sector and restricting to CP-even operators with at most four derivatives. Indeed, \mathcal{L}_{low} describes an extended class of “Higgs” models, ranging from the SM scenario to technicolor-like ansatzs and intermediate situations such as dilaton-like scalar frameworks and CH models.

Notice that here, for later convenience, a slightly different notation is adopted with respect to that in refs. [36, 42] for the definition of the $\mathcal{F}_i(h)$ functions. Here the $\mathcal{F}_i(h)$ functions are not part of the definition of the operators \mathcal{P}_i , but instead are left outside as

multiplicative terms in the Lagrangian. The only dependence on h left inside the operators \mathcal{P}_i is that corresponding to derivatives of h . Furthermore, in refs. [36, 42] the dependence on the parameter ξ was made explicit at the Lagrangian level in order to show the connection with the linear effective Lagrangian. Here instead, the ξ weights are reabsorbed in the coefficients c_i and in the functions $\mathcal{F}_i(h)$. The role of ξ will become clear in the following sections, once specific dynamical Higgs models will be considered.

According to NDA [18, 46], the weight in front of each four-derivative operator is estimated to be $f^2/\Lambda_s^2 \gtrsim 1/(4\pi)^2$. This is true for all terms above even if obscured for those operators in eq. (2.5) which include $\partial(h/v)$: their associated c_i have already absorbed a dependence on ξ , as mentioned above. To illustrate this, let us consider the example of \mathcal{P}_5 : on physics grounds, factors of h are expected to enter the operators weighted down by f , which is the associated Goldstone boson scale, and the “natural” definition of the operator would have been

$$\mathcal{P}_5 = ig \text{Tr}(\mathbf{W}_{\mu\nu} \mathbf{V}^\mu) \partial^\nu(h/f), \quad (2.11)$$

for whose coefficient NDA would indicate a f^2/Λ_s^2 weight. Now, the operator definition chosen with $\partial^\nu(h/v)$ instead of $\partial^\nu(h/f)$, implies that c_5 has already been redefined in order to reabsorb a factor of $\sqrt{\xi}$, and the overall weight expected for the coefficient of the \mathcal{P}_5 operator as defined in eq. (2.5) is $c_5 \sim \sqrt{\xi} f^2/\Lambda_s^2 \gtrsim (v/f) \times 1/(4\pi)^2$.

3 Effective chiral Lagrangian for symmetric cosets

This section is dedicated to the construction of the high-energy effective Lagrangian in a generic CH setup: a global symmetry group \mathcal{G} is spontaneously broken by some strong dynamics mechanism at the scale Λ_s , to a subgroup \mathcal{H} , such that the coset \mathcal{G}/\mathcal{H} is symmetric; the minimum requisite is that $\dim(\mathcal{G}/\mathcal{H}) \geq 4$, i.e. at least four GBs arise from the global symmetry breaking, such that three of them would be then identified with the longitudinal components of the SM gauge bosons and one with the light scalar resonance observed at LHC. No fermionic operators will be considered, and only CP-even ones will be retained among the set of bosonic operators, up to four derivatives.

This generic effective chiral Lagrangian for symmetric cosets will be applied in the subsequent sections to specific CH models.

3.1 Non-linear realisations of the \mathcal{G}/\mathcal{H} symmetry breaking

Following the general CCWZ construction [47, 48], the GB degrees of freedom arising from the global symmetry breaking of the group \mathcal{G} down to the subgroup \mathcal{H} can be described by the field $\Omega(x)$:

$$\Omega(x) \equiv e^{i\Xi(x)/2f}, \quad (3.1)$$

transforming under the global groups \mathcal{G} and \mathcal{H} as⁴

$$\Omega(x) \rightarrow \mathbf{g} \Omega(x) \mathbf{h}^{-1}(\Xi, \mathbf{g}), \quad (3.2)$$

⁴Depending on whether the group $\text{SU}(N)$ or $\text{SO}(N)$ is considered, $\mathbf{h}^{-1} = \mathbf{h}^\dagger$ or $\mathbf{h}^{-1} = \mathbf{h}^T$ should be used, respectively.

where \mathfrak{g} is a (global) element of \mathcal{G} while $\mathfrak{h}(\Xi, \mathfrak{g})$ is a (local) element of \mathcal{H} depending explicitly on \mathfrak{g} and on the Goldstone boson field $\Xi(x)$. For the sake of brevity, in what follows it will be understood $\mathfrak{h} \equiv \mathfrak{h}(\Xi, \mathfrak{g})$ unless otherwise stated. Eq. (3.2) defines the non-linear transformation of $\Xi(x)$. Denoting by T_a (with $a = 1, \dots, \dim(\mathcal{H})$) the generators of \mathcal{H} and by $X_{\hat{a}}$ (with $\hat{a} = 1, \dots, \dim(\mathcal{G}/\mathcal{H})$) the generators of the coset \mathcal{G}/\mathcal{H} in such a way that $(T_a, X_{\hat{a}})$ form an orthonormal basis of \mathcal{G} , the GB field matrix explicitly reads:

$$\Xi(x) = \Xi^{\hat{a}}(x) X_{\hat{a}}. \quad (3.3)$$

In all realistic models considered in the literature, either in the context of QCD, EW chiral Lagrangian or CH models, the generators satisfy the following schematic conditions:

$$[T, T] \propto T, \quad [T, X] \propto X, \quad [X, X] \propto T, \quad (3.4)$$

the last one being the condition for a symmetric coset.⁵ In other words, a symmetric \mathcal{G}/\mathcal{H} coset admits the automorphism (usually dubbed “grading”) $\mathfrak{g} \rightarrow \mathcal{R}(\mathfrak{g}) = \mathfrak{g}\mathcal{R}$,

$$\mathcal{R}: \quad \begin{cases} T_a \rightarrow +T_a \\ X_{\hat{a}} \rightarrow -X_{\hat{a}} \end{cases} \quad (3.5)$$

consistent with the commutation relations in eq. (3.4). For instance, in the case of chiral groups like $SU(N)_L \times SU(N)_R \rightarrow SU(N)_V$ this grading corresponds to the parity operator that leaves invariant the vector generators, while changing the sign to the axial-vector ones.

As already pointed out in ref. [47], it can be shown that in the presence of such an automorphism the non-linear field transformations of $\Omega(x)$ can also be recast as:

$$\Omega(x) \rightarrow \mathfrak{h} \Omega(x) \mathfrak{g}_{\mathcal{R}}^{-1}. \quad (3.6)$$

From eqs. (3.2) and (3.6), it is thus possible to define for all symmetric cosets a “squared” non-linear field $\Sigma(x)$:

$$\Sigma(x) \equiv \Omega(x)^2, \quad (3.7)$$

transforming under \mathcal{G} as,

$$\Sigma(x) \rightarrow \mathfrak{g} \Sigma(x) \mathfrak{g}_{\mathcal{R}}^{-1}, \quad (3.8)$$

showing explicitly that the transformation on $\Xi(x)$ is a realisation of \mathcal{G} , and that it is linear when restricted to \mathcal{H} . Notice that the GB field matrix $\Sigma(x)$ transforms under the grading \mathcal{R} as:

$$\Sigma(x) \rightarrow \Sigma(x)^{-1}. \quad (3.9)$$

It is then a matter of taste, in a symmetric coset framework, to use $\Omega(x)$ or $\Sigma(x)$ for describing the GBs degrees of freedom and the interactions between the GB fields and the gauge/matter fields. The Ω -representation to derive \mathcal{H} -covariant quantities entering the model Lagrangian has been used in several examples. However, when discussing QCD or

⁵The first condition follows from \mathcal{H} being closed. The second one can be deduced from the first one together with the fact that for compact groups the structure constants are completely antisymmetric.

EW chiral Lagrangians, the Σ -representation has been more often adopted. To make a straightforward comparison with \mathcal{L}_{low} introduced in section 2, the Σ -representation will be kept in the following.

One can introduce the vector chiral field:⁶

$$\tilde{\mathbf{V}}_\mu = (\partial_\mu \Sigma) \Sigma^{-1}, \quad \tilde{\mathbf{V}}_\mu \rightarrow \mathfrak{g} \tilde{\mathbf{V}}_\mu \mathfrak{g}^{-1}, \quad (3.10)$$

transforming in the adjoint of \mathcal{G} . The effective Lagrangian describing the GB interactions in the context of the non-linearly realised \mathcal{G} breaking mechanism, with symmetric coset \mathcal{G}/\mathcal{H} , can then be constructed solely from $\tilde{\mathbf{V}}_\mu$.

In a realistic context, however, gauge interactions should be introduced, and to assign quantum numbers it is convenient to formally gauge the full group \mathcal{G} . In the symmetric coset case, it is possible to define both the \mathcal{G} gauge fields $\tilde{\mathbf{S}}_\mu$, and the graded siblings $\tilde{\mathbf{S}}_\mu^{\mathcal{R}} \equiv \mathcal{R}(\tilde{\mathbf{S}}_\mu)$, transforming under \mathcal{G} , respectively, as:

$$\tilde{\mathbf{S}}_\mu \rightarrow \mathfrak{g} \tilde{\mathbf{S}}_\mu \mathfrak{g}^{-1} - \frac{i}{g_S} \mathfrak{g} (\partial_\mu \mathfrak{g}^{-1}), \quad \tilde{\mathbf{S}}_\mu^{\mathcal{R}} \rightarrow \mathfrak{g} \mathcal{R} \tilde{\mathbf{S}}_\mu^{\mathcal{R}} \mathfrak{g}^{-1} - \frac{i}{g_S} \mathfrak{g} \mathcal{R} (\partial_\mu \mathfrak{g}^{-1}), \quad (3.11)$$

with g_S denoting the associated gauge coupling constant. The (gauged) version of the chiral vector field $\tilde{\mathbf{V}}_\mu$ can then be defined as:

$$\tilde{\mathbf{V}}_\mu = (\mathbf{D}_\mu \Sigma) \Sigma^{-1}, \quad (3.12)$$

with the covariant derivative of the non-linear field $\Sigma(x)$ being,

$$\mathbf{D}_\mu \Sigma = \partial_\mu \Sigma + i g_S (\tilde{\mathbf{S}}_\mu \Sigma - \Sigma \tilde{\mathbf{S}}_\mu^{\mathcal{R}}). \quad (3.13)$$

The following three \mathcal{G} -covariant objects can thus be used as building blocks for the (gauged) effective chiral Lagrangian:

$$\tilde{\mathbf{V}}_\mu, \quad \tilde{\mathbf{S}}_{\mu\nu} \quad \text{and} \quad \Sigma \tilde{\mathbf{S}}_{\mu\nu}^{\mathcal{R}} \Sigma^{-1}. \quad (3.14)$$

The introduction of the graded vector chiral field $\tilde{\mathbf{V}}_\mu^{\mathcal{R}}$ does not add any further independent structure, as indeed

$$\tilde{\mathbf{V}}_\mu^{\mathcal{R}} \equiv \mathcal{R}(\tilde{\mathbf{V}}_\mu) = (\mathbf{D}_\mu \Sigma)^{-1} \Sigma \quad \text{with} \quad \Sigma \tilde{\mathbf{V}}_\mu^{\mathcal{R}} \Sigma^{-1} = -\tilde{\mathbf{V}}_\mu. \quad (3.15)$$

3.2 Basis of independent operators

It is now possible to derive the most general operator basis describing the interactions of the \mathcal{G} gauge fields and of the GBs of a non-linear realisation of the symmetric coset \mathcal{G}/\mathcal{H} . Performing an expansion in momenta and considering CP even operators with at most four derivatives, one obtains the following nine independent operators:

2-momenta operator

$$\text{Tr} \left(\tilde{\mathbf{V}}_\mu \tilde{\mathbf{V}}^\mu \right). \quad (3.16)$$

This operator describes the kinetic terms for the GBs and, once the gauge symmetry is broken, results in masses for those GBs associated to the broken generators.

⁶In order to avoid confusion we will denote with “ \sim ” gauge bosons and chiral fields embedded in \mathcal{G} .

4-momenta operators with explicit gauge field strength $\tilde{\mathbf{S}}_{\mu\nu}$

$$\text{Tr} \left(\tilde{\mathbf{S}}_{\mu\nu} \tilde{\mathbf{S}}^{\mu\nu} \right), \quad \text{Tr} \left(\Sigma \tilde{\mathbf{S}}_{\mu\nu}^R \Sigma^{-1} \tilde{\mathbf{S}}^{\mu\nu} \right), \quad \text{Tr} \left(\tilde{\mathbf{S}}_{\mu\nu} \left[\tilde{\mathbf{V}}^\mu, \tilde{\mathbf{V}}^\nu \right] \right). \quad (3.17)$$

The first operator describes the kinetic terms for the gauge bosons $\tilde{\mathbf{S}}_\mu$. The other two contain gauge-GB and pure-gauge interactions.

4-momenta operators without explicit gauge field strength $\tilde{\mathbf{S}}_{\mu\nu}$

$$\begin{aligned} & \text{Tr} \left(\tilde{\mathbf{V}}_\mu \tilde{\mathbf{V}}^\mu \right) \text{Tr} \left(\tilde{\mathbf{V}}_\nu \tilde{\mathbf{V}}^\nu \right), \quad \text{Tr} \left(\tilde{\mathbf{V}}_\mu \tilde{\mathbf{V}}_\nu \right) \text{Tr} \left(\tilde{\mathbf{V}}^\mu \tilde{\mathbf{V}}^\nu \right), \\ & \text{Tr} \left((\mathcal{D}_\mu \tilde{\mathbf{V}}^\mu)^2 \right), \quad \text{Tr} \left(\tilde{\mathbf{V}}_\mu \tilde{\mathbf{V}}^\mu \tilde{\mathbf{V}}_\nu \tilde{\mathbf{V}}^\nu \right), \quad \text{Tr} \left(\tilde{\mathbf{V}}_\mu \tilde{\mathbf{V}}_\nu \tilde{\mathbf{V}}^\mu \tilde{\mathbf{V}}^\nu \right), \end{aligned} \quad (3.18)$$

where the adjoint covariant derivative acting on $\tilde{\mathbf{V}}^\mu$ is defined as

$$\mathcal{D}_\mu \tilde{\mathbf{V}}^\mu = \partial_\mu \tilde{\mathbf{V}}^\mu + i g_S \left[\tilde{\mathbf{S}}_\mu, \tilde{\mathbf{V}}^\mu \right].$$

The operators listed in eqs. (3.16)–(3.18) represent a complete set of independent structures describing the interactions among \mathcal{G} gauge bosons and the GBs associated to \mathcal{G}/\mathcal{H} in the Σ -representation. Additional Lorentz and \mathcal{G} -invariant structures could be *a priori* considered beyond those in the previous list (aside from those that are trivially not independent). Of particular interest are the operator $\text{Tr}((\mathcal{D}_\mu \tilde{\mathbf{V}}^\mu) \tilde{\mathbf{V}}_\nu \tilde{\mathbf{V}}^\nu)$ and operators containing determinants. However, the first one is not invariant under the grading \mathcal{R} (see eq. (3.15)) and therefore cannot be retained in the previous set of independent operators. Moreover, invariants of the second type are redundant once restricting only to couplings with at most four derivatives: the Cayley-Hamilton theorem to reduce determinants in terms of traces is a useful tool to prove it.

It is worth noticing that in specific \mathcal{G}/\mathcal{H} realisations, some of the operators listed may not be independent. For example the operators with traces of four $\tilde{\mathbf{V}}^\mu$ appearing in the second line of eq. (3.18) are redundant in the case $\mathcal{G} = \text{SU}(2)_L \times \text{SU}(2)_R$ and $\mathcal{H} = \text{SU}(2)_V$, as they decompose in products of traces of two $\tilde{\mathbf{V}}^\mu$. It may not be true in models with larger group \mathcal{G} , as it depends on the specific algebra relations of the generators.

Finally, some caution should be also used when fermions are introduced. In this case all operators containing $\mathcal{D}_\mu \tilde{\mathbf{V}}^\mu$ can be traded, via equations of motion, by operators containing fermions and a careful analysis should be performed to avoid the presence of redundant terms.

3.3 General EW effective Lagrangian for a symmetric \mathcal{G}/\mathcal{H} coset

The list of operators in eqs. (3.16)–(3.18) is valid on general grounds when formally gauging the full group \mathcal{G} . Nevertheless, in most realisations of CH models only the SM gauge group is gauged. Consequently, in the generic gauge field $\tilde{\mathbf{S}}_\mu$, only the EW components should be retained. While no new operator structures appear in the sector made out exclusively of $\tilde{\mathbf{V}}_\mu$ fields (see eqs. (3.16) and (3.18)), all operators where the gauge field strength appears

explicitly, such as those in eq. (3.17), should be “doubled” by substituting $\tilde{\mathbf{S}}_\mu$ either with $\tilde{\mathbf{W}}_\mu$ or $\tilde{\mathbf{B}}_\mu$, defined by

$$\tilde{\mathbf{W}}_\mu \equiv W_\mu^a Q_L^a \quad \text{and} \quad \tilde{\mathbf{B}}_\mu \equiv B_\mu Q_Y, \quad (3.19)$$

where Q_L^a and Q_Y denote the embedding in \mathcal{G} of the $\text{SU}(2)_L \times \text{U}(1)_Y$ generators. It follows that a larger number of invariants can be written in this case. In consequence, the CP-even EW high-energy chiral Lagrangian describing up to four-derivative bosonic interactions, $\mathcal{L}_{\text{high}}$, contains in total thirteen operators:

$$\mathcal{L}_{\text{high}} = \mathcal{L}_{\text{high}}^{p^2} + \mathcal{L}_{\text{high}}^{p^4}, \quad (3.20)$$

where

$$\mathcal{L}_{\text{high}}^{p^2} = \tilde{\mathcal{A}}_C, \quad (3.21)$$

$$\mathcal{L}_{\text{high}}^{p^4} = \tilde{\mathcal{A}}_B + \tilde{\mathcal{A}}_W + \tilde{c}_{B\Sigma} \tilde{\mathcal{A}}_{B\Sigma} + \tilde{c}_{W\Sigma} \tilde{\mathcal{A}}_{W\Sigma} + \sum_{i=1}^8 \tilde{c}_i \tilde{\mathcal{A}}_i, \quad (3.22)$$

with

$$\begin{aligned} \tilde{\mathcal{A}}_C &= -\frac{f^2}{4} \text{Tr} \left(\tilde{\mathbf{V}}_\mu \tilde{\mathbf{V}}^\mu \right), & \tilde{\mathcal{A}}_3 &= i g \text{Tr} \left(\tilde{\mathbf{W}}_{\mu\nu} \left[\tilde{\mathbf{V}}^\mu, \tilde{\mathbf{V}}^\nu \right] \right), \\ \tilde{\mathcal{A}}_B &= -\frac{1}{4} \text{Tr} \left(\tilde{\mathbf{B}}_{\mu\nu} \tilde{\mathbf{B}}^{\mu\nu} \right), & \tilde{\mathcal{A}}_4 &= \text{Tr} \left(\tilde{\mathbf{V}}_\mu \tilde{\mathbf{V}}^\mu \right) \text{Tr} \left(\tilde{\mathbf{V}}_\mu \tilde{\mathbf{V}}^\mu \right), \\ \tilde{\mathcal{A}}_W &= -\frac{1}{4} \text{Tr} \left(\tilde{\mathbf{W}}_{\mu\nu} \tilde{\mathbf{W}}^{\mu\nu} \right), & \tilde{\mathcal{A}}_5 &= \text{Tr} \left(\tilde{\mathbf{V}}_\mu \tilde{\mathbf{V}}_\nu \right) \text{Tr} \left(\tilde{\mathbf{V}}^\mu \tilde{\mathbf{V}}^\nu \right), \\ \tilde{\mathcal{A}}_{B\Sigma} &= g'^2 \text{Tr} \left(\Sigma \tilde{\mathbf{B}}_{\mu\nu} \Sigma^{-1} \tilde{\mathbf{B}}^{\mu\nu} \right), & \tilde{\mathcal{A}}_6 &= \text{Tr} \left((\mathcal{D}_\mu \tilde{\mathbf{V}}^\mu)^2 \right), \\ \tilde{\mathcal{A}}_{W\Sigma} &= g^2 \text{Tr} \left(\Sigma \tilde{\mathbf{W}}_{\mu\nu} \Sigma^{-1} \tilde{\mathbf{W}}^{\mu\nu} \right), & \tilde{\mathcal{A}}_7 &= \text{Tr} \left(\tilde{\mathbf{V}}_\mu \tilde{\mathbf{V}}^\mu \tilde{\mathbf{V}}_\nu \tilde{\mathbf{V}}^\nu \right), \\ \tilde{\mathcal{A}}_1 &= g g' \text{Tr} \left(\Sigma \tilde{\mathbf{B}}_{\mu\nu} \Sigma^{-1} \tilde{\mathbf{W}}^{\mu\nu} \right), & \tilde{\mathcal{A}}_8 &= \text{Tr} \left(\tilde{\mathbf{V}}_\mu \tilde{\mathbf{V}}_\nu \tilde{\mathbf{V}}^\mu \tilde{\mathbf{V}}^\nu \right), \\ \tilde{\mathcal{A}}_2 &= i g' \text{Tr} \left(\tilde{\mathbf{B}}_{\mu\nu} \left[\tilde{\mathbf{V}}^\mu, \tilde{\mathbf{V}}^\nu \right] \right), \end{aligned} \quad (3.23)$$

with the EW covariant derivative in eq. (3.23) defined as

$$\mathcal{D}_\mu \tilde{\mathbf{V}}^\mu = \partial_\mu \tilde{\mathbf{V}}^\mu + i g \left[\tilde{\mathbf{W}}_\mu, \tilde{\mathbf{V}}^\mu \right] + i g' \left[\tilde{\mathbf{B}}_\mu, \tilde{\mathbf{V}}^\mu \right]. \quad (3.24)$$

The coefficients \tilde{c}_i are expected to be all of the same order of magnitude, according to the effective field theory approach.⁷ NDA [18, 46] applies and indicates that the four-derivative operator coefficients are expected to be of order $f^2/\Lambda_s^2 \gtrsim 1/(4\pi)^2$.

It is remarkable that, aside from kinetic terms, $\mathcal{L}_{\text{high}}$ contains only ten independent operators, and thus at most ten arbitrary coefficients \tilde{c}_i need to be determined. They will govern the projection of $\mathcal{L}_{\text{high}}$ into \mathcal{L}_{low} (in addition to the parameter(s) of the explicit breaking of the global symmetry).

⁷The coefficients of the operators $\tilde{\mathcal{A}}_C$, $\tilde{\mathcal{A}}_B$ and $\tilde{\mathcal{A}}_W$ are taken equal to 1, which leads to canonical kinetic terms.

It is also worth to note that the gauging of the SM symmetry breaks explicitly the custodial and the grading symmetries. As a result, custodial and/or grading symmetry breaking operators can arise once quantum corrections induced by SM interactions are considered.

In the case $\mathcal{G} = \text{SU}(2)_L \times \text{SU}(2)_R$ and $\mathcal{H} = \text{SU}(2)_V$, the Lagrangian $\mathcal{L}_{\text{high}}$ reduces to the custodial preserving sector of the ALF basis, with the three GBs described by the non-linear realisation of the EWSB mechanism corresponding to the longitudinal degrees of freedom of the SM gauge bosons. In this case, $\dim(\mathcal{G}/\mathcal{H}) = 3$ and the h field cannot arise as a GB of the spontaneous \mathcal{G} symmetry breaking.

CH models are, instead, built upon cosets with $\dim(\mathcal{G}/\mathcal{H}) \geq 4$, the minimal ones being for example $\text{SO}(5)/\text{SO}(4)$ and $\text{SU}(3)/(\text{SU}(2) \times \text{U}(1))$ for the intrinsically custodial preserving and custodial breaking setups, respectively. The four GBs resulting from the non-linear symmetry breaking mechanism will then correspond to the three would-be SM GBs and the Higgs particle. In non-minimal models, such as the $\text{SU}(5)/\text{SO}(5)$ Georgi-Kaplan model, additional GBs appear in the symmetry breaking sector. Either they are light degrees of freedom and then provide interesting candidates for dark matter (see for instance ref. [49, 50]) or for other exotic particles, or they should become heavy enough through some “ad hoc” global symmetry breaking effect associated to the strong interacting sector [10], leaving a negligible impact on low-energy physics.

In the next sections, $\mathcal{L}_{\text{high}}$ will be particularised to the case of three well-known CH models, by decomposing the field matrix Σ in eq. (3.7) into its SM and BSM fields, and projecting into the former: the title of this paper refers to this procedure.

4 The $\text{SU}(5)/\text{SO}(5)$ composite Higgs model

The first CH model was proposed by Georgi and Kaplan [10] more than 30 years ago. They assumed a global $\mathcal{G} = \text{SU}(5)$ symmetry spontaneously broken to the $\mathcal{H} = \text{SO}(5)$ subgroup. It is clearly a non-minimal model as fourteen GBs arise from the $\text{SU}(5) \rightarrow \text{SO}(5)$ breaking: three of them are then identified with the GBs of the SM, a fourth one with the physical Higgs, while the remaining ten are potentially light states. In ref. [10], it was shown that strong dynamical effects can induce large (i.e. $\mathcal{O}(f)$) masses for these extra degrees of freedom, that therefore can be safely disregarded at low-energies. The discussion of this mechanism is beyond the scope of our paper and can be found in that reference. In what follows all those ten extra GBs are removed from the spectrum and only the three plus one physical degrees of freedom relevant at low energies are considered.

The global $\text{SU}(2)_L \times \text{SU}(2)_R$ symmetry can be embedded in the unbroken $\text{SO}(5)$ residual group and therefore the model benefits of an approximate custodial symmetry. We will first review in some detail the original Georgi-Kaplan construction, as this will be the playground for generic (minimal or non-minimal) CH models.

4.1 Spontaneous $\text{SU}(5)/\text{SO}(5)$ symmetry breaking setup

Mimicking the detailed discussion presented in ref. [11], the spontaneous (global) symmetry breaking pattern $\text{SU}(5) \rightarrow \text{SO}(5)$ can be associated to a scalar field⁸ belonging to the

⁸This scalar field could result for example from fermionic condensates.

symmetric representation of \mathcal{G} and acquiring a vev Δ_0 . The vev can be taken in all generality to be a real, symmetric and orthogonal 5×5 matrix:

$$\Delta_0 = \Delta_0^\dagger = \Delta_0^T = \Delta_0^{-1}. \quad (4.1)$$

A convenient choice, which facilitates the identification of the $SU(2)_L \times U(1)_Y$ quantum numbers in the $SU(5)$ embedding, is given by

$$\Delta_0 = \begin{pmatrix} 0 & i\sigma_2 & 0 \\ -i\sigma_2 & 0 & 0 \\ 0 & 0 & 1 \end{pmatrix}. \quad (4.2)$$

It is then possible to describe the massless excitations around the vacuum with a symmetric field $\Delta(x)$, obtained “rotating” the vacuum by means of the GB non-linear field $\Omega(x)$:

$$\Delta(x) = \Omega(x) \Delta_0 \Omega(x)^T, \quad \Delta(x) \rightarrow \mathbf{g} \Delta(x) \mathbf{g}^T. \quad (4.3)$$

The field $\Delta(x)$ describes all fourteen GBs stemming from the $SU(5)/SO(5)$ breaking. Its transformation properties under $SU(5)$, i.e. in the symmetric representation, follow from the invariance of the vacuum under $SO(5)$. Using the following relations between the vacuum Δ_0 and the broken and unbroken generators,

$$\Delta_0 T_a \Delta_0 = -T_a^T, \quad \Delta_0 X_{\hat{a}} \Delta_0 = X_{\hat{a}}^T, \quad (4.4)$$

and because of the relations in eq. (4.1), the excitations around the vacuum can be rewritten in terms of the GB field $\Sigma(x)$:

$$\Delta(x) = \Omega(x)^2 \Delta_0 \equiv \Sigma(x) \Delta_0. \quad (4.5)$$

The vector chiral field $\tilde{\mathbf{V}}_\mu$ is then related to the vacuum excitations,

$$\tilde{\mathbf{V}}_\mu(x) \equiv (\mathbf{D}_\mu \Sigma(x)) \Sigma^\dagger(x) = (\mathbf{D}_\mu \Delta(x)) \Delta^*(x), \quad (4.6)$$

from which it follows that the GB kinetic term can be written as:

$$\text{Tr}((\mathbf{D}_\mu \Delta)(\mathbf{D}_\mu \Delta)^*) = \text{Tr}((\mathbf{D}_\mu \Sigma)(\mathbf{D}_\mu \Sigma)^\dagger) = -\text{Tr}(\tilde{\mathbf{V}}_\mu \tilde{\mathbf{V}}^\mu). \quad (4.7)$$

Considering the fourteen GBs arising from the $SU(5)/SO(5)$ breaking and described by $\Omega(x)$ (or $\Sigma(x)$), the three would-be SM GBs $\mathcal{X}(x)$ and the scalar singlet field $\varphi(x)$ can be split from the other d.o.f. denoted collectively by $\mathcal{K}(x)$, by decomposing $\Omega(x)$ as [11]:

$$\Omega(x) = e^{i\frac{\varphi(x)}{2f}} e^{i\frac{\mathcal{K}(x)}{2f}}. \quad (4.8)$$

Strong dynamics effects may induce a heavy mass term for the GBs described by $\mathcal{K}(x)$ [10]. The GB field $\Omega(x)$, and $\Sigma(x)$, can then be approximated at energies below f by:

$$\Omega(x) \approx e^{i\frac{\varphi(x)}{2f}} e^{i\frac{\mathcal{K}(x)}{2f}}, \quad \Sigma(x) \approx e^{i\frac{\varphi(x)}{f}} e^{i\frac{\mathcal{K}(x)}{f}}. \quad (4.9)$$

Furthermore, the explicit breaking of the global high-energy symmetry is assumed to induce a potential for the singlet field $\varphi(x)$, which eventually acquires dynamically a non-vanishing vev,

$$\frac{\varphi(x)}{f} \equiv \frac{h(x) + \langle \varphi \rangle}{f} = \left(\frac{h(x) + \langle \varphi \rangle}{v} \right) \sqrt{\xi}, \quad (4.10)$$

where $h(x)$ refers to the physical Higgs (denoted often simply as h in what follows).

Denoting by X the broken generator along which the EW symmetry breaking occurs,

$$X = \frac{1}{2} \begin{pmatrix} 0 & 0 & e_1 \\ 0 & 0 & e_2 \\ e_1^T & e_2^T & 0 \end{pmatrix} \quad \text{with} \quad e_1 = \begin{pmatrix} 1 \\ 0 \end{pmatrix}, \quad e_2 = \begin{pmatrix} 0 \\ 1 \end{pmatrix}, \quad (4.11)$$

the SU(5) embedding of the SM GB fields can be parametrised as

$$\mathcal{X}(x) = \sqrt{2} \begin{pmatrix} \mathbf{U} & & \\ & \mathbf{U} & \\ & & 1 \end{pmatrix} X \begin{pmatrix} \mathbf{U}^\dagger & & \\ & \mathbf{U}^\dagger & \\ & & 1 \end{pmatrix} = \frac{1}{\sqrt{2}} \begin{pmatrix} 0 & 0 & \mathbf{U}(x)e_1 \\ 0 & 0 & \mathbf{U}(x)e_2 \\ (\mathbf{U}(x)e_1)^\dagger & (\mathbf{U}(x)e_2)^\dagger & 0 \end{pmatrix}, \quad (4.12)$$

with $\mathbf{U}(x)$ defined in eq. (2.1). In the unitary gauge, $\mathcal{X} = \sqrt{2}X$. Given the peculiar structure of the matrix X , the Σ field can be written uniquely in terms of linear and quadratic powers of \mathcal{X} because $\mathcal{X}^3 = \mathcal{X}$:

$$\Sigma \equiv \mathbb{1} + i \sin\left(\frac{\varphi}{f}\right) \mathcal{X} + \left(\cos\left(\frac{\varphi}{f}\right) - 1\right) \mathcal{X}^2. \quad (4.13)$$

The last ingredient needed to fully specify the setup is the embedding of the SM fields in \mathcal{G} . Given the choice of vacuum, the SU(2)_L × U(1)_Y generators can be expressed as

$$Q_L^a = \frac{1}{2} \begin{pmatrix} \sigma_a & & \\ & \sigma_a & \\ & & 0 \end{pmatrix}, \quad Q_Y = \frac{1}{2} \begin{pmatrix} -\mathbb{1}_2 & & \\ & \mathbb{1}_2 & \\ & & 0 \end{pmatrix}, \quad (4.14)$$

where in these expressions σ_a denote the Pauli matrices and the normalisation of the generators is $\text{Tr}(Q_a Q_a) = 1$.

4.2 The low-energy effective EW chiral Lagrangian

One can now substitute the explicit expression for Σ , $\tilde{\mathbf{V}}_\mu$, $\tilde{\mathbf{W}}_\mu$ and $\tilde{\mathbf{B}}_\mu$ in the operators of the high-energy basis in eq. (3.23) and obtain \mathcal{L}_{low} for the Georgi-Kaplan model as a function of the SM would-be GBs, the light scalar singlet field $\varphi(x)$ and the SM gauge fields.

4.2.1 The two-derivative low-energy projection

For SU(5)/SO(5), the low-energy projection of the custodial preserving two-derivative operator reads [51]

$$\tilde{\mathcal{A}}_C \equiv -\frac{f^2}{4} \text{Tr}(\tilde{\mathbf{V}}_\mu \tilde{\mathbf{V}}^\mu) = \frac{4}{\xi} \sin^2 \left[\frac{\varphi}{2f} \right] \mathcal{P}_C + \mathcal{P}_H, \quad (4.15)$$

with \mathcal{P}_C and \mathcal{P}_H being the operators in \mathcal{L}_{low} defined in eqs. (2.4) and (2.7), respectively. Having assumed the absence of any sources of custodial breaking besides the SM ones, no other two-derivative operators arise in the low-energy effective chiral Lagrangian.

Besides giving rise to the (correctly normalised) h kinetic term described by \mathcal{P}_H , the operator $\tilde{\mathcal{A}}_C$ intervenes also in the definition of the SM gauge boson masses. To provide a consistent definition for the SM W mass $m_W^2 \equiv g^2 v^2/4$, it is necessary to impose that

$$\xi \equiv \frac{v^2}{f^2} = 4 \sin^2 \frac{\langle \varphi \rangle}{2f}, \quad (4.16)$$

providing a strict and model-dependent relation between the EW scale v , the vev of the scalar field φ and the NP scale f . Note that in the $\xi \ll 1$ limit the usual SM result $\langle \varphi \rangle = v$ is recovered. Using eq. (4.16), the functional dependence on φ/f can be nicely translated in terms of the physical h excitation and the EW scale v , and the following expressions will be useful later on:

$$\begin{aligned}\sin\left(\frac{\varphi}{2f}\right) &= \sin\left(\arcsin\left(\frac{v}{2f}\right) + \frac{h}{2f}\right) = \frac{v}{2f} \cos\left(\frac{h}{2f}\right) + \sqrt{1 - \frac{v^2}{4f^2}} \sin\left(\frac{h}{2f}\right), \\ \cos\left(\frac{\varphi}{2f}\right) &= \cos\left(\arcsin\left(\frac{v}{2f}\right) + \frac{h}{2f}\right) = \sqrt{1 - \frac{v^2}{4f^2}} \cos\left(\frac{h}{2f}\right) - \frac{v}{2f} \sin\left(\frac{h}{2f}\right).\end{aligned}\tag{4.17}$$

4.2.2 The four-derivative low-energy projection

The low-energy projection of the four-derivative effective operators of eq. (3.23) gives:

$$\begin{aligned}\tilde{\mathcal{A}}_B &= \mathcal{P}_B, \\ \tilde{\mathcal{A}}_W &= \mathcal{P}_W, \\ \tilde{\mathcal{A}}_{B\Sigma} &= -4g'^2 \cos^2\left[\frac{\varphi}{2f}\right] \mathcal{P}_B, \\ \tilde{\mathcal{A}}_{W\Sigma} &= -4g^2 \cos^2\left[\frac{\varphi}{2f}\right] \mathcal{P}_W, \\ \tilde{\mathcal{A}}_1 &= \sin^2\left[\frac{\varphi}{2f}\right] \mathcal{P}_1, \\ \tilde{\mathcal{A}}_2 &= \sin^2\left[\frac{\varphi}{2f}\right] \mathcal{P}_2 + \sqrt{\xi} \sin\left[\frac{\varphi}{f}\right] \mathcal{P}_4, \\ \tilde{\mathcal{A}}_3 &= 2\sin^2\left[\frac{\varphi}{2f}\right] \mathcal{P}_3 - 2\sqrt{\xi} \sin\left[\frac{\varphi}{f}\right] \mathcal{P}_5, \\ \tilde{\mathcal{A}}_4 &= 4\xi^2 \mathcal{P}_{DH} + 16\sin^4\left[\frac{\varphi}{2f}\right] \mathcal{P}_6 - 16\xi \sin^2\left[\frac{\varphi}{2f}\right] \mathcal{P}_{20}, \\ \tilde{\mathcal{A}}_5 &= 4\xi^2 \mathcal{P}_{DH} - 16\xi \sin^2\left[\frac{\varphi}{2f}\right] \mathcal{P}_8 + 16\sin^4\left[\frac{\varphi}{2f}\right] \mathcal{P}_{11}, \\ \tilde{\mathcal{A}}_6 &= -2\xi \mathcal{P}_{\square H} - \frac{1}{2} \sin^2\left[\frac{\varphi}{f}\right] \mathcal{P}_6 + 4\xi \cos^2\left[\frac{\varphi}{2f}\right] \mathcal{P}_8 + 4\sin^2\left[\frac{\varphi}{2f}\right] \mathcal{P}_9 + \\ &\quad - 2\sqrt{\xi} \sin\left[\frac{\varphi}{f}\right] (\mathcal{P}_7 - 2\mathcal{P}_{10}),\end{aligned}\tag{4.18}$$

while the remaining two high-energy operators are not independent when focusing only on the light GBs remaining at low-energies:

$$\tilde{\mathcal{A}}_7 = \frac{1}{4} (\tilde{\mathcal{A}}_4 + \tilde{\mathcal{A}}_5), \quad \tilde{\mathcal{A}}_8 = \frac{1}{2} \tilde{\mathcal{A}}_5.\tag{4.19}$$

The fact that $\tilde{\mathcal{A}}_7$ and $\tilde{\mathcal{A}}_8$ do not give independent contributions as they are linear combinations of other high-energy operators is connected with the peculiar structure of the \mathcal{G}/\mathcal{H} breaking and has to be inferred case by case. This specific example is similar to the ALF

case, where it can be proven that traces of four \mathbf{V}_μ can be expressed as products of traces of two \mathbf{V}_μ . In resume, \mathcal{L}_{low} for the SU(5)/SO(5) scenario considered here depends on only eight independent operators, besides the kinetic terms for gauge bosons and GB fields.

It is useful to explicit the dependence on the φ field of the expressions in eq. (4.18), so as to identify easily the correlations to be expected in experimental signals involving the same number of Higgs external fields, and compare with those involving a different number of Higgs particles. To illustrate it, let us momentarily adopt a slightly different notation for the following operators in \mathcal{L}_{low} :

$$\begin{aligned}\mathcal{P}_i &\equiv \hat{\mathcal{P}}_{i\nu} \partial^\nu (h/v) & \text{for } i = 4, 5, 10, \\ \mathcal{P}_7 &\equiv \hat{\mathcal{P}}_7 \partial_\nu \partial^\nu (h/v), \\ \mathcal{P}_8 &\equiv \hat{\mathcal{P}}_{8\nu\mu} \partial^\mu (h/v) \partial^\nu (h/v).\end{aligned}\tag{4.20}$$

The operators $\tilde{\mathcal{A}}_2$, $\tilde{\mathcal{A}}_3$ and $\tilde{\mathcal{A}}_6$ can then be rewritten as

$$\begin{aligned}\tilde{\mathcal{A}}_2 &= \left(\mathcal{P}_2 + 2 \hat{\mathcal{P}}_{4\nu} \partial^\nu \right) \sin^2 \left[\frac{\varphi}{2f} \right], \\ \tilde{\mathcal{A}}_3 &= 2 \left(\mathcal{P}_3 - 2 \hat{\mathcal{P}}_{5\nu} \partial^\nu \right) \sin^2 \left[\frac{\varphi}{2f} \right], \\ \tilde{\mathcal{A}}_6 &= -2\xi \mathcal{P}_{\square H} - \left(\frac{1}{2} \mathcal{P}_6 - 4\mathcal{P}_9 + 4 \hat{\mathcal{P}}_7 \partial_\nu \partial^\nu - 8 \hat{\mathcal{P}}_{10\nu} \partial^\nu \right) \sin^2 \left[\frac{\varphi}{2f} \right] + \\ &\quad + 16 \hat{\mathcal{P}}_{8\mu\nu} \partial^\mu \sin \left[\frac{\varphi}{2f} \right] \partial^\nu \sin \left[\frac{\varphi}{2f} \right].\end{aligned}\tag{4.21}$$

This decomposition shows that, for any given number of φ external legs, the gauge interactions stemming -for instance- from \mathcal{P}_2 and \mathcal{P}_4 in $\tilde{\mathcal{A}}_2$ combine with a fixed relative weight, independently of the size of f and of the ratio $\langle\varphi\rangle/f$. That relative weight is equal to that holding for the same set of gauge interactions within the $d = 6$ operators of the linear Lagrangian, as it will be discussed in section 7. This correlation is intimately related to the fact that the φ field was embedded as a $\text{SU}(2)_L$ doublet in the high-energy theory. An analogous discussion applies to $\tilde{\mathcal{A}}_3$ and $\tilde{\mathcal{A}}_6$ in eq. (4.21).

5 The minimal SO(5)/SO(4) composite Higgs model

Most of the recent literature in CH models deals with the minimal SO(5)/SO(4) [15] setup. The features that make this model appealing are its custodial symmetry approximate conservation and its minimality in terms of number of GBs that arise from the global symmetry breaking: only four to be associated with the SM would-be GBs and the Higgs field.

5.1 Spontaneous SO(5)/SO(4) symmetry breaking setup

The spontaneous SO(5)/SO(4) symmetry breaking can be obtained giving a vev to a scalar field either in a fundamental or in the symmetric adjoint representation. To resemble most the discussion of the SU(5)/SO(5) model the latter representation is chosen here. Also for

this setup, the vacuum can be taken in all generality to be a real, symmetric and orthogonal 5×5 matrix satisfying eq. (4.1), and a convenient choice is to set

$$\Delta_0 = \begin{pmatrix} \mathbb{1}_4 & 0 \\ 0 & -1 \end{pmatrix}. \quad (5.1)$$

As in the previous case, it is then possible to describe the massless excitations around the vacuum with a symmetric field $\Delta(x)$ obtained “rotating” the vacuum with the GB non-linear field $\Omega(x)$: eq. (4.3) also holds here, with \mathbf{g} being now a transformation of $\text{SO}(5)$. $\Delta(x)$ transforms in the adjoint of $\text{SO}(5)$, as a consequence of the invariance of the vacuum under $\text{SO}(4)$, and describes only four GBs.

The relations between the vacuum Δ_0 and the broken and unbroken generators presented in eq. (4.4) are valid also for this model, and because of the relations in eq. (4.1) the excitations around the vacuum can be reparametrised in the Σ -representation as in eq. (4.5), where now $\Omega(x)$ and $\Sigma(x)$ are given by

$$\Omega(x) = e^{i \frac{\varphi(x)}{2f} \mathcal{X}(x)}, \quad \Sigma(x) = e^{i \frac{\varphi(x)}{f} \mathcal{X}(x)}. \quad (5.2)$$

The $\text{SO}(5)/\text{SO}(4)$ generators can be written in a compact form as

$$(X_{\hat{a}})_{ij} = \frac{i}{\sqrt{2}} (\delta_{i5} \delta_{j\hat{a}} - \delta_{j5} \delta_{i\hat{a}}), \quad \hat{a} = 1, \dots, 4, \quad (5.3)$$

and denoting the broken generator along which the EW symmetry breaking occurs as $X_{\hat{4}}$,

$$X_{\hat{4}} = \frac{i}{\sqrt{2}} \begin{pmatrix} 0 & 0 & 0 \\ 0 & 0 & -e_2 \\ 0 & e_2^T & 0 \end{pmatrix}, \quad (5.4)$$

the GB non-linear field reads

$$\mathcal{X}(x) = -\frac{i}{\sqrt{2}} \text{Tr}(\mathbf{U} \sigma_{\hat{a}}) X_{\hat{a}}, \quad \hat{a} = 1, \dots, 4, \quad (5.5)$$

where $\sigma_{\hat{a}} \equiv \{\sigma_1, \sigma_2, \sigma_3, i\mathbb{1}_2\}$ and which reduces to $\mathcal{X} = \sqrt{2} X_{\hat{4}}$ in the unitary gauge. Alike to the case of the Georgi-Kaplan model, the field Σ takes the simple form in terms of linear and quadratic powers of \mathcal{X} shown in eq. (4.13). Finally, with this convention the embedding of the $\text{SU}(2)_L \times \text{U}(1)_Y$ generators in $\text{SO}(5)$ reads

$$\begin{aligned} Q_L^1 &= \frac{1}{2} \begin{pmatrix} & -i\sigma_1 & \\ i\sigma_1 & & \\ & & 0 \end{pmatrix}, & Q_L^2 &= \frac{1}{2} \begin{pmatrix} & i\sigma_3 & \\ -i\sigma_3 & & \\ & & 0 \end{pmatrix}, \\ Q_L^3 &= \frac{1}{2} \begin{pmatrix} \sigma_2 & & \\ & \sigma_2 & \\ & & 0 \end{pmatrix}, & Q_Y &= \frac{1}{2} \begin{pmatrix} \sigma_2 & & \\ & -\sigma_2 & \\ & & 0 \end{pmatrix}. \end{aligned} \quad (5.6)$$

5.2 The low-energy effective EW chiral Lagrangian

Having chosen the explicit realisation of the $\text{SO}(5)/\text{SO}(4)$ symmetry breaking mechanism and the representation of the embedding of the SM group charges into $\text{SO}(5)$, the substitution of the explicit expressions for Σ , $\tilde{\mathbf{V}}_\mu$, $\tilde{\mathbf{W}}_\mu$ and $\tilde{\mathbf{B}}_\mu$ into the operators of the high-energy basis in eq. (3.23) produces \mathcal{L}_{low} for the minimal $\text{SO}(5)/\text{SO}(4)$ CH model, as a function of the SM would-be GBs and the light scalar resonance φ .

The low-energy projection of the $\text{SO}(5)/\text{SO}(4)$ Lagrangian turns out to be exactly the same as that for the $\text{SU}(5)/\text{SO}(5)$ model. This result depends on the strict connection between $\text{SO}(5)$ and $\text{SU}(5)$, as indeed the GB matrix fields of the two theories are linked by a unitary global transformation, once decoupling the extra GBs arising in the $\text{SU}(5) \rightarrow \text{SO}(5)$ breaking. Moreover, the gauging of the SM symmetry represents an explicit breaking of the global symmetries and it produces the effect of washing out the differences between the two preserved subgroups, once focusing only on the SM particle spectrum. This also suggests that any model with the minimal number of GBs that can be arranged in a doublet of $\text{SU}(2)_L$ and approximate custodial symmetry will yield the same low-energy effective chiral Lagrangian regardless of the specific ultraviolet completion.

6 The $\text{SU}(3)/(\text{SU}(2) \times \text{U}(1))$ composite Higgs model

As a final example, the $\text{SU}(3)/(\text{SU}(2) \times \text{U}(1))$ CH model is now considered. As only four GBs arise from the breaking of the global symmetry, also this model is minimal. However, contrary to the previously discussed CH models, the preserved subgroup \mathcal{H} does not contain the custodial $\text{SO}(4)$ term and therefore no (approximate) custodial symmetry is embeddable in this model. This feature disfavours phenomenologically the $\text{SU}(3)/(\text{SU}(2) \times \text{U}(1))$ CH model as large tree-level contributions to the T parameter occur. Nevertheless, the study of its low-energy projection is instructive in order to discuss the custodial breaking operators of the effective Lagrangian \mathcal{L}_{low} in eq. (2.9). Indeed, although in the initial high-energy $\text{SU}(3)/(\text{SU}(2) \times \text{U}(1))$ Lagrangian no extra sources of custodial breaking (besides the SM ones) are introduced, these operators appear at tree-level in the low-energy effective Lagrangian.

6.1 Spontaneous $\text{SU}(3)/(\text{SU}(2) \times \text{U}(1))$ symmetry breaking setup

An appropriate choice for the vacuum that breaks $\text{SU}(3) \rightarrow \text{SU}(2) \times \text{U}(1)$ is given by the following hermitian and orthogonal matrix:

$$\Delta_0 = \begin{pmatrix} \mathbb{1}_2 & 0 \\ 0 & -1 \end{pmatrix}, \quad (6.1)$$

that satisfies the relations in eq. (4.1). As in the previous cases, it is then possible to describe the massless excitations around the vacuum with a unitary field $\Delta(x)$ obtained “rotating” the vacuum with the GB non-linear field $\Omega(x)$:

$$\Delta(x) = \Omega(x) \Delta_0 \Omega(x)^\dagger, \quad \Delta(x) \rightarrow \mathbf{g} \Delta(x) \mathbf{g}^\dagger. \quad (6.2)$$

As the vacuum is invariant under $SU(2) \times U(1)$ transformations, $\Delta(x)$ belongs to the adjoint of $SU(3)$. Being $\dim(SU(3)/(SU(2) \times U(1))) = 4$, the field $\Delta(x)$ describes the dynamics of only four GBs, which will be then identified with the longitudinal components of the SM gauge bosons and the physical Higgs particle. Using the following relations between the vacuum Δ_0 and the broken and unbroken generators,

$$\Delta_0 T_a \Delta_0 = T_a, \quad \Delta_0 X_{\hat{a}} \Delta_0 = -X_{\hat{a}}, \quad (6.3)$$

and because of the relations in eq. (4.1), the excitations around the vacuum can be arranged in the Σ -representation as in eq. (4.5) with Ω and Σ given as in eq. (5.2). Choosing the following direction of EW symmetry breaking,

$$X = \frac{1}{\sqrt{2}} \begin{pmatrix} 0 & e_2 \\ e_2^T & 0 \end{pmatrix}, \quad (6.4)$$

it is possible to write the $SU(3)$ embedding of the SM GB fields as

$$\mathcal{X}(x) = \sqrt{2} \begin{pmatrix} \mathbf{U}(x) \\ 1 \end{pmatrix} X \begin{pmatrix} \mathbf{U}(x)^\dagger \\ 1 \end{pmatrix} = \begin{pmatrix} 0 & \mathbf{U}(x)e_2 \\ (\mathbf{U}(x)e_2)^\dagger & 0 \end{pmatrix}, \quad (6.5)$$

reducing to $\mathcal{X} = \sqrt{2}X$ in the unitary gauge. As for the two models previously analysed, the GB field matrix Σ can be expressed in terms of \mathcal{X} as in eq. (4.13). Finally the $SU(3)$ -embedding of the $SU(2)_L \times U(1)_Y$ generators are given by

$$Q_L^a = \frac{1}{2} \begin{pmatrix} \sigma_a \\ 0 \end{pmatrix}, \quad Q_Y = \frac{1}{6} \begin{pmatrix} \mathbb{1}_2 & \\ & -2 \end{pmatrix}, \quad (6.6)$$

with $\text{Tr}(Q_L^a Q_L^a) = 1$ and $\text{Tr}(Q_Y Q_Y) = 1/6$.

6.2 The low-energy effective EW chiral Lagrangian

By substituting the explicit expressions for Σ , $\tilde{\mathbf{V}}_\mu$, $\tilde{\mathbf{W}}_\mu$ and $\tilde{\mathbf{B}}_\mu$ into the operators of the high-energy basis in eq. (3.23), \mathcal{L}_{low} is obtained for the $SU(3)/(SU(2) \times U(1))$ model as a function of the SM would-be GBs and the light physical Higgs φ .

6.2.1 The two-derivative low-energy projection

The low-energy projection of this CH model, where the custodial symmetry is not approximately conserved, underlines some peculiarities that can be already seen in the resulting expression for the dimension-two operator $\tilde{\mathcal{A}}_C$:

$$\tilde{\mathcal{A}}_C = -\frac{f^2}{4} \text{Tr}(\tilde{\mathbf{V}}_\mu \tilde{\mathbf{V}}^\mu) = \mathcal{P}_H + \frac{4}{\xi} \sin^2 \left[\frac{\varphi}{2f} \right] \mathcal{P}_C + \frac{2}{\xi} \sin^4 \left[\frac{\varphi}{2f} \right] \mathcal{P}_T. \quad (6.7)$$

It projects at low-energy not only into the h and GBs kinetic terms as expected, but also into the two-derivative custodial violating operator \mathcal{P}_T in eq. (2.4).

Alike to the situation for the models previously studied, $\tilde{\mathcal{A}}_C$ contains the term that describes the masses of the gauge bosons once the EW symmetry is broken. Requiring consistency with the definition of the W -mass, the link given in eq. (4.16) among the EW scale v , the Higgs VEV $\langle \varphi \rangle$ and the strong dynamic scale f also follows here.

6.2.2 The four-derivative low-energy projection

The low-energy projection of the four-derivative operators listed in eq. (3.23) results in the following decomposition for the $SU(3)/(SU(2) \times U(1))$ model:

$$\begin{aligned}
 \tilde{\mathcal{A}}_B &= \frac{2}{3} \mathcal{P}_B, \\
 \tilde{\mathcal{A}}_W &= \mathcal{P}_W, \\
 \tilde{\mathcal{A}}_{B\Sigma} &= -\frac{g'^2}{6} \left(1 + 3 \cos \left[\frac{2\varphi}{f} \right] \right) \mathcal{P}_B, \\
 \tilde{\mathcal{A}}_{W\Sigma} &= -2g^2 \cos \left[\frac{\varphi}{f} \right] \mathcal{P}_W + \sin^4 \left[\frac{\varphi}{2f} \right] \mathcal{P}_{12}, \\
 \tilde{\mathcal{A}}_1 &= \frac{1}{4} \sin^2 \left[\frac{\varphi}{f} \right] \mathcal{P}_1, \\
 \tilde{\mathcal{A}}_2 &= \frac{1}{4} \sin^2 \left[\frac{\varphi}{f} \right] \mathcal{P}_2 + \frac{\sqrt{\xi}}{2} \sin \left[\frac{2\varphi}{f} \right] \mathcal{P}_4, \\
 \tilde{\mathcal{A}}_3 &= \frac{1}{2} \sin^2 \left[\frac{\varphi}{f} \right] \mathcal{P}_3 - 2\sqrt{\xi} \sin \left[\frac{\varphi}{f} \right] \mathcal{P}_5 + 2 \sin^4 \left[\frac{\varphi}{2f} \right] \mathcal{P}_{13} + 2\sqrt{\xi} \sin \left[\frac{\varphi}{f} \right] \sin^2 \left[\frac{\varphi}{2f} \right] \mathcal{P}_{17}, \\
 \tilde{\mathcal{A}}_4 &= 4\xi^2 \mathcal{P}_{DH} + 16 \sin^4 \left[\frac{\varphi}{2f} \right] \mathcal{P}_6 - 16\xi \sin^2 \left[\frac{\varphi}{2f} \right] \mathcal{P}_{20} + 8\xi \sin^4 \left[\frac{\varphi}{2f} \right] \mathcal{P}_{21} + \\
 &\quad - 16 \sin^6 \left[\frac{\varphi}{2f} \right] \mathcal{P}_{23} + 4 \sin^8 \left[\frac{\varphi}{2f} \right] \mathcal{P}_{26}, \\
 \tilde{\mathcal{A}}_5 &= 4\xi^2 \mathcal{P}_{DH} - 16\xi \sin^2 \left[\frac{\varphi}{2f} \right] \mathcal{P}_8 + 16 \sin^4 \left[\frac{\varphi}{2f} \right] \mathcal{P}_{11} + 8\xi \sin^4 \left[\frac{\varphi}{2f} \right] \mathcal{P}_{22} + \\
 &\quad - 16 \sin^6 \left[\frac{\varphi}{2f} \right] \mathcal{P}_{24} + 4 \sin^8 \left[\frac{\varphi}{2f} \right] \mathcal{P}_{26}, \\
 \tilde{\mathcal{A}}_6 &= -2\xi \mathcal{P}_{\square h} - \frac{1}{2} \sin^2 \left[\frac{\varphi}{f} \right] \mathcal{P}_6 - 2\sqrt{\xi} \sin \left[\frac{\varphi}{f} \right] (\mathcal{P}_7 - 2\mathcal{P}_{10}) + 4\xi \cos^2 \left[\frac{\varphi}{2f} \right] \mathcal{P}_8 + \\
 &\quad + 4 \sin^2 \left[\frac{\varphi}{2f} \right] \mathcal{P}_9 - 2 \sin^4 \left[\frac{\varphi}{2f} \right] (\mathcal{P}_{15} - 2\mathcal{P}_{16}) - 2\xi \left(1 + 2 \cos \left[\frac{\varphi}{f} \right] \right) \sin^2 \left[\frac{\varphi}{2f} \right] \mathcal{P}_{22} + \\
 &\quad + 2\sqrt{\xi} \sin \left[\frac{\varphi}{f} \right] \sin^2 \left[\frac{\varphi}{2f} \right] (\mathcal{P}_{18} - 2\mathcal{P}_{19} + \mathcal{P}_{25}) + \sin^2 \left[\frac{\varphi}{f} \right] \sin^2 \left[\frac{\varphi}{2f} \right] \mathcal{P}_{23} + \\
 &\quad - 4 \sin^6 \left[\frac{\varphi}{2f} \right] \mathcal{P}_{24} + 2 \sin^8 \left[\frac{\varphi}{2f} \right] \mathcal{P}_{26}, \\
 \tilde{\mathcal{A}}_7 &= 2\xi^2 \mathcal{P}_{DH} + 8 \sin^4 \left[\frac{\varphi}{2f} \right] \mathcal{P}_6 - 4\xi \sin^2 \left[\frac{\varphi}{2f} \right] \mathcal{P}_8 - 2\sqrt{\xi} \sin \left[\frac{\varphi}{f} \right] \sin^2 \left[\frac{\varphi}{2f} \right] \mathcal{P}_{18} + \\
 &\quad - 4\xi \sin^2 \left[\frac{\varphi}{2f} \right] \mathcal{P}_{20} - 2\xi \cos \left[\frac{\varphi}{f} \right] \sin^2 \left[\frac{\varphi}{2f} \right] \mathcal{P}_{21} + 2\xi \sin^2 \left[\frac{\varphi}{2f} \right] \mathcal{P}_{22} - \\
 &\quad - 2 \left(3 - \cos \left[\frac{\varphi}{f} \right] \right) \sin^4 \left[\frac{\varphi}{2f} \right] \mathcal{P}_{23} + \sin^2 \left[\frac{\varphi}{f} \right] \sin^2 \left[\frac{\varphi}{2f} \right] \mathcal{P}_{24} + 2 \sin^2 \left[\frac{\varphi}{2f} \right]^8 \mathcal{P}_{26}
 \end{aligned} \tag{6.8}$$

The remaining operator in the list in eq. (3.23) is not independent in this case, as it can be expressed as the combination

$$\tilde{\mathcal{A}}_8 = \frac{1}{2} \tilde{\mathcal{A}}_4 + \tilde{\mathcal{A}}_5 - 2\tilde{\mathcal{A}}_7, \tag{6.9}$$

which in summary implies that the low-energy physical consequences of this model depend on nine arbitrary coefficients.

7 Matching the high- and the low-energy Lagrangians

The remnant of the GB nature of the Higgs field can be tracked down to the trigonometric functions that enter into the low-energy EW chiral Lagrangian for the specific CH models: indeed, one given gauge vertex can involve an arbitrary number of h legs, with a suppression in terms of powers of the GB scale f . The explicit dependence on the h field is easily recovered using eq. (4.10) in combination with trigonometric function properties. In the general \mathcal{L}_{low} basis, the dependence on the h field is encoded into the generic functions $\mathcal{F}_i(h)$ in eq. (2.10) and into some operators which contain derivatives of h . The matching between the low-energy EW chiral Lagrangian of the specific CH models and the general \mathcal{L}_{low} basis in eq. (2.9) allows to identify the products $c_i \mathcal{F}_i(h)$ in terms of the high-energy parameters. The existence of peculiar correlations between the low-energy chiral effective operators could indeed provide very valuable information when trying to unveil the nature of the EWSB mechanism [37, 42, 43].

7.1 The SU(5)/SO(5) and SO(5)/SO(4) models

For the specific case of the SU(5)/SO(5) model discussed in section 4 and the terms in its two-derivative Lagrangian it results

$$\mathcal{F}_C(h) = \frac{4}{\xi} \sin^2 \left[\frac{\varphi}{2f} \right], \quad \mathcal{F}_H(h) = 1, \quad (7.1)$$

for the custodial preserving sector, while

$$c_T \mathcal{F}_T(h) = 0 \quad (7.2)$$

for the custodial breaking term, as expected from a model which was formulated with an embedded custodial symmetry.

A superficial look to the ξ dependence of the right-hand side of eq. (4.15) (or equivalently of $\mathcal{F}_C(h)$ in eq. (7.1)) may raise questions about an apparent unphysical behaviour for $\xi \ll 1$. However, this is not the case as for $\xi \rightarrow 0$ eq. (4.15) reduces to

$$\tilde{\mathcal{A}}_C \approx \left[\left(1 + \frac{h}{v} \right)^2 - \frac{\xi}{12} \frac{h}{v} \left(1 + \frac{h}{v} \right) \left(3 + 3 \frac{h}{v} + \frac{h^2}{v^2} \right) + \mathcal{O}(\xi^2) \right] \mathcal{P}_C + \mathcal{P}_H, \quad (7.3)$$

with the SM gauge boson-Higgs couplings exactly recovered⁹ for $\xi = 0$. This is consistent, as in this model the three would-be SM GBs and the Higgs field were introduced in a $\text{SU}(2)_L$ doublet structure embedded into the SU(5) representation (see eq. (4.12)). Any deviation from the SM (doublet) predictions should thus appear weighted by powers of ξ .

⁹Equivalently, rewriting $\mathcal{F}_C(h)$ in eq. (7.1) as $\mathcal{F}_C(h) = (\varphi^2/v^2)[\sin(x)/x]^2$ with $x \equiv \sqrt{\xi}\varphi/(2v)$ shows that its $\xi \rightarrow 0$ limit is safe, as $\sin(x)/x$ is an analytic function for any value of x and in particular $x = 0$.

$c_i \mathcal{F}_i(h)$	SU(5)/SO(5) SO(5)/SO(4)	SU(3)/SU(2) \times U(1)	linear $d \leq 6$
$\mathcal{F}_C(h)$	$\frac{4}{\xi} \sin^2 \frac{\varphi}{2f}$	$\frac{4}{\xi} \sin^2 \frac{\varphi}{2f}$	$1 + \frac{(v+h)^2}{2\Lambda^2} c_{\Phi 4}$
$\mathcal{F}_H(h)$	1	1	$1 + \frac{(v+h)^2}{2\Lambda^2} (c_{\Phi 1} + 2c_{\Phi 2} + c_{\Phi 4})$
$\mathcal{F}_B(h)$	$1 - 4g'^2 \tilde{c}_{B\Sigma} \cos^2 \frac{\varphi}{2f}$	$1 - g'^2 \frac{\tilde{c}_{B\Sigma}}{6} \left(1 + 3 \cos \frac{2\varphi}{f}\right)$	$1 + \frac{(v+h)^2}{2\Lambda^2} g'^2 c_{BB}$
$\mathcal{F}_W(h)$	$1 - 4g^2 \tilde{c}_{W\Sigma} \cos^2 \frac{\varphi}{2f}$	$1 - 2g^2 \tilde{c}_{W\Sigma} \cos \frac{\varphi}{f}$	$1 + \frac{(v+h)^2}{2\Lambda^2} g^2 c_{WW}$
$c_{\square H} \mathcal{F}_{\square H}(h)$	$-2\tilde{c}_6 \xi$	$-2\tilde{c}_6 \xi$	$\frac{v^2}{2\Lambda^2} c_{\square \Phi}$
$c_{\Delta H} \mathcal{F}_{\Delta H}(h)$	—	—	—
$c_{DH} \mathcal{F}_{DH}(h)$	$4(\tilde{c}_4 + \tilde{c}_5) \xi^2$	$2(2\tilde{c}_4 + 2\tilde{c}_5 + \tilde{c}_7) \xi^2$	—
$c_1 \mathcal{F}_1(h)$	$\tilde{c}_1 \sin^2 \frac{\varphi}{2f}$	$\frac{\tilde{c}_1}{4} \sin^2 \frac{\varphi}{f}$	$\frac{(v+h)^2}{4\Lambda^2} c_{BW}$
$c_2 \mathcal{F}_2(h)$	$\tilde{c}_2 \sin^2 \frac{\varphi}{2f}$	$\frac{\tilde{c}_2}{4} \sin^2 \frac{\varphi}{f}$	$\frac{(v+h)^2}{8\Lambda^2} c_B$
$c_3 \mathcal{F}_3(h)$	$2\tilde{c}_3 \sin^2 \frac{\varphi}{2f}$	$\frac{\tilde{c}_3}{2} \sin^2 \frac{\varphi}{f}$	$\frac{(v+h)^2}{8\Lambda^2} c_W$
$c_4 \mathcal{F}_4(h)$	$\tilde{c}_2 \sqrt{\xi} \sin \frac{\varphi}{f}$	$\frac{\tilde{c}_2}{2} \sqrt{\xi} \sin \frac{2\varphi}{f}$	$\frac{v(v+h)}{2\Lambda^2} c_B$
$c_5 \mathcal{F}_5(h)$	$-2\tilde{c}_3 \sqrt{\xi} \sin \frac{\varphi}{f}$	$-2\tilde{c}_3 \sqrt{\xi} \sin \frac{\varphi}{f}$	$-\frac{v(v+h)}{2\Lambda^2} c_W$
$c_6 \mathcal{F}_6(h)$	$16\tilde{c}_4 \sin^4 \frac{\varphi}{2f} - \frac{1}{2} \tilde{c}_6 \sin^2 \frac{\varphi}{f}$	$8(2\tilde{c}_4 + \tilde{c}_7) \sin^4 \frac{\varphi}{2f} - \frac{1}{2} \tilde{c}_6 \sin^2 \frac{\varphi}{f}$	$\frac{(v+h)^2}{8\Lambda^2} c_{\square \Phi}$
$c_7 \mathcal{F}_7(h)$	$-2\tilde{c}_6 \sqrt{\xi} \sin \frac{\varphi}{f}$	$-2\tilde{c}_6 \sqrt{\xi} \sin \frac{\varphi}{f}$	$\frac{v(v+h)}{2\Lambda^2} c_{\square \Phi}$
$c_8 \mathcal{F}_8(h)$	$-16\tilde{c}_5 \xi \sin^2 \frac{\varphi}{2f} + 4\tilde{c}_6 \xi \cos^2 \frac{\varphi}{2f}$	$-4(4\tilde{c}_5 + \tilde{c}_7) \xi \sin^2 \frac{\varphi}{2f} + 4\tilde{c}_6 \xi \cos^2 \frac{\varphi}{2f}$	$-\frac{v^2}{\Lambda^2} c_{\square \Phi}$
$c_9 \mathcal{F}_9(h)$	$4\tilde{c}_6 \sin^2 \frac{\varphi}{2f}$	$4\tilde{c}_6 \sin^2 \frac{\varphi}{2f}$	$-\frac{(v+h)^2}{4\Lambda^2} c_{\square \Phi}$
$c_{10} \mathcal{F}_{10}(h)$	$4\tilde{c}_6 \sqrt{\xi} \sin \frac{\varphi}{f}$	$4\tilde{c}_6 \sqrt{\xi} \sin \frac{\varphi}{f}$	$-\frac{v(v+h)}{\Lambda^2} c_{\square \Phi}$
$c_{11} \mathcal{F}_{11}(h)$	$16\tilde{c}_5 \sin^4 \frac{\varphi}{2f}$	$16\tilde{c}_5 \sin^4 \frac{\varphi}{2f}$	—
$c_{20} \mathcal{F}_{20}(h)$	$-16\tilde{c}_4 \xi \sin^2 \frac{\varphi}{2f}$	$-4(4\tilde{c}_4 + \tilde{c}_7) \xi \sin^2 \frac{\varphi}{2f}$	—

Table 1. Expressions for the products $c_i \mathcal{F}_i(h)$ of custodial preserving operators: SU(5)/SO(5) and SO(5)/SO(4) in the second column, SU(3)/(SU(2) \times U(1)) in the third column, and the $d = 6$ effective linear Lagrangian in the fourth column. The “—” entries indicate no leading order contributions at low-energy to the corresponding operator. Notice that the kinetic terms are not canonically normalised at this stage.

For completeness, it may be useful to provide the expression for the $\mathcal{F}_C(h)$ function in the notation usually adopted in the literature:¹⁰

$$\mathcal{F}_C(h) = 1 + 2a_C \frac{h}{v} + b_C \frac{h^2}{v^2} + \dots, \quad \text{with} \quad a_C = 1 - \frac{\xi}{8}, \quad b_C = 1 - \frac{\xi}{2}. \quad (7.4)$$

For the terms in the four-derivative Lagrangian, the expressions for the products $c_i \mathcal{F}_i(h)$ are reported in table 1 (second column). Some relevant conclusions can be inferred from these results:

- i) All custodial preserving operators entering the low-energy Lagrangian \mathcal{L}_{low} , eq. (2.10), are generated from the high-energy one $\mathcal{L}_{\text{high}}$ for the SU(5)/SO(5) CH

¹⁰In ref. [51], a slightly different result is reported: $a_C = 1 - \xi/2$ and $b_C = 1 - 2\xi$. This is due to a different normalisation chosen for the operator $\tilde{\mathcal{A}}_C$ in ref. [51] (see eq. (A.34)). By a redefinition of the Higgs field, $\varphi \rightarrow \varphi/2$, the two expressions for a_C and b_C coincide.

model, with the exception of the operator $\mathcal{P}_{\Delta H}$ in eq. (2.8) and $\mathcal{F}_H(h)$, $\mathcal{F}_{\square H}$ and \mathcal{F}_{DH} . They cannot be originated due to the GB nature of the φ field in that model, which forbids couplings with an odd number of Goldstone bosons, plus the fact that the departure from a pure Goldstone boson nature is through its vev $\langle\varphi\rangle \neq 0$, and not from any source containing derivatives.¹¹

- ii) All other operators present in $\mathcal{L}_{\text{low}}^{p^4}$ in eq. (2.10) and not appearing in table 1 describe effects of tree-level custodial breaking beyond the SM ones, and are thus absent in the low-energy SU(5)/SO(5) effective chiral Lagrangian discussed.
- iii) The arbitrary functions $\mathcal{F}_i(h)$ of the generic low-energy effective chiral Lagrangian \mathcal{L}_{low} in eq. (2.10) become now a constrained set. Having chosen a specific CH model reduces the number of free parameters in \mathcal{L}_{low} : sixteen low-energy generic parameters contained in $c_i \mathcal{F}_i(h)$ are now described in terms of the eight high-energy parameters \tilde{c}_i .

As the EW chiral Lagrangian for the minimal SO(5)/SO(4) model is the same of the one for the SU(5)/SO(5) model, the results presented here also apply to the minimal SO(5)/SO(4) model.

7.2 The SU(3)/(SU(2) × U(1)) model

The $\mathcal{F}_C(h)$ and $\mathcal{F}_H(h)$ functions of the two-derivative low-energy chiral Lagrangian eq. (2.10) stemming from the high-energy SU(3)/(SU(2) × U(1)) model turn out to be

$$\mathcal{F}_C(h) = \frac{4}{\xi} \sin^2 \left[\frac{\varphi}{2f} \right], \quad \mathcal{F}_H(h) = 1, \quad (7.5)$$

for the custodial preserving sector, and thus equal to that for SU(5)/SO(5) and SO(5)/SO(4) in eq. (7.1). This suggests that they are universal for composite models in which the Higgs is embedded as a SU(2)_L doublet. For the custodial breaking sector, instead, it results

$$c_T \mathcal{F}_T(h) = \frac{2}{\xi} \sin^4 \left[\frac{\varphi}{2f} \right], \quad (7.6)$$

and in this case the coefficient c_T is not a free parameter, but is fixed by the high-energy operator $\tilde{\mathcal{A}}_C$. In consequence, the experimental bounds on the T parameter [52] translate into strong constraints on the parameter ξ and on the strong dynamics scale f :

$$\alpha_{\text{em}} \Delta T = \frac{\xi}{4} \quad \Longrightarrow \quad \xi \lesssim 0.014, \quad f \gtrsim 2 \text{ TeV}. \quad (7.7)$$

For the terms in the four-derivative Lagrangian, the expressions for the products $c_i \mathcal{F}_i(h)$ corresponding to custodial invariant operators are reported in table 1 (third column), while those corresponding to custodial-breaking ones are collected in table 2.

¹¹Even when fermions will be considered explicitly, it is not expected to result in $\mathcal{P}_{\Delta H}$ generated at low energies; but the additional fermionic operators expected could be rewritten in terms of $\mathcal{P}_{\Delta H}$ (and other operators) via EOM. A similar reasoning applies to $\mathcal{F}_H(h)$, $\mathcal{F}_{\square H}$ and \mathcal{F}_{DH} . We thus keep them here for generality.

$c_i \mathcal{F}_i(h)$	SU(3)/(SU(2) × U(1))	$c_i \mathcal{F}_i(h)$	SU(3)/(SU(2) × U(1))
$c_T \mathcal{F}_T(h)$	$\frac{2}{\xi} \sin^4 \frac{\varphi}{2f}$	$c_{21} \mathcal{F}_{21}(h)$	$8\tilde{c}_4 \xi \sin^4 \frac{\varphi}{2f} - 2\tilde{c}_7 \xi \cos \frac{\varphi}{f} \sin^2 \frac{\varphi}{2f}$
$c_{12} \mathcal{F}_{12}(h)$	$\tilde{c}_{W\Sigma} \sin^4 \frac{\varphi}{2f}$	$c_{22} \mathcal{F}_{22}(h)$	$8\tilde{c}_5 \xi \sin^4 \frac{\varphi}{2f} + 2\xi \tilde{c}_7 \sin^2 \frac{\varphi}{2f} - 2\tilde{c}_6 \xi \sin^2 \frac{\varphi}{2f} \left(1 + 2 \cos \frac{\varphi}{f}\right)$
$c_{13} \mathcal{F}_{13}(h)$	$2\tilde{c}_3 \sin^4 \frac{\varphi}{2f}$	$c_{23} \mathcal{F}_{23}(h)$	$-16\tilde{c}_4 \sin^6 \frac{\varphi}{2f} + \tilde{c}_6 \sin^2 \frac{\varphi}{2f} \sin^2 \frac{\varphi}{f} + 2\tilde{c}_7 \sin^4 \frac{\varphi}{2f} \left(\cos \frac{\varphi}{f} - 3\right)$
$c_{15} \mathcal{F}_{15}(h)$	$-2\tilde{c}_6 \sin^4 \frac{\varphi}{2f}$	$c_{24} \mathcal{F}_{24}(h)$	$-4(4\tilde{c}_5 + \tilde{c}_6) \sin^6 \frac{\varphi}{2f} + \tilde{c}_7 \sin^2 \frac{\varphi}{2f} \sin^2 \frac{\varphi}{f}$
$c_{16} \mathcal{F}_{16}(h)$	$4\tilde{c}_6 \sin^4 \frac{\varphi}{2f}$	$c_{25} \mathcal{F}_{25}(h)$	$2\tilde{c}_6 \sqrt{\xi} \sin^2 \frac{\varphi}{2f} \sin \frac{\varphi}{f}$
$c_{17} \mathcal{F}_{17}(h)$	$2\tilde{c}_3 \sqrt{\xi} \sin^2 \frac{\varphi}{2f} \sin \frac{\varphi}{f}$	$c_{26} \mathcal{F}_{26}(h)$	$2(2(\tilde{c}_4 + \tilde{c}_5) + \tilde{c}_6 + \tilde{c}_7) \sin^8 \frac{\varphi}{2f}$
$c_{18} \mathcal{F}_{18}(h)$	$2(\tilde{c}_6 - \tilde{c}_7) \sqrt{\xi} \sin^2 \frac{\varphi}{2f} \sin \frac{\varphi}{f}$		
$c_{19} \mathcal{F}_{19}(h)$	$-4\tilde{c}_6 \sqrt{\xi} \sin^2 \frac{\varphi}{2f} \sin \frac{\varphi}{f}$		

Table 2. Expressions for the products $c_i \mathcal{F}_i(h)$ for the custodial symmetry breaking operators of SU(3)/(SU(2) × U(1)) CH model. No analogous contributions are present neither for the SU(5)/SO(5) and SO(5)/SO(4) model, nor for the linear $d = 6$ effective Lagrangian, but for the combination $c_T \mathcal{F}_T(h)$ that receives contributions from $\mathcal{O}_{\Phi 1}$.

Contrary to the case of the two models previously analysed, all custodial preserving and all custodial breaking operators entering the low-energy Lagrangian \mathcal{L}_{low} in eq. (2.10) are generated from the high-energy one for the SU(3)/(SU(2) × U(1)) CH model, with the exception of the operator $\mathcal{P}_{\Delta H}$ in eq. (2.8) and $\mathcal{F}_H(h)$, $\mathcal{F}_{\square H}$ and \mathcal{F}_{DH} . On the other side, also in this case the a priori many arbitrary combinations $c_i \mathcal{F}_i(h)$ can be written in terms of the small set of nine high-energy parameters \tilde{c}_i .

In summary, a quite universal pattern is suggested by our results as to the form of the $c_i \mathcal{F}_i(h)$ functions, at least for the custodial preserving sector. Table 1 encompasses the main results and allows a direct comparison of the low-energy impact of the models considered (as well as of the BSM physics expected from linear realisations of EWSB). Not only $\mathcal{F}_C(h)$ coincides exactly for all three chiral models considered, see eqs. (7.1) and (7.5), but the $c_i \mathcal{F}_i(h)$ functions for *all* four-derivative chiral operators do as well, except for the couplings which involve gauge field-strengths for which the intrinsically custodial-invariant groups and SU(3)/(SU(2) × U(1)) differ simply by a rescaling of the scale f and multiplicative factors, see table 1.

7.3 The $\xi \ll 1$ limit and the linear effective Lagrangian

As anticipated in section 2, the low-energy effective Lagrangian \mathcal{L}_{low} is suitable to describe a large class of Higgs models, including the case of a linearly realised EWSB. In the limit of small ξ , the trigonometric functions containing the Higgs field φ can be expanded in Taylor series. If only the first terms in this expansion are retained, the resulting effective chiral Lagrangian describes similar interactions as the effective $d = 6$ linear Lagrangian [53, 54] — and with similar features. For definiteness, let us refer to a specific basis for the bosonic sector of the effective $d = 6$ linear Lagrangian — the so-called Hagiwara-Ishihara-Szalapski-Zeppenfeld (HISZ) basis [55, 56]. The effective linear Lagrangian including the leading corrections can be decomposed as the SM part plus a piece containing operators with canonical dimension $d = 6$, weighted down by suitable powers of the ultraviolet cut-off

scale Λ :

$$\mathcal{L}_{\text{linear}} = \mathcal{L}_{SM} + \Delta\mathcal{L}_{\text{linear}}, \quad (7.8)$$

where

$$\Delta\mathcal{L}_{\text{linear}} = \sum_i \frac{c_i}{\Lambda^2} \mathcal{O}_i, \quad (7.9)$$

with c_i being order one parameters and \mathcal{O}_i denoting operators defined as follows [54–56]:

$$\begin{aligned} \mathcal{O}_{BB} &= \Phi^\dagger \hat{B}_{\mu\nu} \hat{B}^{\mu\nu} \Phi, & \mathcal{O}_{WW} &= \Phi^\dagger \hat{W}_{\mu\nu} \hat{W}^{\mu\nu} \Phi, \\ \mathcal{O}_W &= (\mathbf{D}_\mu \Phi)^\dagger \hat{W}^{\mu\nu} (\mathbf{D}_\nu \Phi), & \mathcal{O}_{BW} &= \Phi^\dagger \hat{B}_{\mu\nu} \hat{W}^{\mu\nu} \Phi, \\ \mathcal{O}_B &= (\mathbf{D}_\mu \Phi)^\dagger \hat{B}^{\mu\nu} (\mathbf{D}_\nu \Phi), & \mathcal{O}_{\Phi,1} &= (\mathbf{D}_\mu \Phi)^\dagger \Phi \Phi^\dagger (\mathbf{D}^\mu \Phi), \\ \mathcal{O}_{\Phi,2} &= \frac{1}{2} \partial^\mu (\Phi^\dagger \Phi) \partial_\mu (\Phi^\dagger \Phi), & \mathcal{O}_{\Phi,3} &= \frac{1}{3} (\Phi^\dagger \Phi)^3, \\ \mathcal{O}_{\Phi,4} &= (\mathbf{D}_\mu \Phi)^\dagger (\mathbf{D}^\mu \Phi) (\Phi^\dagger \Phi), & \mathcal{O}_{\square\Phi} &= (\mathbf{D}_\mu \mathbf{D}^\mu \Phi)^\dagger (\mathbf{D}_\nu \mathbf{D}^\nu \Phi), \end{aligned} \quad (7.10)$$

with $\mathbf{D}_\mu \Phi \equiv (\partial_\mu + \frac{i}{2} g' B_\mu + \frac{i}{2} g \sigma_i W_\mu^i) \Phi$. Among these, $\mathcal{O}_{\Phi,1}$ is custodial breaking and $\mathcal{O}_{\Phi,3}$ is a pure potential-like Higgs term; assuming custodial symmetry it remains a total of eight independent operators.¹²

After the $SU(2)_L$ Higgs doublet Φ acquires a vev, $\langle \Phi \rangle = (v + h)/\sqrt{2}$, the interactions resulting from this set of linear operators can be also described by \mathcal{L}_{low} in eq. (2.10), with the products $c_i \mathcal{F}_i(h)$ taking the values shown in the last column of table 1. In the small ξ limit, the low-energy effective chiral Lagrangian associated to the considered CH models converges to the linear one, with the correspondence

$$\tilde{c}_{B\Sigma} \rightarrow c_{BB}, \quad \tilde{c}_{W\Sigma} \rightarrow c_{WW}, \quad \tilde{c}_1 \rightarrow c_{BW}, \quad \tilde{c}_2 \rightarrow c_B, \quad \tilde{c}_3 \rightarrow c_W, \quad \tilde{c}_6 \rightarrow c_{\square\Phi}. \quad (7.11)$$

The parameters \tilde{c}_4 and \tilde{c}_5 are not relevant, because they appear in contributions of order $\xi^{\geq 2}$, that correspond to linear operators of $d \geq 8$. Notice in addition that the products $c_i \mathcal{F}_i(h)$ corresponding to custodial-breaking operators and appearing in table 2 are suppressed by $\xi^{\geq 2}$ and are therefore negligible in the small ξ limit. Consistently, the corresponding contributions from the effective linear Lagrangian come from operators with dimensions $d \geq 8$. Notice that a complete comparison is only possible in the basis where the kinetic terms are canonical: in table 1, $\mathcal{F}_H(h)$ is 1 for the CH models, but not for the linear Lagrangian.

Eq. (6.8) together with the decomposition in eq. (4.21) allow to appreciate the coincidences and the differences between the low-energy effective chiral Lagrangian and the effective linear one: i) the gauge interactions stemming from some chiral operators combine with fixed weights, even for large ξ values, which are precisely those predicted by the linear Lagrangian (see table 1); this is because the φ field was embedded in the high energy theory as a $SU(2)_L$ doublet; ii) the low-energy differences stem from the h dependence, given via functions of $\sin[(\langle \varphi \rangle + h)/2f]$ for the low-energy chiral Lagrangian versus

¹²The original HISZ basis includes in addition the gluonic operator $\mathcal{O}_{GG} = \Phi^\dagger \Phi G_{\mu\nu}^a G^{a\mu\nu}$, which is not considered here as only the EW sector is analysed in this paper.

powers of $(v + h)/2$ for linear realisations of BSM theories. Therefore, although the number of free parameters is the same in the two Lagrangians, the h -couplings have different dependencies [35, 44].

To illustrate it, consider the \mathcal{O}_B operator of the linear realisation. Expressing Φ in terms of the GB matrix \mathbf{U} and the physical scalar h ,

$$\Phi = \frac{(v + h)}{\sqrt{2}} \mathbf{U} \begin{pmatrix} 0 \\ 1 \end{pmatrix}, \quad (7.12)$$

\mathcal{O}_B can be rewritten in the chiral notation as

$$\begin{aligned} \mathcal{O}_B &= B_{\mu\nu} \text{Tr}(\mathbf{T}[\mathbf{V}^\mu, \mathbf{V}^\nu]) \frac{(v + h)^2}{4} + B_{\mu\nu} \text{Tr}(\mathbf{T}\mathbf{V}^\mu) \partial^\nu \frac{(v + h)^2}{4} \\ &= \left(\mathcal{P}_2 + 2\hat{\mathcal{P}}_{4\nu} \partial^\nu \right) \frac{(v + h)^2}{4}, \end{aligned} \quad (7.13)$$

to be compared with $\tilde{\mathcal{A}}_2$ in eq. (4.21). This pattern is general for the complete set of operators: same gauge couplings as in $d = 6$ linear basis for a fixed number of h legs, while the relative strength of couplings involving different number of h external legs differs from that in linear expansions. The results support the approach to the effective Lagrangian for composite Higgs models based in the linear expansion in ref. [54–57] only if the Higgs is assumed to be a pure $\text{SU}(2)_L$ doublet. Indeed in this case $\xi \ll 1$ and the trigonometric dependence on h reduces exactly to the linear one, as $\sin^2(\varphi/f) = \xi(1 + h/v)^2 + \mathcal{O}(\xi^2)$ and the higher order terms in ξ can be safely neglected.

Promising discriminating signals include then some pure-gauge versus gauge-Higgs couplings [37, 42, 43], whose precise form we have determined here for the specific CH models considered. The strength of this type of departures from the SM expectations depends on ξ and therefore the larger ξ the sooner it will be possible to disentangle at colliders a composite from an elementary nature of the Higgs particle.

For the more general case in which the observed light Higgs particle is not an exact $\text{SU}(2)_L$ doublet, linear $d = 6$ expansions will be insufficient to describe the leading corrections. There are then more independent parameters, as given by the general low-energy non-linear Lagrangian [36, 37, 42], and further decorrelations are expected, including among vertices with the same number of Higgs legs.

8 Conclusions

For a simple group \mathcal{G} broken to a subgroup \mathcal{H} , we have constructed the effective chiral Lagrangian for a generic symmetric coset \mathcal{G}/\mathcal{H} , restricting to CP-even bosonic operators with at most four derivatives: at most seven independent operators result, aside from the kinetic terms. After gauging the $\text{SU}(2)_L \times \text{U}(1)_Y$ symmetry and considering the induced custodial symmetry breaking terms, the total number of operators increases up to ten, plus three kinetic terms. This finding is independent of the specific choice of \mathcal{G} . It applies to composite Higgs scenarios in which the Higgs particle is a pseudo-Goldstone boson of the spontaneous breaking of \mathcal{G} , irrespective of the $\text{SU}(2)_L$ representation to which it may belong.

One consequence is that for any composite model in which the Higgs is embedded as a Goldstone boson of the high-energy theory, we predict strong relations among the dozens of low-energy parameters of the general low-energy effective chiral Lagrangian with a light Higgs particle.

Under the assumptions of no new sources of custodial non-invariance other than the SM gauge ones, we then particularised to the case of three specific composite Higgs models: two intrinsically custodial-preserving ones, $SU(5)/SO(5)$ and $SO(5)/SO(4)$, and another which by construction breaks custodial symmetry, $SU(3)/(SU(2) \times U(1))$. For the latter group the number of independent operators is nine (aside from possible sources of explicit subsequent breaking and from kinetic terms), while for the former two groups it is eight.

This analysis has allowed to confirm that the general low-energy Lagrangian for a dynamical Higgs particle developed in refs. [36, 42] is complete: all operators of that basis and nothing else result at low-energies. The exceptions are $\mathcal{P}_{\Delta H}$ in eq. (3.19) and $\mathcal{F}_H(h)$, $\mathcal{F}_{\square H}$ and \mathcal{F}_{DH} , which are not generated: these couplings are forbidden by the original Goldstone boson nature of the Higgs particle, and also by the particular way in which the global symmetry is subsequently explicitly broken in the models considered (as a vev for the Higgs particle). The results of the sigma decomposition confirm as well the powers of ξ predicted in ref. [36, 42] as weights for each operator of the low-energy effective chiral Lagrangian, allowing an immediate comparison with linear expansions. Note that, for the scalar sector, a different and fully model-independent proof of the completeness of that effective Lagrangian is provided by the recent analysis in ref. [58] of one-loop induced four-derivative counterterms.

The present work also sheds light on the relevance of the Higgs particle being a Goldstone boson embedded as a part of an $SU(2)_L$ doublet in a representation of the high-energy group, versus scenarios in which it is also a Goldstone boson albeit a $SU(2)$ singlet, or the most general case in which h is a generic singlet scalar, such as a Higgs “impostor”, or a dilaton or a dark sector scalar. Data strongly suggest that h belongs to an electroweak doublet and it is thus especially interesting to further explore the consequences of this restriction for BSM physics. Our results show that:

- i) For vertices with a fixed number of external Higgs legs, the gauge couplings combine with the same relative weights as in the case of the $d = 6$ linear effective Lagrangian for BSM physics. This is so irrespective of the size of ξ for the intrinsically custodial preserving groups considered, while for the $SU(3)/(SU(2) \times U(1))$ model it only holds at leading order in ξ .
- ii) Conversely, vertices with different number of h external legs get different relative weights than in linear realisations of BSM physics. While the latter show a generic polynomial Higgs dependence on $(v + h)$ and its derivatives, composite Higgs models induce a functional $c_i \mathcal{F}_i(h)$ dependence in the effective Lagrangian. We have explicitly determined all $c_i \mathcal{F}_i(h)$ functions of the low-energy effective Lagrangian up to four-derivative couplings, for the three composite models considered.

- iii) The determined $\mathcal{F}_i(h)$ are trigonometric functions, as befits a Goldstone boson origin of the Higgs field, and it is tantalising that they turn out to be basically exactly equal for the three models considered, except in the set of operators which include gauge field strengths; even the latter differ at most by a rescaling of f (aside from custodial breaking ingredients).

The latter point suggests that the $\mathcal{F}_i(h)$ determined here may be universal to any composite Higgs model. Table 1 encompasses the main results and allows a direct comparison of the low-energy impact of the composite Higgs models considered (as well as of BSM linear realisations of EWSB). This universality may be very relevant for the analysis of experimental data, as it predicts the precise form in which anomalies in Higgs-gauge couplings and self-couplings would point to composite Higgs models, and in an almost model-independent way.

The present work illuminates as well the relation between non-linear realisations of electroweak symmetry breaking with a light Higgs embedded as an electroweak doublet of the high-energy strong dynamics, and linear ones. The former approximates the latter when the strong dynamics scale grows, that is for $\xi \rightarrow 0$. We have shown here that the precise -and almost universal- $\mathcal{F}_i(h)$ functions determined for three composite Higgs models shows the specific form of the convergence towards the Higgs dependence of linear realisations, in the limit $\xi \ll 1$.

If the Higgs particle is a Goldstone boson of the high-energy group, although not an electroweak doublet -for instance a singlet- then point i) above would not hold: while the number of arbitrary operator coefficients would still be restricted to the small number predicted for a generic symmetric coset, the relative weight of gauge couplings for a fixed number of external h legs would be different with respect to that in linear analysis [54–57], with gauge decorrelations predicted alike to those in refs. [36, 42, 43]. Finally, for the completely general case in which the Higgs field is a generic SM scalar singlet at low energies, again the linear-based analysis is not an appropriate tool as both the relative weights of gauge couplings with and without the same number of h legs are completely free parameters, described (in the absence of a concrete model) by the most general low-energy bosonic effective Lagrangian for a dynamical Higgs [36, 42]. Further experimental decorrelations and signals follow in these last two cases [42, 43]. It is particularly relevant to keep tracking the possible non-doublet components of the Higgs particle, in view of the present large error bars and the theoretical challenge set by the electroweak hierarchy problem.

Acknowledgments

We acknowledge illuminating conversations with Roberto Contino, Ferruccio Feruglio, Howard Georgi, Concha Gonzalez-García, Christophe Grojean, Gino Isidori, Kirill Kanishin, Pedro Machado, Luciano Maiani, Aneesh Manohar, Sara Saa and Michael Trott. We also thank Oscar Catà for a clarifying discussion on the issues risen in ref. [41]. We also acknowledge partial support of the European Union network FP7 ITN INVISIBLES (Marie Curie Actions, PITN-GA-2011-289442), of CiCYT through the project FPA2012-31880, of

the European Union FP7 ITN UNILHC (Marie Curie Actions, PITN-GA-2009-237920), of MICINN through the grant BES-2010-037869, of the Spanish MINECO's "Centro de Excelencia Severo Ochoa" Programme under grant SEV-2012-0249, and of the Italian Ministero dell'Università e della Ricerca Scientifica through the COFIN program (PRIN 2008) and the contract MRTN-CT-2006-035505. RA acknowledges support by the DOE grant DE-SC0009919. The work of I.B. is supported by an ESR contract of the European Union network FP7 ITN INVISIBLES mentioned above. The work of L.M. is supported by the Juan de la Cierva programme (JCI-2011-09244). I.B., B.G., L.M. and S.R. acknowledge the Galileo Galilei Institute (Florence) and CERN TH department for hospitality during the initial stages of this work.

A The Ω -representation

The CCWZ construction allows to identify a non-redundant parametrisation of the GB fields arising from the breaking $\mathcal{G} \rightarrow \mathcal{H}$ in terms of the GB matrix Ω , or in terms of Σ . Although the choice between the Ω -representation or the Σ -representation is not discriminant to construct the most general effective Lagrangian for the \mathcal{G}/\mathcal{H} coset, much of the CH models in the literature have been presented in the Ω -representation. In the following, we will rewrite the effective Lagrangians in eqs. (3.16)–(3.18) and in eq. (3.20) in the Ω -representation and compare them with other effective Lagrangians presented in the literature for the case of $\text{SO}(5)/\text{SO}(4)$ model.

A.1 The high-energy effective chiral Lagrangian

The building blocks used to construct the effective Lagrangian in eqs. (3.16)–(3.18) are the gauge field strength $\tilde{\mathbf{S}}_{\mu\nu}$ and the vector chiral field $\tilde{\mathbf{V}}_\mu$, which in the Σ -representation transform in the adjoint of the group \mathcal{G} (see eqs. (3.11) and (3.10), respectively). To move to the Ω -representation, it is then necessary to translate $\tilde{\mathbf{S}}_{\mu\nu}$ and $\tilde{\mathbf{V}}_\mu$, and their graded versions, into building blocks that transform in the adjoint of the preserved subgroup \mathcal{H} . The GB matrix Ω can be exploited to this end:

$$\begin{aligned} s_{\mu\nu} &\equiv \Omega^{-1} \tilde{\mathbf{S}}_{\mu\nu} \Omega, & v_\mu &\equiv \Omega^{-1} \tilde{\mathbf{V}}_\mu \Omega = \Omega^{-1} \mathbf{D}_\mu \Omega - \Omega \mathbf{D}_\mu \Omega^{-1}, \\ s_{\mu\nu}^{\mathcal{R}} &\equiv \Omega \tilde{\mathbf{S}}_{\mu\nu}^{\mathcal{R}} \Omega^{-1}, & v_\mu^{\mathcal{R}} &\equiv \Omega \tilde{\mathbf{V}}_\mu^{\mathcal{R}} \Omega^{-1} = \Omega \mathbf{D}_\mu \Omega^{-1} - \Omega^{-1} \mathbf{D}_\mu \Omega. \end{aligned} \quad (\text{A.1})$$

From the relation $v_\mu + v_\mu^{\mathcal{R}} = 0$, one can deduce that v_μ runs only over the broken generators and not over the preserved ones. It is then useful to introduce the following notation:

$$\Omega^{-1} \mathbf{D}_\mu \Omega \equiv \frac{v_\mu}{2} + i p_\mu = \frac{v_\mu^{\hat{a}}}{2} X_{\hat{a}} + i p_\mu^a T_a, \quad (\text{A.2})$$

with v_μ and p_μ transforming under \mathcal{H} as:

$$v_\mu \rightarrow \mathfrak{h} v_\mu \mathfrak{h}^{-1}, \quad p_\mu \rightarrow \mathfrak{h} (p_\mu - i \partial_\mu) \mathfrak{h}^{-1}. \quad (\text{A.3})$$

The field p_μ transforms as a connection and therefore it is possible to define the extended covariant derivative of v_μ as

$$\nabla_\mu v_\nu = \mathbf{D}_\mu v_\nu + i [e_\mu, v_\nu]. \quad (\text{A.4})$$

From eq. (A.1), it follows that

$$v_\mu^{\mathcal{R}} = -v_\mu, \quad (\text{A.5})$$

and therefore the list of building blocks necessary to construct the effective Lagrangian in the Ω -representation reduces to only three elements: $\{v_\mu, s_{\mu\nu}, s_{\mu\nu}^{\mathcal{R}}\}$.

The high-energy basis for a generic symmetric coset \mathcal{G}/\mathcal{H} in the custodial preserving framework presented in eqs. (3.16)–(3.18) reads in the Ω -representation:

$$\begin{aligned} \text{Tr} \left(\tilde{\mathbf{V}}_\mu \tilde{\mathbf{V}}^\mu \right) &\rightarrow \text{Tr} (v_\mu v^\mu), \\ \text{Tr} \left(\tilde{\mathbf{S}}_{\mu\nu} \tilde{\mathbf{S}}^{\mu\nu} \right) &\rightarrow \text{Tr} (s_{\mu\nu} s^{\mu\nu}), \\ \text{Tr} \left(\Sigma \tilde{\mathbf{S}}_{\mu\nu}^R \Sigma^{-1} \tilde{\mathbf{S}}^{\mu\nu} \right) &\rightarrow \text{Tr} (s_{\mu\nu}^{\mathcal{R}} s^{\mu\nu}), \\ \text{Tr} \left(\tilde{\mathbf{S}}_{\mu\nu} [\tilde{\mathbf{V}}^\mu, \tilde{\mathbf{V}}^\nu] \right) &\rightarrow \text{Tr} (s_{\mu\nu} [v^\mu, v^\nu]), \\ \text{Tr} \left(\tilde{\mathbf{V}}_\mu \tilde{\mathbf{V}}^\mu \right) \text{Tr} \left(\tilde{\mathbf{V}}_\nu \tilde{\mathbf{V}}^\nu \right) &\rightarrow \text{Tr} (v_\mu v^\mu) \text{Tr} (v_\nu v^\nu), \\ \text{Tr} \left(\tilde{\mathbf{V}}_\mu \tilde{\mathbf{V}}_\nu \right) \text{Tr} \left(\tilde{\mathbf{V}}^\mu \tilde{\mathbf{V}}^\nu \right) &\rightarrow \text{Tr} (v_\mu v_\nu) \text{Tr} (v^\mu v^\nu), \\ \text{Tr} \left((\mathcal{D}_\mu \tilde{\mathbf{V}}^\mu)^2 \right) &\rightarrow \text{Tr} ((\nabla_\mu v^\mu)^2), \\ \text{Tr} \left(\tilde{\mathbf{V}}_\mu \tilde{\mathbf{V}}^\mu \tilde{\mathbf{V}}_\nu \tilde{\mathbf{V}}^\nu \right) &\rightarrow \text{Tr} (v_\mu v^\mu v_\nu v^\nu), \\ \text{Tr} \left(\tilde{\mathbf{V}}_\mu \tilde{\mathbf{V}}_\nu \tilde{\mathbf{V}}^\mu \tilde{\mathbf{V}}^\nu \right) &\rightarrow \text{Tr} (v_\mu v_\nu v^\mu v^\nu). \end{aligned} \quad (\text{A.6})$$

In realistic realisations of CH models only the SM gauge group is gauged, and in this case the previous basis is augmented by operators constructed with

$$b_{\mu\nu} \equiv \Omega^{-1} \mathbf{B}_{\mu\nu} \Omega, \quad \text{and} \quad w_{\mu\nu} \equiv \Omega^{-1} \mathbf{W}_{\mu\nu} \Omega, \quad (\text{A.7})$$

in substitution of those containing explicit gauge field strength $s_{\mu\nu}$. As a result, the effective Lagrangian in eq. (3.20) reads in the Ω -representation:

$$\begin{aligned} \tilde{\mathcal{A}}_C &\rightarrow -\frac{f^2}{4} \text{Tr} (v_\mu v^\mu), & \tilde{\mathcal{A}}_3 &\rightarrow g \text{Tr} (w_{\mu\nu} [v^\mu, v^\nu]), \\ \tilde{\mathcal{A}}_B &\rightarrow g'^2 \text{Tr} (b_{\mu\nu} b^{\mu\nu}), & \tilde{\mathcal{A}}_4 &\rightarrow \text{Tr} (v_\mu v^\mu) \text{Tr} (v_\nu v^\nu), \\ \tilde{\mathcal{A}}_W &\rightarrow g^2 \text{Tr} (w_{\mu\nu} w^{\mu\nu}), & \tilde{\mathcal{A}}_5 &\rightarrow \text{Tr} (v_\mu v_\nu) \text{Tr} (v^\mu v^\nu), \\ \tilde{\mathcal{A}}_{B\Sigma} &\rightarrow g'^2 \text{Tr} (b_{\mu\nu}^{\mathcal{R}} b^{\mu\nu}), & \tilde{\mathcal{A}}_6 &\rightarrow \text{Tr} ((\nabla_\mu v^\mu)^2), \\ \tilde{\mathcal{A}}_{W\Sigma} &\rightarrow g^2 \text{Tr} (w_{\mu\nu}^{\mathcal{R}} w^{\mu\nu}), & \tilde{\mathcal{A}}_7 &\rightarrow \text{Tr} (v_\mu v^\mu v_\nu v^\nu), \\ \tilde{\mathcal{A}}_1 &\rightarrow g g' \text{Tr} (b_{\mu\nu}^{\mathcal{R}} w^{\mu\nu}), & \tilde{\mathcal{A}}_8 &\rightarrow \text{Tr} (v_\mu v_\nu v^\mu v^\nu), \\ \tilde{\mathcal{A}}_2 &\rightarrow g' \text{Tr} (b_{\mu\nu} [v^\mu, v^\nu]), \end{aligned} \quad (\text{A.8})$$

where $b_{\mu\nu}^{\mathcal{R}} \equiv \Omega \mathbf{B}_{\mu\nu} \Omega^{-1}$ and $w_{\mu\nu}^{\mathcal{R}} \equiv \Omega \mathbf{W}_{\mu\nu} \Omega^{-1}$, and the gauge constants g and g' have been explicitly reported.

A.2 SO(5)/SO(4) model in the Ω -representation by refs. [49,57]

An effective Lagrangian for the SO(5)/SO(4) CH model has been explicitly derived in the Ω -representation in refs. [51, 59], even if slightly different operator bases have been reported in the two articles. Furthermore, a different notation has been adopted in these references with respect to the notation used in this paper. In this section, we will comment on the differences among the two bases in refs. [51, 59]. In the next section, we will discuss the different notations used and compare between the operators basis in ref. [51] and the one presented in appendix A.1.

Equivalently to the definition in eq. (A.2), it is possible to introduce the following expression, according to refs. [51, 59],

$$-i U^{-1} \mathbf{D}_\mu U \equiv d_\mu + e_\mu = d_\mu^{\hat{a}} X_{\hat{a}} + e_\mu^a T_a, \quad (\text{A.9})$$

where U stands for the GB matrix of the SO(5)/SO(4) coset, defined in eq. (11) of ref. [51], and d_μ and e_μ transform under a global transformation of $\mathcal{H} = \text{SO}(4)$ as

$$d_\mu \rightarrow \mathfrak{h} d^\mu \mathfrak{h}^{-1}, \quad e_\mu \rightarrow \mathfrak{h} (e_\mu - i \partial_\mu) \mathfrak{h}^{-1}. \quad (\text{A.10})$$

The field e_μ transforms as a connection, opening the possibility to define the field strength

$$e_{\mu\nu} \equiv \partial_\mu e_\nu - \partial_\nu e_\mu + i [e_\mu, e_\nu], \quad (\text{A.11})$$

and the extended covariant derivative of d_μ as

$$\nabla_\mu d_\nu = \mathbf{D}_\mu d_\nu + i [e_\mu, d_\nu], \quad (\text{A.12})$$

where the covariant derivative $\mathbf{D}_\mu d_\nu$ is defined in terms of the gauge fields F_μ associated to the gauging of a subgroup $\text{SO}(4)'$ of $\text{SO}(5)$:

$$\mathbf{D}_\mu d_\nu = \partial_\mu d_\nu + i g_S F_\mu d_\nu. \quad (\text{A.13})$$

It is then possible to introduce the $F_{\mu\nu}$ gauge field strength, albeit transforming in the adjoint of the group $\text{SO}(4)$:

$$\begin{aligned} f_{\mu\nu} &= \Omega^{-1} F_{\mu\nu} \Omega, & f_{\mu\nu} &\rightarrow \mathfrak{h} f_{\mu\nu} \mathfrak{h}^{-1}, \\ f_{\mu\nu}^{\mathcal{R}} &= \Omega F_{\mu\nu}^{\mathcal{R}} \Omega^{-1}, & f_{\mu\nu}^{\mathcal{R}} &\rightarrow \mathfrak{h} f_{\mu\nu}^{\mathcal{R}} \mathfrak{h}^{-1}, \end{aligned} \quad (\text{A.14})$$

where in the second line the graded version of the gauge field strength is shown. The gauge field strength can be expressed in the same notation as that in eq. (A.9), i.e. distinguishing between the preserved and the broken parts:

$$f_{\mu\nu}^+ = \frac{f_{\mu\nu} + f_{\mu\nu}^{\mathcal{R}}}{2}, \quad f_{\mu\nu}^- = \frac{f_{\mu\nu} - f_{\mu\nu}^{\mathcal{R}}}{2}. \quad (\text{A.15})$$

The preserved part of the field strength $f_{\mu\nu}^+$ and the covariant field $e_{\mu\nu}$ are related by an identity,

$$e_{\mu\nu} = f_{\mu\nu}^+ - i [d_\mu, d_\nu], \quad (\text{A.16})$$

and, as a consequence, there is a certain degree of freedom in the choice of the building blocks necessary to construct the Lagrangian: two distinct sets of covariant objects can be adopted, either $\{f_{\mu\nu}^+, f_{\mu\nu}^-, d_\mu\}$ or $\{e_{\mu\nu}, f_{\mu\nu}^-, d_\mu\}$.

Since $\text{SO}(4)$ is isomorphic to $\text{SU}(2)_L \times \text{SU}(2)_R$, the custodial symmetry is embeddable in this model. However, as it is explicitly broken by the gauging of the SM group, the left and the right components of the covariant objects defined just above can be treated independently, adding more freedom in writing the effective Lagrangian. The following structures can then be introduced:

$$\begin{aligned} f_{\mu\nu}^+ &= f_{\mu\nu}^L + f_{\mu\nu}^R, & \hat{f}_{\mu\nu}^+ &= f_{\mu\nu}^L - f_{\mu\nu}^R, \\ e_{\mu\nu} &= e_{\mu\nu}^L + e_{\mu\nu}^R, & \hat{e}_{\mu\nu} &= e_{\mu\nu}^L - e_{\mu\nu}^R, \end{aligned} \quad (\text{A.17})$$

with the obvious relations

$$e_{\mu\nu}^L = f_{\mu\nu}^L - i [d_\mu, d_\nu]_L, \quad e_{\mu\nu}^R = f_{\mu\nu}^R - i [d_\mu, d_\nu]_R. \quad (\text{A.18})$$

These covariant terms complete the list of building blocks necessary to write the effective chiral Lagrangian up to four derivatives for the $\text{SO}(5)/\text{SO}(4)$ model in the Ω -representation:

- i) The kinetic term for the GBs is described by the operator

$$\mathcal{L}^{(2)} = \frac{f^2}{4} \text{Tr} (d_\mu d^\mu). \quad (\text{A.19})$$

- ii) The kinetic terms for the gauge fields are described by the operator

$$\mathcal{O}_k = \text{Tr} [f_{\mu\nu} f^{\mu\nu}] = \text{Tr} [f_{\mu\nu}^L f_L^{\mu\nu}] + \text{Tr} [f_{\mu\nu}^R f_R^{\mu\nu}] + \text{Tr} [f_{\mu\nu}^- f_-^{\mu\nu}] \equiv \text{L}^2 + \text{R}^2 + \text{B}^2 \quad (\text{A.20})$$

where the definition for L, R, and B can be easily deduced. In the following, the compact notation L, R, and B will be adopted for shortness when necessary.

- iii) The following two operators describing gauge-GB interactions,

$$\mathcal{O}_1 = \text{Tr} (d_\mu d^\mu) \text{Tr} (d_\nu d^\nu), \quad \mathcal{O}_2 = \text{Tr} (d_\mu d_\nu) \text{Tr} (d^\mu d^\nu), \quad (\text{A.21})$$

belong to the operator basis presented both in ref. [51] and in ref. [59].

- iv-a) In ref. [51], focussing only on CP-even operators with at most four derivatives, the following list has been considered:

$$\begin{aligned} \mathcal{O}_3 &= \text{Tr} (\hat{e}_{\mu\nu} e^{\mu\nu}) = \text{Tr} ((e_{\mu\nu}^L)^2 - (e_{\mu\nu}^R)^2), \\ \mathcal{O}_4^+ &= i \text{Tr} (f_{\mu\nu}^+ [d^\mu, d^\nu]) = i \text{Tr} ((f_{\mu\nu}^L + f_{\mu\nu}^R) [d^\mu, d^\nu]), \\ \mathcal{O}_4^- &= i \text{Tr} (\hat{f}_{\mu\nu}^+ [d^\mu, d^\nu]) = i \text{Tr} ((f_{\mu\nu}^L - f_{\mu\nu}^R) [d^\mu, d^\nu]), \\ \mathcal{O}_5^+ &= \text{Tr} ((f_{\mu\nu}^-)^2), \\ \mathcal{O}_5^- &= \text{Tr} (\hat{f}_{\mu\nu}^+ f^{+\mu\nu}) = \text{Tr} ((f_{\mu\nu}^L)^2 - (f_{\mu\nu}^R)^2). \end{aligned} \quad (\text{A.22})$$

Although two additional operators with four d_μ fields could be included in general,

$$\begin{aligned}\mathcal{O}_{1a}^+ &= \text{Tr}([d_\mu, d_\nu][d^\mu, d^\nu]) = \text{Tr}([d_\mu, d_\nu]_L)^2 + ([d_\mu, d_\nu]_R)^2, \\ \mathcal{O}_{1a}^- &= \text{Tr}([d_\mu, d_\nu]_L)^2 - ([d_\mu, d_\nu]_R)^2,\end{aligned}\quad (\text{A.23})$$

in the particular case of $\text{SO}(5)/\text{SO}(4)$ CH model these operators are redundant or vanishing:

$$\mathcal{O}_{1a}^+ = \frac{1}{2}(\mathcal{O}_2 - \mathcal{O}_1), \quad \mathcal{O}_{1a}^- = 0. \quad (\text{A.24})$$

It is useful to rewrite the operators in eqs. (A.22) and (A.23) in terms of the $\text{SU}(2)_L \times \text{SU}(2)_R$ projections. Defining for shortness,

$$\begin{aligned}\text{LD}_L &= i \text{Tr}(f_{\mu\nu}^L [d_\mu, d_\nu]_L), & \text{RD}_R &= i \text{Tr}(f_{\mu\nu}^R [d_\mu, d_\nu]_R) \\ \text{D}_L^2 &= \text{Tr}([d_\mu, d_\nu]_L [d_\mu, d_\nu]_L), & \text{D}_R^2 &= \text{Tr}([d_\mu, d_\nu]_R [d_\mu, d_\nu]_R),\end{aligned}\quad (\text{A.25})$$

it is possible to write:

$$\begin{aligned}\mathcal{O}_3 &= \text{L}^2 - \text{R}^2 - 2(\text{LD}_L - \text{RD}_R) + (\text{D}_L^2 - \text{D}_R^2), \\ \mathcal{O}_4^+ &= (\text{LD}_L + \text{RD}_R), \\ \mathcal{O}_4^- &= (\text{LD}_L - \text{RD}_R), \\ \mathcal{O}_5^+ &= \text{B}^2, \\ \mathcal{O}_5^- &= \text{L}^2 - \text{R}^2, \\ \mathcal{O}_{1a}^+ &= \text{D}_L^2 + \text{D}_R^2 = \frac{1}{2}(\mathcal{O}_2 - \mathcal{O}_1), \\ \mathcal{O}_{1a}^- &= \text{D}_L^2 - \text{D}_R^2 = 0.\end{aligned}\quad (\text{A.26})$$

The set of operators $\{\mathcal{L}^{(2)}, \mathcal{O}_k, \mathcal{O}_1, \mathcal{O}_2, \mathcal{O}_4^+, \mathcal{O}_4^-, \mathcal{O}_5^+, \mathcal{O}_5^-\}$ constitutes a basis for the $\text{SO}(5)/\text{SO}(4)$ CH model, while the invariants $\{\mathcal{O}_3, \mathcal{O}_{1a}^+, \mathcal{O}_{1a}^-\}$ are redundant or vanishing. In particular, contrary to what is stated in ref. [51], \mathcal{O}_3 is not an independent operator of the basis as it can be expressed as a linear combination of other operators:

$$\mathcal{O}_3 = \mathcal{O}_5^- - 2\mathcal{O}_4^-. \quad (\text{A.27})$$

iv-b) The operator basis for the $\text{SO}(5)/\text{SO}(4)$ CH model presented in ref. [59] is slightly different. Besides $\mathcal{L}^{(2)}$, \mathcal{O}_k , \mathcal{O}_1 and \mathcal{O}_2 , the operators in eq. (A.22) have been substituted by the following ones:¹³

$$\begin{aligned}\mathcal{O}_3'^+ &= \text{Tr}(e_{\mu\nu} e^{\mu\nu}) = \text{Tr}((e_{\mu\nu}^L)^2 + (e_{\mu\nu}^R)^2), \\ \mathcal{O}_3'^- &\equiv \mathcal{O}_3 = \text{Tr}(\hat{e}_{\mu\nu} e^{\mu\nu}) = \text{Tr}((e_{\mu\nu}^L)^2 - (e_{\mu\nu}^R)^2), \\ \mathcal{O}_4'^+ &= i \text{Tr}(e_{\mu\nu} [d^\mu, d^\nu]) = i \text{Tr}((e_{\mu\nu}^L + e_{\mu\nu}^R) [d^\mu, d^\nu]), \\ \mathcal{O}_4'^- &= i \text{Tr}(\hat{e}_{\mu\nu} [d^\mu, d^\nu]) = i \text{Tr}((e_{\mu\nu}^L - e_{\mu\nu}^R) [d^\mu, d^\nu]), \\ \mathcal{O}_5' &\equiv \mathcal{O}_{1a}^- = \text{Tr}([d_\mu, d_\nu]_L)^2 - ([d_\mu, d_\nu]_R)^2.\end{aligned}\quad (\text{A.28})$$

¹³The operators of the basis in ref. [59] will be denoted with a “'” to avoid confusion with the ones in ref. [51].

By rewriting these operators in terms of the $SU(2)_L \times SU(2)_R$ projections, it follows that

$$\begin{aligned}
 \mathcal{O}_3'^+ &= L^2 + R^2 - 2(LD_L + RD_R) + (D_L^2 + D_R^2), \\
 \mathcal{O}_3'^- &= L^2 - R^2 - 2(LD_L - RD_R) + (D_L^2 - D_R^2), \\
 \mathcal{O}_4'^+ &= (LD_L + RD_R) + D_L^2 + D_R^2, \\
 \mathcal{O}_4'^- &= (LD_L - RD_R) + D_L^2 - D_R^2, \\
 \mathcal{O}_5' &= D_L^2 - D_R^2 = 0.
 \end{aligned} \tag{A.29}$$

With respect to the basis in ref. [51], the operator $\mathcal{O}_3'^- = \mathcal{O}_3$ should now be taken as part of the basis, as it is the only one containing the combination $L^2 - R^2$ (\mathcal{O}_5^- does not have a counterpart in this basis). The total number of operators entering the basis is the same as in the previous case: $\{\mathcal{L}^{(2)}, \mathcal{O}_k, \mathcal{O}_1, \mathcal{O}_2, \mathcal{O}_3'^+, \mathcal{O}_3'^-, \mathcal{O}_4'^+, \mathcal{O}_4'^-\}$, as \mathcal{O}_5' is automatically vanishing.

A.3 Comparison with the basis in ref. [49]

As described in ref. [51], the EWSB is induced due to a misalignment between the $SO(4)$ subgroup, left unbroken in the global $SO(5)$ breaking, and the $SO(4)'$ subgroup that contains the SM gauged group. A rotation between these two directions can be defined and it can be parametrised by an angle θ . Accordingly, the $SO(4)$ generators and the $SO(4)'$ ones are connected to each other through the rotation R_θ and, to recover the results in eq. (13) of ref. [51], the following relation between the GB matrices U , introduced in appendix A.2, and Ω should be adopted:

$$U = \Omega R_\theta^\dagger, \tag{A.30}$$

and it follows that

$$U^\dagger \mathbf{D}_\mu U = R_\theta \left(\Omega^\dagger \mathbf{D}_\mu \Omega \right) R_\theta^\dagger \longrightarrow d_\mu = -\frac{i}{2} R_\theta v_\mu R_\theta^\dagger, \quad e_\mu = R_\theta p_\mu R_\theta^\dagger. \tag{A.31}$$

Furthermore, a link between the gauge field strengths $s_{\mu\nu}$ and $f_{\mu\nu}$ can be found:

$$f_{\mu\nu} = R_\theta s_{\mu\nu} R_\theta^\dagger. \tag{A.32}$$

It is now possible to identify the relation among the operator basis in ref. [51] and reported in eq. (A.26) (excluding the redundant operator \mathcal{O}_3) and the operators in eqs. (A.6) and (A.8). A similar discussion can be performed for the operators basis in ref. [59]. Focussing to the case in which the full group $SO(5)$ is gauged, i.e. any source of custodial breaking, SM or beyond, is neglected, it follows that the two bases are equivalent:

$$\begin{aligned}
 \mathcal{L}^{(2)} &\rightarrow -\frac{f^2}{16} \text{Tr}(v_\mu v^\mu), \\
 \mathcal{O}_k &\rightarrow \text{Tr}(s_{\mu\nu} s^{\mu\nu}), \\
 \mathcal{O}_1 &\rightarrow \frac{1}{16} \text{Tr}(v_\mu v^\mu) \text{Tr}(v_\mu v^\mu), \\
 \mathcal{O}_2 &\rightarrow \frac{1}{16} \text{Tr}(v_\mu v_\nu) \text{Tr}(v^\mu v^\nu), \\
 \mathcal{O}_4^+ &\rightarrow -\frac{i}{4} \text{Tr}(s_{\mu\nu} [v^\mu, v^\nu]), \\
 \mathcal{O}_5^+ &\rightarrow 2\text{Tr}(s_{\mu\nu} s^{\mu\nu}) - 2\text{Tr}(s_{\mu\nu}^{\mathcal{R}} s^{\mu\nu}).
 \end{aligned} \tag{A.33}$$

Indeed the last three operators in eq. (A.6), that do not appear in the list above, are vanishing or redundant due to the fact that fermions are neglected in ref. [51] and due to the algebra of the SO(4) generators (see appendix A.2).

In the case in which only the SM symmetry is gauged, introducing then an explicit breaking of the custodial symmetry due to the hypercharge group, the two bases do not coincide anymore:

$$\begin{aligned}
\mathcal{L}^{(2)} &\rightarrow \frac{1}{4} \tilde{\mathcal{A}}_C, \\
\mathcal{O}_k &\rightarrow \tilde{\mathcal{A}}_B + \tilde{\mathcal{A}}_W, \\
\mathcal{O}_1 &\rightarrow \frac{1}{16} \tilde{\mathcal{A}}_4, \\
\mathcal{O}_2 &\rightarrow \frac{1}{16} \tilde{\mathcal{A}}_5, \\
\mathcal{O}_4^+ &\rightarrow -\frac{1}{4} (\tilde{\mathcal{A}}_2 + \tilde{\mathcal{A}}_3), \\
\mathcal{O}_4^- &\rightarrow \frac{1}{4} (\tilde{\mathcal{A}}_2 - \tilde{\mathcal{A}}_3), \\
\mathcal{O}_5^+ &\rightarrow 2 (\tilde{\mathcal{A}}_B + \tilde{\mathcal{A}}_W) - 2 (\tilde{\mathcal{A}}_{B\Sigma} + \tilde{\mathcal{A}}_{W\Sigma} + 2\tilde{\mathcal{A}}_1), \\
\mathcal{O}_5^- &\rightarrow -\tilde{\mathcal{A}}_B + \tilde{\mathcal{A}}_W.
\end{aligned} \tag{A.34}$$

The operators $\mathcal{L}^{(2)}$, \mathcal{O}_1 and \mathcal{O}_2 are in a one-to-one correspondence with the operators $\tilde{\mathcal{A}}_C$, $\tilde{\mathcal{A}}_4$ and $\tilde{\mathcal{A}}_5$; the two operators \mathcal{O}_k and \mathcal{O}_5^- (\mathcal{O}_4^+ and \mathcal{O}_4^-) are connected to two linear independent combinations of $\tilde{\mathcal{A}}_B$ and $\tilde{\mathcal{A}}_W$ ($\tilde{\mathcal{A}}_2$ and $\tilde{\mathcal{A}}_3$); finally, the operator \mathcal{O}_5^+ is connected with a linear combination of five operators of the basis in eq. (A.8), identifying therefore a relation among $\tilde{\mathcal{A}}_{B\Sigma}$, $\tilde{\mathcal{A}}_{W\Sigma}$ and $\tilde{\mathcal{A}}_1$.

In summary, the analysis in this appendix has clarified the connection with previous literature. The differences between the basis presented here and that in ref. [51] are understood in terms of the different sources of custodial breaking assumed:

- Ref. [51] describes an explicit breaking of the SO(4) subgroup (this is encoded in their definition of $\hat{f}_{\mu\nu}^+$). As a result, their basis is composed of eight independent operators.
- This work instead implements an explicit breaking of SO(4)' in the language of ref. [51]. This originates from treating independently the gauge fields \mathbf{W}_μ and \mathbf{B}_μ . This choice closely follows the approach of Appelquist and Longhitano of considering all possible SM $SU(2)_L \times U(1)_Y$ invariant operators: operators $\tilde{\mathcal{A}}_{W\Sigma}$ and $\tilde{\mathcal{A}}_{B\Sigma}$ arise then as independent structures. As a consequence, the basis requires ten independent operators.

Open Access. This article is distributed under the terms of the Creative Commons Attribution License ([CC-BY 4.0](https://creativecommons.org/licenses/by/4.0/)), which permits any use, distribution and reproduction in any medium, provided the original author(s) and source are credited.

References

- [1] ATLAS collaboration, *Observation of a new particle in the search for the Standard Model Higgs boson with the ATLAS detector at the LHC*, *Phys. Lett. B* **716** (2012) 1 [[arXiv:1207.7214](#)] [[INSPIRE](#)].
- [2] CMS collaboration, *Observation of a new boson at a mass of 125 GeV with the CMS experiment at the LHC*, *Phys. Lett. B* **716** (2012) 30 [[arXiv:1207.7235](#)] [[INSPIRE](#)].
- [3] F. Englert and R. Brout, *Broken Symmetry and the Mass of Gauge Vector Mesons*, *Phys. Rev. Lett.* **13** (1964) 321 [[INSPIRE](#)].
- [4] P.W. Higgs, *Broken symmetries, massless particles and gauge fields*, *Phys. Lett.* **12** (1964) 132 [[INSPIRE](#)].
- [5] P.W. Higgs, *Broken Symmetries and the Masses of Gauge Bosons*, *Phys. Rev. Lett.* **13** (1964) 508 [[INSPIRE](#)].
- [6] D.B. Kaplan and H. Georgi, *SU(2) \times U(1) Breaking by Vacuum Misalignment*, *Phys. Lett. B* **136** (1984) 183 [[INSPIRE](#)].
- [7] D.B. Kaplan, H. Georgi and S. Dimopoulos, *Composite Higgs Scalars*, *Phys. Lett. B* **136** (1984) 187 [[INSPIRE](#)].
- [8] T. Banks, *Constraints on SU(2) \times U(1) breaking by vacuum misalignment*, *Nucl. Phys. B* **243** (1984) 125 [[INSPIRE](#)].
- [9] H. Georgi, D.B. Kaplan and P. Galison, *Calculation of the Composite Higgs Mass*, *Phys. Lett. B* **143** (1984) 152 [[INSPIRE](#)].
- [10] H. Georgi and D.B. Kaplan, *Composite Higgs and Custodial SU(2)*, *Phys. Lett. B* **145** (1984) 216 [[INSPIRE](#)].
- [11] M.J. Dugan, H. Georgi and D.B. Kaplan, *Anatomy of a Composite Higgs Model*, *Nucl. Phys. B* **254** (1985) 299 [[INSPIRE](#)].
- [12] N. Arkani-Hamed, A.G. Cohen and H. Georgi, *Electroweak symmetry breaking from dimensional deconstruction*, *Phys. Lett. B* **513** (2001) 232 [[hep-ph/0105239](#)] [[INSPIRE](#)].
- [13] N. Arkani-Hamed, A.G. Cohen, E. Katz and A.E. Nelson, *The Littlest Higgs*, *JHEP* **07** (2002) 034 [[hep-ph/0206021](#)] [[INSPIRE](#)].
- [14] R. Contino, Y. Nomura and A. Pomarol, *Higgs as a holographic pseudoGoldstone boson*, *Nucl. Phys. B* **671** (2003) 148 [[hep-ph/0306259](#)] [[INSPIRE](#)].
- [15] K. Agashe, R. Contino and A. Pomarol, *The Minimal composite Higgs model*, *Nucl. Phys. B* **719** (2005) 165 [[hep-ph/0412089](#)] [[INSPIRE](#)].
- [16] R. Contino, L. Da Rold and A. Pomarol, *Light custodians in natural composite Higgs models*, *Phys. Rev. D* **75** (2007) 055014 [[hep-ph/0612048](#)] [[INSPIRE](#)].
- [17] B. Gripaios, A. Pomarol, F. Riva and J. Serra, *Beyond the Minimal Composite Higgs Model*, *JHEP* **04** (2009) 070 [[arXiv:0902.1483](#)] [[INSPIRE](#)].
- [18] A. Manohar and H. Georgi, *Chiral Quarks and the Nonrelativistic Quark Model*, *Nucl. Phys. B* **234** (1984) 189 [[INSPIRE](#)].
- [19] R. Contino, *The Higgs as a Composite Nambu-Goldstone Boson*, [arXiv:1005.4269](#) [[INSPIRE](#)].

- [20] O. Matsedonskyi, G. Panico and A. Wulzer, *Light Top Partners for a Light Composite Higgs*, *JHEP* **01** (2013) 164 [[arXiv:1204.6333](#)] [[INSPIRE](#)].
- [21] A. Pomarol and F. Riva, *The Composite Higgs and Light Resonance Connection*, *JHEP* **08** (2012) 135 [[arXiv:1205.6434](#)] [[INSPIRE](#)].
- [22] M. Redi and A. Tesi, *Implications of a Light Higgs in Composite Models*, *JHEP* **10** (2012) 166 [[arXiv:1205.0232](#)] [[INSPIRE](#)].
- [23] D. Marzocca, M. Serone and J. Shu, *General Composite Higgs Models*, *JHEP* **08** (2012) 013 [[arXiv:1205.0770](#)] [[INSPIRE](#)].
- [24] G. Panico, M. Redi, A. Tesi and A. Wulzer, *On the Tuning and the Mass of the Composite Higgs*, *JHEP* **03** (2013) 051 [[arXiv:1210.7114](#)] [[INSPIRE](#)].
- [25] D. Pappadopulo, A. Thamm and R. Torre, *A minimally tuned composite Higgs model from an extra dimension*, *JHEP* **07** (2013) 058 [[arXiv:1303.3062](#)] [[INSPIRE](#)].
- [26] R. Contino, C. Grojean, D. Pappadopulo, R. Rattazzi and A. Thamm, *Strong Higgs Interactions at a Linear Collider*, *JHEP* **02** (2014) 006 [[arXiv:1309.7038](#)] [[INSPIRE](#)].
- [27] O. Matsedonskyi, F. Riva and T. Vantalón, *Composite Charge 8/3 Resonances at the LHC*, *JHEP* **04** (2014) 059 [[arXiv:1401.3740](#)] [[INSPIRE](#)].
- [28] T. Appelquist and C.W. Bernard, *Strongly Interacting Higgs Bosons*, *Phys. Rev. D* **22** (1980) 200 [[INSPIRE](#)].
- [29] A.C. Longhitano, *Heavy Higgs Bosons in the Weinberg-Salam Model*, *Phys. Rev. D* **22** (1980) 1166 [[INSPIRE](#)].
- [30] A.C. Longhitano, *Low-Energy Impact of a Heavy Higgs Boson Sector*, *Nucl. Phys. B* **188** (1981) 118 [[INSPIRE](#)].
- [31] F. Feruglio, *The Chiral approach to the electroweak interactions*, *Int. J. Mod. Phys. A* **8** (1993) 4937 [[hep-ph/9301281](#)] [[INSPIRE](#)].
- [32] T. Appelquist and G.-H. Wu, *The Electroweak chiral Lagrangian and new precision measurements*, *Phys. Rev. D* **48** (1993) 3235 [[hep-ph/9304240](#)] [[INSPIRE](#)].
- [33] B. Grinstein and M. Trott, *A Higgs-Higgs bound state due to new physics at a TeV*, *Phys. Rev. D* **76** (2007) 073002 [[arXiv:0704.1505](#)] [[INSPIRE](#)].
- [34] R. Contino, C. Grojean, M. Moretti, F. Piccinini and R. Rattazzi, *Strong Double Higgs Production at the LHC*, *JHEP* **05** (2010) 089 [[arXiv:1002.1011](#)] [[INSPIRE](#)].
- [35] A. Azatov, R. Contino and J. Galloway, *Model-Independent Bounds on a Light Higgs*, *JHEP* **04** (2012) 127 [Erratum *ibid.* **1304** (2013) 140] [[arXiv:1202.3415](#)] [[INSPIRE](#)].
- [36] R. Alonso, M.B. Gavela, L. Merlo, S. Rigolin and J. Yepes, *The Effective Chiral Lagrangian for a Light Dynamical “Higgs Particle”*, *Phys. Lett. B* **722** (2013) 330 [Erratum *ibid.* **B 726** (2013) 926] [[arXiv:1212.3305](#)] [[INSPIRE](#)].
- [37] M.B. Gavela et al., *CP violation with a dynamical Higgs*, *JHEP* **1410** (2014) 44 [[arXiv:1406.6367](#)] [[INSPIRE](#)].
- [38] G. Buchalla and O. Catà, *Effective Theory of a Dynamically Broken Electroweak Standard Model at NLO*, *JHEP* **07** (2012) 101 [[arXiv:1203.6510](#)] [[INSPIRE](#)].
- [39] R. Alonso, M.B. Gavela, L. Merlo, S. Rigolin and J. Yepes, *Minimal Flavour Violation with Strong Higgs Dynamics*, *JHEP* **06** (2012) 076 [[arXiv:1201.1511](#)] [[INSPIRE](#)].

- [40] R. Alonso, M.B. Gavela, L. Merlo, S. Rigolin and J. Yepes, *Flavor with a light dynamical “Higgs particle”*, *Phys. Rev. D* **87** (2013) 055019 [[arXiv:1212.3307](#)] [[INSPIRE](#)].
- [41] G. Buchalla, O. Catà and C. Krause, *Complete Electroweak Chiral Lagrangian with a Light Higgs at NLO*, *Nucl. Phys. B* **880** (2014) 552 [[arXiv:1307.5017](#)] [[INSPIRE](#)].
- [42] I. Brivio et al., *Disentangling a dynamical Higgs*, *JHEP* **03** (2014) 024 [[arXiv:1311.1823](#)] [[INSPIRE](#)].
- [43] I. Brivio et al., *Higgs ultraviolet softening*, [arXiv:1405.5412](#) [[INSPIRE](#)].
- [44] G. Isidori and M. Trott, *Higgs form factors in Associated Production*, *JHEP* **02** (2014) 082 [[arXiv:1307.4051](#)] [[INSPIRE](#)].
- [45] G. Cvetič and R. Kogerler, *Fermionic Couplings in an Electroweak Theory With Nonlinear Spontaneous Symmetry Breaking*, *Nucl. Phys. B* **328** (1989) 342 [[INSPIRE](#)].
- [46] E.E. Jenkins, A.V. Manohar and M. Trott, *Naive Dimensional Analysis Counting of Gauge Theory Amplitudes and Anomalous Dimensions*, *Phys. Lett. B* **726** (2013) 697 [[arXiv:1309.0819](#)] [[INSPIRE](#)].
- [47] S.R. Coleman, J. Wess and B. Zumino, *Structure of phenomenological Lagrangians. 1.*, *Phys. Rev.* **177** (1969) 2239 [[INSPIRE](#)].
- [48] C.G. Callan Jr., S.R. Coleman, J. Wess and B. Zumino, *Structure of phenomenological Lagrangians. 2.*, *Phys. Rev.* **177** (1969) 2247 [[INSPIRE](#)].
- [49] M. Frigerio, A. Pomarol, F. Riva and A. Urbano, *Composite Scalar Dark Matter*, *JHEP* **07** (2012) 015 [[arXiv:1204.2808](#)] [[INSPIRE](#)].
- [50] D. Marzocca and A. Urbano, *Composite Dark Matter and LHC Interplay*, *JHEP* **07** (2014) 107 [[arXiv:1404.7419](#)] [[INSPIRE](#)].
- [51] R. Contino, D. Marzocca, D. Pappadopulo and R. Rattazzi, *On the effect of resonances in composite Higgs phenomenology*, *JHEP* **10** (2011) 081 [[arXiv:1109.1570](#)] [[INSPIRE](#)].
- [52] PARTICLE DATA GROUP collaboration, J. Beringer et al., *Review of Particle Physics (RPP)*, *Phys. Rev. D* **86** (2012) 010001 [[INSPIRE](#)].
- [53] W. Buchmüller and D. Wyler, *Effective Lagrangian Analysis of New Interactions and Flavor Conservation*, *Nucl. Phys. B* **268** (1986) 621 [[INSPIRE](#)].
- [54] B. Grzadkowski, M. Iskrzynski, M. Misiak and J. Rosiek, *Dimension-Six Terms in the Standard Model Lagrangian*, *JHEP* **10** (2010) 085 [[arXiv:1008.4884](#)] [[INSPIRE](#)].
- [55] K. Hagiwara, S. Ishihara, R. Szalapski and D. Zeppenfeld, *Low-energy effects of new interactions in the electroweak boson sector*, *Phys. Rev. D* **48** (1993) 2182 [[INSPIRE](#)].
- [56] K. Hagiwara, T. Hatsukano, S. Ishihara and R. Szalapski, *Probing nonstandard bosonic interactions via W boson pair production at lepton colliders*, *Nucl. Phys. B* **496** (1997) 66 [[hep-ph/9612268](#)] [[INSPIRE](#)].
- [57] G.F. Giudice, C. Grojean, A. Pomarol and R. Rattazzi, *The Strongly-Interacting Light Higgs*, *JHEP* **06** (2007) 045 [[hep-ph/0703164](#)] [[INSPIRE](#)].
- [58] M.B. Gavela, K. Kanshin, P.A.N. Machado and S. Saa, *On the renormalization of the electroweak chiral lagrangian with a light higgs*, [arXiv:1409.1571](#) [[INSPIRE](#)].
- [59] A. Azatov, R. Contino, A. Di Iura and J. Galloway, *New Prospects for Higgs Compositeness in $h \rightarrow Z\gamma$* , *Phys. Rev. D* **88** (2013) 075019 [[arXiv:1308.2676](#)] [[INSPIRE](#)].

The complete HEFT Lagrangian after the LHC Run I

This Chapter contains the publication in Ref. [31]. This work extends the analysis of Ref. [28] (Chapter 4) with the addition of fermionic operators and of CP-odd interactions. The basis for the bosonic sector has been obtained merging the sets of Refs. [28] (CP-even) and Ref. [105] (CP-odd), while the invariants for the fermionic sectors have been constructed independently, assuming baryon and lepton number conservation. Subsequently, the equations of motion have been employed to remove redundancies across the two sectors, leaving a complete basis composed, altogether, of 148 independent flavor-blind operators (188 if right-handed neutrinos are included in the spectrum), listed in Sec. 2 of this chapter. The correspondence between this basis and the linear $d = 6$ ones in Refs. [98] and [111, 112] is reported in Table 9.

Sec. 3 contains a phenomenological study that follows the same lines as that in Chapter 4. In this case, electroweak precision data allow to constrain up to 8 combinations of fermionic operators, plus 3 bosonic ones. An interesting feature is the simultaneous presence of independent contributions to the oblique parameter U and to the Fermi constant G_F . This condition creates a blind direction in the parameter space that eventually weakens the bounds on T and U by more than a factor 20 compared to the results of the standard fit reported in Eq. (2.2.55). The impact on Higgs physics has been studied with a fit similar to that in Chapter 4 but with an enlarged parameter space: here we include the three heavy Yukawa couplings Y_t , Y_b , Y_τ and the coefficient a_{17} that enters ZZh and $Z\gamma h$ couplings. As for the discriminating signals between the two EFTs, it is worth noticing how the improvement in Higgs data (in particular the information from kinematic distributions in Higgs decays) impacts on the bounds drawn in Fig. 3, compared to the same plot produced two years earlier, namely Fig. 2 of Chapter 4. Finally, this work contains the first systematic analysis of the validity of the chiral EFT, illustrated in Sec. 4 of this chapter.

A final remark: the notation adopted here differs slightly from that of Chapter 4: the explicit dependence on the ξ parameter has been omitted and the operators have been normalized according to the prescriptions of Naive Dimensional Analysis. Moreover, the bosonic operators \mathcal{P}_C and \mathcal{P}_H are not present due to a different choice in the parameterization of the LO Lagrangian. Another major difference with Ref. [28] originates from a modification in the counting rules adopted in the construction of the NLO basis, which in this case is based on the results of Ref. [103], that were not available at the time of publication of the previous paper. The main adjustment is the inclusion in the NLO basis of the operators \mathcal{P}_{WWW} and \mathcal{P}_{GGG} , in spite of the fact that they technically contain six derivatives. More details can be found in the text.

The Complete HEFT Lagrangian after the LHC Run I

I. Brivio ^{a)}, J. Gonzalez–Fraile ^{b)}, M. C. Gonzalez–Garcia ^{c),d),e)}, L. Merlo ^{a)}

^{a)} Departamento de Física Teórica and Instituto de Física Teórica, IFT-UAM/CSIC,
Universidad Autónoma de Madrid, Cantoblanco, 28049, Madrid, Spain

^{b)} Institut für Theoretische Physik, Universität Heidelberg, Germany

^{c)} C.N. Yang Institute for Theoretical Physics and Department of Physics and Astronomy, SUNY at
Stony Brook, Stony Brook, NY 11794-3840, USA

^{d)} Departament d'Estructura i Constituents de la Matèria and ICC-UB, Universitat de Barcelona, 647
Diagonal, E-08028 Barcelona, Spain

^{e)} Institució Catalana de Recerca i Estudis Avançats (ICREA)

E-mail: ilaria.brivio@uam.es, fraile@thphys.uni-heidelberg.de,
concha@insti.physics.sunysb.edu, luca.merlo@uam.es

Abstract

The complete effective chiral Lagrangian for a dynamical Higgs is presented and constrained by means of a global analysis including electroweak precision data together with Higgs and triple gauge boson coupling data from the LHC Run I. The operators' basis up to next-to-leading order in the expansion consists of 148 (188 considering right-handed neutrinos) flavour universal terms and it is presented here making explicit the custodial nature of the operators. This effective Lagrangian provides the most general description of the physical Higgs couplings once the electroweak symmetry is assumed, and it allows for deviations from the $SU(2)_L$ doublet nature of the Standard Model Higgs. The comparison with the effective linear Lagrangian constructed with an exact $SU(2)_L$ doublet Higgs and considering operators with at most canonical dimension six is presented. A promising strategy to disentangle the two descriptions consists in analysing i) anomalous signals present only in the chiral Lagrangian and not expected in the linear one, that are potentially relevant for LHC searches, and ii) decorrelation effects between observables that are predicted to be correlated in the linear case and not in the chiral one. The global analysis presented here, that includes several kinematic distributions, is crucial for reducing the allowed parameter space and for controlling the correlations between parameters. This improves previous studies aimed at investigating the Higgs Nature and the origin of the electroweak symmetry breaking.

Contents

1	Introduction	2
2	The Complete HEFT Lagrangian	4
2.1	The NLO Lagrangian	7
2.2	NLO basis: bosonic sector $\Delta\mathcal{L}_{\text{bos}}$	9
2.2.1	CP even bosonic basis $\Delta\mathcal{L}_{\text{bos}}^{CP}$	9
2.2.2	CP odd bosonic basis $\Delta\mathcal{L}_{\text{bos}}^{CP}$	11
2.3	NLO basis: fermionic sector $\Delta\mathcal{L}_{\text{fer}}$	12
2.3.1	Single fermionic current $\Delta\mathcal{L}_{2F}$	13
2.3.2	Four-fermion operators $\Delta\mathcal{L}_{4F}$	15
2.4	Comparison with the SMEFT basis	17
3	Phenomenology	20
3.1	Renormalisation procedure	20
3.2	Constraints from EWPD	21
3.3	Effects in Higgs Physics	26
3.4	Triple gauge boson couplings and Higgs interplay	30
4	Higher order operators and expansion validity	33
5	Conclusions	36
A	Additional operators in presence of RH neutrinos	38
B	Removal of $\mathcal{F}(\text{h})$ from the Higgs and fermions kinetic terms	39
C	Construction of the fermionic basis	41
C.1	Useful identities	41
C.2	Construction of $\Delta\mathcal{L}_{2F}$	42
C.3	Construction of $\Delta\mathcal{L}_{4F}$	43
D	Application of the Equations of Motion	46
E	Feynman rules	49

1 Introduction

The discovery of a resonance at LHC [1, 2] compatible with the Standard Model (SM) scalar boson (“Higgs” for short) [3–5] opened a new era in particle physics. Now, the on going LHC measurements of the Higgs properties are a crucial step to understand the nature of the Higgs boson and of the Electroweak (EW) symmetry breaking (EWSB).

Without entering into details of specific scenarios, the formalism of Effective Field Theories (EFT) represents an optimal tool for studying the phenomenology of the Higgs sector. In particular, an appropriate description of scenarios in which the Higgs belongs to an elementary $SU(2)$ doublet is provided by the Standard Model EFT (SMEFT). This consists of operators constructed with the SM spectrum, invariant under the Lorentz and SM gauge symmetries and respecting an expansion in canonical mass dimensions d . Assuming lepton and baryon number conservation, the first corrections to the SM are provided by operators of dimension six [6, 7], suppressed by two powers of the cutoff scale Λ . Weakly coupled theories are the typical underlying scenarios that can be matched to the SMEFT (also referred to as “linear” Lagrangian) at low energy.

Scenarios where the Higgs does not belong to an elementary exact $SU(2)_L$ doublet are still allowed within the current experimental accuracy. This is the case, for example, of Composite Higgs models [8–12] or dilaton constructions [13, 14]. It is then fundamental and necessary to identify observables that allow to disentangle these different possibilities. When the Higgs is not required to belong to an exact EW doublet, instead, a useful tool is the so-called Higgs EFT (HEFT) (also dubbed “chiral” Lagrangian). The main difference between SMEFT and HEFT resides in the fact that, in the latter formalism, the physical Higgs h and the ensemble of the three EW Goldstone bosons $\vec{\pi}$ are treated as independent objects, rather than being collectively described by the Higgs doublet. In particular, the physical Higgs h is assigned to a singlet representation of the SM gauge groups. The Goldstone bosons’ sector has been studied deeply in the past [15–18] in the context of Higgs-less EWSB scenarios. These works were the first to describe the GBs by means of a dimensionless unitary matrix transforming as a bi-doublet of the global symmetry $SU(2)_L \times SU(2)_R$,

$$\mathbf{U}(x) \equiv e^{i\sigma_a \pi^a(x)/f_\pi}, \quad \mathbf{U}(x) \rightarrow L\mathbf{U}(x)R^\dagger, \quad (1.1)$$

being f_π the scale associated to the SM GBs, and L, R the $SU(2)_{L,R}$ transformations. After EWSB, the invariance under the group $SU(2)_L \times SU(2)_R$ is broken down to the diagonal $SU(2)_C$, commonly called Custodial symmetry, and explicitly broken by the gauging of the hypercharge $U(1)_Y$ and by the fermion mass splittings. It is customary to introduce two objects, the vector and scalar chiral fields, that transform in the adjoint of $SU(2)_L$. They are defined respectively as

$$\mathbf{V}_\mu \equiv (\mathbf{D}_\mu \mathbf{U})\mathbf{U}^\dagger, \quad \mathbf{T} \equiv \mathbf{U}\sigma_3\mathbf{U}^\dagger, \quad (1.2)$$

where

$$\mathbf{D}_\mu \mathbf{U}(x) \equiv \partial_\mu \mathbf{U}(x) + igW_\mu(x)\mathbf{U}(x) - \frac{ig'}{2}B_\mu(x)\mathbf{U}(x)\sigma_3. \quad (1.3)$$

Unlike \mathbf{V}_μ , \mathbf{T} is not invariant under $SU(2)_C$ and can therefore be considered a custodial symmetry breaking spurion. The bosonic Higgs-less EW chiral Lagrangian can then be constructed with \mathbf{V}_μ , \mathbf{T} and the gauge boson field strengths as building blocks, and the tower of invariant operators shall be organised according to a chiral (derivative) expansion [19].

In the last decade, the EW chiral Lagrangian has been extended with the introduction of a light physical Higgs h [20–28], treated as an isosinglet of the SM gauge symmetries. The dependence on the h field is customarily encoded in generic functions $\mathcal{F}(h)$, that are used as building blocks for the construction of the effective operators. These functions are made adimensional by implicitly weighting the insertions of the Higgs field with an opportune suppression scale f_h , so that one may rewrite the dependence as $\mathcal{F}(h/f_h)$. It is worth underlining that the dependence on the structure $(1 + h/v)$, where v is the EW vacuum expectation value (vev), that characterises the SMEFT Lagrangian is lost in the HEFT and substituted by a generic h/f_h expansion.

The typical underlying scenarios that can be described at low-energy in terms of the matrix $\mathbf{U}(x)$, the Higgs functions $\mathcal{F}(h)$ and the rest of the SM fields, are those of Composite Higgs models [8–12]. These assume the existence of some strong (“ultracoulour”) interaction at a high energy, and initially invariant under some global symmetry group \mathcal{G} . At the scale Λ_s , the formation of ultracoulour condensates breaks spontaneously this invariance, leaving a residual symmetry \mathcal{H} that can embed the EW group. This triggers the appearance of a certain number of Goldstone bosons, among which three can be identified with the would-be GBs of the EW group and a fourth one with the Higgs. In such scenarios, all the SM scalars are naturally associated to the same scale $f_\pi = f_h \equiv f$, with $\Lambda_s \leq 4\pi f$. Spontaneous EWSB is triggered by some explicit breaking of the \mathcal{H} symmetry (provided either by external symmetries [8] or by gauging the SM symmetry together with fermion interactions [11]) and takes place in a second stage. At this level, the Higgs field acquires a vev $\langle h \rangle$ that does not need to coincide with the EW scale v , defined by the EW gauge boson mass: the three quantities v , f and $\langle h \rangle$ are instead related by a model-dependent function. The splitting between v and f constitutes the well-known fine-tuning of Composite Higgs models. It is usually expressed in terms of the parameter

$$\xi \equiv \frac{v^2}{f^2}, \quad (1.4)$$

that substantially quantifies the degree of non-linearity of the Higgs dynamics. The low-energy projection of composite Higgs models can be described by the HEFT Lagrangian [29, 30] and the matching conditions allow to write the low-energy effective operator coefficients in terms of the high-energy parameters, and the generic functions $\mathcal{F}(h)$ as trigonometric functions of h/f . The HEFT Lagrangian can also be used to describe the SMEFT [22–25, 29–31], after identifying the operator coefficients of the effective Lagrangians and writing all the $\mathcal{F}(h)$ functions in terms of $(1 + h/v)$. Dilaton constructions [13, 14] or even more exotic models, where the Higgs is an EW singlet, can also be described by the HEFT Lagrangian.

Without assuming any specific underlying scenario or comparing with HEFT, the v/f_h and v/f_π parameters are not physical and can be reabsorbed in the operators coefficients

and in the coefficients of the $\mathcal{F}(h)$ functions. This is tantamount to assuming

$$f_\pi = v, \quad f_h = v, \quad (1.5)$$

which ensures canonical kinetic terms for the GBs and fixes the correct order of magnitude for the gauge bosons masses, without fine-tunings. This notation will be employed in what follows, unless otherwise specified.

The disparities between the SMEFT and the HEFT originate from the different nature of the building blocks used in the construction of the effective operators. The independence between the GB field $\mathbf{U}(x)$ and the physical h , together with the fact that h does not transform under the SM gauge symmetries, leads to a different ordering of the chiral effective operators compared to the linear ones. As a result, at any given order in the expansion the number of chiral independent operators is much larger than in the SMEFT case. The corresponding phenomenology, focussing on the bosonic part of the Lagrangian, has been studied in Refs. [24,25], where signatures that may allow to discriminate between an elementary and a dynamical Higgs have also been identified. These signatures include sets of couplings that are predicted to be correlated in an elementary Higgs scenario but are generically decorrelated in the dynamical case, as well as effects that are expected to be suppressed in the linear realisation but may appear at the lowest order in the chiral expansion.

The complete non-redundant HEFT Lagrangian including both bosonic and fermionic operators has been constructed in this work and is presented in Sect. 2, making explicit the custodial nature of the operators. The HEFT basis is formed by 148 independent flavour universal operators altogether, whose extension to generic flavour contractions is straightforward. The Lagrangian does not account for the presence of right-handed neutrinos, whose inclusion in the spectrum would imply the addition 40 extra operators to the basis, listed in Appendix A. Section 2 also contains a comparison between the HEFT Lagrangian and the SMEFT one, while a phenomenological analysis of the HEFT basis is presented in Sect. 3. The study considers all the available collider data, which includes electroweak precision measurements and Higgs and triple gauge boson vertex (TGV) data from the LHC Run I. To our knowledge, this is the first time that such analysis has been done for the complete HEFT description. Finally, Sect. 4, contains a discussion on the impact of higher order operators: a set of invariants that may become relevant at the increased energies foreseen for the LHC and future colliders is also pointed out. The conclusions are presented in Sect. 5, while some more technical details are deferred to the Appendices, together with the Feynman Rules for the CP-even subset of HEFT operators.

2 The Complete HEFT Lagrangian

In this section we review the construction of the HEFT Lagrangian, in a notation similar to that of Refs. [22–25, 31, 32]. The bosonic building blocks are the gauge field strengths $B_{\mu\nu}$, $W_{\mu\nu}$, $G_{\mu\nu}$, the vector and scalar chiral fields \mathbf{V}_μ and \mathbf{T} defined in Eq. (1.2) and the functions $\mathcal{F}(h)$ introduced in the previous section. The SM fermions are conveniently

grouped into doublets of the global $SU(2)_{L,R}$ symmetries:

$$Q_L = \begin{pmatrix} U_L \\ D_L \end{pmatrix}, \quad Q_R = \begin{pmatrix} U_R \\ D_R \end{pmatrix}, \quad L_L = \begin{pmatrix} \nu_L \\ E_L \end{pmatrix}, \quad L_R = \begin{pmatrix} 0 \\ E_R \end{pmatrix}. \quad (2.1)$$

This choice allows to have a more compact notation for the fermionic operators. The $SU(2)_R$ doublet structure can be easily broken with the insertion of the custodial symmetry breaking spurion \mathbf{T} . Notice that the L_R doublet only includes right-handed charged leptons. The inclusion of right-handed neutrinos requires an extension of the fermionic basis presented in Sec. 2.3 with the addition of the operators listed in App. A.

The HEFT Lagrangian can be written as a sum of two terms,

$$\mathcal{L}_{\text{HEFT}} \equiv \mathcal{L}_0 + \Delta\mathcal{L}, \quad (2.2)$$

where the first term contains the leading order (LO) operators and the second one accounts for new interactions and for deviations from the LO.

The LO Lagrangian includes the kinetic terms for all the particles in the spectrum, the Yukawa couplings and the scalar potential¹:

$$\begin{aligned} \mathcal{L}_0 = & -\frac{1}{4}\mathcal{G}_{\mu\nu}^\alpha\mathcal{G}^{\alpha\mu\nu} - \frac{1}{4}W_{\mu\nu}^a W^{a\mu\nu} - \frac{1}{4}B_{\mu\nu}B^{\mu\nu} + \\ & + \frac{1}{2}\partial_\mu h \partial^\mu h - \frac{v^2}{4}\text{Tr}(\mathbf{V}_\mu\mathbf{V}^\mu)\mathcal{F}_C(h) - V(h) + \\ & + i\bar{Q}_L \not{D} Q_L + i\bar{Q}_R \not{D} Q_R + i\bar{L}_L \not{D} L_L + i\bar{L}_R \not{D} L_R + \\ & - \frac{v}{\sqrt{2}}(\bar{Q}_L \mathbf{U} \mathcal{Y}_Q(h) Q_R + \text{h.c.}) - \frac{v}{\sqrt{2}}(\bar{L}_L \mathbf{U} \mathcal{Y}_L(h) L_R + \text{h.c.}) + \\ & - \frac{g_s^2}{16\pi^2} \lambda_s \mathcal{G}_{\mu\nu}^\alpha \tilde{\mathcal{G}}^{\alpha\mu\nu}, \end{aligned} \quad (2.3)$$

where $\tilde{\mathcal{G}}^{\mu\nu} \equiv \frac{1}{2}\epsilon^{\mu\nu\rho\sigma}\mathcal{G}_{\rho\sigma}$. The first line describes the kinetic terms of the gauge bosons; the second line contains the Higgs and Goldstone bosons' kinetic term, the scalar potential, and the mass terms for the EW gauge bosons; the third line presents the kinetic terms for all the fermions, while the fourth line accounts for the Yukawa interactions. Finally, the last line contains the theta term of QCD. The function $\mathcal{F}_C(h)$ appearing in the kinetic term for the GBs can be expanded as

$$\mathcal{F}_C(h) = 1 + 2a_C \frac{h}{v} + b_C \frac{h^2}{v^2} + \dots \quad (2.4)$$

where the dots account for higher powers of (h/v) . For the the phenomenological analysis it is convenient to single out the BSM part of the coefficients a_C , b_C , using the notation

$$a_C = 1 + \Delta a_C, \quad b_C = 1 + \Delta b_C, \quad (2.5)$$

where Δa_C , Δb_C will be assumed to be of the same order as the coefficients accompanying the operators appearing in $\Delta\mathcal{L}$. The functions $\mathcal{Y}_{Q,L}(h)$ appearing in the Yukawa couplings

¹Comments on the construction of the LO Lagrangian in Eq. (2.3) are given in App. B.

have an analogous structure to $\mathcal{F}_C(h)$:

$$\mathcal{Y}_Q(h) \equiv \text{diag} \left(\sum_n Y_U^{(n)} \frac{h^n}{v^n}, \sum_n Y_D^{(n)} \frac{h^n}{v^n} \right), \quad \mathcal{Y}_L(h) \equiv \text{diag} \left(0, \sum_n Y_\ell^{(n)} \frac{h^n}{v^n} \right). \quad (2.6)$$

The $n = 0$ terms yield fermion masses, while the higher orders describe the interaction with n insertions of the Higgs field h , accounting in general for non-aligned contributions.

The kinetic terms of the fermions and of the physical Higgs are not accompanied by any $\mathcal{F}(h)$ since, as shown in App. B, it is always possible to reabsorb their contributions inside the generic functions $\mathcal{F}_C(h)$ and $\mathcal{Y}_{Q,L}(h)$. This can be done either via a field redefinition or, alternatively, applying the Equations of Motion (EOMs) (the two procedures are *not* equivalent in general, but lead to the same result at first order in the deviations from the LO). Moreover, the kinetic terms of the gauge bosons in the first line of Eq. (2.3) do not come associated with any $\mathcal{F}(h)$, assuming that the transverse components of the gauge fields, described by the gauge field strength, do not couple strongly to the Higgs sector. These couplings can be neglected at the LO and be considered, instead, at the next-to-leading order (NLO).

$\Delta\mathcal{L}$ contains higher order operators with respect to those appearing in \mathcal{L}_0 . The precise ordering of these operators depends on the choice of a specific power counting rule. The HEFT can be seen as a fusion of two theories, the chiral perturbation approach associated to the SM GBs – i.e. the longitudinal components of the gauge bosons – and the traditional linear description that applies to the transverse components of the gauge bosons and to fermions. The physical h should also undergo the chiral perturbation description as it enters in the Lagrangian via the adimensional functions $\mathcal{F}(h)$: the latter can be interpreted as playing the same role as the adimensional GB matrix field $\mathbf{U}(x)$. Indeed, in concrete Composite Higgs models, the pseudo-GB nature of the Higgs forces the $\mathcal{F}(h)$ functions to take trigonometric structures [29]. Being the HEFT a merging between linear and chiral descriptions, the counting rules which apply singularly to each of the expansions hold simultaneously for the HEFT [33]. As a result, the LO Lagrangian in Eq. (2.3) itself does not strictly respect the chiral expansion: \mathcal{L}_0 contains both operators with two derivatives and the gauge boson kinetic terms, which has four derivatives; at the same time, some two-derivative operators have been excluded from the LO. On the other hand, \mathcal{L}_0 does not even follow an expansion in canonical dimensions, as for instance the Yukawa interactions and the gauge boson mass term present an infinite series of h legs, contrary to all the other terms in the LO Lagrangian.

The renormalisability conditions are also different in the two descriptions. In the linear expansion an n -loop diagram containing one single $d = 6$ vertex generates divergent contributions that can be reabsorbed by other $d = 6$ operators and do not require the introduction of any higher-dimensional operator. On the contrary, in the chiral case, 1-loop diagrams with n insertions of a two-derivative coupling, usually listed in the LO Lagrangian, produce divergences that require the introduction of operators with four-derivatives, which generically constitute the NLO Lagrangian.

Finally, the HEFT presents an additional aspect that makes it hard to identify a proper counting rule: the presence of multiple scales. Besides the cut-off of the theory Λ , one should consider the presence of the GB scale f_π and of the h -scale f_h . Although it may

happen that the last two coincide with $f_\pi = f_h = f$ and that they are related to the first one by the constraint $\Lambda \leq 4\pi f$ (which is the case in composite Higgs models), the three scales are in principle independent and associated to different physical quantities. On top of this, one should not forget the fine-tuning associated to the EW scale v and parametrised by ξ defined in Eq. (1.4). In practice, the counting rule associated to the HEFT depends on more than one expansion parameters and may vary depending on the typical energy scale of the observables considered in the phenomenological analysis.

In conclusion, rather than basing the choice of the NLO Lagrangian operators on a sophisticated counting rule whose applicability is not valid in full generality, here the selection is performed with the following strategy. An NLO operator should satisfy at least one of the criteria below:

- It is necessary for reabsorbing 1-loop divergences arising from the renormalisation of \mathcal{L}_0 .
- It presents the same suppression as the operators in the first class and receives finite 1-loop contributions: for instance, all the four-fermion operators are included in the NLO, in spite of the fact that only a subset of these is required to reabsorb 1-loop divergences.
- It has been left out from the LO Lagrangian due to phenomenological reasons.

The suppression factor of each operator is determined using the NDA master formula, first proposed in Ref. [34] and later modified in Refs. [35] and [33]. Following the notation of Ref. [33]:

$$\frac{\Lambda^4}{16\pi^2} \left[\frac{\partial}{\Lambda} \right]^{N_p} \left[\frac{4\pi \phi}{\Lambda} \right]^{N_\phi} \left[\frac{4\pi A}{\Lambda} \right]^{N_A} \left[\frac{4\pi \psi}{\Lambda^{3/2}} \right]^{N_\psi} \left[\frac{g}{4\pi} \right]^{N_g} \left[\frac{y}{4\pi} \right]^{N_y}, \quad (2.7)$$

where ϕ represents either the SM GBs or h , ψ a generic fermion, A a generic gauge field, g the gauge couplings and y the Yukawa couplings. All the operators appearing in the LO Lagrangian in Eq. (2.3) are normalised according to this formula, apart from the operators providing gauge bosons' masses, $(v^2/4)\text{Tr}(\mathbf{V}_\mu \mathbf{V}^\mu) \mathcal{F}_C(h)$, and fermions' masses $(v\sqrt{2})\bar{\psi}_L \mathbf{U} \mathcal{Y}_\psi(h) \psi_R$, which are multiplied by powers of the EW scale v and not by Λ or f as expected. This is due to the well-known fine-tuning, typical of theories where the EWSB sector is non-linearly realised. Notice that with these conventions all the kinetic terms are canonically normalised, differently from what follows using the original version of the NDA master formula from Ref. [34].

The master formula also ensures that the operators belonging to the NLO Lagrangian are typically suppressed with respect to those of \mathcal{L}_0 by powers of $(4\pi)^{(n \leq 2)}$, reflecting the renormalisation of the chiral sector, and/or by powers of $\Lambda^{(n \leq 2)}$, associated to possible new physics contributions. Different cases will be discussed when necessary.

2.1 The NLO Lagrangian

The second part of the HEFT Lagrangian, $\Delta\mathcal{L}$, contains in general all the invariant operators appearing beyond the leading order. They include corrections to the interactions

contained in \mathcal{L}_0 as well as completely new couplings. This Lagrangian can be generically written as a sum of two parts

$$\Delta\mathcal{L} = \Delta\mathcal{L}_{\text{bos}} + \Delta\mathcal{L}_{\text{fer}} , \quad (2.8)$$

where $\Delta\mathcal{L}_{\text{bos}}$ contains all the purely-bosonic operators, while $\Delta\mathcal{L}_{\text{fer}}$ accounts for the interactions that involve fermions.

In this work, $\Delta\mathcal{L}$ will be restricted to the NLO, defined according to the rules presented in the previous section. We present a set of invariants that forms a complete, non-redundant basis at this order in the effective expansion, which has been constructed identifying first a complete basis for each of the two sectors individually (bosonic and fermionic) and subsequently employing the EOMs to remove redundant terms.

Given the large number of invariants, the operators are classified as follows: the bosonic basis is split into CP conserving and CP violating subsets (the field h is assumed to be a CP-even scalar):

$$\Delta\mathcal{L}_{\text{bos}} = \Delta\mathcal{L}_{\text{bos}}^{CP} + \Delta\mathcal{L}_{\text{bos}}^{CP\mathcal{P}} , \quad (2.9)$$

while in the fermionic sector the distinction is between fermionic single- and double-current structures:

$$\Delta\mathcal{L}_{\text{fer}} = \Delta\mathcal{L}_{2F} + \Delta\mathcal{L}_{4F} . \quad (2.10)$$

The operators are named differently according to the category to which they belong and each of them includes a function $\mathcal{F}_i(h)$ conventionally parametrised as

$$\mathcal{F}_i(h) = 1 + 2a_i \frac{h}{v} + b_i \frac{h^2}{v^2} + \dots \quad (2.11)$$

Moreover, each effective operator is multiplied with a real coefficient, indicated with a lowercase letter (c , \tilde{c} , n , r) associated to each class. The following table defines the notation and summarises the number of independent invariants for each set, in the absence of right-handed neutrinos and after the application of the EOMs.

\mathcal{L}	sub-category	notation	# operators
$\Delta\mathcal{L}_{\text{bos}}^{CP}$		$c_j \mathcal{P}_j$	26
$\Delta\mathcal{L}_{\text{bos}}^{CP\mathcal{P}}$		$\tilde{c}_j \mathcal{S}_j$	16
$\Delta\mathcal{L}_{2F}$	quark current	$n_j^{\mathcal{Q}} \mathcal{N}_j^{\mathcal{Q}}$	36
	lepton current	$n_j^{\ell} \mathcal{N}_j^{\ell}$	14
$\Delta\mathcal{L}_{4F}$	four quarks	$r_j^{\mathcal{Q}} R_j^{\mathcal{Q}}$	26
	four leptons	$r_j^{\ell} R_j^{\ell}$	7
	two quarks and two leptons	$r_j^{\mathcal{Q}\ell} R_j^{\mathcal{Q}\ell}$	23
Tot			148

Forty additional operators should be considered if right-handed neutrinos are added to the spectrum: 17 in \mathcal{L}_{2F} , 8 four-leptons interactions and 15 mixed two-quark-two-lepton terms.

The complete list of NLO operators is provided in what follows: Sects. 2.2 and 2.3 are respectively dedicated to the bosonic and fermionic sectors. Further details on the construction of the invariants and on how the EOMs have been employed to remove redundant terms can be found in Appendices C and D. The Feynman rules of the complete CP conserving basis are reported in Appendix E, in unitary gauge and for vertices with up to four legs.

2.2 NLO basis: bosonic sector $\Delta\mathcal{L}_{\text{bos}}$

At NLO in the chiral expansion, the Lagrangian $\Delta\mathcal{L}_{\text{bos}}$ contains purely bosonic operators. Complete bases for the CP even and CP odd sectors have been already constructed in Refs. [22, 24] and [25] respectively. In this work only a subset of those ensembles are retained as, once the fermionic sector is introduced, some of the terms become redundant and can be removed using the EOMs (see App. D). Nonetheless, the original numeration of the operators has been kept, in order to simplify the comparison with the literature. Finally, the explicit formal dependence on h in the generic functions $\mathcal{F}_i(h)$ is dropped in what follows for brevity.

2.2.1 CP even bosonic basis $\Delta\mathcal{L}_{\text{bos}}^{CP}$

The CP even NLO Lagrangian reads

$$\Delta\mathcal{L}_{\text{bos}}^{CP} = \sum_j c_j \mathcal{P}_j(h), \quad (2.12)$$

with

$$j = \{T, B, W, G, DH, 1-6, 8, 11-14, 17, 18, 20-24, 26, WWW, GGG\} \quad (2.13)$$

where all the operators contain four derivatives, with the exception of

$$\mathcal{P}_T(h) = \frac{v^2}{4} \text{Tr}(\mathbf{T}\mathbf{V}_\mu) \text{Tr}(\mathbf{T}\mathbf{V}^\mu) \mathcal{F}_T, \quad (2.14)$$

and

$$\begin{aligned} \mathcal{P}_{WWW}(h) &= \frac{4\pi\epsilon_{abc}}{\Lambda^2} W_\mu^{a\nu} W_\nu^{b\rho} W_\rho^{c\mu} \mathcal{F}_{WWW}, \\ \mathcal{P}_{GGG}(h) &= \frac{4\pi f_{\alpha\beta\gamma}}{\Lambda^2} G_\mu^{\alpha\nu} G_\nu^{\beta\rho} G_\rho^{\gamma\mu} \mathcal{F}_{GGG}, \end{aligned} \quad (2.15)$$

where $f_{\alpha\beta\gamma}$ denotes the structure constants of $SU(3)$.

The two-derivative operator $\mathcal{P}_T(h)$ is very similar to $v^2 \text{Tr}(\mathbf{V}_\mu \mathbf{V}^\mu) \mathcal{F}_C$ and, therefore, it could have been included in \mathcal{L}_0 *a priori*. However, it is customary to move it to $\Delta\mathcal{L}$ because the bounds existing on its coefficient are quite strong: $c_T \lesssim 10^{-2}$. In fact, this operator violates the custodial symmetry and contributes to the T parameter, which is

constrained to a high accuracy by electroweak precision data (EWPD). The two operators $\mathcal{P}_{WW}(h)$ and $\mathcal{P}_{GG}(h)$ are not required to absorb divergences due to the 1-loop renormalisation. However, they can be listed among the NLO operators: containing only the transverse components of the gauge bosons, they follow the linear description; then, they come suppressed by Λ^2 , on the same foot as the four-fermion operators. It will be shown in the following that they have a non-trivial impact at the phenomenological level.

The remaining 23 operators in $\Delta\mathcal{L}_{\text{bos}}^{CP}$, in the numeration of Ref. [24], are the following:

$$\begin{aligned}
\mathcal{P}_B(h) &= -\frac{1}{4}B_{\mu\nu}B^{\mu\nu}\mathcal{F}_B & \mathcal{P}_W(h) &= -\frac{1}{4}W_{\mu\nu}^a W^{a\mu\nu}\mathcal{F}_W \\
\mathcal{P}_G(h) &= -\frac{1}{4}G_{\mu\nu}^a G^{a\mu\nu}\mathcal{F}_G & \mathcal{P}_{DH}(h) &= (\partial_\mu\mathcal{F}_{DH}(h)\partial^\mu\mathcal{F}'_{DH}(h))^2 \\
\mathcal{P}_1(h) &= B_{\mu\nu}\text{Tr}(\mathbf{T}W^{\mu\nu})\mathcal{F}_1 & \mathcal{P}_2(h) &= \frac{i}{4\pi}B_{\mu\nu}\text{Tr}(\mathbf{T}[\mathbf{V}^\mu, \mathbf{V}^\nu])\mathcal{F}_2 \\
\mathcal{P}_3(h) &= \frac{i}{4\pi}\text{Tr}(W_{\mu\nu}[\mathbf{V}^\mu, \mathbf{V}^\nu])\mathcal{F}_3 & \mathcal{P}_4(h) &= \frac{i}{4\pi}B_{\mu\nu}\text{Tr}(\mathbf{T}\mathbf{V}^\mu)\partial^\nu\mathcal{F}_4 \\
\mathcal{P}_5(h) &= \frac{i}{4\pi}\text{Tr}(W_{\mu\nu}\mathbf{V}^\mu)\partial^\nu\mathcal{F}_5 & \mathcal{P}_6(h) &= \frac{1}{(4\pi)^2}(\text{Tr}(\mathbf{V}_\mu\mathbf{V}^\mu))^2\mathcal{F}_6 \\
\mathcal{P}_8(h) &= \frac{1}{(4\pi)^2}\text{Tr}(\mathbf{V}_\mu\mathbf{V}_\nu)\partial^\mu\mathcal{F}_8\partial^\nu\mathcal{F}'_8 & \mathcal{P}_{11}(h) &= \frac{1}{(4\pi)^2}(\text{Tr}(\mathbf{V}_\mu\mathbf{V}_\nu))^2\mathcal{F}_{11} \\
\mathcal{P}_{12}(h) &= (\text{Tr}(\mathbf{T}W_{\mu\nu}))^2\mathcal{F}_{12} & \mathcal{P}_{13}(h) &= \frac{i}{4\pi}\text{Tr}(\mathbf{T}W_{\mu\nu})\text{Tr}(\mathbf{T}[\mathbf{V}^\mu, \mathbf{V}^\nu])\mathcal{F}_{13} \\
\mathcal{P}_{14}(h) &= \frac{\varepsilon^{\mu\nu\rho\lambda}}{4\pi}\text{Tr}(\mathbf{T}\mathbf{V}_\mu)\text{Tr}(\mathbf{V}_\nu W_{\rho\lambda})\mathcal{F}_{14} & \mathcal{P}_{17}(h) &= \frac{i}{4\pi}\text{Tr}(\mathbf{T}W_{\mu\nu})\text{Tr}(\mathbf{T}\mathbf{V}^\mu)\partial^\nu\mathcal{F}_{17} \\
\mathcal{P}_{18}(h) &= \frac{1}{(4\pi)^2}\text{Tr}(\mathbf{T}[\mathbf{V}_\mu, \mathbf{V}_\nu])\text{Tr}(\mathbf{T}\mathbf{V}^\mu)\partial^\nu\mathcal{F}_{18} & \mathcal{P}_{20}(h) &= \frac{1}{(4\pi)^2}\text{Tr}(\mathbf{V}_\mu\mathbf{V}^\mu)\partial_\nu\mathcal{F}_{20}\partial^\nu\mathcal{F}'_{20} \\
\mathcal{P}_{21}(h) &= \frac{1}{(4\pi)^2}(\text{Tr}(\mathbf{T}\mathbf{V}_\mu))^2\partial_\nu\mathcal{F}_{21}\partial^\nu\mathcal{F}'_{21} & \mathcal{P}_{22}(h) &= \frac{1}{(4\pi)^2}\text{Tr}(\mathbf{T}\mathbf{V}_\mu)\text{Tr}(\mathbf{T}\mathbf{V}_\nu)\partial^\mu\mathcal{F}_{22}\partial^\nu\mathcal{F}'_{22} \\
\mathcal{P}_{23}(h) &= \frac{1}{(4\pi)^2}\text{Tr}(\mathbf{V}_\mu\mathbf{V}^\mu)(\text{Tr}(\mathbf{T}\mathbf{V}_\nu))^2\mathcal{F}_{23} & \mathcal{P}_{24}(h) &= \frac{1}{(4\pi)^2}\text{Tr}(\mathbf{V}_\mu\mathbf{V}_\nu)\text{Tr}(\mathbf{T}\mathbf{V}^\mu)\text{Tr}(\mathbf{T}\mathbf{V}^\nu)\mathcal{F}_{24} \\
\mathcal{P}_{26}(h) &= \frac{1}{(4\pi)^2}(\text{Tr}(\mathbf{T}\mathbf{V}_\mu)\text{Tr}(\mathbf{T}\mathbf{V}_\nu))^2\mathcal{F}_{26} .
\end{aligned}$$

As anticipated in the previous section, while the kinetic terms for the gauge bosons are listed at the LO, the interactions obtained after introducing the dependence on h are reported in the list of NLO operators, under the assumption that the coupling of the transverse components of the gauge fields with the Higgs sector is a subleading effect.

It is also worth commenting on the operators $\mathcal{P}_1(h)$ and $\mathcal{P}_{12}(h)$: these two structures, including the terms without h insertions, are customarily listed among the NLO terms despite their similarity with the gauge bosons' kinetic terms. This is justified, *a posteriori*, by the fact that they contribute to the S and U parameters respectively (see Sect. 3.2), which are strongly constrained. In this sense, their treatment is analogous to that of $\mathcal{P}_T(h)$.

The operators $\mathcal{P}_C(h)$ and $\mathcal{P}_H(h)$ of Ref. [24] have not been included in this list, as their effects can be reabsorbed in redefinitions of the arbitrary functions $\mathcal{F}_C(h)$ and $\mathcal{Y}_{Q,L}(h)$ appearing in \mathcal{L}_0 in eq. (2.3) (see App. B). Moreover, compared to Ref. [24], a different normalisation for the operators has been chosen: the 4π suppression factors determined by

the NDA master formula in Eq. (2.7) have been made explicit (see Ref. [33] for details on the advantages of the NDA normalisation), while the dependence on the coupling constants has been removed, in order to emphasise the generality of the EFT approach. It is customary, indeed, to include in the definition of the HEFT operators the numerical factors arising from the 1-loop renormalisation procedure: for instance, the operator $\mathcal{P}_1(h)$ is often defined proportionally to $gg'/(4\pi)^2$ [17, 18, 22, 24]. However, in principle the coefficients c_i account not only for renormalisation effects, but also for possible external contributions, originated by sources that do not need to share the same dependence on the gauge couplings. This normalisation choice is common in many EFTs, such as Fermi's Theory, the EFT for mesons processes and the SMEFT.

2.2.2 CP odd bosonic basis $\Delta\mathcal{L}_{\text{bos}}^{\text{CP}}$

In the CP-odd sector the bosonic Lagrangian contains 16 operators: according to Ref. [25],

$$\Delta\mathcal{L}_{\text{bos}}^{\text{CP}} = \sum_j \tilde{c}_j \mathcal{S}_j, \quad j = \{2D, \tilde{B}, \tilde{W}, \tilde{G}, 1-9, 15, \tilde{W}WW, \tilde{G}GG\}, \quad (2.16)$$

where, as for $\Delta\mathcal{L}_{\text{bos}}^{\text{CP}}$, all the operators have four derivatives, with the exception of

$$\mathcal{S}_{2D}(h) \equiv i \frac{v^2}{4} \text{Tr}(\mathbf{T} \mathbf{V}_\mu) \partial^\mu \mathcal{F}_{2D} \quad (2.17)$$

and

$$\begin{aligned} \mathcal{S}_{\tilde{W}WW}(h) &= \frac{4\pi\varepsilon_{abc}}{\Lambda^2} \tilde{W}_\mu^{a\nu} W_\nu^{b\rho} W_\rho^{c\mu} \mathcal{F}_{\tilde{W}WW}, \\ \mathcal{S}_{\tilde{G}GG}(h) &= \frac{4\pi f_{\alpha\beta\gamma}}{\Lambda^2} \tilde{G}_\mu^{\alpha\nu} G_\nu^{\beta\rho} G_\rho^{\gamma\mu} \mathcal{F}_{\tilde{G}GG}. \end{aligned} \quad (2.18)$$

The rest of operators entering $\Delta\mathcal{L}_{\text{bos}}^{\text{CP}}$ are

$$\begin{aligned} \mathcal{S}_{\tilde{B}}(h) &\equiv -B^{\mu\nu} \tilde{B}_{\mu\nu} \mathcal{F}_{\tilde{B}} & \mathcal{S}_{\tilde{W}}(h) &\equiv -\text{Tr}(W^{\mu\nu} \tilde{W}_{\mu\nu}) \mathcal{F}_{\tilde{W}} \\ \mathcal{S}_{\tilde{G}}(h) &\equiv -G^{a\mu\nu} \tilde{G}_{\mu\nu}^a \mathcal{F}_{\tilde{G}} & \mathcal{S}_1(h) &\equiv \tilde{B}^{\mu\nu} \text{Tr}(\mathbf{T} W_{\mu\nu}) \mathcal{F}_1 \\ \mathcal{S}_2(h) &\equiv \frac{i}{4\pi} \tilde{B}^{\mu\nu} \text{Tr}(\mathbf{T} \mathbf{V}_\mu) \partial_\nu \mathcal{F}_2 & \mathcal{S}_3(h) &\equiv \frac{i}{4\pi} \text{Tr}(\tilde{W}^{\mu\nu} \mathbf{V}_\mu) \partial_\nu \mathcal{F}_3 \\ \mathcal{S}_4(h) &\equiv \frac{1}{4\pi} \text{Tr}(W^{\mu\nu} \mathbf{V}_\mu) \text{Tr}(\mathbf{T} \mathbf{V}_\nu) \mathcal{F}_4 & \mathcal{S}_5(h) &\equiv \frac{i}{(4\pi)^2} \text{Tr}(\mathbf{V}^\mu \mathbf{V}^\nu) \text{Tr}(\mathbf{T} \mathbf{V}_\mu) \partial_\nu \mathcal{F}_5 \\ \mathcal{S}_6(h) &\equiv \frac{i}{(4\pi)^2} \text{Tr}(\mathbf{V}^\mu \mathbf{V}_\mu) \text{Tr}(\mathbf{T} \mathbf{V}^\nu) \partial_\nu \mathcal{F}_6 & \mathcal{S}_7(h) &\equiv \frac{1}{4\pi} \text{Tr}(\mathbf{T} [W^{\mu\nu}, \mathbf{V}_\mu]) \partial_\nu \mathcal{F}_7 \\ \mathcal{S}_8(h) &\equiv \text{Tr}(\mathbf{T} \tilde{W}^{\mu\nu}) \text{Tr}(\mathbf{T} W_{\mu\nu}) \mathcal{F}_8 & \mathcal{S}_9(h) &\equiv \frac{i}{4\pi} \text{Tr}(\mathbf{T} \tilde{W}^{\mu\nu}) \text{Tr}(\mathbf{T} \mathbf{V}_\mu) \partial_\nu \mathcal{F}_9 \\ \mathcal{S}_{15}(h) &\equiv \frac{i}{(4\pi)^2} \text{Tr}(\mathbf{T} \mathbf{V}^\mu) (\text{Tr}(\mathbf{T} \mathbf{V}^\nu))^2 \partial_\mu \mathcal{F}_{15}. \end{aligned}$$

As for the CP-even part of the bosonic basis, the explicit dependence on the gauge couplings is not part of the definition of the operators, while the 4π factors are reported according to Eq. (2.7).

The operator $\mathcal{S}_{2D}(h)$ deserves a special remark. Being a two-derivative operator, it would be naturally listed at the LO. However, restricting for simplicity the discussion to the unitary gauge, $\mathcal{S}_{2D}(h)$ introduces a mixing between the gauge boson Z and the physical h , that can be rotated away via a proper redefinition of the Goldstone bosons' matrix, as detailed in Ref. [25, 36]:

$$\mathbf{U} \rightarrow \tilde{\mathbf{U}} \exp \left[-ia_{2D} \tilde{c}_{2D} \frac{h}{v} \sigma_3 \right]. \quad (2.19)$$

At leading order in the effective coefficients, the effects of this operator are eventually recast into CP-odd contributions to the Yukawa couplings with arbitrary number of h legs and to the vertices Zh^n , $n \geq 2$. Furthermore, $\mathcal{S}_{2D}(h)$ induces, at 1-loop, corrections to the Higgs gauge-boson couplings that are bounded by the strong experimental limits on fermionic EDMs, as discussed in Ref. [25]. For this reason is listed at the NLO, similarly to $\mathcal{P}_T(h)$.

Finally, the two operators $\mathcal{P}_{\tilde{W}WW}(h)$ and $\mathcal{P}_{\tilde{G}GG}(h)$ are the CP-odd counterparts of $\mathcal{P}_{WW}(h)$ and $\mathcal{P}_{GG}(h)$; comments similar to those given for the latter apply here too.

2.3 NLO basis: fermionic sector $\Delta\mathcal{L}_{\text{fer}}$

The fermionic Lagrangian at NLO is constituted by single-current operators with up to two derivatives and by four-fermion operators. Flavour indices are left implicit, unless necessary for the discussion. This section presents a set of independent terms that completes the NLO basis in the bosonic sector $\Delta\mathcal{L}_{\text{bos}}$: some redundant structures have been removed using the EOMs, as detailed in App. D. Only baryon and lepton number conserving operators are considered (see Ref. [37] for the baryon and lepton number violating basis). Moreover, as already stated in the previous sections, right-handed neutrinos are not considered in the present description. Their inclusion in the spectrum would require an extension of the basis presented in this section, with the addition of the operators in App. A.

The numbering of the functions $\mathcal{F}_i(h)$ is dropped in what follows for brevity. The Pauli matrices that act on the $SU(2)_L$ components are denoted by σ^i , while the Gell-Mann matrices that contract colour indices are indicated by λ^A . Whenever they are not specified, the colour (uppercase) and isospin (lowercase) contractions are understood to be diagonal. Flavour contractions are also assumed to be diagonal. The tensor structure $\sigma^{\mu\nu}$ entering the dipole operators is defined as $\sigma^{\mu\nu} = \frac{i}{2}[\gamma^\mu, \gamma^\nu]$. Finally, the mark \mathcal{CP} on the left of an operator indicates that it is intrinsically CP-odd.

2.3.1 Single fermionic current $\Delta\mathcal{L}_{2F}$

The operators with a single fermionic current and up to two derivatives (including those in \mathbf{V}_μ) are contained in the Lagrangian

$$\begin{aligned}\Delta\mathcal{L}_{2F} = & \sum_{j=1}^8 n_j^{\mathcal{Q}} \mathcal{N}_j^{\mathcal{Q}} + \sum_{j=9}^{28} \frac{1}{\Lambda} (n_j^{\mathcal{Q}} + i\tilde{n}_j^{\mathcal{Q}}) \mathcal{N}_j^{\mathcal{Q}} + \sum_{j=29}^{36} \frac{4\pi}{\Lambda} (n_j^{\mathcal{Q}} + i\tilde{n}_j^{\mathcal{Q}}) \mathcal{N}_j^{\mathcal{Q}} \\ & + \sum_{j=1}^2 n_j^{\ell} \mathcal{N}_j^{\ell} + \sum_{j=3}^{11} \frac{1}{\Lambda} (n_j^{\ell} + i\tilde{n}_j^{\ell}) \mathcal{N}_j^{\ell} + \sum_{j=12}^{14} \frac{4\pi}{\Lambda} (n_j^{\ell} + i\tilde{n}_j^{\ell}) \mathcal{N}_j^{\ell} + \text{h.c.},\end{aligned}\quad (2.20)$$

where we recall that the coefficients $n_j^{\mathcal{Q}}$, n_j^{ℓ} , $\tilde{n}_j^{\mathcal{Q}}$, \tilde{n}_j^{ℓ} are real and smaller than unity. The terms with two derivatives have overall canonical mass dimension 5 and are therefore suppressed by Λ^{-1} . Moreover, they necessarily require chirality-flipping (scalar or tensor) Lorentz structures. These structures do not have definite CP character, as the scalar ($\bar{\psi}\psi$) and pseudo-scalar ($\bar{\psi}i\gamma_5\psi$) contractions have opposite parity. As a consequence, each $SU(2)$ structure yields two contributions with opposite CP properties, that have been parameterised by two independent real coefficients: for the quark bilinears, the terms $n_j^{\mathcal{Q}}(\mathcal{N}_j^{\mathcal{Q}} + \text{h.c.})$ with the $\mathcal{N}_j^{\mathcal{Q}}$'s defined below are CP even, while the combinations $\tilde{n}_j^{\mathcal{Q}}(i\mathcal{N}_j^{\mathcal{Q}} + \text{h.c.})$ are CP odd. A similar notation has been adopted for the lepton bilinears.

Quark Current Operators

All the non-redundant terms that can be constructed coupling one derivative or one chiral vector field \mathbf{V}_μ to a fermionic bilinear necessarily have a vector-axial Lorentz structure, that preserves chirality. For the quarks case, they are:

$$\begin{aligned}\mathcal{N}_1^{\mathcal{Q}}(h) &\equiv i\bar{Q}_L \gamma_\mu \mathbf{V}^\mu Q_L \mathcal{F} & \mathcal{N}_2^{\mathcal{Q}}(h) &\equiv i\bar{Q}_R \gamma_\mu \mathbf{U}^\dagger \mathbf{V}^\mu \mathbf{U} Q_R \mathcal{F} \\ \mathcal{CP} \quad \mathcal{N}_3^{\mathcal{Q}}(h) &\equiv \bar{Q}_L \gamma_\mu [\mathbf{V}^\mu, \mathbf{T}] Q_L \mathcal{F} & \mathcal{CP} \quad \mathcal{N}_4^{\mathcal{Q}}(h) &\equiv \bar{Q}_R \gamma_\mu \mathbf{U}^\dagger [\mathbf{V}^\mu, \mathbf{T}] \mathbf{U} Q_R \mathcal{F} \\ \mathcal{N}_5^{\mathcal{Q}}(h) &\equiv i\bar{Q}_L \gamma_\mu \{\mathbf{V}^\mu, \mathbf{T}\} Q_L \mathcal{F} & \mathcal{N}_6^{\mathcal{Q}}(h) &\equiv i\bar{Q}_R \gamma_\mu \mathbf{U}^\dagger \{\mathbf{V}^\mu, \mathbf{T}\} \mathbf{U} Q_R \mathcal{F} \\ \mathcal{N}_7^{\mathcal{Q}}(h) &\equiv i\bar{Q}_L \gamma_\mu \mathbf{T} \mathbf{V}^\mu \mathbf{T} Q_L \mathcal{F} & \mathcal{N}_8^{\mathcal{Q}}(h) &\equiv i\bar{Q}_R \gamma_\mu \mathbf{U}^\dagger \mathbf{T} \mathbf{V}^\mu \mathbf{T} \mathbf{U} Q_R \mathcal{F}.\end{aligned}$$

Invariants with a derivative acting on a fermion field or on a $\mathcal{F}(h)$ function are redundant upon application of the EOMs and integration by parts, and have therefore been removed from the final basis.

Operators with two derivatives require a fermionic current with an even number (zero or two) of gamma matrices: therefore only chirality-flipping Lorentz structures are allowed. All the operators with a scalar structure are required as counterterms in the 1-loop renormalisation of \mathcal{L}_0 :

$$\begin{aligned}\mathcal{N}_9^{\mathcal{Q}}(h) &\equiv \bar{Q}_L \mathbf{U} Q_R \partial_\mu \mathcal{F} \partial^\mu \mathcal{F}' & \mathcal{N}_{10}^{\mathcal{Q}}(h) &\equiv \bar{Q}_L \mathbf{T} \mathbf{U} Q_R \partial_\mu \mathcal{F} \partial^\mu \mathcal{F}' \\ \mathcal{N}_{11}^{\mathcal{Q}}(h) &\equiv \bar{Q}_L \mathbf{V}_\mu \mathbf{U} Q_R \partial^\mu \mathcal{F} & \mathcal{N}_{12}^{\mathcal{Q}}(h) &\equiv \bar{Q}_L \{\mathbf{V}_\mu, \mathbf{T}\} \mathbf{U} Q_R \partial^\mu \mathcal{F} \\ \mathcal{N}_{13}^{\mathcal{Q}}(h) &\equiv \bar{Q}_L [\mathbf{V}_\mu, \mathbf{T}] \mathbf{U} Q_R \partial^\mu \mathcal{F} & \mathcal{N}_{14}^{\mathcal{Q}}(h) &\equiv \bar{Q}_L \mathbf{T} \mathbf{V}_\mu \mathbf{T} \mathbf{U} Q_R \partial^\mu \mathcal{F}\end{aligned}$$

$$\begin{aligned}
\mathcal{N}_{15}^{\mathcal{Q}}(h) &\equiv \bar{Q}_L \mathbf{V}_\mu \mathbf{V}^\mu \mathbf{U} Q_R \mathcal{F} & \mathcal{N}_{16}^{\mathcal{Q}}(h) &\equiv \bar{Q}_L \mathbf{V}_\mu \mathbf{V}^\mu \mathbf{T} \mathbf{U} Q_R \mathcal{F} \\
\mathcal{N}_{17}^{\mathcal{Q}}(h) &\equiv \bar{Q}_L \mathbf{T} \mathbf{V}_\mu \mathbf{T} \mathbf{V}^\mu \mathbf{U} Q_R \mathcal{F} & \mathcal{N}_{18}^{\mathcal{Q}}(h) &\equiv \bar{Q}_L \mathbf{T} \mathbf{V}_\mu \mathbf{T} \mathbf{V}^\mu \mathbf{T} \mathbf{U} Q_R \mathcal{F} \\
\mathcal{N}_{19}^{\mathcal{Q}}(h) &\equiv \bar{Q}_L \mathbf{V}_\mu \mathbf{T} \mathbf{V}^\mu \mathbf{U} Q_R \mathcal{F} & \mathcal{N}_{20}^{\mathcal{Q}}(h) &\equiv \bar{Q}_L \mathbf{V}_\mu \mathbf{T} \mathbf{V}^\mu \mathbf{T} \mathbf{U} Q_R \mathcal{F}.
\end{aligned}$$

Operators with tensor structure are also included in the NLO basis, although they are not needed to reabsorb the 1-loop divergences of \mathcal{L}_0 , as the loop diagrams that generate them in the EFT are finite. Nonetheless, these interactions may result from the (tree-level) exchange of a heavy BSM resonance and therefore they may be as relevant as those in the previous lists:

$$\begin{aligned}
\mathcal{N}_{21}^{\mathcal{Q}}(h) &\equiv \bar{Q}_L \sigma^{\mu\nu} \mathbf{V}_\mu \mathbf{U} Q_R \partial_\nu \mathcal{F} & \mathcal{N}_{22}^{\mathcal{Q}}(h) &\equiv \bar{Q}_L \sigma^{\mu\nu} [\mathbf{V}_\mu, \mathbf{T}] \mathbf{U} Q_R \partial_\nu \mathcal{F} \\
\mathcal{N}_{23}^{\mathcal{Q}}(h) &\equiv \bar{Q}_L \sigma^{\mu\nu} \{\mathbf{V}_\mu, \mathbf{T}\} \mathbf{U} Q_R \partial_\nu \mathcal{F} & \mathcal{N}_{24}^{\mathcal{Q}}(h) &\equiv \bar{Q}_L \sigma^{\mu\nu} \mathbf{T} \mathbf{V}_\mu \mathbf{T} \mathbf{U} Q_R \partial_\nu \mathcal{F} \\
\mathcal{N}_{25}^{\mathcal{Q}}(h) &\equiv \bar{Q}_L \sigma^{\mu\nu} \mathbf{V}_\mu \mathbf{T} \mathbf{V}_\nu \mathbf{U} Q_R \mathcal{F} & \mathcal{N}_{26}^{\mathcal{Q}}(h) &\equiv \bar{Q}_L \sigma^{\mu\nu} \mathbf{V}_\mu \mathbf{T} \mathbf{V}_\nu \mathbf{T} \mathbf{U} Q_R \mathcal{F} \\
\mathcal{N}_{27}^{\mathcal{Q}}(h) &\equiv \bar{Q}_L \sigma^{\mu\nu} [\mathbf{V}_\mu, \mathbf{V}_\nu] \mathbf{U} Q_R \mathcal{F} & \mathcal{N}_{28}^{\mathcal{Q}}(h) &\equiv \bar{Q}_L \sigma^{\mu\nu} [\mathbf{V}_\mu, \mathbf{V}_\nu] \mathbf{T} \mathbf{U} Q_R \mathcal{F} \\
\mathcal{N}_{29}^{\mathcal{Q}}(h) &\equiv ig' \bar{Q}_L \sigma^{\mu\nu} \mathbf{U} Q_R \mathcal{F} B_{\mu\nu} & \mathcal{N}_{30}^{\mathcal{Q}}(h) &\equiv ig' \bar{Q}_L \sigma^{\mu\nu} \mathbf{T} \mathbf{U} Q_R \mathcal{F} B_{\mu\nu} \\
\mathcal{N}_{31}^{\mathcal{Q}}(h) &\equiv ig_s \bar{Q}_L \sigma^{\mu\nu} \mathcal{G}_{\mu\nu} \mathbf{U} Q_R \mathcal{F} & \mathcal{N}_{32}^{\mathcal{Q}}(h) &\equiv ig_s \bar{Q}_L \sigma^{\mu\nu} \mathcal{G}_{\mu\nu} \mathbf{T} \mathbf{U} Q_R \mathcal{F} \\
\mathcal{N}_{33}^{\mathcal{Q}}(h) &\equiv ig \bar{Q}_L \sigma^{\mu\nu} W_{\mu\nu} \mathbf{U} Q_R \mathcal{F} & \mathcal{N}_{34}^{\mathcal{Q}}(h) &\equiv ig \bar{Q}_L \sigma^{\mu\nu} \{W_{\mu\nu}, \mathbf{T}\} \mathbf{U} Q_R \mathcal{F} \\
\mathcal{N}_{35}^{\mathcal{Q}}(h) &\equiv ig \bar{Q}_L \sigma^{\mu\nu} [W_{\mu\nu}, \mathbf{T}] \mathbf{U} Q_R \mathcal{F} & \mathcal{N}_{36}^{\mathcal{Q}}(h) &\equiv ig \bar{Q}_L \sigma^{\mu\nu} \mathbf{T} W_{\mu\nu} \mathbf{T} \mathbf{U} Q_R \mathcal{F}.
\end{aligned}$$

Leptonic Current Operators

Leptonic bilinears can be constructed along the same lines as the quark ones. The absence of right-handed neutrinos, however, reduces notably the number of independent invariants. Making use of Eq. (D.14), only two independent operators can be constructed with the insertion of a single derivative or \mathbf{V}_μ :

$$\mathcal{CP} \quad \mathcal{N}_1^\ell(h) \equiv \bar{L}_L \gamma_\mu [\mathbf{V}^\mu, \mathbf{T}] L_L \mathcal{F} \quad \mathcal{N}_2^\ell(h) \equiv i \bar{L}_R \gamma_\mu \mathbf{U}^\dagger \{\mathbf{V}^\mu, \mathbf{T}\} \mathbf{U} L_R \mathcal{F}.$$

Notice that, if flavour effects are also taken into consideration, two other structures should be considered:

$$i \bar{L}_{Li} \gamma_\mu \mathbf{V}^\mu L_{Lj} \mathcal{F}, \quad i \bar{L}_{Li} \gamma_\mu \{\mathbf{T}, \mathbf{V}^\mu\} L_{Lj} \mathcal{F}. \quad (2.21)$$

only for the case with $i \neq j$. Indeed, as shown in Eq. (D.14), the flavour diagonal contractions do not represent independent terms as they are related via EOMs to bosonic operators that have been retained in the basis.

With two derivatives, two \mathbf{V}_μ or a combination of them, the following structures can be constructed:

$$\begin{aligned}
\mathcal{N}_3^\ell(h) &\equiv \bar{L}_L \mathbf{U} L_R \partial_\mu \mathcal{F} \partial^\mu \mathcal{F}' & \mathcal{N}_4^\ell(h) &\equiv \bar{L}_L \{\mathbf{V}_\mu, \mathbf{T}\} \mathbf{U} L_R \partial^\mu \mathcal{F} \\
\mathcal{N}_5^\ell(h) &\equiv \bar{L}_L [\mathbf{V}_\mu, \mathbf{T}] \mathbf{U} L_R \partial^\mu \mathcal{F} & \mathcal{N}_6^\ell(h) &\equiv \bar{L}_L \mathbf{V}_\mu \mathbf{V}^\mu \mathbf{U} L_R \mathcal{F}
\end{aligned}$$

$$\begin{aligned}
\mathcal{N}_7^\ell(h) &\equiv \bar{L}_L \mathbf{T} \mathbf{V}_\mu \mathbf{T} \mathbf{V}^\mu \mathbf{U} L_R \mathcal{F} & \mathcal{N}_8^\ell(h) &\equiv \bar{L}_L \sigma^{\mu\nu} [\mathbf{V}_\mu, \mathbf{T}] \mathbf{U} L_R \partial_\nu \mathcal{F} \\
\mathcal{N}_9^\ell(h) &\equiv \bar{L}_L \sigma^{\mu\nu} \{\mathbf{V}_\mu, \mathbf{T}\} \mathbf{U} L_R \partial_\nu \mathcal{F} & \mathcal{N}_{10}^\ell(h) &\equiv \bar{L}_L \sigma^{\mu\nu} \mathbf{V}_\mu \mathbf{T} \mathbf{V}_\nu \mathbf{U} L_R \mathcal{F} \\
\mathcal{N}_{11}^\ell(h) &\equiv \bar{L}_L \sigma^{\mu\nu} [\mathbf{V}_\mu, \mathbf{V}_\nu] \mathbf{U} L_R \mathcal{F} & \mathcal{N}_{12}^\ell(h) &\equiv ig' \bar{L}_L \sigma^{\mu\nu} \mathbf{U} L_R \mathcal{F} B_{\mu\nu} \\
\mathcal{N}_{13}^\ell(h) &\equiv ig \bar{L}_L \sigma^{\mu\nu} W_{\mu\nu} \mathbf{U} L_R \mathcal{F} & \mathcal{N}_{14}^\ell(h) &\equiv ig \bar{L}_L \sigma^{\mu\nu} [W_{\mu\nu}, \mathbf{T}] \mathbf{U} L_R \mathcal{F}.
\end{aligned}$$

where, as explained above, all these operators are required as counterterms in the 1-loop renormalisation of \mathcal{L}_0 with the exception of those with tensor structure, that correspond to finite contributions. It is also worth recalling that all the chirality-flipping structures listed here are CP even in the combination $(\mathcal{N}_j^\ell + \text{h.c.})$ but independent CP violating terms of the form $(i\mathcal{N}_j^\ell + \text{h.c.})$ should also be considered.

2.3.2 Four-fermion operators $\Delta\mathcal{L}_{4F}$

Four fermion operators can be classified into four-quarks, four-leptons and two-quark-two-lepton sets. The overall Lagrangian reads:

$$\begin{aligned}
\Delta\mathcal{L}_{4F} = \frac{(4\pi)^2}{\Lambda^2} &\left[\sum_{j=1}^8 (r_j^{\mathcal{Q}} + i\tilde{r}_j^{\mathcal{Q}}) R_j^{\mathcal{Q}} + \sum_{j=9}^{26} r_j^{\mathcal{Q}} R_j^{\mathcal{Q}} + (r_1^\ell + i\tilde{r}_1^\ell) R_1^\ell + \sum_{j=2}^7 r_j^\ell R_j^\ell + \right. \\
&\left. + \sum_{j=1}^6 (r_j^{\mathcal{Q}\ell} + i\tilde{r}_j^{\mathcal{Q}\ell}) R_j^{\mathcal{Q}\ell} + \sum_{j=7}^{23} r_j^{\mathcal{Q}\ell} R_j^{\mathcal{Q}\ell} + \text{h.c.} \right]. \quad (2.22)
\end{aligned}$$

Details on the construction and reduction of this subset of operators can be found in App. C.3. As for the bilinears case, the chirality-flipping contractions $(\bar{\psi}_L \psi_R)(\bar{\psi}_L \psi_R)$ listed here are CP even in the combination $(R_j^f + \text{h.c.})$ but independent CP violating terms of the form $(iR_j^f + \text{h.c.})$ should also be considered.

Pure Quark Operators

The only four-quark operators required to remove divergences originated at 1-loop are the following:

$$\begin{aligned}
R_1^{\mathcal{Q}}(h) &\equiv (\bar{Q}_L \mathbf{U} Q_R)(\bar{Q}_L \mathbf{U} Q_R) \mathcal{F} & R_2^{\mathcal{Q}}(h) &\equiv (\bar{Q}_L \sigma^i \mathbf{U} Q_R)(\bar{Q}_L \sigma^i \mathbf{U} Q_R) \mathcal{F} \\
R_3^{\mathcal{Q}}(h) &\equiv (\bar{Q}_L \mathbf{U} Q_R)(\bar{Q}_L \mathbf{TU} Q_R) \mathcal{F} & R_4^{\mathcal{Q}}(h) &\equiv (\bar{Q}_L \mathbf{TU} Q_R)(\bar{Q}_L \mathbf{TU} Q_R) \mathcal{F} \\
R_5^{\mathcal{Q}}(h) &\equiv (\bar{Q}_L \lambda^A \mathbf{U} Q_R)(\bar{Q}_L \lambda^A \mathbf{U} Q_R) \mathcal{F} & R_6^{\mathcal{Q}}(h) &\equiv (\bar{Q}_L \lambda^A \sigma^i \mathbf{U} Q_R)(\bar{Q}_L \lambda^A \sigma^i \mathbf{U} Q_R) \mathcal{F} \\
R_7^{\mathcal{Q}}(h) &\equiv (\bar{Q}_L \lambda^A \mathbf{U} Q_R)(\bar{Q}_L \lambda^A \mathbf{TU} Q_R) \mathcal{F} & R_8^{\mathcal{Q}}(h) &\equiv (\bar{Q}_L \lambda^A \mathbf{TU} Q_R)(\bar{Q}_L \lambda^A \mathbf{TU} Q_R) \mathcal{F}.
\end{aligned}$$

A large number of additional structures can be constructed, that are listed below and included in the basis. Although they do not correspond to counterterms in the renormalisation of \mathcal{L}_0 , they are potentially generated by the exchange of BSM resonances:

$$\begin{aligned}
R_9^{\mathcal{Q}}(h) &\equiv (\bar{Q}_L \gamma_\mu Q_L)(\bar{Q}_L \gamma^\mu Q_L) \mathcal{F} & R_{10}^{\mathcal{Q}}(h) &\equiv (\bar{Q}_L \gamma_\mu Q_L)(\bar{Q}_L \gamma^\mu \mathbf{T} Q_L) \mathcal{F} \\
R_{11}^{\mathcal{Q}}(h) &\equiv (\bar{Q}_L \gamma_\mu \mathbf{T} Q_L)(\bar{Q}_L \gamma^\mu \mathbf{T} Q_L) \mathcal{F} & R_{12}^{\mathcal{Q}}(h) &\equiv (\bar{Q}_L \gamma_\mu \sigma^j Q_L)(\bar{Q}_L \gamma^\mu \sigma^j Q_L) \mathcal{F} \\
R_{13}^{\mathcal{Q}}(h) &\equiv (\bar{Q}_R \gamma_\mu Q_R)(\bar{Q}_R \gamma^\mu Q_R) \mathcal{F} & R_{14}^{\mathcal{Q}}(h) &\equiv (\bar{Q}_R \gamma_\mu Q_R)(\bar{Q}_R \gamma^\mu \mathbf{U}^\dagger \mathbf{T} \mathbf{U} Q_R) \mathcal{F} \\
R_{15}^{\mathcal{Q}}(h) &\equiv (\bar{Q}_R \gamma_\mu \mathbf{U}^\dagger \mathbf{T} \mathbf{U} Q_R)(\bar{Q}_R \gamma^\mu \mathbf{U}^\dagger \mathbf{T} \mathbf{U} Q_R) \mathcal{F} & R_{16}^{\mathcal{Q}}(h) &\equiv (\bar{Q}_R \gamma_\mu \sigma^j Q_R)(\bar{Q}_R \gamma^\mu \mathbf{U}^\dagger \sigma^j \mathbf{U} Q_R) \mathcal{F} \\
R_{17}^{\mathcal{Q}}(h) &\equiv (\bar{Q}_L \gamma_\mu Q_L)(\bar{Q}_R \gamma^\mu Q_R) \mathcal{F} & R_{18}^{\mathcal{Q}}(h) &\equiv (\bar{Q}_L \gamma_\mu Q_L)(\bar{Q}_R \gamma^\mu \mathbf{U}^\dagger \mathbf{T} \mathbf{U} Q_R) \mathcal{F} \\
R_{19}^{\mathcal{Q}}(h) &\equiv (\bar{Q}_L \gamma^\mu \mathbf{T} Q_L)(\bar{Q}_R \gamma_\mu Q_R) \mathcal{F} & R_{20}^{\mathcal{Q}}(h) &\equiv (\bar{Q}_L \gamma_\mu \mathbf{T} Q_L)(\bar{Q}_R \gamma^\mu \mathbf{U}^\dagger \mathbf{T} \mathbf{U} Q_R) \mathcal{F} \\
R_{21}^{\mathcal{Q}}(h) &\equiv (\bar{Q}_L \gamma_\mu \sigma^i Q_L)(\bar{Q}_R \gamma^\mu \mathbf{U}^\dagger \sigma^i \mathbf{U} Q_R) \mathcal{F} & R_{22}^{\mathcal{Q}}(h) &\equiv (\bar{Q}_L \gamma_\mu \lambda^A Q_L)(\bar{Q}_R \gamma^\mu \lambda^A Q_R) \mathcal{F} \\
R_{23}^{\mathcal{Q}}(h) &\equiv (\bar{Q}_L \gamma_\mu \lambda^A Q_L)(\bar{Q}_R \gamma^\mu \lambda^A \mathbf{U}^\dagger \mathbf{T} \mathbf{U} Q_R) \mathcal{F} & R_{24}^{\mathcal{Q}}(h) &\equiv (\bar{Q}_L \gamma^\mu \lambda^A \mathbf{T} Q_L)(\bar{Q}_R \gamma_\mu \lambda^A Q_R) \mathcal{F} \\
R_{25}^{\mathcal{Q}}(h) &\equiv (\bar{Q}_L \gamma_\mu \lambda^A \mathbf{T} Q_L)(\bar{Q}_R \gamma^\mu \lambda^A \mathbf{U}^\dagger \mathbf{T} \mathbf{U} Q_R) \mathcal{F} & R_{26}^{\mathcal{Q}}(h) &\equiv (\bar{Q}_L \gamma_\mu \lambda^A \sigma^i Q_L)(\bar{Q}_R \gamma^\mu \lambda^A \mathbf{U}^\dagger \sigma^i \mathbf{U} Q_R) \mathcal{F}.
\end{aligned}$$

Pure Leptonic Operators

The set of independent four-lepton operators is considerably smaller than that with four quarks, due to the absence of right-handed neutrinos and of colour charges. Only one operator is required as a 1-loop counterterm:

$$R_1^\ell(h) \equiv (\bar{L}_L \mathbf{U} L_R)(\bar{L}_L \mathbf{U} L_R) \mathcal{F}.$$

Six additional structures, that are not required as counterterms, complete the list of possible invariants:

$$\begin{aligned}
R_2^\ell(h) &\equiv (\bar{L}_L \gamma_\mu L_L)(\bar{L}_L \gamma^\mu L_L) \mathcal{F} & R_3^\ell(h) &\equiv (\bar{L}_R \gamma_\mu L_R)(\bar{L}_R \gamma^\mu L_R) \mathcal{F} \\
R_4^\ell(h) &\equiv (\bar{L}_L \gamma_\mu L_L)(\bar{L}_L \gamma^\mu \mathbf{T} L_L) \mathcal{F} & R_5^\ell(h) &\equiv (\bar{L}_L \gamma_\mu \mathbf{T} L_L)(\bar{L}_L \gamma^\mu \mathbf{T} L_L) \mathcal{F} \\
R_6^\ell(h) &\equiv (\bar{L}_L \gamma_\mu L_L)(\bar{L}_R \gamma^\mu L_R) \mathcal{F} & R_7^\ell(h) &\equiv (\bar{L}_L \gamma^\mu \mathbf{T} L_L)(\bar{L}_R \gamma_\mu L_R) \mathcal{F}.
\end{aligned}$$

Mixed Quark-Lepton Operators

Finally, barring any B or L violation effects, mixed four-fermion operators can only contain two quarks and two leptons in either of the current structures $\bar{L}L\bar{Q}Q$ and $\bar{L}Q\bar{Q}L$.

Among the constructed invariants, the following are required to reabsorb 1-loop divergences:

$$\begin{aligned}
R_1^{\mathcal{Q}\ell}(h) &\equiv (\bar{L}_L \mathbf{U} L_R)(\bar{Q}_L \mathbf{U} Q_R) \mathcal{F} & R_2^{\mathcal{Q}\ell}(h) &\equiv (\bar{L}_L \mathbf{U} Q_R)(\bar{Q}_L \mathbf{U} L_R) \mathcal{F} \\
R_3^{\mathcal{Q}\ell}(h) &\equiv (\bar{L}_L \mathbf{U} L_R)(\bar{Q}_L \mathbf{T} \mathbf{U} Q_R) \mathcal{F} & R_4^{\mathcal{Q}\ell}(h) &\equiv (\bar{L}_L \mathbf{T} \mathbf{U} Q_R)(\bar{Q}_L \mathbf{U} L_R) \mathcal{F} \\
R_5^{\mathcal{Q}\ell}(h) &\equiv (\bar{L}_L \sigma^i \mathbf{U} L_R)(\bar{Q}_L \sigma^i \mathbf{U} Q_R) \mathcal{F} & R_6^{\mathcal{Q}\ell}(h) &\equiv (\bar{L}_L \sigma^i \mathbf{U} Q_R)(\bar{Q}_L \sigma^i \mathbf{U} L_R) \mathcal{F},
\end{aligned}$$

while the remaining correspond to finite diagrams and are included for completeness:

$$\begin{aligned}
R_7^{\mathcal{Q}\ell}(h) &\equiv (\bar{L}_L \gamma_\mu L_L)(\bar{Q}_L \gamma^\mu Q_L) \mathcal{F} & R_8^{\mathcal{Q}\ell}(h) &\equiv (\bar{L}_R \gamma_\mu L_R)(\bar{Q}_R \gamma^\mu Q_R) \mathcal{F} \\
R_9^{\mathcal{Q}\ell}(h) &\equiv (\bar{L}_L \gamma_\mu L_L)(\bar{Q}_L \gamma^\mu \mathbf{T} Q_L) \mathcal{F} & R_{10}^{\mathcal{Q}\ell}(h) &\equiv (\bar{L}_R \gamma_\mu L_R)(\bar{Q}_R \gamma^\mu \mathbf{U}^\dagger \mathbf{T} \mathbf{U} Q_R) \mathcal{F} \\
R_{11}^{\mathcal{Q}\ell}(h) &\equiv (\bar{L}_L \gamma_\mu \mathbf{T} L_L)(\bar{Q}_L \gamma^\mu Q_L) \mathcal{F} & R_{12}^{\mathcal{Q}\ell}(h) &\equiv (\bar{L}_L \gamma_\mu \mathbf{T} L_L)(\bar{Q}_L \gamma^\mu \mathbf{T} Q_L) \mathcal{F} \\
R_{13}^{\mathcal{Q}\ell}(h) &\equiv (\bar{L}_L \gamma_\mu \sigma^i L_L)(\bar{Q}_L \gamma^\mu \sigma^i Q_L) \mathcal{F} & R_{14}^{\mathcal{Q}\ell}(h) &\equiv (\bar{L}_L \gamma_\mu L_L)(\bar{Q}_R \gamma^\mu Q_R) \mathcal{F} \\
R_{15}^{\mathcal{Q}\ell}(h) &\equiv (\bar{Q}_L \gamma_\mu Q_L)(\bar{L}_R \gamma^\mu L_R) \mathcal{F} & R_{16}^{\mathcal{Q}\ell}(h) &\equiv (\bar{L}_L \gamma^\mu \mathbf{T} L_L)(\bar{Q}_R \gamma_\mu Q_R) \mathcal{F} \\
R_{17}^{\mathcal{Q}\ell}(h) &\equiv (\bar{Q}_L \gamma_\mu \mathbf{T} Q_L)(\bar{L}_R \gamma^\mu L_R) \mathcal{F} & R_{18}^{\mathcal{Q}\ell}(h) &\equiv (\bar{L}_L \gamma_\mu L_L)(\bar{Q}_R \gamma^\mu \mathbf{U}^\dagger \mathbf{T} \mathbf{U} Q_R) \mathcal{F} \\
R_{19}^{\mathcal{Q}\ell}(h) &\equiv (\bar{L}_L \gamma^\mu \mathbf{T} L_L)(\bar{Q}_R \gamma_\mu \mathbf{U}^\dagger \mathbf{T} \mathbf{U} Q_R) \mathcal{F} & R_{20}^{\mathcal{Q}\ell}(h) &\equiv (\bar{L}_L \gamma^\mu \sigma^j L_L)(\bar{Q}_R \gamma_\mu \mathbf{U}^\dagger \sigma^j \mathbf{U} Q_R) \mathcal{F} \\
R_{21}^{\mathcal{Q}\ell}(h) &\equiv (\bar{Q}_L \gamma_\mu L_L)(\bar{L}_R \gamma^\mu Q_R) \mathcal{F} & R_{22}^{\mathcal{Q}\ell}(h) &\equiv (\bar{Q}_L \gamma_\mu \mathbf{T} L_L)(\bar{L}_R \gamma^\mu Q_R) \mathcal{F} \\
R_{23}^{\mathcal{Q}\ell}(h) &\equiv (\bar{Q}_L \gamma^\mu \sigma^j L_L)(\bar{L}_R \gamma_\mu \mathbf{U}^\dagger \sigma^j \mathbf{U} Q_R) \mathcal{F}.
\end{aligned}$$

2.4 Comparison with the SMEFT basis

The comparison with the SMEFT is crucial for the identification of signals able to shed some light on the Higgs nature.

For the bosonic sector, the relation between the HEFT and its linear counterpart has already been identified in Ref. [24], adopting the so-called HISZ basis [38, 39], which is also used in Refs. [40–42]. Those results still hold here, up to the fact that some operators have been traded for fermionic ones: the correspondence is summarised in Table 1, where the relation to the basis of Ref. [7] is also reported. The fermionic sector of the HEFT has also been matched with the linear bases of Refs. [7] and [40–42], as indicated in Table 2.

It is worth pointing out a few points that should be kept into account when performing this comparison:

- In the HEFT, right-handed fermions are grouped in the $SU(2)_R$ doublets L_R and Q_R and the up and down components are disentangled inserting the object $\mathbf{U}^\dagger \mathbf{T} \mathbf{U} = \sigma^3$ in the bilinear structures. Each linear operator, written in the traditional notation, is then easily matched with a linear combination of HEFT invariants.

On the other hand, it is worth noticing that the HEFT notation allows to construct invariants that contain the structure $\mathbf{U}^\dagger \sigma^j \mathbf{U}$, that in general does not have an equivalent in the SMEFT. In particular, this can induce RH charged currents, that are absent in the linear case.

- The adimensional scalar field \mathbf{T} corresponds, in the linear context, to a quadratic combination of Higgs doublets. As a consequence, the counterparts of fermionic invariants containing \mathbf{T} are mostly linear operators of dimension $d > 6$, that are therefore not present in the list of Refs. [7], [41, 42].

The insertions of \mathbf{T} into right-handed currents, mentioned in the previous point, represent an exception. In fact, in these cases \mathbf{T} appears in the combination $\mathbf{U}^\dagger \mathbf{T} \mathbf{U} = \sigma^3$, that does not contain any field and in fact is not associated to dimensional objects in the linear language.

Ref. [7]	Refs. [41, 42]	HEFT	Ref. [7]	Refs. [41, 42]	HEFT
\mathcal{Q}_φ	$\mathcal{O}_{\Phi,3}$	scalar pot.	$\mathcal{Q}_{\varphi\Box}$	\mathcal{O}_{Φ_2}	$\mathcal{F}_C + \mathcal{F}_Y(\mathcal{P}_H)$
$\mathcal{Q}_{\varphi D}$	$\mathcal{O}_{\Phi,1}$	\mathcal{P}_T	$\mathcal{Q}_{\varphi G}$	\mathcal{O}_{GG}	\mathcal{P}_G
$\mathcal{Q}_{\varphi W}$	\mathcal{O}_{WW}	\mathcal{P}_W	$\mathcal{Q}_{\varphi B}$	\mathcal{O}_{BB}	\mathcal{P}_B
$\mathcal{Q}_{\varphi WB}$	\mathcal{O}_{BW}	\mathcal{P}_1	—	\mathcal{O}_B	$\mathcal{P}_2 + \mathcal{P}_4$
—	\mathcal{O}_W	$\mathcal{P}_3 + \mathcal{P}_5$			
\mathcal{Q}_G	“ \mathcal{Q}_G ”	\mathcal{P}_{GGG}	\mathcal{Q}_W	\mathcal{O}_{WWW}	\mathcal{P}_{WWW}
$\mathcal{Q}_{\varphi\tilde{G}}$	“ $\mathcal{Q}_{\varphi\tilde{G}}$ ”	$\mathcal{S}_{\tilde{G}}$	$\mathcal{Q}_{\varphi\tilde{B}}$	“ $\mathcal{Q}_{\varphi\tilde{B}}$ ”	$\mathcal{S}_{\tilde{B}}$
$\mathcal{Q}_{\varphi\tilde{W}}$	“ $\mathcal{Q}_{\varphi\tilde{W}}$ ”	$\mathcal{S}_{\tilde{W}}$	$\mathcal{Q}_{\varphi\tilde{W}B}$	“ $\mathcal{Q}_{\varphi\tilde{W}B}$ ”	\mathcal{S}_1
$\mathcal{Q}_{\tilde{G}}$	“ $\mathcal{Q}_{\tilde{G}}$ ”	$\mathcal{P}_{\tilde{G}GG}$	$\mathcal{Q}_{\tilde{W}}$	“ $\mathcal{Q}_{\tilde{W}}$ ”	$\mathcal{P}_{\tilde{W}WW}$

Table 1: Correspondence between the SMEFT operators from Refs. [7] and [41, 42], and the HEFT terms presented here for the bosonic sector. The - refers to the absence of an equivalent operator. The use of “ \mathcal{Q}_i ” notation for the second column means that a particular operator does not explicitly appear in Refs. [41, 42], but that anyway enters the SMEFT basis and is defined as in Ref. [7]. Numerical coefficients and signs in the combinations of the HEFT operators are not indicated.

- The two-derivative object $\mathbf{V}_\mu \mathbf{V}^\mu$ is typically described, in the SMEFT, by a quantity proportional to $D_\mu \Phi^\dagger D^\mu \Phi$, which has canonical dimension 4. Thus, fermionic bilinears containing this structure correspond to SMEFT operators with $d \geq 7$.

Tables 1 and 2 summarise the relations between operators of the HEFT, defined in the previous section, and those of the SMEFT from Refs. [7] and [41, 42]. The only difference between these two linear bases (the first two columns in both tables) lies in the choice of two invariants: in Refs. [41, 42] the EOMs have been used for removing the fermionic terms corresponding to $\mathcal{Q}_{\varphi l, ii}^{(1)}$ and $\mathcal{Q}_{\varphi l, ii}^{(3)}$ in Ref. [7], replacing them with the bosonic operators \mathcal{O}_B and \mathcal{O}_W . In the HEFT construction, the EOMs have been applied analogously to Refs. [41, 42], namely retaining \mathcal{P}_B and \mathcal{P}_W , rather than two leptonic invariants (see Eq. (D.14)).

All the HEFT operators that do not appear in this list have SMEFT counterparts (dubbed also “linear siblings”) of dimension larger than six and therefore are not contained in the bases of Refs. [7] and [41, 42].

Ref. [7]	Refs. [41, 42]	HEFT	Ref. [7]	Refs. [41, 42]	HEFT
$\mathcal{Q}_{\varphi u}$	$\mathcal{O}_{u\Phi}$	$\mathcal{Y}_U(h)$	$\mathcal{Q}_{\varphi e}$	$\mathcal{O}_{e\Phi}$	$\mathcal{Y}_E(h)$
$\mathcal{Q}_{\varphi d}$	$\mathcal{O}_{d\Phi}$	$\mathcal{Y}_D(h)$	$\mathcal{Q}_{\varphi l, ii}^{(1)}$	—	—
$\mathcal{Q}_{\varphi q}^{(1)}$	$\mathcal{O}_{\Phi Q}^{(1)}$	$\mathcal{N}_5^{\mathcal{Q}}$	$\mathcal{Q}_{\varphi l, ij}^{(1)}$	$\mathcal{O}_{\Phi L, ij}^{(1)}$	$i\bar{L}_{L_i}\gamma_\mu\{\mathbf{T}, \mathbf{V}^\mu\}L_{L_j}\mathcal{F}$
$\mathcal{Q}_{\varphi q}^{(3)}$	$\mathcal{O}_{\Phi Q}^{(3)}$	$\mathcal{N}_1^{\mathcal{Q}}$	$\mathcal{Q}_{\varphi l, ii}^{(3)}$	—	—
$\mathcal{Q}_{\varphi u}$	$\mathcal{O}_{\Phi u}^{(1)}$	$\mathcal{N}_2^{\mathcal{Q}} + \mathcal{N}_6^{\mathcal{Q}} + \mathcal{N}_8^{\mathcal{Q}}$	$\mathcal{Q}_{\varphi l, ij}^{(3)}$	$\mathcal{O}_{\Phi L, ij}^{(3)}$	$i\bar{L}_{L_i}\gamma_\mu\mathbf{V}^\mu L_{L_j}\mathcal{F}$
$\mathcal{Q}_{\varphi d}$	$\mathcal{O}_{\Phi d}^{(1)}$	$\mathcal{N}_2^{\mathcal{Q}} + \mathcal{N}_6^{\mathcal{Q}} + \mathcal{N}_8^{\mathcal{Q}}$	$\mathcal{Q}_{\varphi e}$	$\mathcal{O}_{\Phi e}^{(1)}$	\mathcal{N}_2^ℓ
$\mathcal{Q}_{\varphi ud}$	$\mathcal{O}_{\Phi ud}^{(1)}$	$\mathcal{N}_2^{\mathcal{Q}} + \mathcal{N}_8^{\mathcal{Q}}$			
\mathcal{Q}_{uG}	“ \mathcal{Q}_{uG} ”	$\mathcal{N}_{31}^{\mathcal{Q}} + \mathcal{N}_{32}^{\mathcal{Q}}$			
\mathcal{Q}_{dG}	“ \mathcal{Q}_{dG} ”	$\mathcal{N}_{31}^{\mathcal{Q}} + \mathcal{N}_{32}^{\mathcal{Q}}$			
\mathcal{Q}_{uW}	“ \mathcal{Q}_{uW} ”	$\mathcal{N}_{33}^{\mathcal{Q}} + \mathcal{N}_{34}^{\mathcal{Q}} + \mathcal{N}_{35}^{\mathcal{Q}}$			
\mathcal{Q}_{dW}	“ \mathcal{Q}_{dW} ”	$\mathcal{N}_{33}^{\mathcal{Q}} + \mathcal{N}_{34}^{\mathcal{Q}} + \mathcal{N}_{35}^{\mathcal{Q}}$	\mathcal{Q}_{eW}	“ \mathcal{Q}_{eW} ”	\mathcal{N}_{13}^ℓ
\mathcal{Q}_{uB}	“ \mathcal{Q}_{uB} ”	$\mathcal{N}_{29}^{\mathcal{Q}} + \mathcal{N}_{30}^{\mathcal{Q}}$			
\mathcal{Q}_{dB}	“ \mathcal{Q}_{dB} ”	$\mathcal{N}_{29}^{\mathcal{Q}} + \mathcal{N}_{30}^{\mathcal{Q}}$	\mathcal{Q}_{eB}	“ \mathcal{Q}_{eB} ”	\mathcal{N}_{12}^ℓ
$\mathcal{Q}_{qq}^{(1)}$	“ $\mathcal{Q}_{qq}^{(1)}$ ”	$R_9^{\mathcal{Q}}$	\mathcal{Q}_{ll}	“ \mathcal{Q}_{ll} ”	R_2^ℓ
$\mathcal{Q}_{qq}^{(3)}$	“ $\mathcal{Q}_{qq}^{(3)}$ ”	$R_{12}^{\mathcal{Q}}$	$\mathcal{Q}_{lq}^{(1)}$	“ $\mathcal{Q}_{lq}^{(1)}$ ”	$R_7^{\mathcal{Q}\ell}$
\mathcal{Q}_{uu}	“ \mathcal{Q}_{uu} ”	$R_{13}^{\mathcal{Q}} + R_{14}^{\mathcal{Q}} + R_{15}^{\mathcal{Q}}$	$\mathcal{Q}_{lq}^{(3)}$	“ $\mathcal{Q}_{lq}^{(3)}$ ”	$R_{13}^{\mathcal{Q}\ell}$
\mathcal{Q}_{dd}	“ \mathcal{Q}_{dd} ”	$R_{13}^{\mathcal{Q}} + R_{14}^{\mathcal{Q}} + R_{15}^{\mathcal{Q}}$	\mathcal{Q}_{ee}	“ \mathcal{Q}_{ee} ”	R_3^ℓ
$\mathcal{Q}_{ud}^{(1)}$	“ $\mathcal{Q}_{ud}^{(1)}$ ”	$R_{13}^{\mathcal{Q}} + R_{15}^{\mathcal{Q}}$	\mathcal{Q}_{eu}	“ \mathcal{Q}_{eu} ”	$R_8^{\mathcal{Q}\ell} + R_{10}^{\mathcal{Q}\ell}$
$\mathcal{Q}_{ud}^{(8)}$	“ $\mathcal{Q}_{ud}^{(8)}$ ”	$R_{13}^{\mathcal{Q}} + R_{16}^{\mathcal{Q}} + R_{15}^{\mathcal{Q}}$	\mathcal{Q}_{ed}	“ \mathcal{Q}_{ed} ”	$R_8^{\mathcal{Q}\ell} + R_{10}^{\mathcal{Q}\ell}$
$\mathcal{Q}_{qu}^{(1)}$	“ $\mathcal{Q}_{qu}^{(1)}$ ”	$R_{17}^{\mathcal{Q}} + R_{18}^{\mathcal{Q}}$	\mathcal{Q}_{le}	“ \mathcal{Q}_{le} ”	R_6^ℓ
$\mathcal{Q}_{qu}^{(8)}$	“ $\mathcal{Q}_{qu}^{(8)}$ ”	$R_{22}^{\mathcal{Q}} + R_{23}^{\mathcal{Q}}$	\mathcal{Q}_{lu}	“ \mathcal{Q}_{lu} ”	$R_{14}^{\mathcal{Q}\ell} + R_{18}^{\mathcal{Q}\ell}$
$\mathcal{Q}_{qd}^{(1)}$	“ $\mathcal{Q}_{qd}^{(1)}$ ”	$R_{17}^{\mathcal{Q}} + R_{18}^{\mathcal{Q}}$	\mathcal{Q}_{ld}	“ \mathcal{Q}_{ld} ”	$R_{14}^{\mathcal{Q}\ell} + R_{18}^{\mathcal{Q}\ell}$
$\mathcal{Q}_{qd}^{(8)}$	“ $\mathcal{Q}_{qd}^{(8)}$ ”	$R_{22}^{\mathcal{Q}} + R_{23}^{\mathcal{Q}}$	\mathcal{Q}_{qe}	“ \mathcal{Q}_{qe} ”	$R_{15}^{\mathcal{Q}\ell}$
$\mathcal{Q}_{quqd}^{(1)}$	“ $\mathcal{Q}_{quqd}^{(1)}$ ”	$R_1^{\mathcal{Q}} + R_2^{\mathcal{Q}}$	\mathcal{Q}_{ledq}	“ \mathcal{Q}_{ledq} ”	$R_{21}^{\mathcal{Q}\ell} + R_{22}^{\mathcal{Q}\ell}$
$\mathcal{Q}_{quqd}^{(8)}$	“ $\mathcal{Q}_{quqd}^{(8)}$ ”	$R_5^{\mathcal{Q}} + R_6^{\mathcal{Q}}$	$\mathcal{Q}_{lequ}^{(1)}$	“ $\mathcal{Q}_{lequ}^{(1)}$ ”	$R_2^{\mathcal{Q}\ell} + R_6^{\mathcal{Q}\ell}$
			$\mathcal{Q}_{lequ}^{(3)}$	“ $\mathcal{Q}_{lequ}^{(3)}$ ”	$R_1^{\mathcal{Q}\ell} + R_2^{\mathcal{Q}\ell} + R_3^{\mathcal{Q}\ell} + R_5^{\mathcal{Q}\ell} + R_6^{\mathcal{Q}\ell}$

Table 2: Correspondence between the SMEFT operators from Refs. [7] and [41, 42], and the HEFT terms presented here for the fermionic sector. The - refers to the absence of an equivalent operator. The use of “ \mathcal{Q}_i ” notation for the second column means that a particular operator does not explicitly appear in Refs. [41, 42], but that anyway enters the SMEFT basis and is defined as in Ref. [7]. Flavour indices are omitted, unless explicitly indicated. Numerical coefficients and signs in the combinations of the HEFT operators are not indicated.

3 Phenomenology

3.1 Renormalisation procedure

The phenomenological analysis is carried out in the Z-scheme, defined by the following set of observables, that are taken as input parameters:

$$\begin{aligned}
\alpha_s & \text{ world average [43],} \\
G_F & \text{ extracted from the muon decay rate [43],} \\
\alpha_{\text{em}} & \text{ extracted from Thomson scattering [43],} \\
M_Z & \text{ extracted from the } Z \text{ lineshape at LEP I [43],} \\
M_h & \text{ measured at LHC [44].}
\end{aligned} \tag{3.1}$$

All the other quantities appearing in the Lagrangian will be implicitly interpreted as corresponding to the combinations of experimental inputs as follows:

$$\begin{aligned}
e^2 &= 4\pi\alpha_{\text{em}}, & \sin^2 \theta_W &= \frac{1}{2} \left(1 - \sqrt{1 - \frac{4\pi\alpha_{\text{em}}}{\sqrt{2}G_F M_Z^2}} \right), \\
v^2 &= \frac{1}{\sqrt{2}G_F}, & \left(g = \frac{e}{\sin \theta_W}, \quad g' = \frac{e}{\cos \theta_W} \right) & \Big|_{\theta_W, e \text{ as above}}.
\end{aligned} \tag{3.2}$$

The trigonometric functions $\sin \theta_W$, $\cos \theta_W$ will be conveniently shortened to s_θ , c_θ .

The kinetic terms are made canonical and diagonal with the following field redefinitions:

$$\begin{aligned}
A_\mu &\rightarrow A_\mu \left[1 + s_{2\theta}c_1 + 2s_\theta^2c_{12} - \frac{1}{2}(c_\theta^2c_B + s_\theta^2c_W) \right] + \\
&\quad + Z_\mu 2 \left[c_{2\theta}c_1 + s_{2\theta} \left(c_{12} + \frac{c_B - c_W}{4} \right) \right] + \mathcal{O}(c_i^2) \\
Z_\mu &\rightarrow Z_\mu \left[1 - s_{2\theta}c_1 + 2c_\theta^2c_{12} - \frac{1}{2}(c_\theta^2c_W + s_\theta^2c_B) \right] + \mathcal{O}(c_i^2) \\
W_\mu^+ &\rightarrow W_\mu^+ \left[1 - \frac{1}{2}c_W \right] + \mathcal{O}(c_i^2).
\end{aligned} \tag{3.3}$$

The contributions to the input parameters at first order in the effective coefficients read:

$$\begin{aligned}
\frac{\delta\alpha_{\text{em}}}{\alpha_{\text{em}}} &\simeq 2s_{2\theta}c_1 + 4s_\theta^2c_{12} - c_\theta^2c_B - s_\theta^2c_W & \frac{\delta G_F}{G_F} &\simeq -64\sqrt{2}\pi^2 \frac{v^2}{\Lambda^2} (r_2^\ell - r_5^\ell) \\
\frac{\delta M_Z}{M_Z} &\simeq -c_T - s_{2\theta}c_1 + 2c_\theta^2c_{12} - \frac{1}{2}(c_\theta^2c_W + s_\theta^2c_B) & \frac{\delta M_h}{M_h} &\simeq 0.
\end{aligned} \tag{3.4}$$

The resulting shifts for the W mass and fermion couplings to gauge bosons with respect to their corresponding SM expectations due to these finite renormalisation effects are summarised below:

W mass:

$$\frac{\Delta M_W}{M_W} = \frac{c_\theta^2}{c_{2\theta}}c_T + \frac{s_{2\theta}}{c_{2\theta}}c_1 - 2c_{12} + \frac{32\pi^2\sqrt{2}s_\theta^2}{c_{2\theta}} \frac{v^2}{\Lambda^2} (r_2^\ell - r_5^\ell). \tag{3.5}$$

Fermionic couplings:

It is convenient to adopt the following compact notation:

$$\begin{aligned}\Delta g_1 &= c_T + 32\pi^2 \sqrt{2} \frac{v^2}{\Lambda^2} (r_2^\ell - r_5^\ell) \\ \Delta g_W &= \frac{c_\theta^2}{c_{2\theta}} c_T + t_{2\theta} c_1 - 2c_{12} + \frac{32\pi^2 \sqrt{2} c_\theta^2 v^2}{c_{2\theta} \Lambda^2} (r_2^\ell - r_5^\ell) \\ \Delta g_2 &= -s_\theta^2 \left(-\frac{\delta s_\theta^2}{s_\theta^2} - \frac{\beta}{t_\theta} \right) = \frac{s_{2\theta}^2}{2c_{2\theta}} \left(c_T + \frac{2c_1}{s_{2\theta}} + 32\pi^2 \sqrt{2} \frac{v^2}{\Lambda^2} (r_2^\ell - r_5^\ell) \right),\end{aligned}\tag{3.6}$$

where Δg_1 accounts for the renormalisation of Z_μ , g and c_θ in the combination gZ_μ/c_θ ; Δg_W for the renormalisation of W_μ and g in the combination gW_μ ; Δg_2 for the renormalisation of s_θ^2 and for the contribution to the Z couplings that comes from the redefinition of the photon field: $A \rightarrow \alpha A + \beta Z$ (see Eq. (3.3)). With this notation, the renormalisation of Z couplings to left-handed and right-handed fermions, $g_L^f = (T_3^f - s_\theta^2 Q^f)$ and $g_R^f = -s_\theta^2 Q^f$, and of the W to left handed fermions can be written as

$$\Delta g_{L,R}^f = g_{L,R}^f \Delta g_1 + Q^f \Delta g_2 \quad \Delta g_W^{ff'} = \Delta g_W, \tag{3.7}$$

where Q_f and T_{3f} are respectively the electric and isospin charges of the fermion f , and where the W couplings to left-handed fermions is normalised to 1 in the SM.

The next sections are dedicated to the discussion of the constraints imposed on the operator coefficients considering respectively electroweak precision data, Higgs results from the LHC and the Tevatron, and measurements of the triple gauge bosons couplings. For the sake of simplicity we will assume fermion universality as well as the absence of new sources of flavour violation.

3.2 Constraints from EWPD

After accounting for finite renormalisation effects in the gauge bosons' wavefunctions and couplings as well as for direct contributions to the vertices, 12 operators modify the Z and W gauge boson couplings to fermions with the same Lorentz structure as the SM and the W mass, which correspondingly lead to linear modifications of the EWPD.

Five operators, $\mathcal{P}_T(h)$, $\mathcal{P}_1(h)$, $\mathcal{P}_{12}(h)$, $\mathcal{R}_2^\ell(h)$, $\mathcal{R}_5^\ell(h)$ give tree level contributions to universal modifications of the couplings and of the W mass, which can be recast in terms of the oblique S, T, U parameters [45, 46] and of the shift in the Fermi constant ΔG_F . In particular

$$\alpha S = -8s_\theta c_\theta c_1, \quad \alpha T = 2c_T, \quad \alpha U = -16s_\theta^2 c_{12}, \quad \frac{\delta G_F}{G_F} = -64\pi^2 \sqrt{2} \frac{v^2}{\Lambda^2} (r_2^\ell - r_5^\ell), \tag{3.8}$$

so, for example, the correction to the W mass in Eq. (3.5) reads

$$\frac{\Delta M_W}{M_W} = \frac{c_\theta^2}{2c_{2\theta}} \alpha T - \frac{1}{4c_{2\theta}} \alpha S + \frac{1}{8s_\theta^2} \alpha U - \frac{s_\theta^2}{2c_{2\theta}} \frac{\delta G_F}{G_F}. \tag{3.9}$$

The other seven operators, $\mathcal{N}_1^{\mathcal{Q}}(h)$, $\mathcal{N}_2^{\mathcal{Q}}(h)$, $\mathcal{N}_5^{\mathcal{Q}}(h)$, $\mathcal{N}_6^{\mathcal{Q}}(h)$, $\mathcal{N}_7^{\mathcal{Q}}(h)$, $\mathcal{N}_8^{\mathcal{Q}}(h)$, $\mathcal{N}_2^{\ell}(h)$, give fermion dependent contributions to the W and Z couplings. Altogether the shifts to the SM Z couplings can be written as

$$\Delta g_{L,R}^f = g_{L,R}^f \Delta g_1 + Q^f \Delta g_2 + \Delta \tilde{g}_{L,R}^f, \quad (3.10)$$

where the finite renormalisation shifts of the fermion couplings in Eq. (3.6) can be rewritten as:

$$\Delta g_1 = \frac{1}{2} \left(\alpha T - \frac{\delta G_F}{G_F} \right), \quad \Delta g_2 = \frac{s_\theta^2}{c_{2\theta}} \left(c_\theta^2 \left(\alpha T - \frac{\delta G_F}{G_F} \right) - \frac{1}{4s_\theta^2} \alpha S \right), \quad (3.11)$$

while the fermion dependent modification of the couplings read²

$$\begin{aligned} \Delta \tilde{g}_L^u &= n_1^{\mathcal{Q}} + 2n_5^{\mathcal{Q}} + n_7^{\mathcal{Q}}, & \Delta \tilde{g}_R^u &= n_2^{\mathcal{Q}} + 2n_6^{\mathcal{Q}} + n_8^{\mathcal{Q}}, \\ \Delta \tilde{g}_L^d &= -n_1^{\mathcal{Q}} + 2n_5^{\mathcal{Q}} - n_7^{\mathcal{Q}}, & \Delta \tilde{g}_R^d &= -n_2^{\mathcal{Q}} + 2n_6^{\mathcal{Q}} - n_8^{\mathcal{Q}}, \\ \Delta \tilde{g}_L^\nu &= 0, & \Delta \tilde{g}_R^\nu &= 0, \\ \Delta \tilde{g}_L^e &= 0, & \Delta \tilde{g}_R^e &= 2n_2^\ell. \end{aligned} \quad (3.12)$$

The corresponding shifts to the W couplings to left-handed fermions (normalised to 1 in the SM) are

$$\Delta g_W^{ff'} = \Delta g_W + \Delta \tilde{g}_W^{ff'}, \quad (3.13)$$

with the universal shift due to the finite renormalisation defined in Eq. (3.6) given by

$$\Delta g_W = \frac{\Delta M_W}{M_W} - \frac{1}{2} \frac{\delta G_F}{G_F}, \quad (3.14)$$

and the fermion dependent shifts induced by the fermionic operators by

$$\Delta \tilde{g}_W^{ud} = 2n_1^{\mathcal{Q}} - 2n_7^{\mathcal{Q}}, \quad \Delta \tilde{g}_W^{e\nu} = 0. \quad (3.15)$$

There are two main differences with respect to the corresponding contributions to EWPD obtained assuming a linear realisation of the $SU(2)_L \times U(1)_Y$ gauge symmetry breaking with operators up to dimension six (see for example Refs. [47, 48]). First, in the SMEFT no contribution to the U parameter is generated at dimension six, while a contribution is generated in the HEFT at NLO, $\mathcal{O}(p^4)$. Second, in the linear description and assuming universality, the fermion dependent shifts of the W couplings to fermions are directly determined by those of the Z as there are only five independent dimension-six operators entering those vertices with SM Lorentz structure (which can be chosen for example to be $\mathcal{O}_{\phi q}^{(3)}$, $\mathcal{O}_{\phi q}^{(1)}$, $\mathcal{O}_{\phi u}$, $\mathcal{O}_{\phi d}$, $\mathcal{O}_{\phi e}$ in the notation of Ref. [7]). In the chiral description at order p^4 the fermion dependent contributions come in contrast from the seven operators given above, of which six combinations contribute independently to EWPD.

So altogether 10 combinations of the 12 operator coefficients can be determined by the analysis of EWPD which have been chosen here to be c_T , c_1 , c_{12} , $(r_2^\ell - r_5^\ell)$, $n_1^{\mathcal{Q}}$, $(n_2^{\mathcal{Q}} + n_8^{\mathcal{Q}})$, $n_5^{\mathcal{Q}}$,

²One could expect $\Delta \tilde{g}_L^{\nu,e}$ to have a similar contributions as $\Delta \tilde{g}_L^{u,d}$. This is not the case as the corresponding leptonic operators have been removed from the basis by using the EOMs, as discussed in Eq. (D.14). This choice simplifies the renormalisation procedure as $\Delta \tilde{g}_L^{\nu,e}$ are vanishing.

n_6^Q , n_7^Q and n_2^ℓ . In order to obtain the corresponding constraints on these 10 parameters a fit including 16 experimental data points is performed. These are 13 Z observables: Γ_Z , σ_h^0 , P_τ^{pol} , $\sin^2 \theta_{\text{eff}}^\ell$, R_l^0 , \mathcal{A}_l (SLD), $A_{\text{FB}}^{0,l}$, R_c^0 , R_b^0 , \mathcal{A}_c , \mathcal{A}_b , $A_{\text{FB}}^{0,c}$, and $A_{\text{FB}}^{0,b}$ from SLD/LEP-I [49], plus three W observables: the average of the W -boson mass, from [50], the W width, Γ_W , from LEP-II/Tevatron [51], and the leptonic W branching ratio, $Br_W^{e\nu}$, for which the average in Ref. [43] is taken. The correlations among the inputs can be found in Ref. [49] and have been taken into consideration in the analysis. As mentioned above, unlike in the fits to dimension-6 SMEFT operators, the independent experimental information on the W couplings to fermions have been included in the present study: this is done by considering in the fit the leptonic W branching ratio, as it is measured independently of the total W width, which is determined from kinematic distributions. The corresponding predictions for the observables in the analysis in terms of the shifts of the SM couplings defined above are given by:

$$\Delta\Gamma_Z = 2\Gamma_{Z,\text{SM}} \left(\frac{\sum_f (g_L^f \Delta g_L^f + g_R^f \Delta g_R^f) N_C^f}{\sum_f (|g_L^f|^2 + |g_R^f|^2) N_C^f} \right) \quad (3.16)$$

$$\Delta\sigma_h^0 = 2\sigma_{h,\text{SM}}^0 \left(\frac{(g_L^e \Delta g_L^e + g_R^e \Delta g_R^e)}{|g_L^e|^2 + |g_R^e|^2} + \frac{\sum_q (g_L^q \Delta g_L^q + g_R^q \Delta g_R^q)}{\sum_q (|g_L^q|^2 + |g_R^q|^2)} - \frac{\Delta\Gamma_Z}{\Gamma_{Z,\text{SM}}} \right) \quad (3.17)$$

$$\Delta R_l^0 \equiv \Delta \left(\frac{\Gamma_Z^{\text{had}}}{\Gamma_Z^l} \right) = 2R_{l,\text{SM}}^0 \left(\frac{\sum_q (g_L^q \Delta g_L^q + g_R^q \Delta g_R^q)}{\sum_q (|g_L^q|^2 + |g_R^q|^2)} - \frac{(g_L^l \Delta g_L^l + g_R^l \Delta g_R^l)}{|g_L^l|^2 + |g_R^l|^2} \right) \quad (3.18)$$

$$\Delta R_q^0 \equiv \Delta \left(\frac{\Gamma_Z^q}{\Gamma_Z^{\text{had}}} \right) = 2R_{q,\text{SM}}^0 \left(\frac{(g_L^q \Delta g_L^q + g_R^q \Delta g_R^q)}{|g_L^q|^2 + |g_R^q|^2} - \frac{\sum_{q'} (g_L^{q'} \Delta g_L^{q'} + g_R^{q'} \Delta g_R^{q'})}{\sum_{q'} (|g_L^{q'}|^2 + |g_R^{q'}|^2)} \right) \quad (3.19)$$

$$\Delta \sin^2 \theta_{\text{eff}}^l = \sin^2 \theta_{\text{eff},\text{SM}}^l \frac{g_L^l}{g_L^l - g_R^l} \left(\frac{\Delta g_R^f}{g_R^f} - \frac{\Delta g_L^f}{g_L^f} \right) \quad (3.20)$$

$$\Delta \mathcal{A}_f = 4\mathcal{A}_{f,\text{SM}} \frac{g_L^f g_R^f}{|g_L^f|^4 - |g_R^f|^4} \left(g_R^f \Delta g_L^f - g_L^f \Delta g_R^f \right) \quad (3.21)$$

$$\Delta P_\tau^{\text{pol}} = \Delta \mathcal{A}_l \quad (3.22)$$

$$\Delta A_{\text{FB}}^{0,f} = A_{\text{FB},\text{SM}}^{0,f} \left(\frac{\Delta \mathcal{A}_l}{\mathcal{A}_l} + \frac{\Delta \mathcal{A}_f}{\mathcal{A}_f} \right) \quad (3.23)$$

$$\Delta\Gamma_W = \Gamma_{W,\text{SM}} \left(\frac{4}{3} \Delta g_W^{ud} + \frac{2}{3} \Delta g_W^{e\nu} + \Delta M_W \right) \quad (3.24)$$

$$\Delta Br_W^{e\nu} = Br_{W,\text{SM}}^{e\nu} \left(-\frac{4}{3} \Delta g_W^{ud} + \frac{4}{3} \Delta g_W^{e\nu} \right). \quad (3.25)$$

When performing the fit within the context of the SM the result is $\chi_{\text{EWP,SM}}^2 = 18.3$, while when including the ten new parameters it gets reduced to $\chi_{\text{EWP,min}}^2 = 6$. The results of the analysis are shown in Fig. 1 which displays the $\Delta\chi_{\text{EWP}}^2$ dependence of the 10 independent operator coefficients. In each panel $\Delta\chi_{\text{EWP}}^2$ is shown after marginalizing over the other nine coefficients. The figure shows the corresponding 95% allowed ranges given in Table 3: the only operator coefficient not compatible with zero at 2σ is $n_2^Q + n_8^Q$, a result driven by the 2.7σ discrepancy between the observed $A_{\text{FB}}^{0,b}$ and the SM expectation.

It is interesting to notice that the resulting constraints on the coefficients contributing to T , U and δG_F are considerably weaker than what one would obtain in the standard 3 parameter fits to S , T , U . Quantitatively, the results of the 10 parameter analysis performed here give the following 1σ ranges for S, T, U and δG_F :

$$S = -0.45 \pm 0.37, \quad T = -0.3 \pm 2.8, \quad U = -0.1 \pm 2.5, \quad \frac{\delta G_F}{G_F} = (0.08 \pm 2.2) \times 10^{-2}, \quad (3.26)$$

to be compared with the results of the standard 3 parameter fit for S, T, U [48],

$$S = 0.08 \pm 0.1, \quad T = -0.1 \pm 0.12, \quad U = 0.0 \pm 0.09. \quad (3.27)$$

While the range for S is only about 4 times broader when including the effects of all the additional operators, the bounds on T and U are weakened by more than a factor 20. The main reason is that when δG_F is also included in the analysis cancellations can occur. In particular for $\alpha T = \frac{\delta G_F}{G_F} = -\frac{1}{4s_\theta^2} \alpha U$ the contributions from T , U , and δG_F cancel both in the Z observables and in ΔM_W as can be seen from Eqs. (3.9) and (3.11). Therefore, along this direction in the parameter space, the bounds on these three quantities come from the contribution of δG_F to Γ_W and $Br_W^{\nu\ell}$ in Eq. (3.15), but these observables are less precisely determined.

It is important to notice that this “weakening” arises even if the n_i^f coefficients, that is all the fermion dependent contributions, but the four-fermionic ones, are set to zero and only the four contributions c_1 , c_T , c_{12} and $r_2^\ell - r_5^\ell$ are retained. In this particular case, the result of the fit is

$$S = -0.1 \pm 0.1, \quad T = 0.43 \pm 2.86, \quad U = -0.3 \pm 2.4, \quad \frac{\delta G_F}{G_F} = (-0.26 \pm 2.0) \times 10^{-2}, \quad (3.28)$$

to be compared with Eq. (3.26). On the contrary, in the framework of linear dimension-6 operators, the condition $U = 0$ makes this cancellation not possible, so bounds on the corresponding operator coefficients are generically stronger. In other words, when making the EWP analysis in the context of HEFT at $\mathcal{O}(p^4)$ the bounds on the operators contributing to T and U are generically weaker by more than one order of magnitude.

The fermionic operators can also lead to modifications of the semileptonic decay amplitudes used to determine the elements of the CKM matrix and to test its unitarity. In particular, $\mathcal{N}_1^Q(h)$, $\mathcal{N}_7^Q(h)$, $\mathcal{R}_2^\ell(h)$, $\mathcal{R}_5^\ell(h)$, $\mathcal{R}_{13}^Q(h)$ induce linear shifts to the corresponding amplitudes (normalised to G_F as determined from μ decay) which can be parameterised as a shift in the effective CKM matrix,

$$\Delta V_{\text{CKM},ij} = V_{\text{CKM,SM},ij} \left(-64\pi^2 \sqrt{2} \frac{v^2}{\Lambda^2} r_{13}^{Q\ell} + \Delta \tilde{g}_W^{ud} - \frac{\delta G_F}{G_F} \right), \quad (3.29)$$

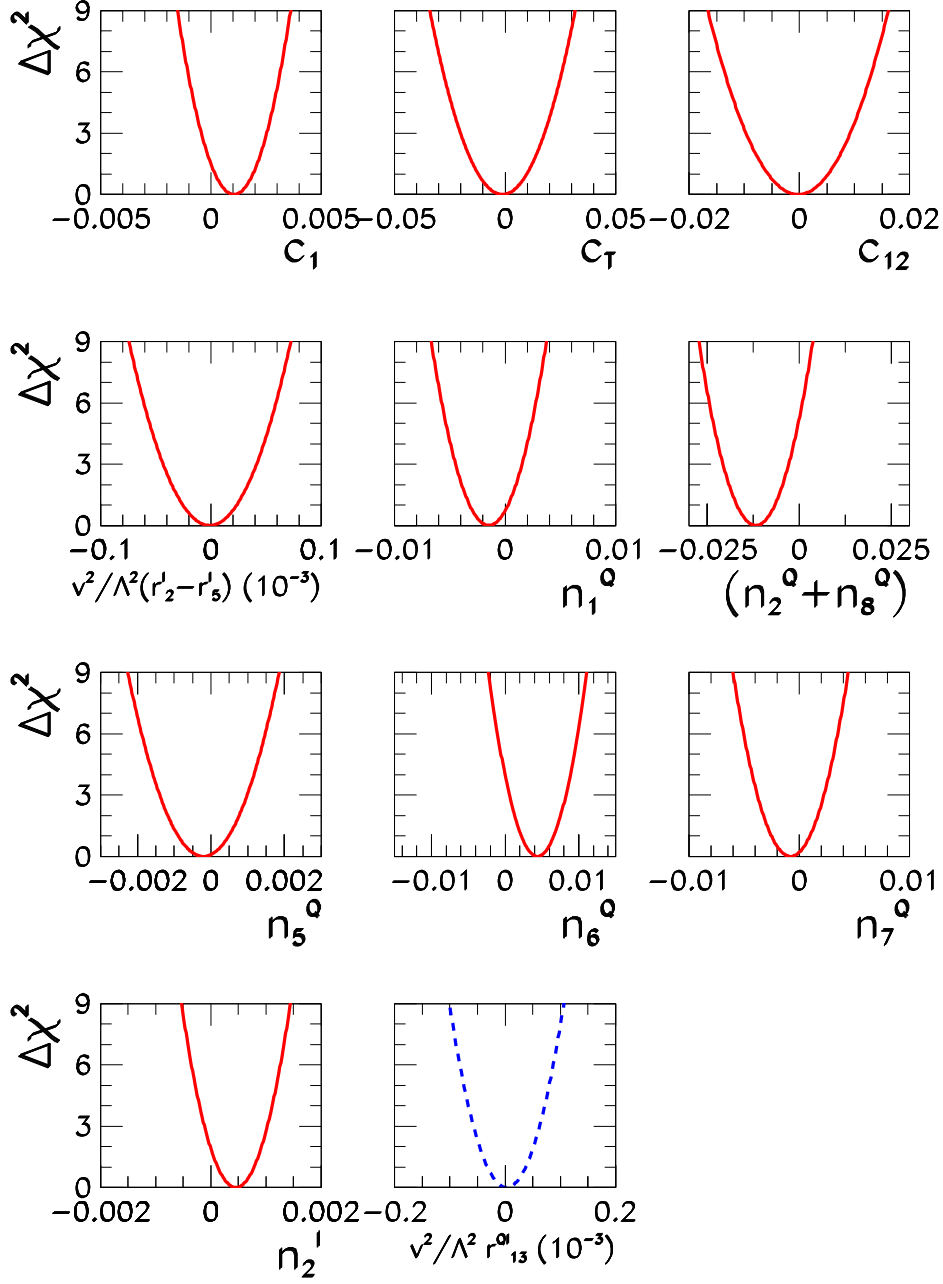


Figure 1: *Dependence of $\Delta\chi^2_{\text{EWP}+\text{CKM}}$ ($= \Delta\chi^2_{\text{EWP}}$ for all, but last panel) on the 11 independent operator coefficients as labeled in the figure. In each panel $\Delta\chi^2_{\text{EWP}+\text{CKM}}$ is shown after marginalizing over the other undisplayed parameters.*

coupling	95% allowed range
c_1	$(-0.66, 2.7) \times 10^{-3}$
c_T	$(-0.023, 0.021)$
c_{12}	$(-0.011, 0.011)$
$\frac{v^2}{\Lambda^2} (r_2^\ell - r_5^\ell)$	$(-4.9, 4.7) \times 10^{-5}$
$n_1^{\mathcal{Q}}$	$(-4.9, 2.0) \times 10^{-3}$
$n_2^{\mathcal{Q}} + n_8^{\mathcal{Q}}$	$(-22, -1.5) \times 10^{-3}$
$n_5^{\mathcal{Q}}$	$(-1.6, 1.2) \times 10^{-3}$
$n_6^{\mathcal{Q}}$	$(-0.025, 8.8) \times 10^{-3}$
$n_7^{\mathcal{Q}}$	$(-4.2, 2.7) \times 10^{-3}$
n_2^ℓ	$(-0.2, 1.1) \times 10^{-3}$
$\frac{v^2}{\Lambda^2} r_{13}^{\mathcal{Q}\ell}$	$(-7.1, 6.6) \times 10^{-5}$

Table 3: 95% allowed ranges for the combinations of operator coefficients entering the EWPD analysis and the CKM unitarity test.

and which can lead to violations of unitarity of the CKM matrix which are strongly constrained. In the case of SMEFT with operators up to dimension six, three operators enter this observable after equivalent application of the EOMs [47, 48] (which can be chosen for example to be $\mathcal{O}_{\phi q}^{(3)}$, \mathcal{O}_l , and, $\mathcal{O}_{lq}^{(3)}$ Ref. [7]). From the global analysis in Ref. [43]

$$\sum_i |V_{ui}|^2 - 1 = 2 \left(-64\pi^2 \sqrt{2} \frac{v^2}{\Lambda^2} r_{13}^{\mathcal{Q}\ell} + \Delta \tilde{g}_W^{ud} - \frac{\delta G_F}{G_F} \right) = (-1 \pm 6) \times 10^{-4}. \quad (3.30)$$

In combination with the analysis of the EWPD, this allows for constraining the coefficient of an 11th operator $\mathcal{R}_{13}^{\mathcal{Q}\ell}(h)$. Adding this data point to the 16 of the EWPD allows to construct $\chi_{\text{EWPD+CKM}}^2$, which is now a function of 11 parameters (with $\chi_{\text{EWPD+CKM,SM}}^2 = 18.4$ and $\chi_{\text{EWPD+CKM,min}}^2 = 6$). The marginalised distributions verify $\Delta \chi_{\text{EWPD+CKM}}^2(x) = \Delta \chi_{\text{EWPD}}^2(x)$ for the first ten parameters, i.e. the inclusion of the CKM unitarity constraint has no impact in the previous analysis as long as $r_{13}^{\mathcal{Q}\ell}$ is allowed to vary free in the fit. The new $\Delta \chi_{\text{EWPD+CKM}}^2(r_{13}^{\mathcal{Q}\ell})$ is shown in the curve in the last panel in Fig. 1 and its 95% CL range is listed in the last row in Table 3.

3.3 Effects in Higgs Physics

This section is dedicated to the study of the current bounds stemming from the Higgs searches at the LHC. Restricting the analysis to the subset of C and P -even operators³, the focus is on those terms that contribute to the trilinear Higgs interactions with fermions and gauge bosons (deviations in the Higgs triple vertex will only become observable in the future). This list of operators includes $\mathcal{P}_T(h)$, $\mathcal{P}_{B,G,W}(h)$ and $\mathcal{P}_{1,4,5,12,17}(h)$, in addition

³The extension of the analysis to CP -odd non linear operators could be performed after the inclusion of CP sensitive observables, see Ref. [25].

to the contributions from $Y_U^{(1)}$, $Y_D^{(1)}$, $Y_\ell^{(1)}$ and to the deviations in the GBs kinetic term parameterised by Δa_C . This set can be further reduced considering the strong constraints imposed on $\mathcal{P}_{T,1,12}(h)$ by the global analysis of EWPD at the Z pole: the impact of these operators on Higgs physics can be safely neglected, given the accuracy at which these observables are currently measured. Moreover, the current Higgs searches are only sensitive to Hff vertices with $f = t, b, \tau$ (the addition of μ to the analysis will be straightforward once the sensitivity to this coupling increases). Therefore, only a subset of 10 operators is relevant for the analysis of the available Higgs data. Their contributions to the several Higgs trilinear interactions can be illustrated with the usual HVV phenomenological Lagrangian in the unitary gauge:

$$\begin{aligned} \mathcal{L} = & g_{Hgg} H G_{\mu\nu}^a G^{a\mu\nu} + g_{H\gamma\gamma} H A_{\mu\nu} A^{\mu\nu} + g_{HZ\gamma}^{(1)} A_{\mu\nu} Z^\mu \partial^\nu H + g_{HZ\gamma}^{(2)} H A_{\mu\nu} Z^{\mu\nu} \\ & + g_{HZZ}^{(1)} Z_{\mu\nu} Z^\mu \partial^\nu H + g_{HZZ}^{(2)} H Z_{\mu\nu} Z^{\mu\nu} + g_{HZZ}^{(3)} H Z_\mu Z^\mu \\ & + g_{HWW}^{(1)} (W_{\mu\nu}^+ W^{-\mu} \partial^\nu H + \text{h.c.}) + g_{HWW}^{(2)} H W_{\mu\nu}^+ W^{-\mu\nu} + g_{HWW}^{(3)} H W_\mu^+ W^{-\mu} \\ & + \sum_{f=\tau,b,t} (g_f H \bar{f}_L f_R + \text{h.c.}) . \end{aligned} \quad (3.31)$$

The 13 parameters in this Lagrangian can be re-written in terms of the following ten coefficients⁴:

$$\Delta a_C, a_B, a_G, a_W, a_4, a_5, a_{17}, Y_t^{(1)}, Y_b^{(1)}, Y_\tau^{(1)}, \quad (3.32)$$

and explicitly they read

$$\begin{aligned} g_{Hgg} &= -\frac{1}{2v} a_G, & g_{HZ\gamma}^{(1)} &= -\frac{gs_\theta}{4\pi v c_\theta} \left(a_5 + 2\frac{c_\theta}{s_\theta} a_4 + 2a_{17} \right), & g_{HZ\gamma}^{(2)} &= \frac{s_\theta c_\theta}{v} (a_B - a_W), \\ g_{HZZ}^{(1)} &= \frac{g}{4\pi v} \left(2\frac{s_\theta}{c_\theta} a_4 - a_5 - 2a_{17} \right), & g_{HZZ}^{(2)} &= -\frac{1}{2v} (s_\theta^2 a_B + c_\theta^2 a_W), \\ g_{HZZ}^{(3)} &= M_Z^2 \left(\sqrt{2} G_F \right)^{1/2} (1 + \Delta a_C), & g_{H\gamma\gamma} &= -\frac{1}{2v} (s_\theta^2 a_W + c_\theta^2 a_B), \\ g_{HWW}^{(1)} &= -\frac{g}{4\pi v} a_5, & g_{HWW}^{(2)} &= \frac{1}{v} a_W, & g_{HWW}^{(3)} &= 2M_W^2 \left(\sqrt{2} G_F \right)^{1/2} (1 + \Delta a_C), \\ & & g_f &= -\frac{Y_f^{(1)}}{\sqrt{2}}. \end{aligned} \quad (3.33)$$

The anomalous Higgs interactions described by these 10 operators can be studied and constrained in a model independent way by means of a global analysis of all the Higgs experimental measurements that were performed at the LHC during the Run I. This includes not only event rate data in several Higgs production and decay categories, but also some kinematic distributions, that have an interesting phenomenological impact, as shown in the context of SMEFT in Ref. [52–57]. Indeed, they are important for allowing to obtain finite constraints in the large-dimensional parameter space spanned in the global analysis [52]. Moreover, they make it possible to disentangle the non-SM Lorentz structures from the SM-like shifts.

⁴Notice the implicit redefinitions $a_i \equiv c_i a_i$ for the bosonic operators.

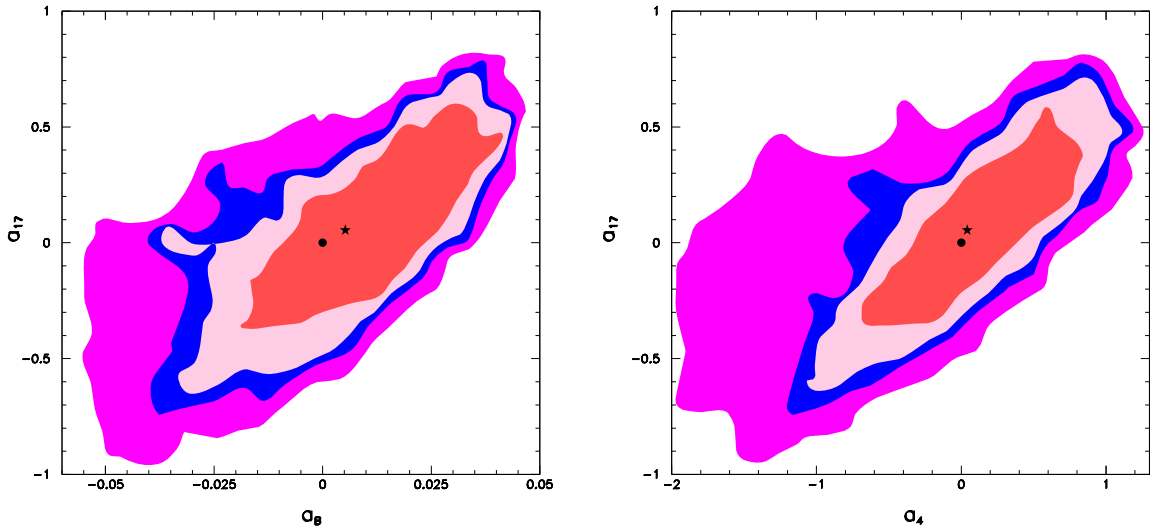


Figure 2: *Results of the global analysis of LHC Higgs run I data, including kinematic distributions, for $\{a_B, a_4, a_{17}\}$, profiling on the undisplayed parameters. The colours refers to the different C.L. regions: from the inner to outer, 68%, 90%, 95%, 99% C.L..*

The global analysis of all Run I Higgs, data using the SFITTER framework [58–62] for the SMEFT [41, 42], has been presented in Ref. [52]: in that case, the 13 parameters of the phenomenological Lagrangian in Eq. (3.31) received contributions from 9 linear operators. Here, that analysis is extended to account for the 10th coefficient a_{17} . All the details regarding the data set and the kinematic distributions analysed, as well as the statistical treatment performed in this log-likelihood analysis follow exactly the description presented in Ref. [52] and will not be repeated here.

The results of the global analysis on the parameters in Eq. (3.32) using the available Higgs data, including all the kinematic distributions described in Ref. [52], are reported in Table 4. On the right figure we graphically display the corresponding values where error bars refer to the 95% C.L. allowed ranges, obtained profiling for each coefficient on the other 9 parameters that are included in the global analysis. The off-shell $m_{4\ell}$ distributions, which have been implemented in Ref. [52], are not included here, as their impact in the present analysis is subdominant with respect to the rest of kinematic distributions considered.

The addition of the extra parameter a_{17} has enlarged the allowed range for all the rest of coefficients contributing to the bosonic Higgs trilinear interactions (a_4, a_5, a_W, a_B and Δa_C) in comparison with the results in Ref. [52, 63] (after taking into account the different normalizations used between the two analyses). This was expected given the larger dimensionality of the parameter space analysed in here. The new contributions from $\mathcal{P}_{17}(h)$ are consequently strongly correlated to some of the other operators, as illustrated in Figure 2, where the 2-dimensional planes a_B vs. a_{17} and a_4 vs. a_{17} are shown, after profiling on the rest of undisplayed coefficients for each of the panels.

In the present analysis the addition of kinematic distributions is crucial both for closing the allowed regions on all the considered parameters, and for controlling the correlations

	Best fit	95% CL region
a_G	-0.0125	$(-0.018, -0.0080)$
	-0.0030	$(-0.0054, 0.0058)$
	0.0029	
	0.0123	$(0.0091, 0.017)$
a_W	-0.017	$(-0.11, 0.088)$
a_B	0.0052	$(-0.025, 0.041)$
a_4	0.041	$(-0.85, 1.1)$
a_5	0.13	$(-0.81, 0.60)$
Δa_C	-0.13	$(-0.30, 0.23)$
a_{17}	0.055	$(-0.52, 0.65)$
$Y_t^{(1)}/Y_t^{(0)}$	-1.11	$(-1.7, -0.53)$
	1.31	$(0.56, 1.7)$
$Y_b^{(1)}/Y_b^{(0)}$	-0.70	$(-1.7, -0.39)$
	0.66	$(0.35, 1, 7)$
$Y_\tau^{(1)}/Y_\tau^{(0)}$	-0.94	$(-1.37, -0.63)$
	0.82	$(0.66, 1.47)$
c_2	0.041	$(-0.24, 0.27)$
c_3	0.15	$(-0.093, 0.39)$
c_{WWW}	0.006	$(-0.013, 0.018)$

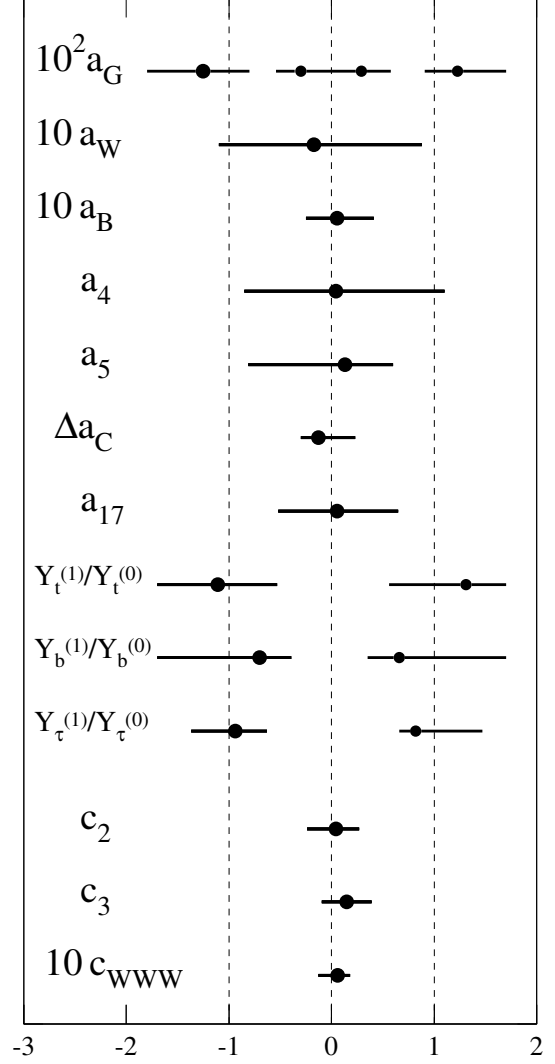


Table 4: *Best fit and 95% C.L. allowed ranges of the coefficients of the operators contributing to Higgs data (a_G , a_W , a_B , a_4 , a_5 , a_{17} , Δa_C , $Y_t^{(1)}$, $Y_b^{(1)}$ and $Y_\tau^{(1)}$) and to TGV analyses (c_2 , c_3 and c_{WWW}). $Y_t^{(1)}$, $Y_b^{(1)}$ and $Y_\tau^{(1)}$ are normalised to the SM expectation.*

among the anomalous couplings [52]. To our knowledge, the results derived here present the most complete set of Higgs based constraints on the set of operators of the HEFT Lagrangian. They highlight, in addition, the potential of the EFT expansion to describe and study the Higgs interactions at the LHC.

3.4 Triple gauge boson couplings and Higgs interplay

The study of triple gauge boson vertices is complementary to the analysis of Higgs physics, and it is fundamental for obtaining a more complete description of the EWSB sector. Focusing again on the C and P even operators and after including the strong constraints from EWPD, only four operators, $\mathcal{P}_2(h)$, $\mathcal{P}_3(h)$, $\mathcal{P}_{13}(h)$ and $\mathcal{P}_{WWW}(h)$, enter this analysis⁵. They can give observable deviations from the SM predictions for the triple gauge boson vertices WWZ and $WW\gamma$. These anomalous contributions can be parameterised in terms of the usual phenomenological TGV Lagrangian presented in Ref. [65]:

$$\mathcal{L}_{WWV} = -ig_{WWV} \left\{ g_1^V \left(W_{\mu\nu}^+ W^{-\mu} V^\nu - W_\mu^+ V_\nu W^{-\mu\nu} \right) + \kappa_V W_\mu^+ W_\nu^- V^{\mu\nu} + \frac{\lambda_V}{2m_W^2} W_{\mu\nu}^+ W^{-\nu\rho} V_\rho^\mu \right\}, \quad (3.34)$$

with deviations from the SM predictions $g_1^Z = \kappa_Z = \kappa_\gamma = 1$, $\lambda_\gamma = \lambda_Z = 1$

$$\begin{aligned} \Delta g_1^Z &= g_1^Z - 1 \equiv \frac{g}{4\pi c_\theta^2} c_3, \\ \Delta \kappa_Z &= \kappa_Z - 1 \equiv \frac{g}{4\pi} (c_3 + 2c_{13} - 2t_\theta c_2), \\ \Delta \kappa_\gamma &= \kappa_\gamma - 1 \equiv \frac{g}{4\pi} \left(c_3 + 2c_{13} + 2\frac{c_2}{t_\theta} \right), \\ \lambda_\gamma &= \lambda_Z \equiv \frac{6\pi g v^2}{\Lambda^2} c_{WWW}. \end{aligned} \quad (3.35)$$

Electromagnetic gauge invariance enforces $g_1^\gamma = 1$, both in the SM and in the presence of the new operators. In Eq. (3.34), $V \equiv \{\gamma, Z\}$, $g_{WW\gamma} = e$, $g_{WWZ} = g \cos \theta_W$, and $W_{\mu\nu}^\pm$ and $V_{\mu\nu}$ refer exclusively to the kinetic part of the gauge field strengths.

The combination of all the most sensitive searches for anomalous TGV deviations in WV diboson production has been performed in Ref. [66], presenting the results obtained in the SMEFT framework. These results show that at present the most stringent constraints on the anomalous TGV are set by the LHC Run I searches, whose combined sensitivity has clearly surpassed that of LEP. Even more relevant is the fact that, while the LHC Higgs data and gauge boson pair production searches are able to separately set stringent constraints on the HEFT operators, the combined study of the two sets of data could be used to improve the understanding of the nature of the Higgs boson state, as already emphasised in Ref. [24].

In brief, three CP-even SMEFT operators with $d = 6$ can lead to sizeable corrections to the TGV vertices after considering all bounds from EWPD [40–42, 52, 66]:

$$\begin{aligned} \mathcal{O}_W &= \frac{ig}{2} (D_\mu \Phi)^\dagger W^{\mu\nu} (D_\nu \Phi), & \mathcal{O}_B &= \frac{ig'}{2} (D_\mu \Phi)^\dagger B^{\mu\nu} (D_\nu \Phi), \\ \mathcal{O}_{WWW} &= -\frac{ig^3}{8} \text{Tr} (W_{\mu\nu} W^{\nu\rho} W_\rho^\mu), \end{aligned} \quad (3.36)$$

where the notation of the original papers has been kept.

⁵An additional operator, $\mathcal{P}_{14}(h)$, generates a CP conserving but C and P violating coupling, whose effects and numerical analysis have been discussed in Ref. [24, 64] and also hold here.

As pointed out in Ref. [24], comparing the interactions generated by these three operators with those induced by the relevant operators in the HEFT basis, one finds two differences: (i) for the TGV phenomenology \mathcal{O}_W and \mathcal{O}_B give corrections to the vertices equivalent to those induced by $\mathcal{P}_2(h)$ and $\mathcal{P}_3(h)$, while for the HVV couplings their effects are equivalent to those of $\mathcal{P}_4(h)$ and $\mathcal{P}_5(h)$; (ii) the $\mathcal{O}(p^4)$ chiral operator $\mathcal{P}_{13}(h)$ has no equivalent in the linear expansion at dimension 6.

In other words, (i) implies that, as it is well known from the pre-LHC times [67], and recently emphasised in some of the post-Higgs discovery analyses [42, 56, 68], the operators \mathcal{O}_W and \mathcal{O}_B lead at the same time to anomalous contributions to both Higgs physics and TGV anomalous measurements. Thus, any deviation generated by them should be correlated in data from both sectors, and consequently the combined analysis of Higgs data and TGV measurements becomes mandatory in order to obtain constraints as strong as possible on their coefficients [66]. Conversely, in the HEFT case, the anomalous TGV deviations induced by \mathcal{O}_W and \mathcal{O}_B are generated by $\mathcal{P}_2(h)$ and $\mathcal{P}_3(h)$, while their effects on Higgs physics originate from $\mathcal{P}_4(h)$ and $\mathcal{P}_5(h)$. Therefore, deviations in TGV and in Higgs physics could remain completely uncorrelated in the HEFT context [24]. This means that the nature of the Higgs boson can be directly probed by testing the presence of this (de)-correlated pattern of interactions in the event of an anomalous observation in any of the two sectors.

To illustrate the present status of such comparison, a global analysis of the data available both on the Higgs interactions and on the searches for anomalous TGV has been performed. The analysis spans the 10 coefficients relevant for Higgs physics in the HEFT scenario, see Eq. (3.32), together with the 3 parameters relevant for the TGV sector, which have an equivalent in the SMEFT Lagrangian, c_2 , c_3 and c_{WWW} (i.e. setting c_{13} to zero)⁶.

In what respects the TGV analysis, the simulation of the relevant distributions and the statistical fit follow those of Ref. [66]. The best fit values and 95% C.L. intervals obtained for c_2 , c_3 and c_{WWW} are quoted for completeness in Table 4. As can be seen comparing the results in Table 4 with Table 4 of Ref. [24], derived considering only the LEP based TGV bounds on c_2 and c_3 , the new combination of LHC Run I searches is able to improve substantially the constraints on $\mathcal{P}_2(h)$ and $\mathcal{P}_3(h)$.

It was already shown in Ref. [24] that four specific combinations of the coefficients $\mathcal{P}_2(h)$, $\mathcal{P}_3(h)$, $\mathcal{P}_4(h)$ and $\mathcal{P}_5(h)$ are meaningful for illustrating the Higgs+TGV results:⁷

$$\begin{aligned}\Sigma_B &\equiv \frac{1}{\pi g t_\theta} (2c_2 + a_4), & \Sigma_W &\equiv \frac{1}{2\pi g} (2c_3 - a_5), \\ \Delta_B &\equiv \frac{1}{\pi g t_\theta} (2c_2 - a_4), & \Delta_W &\equiv \frac{1}{2\pi g} (2c_3 + a_5).\end{aligned}\tag{3.37}$$

These four parameters were defined in such a way that, at $d = 6$ order in the SMEFT expansion, the two Δ 's are zero because of gauge invariance and of the doublet nature of

⁶Notice that the operator belonging to the SMEFT expansion which contains the same interactions described by $\mathcal{P}_{13}(h)$, also called “linear sibling”, arises only at $d = 8$.

⁷For the sake of comparison with Ref. [24], the four combinations have been defined to be quantitatively equivalent to those in Ref. [24], in spite of the different normalisation for the c_i and a_i coefficients used in here.

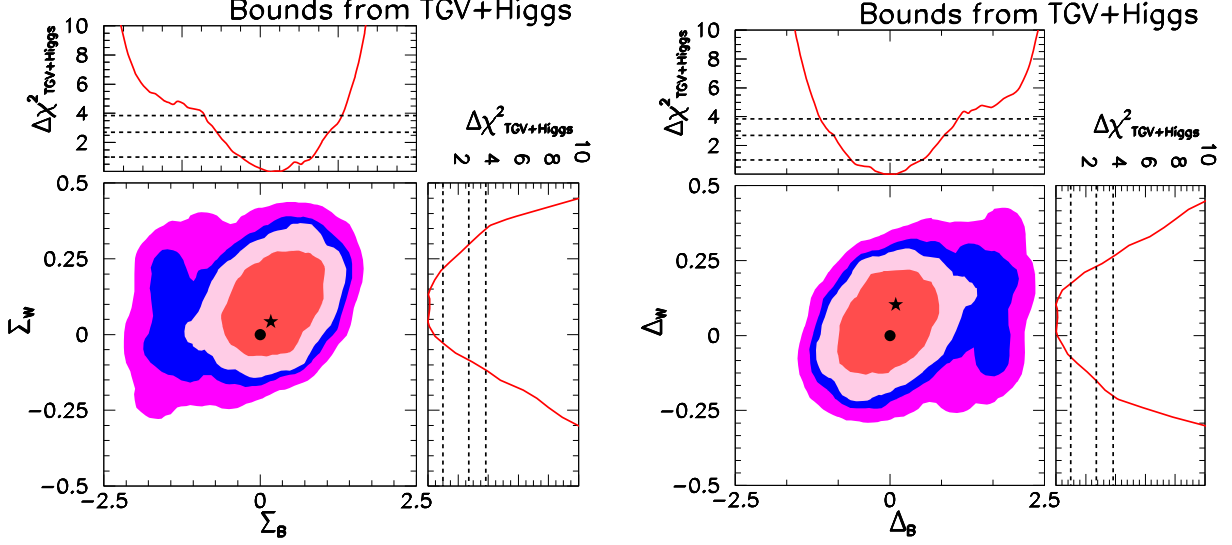


Figure 3: *Present bounds on Σ_B , Σ_W , Δ_B and Δ_W (see text for the details on their definition) as obtained from the most recent combined global analysis of Higgs and TGV data. The rest of undisplayed parameters spanned in the global analysis (Δa_C , a_B , a_G , a_W , a_{17} , $Y_t^{(1)}$, $Y_b^{(1)}$, $Y_\tau^{(1)}$ and c_{WW}) have been profiled. The black dots signal the (0,0) point, while the stars signal the current best fit point obtained in the analysis.*

the Higgs, $\Delta_B = \Delta_W = 0$. On the other hand, the operators \mathcal{O}_W and \mathcal{O}_B contribute to the Σ 's leading to $\Sigma_B = v^2 \frac{f_B}{\Lambda^2}$ and $\Sigma_W = v^2 \frac{f_W}{\Lambda^2}$, being f_i the associated Wilson coefficients. In contrast, the HEFT operators could generate independent modifications to each of these four variables. Figure 3 shows the current status of the bounds on the two relevant planes of coefficients after taking into consideration all the Higgs measurements included in the presented Higgs global analysis (based on Ref. [52]), together with the most recent combination of TGV searches presented in the previous subsection (based on Ref. [66]).

As described in Ref. [24], in the left panel of Figure 3 the (0,0) point corresponds to no deviation from the SM, while in the right one it represents the limit in which TGV and HVV couplings show a SMEFT-like correlation. Therefore, any deviation from (0,0) in the left panel would indicate BSM physics irrespectively of the nature of the EWSB realisation, while a similar departure in the right panel would disfavour a linear EWSB. As the Δ 's and the Σ 's are orthogonal combinations of parameters, the two panels of Fig. 3 are in principle independent of each other. In particular, deviations from (0,0) may occur arbitrarily in only one plane or in both at the same time.

The constraints of Σ_B , Σ_W , Δ_B and Δ_W shown in Fig. 3 present a significant improvement with respect to the bounds previously shown in Fig. 2 of Ref. [24]. The reason for such a sizeable improvement relies on two key points. First, the strength of the derived results is increased by the inclusion of the more complete set of run I LHC Higgs event rate measurement and by the addition of relevant kinematic distributions, that are sensitive to the anomalous SM Lorentz structures generated by a_3 and a_5 [52]. Second, the combination of the significant LHC Run I diboson production analysis as described in Ref. [66] also

has a huge impact in the analysis. The combination of these two ameliorations enhances significantly the accuracy of the combined results shown in Figure 3, in spite of the larger dimensionality of the parameter space considered in the present study with respect to the global analysis in Ref. [24].

4 Higher order operators and expansion validity

An important issue for numerical analyses performed in an EFT approach is that of establishing whether the EFT description is valid at the typical energies of the processes considered. The task is particularly relevant when collider data is included in the analysis, as the corresponding measurements are typically taken at energies significantly higher than the EW scale.

In general, the validity of the expansion can be discussed studying the impact of operators which belong to different expansion orders. In the context of the SMEFT, this is tantamount to analysing operators with dimension $d > 6$. As discussed in Refs. [69–73], this analysis sets different constraints on the cutoff of the theory, depending on the observables and of the operators considered: the strongest bounds are associated to observables that receive contributions from $d = 8$ operators with a larger number of derivatives, as they induce a strong energy-dependence.

Similar general considerations also apply to the HEFT. However, in this case the discussion is complicated by the simultaneous presence of several characteristic scales and, consequently, of multiple expansion parameters. Although the only physical scales of the HEFT are Λ and v , as explained in Sect. 1, it is useful to keep momentarily the scale f ($\Lambda \leq 4\pi f$) as an independent quantity. The limit $f \rightarrow v$ will be discussed later on.

In realistic Composite Higgs models, that can be considered as a benchmark for understanding the role played by each scale, v , f and Λ enter the low-energy Lagrangian in three different combinations: $v/f = \sqrt{\xi}$, $1/4\pi \leq f/\Lambda \leq 1$, and E/Λ , where E is the characteristic energy scale of a given observable. As shown in Ref. [33], cross sections of physical processes only depend on scale suppressions: the generic expression, adopting the NDA normalisation of Eq. (2.7), is given by

$$\sigma \sim \frac{\pi(4\pi)^2}{E^2} \left(\frac{E^2}{\Lambda^2} \right)^{-N_\Lambda}, \quad (4.1)$$

where $(-N_\Lambda)$ is the number of powers of Λ that suppress an interaction term. The NDA master formula takes automatically care of all the 4π factors appearing in the cross-section (see Ref. [33] for further details and for generalisations), so that $(-N_\Lambda)$ actually counts both powers of Λ and of f indifferently. As a result, the only quantities that can be considered as proper suppression factors are $\sqrt{\xi}$ and E/Λ . The physical relevance of a given cross-sections is basically determined by its dependence on these two parameters.

While the dependence on $1/\Lambda$ is explicit in HEFT operators, it is less trivial to trace that on $\sqrt{\xi} = v/f$. To this aim, it is useful to recall (see Sect. 1) that f is the scale associated to both the SM GBs and the Higgs and, as such, it is always hidden inside the GB matrix $\mathbf{U}(x)$ and the generic Higgs functions $\mathcal{F}(h)$. The dependence on f can be

explicitly expanding these structures:

$$\mathbf{U} = \mathbb{1} + 2i \frac{\sigma_a \pi^a}{f} + \dots, \quad \mathcal{F}(h) = 1 + 2a \frac{h}{f} + \dots. \quad (4.2)$$

Within \mathbf{V}_μ and upon going to unitary gauge, the powers on $1/f$ are converted into factors of $\sqrt{\xi}$. This is due to the fact that, in the kind of scenarios considered here, ξ represents a fine-tuning, that necessarily weights insertions of longitudinal components of the gauge bosons [33]. This indeed occurs in composite Higgs models (see Refs. [29, 30]), where analogous conclusions are found to hold also for $\partial_\mu \mathcal{F}(h)$.

It is worth noticing that, while $\mathbf{U}(x)$ and $\mathcal{F}(h)$, considered globally, are adimensional quantities, their expansions contain terms with different canonical dimensions that come suppressed by powers of f . As a result, the leading terms of \mathbf{V}_μ and $\partial_\mu \mathcal{F}(h)$, obtained applying one derivative to the series of Eq. (4.2), have canonical dimension two: one dimension being associated to the derivative and the other to the first non-vanishing term in the expansion of either \mathbf{U} or $\mathcal{F}(h)$. This observation can be generalised introducing the primary dimension d_p , defined in Ref. [33] as the canonical dimension of the leading term in the expansion of a given object. For fundamental elements, such as derivatives, gauge fields and fermions, the primary dimension coincides with the traditional canonical dimension. Table 5 contains a summary of the primary dimensions for the building blocks used in the construction of the HEFT Lagrangian, together with the associated suppression factors. It follows from the discussion above that a term suppressed by $\xi^{\alpha/2} (p/\Lambda)^\beta$ must have $d_p = \alpha + \beta$.

With the information provided by Table 5, it is easy to infer the dependences for all the HEFT operators, that can be thus organised in a two-parameter expansion as indicated, schematically, in Table 6. The colours discriminate between two sets of operators: the structures reported in the cyan boxes correspond to the NLO Lagrangian considered in this work; the structures in the white cells, instead, are customarily considered as higher order terms, but their impact may be comparable to that of the NLO terms for sufficiently high energies. Depending on the observables considered, it may be necessary to include (part of) the second set of operators into the phenomenological analysis (see also Ref. [74]), even if this would mean working with a ill-defined basis from a renormalisation point of view.

Building block	d_p	Factors of ξ	Factors of p/Λ
$\mathbf{U}(x)$	0	1	1
$\mathcal{F}(h)$	0	1	1
∂_μ	1	1	(p/Λ)
ψ	3/2	1	$(p/\Lambda)^{3/2}$
$X_{\mu\nu}$	2	1	$(p/\Lambda)^2$
\mathbf{V}_μ	2	$\sqrt{\xi}$	(p/Λ)
$\partial_\mu \mathcal{F}(h)$	2	$\sqrt{\xi}$	(p/Λ)

Table 5: *Different HEFT building blocks and their primary dimensions. The two last columns report the suppression factors associated to each object.*

ξ^2	$(\partial\mathcal{F})^2(\mathbf{V})^2$ $(\mathbf{V})^4$ $(\partial\mathcal{F})^4$				
$\xi^{3/2}$					
ξ	$(\mathbf{V}^2)(X)^2$ $(\partial\mathcal{F})(\mathbf{V})(X)$	$(\partial\mathcal{F})(\mathbf{V})(\bar{\psi}\psi)$ $(\mathbf{V})^2(\bar{\psi}\psi)$ $(\partial\mathcal{F})^2(\bar{\psi}\psi)$	$(X)^2(\mathbf{V})^2$ $(\partial\mathcal{F})(\mathbf{V})(X)^2$ $(\partial\mathcal{F})^2(X)^2$		
$\sqrt{\xi}$	$(\bar{\psi}\psi)(\mathbf{V})$		$(\mathbf{V})(X)(\bar{\psi}\psi)$ $(\partial\mathcal{F})(X)(\bar{\psi}\psi)$	$(\mathbf{V})(\bar{\psi}\psi)^2$ $(\partial\mathcal{F})(\bar{\psi}\psi)^2$	
1	$(X)^2$	$(X)(\bar{\psi}\psi)$	$(\bar{\psi}\psi)^2$ $(X)^3$	$(X)^2(\bar{\psi}\psi)$	$(X)(\bar{\psi}\psi)^2$ $(X)^4$
	1	$\left(\frac{p}{\Lambda}\right)$	$\left(\frac{p}{\Lambda}\right)^2$	$\left(\frac{p}{\Lambda}\right)^3$	$\left(\frac{p}{\Lambda}\right)^4$

Table 6: *HEFT operators distributed according to their ξ and p/Λ suppressing factors. A schematic notation has been adopted for categorising the operators based on the building blocks they contain. The terms appearing in the cyan boxes correspond to the NLO operators listed in the previous sections. The other terms refer to operators that usually belong to higher Lagrangian orders, but that can have an impact similar to that of the NLO ones for sufficiently high energies. EOMs have been employed to remove redundant structures.*

This should not be seen as a concern, as, even considering a complete, non-redundant basis at NNLO, only the subcategories listed in Table 6 would be physically relevant. Effects due to operator mixing under the renormalisation group running are also expected to be completely negligible at the experimental sensitivities foreseen for the near future.

In the limit $f \rightarrow v$, the dependence on ξ does not represent a suppression anymore and the physical impact of an operator is determined only by the factors of p/Λ . In this case, one recovers a pure chiral expansion, which is organised “horizontally” in the representation of Table 6.

On the contrary, in the limit $p/\Lambda \simeq \sqrt{\xi}$, all the operators with the same d_p are equally suppressed and therefore one recovers, altogether, the linear expansion organised in canonical (or primary) dimensions. In this case, *all* the operators in the white boxes of Table 6 should be considered. This condition is for instance fulfilled for $\Lambda = 10 \text{ TeV}$ and $E \simeq 1 \text{ TeV}$, which is within the range of energies that are relevant for processes to be observed at LHC13.

The introduction of the primary dimension, i.e. of a counting on explicit and implicit

scale suppressions, allows to link the particular structure of an operator to the strength of a physical signal in terms of cross sections. Indeed, if an observable receives contributions from a single operator, then the corresponding cross section is uniquely determined by the primary dimension of that operator, according to Eq. (4.1). As a consequence, the d_p is a useful phenomenological tool to indicate whether the strength of an observable, that receive contributions only from operators belonging to higher expansion orders, is expected to be of the same order or more suppressed with respect to the other processes already considered in the phenomenological analysis.

An interesting application of the primary dimension is that if the d_p of an HEFT operator is smaller than the canonical dimension of the corresponding linear sibling, then the processes described by these operators represent smoking guns to test the linearity of the EWSB realisation. This is the case of the operator $\mathcal{P}_{14}(h)$ discussed in Ref. [33]: it induces an anomalous TGV, commonly called g_5^Z , that is expected to be strongly suppressed in the SMEFT description, but not in the HEFT one.

5 Conclusions

The complete effective Lagrangian for a non-linear realisation of the EWSB (shortened into HEFT) has been presented. It provides the most general description of the Higgs couplings and it can be used for investigating a large spectrum of distinct theories, ranging from the SM to technicolour constructions, including Composite Higgs realisations and dilaton-like frameworks. In contrast with the effective Lagrangian for a linearly realised EWSB (also SMEFT), in which the Higgs belongs to an exact $SU(2)_L$ doublet, in the HEFT the physical Higgs is assigned to a singlet representation of the EW group and it is treated as an object independent of the Goldstone bosons' matrix.

Assuming invariance under the Lorentz and SM gauge symmetries, as well as the conservation of Baryon and Lepton numbers, the complete chiral basis at the next to leading order contains a total number of 148 independent, flavour universal terms. When extending the SM spectrum to include three right-handed neutrinos, 40 more operators enrich the basis. The generalisation to arbitrary flavour contractions is straightforward.

Conversely, the SMEFT basis up to $d = 6$ consists of only 59 flavour universal terms, in absence of right-handed neutrinos. The different number of operators and of building blocks used for the construction of the two bases lead to fundamental differences between the SMEFT and the HEFT. The possibility of distinguishing between them has been discussed performing a global fit including all the available data from colliders, including EWPD, Higgs and TGV measurements taken at the LHC Run I. The main outcomes are summarised in the following points:

- The Electroweak precision data analysis together with the study of the CKM matrix unitarity allows to constrain 11 parameters of the HEFT Lagrangian. The corresponding value of the χ^2 at the minimum is 6. This can be compared with the corresponding analysis within the SM, whose χ^2 is 18.4.
- The results for the S , T and U parameters are significantly different with respect to the standard analysis in the SMEFT with operators up to dimension 6, due to the

presence of extra free parameters: the allowed range for S is about 4 times broader, while the bounds on T and U are about 20 times weaker.

- The analysis of Higgs data depends on a total of 10 parameters, with one bosonic operator more compared to the same analysis in the SMEFT case at dimension six. Although the final results are quite similar to those obtained for the SMEFT, the addition of the extra parameter broadens the allowed range for the remaining 9 coefficients, as expected.
- The interplay between triple gauge boson vertices and Higgs couplings provides an interesting way of investigating the nature of EWSB. Although this analysis is not conclusive yet due to the limited sensitivity on the observables considered, the introduction of kinematic distributions is seen to improve considerably the results. Would the accuracy of Higgs measurements improve significantly in the future, this kind of analysis may reveal signatures of non-linearity in the Higgs sector.
- It has been underlined that with the increase in energy at colliders, it may be necessary to consider several operators that, in spite of being usually considered as higher order effects, may have a non-negligible phenomenological impact. The list of the relevant structures has been given in Table 6.

In summary, this work extends the chiral basis of Refs. [24, 25] with the introduction of fermionic operators. Moreover, the analysis presented here updates and extends that contained in Ref. [24] with the inclusion of more recent collider data and of fermionic observables. A strategy for disentangling the nature of the EWSB has been discussed, based on the presence of new anomalous signals and of decorrelations among observables. It has also been discussed how the phenomenological analysis should be modified when higher energy data is kept into account, specifying the relevant operator structures that should be added to the basis in this case. The analysis presented here represents the first phenomenological study performed with the complete HEFT Lagrangian and it could be taken as a reference for dedicated experimental analyses aimed at shedding light on the Electroweak symmetry breaking sector and the Higgs nature.

Acknowledgements

We thank M.B. Gavela for useful discussions during the development of the project, as well as Anja Butter, Tilman Plehn and Michael Rauch for their crucial assistance with both the Higgs and the TGV analyses. I.B. research was supported by an ESR contract of the EU network FP7 ITN INVISIBLES (Marie Curie Actions, PITN-GA-2011-289442). M.C.G-G is supported by USA-NSF grant PHY-13-16617, by grants 2014-SGR-104 and by FPA2013-46570 and consolidator-ingenio 2010 program CSD-2008-0037. L.M. acknowledge partial support of CiCYT through the project FPA2012-31880 and of the Spanish MINECO's "Centro de Excelencia Severo Ochoa" Programme under grant SEV-2012-0249. M.C.G-G and L.M. acknowledge partial support by FP7 ITN INVISIBLES (PITN-GA-2011-289442),

A Additional operators in presence of RH neutrinos

Adding right-handed neutrinos to the spectrum amounts to declaring a non-zero upper component for the L_R doublet, which shall be defined as $L_R = (N_R, E_R)^T$. Consequently, the lepton Yukawa matrix in the LO Lagrangian Eq. (2.3) has to be generalised to account for the masses and interactions of the neutrinos with the Higgs

$$\mathcal{Y}_L(h) \equiv \text{diag} \left(\sum_n Y_\nu^{(n)} \frac{h^n}{v^n}, \sum_n Y_\ell^{(n)} \frac{h^n}{v^n} \right). \quad (\text{A.1})$$

In addition, the fermionic basis presented in Sec. 2.3 must be enlarged in order to account for the increased number of possible invariants, as follows:

$$\Delta \mathcal{L}_{2F} = \sum_{j=15}^{17} n_j^\ell \mathcal{N}_j^\ell + \sum_{j=18}^{28} \frac{1}{\Lambda} (n_j^\ell + i\tilde{n}_j^\ell) \mathcal{N}_j^\ell + \sum_{j=29}^{31} \frac{4\pi}{\Lambda} (n_j^\ell + i\tilde{n}_j^\ell) \mathcal{N}_j^\ell, \quad (\text{A.2})$$

$$\Delta \mathcal{L}_{4F} = \frac{(4\pi)^2}{\Lambda^2} \left[\sum_{j=8}^{10} (r_j^\ell + i\tilde{r}_j^\ell) R_j^\ell + \sum_{j=1}^{15} r_j^\ell R_j^\ell + \sum_{j=24}^{29} (r_j^{\mathcal{Q}\ell} + i\tilde{r}_j^{\mathcal{Q}\ell}) R_j^{\mathcal{Q}\ell} + \sum_{j=30}^{38} r_j^{\mathcal{Q}\ell} R_j^{\mathcal{Q}\ell} \right]. \quad (\text{A.3})$$

The complete list of additional operators is provided in this Appendix.

Single Leptonic Current Operators

With one derivative

$$\begin{aligned} \mathcal{N}_{15}^\ell(h) &\equiv i\bar{L}_R \gamma_\mu \mathbf{U}^\dagger \mathbf{V}^\mu \mathbf{U} L_R \mathcal{F} & \mathcal{O}^\ell \mathcal{N}_{16}^\ell(h) &\equiv \bar{L}_R \gamma_\mu \mathbf{U}^\dagger [\mathbf{V}^\mu, \mathbf{T}] \mathbf{U} L_R \mathcal{F} \\ \mathcal{N}_{17}^\ell(h) &\equiv i\bar{L}_R \gamma_\mu \mathbf{U}^\dagger \mathbf{T} \mathbf{V}^\mu \mathbf{T} \mathbf{U} L_R \mathcal{F} \end{aligned}$$

With two derivatives

$$\begin{aligned} \mathcal{N}_{18}^\ell(h) &\equiv \bar{L}_L \mathbf{T} \mathbf{U} L_R \partial_\mu \mathcal{F} \partial^\mu \mathcal{F}' & \mathcal{N}_{19}^\ell(h) &\equiv \bar{L}_L \mathbf{V}_\mu \mathbf{U} L_R \partial^\mu \mathcal{F} \\ \mathcal{N}_{20}^\ell(h) &\equiv \bar{L}_L \mathbf{T} \mathbf{V}_\mu \mathbf{T} \mathbf{U} L_R \partial^\mu \mathcal{F} & \mathcal{N}_{21}^\ell(h) &\equiv \bar{L}_L \mathbf{V}_\mu \mathbf{V}^\mu \mathbf{T} \mathbf{U} L_R \mathcal{F} \\ \mathcal{N}_{22}^\ell(h) &\equiv \bar{L}_L \mathbf{T} \mathbf{V}_\mu \mathbf{T} \mathbf{V}^\mu \mathbf{T} \mathbf{U} L_R \mathcal{F} & \mathcal{N}_{23}^\ell(h) &\equiv \bar{L}_L \mathbf{V}_\mu \mathbf{T} \mathbf{V}^\mu \mathbf{U} L_R \mathcal{F} \\ \mathcal{N}_{24}^\ell(h) &\equiv \bar{L}_L \mathbf{V}_\mu \mathbf{T} \mathbf{V}^\mu \mathbf{T} \mathbf{U} L_R \mathcal{F} & \mathcal{N}_{25}^\ell(h) &\equiv \bar{L}_L \sigma^{\mu\nu} \mathbf{V}_\mu \mathbf{U} L_R \partial_\nu \mathcal{F} \\ \mathcal{N}_{26}^\ell(h) &\equiv \bar{L}_L \sigma^{\mu\nu} \mathbf{T} \mathbf{V}_\mu \mathbf{T} \mathbf{U} L_R \partial_\nu \mathcal{F} & \mathcal{N}_{27}^\ell(h) &\equiv \bar{L}_L \sigma^{\mu\nu} \mathbf{V}_\mu \mathbf{T} \mathbf{V}_\nu \mathbf{T} \mathbf{U} L_R \mathcal{F} \\ \mathcal{N}_{28}^\ell(h) &\equiv \bar{L}_L \sigma^{\mu\nu} [\mathbf{V}_\mu, \mathbf{V}_\nu] \mathbf{T} \mathbf{U} L_R \mathcal{F} & \mathcal{N}_{29}^\ell(h) &\equiv ig' \bar{L}_L \sigma^{\mu\nu} \mathbf{T} \mathbf{U} L_R \mathcal{F} B_{\mu\nu} \\ \mathcal{N}_{30}^\ell(h) &\equiv ig \bar{L}_L \sigma^{\mu\nu} \{W_{\mu\nu}, \mathbf{T}\} \mathbf{U} L_R \mathcal{F} & \mathcal{N}_{31}^\ell(h) &\equiv ig \bar{L}_L \sigma^{\mu\nu} \mathbf{T} W_{\mu\nu} \mathbf{T} \mathbf{U} L_R \mathcal{F} \end{aligned}$$

Four-fermion Operators

Additional operators with four leptons:

$$\begin{aligned}
R_8^\ell(h) &\equiv (\bar{L}_L \sigma^i \mathbf{U} L_R)(\bar{L}_L \sigma^i \mathbf{U} L_R) \mathcal{F} & R_9^\ell(h) &\equiv (\bar{L}_L \mathbf{U} L_R)(\bar{L}_L \mathbf{TU} L_R) \mathcal{F} \\
R_{10}^\ell(h) &\equiv (\bar{L}_L \mathbf{TU} L_R)(\bar{L}_L \mathbf{TU} L_R) \mathcal{F} & R_{11}^\ell(h) &\equiv (\bar{L}_R \gamma_\mu L_R)(\bar{L}_R \gamma^\mu \mathbf{U}^\dagger \mathbf{TU} L_R) \mathcal{F} \\
R_{12}^\ell(h) &\equiv (\bar{L}_R \gamma_\mu \mathbf{U}^\dagger \mathbf{TU} L_R)(\bar{L}_R \gamma^\mu \mathbf{U}^\dagger \mathbf{TU} L_R) \mathcal{F} & R_{13}^\ell(h) &\equiv (\bar{L}_L \gamma_\mu L_L)(\bar{L}_R \gamma^\mu \mathbf{U}^\dagger \mathbf{TU} L_R) \mathcal{F} \\
R_{14}^\ell(h) &\equiv (\bar{L}_L \gamma_\mu \mathbf{T} L_L)(\bar{L}_R \gamma^\mu \mathbf{U}^\dagger \mathbf{TU} L_R) \mathcal{F} & R_{15}^\ell(h) &\equiv (\bar{L}_L \gamma_\mu \sigma^i L_L)(\bar{L}_R \gamma^\mu \mathbf{U}^\dagger \sigma^i \mathbf{U} L_R) \mathcal{F}
\end{aligned}$$

Additional mixed operators with two quarks and two leptons

$$\begin{aligned}
R_{24}^{\mathcal{Q}\ell}(h) &\equiv (\bar{L}_L \mathbf{U} Q_R)(\bar{Q}_L \mathbf{TU} L_R) \mathcal{F} & R_{25}^{\mathcal{Q}\ell}(h) &\equiv (\bar{L}_L \mathbf{TU} L_R)(\bar{Q}_L \mathbf{U} Q_R) \mathcal{F} \\
R_{26}^{\mathcal{Q}\ell}(h) &\equiv (\bar{L}_L \mathbf{TU} L_R)(\bar{Q}_L \mathbf{TU} Q_R) \mathcal{F} & R_{27}^{\mathcal{Q}\ell}(h) &\equiv (\bar{L}_L \mathbf{TU} Q_R)(\bar{Q}_L \mathbf{TU} L_R) \mathcal{F} \\
R_{28}^{\mathcal{Q}\ell}(h) &\equiv (\bar{L}_L \sigma^i \mathbf{TU} L_R)(\bar{Q}_L \sigma^i \mathbf{U} Q_R) \mathcal{F} & R_{29}^{\mathcal{Q}\ell}(h) &\equiv (\bar{L}_L \sigma^i \mathbf{TU} Q_R)(\bar{Q}_L \sigma^i \mathbf{U} L_R) \mathcal{F} \\
R_{30}^{\mathcal{Q}\ell}(h) &\equiv (\bar{L}_R \gamma_\mu \mathbf{U}^\dagger \mathbf{TU} L_R)(\bar{Q}_R \gamma^\mu Q_R) \mathcal{F} & R_{31}^{\mathcal{Q}\ell}(h) &\equiv (\bar{L}_R \gamma_\mu \mathbf{U}^\dagger \mathbf{TU} L_R)(\bar{Q}_R \gamma^\mu \mathbf{U}^\dagger \mathbf{TU} Q_R) \mathcal{F} \\
R_{32}^{\mathcal{Q}\ell}(h) &\equiv (\bar{L}_R \gamma_\mu \mathbf{U}^\dagger \sigma^j \mathbf{U} L_R)(\bar{Q}_R \gamma^\mu \mathbf{U}^\dagger \sigma^j \mathbf{U} Q_R) \mathcal{F} & R_{33}^{\mathcal{Q}\ell}(h) &\equiv (\bar{Q}_L \gamma_\mu Q_L)(\bar{L}_R \gamma^\mu \mathbf{U}^\dagger \mathbf{TU} L_R) \mathcal{F} \\
R_{34}^{\mathcal{Q}\ell}(h) &\equiv (\bar{Q}_L \gamma_\mu \mathbf{T} Q_L)(\bar{L}_R \gamma^\mu \mathbf{U}^\dagger \mathbf{TU} L_R) \mathcal{F} & R_{35}^{\mathcal{Q}\ell}(h) &\equiv (\bar{Q}_L \gamma_\mu \sigma^j Q_L)(\bar{L}_R \gamma^\mu \mathbf{U}^\dagger \sigma^j \mathbf{U} L_R) \mathcal{F} \\
R_{36}^{\mathcal{Q}\ell}(h) &\equiv (\bar{Q}_L \gamma^\mu L_L)(\bar{L}_R \gamma_\mu \mathbf{U}^\dagger \mathbf{TU} Q_R) \mathcal{F} & R_{37}^{\mathcal{Q}\ell}(h) &\equiv (\bar{Q}_L \gamma_\mu \mathbf{T} L_L)(\bar{L}_R \gamma^\mu \mathbf{U}^\dagger \mathbf{TU} Q_R) \mathcal{F} \\
R_{38}^{\mathcal{Q}\ell}(h) &\equiv (\bar{Q}_L \gamma^\mu \sigma^j \mathbf{T} L_L)(\bar{L}_R \gamma_\mu \mathbf{U}^\dagger \sigma^j \mathbf{U} Q_R) \mathcal{F}
\end{aligned}$$

B Removal of $\mathcal{F}(h)$ from the Higgs and fermions kinetic terms

All the kinetic terms in the LO Lagrangian, Eq. (2.3), are canonically normalised, despite the fact that the singlet nature of the h field in principle allows to couple them to a function $\mathcal{F}(h)$. In the case of the gauge bosons' kinetic term, the absence of a Higgs-dependence is justified in the assumption that the transverse components of the gauge fields do not interact with the Higgs sector at LO. On the other hand, in the cases of the Higgs and of the fermions' kinetic terms, the dependence $\mathcal{F}(h)$ is completely redundant, as it can be removed via a field redefinition (analogously to what was done in Ref. [75]). This appendix provides more details about such redefinition.

The coupling of the fermionic kinetic term to a generic Higgs function would be of the form

$$\frac{i}{2} \left(\bar{\psi} \not{D} \psi - \bar{\psi} \overleftarrow{\not{D}} \psi \right) (1 + \mathcal{F}_\psi(h)) , \quad (\text{B.1})$$

where $\psi = \{Q, L\}$ and

$$\mathcal{F}_\psi(h) = c_\psi + 2a_\psi \frac{h}{v} + b_\psi \frac{h^2}{v^2} + \dots \quad (\text{B.2})$$

The dependence of $\mathcal{F}_\psi(h)$ can therefore be removed via the redefinition

$$\psi \rightarrow \psi' [1 + \mathcal{F}_\psi(h)]^{-1/2} . \quad (\text{B.3})$$

As this substitution is applied to the whole Lagrangian, it induces a modification of all the couplings between fermionic and Higgs fields, which can be reabsorbed in redefinitions of the functions $\mathcal{F}_i(h)$ that accompany fermionic operators. In particular, this is also true for the LO Yukawa couplings, as they are accompanied by arbitrary polynomials $\mathcal{Y}_{Q,L}(h)$. In conclusion, the insertion of a function $\mathcal{F}_\psi(h)$ in the fermionic kinetic term is redundant in the LO Lagrangian of Eq. (2.3).

The Higgs kinetic term may also be written as

$$\frac{1}{2} \partial_\mu h \partial^\mu h (1 + \mathcal{F}_H(h)) , \quad (\text{B.4})$$

with

$$\mathcal{F}_H(h) = c_H + 2a_H \frac{h}{v} + b_H \frac{h^2}{v^2} + \dots \quad (\text{B.5})$$

In this case, the $\mathcal{F}_H(h)$ function can be removed by the field redefinition

$$h' \rightarrow \int_0^h \sqrt{1 + \mathcal{F}_H(s)} ds \quad (\text{B.6})$$

in fact

$$\frac{1}{2} \partial_\mu h' \partial^\mu h' = \frac{1}{2} \left[\partial_\mu h \sqrt{1 + \mathcal{F}_H(h)} \right]^2 = \mathcal{P}_H(h) . \quad (\text{B.7})$$

Although this redefinition looks quite involved, it clearly induces modifications of all the Higgs couplings in the Lagrangian. As these are always described by arbitrary coefficients, the redefinition (B.6) can be entirely reabsorbed into redefinitions of the functions $\mathcal{F}_i(H)$ that appear in the Lagrangian. As seen for the case of $\mathcal{F}_\psi(h)$ above, the presence of $\mathcal{F}_H(h)$ in the Higgs' kinetic term is redundant within the LO Lagrangian chosen in Eq. (2.3).

A practical example

In order to give a practical illustration, one can consider a specific function

$$\mathcal{F}_H(h) = 2a_H \frac{h}{v} . \quad (\text{B.8})$$

Then, the following equation

$$h' = \int_0^h \sqrt{1 + 2a_H s/v} ds = \frac{v}{3a_H} \left[\left(\frac{2a_H h}{v} + 1 \right)^{3/2} - 1 \right] \quad (\text{B.9})$$

can be solved analytically, obtaining

$$h = \frac{v}{2a_H} \left[\left(\frac{3a_H}{v} h' + 1 \right)^{2/3} - 1 \right] . \quad (\text{B.10})$$

Plugging this result into $\mathcal{F}_C(h)$ and re-expanding in h'/v , it gives⁸:

$$\mathcal{F}_C(h) = 1 + 2a_C \frac{h'}{v} + (b_C - a_C a_H) \left(\frac{h'}{v} \right)^2, \quad (\text{B.11})$$

so that the impact of the redefinition can be entirely reabsorbed defining primed coefficients

$$a'_C = a_C, \quad b'_C = b_C - a_C a_H. \quad (\text{B.12})$$

An analogous redefinition allows to reabsorb inside the function $\mathcal{Y}_\psi^{(n)}$ the effects on the Yukawa interactions.

C Construction of the fermionic basis

This appendix provides additional information about the construction of the fermionic basis specifying, in particular, the relation between the structures present in the operators presented in Sec. 2.3 and those that have been removed. In what follows, generic fermion fields are denoted by $\psi = \{Q, L\}$ while Γ stands for an arbitrary $SU(2)$ structure, combination of the blocks $\{\mathbf{T}, \mathbf{V}_\mu, D_\mu, \sigma^j\}$. The Lorentz contractions are always explicated and, whenever they are not specified, chiralities are arbitrary. The correspondence between classes of operators is indicated schematically by an arrow (\rightarrow); signs and numerical coefficients are not specified in these relations.

C.1 Useful identities

A list of useful identities is provided below. Since the building blocks $A = \{\mathbf{T}, \mathbf{V}_\mu, \mathbf{D}_\mu \mathbf{V}^\mu\}$ are traceless, they can be generically rewritten as $A = \frac{1}{2} \text{Tr}[A \sigma^a] \sigma^a$. This yields the relations:

$$[\mathbf{T}, \mathbf{V}_\mu] = \frac{i}{2} \varepsilon^{ijk} \text{Tr}(\mathbf{T} \sigma^i) \text{Tr}(\mathbf{V}_\mu \sigma^j) \sigma^k \quad (\text{C.1})$$

$$\{\mathbf{T}, \mathbf{V}_\mu\} = \text{Tr}(\mathbf{T} \mathbf{V}_\mu) \mathbb{1} \quad (\text{C.2})$$

$$\mathbf{T} \mathbf{V}_\mu \mathbf{T} = \frac{1}{2} [\text{Tr}(\mathbf{T} \mathbf{V}_\mu) \text{Tr}(\mathbf{T} \sigma^i) - \text{Tr}(\mathbf{V}_\mu \sigma^i)] \sigma^i = \mathbf{T} \text{Tr}(\mathbf{T} \mathbf{V}_\mu) - \mathbf{V}_\mu \quad (\text{C.3})$$

The properties of the $SU(2)$ generators additionally lead to the following identities:

$$\begin{aligned} \mathbf{T} \mathbf{V}_\mu \mathbf{V}^\mu &= \mathbf{V}_\mu \mathbf{V}^\mu \mathbf{T} \\ \mathbf{T} \mathbf{V}_{[\mu} \mathbf{T} \mathbf{V}_{\nu]} &= \mathbf{V}_{[\mu} \mathbf{T} \mathbf{V}_{\nu]} \mathbf{T} \\ \mathbf{T} \mathbf{V}_{[\mu} \mathbf{T} \mathbf{V}_{\nu]} \mathbf{T} &= \mathbf{V}_{[\mu} \mathbf{T} \mathbf{V}_{\nu]} \\ \mathbf{T} [\mathbf{V}_\mu, \mathbf{V}_\nu] &= -[\mathbf{V}_\mu, \mathbf{V}_\nu] \mathbf{T} - 2 \mathbf{V}_{[\mu} \mathbf{T} \mathbf{V}_{\nu]}. \end{aligned} \quad (\text{C.4})$$

The transformation properties of \mathbf{T} and \mathbf{V}_μ ensure:

$$\mathbf{D}_\mu \mathbf{T} = [\mathbf{V}_\mu, \mathbf{T}] \quad (\text{C.5})$$

$$\mathbf{V}_{\mu\nu} = \mathbf{D}_\mu \mathbf{V}_\nu - \mathbf{D}_\nu \mathbf{V}_\mu = ig W_{\mu\nu} - ig' B_{\mu\nu}/2 + [\mathbf{V}_\mu, \mathbf{V}_\nu] \quad (\text{C.6})$$

⁸In this computation $a_H > 0$ is assumed. For negative values the third roots give some complications.

Fierz identities for chiral (anticommuting) fields have been employed for the reduction of the four fermion basis

$$(\bar{A}_L B_R)(\bar{C}_L D_R) = -\frac{1}{2}(\bar{A}_L D_R)(\bar{C}_L B_R) - \frac{1}{8}(\bar{A}_L \sigma^{\mu\nu} D_R)(\bar{C}_L \sigma_{\mu\nu} B_R) \quad (C.7)$$

$$(\bar{A}_L B_R)(\bar{C}_R D_L) = -\frac{1}{2}(\bar{A}_L \gamma_\mu D_L)(\bar{C}_R \gamma^\mu B_R) \quad (C.8)$$

$$(\bar{A}_L \gamma_\mu B_L)(\bar{C}_L \gamma^\mu D_L) = (\bar{A}_L \gamma_\mu D_L)(\bar{C}_L \gamma^\mu B_L) \quad (C.9)$$

$$(\bar{A}_R \gamma_\mu B_R)(\bar{C}_R \gamma^\mu D_R) = (\bar{A}_R \gamma_\mu D_R)(\bar{C}_R \gamma^\mu B_R). \quad (C.10)$$

Whenever they are applied to $SU(2)$ doublets (and $SU(3)$ triplets), these identities must be applied together with the completeness relations for the generators of $SU(2)$ (and of $SU(3)$)

$$\sigma_{ij}^a \sigma_{mn}^a = 2\delta_{in}\delta_{mj} - \delta_{ij}\delta_{mn} \quad (C.11)$$

$$\lambda_{ij}^A \lambda_{mn}^A = 2\delta_{in}\delta_{mj} - \frac{2}{3}\delta_{ij}\delta_{mn} \quad (C.12)$$

in order to recover the correct gauge contractions. For example, combining Eq. (C.8) with Eqs. (C.11) and (C.12), the scalar identity for quark doublets reads

$$\begin{aligned} (\bar{Q}_{1L} Q_{2R})(\bar{Q}_{3R} Q_{4L}) &= -\frac{1}{12}(\bar{Q}_{1L} \gamma_\mu Q_{4L})(\bar{Q}_{3R} \gamma^\mu Q_{2R}) - \frac{1}{12}(\bar{Q}_{1L} \gamma_\mu \sigma^k Q_{4L})(\bar{Q}_{3R} \gamma^\mu \sigma^k Q_{2R}) + \\ &\quad - \frac{1}{8}(\bar{Q}_{1L} \gamma_\mu \lambda^A Q_{4L})(\bar{Q}_{3R} \gamma^\mu \lambda^A Q_{2R}) - \frac{1}{8}(\bar{Q}_{1L} \gamma_\mu \lambda^A \sigma^k Q_{4L})(\bar{Q}_{3R} \gamma^\mu \lambda^A \sigma^k Q_{2R}). \end{aligned} \quad (C.13)$$

C.2 Construction of $\Delta\mathcal{L}_{2F}$

- Since for traceless matrices $\text{Tr}(AB)\mathbb{1} = \{A, B\}$, the operators of the type $\bar{\psi}\gamma_\mu\psi\text{Tr}(\Gamma_1\Gamma_2)\mathcal{F}$ with $\Gamma_i = \{\mathbf{T}, \mathbf{V}_\mu, \mathbf{D}_\mu\mathbf{V}_\nu\}$ are always equivalent to the bilinears $\bar{\psi}\gamma_\mu\{\Gamma_1, \Gamma_2\}\psi\mathcal{F}$.
- bilinears with a derivative on the fermion field and a vector current (eg. $(D_\mu\bar{\psi})\gamma^\mu X\psi$) can be removed via intergration by parts and application of the Equations of Motion (see Appendix D)
- operators with a derivative on the fermion field but with no gamma matrices (of the type $\bar{\psi}\Gamma^\mu D_\mu\psi$) are removed using the relation $g^{\mu\nu} = \{\gamma^\mu, \gamma^\nu\}/2$, integration by parts and the Equations of Motion:

$$\begin{aligned} \bar{\psi}\Gamma_\mu D^\mu\psi &= \bar{\psi}g_{\mu\nu}\Gamma^\mu D^\nu\psi = \bar{\psi}\not{\Gamma}(\not{D}\psi) + \bar{\psi}\gamma^\nu\not{\Gamma}(D_\nu\psi) = \\ &= \bar{\psi}\not{\Gamma}(\not{D}\psi) - (\bar{\psi}\overleftarrow{\not{D}})\not{\Gamma}\psi - \bar{\psi}(\not{D}\not{\Gamma})\psi \\ &\rightarrow \bar{\psi}\not{\Gamma}\psi + \bar{\psi}D_\mu\Gamma^\mu\psi + i\bar{\psi}\sigma^{\mu\nu}D_\mu\Gamma_\nu\psi. \end{aligned} \quad (C.14)$$

- bilinears with the structure $\gamma^\mu\gamma^\nu\mathbf{D}_\mu\mathbf{V}_\nu$ can be reduced to a combination of dipole operators (containing field strengths), terms with the structure $\sigma^{\mu\nu}\mathbf{V}_\mu\mathbf{V}_\nu$ and bilinears with the direct contraction $\mathbf{D}_\mu\mathbf{V}^\mu$. In fact:

$$\gamma^\mu\gamma^\nu\mathbf{D}_\mu\mathbf{V}_\nu = (g^{\mu\nu} - i\sigma^{\mu\nu})\mathbf{D}_\mu\mathbf{V}_\nu = \mathbf{D}_\mu\mathbf{V}^\mu - \frac{i}{2}\sigma^{\mu\nu}\mathbf{V}_{\mu\nu} \quad (C.15)$$

where the relation (C.6) shall be applied on the latter term. The former can be also removed using the EOMs.

- the commutator $[D_\mu, D_\nu]$ is always vanishing when applied to $SU(2)$ invariants (right-handed fermions, B and G fields, $\mathcal{F}(h)$ functions), while it is traded for a field strength when it acts on a quantity X with non-trivial isospin transformations: $[D_\mu, D_\nu]X = ig[W_{\mu\nu}, X]$.
- further combinations of \mathbf{T} and \mathbf{V}_μ that do not appear in the basis reported in Sec. 2.3 have been traded for others using the identities (C.1) and (C.4).

C.3 Construction of $\Delta\mathcal{L}_{4F}$

Details about the construction and reduction of the four-fermion operators basis are provided in this section. None of the terms of $\Delta\mathcal{L}_{4F}$ have been removed via Equations of Motion, while the Fierz identities (C.7)-(C.10) have been extensively employed for removing redundant structures. In particular, operators with tensor currents $((\bar{\psi}\sigma^{\mu\nu}\psi)^2)$ were not included in the final basis, as they are always equivalent to combinations of scalar contractions via the Fierz identity (C.7). Similarly, operators with the scalar contraction $(\bar{\psi}_L\psi_R)(\bar{\psi}_R\psi_L)$ have been traded for terms with the vector structure $(\bar{\psi}_L\gamma_\mu\psi_L)(\bar{\psi}_R\gamma^\mu\psi_R)$ employing the identity (C.8).

Four-quark (lepton) operators

- There are four independent $SU(2)$ contractions of four quarks that can be constructed with the scalar structure $(\bar{\psi}_L\psi_R)(\bar{\psi}_L\psi_R)$. They are easily identified in unitary gauge by the $U(1)_{\text{em}}$ invariants

$$(uu)(uu), \quad (dd)(dd), \quad (uu)(dd), \quad (ud)(du).$$

Keeping colour contractions into account, the total number of independent operators in this category is 8.

With four leptons there is only one invariant with this Lorentz structure, due to the absence of right-handed neutrinos: $(ee)(ee)$.

We do not provide the expressions of all the possible $SU(2)$ structures in terms of the invariants selected for the basis of Sect. 2.3. However, it is worth commenting on two contractions that can be constructed without the explicit insertion of Goldstone bosons: in the four-quarks case they are

$$\begin{aligned} R_{\varepsilon 1}^{\mathcal{Q}} &= \varepsilon_{ij}\varepsilon_{ab}(\bar{Q}_{L i} Q_{R a})(\bar{Q}_{L j} Q_{R b})\mathcal{F} \\ R_{\varepsilon 2}^{\mathcal{Q}} &= \varepsilon_{ij}\varepsilon_{ab}(\bar{Q}_{L i}\lambda^A Q_{R a})(\bar{Q}_{L j}\lambda^A Q_{R b})\mathcal{F}. \end{aligned} \quad (\text{C.16})$$

In the four-leptons case, it is possible to introduce a structure analogous to the first one, but only in presence of right-handed neutrinos. this would read:

$$R_{\varepsilon N}^{\ell} = \varepsilon_{ij}\varepsilon_{ab}(\bar{L}_{L i} L_{R a})(\bar{L}_{L j} L_{R b})\mathcal{F}. \quad (\text{C.17})$$

The operators of Eqs. (C.16) and (C.17) are redundant in the basis of Sect. 2.3: in fact, exploiting the properties of the Pauli matrices and the completeness relation (C.11) one has

$$\mathbf{U}_{ia}\mathbf{U}_{jb} - (\mathbf{U}\sigma^k)_{ia}(\mathbf{U}\sigma^k)_{jb} = 2\varepsilon_{ij}\varepsilon_{ab} \left(c_\pi^2 + \frac{|\vec{\pi}|^2}{v^2} s_\pi^2 \right), \quad (\text{C.18})$$

where we have used the compact notation $s_\pi \equiv \sin(|\vec{\pi}|/v)$, $c_\pi \equiv \cos(|\vec{\pi}|/v)$. From Eq. (C.18) it follows immediately that

$$\begin{aligned} \frac{R_1^{\mathcal{Q}} - R_2^{\mathcal{Q}}}{2} &= R_{\varepsilon 1}^{\mathcal{Q}} \left(c_\pi^2 + \frac{|\vec{\pi}|^2}{v^2} s_\pi^2 \right) = R_{\varepsilon 1}^{\mathcal{Q}} \left(1 - \frac{|\vec{\pi}|^2}{v^2} + \frac{4}{3} \frac{|\vec{\pi}|^4}{v^4} + \dots \right) \\ \frac{R_5^{\mathcal{Q}} - R_6^{\mathcal{Q}}}{2} &= R_{\varepsilon 2}^{\mathcal{Q}} \left(c_\pi^2 + \frac{|\vec{\pi}|^2}{v^2} s_\pi^2 \right) = R_{\varepsilon 2}^{\mathcal{Q}} \left(1 - \frac{|\vec{\pi}|^2}{v^2} + \frac{4}{3} \frac{|\vec{\pi}|^4}{v^4} + \dots \right) \\ \frac{R_1^\ell - R_8^\ell}{2} &= R_{\varepsilon N}^\ell \left(c_\pi^2 + \frac{|\vec{\pi}|^2}{v^2} s_\pi^2 \right) = R_{\varepsilon N}^\ell \left(1 - \frac{|\vec{\pi}|^2}{v^2} + \frac{4}{3} \frac{|\vec{\pi}|^4}{v^4} + \dots \right) \end{aligned} \quad (\text{C.19})$$

Therefore, the interactions contained in $R_{\varepsilon 1}^{\mathcal{Q}}$, $R_{\varepsilon 2}^{\mathcal{Q}}$ and $R_{\varepsilon N}^\ell$ are already described by linear combinations of operators in the basis.

- The class of four fermion operators with two left-handed currents contains four independent operators in both the four-quarks and four-leptons cases:

$$\begin{aligned} (\bar{Q}_L \gamma_\mu Q_L)^2 &: (uu)(uu), \quad (dd)(dd), \quad (uu)(dd), \quad (ud)(du) \\ (\bar{L}_L \gamma_\mu L_L)^2 &: (\nu\nu)(\nu\nu), \quad (ee)(ee), \quad (\nu\nu)(ee), \quad (\nu e)(e\nu) \end{aligned}$$

Notice that in this case the octet colour contraction $(\bar{Q}_L \gamma_\mu \lambda^A Q_L)^2$ is not independent. In fact it is equivalent to a combination of invariants with singlet colour contractions. Using Eqs. (C.12) and (C.9):

$$(\bar{Q}_L \gamma_\mu \lambda^a Q_L)(\bar{Q}_L \gamma_\mu \lambda^a Q_L) = \frac{1}{3}(\bar{Q}_L \gamma_\mu Q_L)(\bar{Q}_L \gamma_\mu Q_L) + (\bar{Q}_L \gamma_\mu \sigma^j Q_L)(\bar{Q}_L \gamma_\mu \sigma^j Q_L) \quad (\text{C.20})$$

An analogous relation holds for the structures with right-handed currents.

- The class of four fermion operators with two right-handed currents contains four independent operators in the four-quarks case but only one in the four-leptons sector:

$$\begin{aligned} (\bar{Q}_R \gamma_\mu Q_R)^2 &: (uu)(uu), \quad (dd)(dd), \quad (uu)(dd), \quad (ud)(du) \\ (\bar{L}_R \gamma_\mu L_R)^2 &: (ee)(ee) \end{aligned}$$

- Finally, there are five independent $SU(2)$ contractions for quark vector currents of opposite chirality $(\bar{\psi}_L \gamma_\mu \psi_L)(\bar{\psi}_R \gamma_\mu \psi_R)$, to be doubled when including octet colour contractions:

$$(uu)(uu), \quad (dd)(dd), \quad (uu)(dd), \quad (dd)(uu), \quad (ud)(du) + (du)(ud)$$

The four-leptons counterpart, instead, contains two invariants corresponding to the interactions

$$(ee)(ee), \quad (\nu\nu)(ee).$$

Mixed quark-lepton operators

- Operators with the scalar contraction $(\bar{\psi}_L \psi_R)(\bar{\psi}_L \psi_R)$ can have either the structure $(\bar{Q}Q)(\bar{L}L)$ or $(\bar{Q}L)(\bar{L}Q)$. Each of these yield three independent invariants, that are most easily identified in unitary gauge by the interactions:

$$\begin{aligned} (\bar{Q}Q)(\bar{L}L) : & \quad (uu)(ee), \quad (dd)(ee), \quad (du)(\nu e) \\ (\bar{Q}L)(\bar{L}Q) : & \quad (ue)(eu), \quad (de)(ed), \quad (de)(\nu u) \end{aligned} \quad (\text{C.21})$$

- The two combinations $(\bar{Q}_L \gamma_\mu Q_L)(\bar{L}_L \gamma^\mu L_L)$, $(\bar{Q}_L \gamma_\mu L_L)(\bar{L}_L \gamma^\mu Q_L)$ are related by the Fierz identity (C.9), and therefore only the former structure has been retained. The same holds for the analogous terms constructed with right-handed currents, that are connected by Eq. (C.10).

This class includes five independent left-handed invariants, identified by the hermitian combinations

$$(uu)(ee), \quad (dd)(ee), \quad (uu)(\nu\nu), \quad (dd)(\nu\nu), \quad (du)(\nu e) + (ud)(e\nu).$$

and two right-handed ones:

$$(uu)(ee), \quad (dd)(ee).$$

- Operators with one left-handed and one right-handed current can be constructed in either of the combinations $(\bar{Q}_L \gamma_\mu Q_L)(\bar{L}_R \gamma^\mu L_R)$, $(\bar{L}_L \gamma_\mu L_L)(\bar{Q}_R \gamma^\mu Q_R)$ and $(\bar{Q}_L \gamma_\mu L_L)(\bar{L}_R \gamma^\mu Q_R)$. These provide, respectively, $2 + 5 + 3$ independent interactions:

$$\begin{aligned} (\bar{Q}Q)(\bar{L}L) : & \quad (uu)(ee), \quad (dd)(ee) \\ (\bar{L}L)(\bar{Q}Q) : & \quad (ee)(uu), \quad (ee)(dd), \quad (\nu\nu)(uu), \quad (\nu\nu)(dd), \quad (\nu e)(du) + (e\nu)(ud) \\ (\bar{L}Q)(\bar{Q}L) : & \quad (eu)(ue), \quad (ed)(de), \quad (\nu u)(de) \end{aligned} \quad (\text{C.22})$$

D Application of the Equations of Motion

Given the LO Lagrangian in Eq. (2.3), the fields satisfy the following Equations of Motion (EOMs):

$$i\not{D}\psi_L = \frac{v}{\sqrt{2}}\mathbf{U}\mathcal{Y}_\psi(h)\psi_R \quad (D.1)$$

$$i\not{D}\psi_R = \frac{v}{\sqrt{2}}\mathcal{Y}_Q^\dagger(h)\mathbf{U}^\dagger\psi_L$$

$$(D^\mu W_{\mu\nu})^a = \sum_{\psi=Q,L} \frac{g}{2} \bar{\psi}_L \sigma^a \gamma_\nu \psi_L + \frac{igv^2}{4} \text{Tr}[\mathbf{V}_\nu \sigma^a] \mathcal{F}_C(h) \quad (D.2)$$

$$\partial^\mu B_{\mu\nu} = gc_\theta \sum_{\substack{i=L,R \\ \psi=Q,L}} \bar{\psi}_i \mathbf{h}_{\psi_i} \gamma_\nu \psi_i - \frac{igc_\theta v^2}{4} \text{Tr}[\mathbf{T}\mathbf{V}_\mu] \mathcal{F}_C(h) \quad (D.3)$$

$$\square \frac{h}{v} = -V'(h) - \frac{v}{4} \text{Tr}[\mathbf{V}_\mu \mathbf{V}^\mu] \mathcal{F}'_C(h) - \sum_{\psi=Q,L} \frac{1}{\sqrt{2}} (\bar{\psi}_L \mathbf{U} \mathcal{Y}'_\psi(h) \psi_R + \text{h.c.}) \quad (D.4)$$

where \mathbf{h}_{ψ_i} are the hypercharges in the 2×2 matrix notation:

$$\begin{aligned} h_{Q_L} &= \text{diag}(1/6, 1/6) , & h_{Q_R} &= \text{diag}(2/3, -1/3) , \\ h_{L_L} &= \text{diag}(-1/2, -1/2) , & h_{L_R} &= \text{diag}(0, -1) , \end{aligned} \quad (D.5)$$

and the prime denotes the first derivative with respect to h/v . A consequence of Eqs. (D.2) and (D.1) is

$$\mathbf{D}_\mu (\mathbf{V}^\mu \mathcal{F}_C) = \frac{i}{v^2} D_\mu \left(\sum_{\psi=Q,L} \bar{\psi}_L \sigma^j \gamma^\mu \psi_L \right) \sigma^j = \frac{1}{\sqrt{2}v} \sum_{\psi=Q,L} \left(\bar{\psi}_L \sigma^j \mathbf{U} \mathcal{Y}_\psi(h) \psi_R - \bar{\psi}_R \mathcal{Y}_\psi^\dagger(h) \mathbf{U}^\dagger \sigma^j \psi_L \right) \sigma^j \quad (D.6)$$

which can be recast in the form

$$\text{Tr}(\sigma^j \mathbf{D}_\mu \mathbf{V}^\mu) \mathcal{F}(h) = \frac{\sqrt{2}}{v} \sum_{\psi=Q,L} \left(\bar{\psi}_L \sigma^j \mathbf{U} \mathcal{Y}_\psi(h) \psi_R - \bar{\psi}_R \mathcal{Y}_\psi^\dagger(h) \mathbf{U}^\dagger \sigma^j \psi_L \right) - \text{Tr}(\sigma^j \mathbf{V}_\mu) \partial^\mu \mathcal{F}(h) , \quad (D.7)$$

which is valid order by order in the h expansion.

Operators that have been removed via EOM

The Equations of Motion relate the purely bosonic and the fermionic sectors, and they have been used to eliminate operators that are redundant when both sectors are considered at the same time. In this section we list the categories of operators that have been removed.

Bosonic sector

- Operators containing $\square\mathcal{F}(h)$.

Applying the EOM for the Higgs, Eq. (D.4), these terms can be traded for a combination of other bosonic operators plus fermionic bilinears and four-fermion operators. The following CP even terms have been removed, compared to the basis of Ref. [24]:

$$\begin{aligned}\mathcal{P}_{\square H}(h) &= \frac{\square h \square h}{v^2} \mathcal{F} \\ \mathcal{P}_7(h) &= \text{Tr}(\mathbf{V}_\mu \mathbf{V}^\mu) \square \mathcal{F} \\ \mathcal{P}_{25}(h) &= \text{Tr}(\mathbf{T} \mathbf{V}_\mu) \text{Tr}(\mathbf{T} \mathbf{V}^\mu) \square \mathcal{F}\end{aligned}\tag{D.8}$$

and the CP odd operator

$$\mathcal{S}_{13} = \text{Tr}(\mathbf{T} \mathbf{V}_\mu) \partial^\mu \square \mathcal{F}\tag{D.9}$$

- Operators containing $\mathbf{D}_\mu \mathbf{V}^\mu$.

Rewriting the traceless matrix $\mathbf{D}_\mu \mathbf{V}^\mu$ as

$$\mathbf{D}_\mu \mathbf{V}^\mu = \frac{\sigma^a}{2} \text{Tr}(\sigma^a \mathbf{D}_\mu \mathbf{V}^\mu)\tag{D.10}$$

and applying the identity (D.7), these bosonic operators can be traded by combinations of fermion bilinears, four-fermion operators and other bosonic terms that already belong to the basis. The following CP even terms have been eliminated, in the notation of Ref. [24]:

$$\begin{aligned}\mathcal{P}_9(h) &= \text{Tr}((\mathbf{D}_\mu \mathbf{V}^\mu)^2) \mathcal{F} \\ \mathcal{P}_{10}(h) &= \text{Tr}(\mathbf{V}_\nu \mathbf{D}_\mu \mathbf{V}^\mu) \partial^\nu \mathcal{F} \\ \mathcal{P}_{15}(h) &= \text{Tr}(\mathbf{T} \mathbf{D}_\mu \mathbf{V}^\mu) \text{Tr}(\mathbf{T} \mathbf{D}_\nu \mathbf{V}^\nu) \mathcal{F} \\ \mathcal{P}_{16}(h) &= \text{Tr}([\mathbf{T}, \mathbf{V}_\nu] \mathbf{D}_\mu \mathbf{V}^\mu) \text{Tr}(\mathbf{T} \mathbf{V}^\nu) \mathcal{F} \\ \mathcal{P}_{19}(h) &= \text{Tr}(\mathbf{T} \mathbf{D}_\mu \mathbf{V}^\mu) \text{Tr}(\mathbf{T} \mathbf{V}_\nu) \partial^\nu \mathcal{F}.\end{aligned}\tag{D.11}$$

Analogously, five CP odd operators have been traded for others: in the notation of Ref. [25] they are

$$\begin{aligned}\mathcal{S}_{10} &= i \text{Tr}(\mathbf{V}_\nu \mathbf{D}_\mu \mathbf{V}^\mu) \text{Tr}(\mathbf{T} \mathbf{V}^\nu) \mathcal{F} \\ \mathcal{S}_{11} &= i \text{Tr}(\mathbf{T} \mathbf{D}_\mu \mathbf{V}^\mu) \text{Tr}(\mathbf{V}_\nu \mathbf{V}^\nu) \mathcal{F} \\ \mathcal{S}_{12} &= i \text{Tr}([\mathbf{V}^\mu, \mathbf{T}] \mathbf{D}_\nu \mathbf{V}^\nu) \partial_\mu \mathcal{F} \\ \mathcal{S}_{14} &= i \text{Tr}(\mathbf{T} \mathbf{D}_\mu \mathbf{V}^\mu) \partial_\nu \mathcal{F}(h) \partial^\nu \mathcal{F}' \\ \mathcal{S}_{16} &= i \text{Tr}(\mathbf{T} \mathbf{D}_\mu \mathbf{V}^\mu) \text{Tr}(\mathbf{T} \mathbf{V}_\nu) \text{Tr}(\mathbf{T} \mathbf{V}^\nu) \mathcal{F}.\end{aligned}\tag{D.12}$$

Fermionic sector

- Bilinears of the type $\bar{\psi}\Gamma\gamma_\mu\psi\partial^\mu\mathcal{F}$.

Applying the EOMs for fermions (Eq. (D.1)), these operators can be schematically rewritten as

$$\begin{aligned}\bar{\psi}\Gamma\gamma_\mu\psi\partial^\mu\mathcal{F} &= -\bar{\psi}\overleftarrow{D}\Gamma\psi\mathcal{F} - \bar{\psi}\gamma_\mu(D^\mu\Gamma)\psi\mathcal{F} - \bar{\psi}\Gamma\overrightarrow{D}\psi\mathcal{F} \\ &\rightarrow \bar{\psi}\gamma_\mu(D^\mu\Gamma)\psi\mathcal{F}\bar{\psi}\Gamma\psi\mathcal{F}\end{aligned}\quad (\text{D.13})$$

- Bilinears containing $\square\mathcal{F}$.

Operators in this category are removed applying the EOM for the Higgs field, Eq. (D.4) and traded for other bilinears plus four-fermion operators.

- invariants containing $\mathbf{D}_\mu\mathbf{V}^\mu$

As in the bosonic sector, these operators are removed applying the identity (D.7). and traded for other bilinears plus four-fermion operators.

- Finally, the EOMs for the gauge (Eqs. (D.2), (D.3)) and Higgs (Eq. (D.4)) fields imply the following additional relations (signs and numeric coefficients not specified):

$$\begin{aligned}\mathcal{P}_B + \mathcal{P}_1 + \mathcal{P}_2 + \mathcal{P}_4 + \mathcal{P}_T &\rightarrow i\bar{L}_{L_i}\gamma_\mu\{\mathbf{V}^\mu, \mathbf{T}\}L_{L_i}\mathcal{F} + \mathcal{N}_5^\mathcal{Q} + \mathcal{N}_6^\mathcal{Q} \\ \mathcal{P}_W + \mathcal{P}_1 + \mathcal{P}_3 + \mathcal{P}_5 + \text{Tr}(\mathbf{V}_\mu\mathbf{V}^\mu)\mathcal{F} &\rightarrow i\bar{L}_{L_i}\gamma_\mu\mathbf{V}^\mu L_{L_i}\mathcal{F} + \mathcal{N}_1^\mathcal{Q} \\ \mathcal{P}_T + \mathcal{P}_1 + \mathcal{P}_3 + \mathcal{P}_{12} + \mathcal{P}_{13} + \mathcal{P}_{17} &\rightarrow i\bar{L}_{L_i}\gamma_\mu\mathbf{T}\mathbf{V}^\mu\mathbf{T}L_{L_i}\mathcal{F} + i\bar{L}_{L_i}\gamma_\mu\mathbf{V}^\mu L_{L_i}\mathcal{F} + \mathcal{N}_7^\mathcal{Q} + \mathcal{N}_1^\mathcal{Q}.\end{aligned}\quad (\text{D.14})$$

These have been employed to remove the three (flavour-diagonal contractions of the) leptonic operators specified on the right-hand side. This choice simplifies the renormalisation procedure.



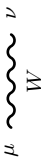

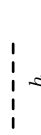

E Feynman rules

This appendix provides a complete list of all the Feynman rules resulting from both fermionic and bosonic operators considered in the present work and listed in Sections 2.2 and 2.3. For compactness we omit CP violating terms, that are not relevant for the phenomenological study presented. The rules are derived in unitary gauge and only vertices with up to four legs are shown. The SM contribution and the renormalization effects are also included, up to first order in the effective coefficients. The latter are sometimes encoded in the quantities Δg_1 , Δg_2 , Δg_W and ΔM_W defined in Eqs. (3.6), (3.5) in the text.

A few comments about the notation and conventions used:

- All momenta are flowing inwards and the convention $\partial_\mu \rightarrow -ip_\mu$ has been used in the derivation.
- We use a shorthand notation for the products $c_i a_i$: for the bosonic operators, we replace $a_i c_i \rightarrow a_i$ and $b_i c_i \rightarrow a_i$. For the fermionic operators, we write $a_i^f n_i^f \rightarrow (na)_i^f$. The structure $\bar{\psi}\psi\partial\mathcal{F}\partial\mathcal{F}'$ gives couplings $hhff$ with the coefficients $n_i^f a_i^f a_i'^f$ that has been shortened in $(naa')_i^f$. For the coefficients of the function $\mathcal{F}_C(h)$, defined in Eq. (2.4), the notation $a_C = 1 + \Delta a_C$, $b_C = 1 + \Delta b_C$ is adopted.
- We have fixed $V_{\text{CKM}} = \mathbb{1}$ for compactness. At the same level, all the effective coefficients are implicitly taken to be flavor-diagonal.
- In the vertices with a single fermion current the spin contractions are obvious. For those with four fermions we use a notation with square brackets and lowercase indices: for example $[P_R]_{ab}[P_L]_{cd}$ means that the right chirality projector contracts the spins of the a and b particle, and the left chirality one shall be inserted between the c and d fields.
- Uppercase indices indicate color and are assumed to be summed over when repeated. Whenever they are not specified, the color (and flavor) contractions go with those of the spin.

FR: propagators

(FR.1)	$\mu \quad \nu$  γ	$\frac{-i}{p^2} \left[g^{\mu\nu} - (1-\eta) \frac{p^\mu p^\nu}{p^2} \right] \quad (\eta \text{ is the gauge fixing parameter})$
(FR.2)	$\mu \quad \nu$  Z	$\frac{-i}{p^2 - m_Z^2} \left[g^{\mu\nu} - \frac{p^\mu p^\nu}{m_Z^2} \right]$
(FR.3)	$\mu \quad \nu$  W	$\frac{-i}{p^2 - M_W^2} \left[g^{\mu\nu} - \frac{p^\mu p^\nu}{M_W^2} \right]; \quad M_W^2 = m_Z^2 c_\theta^2 \left(1 + \frac{\Delta M_W^2}{M_W^2} \right) = m_Z^2 c_\theta^2 \left(1 + 2t_{2\theta} c_1 + \frac{2c_T c_\theta^2}{c_{2\theta}} - 4c_{12} + \frac{64\sqrt{2}\pi^2 s_\theta^2}{\Lambda^2} \frac{v^2}{c_{2\theta}} (r_2^\ell - r_3^\ell) \right)$
(FR.4)	$\mu \quad \nu$  G	$\frac{-i g^{\mu\nu}}{p^2} \left[g^{\mu\nu} - (1-\eta) \frac{p^\mu p^\nu}{p^2} \right]$
(FR.5)	h  h	$\frac{-i}{p^2 - m_h^2}$
(FR.6)	f  f	$\frac{i(\not{p} + m_f)}{p^2 - m_f^2}; \quad m_f = -\frac{v}{\sqrt{2}} Y_f^{(0)}$

FR: Bosonic

$$\begin{aligned}
& A_\rho \sim \left\{ \begin{aligned} & W_\nu^+ \left[i e \left[g_{\mu\nu} (p_+ - p_-)_\rho - g_{\nu\rho} p_{+\nu} + g_{\mu\rho} p_{-\mu} - (g_{\nu\rho} p_{A\mu} - g_{\mu\rho} p_{A\nu}) \left(1 - 2 \left(\frac{c_1}{t_\theta} + 2c_{12} \right) + \frac{g}{4\pi} \left(\frac{2c_2}{t_\theta} + c_3 + 2c_{13} \right) \right) \right] + \right. \\ & - \frac{24\pi s_\theta}{\Lambda^2} c_{WWWW} \left[g_{\rho\mu} ((p_+ \cdot p_-) p_{A\nu} - (p_A \cdot p_-) p_{+\nu}) + g_{\mu\nu} ((p_A \cdot p_-) p_{+\rho} - (p_A \cdot p_+) p_{-\rho}) + g_{\mu\nu} ((p_A \cdot p_+) p_{-\mu} - (p_+ \cdot p_-) p_{A\mu}) + \right. \\ & \left. \left. + p_{A\mu} p_{+\nu} p_{-\rho} - p_{A\nu} p_{+\rho} p_{-\mu} \right] \right. \\ & \left. W_\nu^- \right\} \end{aligned} \quad (\text{FR.7})
\end{aligned}$$

$$\begin{aligned}
& \text{Diagram 1: } Z_\rho \text{ (wavy line) } \rightarrow W_\mu^+ \text{ (solid line)} \\
& \text{Diagram 2: } Z_\rho \text{ (wavy line) } \rightarrow W_\nu^- \text{ (solid line)}
\end{aligned}
\tag{FR.8}$$

[illegible]

$$\begin{array}{ccc}
A_\mu(p_{A1}) & \text{X} & A_\nu(p_{A2}) \\
W_\lambda^+ & & W_\rho^- \\
-e^2[2g_{\mu\nu}g_{\lambda\rho} - (g_{\lambda\mu}g_{\rho\nu} + g_{\lambda\nu}g_{\rho\mu})] - \frac{24\pi i e g_0}{\Lambda^2}{}_{CW}WW \left[g_{\mu\nu}(p_{+\rho}(p_{A1} + p_{A2})_\lambda + p_{-\lambda}(p_{A1} + p_{A2})_\rho) + g_{\lambda\rho}(p_{A1\nu}(p_{+} + p_{-})_\mu + p_{A2\mu}(p_{+} + p_{-})_\nu) + \right. \\
+ g_{\mu\lambda}(p_{A1\rho}(p_{+} - p_{-})_\nu - p_{A2\rho}p_{+\nu} - p_{A1\nu}p_{+\rho}) + g_{\nu\lambda}(p_{A2\rho}(p_{+} - p_{-})_\mu - p_{A1\rho}p_{+\mu} - p_{A2\mu}p_{+\rho}) + \\
+ g_{\mu\rho}(p_{A1\lambda}(p_{-} - p_{+})_\nu - p_{A1\nu}p_{-\lambda} - p_{A2\lambda}p_{-\nu}) + g_{\nu\rho}(p_{A2\lambda}(p_{-} - p_{+})_\mu - p_{A2\mu}p_{-\lambda} - p_{A1\lambda}p_{-\mu}) + \\
\left. - g_{\mu\nu}g_{\lambda\rho}(p_{A1} + p_{A2}) \cdot (p_{+} + p_{-}) + g_{\nu\rho}g_{\lambda\mu}(p_{A1} \cdot p_{-} + p_{A2} \cdot p_{+}) + g_{\mu\rho}g_{\lambda\nu}(p_{A1} \cdot p_{+} + p_{A2} \cdot p_{-}) \right]
\end{array}
\quad (\text{FR.10})$$

(FR.11)

$$\begin{aligned}
& -ig^2c_\theta^2 \left(1 + 2\Delta g_1 + \frac{2}{c_\theta^2} \Delta g_2 + \frac{gc_3}{2\pi c_\theta^2} \right) \left[2g_{\mu\nu}g_{\lambda\rho} \left(1 - \frac{g^2}{16\pi^2c_\theta^4}(c_6 + c_{23}) \right) - (g_{\lambda\mu}g_{\rho\nu} + g_{\lambda\nu}g_{\rho\mu}) \left(1 + \frac{g^2}{16\pi^2c_\theta^4}(c_{11} + c_{24}) \right) \right] + \\
& -\frac{24\pi^4gc_\theta^2}{\Lambda^2} c_{WWWW} \left[g_{\mu\nu} (p_{+\rho}(p_{Z1} + p_{Z2})_\lambda + p_{-\lambda}(p_{Z1} + p_{Z2})_\rho) + g_{\lambda\rho} (p_{Z1\nu}(p_{+} + p_{-})_\mu + p_{Z2\mu}(p_{+} + p_{-})_\nu) + \right. \\
& + g_{\mu\lambda} (p_{Z1\rho}(p_{+} - p_{-})_\nu - p_{Z2\rho}p_{++\nu} - p_{Z1\nu}p_{++\rho}) + g_{\nu\lambda} (p_{Z2\rho}(p_{+} - p_{-})_\mu - p_{Z1\rho}p_{++\mu} - p_{Z2\mu}p_{++\rho}) + \\
& + g_{\mu\rho} (p_{Z1\lambda}(p_{-} - p_{+})_\nu - p_{Z1\nu}p_{-\lambda} - p_{Z2\lambda}p_{-\nu}) + g_{\nu\rho} (p_{Z2\lambda}(p_{-} - p_{+})_\mu - p_{Z2\mu}p_{-\lambda} - p_{Z1\lambda}p_{-\mu}) + \\
& \left. -g_{\mu\nu}g_{\lambda\rho}(p_{Z1} + p_{Z2}) \cdot (p_{+} + p_{-}) + g_{\nu\rho}g_{\lambda\mu} (p_{Z1} \cdot p_{-} + p_{Z2} \cdot p_{+}) + g_{\mu\rho}g_{\lambda\nu} (p_{Z1} \cdot p_{+} + p_{Z2} \cdot p_{-}) \right]
\end{aligned}$$

(FR.12)

$$\begin{aligned}
& -ieg c_\theta \left(1 + \Delta g_1 + \frac{1}{c_\theta^2} \Delta g_2 + \frac{gc_3}{4\pi c_\theta^2} \right) \left[2g_{\mu\nu}g_{\lambda\rho} - (g_{\lambda\nu}g_{\rho\mu} + g_{\lambda\mu}g_{\rho\nu}) \right] - \varepsilon^{\mu\nu\rho\lambda} \frac{eg^2c_{14}}{2\pi c_\theta} + \\
& -\frac{24\pi^4iec_\theta}{\Lambda^2} c_{WWWW} \left[g_{\mu\nu} (p_{+\rho}(p_Z + p_A)_\lambda + p_{-\lambda}(p_Z + p_A)_\rho) + g_{\lambda\rho} (p_{Z\nu}(p_{+} + p_{-})_\mu + p_{A\mu}(p_{+} + p_{-})_\nu) + \right. \\
& + g_{\mu\lambda} (p_{Z\rho}(p_{+} - p_{-})_\nu - p_{A\rho}p_{++\nu} - p_{Z\nu}p_{++\rho}) + g_{\nu\lambda} (p_{A\rho}(p_{+} - p_{-})_\mu - p_{Z\rho}p_{++\mu} - p_{A\mu}p_{++\rho}) + \\
& + g_{\mu\rho} (p_{Z\lambda}(p_{-} - p_{+})_\nu - p_{Z\nu}p_{-\lambda} - p_{A\lambda}p_{-\nu}) + g_{\nu\rho} (p_{A\lambda}(p_{-} - p_{+})_\mu - p_{A\mu}p_{-\lambda} - p_{Z\lambda}p_{-\mu}) + \\
& \left. -g_{\mu\nu}g_{\lambda\rho}(p_Z + p_A) \cdot (p_{+} + p_{-}) + g_{\nu\rho}g_{\lambda\mu} (p_Z \cdot p_{-} + p_A \cdot p_{+}) + g_{\mu\rho}g_{\lambda\nu} (p_Z \cdot p_{+} + p_A \cdot p_{-}) \right]
\end{aligned}$$

(FR.13)

$$\begin{aligned}
& ig^2 \left(1 + 2\Delta g_W + \frac{gc_3}{2\pi} - 4c_{12} + \frac{g^3c_{13}}{\pi} \right) \left[2g_{\lambda\mu}g_{\nu\rho} \left(1 + \frac{g^2}{16\pi^2}c_{11} \right) - (g_{\mu\nu}g_{\lambda\rho} + g_{\lambda\nu}g_{\mu\rho}) \left(1 - \frac{g^2}{16\pi^2}(2c_6 + c_{11}) \right) \right] + \\
& + \frac{24\pi^4ig}{\Lambda^2} c_{WWWW} \left[g_{\mu\nu} (p_{3\rho}(p_1 + p_2)_\lambda + p_{4\lambda}(p_1 + p_2)_\rho) + g_{\lambda\rho} (p_{1\nu}(p_3 + p_4)_\mu + p_{2\mu}(p_3 + p_4)_\nu) + \right. \\
& + g_{\mu\lambda} (p_{1\rho}(p_3 - p_4)_\nu - p_{2\rho}p_{3\nu} - p_{1\nu}p_{3\rho}) + g_{\nu\lambda} (p_{2\rho}(p_3 - p_4)_\mu - p_{1\rho}p_{3\mu} - p_{2\mu}p_{3\rho}) + \\
& + g_{\mu\rho} (p_{1\lambda}(p_4 - p_3)_\nu - p_{1\nu}p_{4\lambda} - p_{2\lambda}p_{4\nu}) + g_{\nu\rho} (p_{2\lambda}(p_4 - p_{+})_\mu - p_{2\mu}p_{4\lambda} - p_{1\lambda}p_{4\mu}) + \\
& \left. -g_{\mu\nu}g_{\lambda\rho}(p_1 + p_2) \cdot (p_3 + p_4) + g_{\nu\rho}g_{\lambda\mu} (p_1 \cdot p_4 + p_2 \cdot p_3) + g_{\mu\rho}g_{\lambda\nu} (p_1 \cdot p_3 + p_2 \cdot p_4) \right]
\end{aligned}$$

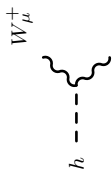
$$\begin{array}{c}
\begin{array}{c} Z_\nu \\ \text{---} \\ Z_\mu \end{array} \begin{array}{c} Z_\lambda \\ \text{---} \\ Z_\rho \end{array} \\
\text{(FR.14)}
\end{array}
\quad
\frac{ig^4}{16\pi^2 c_\theta^4} [g_{\mu\nu} g_{\lambda\rho} + g_{\mu\lambda} g_{\nu\rho} + g_{\mu\rho} g_{\nu\lambda}] (c_6 + c_{11} + 2c_{23} + 2c_{24} + 4c_{26})$$

$$\begin{array}{c}
\begin{array}{c} G_\mu^B(p_2) \\ \text{---} \\ G_\mu^A(p_1) \end{array} \begin{array}{c} G_\lambda^C(p_3) \\ \text{---} \\ G_\rho^D(p_4) \end{array} \\
\text{(FR.15)}
\end{array}
\quad
\begin{aligned}
& ig_s^2 \left[f^{ABX} f^{CDX} (g_{\mu\rho} g_{\nu\lambda} - g_{\mu\lambda} g_{\nu\rho}) + f^{ACX} f^{BDX} (g_{\mu\rho} g_{\nu\lambda} - g_{\mu\lambda} g_{\nu\rho}) + f^{ADX} f^{BCX} (g_{\mu\lambda} g_{\nu\rho} - g_{\mu\nu} g_{\lambda\rho}) \right] (1 + c_G) + \\
& + \frac{24\pi i g_s}{\Lambda^2} c_{GGG} \left[f^{ABX} f^{CDX} (g_{\mu\nu} (p_{1\lambda} p_{2\rho} - p_{1\rho} p_{2\lambda}) + g_{\lambda\rho} (p_{3\mu} p_{4\nu} - p_{4\mu} p_{3\nu}) - g_{\mu\lambda} (p_{1\nu} p_{2\rho} + p_{3\rho} p_{4\nu}) - g_{\nu\rho} (p_{2\mu} p_{1\lambda} + p_{3\mu} p_{4\lambda}) + \right. \\
& + g_{\mu\rho} (p_{1\nu} p_{2\lambda} + p_{4\lambda} p_{3\nu}) + g_{\nu\lambda} (p_{1\rho} p_{2\mu} + p_{3\rho} p_{4\mu}) + (g_{\nu\rho} g_{\mu\lambda} - g_{\nu\lambda} g_{\mu\rho}) (p_1 \cdot p_2 + p_3 \cdot p_4) \left. \right] + \\
& + f^{ACX} f^{BDX} (-g_{\mu\nu} (p_{1\lambda} p_{3\rho} + p_{2\rho} p_{4\lambda}) - g_{\lambda\rho} (p_{1\nu} p_{3\mu} + p_{2\mu} p_{4\nu}) + g_{\mu\lambda} (p_{1\nu} p_{3\rho} - p_{1\rho} p_{3\nu}) + g_{\nu\rho} (p_{2\mu} p_{4\lambda} - p_{2\lambda} p_{4\mu}) + g_{\mu\rho} (p_{4\nu} p_{2\lambda} + p_{1\lambda} p_{3\nu}) + \\
& + g_{\nu\lambda} (p_{1\rho} p_{3\mu} + p_{2\rho} p_{4\mu}) + (g_{\mu\nu} g_{\lambda\rho} - g_{\nu\lambda} g_{\mu\rho}) (p_1 \cdot p_3 + p_2 \cdot p_4) \left. \right) + \\
& + f^{ADX} f^{BCX} (-g_{\mu\nu} (p_{2\lambda} p_{3\rho} + p_{1\rho} p_{4\lambda}) - g_{\lambda\rho} (p_{1\nu} p_{4\mu} + p_{2\mu} p_{3\nu}) + g_{\mu\lambda} (p_{2\rho} p_{3\nu} + p_{1\rho} p_{4\nu}) + g_{\nu\rho} (p_{2\lambda} p_{3\mu} + p_{1\lambda} p_{4\mu}) + g_{\mu\rho} (p_{1\nu} p_{4\lambda} - p_{1\lambda} p_{4\nu}) + \\
& + g_{\nu\lambda} (p_{2\mu} p_{3\rho} - p_{2\rho} p_{3\mu}) + (g_{\mu\nu} g_{\lambda\rho} - g_{\mu\lambda} g_{\nu\rho}) (p_1 \cdot p_4 + p_2 \cdot p_3) \left. \right]
\end{aligned}$$

$$\begin{array}{c}
\begin{array}{c} A_\mu(p_{A1}) \\ \text{---} \\ h \end{array} \begin{array}{c} A_\nu(p_{A2}) \end{array} \\
\text{(FR.16)}
\end{array}
\quad
i \frac{2c_\theta^2}{v} [g^{\mu\nu} p_{A1} \cdot p_{A2} - p_{A1}^\nu p_{A2}^\mu] (a_B - 4t_\theta a_1 + t_\theta^2 (a_W - 4a_{12}))$$

$$\begin{array}{c}
\begin{array}{c} Z_\mu(p_{Z1}) \\ \text{---} \\ h \end{array} \begin{array}{c} Z_\nu(p_{Z2}) \end{array} \\
\text{(FR.17)}
\end{array}
\quad
\begin{aligned}
& 2i \frac{m_Z^2}{v} \left[g^{\mu\nu} (1 + \Delta a_C - 2(a_T - c_T)) + \frac{2c_\theta^4}{g^2 v^2} [g^{\mu\nu} p_{Z1} \cdot p_{Z2} - p_{Z1}^\nu p_{Z2}^\mu] (a_B t_\theta^2 + a_W + 4t_\theta a_1 - 4a_{12}) \right. \\
& \left. - \frac{c_\theta}{4\pi g s_\theta^3 v^2} [p_{Z1}^\nu p_h^\mu + p_{Z2}^\mu p_h^\nu - (p_{Z1} + p_{Z2}) \cdot p_h g^{\mu\nu}] (2s_\theta a_4 - c_\theta (a_5 + 2a_{17})) \right]
\end{aligned}$$

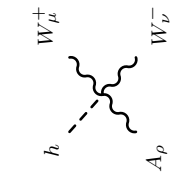
$$\begin{array}{c}
\begin{array}{c} A_\mu \\ \text{---} \\ h \end{array} \begin{array}{c} Z_\nu \end{array} \\
\text{(FR.18)}
\end{array}
\quad
-\frac{i}{v} [g^{\mu\nu} (p_A \cdot p_Z) - p_A^\nu p_Z^\mu] [4a_1 c_{2\theta} + (4a_{12} + a_B - a_W) s_{2\theta}] + \frac{ig}{4\pi v} [p_A^\nu p_h^\mu - p_A \cdot p_h g^{\mu\nu}] (2a_4 + t_\theta (a_5 + 2a_{17}))$$

(FR.19) 

$$i \frac{2m_Z^2 c_\theta^2}{v} \left[g_{\mu\nu} \left(1 + \Delta a_C + \frac{\Delta M_W^2}{M_W^2} \right) + [2g^{\mu\nu}(p_+ \cdot p_-) - 2p_+^\nu p_-^\mu] \frac{a_W}{g^2 v^2} + [(p_+^\nu p_-^\mu + p_-^\mu p_+^\nu) - (p_+ + p_-) \cdot p_\lambda g^{\mu\nu}] \frac{a_5}{4\pi g v^2} \right]$$

(FR.20) 

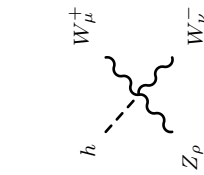
$$i \frac{2}{v} [g^{\mu\nu} p_{G1} \cdot p_{G2} - p_{G1}^\nu p_{G2}^\mu] a_G$$

(FR.21) 

$$-\frac{2ie}{v} [g_{\mu\nu}(p_+ - p_-)_\rho + g_{\mu\rho} p_{-\nu} + g_{\nu\rho} p_{+\mu}] a_W - \frac{2ie}{v} [-g_{\mu\rho} p_{A\nu} + g_{\nu\rho} p_{A\mu}] \left(a_W - 4a_{12} - \frac{2a_1}{t_\theta} + \frac{g}{4\pi} \left(\frac{2a_2}{t_\theta} + a_3 + 2a_{13} \right) \right) +$$

$$-\frac{ieg}{4\pi v} [g_{\mu\rho} p_{h\nu} - g_{\nu\rho} p_{h\mu}] a_5 + \frac{48i\pi s_\theta}{\Lambda^2 v} a_W W W W [g_{\rho\mu} ((p_+ \cdot p_-) p_{A\nu} - (p_A \cdot p_-) p_{+\nu}) + g_{\mu\nu} ((p_A \cdot p_-) p_{+\rho} - (p_A \cdot p_+) p_{-\rho}) +$$

$$+ g_{\rho\nu} ((p_A \cdot p_+) p_{-\mu} - (p_+ \cdot p_-) p_{A\mu}) + p_{A\mu} p_{+\nu} p_{-\rho} - p_{A\nu} p_{+\rho} p_{-\mu}]$$

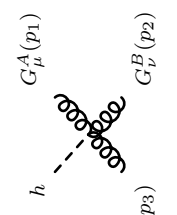
(FR.22) 

$$-\frac{2igc_\theta}{v} [g_{\mu\nu}(p_+ - p_-)_\rho + g_{\mu\rho} p_{-\nu} + g_{\nu\rho} p_{+\mu}] \left(a_W + \frac{ga_3}{4\pi c_\theta} \right) - \frac{2igc_\theta}{v} [-g_{\mu\rho} p_{Z\nu} + g_{\nu\rho} p_{Z\mu}] \left[\frac{g}{4\pi} (a_3 - 2a_2 t_\theta + 2a_{13}) + a_W - 4a_{12} + 2a_1 t_\theta \right]$$

$$+ \frac{ie^2}{4\pi v c_\theta} [g_{\mu\rho} p_{h\nu} - g_{\nu\rho} p_{h\mu}] \left(a_5 + \frac{1}{s_\theta^2} \left(2a_{17} + \frac{ga_{18}}{2\pi} \right) \right) - \frac{g^2}{2\pi v c_\theta} \varepsilon^{\mu\nu\rho\lambda} [p_{+\lambda} - p_{-\lambda}] a_{14} +$$

$$+ \frac{48i\pi c_\theta}{\Lambda^2 v} a_W W W W [g_{\rho\mu} ((p_+ \cdot p_-) p_{Z\nu} - (p_Z \cdot p_-) p_{+\nu}) + g_{\mu\nu} ((p_Z \cdot p_-) p_{+\rho} - (p_Z \cdot p_+) p_{-\rho}) +$$

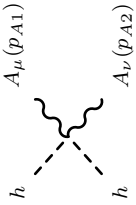
$$+ g_{\rho\nu} ((p_Z \cdot p_+) p_{-\mu} - (p_+ \cdot p_-) p_{Z\mu}) + p_{Z\mu} p_{+\nu} p_{-\rho} - p_{Z\nu} p_{+\rho} p_{-\mu}]$$

(FR.23) 

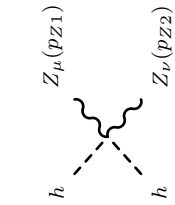
$$2g_s a_G f^{ABC} (g_{\mu\nu} (p_2 - p_1)_\rho + g_{\mu\rho} (p_1 - p_3)_\nu + g_{\nu\rho} (p_3 - p_2)_\mu) +$$

$$+ \frac{48\pi}{\Lambda^2 v} a_G G G f^{ABC} [g_{\rho\mu} ((p_1 \cdot p_2) p_{3\nu} - (p_3 \cdot p_2) p_{1\nu}) + g_{\mu\nu} ((p_3 \cdot p_2) p_{1\rho} - (p_3 \cdot p_1) p_{2\rho}) +$$

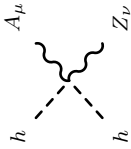
$$+ g_{\rho\nu} ((p_3 \cdot p_1) p_{2\mu} - (p_1 \cdot p_2) p_{3\mu}) + p_{3\mu} p_{1\nu} p_{2\rho} - p_{3\nu} p_{1\rho} p_{2\mu}]$$



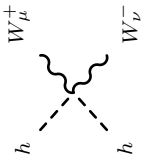
$$(FR.24) \quad i \frac{2c_\theta^2}{v^2} [g^{\mu\nu} p_{A1} \cdot p_{A2} - p_{A1}^\nu p_{A2}^\mu] (b_B - 4t_\theta b_1 + t_\theta^2 (b_W - 4b_{12}))$$



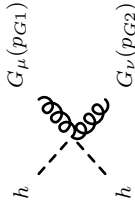
$$(FR.25) \quad i \frac{2m_Z^2}{v^2} g^{\mu\nu} (1 + \Delta b_C - 2(b_T - c_T)) + i \frac{2c_\theta^2}{v^2} [g^{\mu\nu} p_{Z1} \cdot p_{Z2} - p_{Z1}^\nu p_{Z2}^\mu] (b_B t_\theta^2 + b_W + 4t_\theta b_1 - b_{12}) \\ - \frac{ie}{4\pi v^2} [p_{Z1}^\nu (p_{h1} + p_{h2})^\mu + p_{Z2}^\mu (p_{h1} + p_{h2})^\nu - (p_{Z1} + p_{Z2}) \cdot (p_{h1} + p_{h2}) g^{\mu\nu}] \left(\frac{2b_4}{c_\theta} - \frac{b_5 + 2b_{17}}{s_\theta} \right) \\ + \frac{ig^2}{2\pi^2 v^2 c_\theta^2} g_{\mu\nu} p_{h1} \cdot p_{h2} (a_{20} + 2a_{21}) + \frac{ig^2}{4\pi^2 v^2 c_\theta^2} [p_{h1}^\mu p_{h2}^\nu + p_{h1}^\nu p_{h2}^\mu] (a_8 + 2a_{22})$$



$$(FR.26) \quad -\frac{i}{v^2} [g^{\mu\nu} (p_A \cdot p_Z) - p_A^\nu p_Z^\mu] (4b_1 c_{2\theta} + (4b_{12} + b_B - b_W) s_{2\theta}) + \frac{ig}{4\pi v^2} [p_A^\nu (p_{h1} + p_{h2})^\mu - p_A \cdot (p_{h1} + p_{h2}) g^{\mu\nu}] (2b_4 + t_\theta (b_5 + 2b_{17}))$$



$$(FR.27) \quad i \frac{2m_Z^2 c_\theta^2}{v^2} g_{\mu\nu} \left(1 + \Delta b_C + \frac{\Delta M_W^2}{M_W^2} \right) + \frac{i}{v^2} [2g^{\mu\nu} (p_+ \cdot p_-) - 2p_+^\nu p_-^\mu] b_W + \\ + \frac{ig}{4\pi v^2} [p_+^\nu (p_{h1} + p_{h2})^\mu + p_-^\mu (p_{h1} + p_{h2})^\nu - (p_+ + p_-) \cdot (p_{h1} + p_{h2}) g^{\mu\nu}] b_5 + \frac{ig^2}{2\pi^2 v^2} g_{\mu\nu} p_{h1} \cdot p_{h2} a_{20} + \frac{ig^2}{4\pi^2 v^2} [p_{h1}^\mu p_{h2}^\nu + p_{h1}^\nu p_{h2}^\mu] a_8$$



$$(FR.28) \quad i \frac{2}{v^2} [g^{\mu\nu} p_{G1} \cdot p_{G2} - p_{G1}^\nu p_{G2}^\mu] b_G$$

FR: Fermionic

Single quark current

$$(FR.29) \quad \begin{array}{c} d \\ \swarrow \quad \searrow \\ h \text{ --- } \\ \swarrow \quad \searrow \\ d \end{array} \quad -\frac{i}{\sqrt{2}} Y_D^{(1)}$$

$$(FR.30) \quad \begin{array}{c} u \\ \swarrow \quad \searrow \\ h \text{ --- } \\ \swarrow \quad \searrow \\ u \end{array} \quad -\frac{i}{\sqrt{2}} Y_U^{(1)}$$

$$(FR.31) \quad \begin{array}{c} d \\ \swarrow \quad \searrow \\ Z^\mu \\ \swarrow \quad \searrow \\ d \end{array} \quad -\frac{ig}{c_\theta} \left[\left(-\frac{1}{2} + \frac{s_\theta^2}{3} \right) \left(1 + \Delta g_1 + \frac{2}{3-2s_\theta^2} \Delta g_2 + \frac{6}{3-2s_\theta^2} (n_1^Q - 2n_5^Q + n_7^Q) \right) \gamma_\mu P_L + \frac{s_\theta^2}{3} \left(1 + \Delta g_1 - \frac{1}{s_\theta^2} \Delta g_2 - \frac{3}{s_\theta^2} (n_2^Q - 2n_6^Q + n_8^Q) \right) \gamma^\mu P_R + 4\pi c_\theta^2 \left[(n_{33}^Q - 2n_{34}^Q + n_{36}^Q) + 2(n_{29}^Q - n_{30}^Q) t_\theta^2 \right] \frac{p_{Z\nu}}{\Lambda} \sigma^{\mu\nu} \gamma_5 \right]$$

$$(FR.32) \quad \begin{array}{c} u \\ \swarrow \quad \searrow \\ Z^\mu \\ \swarrow \quad \searrow \\ u \end{array} \quad -\frac{ig}{c_\theta} \left[\left(\frac{1}{2} - \frac{2s_\theta^2}{3} \right) \left(1 + \Delta g_1 + \frac{4}{3-4s_\theta^2} \Delta g_2 + \frac{6}{3-4s_\theta^2} (n_1^Q + 2n_5^Q + n_7^Q) \right) \gamma_\mu P_L - \frac{2s_\theta^2}{3} \left(1 + \Delta g_1 - \frac{1}{s_\theta^2} \Delta g_2 - \frac{3}{2s_\theta^2} (n_2^Q + 2n_6^Q + n_8^Q) \right) \gamma^\mu P_R + 4\pi c_\theta^2 \left[(n_{33}^Q + 2n_{34}^Q + n_{36}^Q) - 2(n_{29}^Q + n_{30}^Q) t_\theta^2 \right] \frac{p_{Z\nu}}{\Lambda} \sigma^{\mu\nu} \gamma_5 \right]$$

$$(FR.33) \quad \begin{array}{c} d \\ \swarrow \quad \searrow \\ W_\mu^+ \\ \swarrow \quad \searrow \\ u \end{array} \quad -\frac{ig}{\sqrt{2}} \left[\gamma^\mu P_L \left[1 + \Delta g_W + 2(n_1^Q - n_7^Q) \right] + 2(n_2^Q - n_8^Q) \gamma^\mu P_R - 16\pi n_{35}^Q \frac{p_{W\nu}}{\Lambda} \sigma^{\mu\nu} + 8\pi (n_{33}^Q - n_{36}^Q) \frac{p_{W\nu}}{\Lambda} \sigma^{\mu\nu} \gamma_5 \right]$$

$$(FR.34) \quad \begin{array}{c} u \\ \swarrow \quad \searrow \\ W_\mu^- \\ \swarrow \quad \searrow \\ d \end{array} \quad -\frac{ig}{\sqrt{2}} \left[\gamma^\mu P_L \left[1 + \Delta g_W + 2(n_1^Q - n_7^Q) \right] + 2(n_2^Q - n_8^Q) \gamma^\mu P_R + 16\pi n_{35}^Q \frac{p_{W\nu}}{\Lambda} \sigma^{\mu\nu} + 8\pi (n_{33}^Q - n_{36}^Q) \frac{p_{W\nu}}{\Lambda} \sigma^{\mu\nu} \gamma_5 \right]$$

$$(FR.35) \quad \begin{array}{c} d \\ \swarrow \quad \searrow \\ A^\mu \\ \swarrow \quad \searrow \\ d \end{array} \quad \frac{ie}{3} \left[\gamma^\mu - 12\pi(2n_{29}^Q - 2n_{30}^Q - n_{33}^Q + 2n_{34}^Q - n_{36}^Q) \frac{p_{A\nu}}{\Lambda} \sigma^{\mu\nu} \gamma_5 \right]$$

$$(FR.36) \quad \begin{array}{c} u \\ \swarrow \quad \searrow \\ A^\mu \\ \swarrow \quad \searrow \\ u \end{array} \quad -\frac{2ie}{3} \left[\gamma^\mu + 6\pi(2n_{29}^Q + 2n_{30}^Q + n_{33}^Q + 2n_{34}^Q + n_{36}^Q) \frac{p_{A\nu}}{\Lambda} \sigma^{\mu\nu} \gamma_5 \right]$$

$$(FR.37) \quad \begin{array}{c} d^C \\ \swarrow \quad \searrow \\ G_\mu^A \\ \swarrow \quad \searrow \\ d^B \end{array} \quad -ig_s(\lambda^A)_{BC} \gamma^\mu + 16\pi g_s(n_{31}^Q - n_{32}^Q)(\lambda^A)_{BC} \frac{p_{G\nu}}{\Lambda} \sigma^{\mu\nu} \gamma_5$$

$$(FR.38) \quad \begin{array}{c} u^C \\ \swarrow \quad \searrow \\ G_\mu^A \\ \swarrow \quad \searrow \\ u^B \end{array} \quad -ig_s(\lambda^A)_{BC} \gamma^\mu + 16\pi g_s(n_{31}^Q + n_{32}^Q)(\lambda^A)_{BC} \frac{p_{G\nu}}{\Lambda} \sigma^{\mu\nu} \gamma_5$$

$$(FR.39) \quad \begin{array}{c} d \\ \swarrow \quad \searrow \\ h \\ \swarrow \quad \searrow \\ h \end{array} \quad -\frac{\sqrt{2}i}{v} Y_D^{(2)} - \frac{8i}{v^2 \Lambda} p_{h1} \cdot p_{h2} ((naa')_9^Q - (naa')_{10}^Q)$$

$$(FR.40) \quad \begin{array}{c} u \\ \swarrow \quad \searrow \\ h \\ \swarrow \quad \searrow \\ h \end{array} \quad -\frac{\sqrt{2}i}{v} Y_D^{(2)} - \frac{8i}{v^2 \Lambda} p_{h1} \cdot p_{h2} ((naa')_9^Q + (naa')_{10}^Q)$$

$$(FR.41) \quad \begin{array}{c} d \\ \swarrow \quad \searrow \\ h \\ \swarrow \quad \searrow \\ Z \end{array} \quad \frac{2ig}{v c_\theta} \left[((na)_1^Q - 2(na)_5^Q + (na)_7^Q) \gamma^\mu P_L + ((na)_2^Q - 2(na)_6^Q + (na)_8^Q) \gamma^\mu P_R \right] - \frac{ig}{v c_\theta} ((na)_{11}^Q - 2(na)_{12}^Q + (na)_{14}^Q) \frac{p_h^\mu}{\Lambda} \gamma_5 + \frac{8\pi i g c_\theta}{v} \left[((na)_{33}^Q - 2(na)_{34}^Q + (na)_{36}^Q) + 2((na)_{29}^Q - (na)_{30}^Q) t_\theta^2 \right] \frac{p_{Z\nu}}{\Lambda} \sigma^{\mu\nu} \gamma_5 - \frac{i g c_\theta}{v} ((na)_{21}^Q - 2(na)_{23}^Q + (na)_{24}^Q) \frac{p_{h\nu}}{\Lambda} \sigma^{\mu\nu} \gamma_5$$

$$\begin{aligned}
& \text{Diagram (FR.42): } h \text{ (dashed line) and } u \text{ (solid line) meet at a vertex. A wavy line labeled } Z \text{ connects this vertex to another vertex where } u \text{ (solid line) and } u \text{ (solid line) meet.} \\
& -\frac{2ig}{vc_\theta} \left[((na)_1^Q + 2(na)_5^Q + (na)_7^Q) \gamma^\mu P_L + ((na)_2^Q + 2(na)_6^Q + (na)_8^Q) \gamma^\mu P_R \right] + \frac{ig}{vc_\theta} ((na)_{11}^Q + 2(na)_{12}^Q + (na)_{14}^Q) \frac{p_h^\mu}{\Lambda} \gamma_5 + \\
& -\frac{8\pi ig c_\theta}{v} \left[((na)_{33}^Q + 2(na)_{34}^Q + (na)_{36}^Q) - 2((na)_{29}^Q + (na)_{30}^Q) t_\theta^2 \right] \frac{p_{Z\nu}}{\Lambda} \sigma^{\mu\nu} \gamma_5 + \frac{ig c_\theta}{v} ((na)_{21}^Q + 2(na)_{23}^Q + (na)_{24}^Q) \frac{p_{h\nu}}{\Lambda} \sigma^{\mu\nu} \gamma_5
\end{aligned}
\tag{FR.42}$$

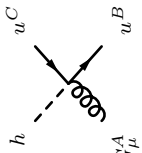
$$\begin{aligned}
& \text{Diagram (FR.43): } h \text{ (dashed line) and } d \text{ (solid line) meet at a vertex. A wavy line labeled } W_\mu^+ \text{ connects this vertex to another vertex where } u \text{ (solid line) and } u \text{ (solid line) meet.} \\
& -\frac{2\sqrt{2}ig}{v} \left[((na)_1^Q + 2i(na)_3^Q - (na)_7^Q) \gamma^\mu P_L + ((na)_2^Q + 2i(na)_4^Q - (na)_8^Q) \gamma^\mu P_R \right] + \frac{\sqrt{2}ig}{v} ((na)_{11}^Q - (na)_{14}^Q) \frac{p_h^\mu}{\Lambda} \gamma_5 - \frac{2\sqrt{2}ig}{v} (na)_{13}^Q \frac{p_h^\mu}{\Lambda} + \\
& -\frac{\sqrt{2}ig}{v} \left[8\pi((na)_{33}^Q - (na)_{36}^Q) \frac{p_{W\nu}}{\Lambda} - ((na)_{21}^Q - (na)_{24}^Q) \frac{p_{h\nu}}{\Lambda} \right] \sigma^{\mu\nu} \gamma_5 + \frac{2\sqrt{2}ig}{v} \left[8\pi(na)_{35}^Q \frac{p_{W\nu}}{\Lambda} - (na)_{22}^Q \frac{p_{h\nu}}{\Lambda} \right] \sigma^{\mu\nu}
\end{aligned}
\tag{FR.43}$$

$$\begin{aligned}
& \text{Diagram (FR.44): } h \text{ (dashed line) and } d \text{ (solid line) meet at a vertex. A wavy line labeled } W_\mu^- \text{ connects this vertex to another vertex where } u \text{ (solid line) and } d \text{ (solid line) meet.} \\
& -\frac{2\sqrt{2}ig}{v} \left[((na)_1^Q - 2i(na)_3^Q - (na)_7^Q) \gamma^\mu P_L + ((na)_2^Q - 2i(na)_4^Q - (na)_8^Q) \gamma^\mu P_R \right] + \frac{\sqrt{2}ig}{v} ((na)_{11}^Q - (na)_{14}^Q) \frac{p_h^\mu}{\Lambda} \gamma_5 + \frac{2\sqrt{2}ig}{v} (na)_{13}^Q \frac{p_h^\mu}{\Lambda} + \\
& -\frac{\sqrt{2}ig}{v} \left[8\pi((na)_{33}^Q - (na)_{36}^Q) \frac{p_{W\nu}}{\Lambda} - ((na)_{21}^Q - (na)_{24}^Q) \frac{p_{h\nu}}{\Lambda} \right] \sigma^{\mu\nu} \gamma_5 - \frac{2\sqrt{2}ig}{v} \left[8\pi(na)_{35}^Q \frac{p_{W\nu}}{\Lambda} - (na)_{22}^Q \frac{p_{h\nu}}{\Lambda} \right] \sigma^{\mu\nu}
\end{aligned}
\tag{FR.44}$$

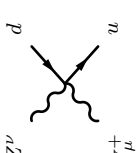
$$\begin{aligned}
& \text{Diagram (FR.45): } h \text{ (dashed line) and } d \text{ (solid line) meet at a vertex. A wavy line labeled } A^\mu \text{ connects this vertex to another vertex where } d \text{ (solid line) and } d \text{ (solid line) meet.} \\
& -\frac{8\pi ie}{v} (2(na)_{29}^Q - 2(na)_{30}^Q - (na)_{33}^Q + 2(na)_{34}^Q - (na)_{36}^Q) \frac{p_{A\nu}}{\Lambda} \sigma^{\mu\nu} \gamma_5
\end{aligned}
\tag{FR.45}$$

$$\begin{aligned}
& \text{Diagram (FR.46): } h \text{ (dashed line) and } u \text{ (solid line) meet at a vertex. A wavy line labeled } A^\mu \text{ connects this vertex to another vertex where } u \text{ (solid line) and } u \text{ (solid line) meet.} \\
& -\frac{8\pi ie}{v} (2(na)_{29}^Q + 2(na)_{30}^Q + (na)_{33}^Q + 2(na)_{34}^Q + (na)_{36}^Q) \frac{p_{A\nu}}{\Lambda} \sigma^{\mu\nu} \gamma_5
\end{aligned}
\tag{FR.46}$$

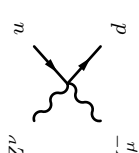
$$\begin{aligned}
& \text{Diagram (FR.47): } h \text{ (dashed line) and } d^C \text{ (solid line) meet at a vertex. A wavy line labeled } G_\mu^A \text{ connects this vertex to another vertex where } d^B \text{ (solid line) and } d^B \text{ (solid line) meet.} \\
& \frac{16\pi g_S}{v} ((na)_{31}^Q - (na)_{32}^Q) (\lambda^A)_{BC} \frac{p_{G\nu}}{\Lambda} \sigma^{\mu\nu} \gamma_5
\end{aligned}
\tag{FR.47}$$

(FR.48) 

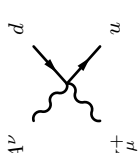
$$\frac{16\pi g_S}{v} ((na)_{31}^Q + (na)_{32}^Q)(\lambda^A)_{BC} \frac{p_{G\nu}}{\Lambda} \sigma^{\mu\nu} \gamma_5$$

(FR.49) 

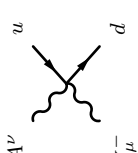
$$\frac{ig^2}{\sqrt{2}c_\theta\Lambda} \left[n_{18}^Q - n_{19}^Q + (n_{20}^Q - n_{17}^Q) \gamma_5 \right] g_{\mu\nu} + \frac{4\sqrt{2}\pi ig^2 c_\theta}{\Lambda} n_{35}^Q \sigma^{\mu\nu} - \frac{\sqrt{2}ig^2}{c_\theta^2\Lambda} \left[n_{28}^Q \sigma^{\mu\nu} - n_{27}^Q \sigma^{\mu\nu} \gamma_5 \right]$$

(FR.50) 

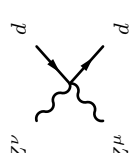
$$\frac{ig^2}{\sqrt{2}c_\theta\Lambda} \left[n_{18}^Q - n_{19}^Q - (n_{20}^Q - n_{17}^Q) \gamma_5 \right] g_{\mu\nu} - \frac{4\sqrt{2}\pi ig^2 c_\theta}{\Lambda} \left[(n_{33}^Q - n_{36}^Q) \sigma^{\mu\nu} \gamma_5 \right] - \frac{8\sqrt{2}\pi ig^2 c_\theta}{\Lambda} n_{35}^Q \sigma^{\mu\nu} - \frac{\sqrt{2}ig^2}{c_\theta^2\Lambda} \left[n_{28}^Q \sigma^{\mu\nu} + n_{27}^Q \sigma^{\mu\nu} \gamma_5 \right]$$

(FR.51) 

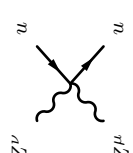
$$\frac{4\sqrt{2}\pi ig e}{\Lambda} (n_{33}^Q - n_{36}^Q) \sigma^{\mu\nu} \gamma_5 - \frac{8\sqrt{2}\pi ig e}{\Lambda} n_{35}^Q \sigma^{\mu\nu}$$

(FR.52) 

$$-\frac{4\sqrt{2}\pi ig e}{\Lambda} (n_{33}^Q - n_{36}^Q) \sigma^{\mu\nu} \gamma_5 - \frac{8\sqrt{2}\pi ig e}{\Lambda} n_{35}^Q \sigma^{\mu\nu}$$

(FR.53) 

$$-\frac{ig^2}{2c_\theta^2\Lambda} (n_{15}^Q - n_{16}^Q + n_{17}^Q - n_{18}^Q - n_{19}^Q + n_{20}^Q) g_{\mu\nu}$$

(FR.54) 

$$-\frac{ig^2}{2c_\theta^2\Lambda} (n_{15}^Q + n_{16}^Q + n_{17}^Q + n_{18}^Q + n_{19}^Q + n_{20}^Q) g_{\mu\nu}$$

$$\begin{array}{c}
\begin{array}{c} W^{-\nu} \\ \diagup \\ d \\ \diagdown \\ W^{+\mu} \\ \diagup \\ d \end{array} \\
\text{(FR.55)}
\end{array}
\quad
-\frac{ig^2}{2\Lambda}(n_{15}^Q - n_{16}^Q - n_{17}^Q - n_{18}^Q + n_{19}^Q - n_{20}^Q)g_{\mu\nu} + \frac{ig^2}{2\Lambda}\left[8\pi(n_{33}^Q - 2n_{34}^Q + n_{36}^Q) + n_{25}^Q - n_{26}^Q + 2(n_{27}^Q - n_{28}^Q)\right]\sigma^{\mu\nu}\gamma_5$$

$$\begin{array}{c}
\begin{array}{c} W^{-\nu} \\ \diagup \\ u \\ \diagdown \\ W^{+\mu} \\ \diagup \\ u \end{array} \\
\text{(FR.56)}
\end{array}
\quad
-\frac{ig^2}{2\Lambda}(n_{15}^Q + n_{16}^Q - n_{17}^Q - n_{18}^Q - n_{19}^Q - n_{20}^Q)g_{\mu\nu} - \frac{ig^2}{2\Lambda}\left[8\pi(n_{33}^Q + 2n_{34}^Q + n_{36}^Q) - n_{25}^Q - n_{26}^Q + 2(n_{27}^Q + n_{28}^Q)\right]\sigma^{\mu\nu}\gamma_5$$

$$\begin{array}{c}
\begin{array}{c} G_\mu^A \\ \diagup \\ d^D \\ \diagdown \\ G_\nu^B \\ \diagup \\ d^C \end{array} \\
\text{(FR.57)}
\end{array}
\quad
\frac{8\pi ig_s^2}{\Lambda}(n_{31}^Q - n_{32}^Q)f_{ABX}(\lambda^X)_{CD}\sigma^{\mu\nu}\gamma_5$$

$$\begin{array}{c}
\begin{array}{c} G_\mu^A \\ \diagup \\ u^D \\ \diagdown \\ G_\nu^B \\ \diagup \\ u^C \end{array} \\
\text{(FR.58)}
\end{array}
\quad
\frac{8\pi ig_s^2}{\Lambda}(n_{31}^Q + n_{32}^Q)f_{ABX}(\lambda^X)_{CD}\sigma^{\mu\nu}\gamma_5$$

Single lepton current

$$(FR.59) \quad \begin{array}{c} l^+ \\ \diagdown \\ \text{---} h \text{---} \\ \diagup \\ l^- \end{array} \quad -\frac{i}{\sqrt{2}} Y_E^{(1)}$$

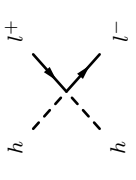
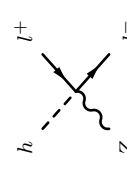
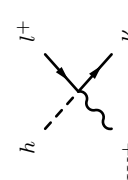
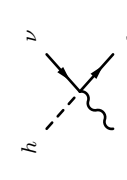
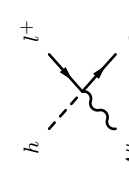
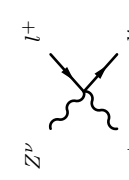
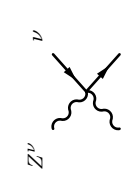
$$(FR.60) \quad \begin{array}{c} l^+ \\ \diagdown \\ \text{---} Z^\mu \text{---} \\ \diagup \\ l^- \end{array} \quad -\frac{ig}{c_\theta} \left[\left(-\frac{1}{2} + s_\theta^2 \right) \left(1 + \Delta g_1 + \frac{2}{1 - 2s_\theta^2} \Delta g_2 \right) \gamma_\mu P_L + s_\theta^2 \left(1 + \Delta g_1 - \frac{1}{s_\theta^2} \Delta g_2 + \frac{2}{s_\theta^2} n_\theta^\ell \right) \gamma_\mu P_R \right. \\ \left. - 4\pi c_\theta^2 \left[n_{13}^\ell + 2n_{12}^\ell t_\theta^2 \right] \frac{p_{Z\nu}}{\Lambda} \sigma^{\mu\nu} \gamma_5 \right]$$

$$(FR.61) \quad \begin{array}{c} \nu \\ \diagdown \\ \text{---} Z^\nu \text{---} \\ \diagup \\ \nu \end{array} \quad -\frac{ig}{2} \gamma_\mu P_L (1 + \Delta g_1)$$

$$(FR.62) \quad \begin{array}{c} l^+ \\ \diagdown \\ \text{---} W_\mu^+ \text{---} \\ \diagup \\ \nu \end{array} \quad -\frac{ig}{\sqrt{2}} \left[\gamma_\mu P_L \left[1 + \Delta g_W - 4in_1^\ell \right] + 8\pi(n_{13}^\ell - 2n_{14}^\ell) \frac{p_{W\nu}}{\Lambda} \sigma^{\mu\nu} P_R \right]$$

$$(FR.63) \quad \begin{array}{c} \nu \\ \diagdown \\ \text{---} W_\mu^- \text{---} \\ \diagup \\ l^- \end{array} \quad -\frac{ig}{\sqrt{2}} \left[\gamma_\mu P_L \left[1 + \Delta g_W + 4in_1^\ell \right] - 8\pi(n_{13}^\ell - 2n_{14}^\ell) \frac{p_{W\nu}}{\Lambda} \sigma^{\mu\nu} P_L \right]$$

$$(FR.64) \quad \begin{array}{c} l^+ \\ \diagdown \\ \text{---} A^\mu \text{---} \\ \diagup \\ l^- \end{array} \quad -ie \left[-\gamma^\mu + (2n_{12}^\ell - n_{13}^\ell) \frac{4\pi p_{A\nu}}{\Lambda} \sigma^{\mu\nu} \gamma_5 \right]$$

	$-\frac{\sqrt{2}i}{v}Y_E^{(2)} - \frac{8i}{v^2\Lambda}p_{h1} \cdot p_{h2}(naa')_3^\ell$	$(FR.65)$
	$-\frac{4ig}{vc_\theta}(na)_2^\ell\gamma^\mu P_R + \frac{2ig}{vc_\theta\Lambda}(na)_4^\ell p_h^\mu\gamma_5 + \frac{8\pi igc_\theta}{v\Lambda}[(na)_{13}^\ell + 2(na)_{12}^\ell t_\theta^2]p_{Z\nu}\sigma^{\mu\nu}\gamma_5 + \frac{2igc_\theta}{v\Lambda}(na)_9^\ell p_{h\nu}\sigma^{\mu\nu}\gamma_5$	$(FR.66)$
	$-\frac{2\sqrt{2}ig}{v\Lambda}(na)_5^\ell p_h^\mu P_R - \frac{2\sqrt{2}ig}{v\Lambda}[4\pi((na)_{13}^\ell - 2(na)_{14}^\ell)p_{W\nu} + (na)_8^\ell p_{h\nu}]\sigma^{\mu\nu}P_R$	$(FR.67)$
	$+\frac{2\sqrt{2}ig}{v\Lambda}(na)_5^\ell p_h^\mu P_L + \frac{2\sqrt{2}ig}{v\Lambda}[4\pi((na)_{13}^\ell - 2(na)_{14}^\ell)p_{W\nu} + (na)_8^\ell p_{h\nu}]\sigma^{\mu\nu}P_L$	$(FR.68)$
	$-\frac{8\pi ie}{v\Lambda}(2(na)_{12}^\ell - (na)_{13}^\ell)p_{A\nu}\sigma^{\mu\nu}\gamma_5$	$(FR.69)$
	$-\frac{ig^2}{\sqrt{2}c_\theta\Lambda}[n_t^\ell g_{\mu\nu} - 2(4\pi c_\theta^2(n_{13}^\ell - 2n_{14}^\ell) + n_{11}^\ell)\sigma^{\mu\nu}]P_R$	$(FR.70)$
	$-\frac{ig^2}{\sqrt{2}c_\theta\Lambda}[n_t^\ell g_{\mu\nu} - 2(4\pi c_\theta^2(n_{13}^\ell - 2n_{14}^\ell) + n_{11}^\ell)\sigma^{\mu\nu}]P_L$	$(FR.71)$

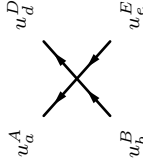
$$(FR.72) \quad \begin{array}{c} A^\nu \\ \diagup \quad \diagdown \\ l^+ \quad \nu \\ \diagdown \quad \diagup \\ W_\mu^+ \end{array} \quad \frac{4\pi i g e \sqrt{2}}{\Lambda} (n_{13}^\ell - 2n_{14}^\ell) \sigma^{\mu\nu} P_R$$

$$(FR.73) \quad \begin{array}{c} A^\nu \\ \diagup \quad \diagdown \\ \nu \quad l^- \\ \diagdown \quad \diagup \\ W_\mu^- \end{array} \quad \frac{4\pi i g e \sqrt{2}}{\Lambda} (n_{13}^\ell - 2n_{14}^\ell) \sigma^{\mu\nu} P_L$$

$$(FR.74) \quad \begin{array}{c} W^{-\nu} \\ \diagup \quad \diagdown \\ l^+ \quad l^- \\ \diagdown \quad \diagup \\ W^{+\mu} \end{array} \quad -\frac{ig^2}{2\Lambda} [(n_6^\ell - n_7^\ell) g_{\mu\nu} - (8\pi n_{13}^\ell + n_{10}^\ell + 2n_{11}^\ell) \sigma^{\mu\nu} \gamma_5]$$

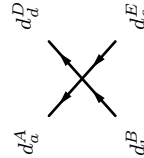
$$(FR.75) \quad \begin{array}{c} Z^\nu \\ \diagup \quad \diagdown \\ l^+ \quad l^- \\ \diagdown \quad \diagup \\ Z^\mu \end{array} \quad -\frac{ig^2}{2c_\theta^2 \Lambda} (n_6^\ell + n_7^\ell) g_{\mu\nu}$$

Four quarks



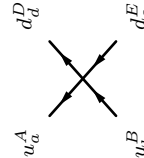
$$\frac{16\pi^2}{\Lambda^2} \left[2i(r_1^Q + r_2^Q + r_3^Q + r_4^Q)([P_L]_{ab}[P_L]_{de} + [P_R]_{ab}[P_R]_{de} + [P_L]_{ae}[P_L]_{db} + [P_R]_{ae}[P_R]_{db}) + \right. \\ + 4i(r_{13}^Q + r_{14}^Q + r_{15}^Q + r_{16}^Q)([\gamma^\mu P_R]_{ab}[\gamma_\mu P_R]_{de} + [\gamma^\mu P_R]_{ae}[\gamma_\mu P_R]_{db}) + 4i(r_9^Q + r_{10}^Q + r_{11}^Q + r_{12}^Q)([\gamma^\mu P_L]_{ab}[\gamma_\mu P_L]_{de} + [\gamma^\mu P_L]_{ae}[\gamma_\mu P_L]_{db}) + \\ + 2i(r_{13}^Q + r_{17}^Q + r_{18}^Q + r_{19}^Q + r_{20}^Q + r_{21}^Q)([\gamma^\mu P_L]_{ab}[\gamma_\mu P_R]_{de} + [\gamma^\mu P_R]_{ab}[\gamma_\mu P_L]_{de} + [\gamma^\mu P_L]_{ae}[\gamma_\mu P_R]_{db} + [\gamma^\mu P_R]_{ae}[\gamma_\mu P_L]_{db}) + \\ + 8i(r_5^Q + r_6^Q + r_7^Q + r_8^Q) \left[\lambda_{AB}^a \lambda_{DE}^a ([P_L]_{ab}[P_L]_{de} + [P_R]_{ab}[P_R]_{de}) + \lambda_{AE}^a \lambda_{DB}^a ([P_L]_{ae}[P_L]_{db} + [P_R]_{ae}[P_R]_{db}) \right] + \\ \left. + 8i(r_{22}^Q + r_{23}^Q + r_{24}^Q + r_{25}^Q + r_{26}^Q) \left[\lambda_{AB}^a \lambda_{DE}^a ([\gamma^\mu P_L]_{ab}[\gamma_\mu P_R]_{de} + [\gamma^\mu P_R]_{ab}[\gamma_\mu P_L]_{de}) + \lambda_{AE}^a \lambda_{DB}^a ([\gamma^\mu P_L]_{ae}[\gamma_\mu P_R]_{db} + [\gamma^\mu P_R]_{ae}[\gamma_\mu P_L]_{db}) \right] \right]$$

(FR.76)



$$\frac{16\pi^2}{\Lambda^2} \left[2i(r_1^Q + r_2^Q - r_3^Q - r_4^Q)([P_L]_{ab}[P_L]_{de} + [P_R]_{ab}[P_R]_{de} + [P_L]_{ae}[P_L]_{db} + [P_R]_{ae}[P_R]_{db}) + \right. \\ + 4i(r_{13}^Q - r_{14}^Q + r_{15}^Q + r_{16}^Q)([\gamma^\mu P_R]_{ab}[\gamma_\mu P_R]_{de} + [\gamma^\mu P_R]_{ae}[\gamma_\mu P_R]_{db}) + 4i(r_9^Q - r_{10}^Q + r_{11}^Q + r_{12}^Q)([\gamma^\mu P_L]_{ab}[\gamma_\mu P_L]_{de} + [\gamma^\mu P_L]_{ae}[\gamma_\mu P_L]_{db}) + \\ + 2i(r_{17}^Q - r_{18}^Q - r_{19}^Q + r_{20}^Q + r_{21}^Q)([\gamma^\mu P_L]_{ab}[\gamma_\mu P_R]_{de} + [\gamma^\mu P_R]_{ab}[\gamma_\mu P_L]_{de} + [\gamma^\mu P_L]_{ae}[\gamma_\mu P_R]_{db} + [\gamma^\mu P_R]_{ae}[\gamma_\mu P_L]_{db}) + \\ + 8i(r_5^Q + r_6^Q - r_7^Q + r_8^Q) \left[\lambda_{AB}^a \lambda_{DE}^a ([P_L]_{ab}[P_L]_{de} + [P_R]_{ab}[P_R]_{de}) + \lambda_{AE}^a \lambda_{DB}^a ([P_L]_{ae}[P_L]_{db} + [P_R]_{ae}[P_R]_{db}) \right] + \\ \left. + 8i(r_{22}^Q - r_{23}^Q - r_{24}^Q + r_{25}^Q + r_{26}^Q) \left[\lambda_{AB}^a \lambda_{DE}^a ([\gamma^\mu P_L]_{ab}[\gamma_\mu P_R]_{de} + [\gamma^\mu P_R]_{ab}[\gamma_\mu P_L]_{de}) + \lambda_{AE}^a \lambda_{DB}^a ([\gamma^\mu P_L]_{ae}[\gamma_\mu P_R]_{db} + [\gamma^\mu P_R]_{ae}[\gamma_\mu P_L]_{db}) \right] \right]$$

(FR.77)



$$\frac{16\pi^2}{\Lambda^2} \left[2i(r_1^Q - r_2^Q - r_4^Q)([P_L]_{ab}[P_L]_{de} + [P_R]_{ab}[P_R]_{de}) + 4i r_2^Q ([P_L]_{ae}[P_L]_{db} + [P_R]_{ae}[P_R]_{db}) + \right. \\ + 4i(r_{13}^Q - r_{15}^Q - r_{16}^Q)([\gamma^\mu P_R]_{ab}[\gamma_\mu P_R]_{de}) + 8i r_{16}^Q ([\gamma^\mu P_R]_{ae}[\gamma_\mu P_R]_{db}) + 4i(r_9^Q - r_{11}^Q - r_{12}^Q)([\gamma^\mu P_L]_{ab}[\gamma_\mu P_L]_{de}) + 8i r_{12}^Q ([\gamma^\mu P_L]_{ae}[\gamma_\mu P_L]_{db}) + \\ + 2i(r_{17}^Q - r_{18}^Q + r_{19}^Q - r_{20}^Q - r_{21}^Q)[\gamma^\mu P_L]_{ab}[\gamma_\mu P_R]_{de} + 2i(r_{17}^Q + r_{18}^Q - r_{19}^Q - r_{20}^Q)[\gamma^\mu P_R]_{ab}[\gamma_\mu P_L]_{de} + \\ + 4i r_{21}^Q ([\gamma^\mu P_L]_{ae}[\gamma_\mu P_R]_{db} + [\gamma^\mu P_R]_{ae}[\gamma_\mu P_L]_{db}) + \\ + 8i(r_5^Q - r_6^Q - r_8^Q) \lambda_{AB}^a \lambda_{DE}^a ([P_L]_{ab}[P_L]_{de} + [P_R]_{ab}[P_R]_{de}) + 16i r_6^Q \lambda_{AE}^a \lambda_{DB}^a ([P_L]_{ae}[P_L]_{db} + [P_R]_{ae}[P_R]_{db}) + \\ + 8i(r_{22}^Q - r_{23}^Q + r_{24}^Q - r_{25}^Q - r_{26}^Q) \lambda_{AB}^a \lambda_{DE}^a ([\gamma^\mu P_L]_{ab}[\gamma_\mu P_R]_{de} + 8i(r_{22}^Q + r_{23}^Q - r_{24}^Q - r_{25}^Q - r_{26}^Q) \lambda_{AB}^a \lambda_{DE}^a [\gamma^\mu P_R]_{ab}[\gamma_\mu P_L]_{de} + \\ + 16i r_{26}^Q \lambda_{AE}^a \lambda_{DB}^a ([\gamma^\mu P_L]_{ae}[\gamma_\mu P_R]_{db} + [\gamma^\mu P_R]_{ae}[\gamma_\mu P_L]_{db}) \left. \right]$$

(FR.78)

Four leptons

$$\begin{array}{c}
 \begin{array}{ccc}
 l_a^+ & & l_d^- \\
 & \swarrow \quad \searrow & \\
 & \text{X} & \\
 & \swarrow \quad \searrow & \\
 l_b^- & & l_e^+
 \end{array} \\
 \text{(FR.79)}
 \end{array}
 \frac{16\pi^2}{\Lambda^2} \left[2i r_1^\ell ([P_L]_{ab} [P_L]_{de} + [P_L]_{ae} [P_L]_{db}) + [P_R]_{ab} [P_R]_{de} + [P_R]_{ae} [P_R]_{db}) + \right.$$

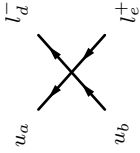
$$\begin{aligned}
 & + 4i r_3^\ell ([\gamma^\mu P_R]_{ab} [\gamma_\mu P_R]_{de} + [\gamma^\mu P_R]_{ae} [\gamma_\mu P_R]_{db}) + 4i (r_2^\ell - r_4^\ell + r_5^\ell) ([\gamma^\mu P_L]_{ab} [\gamma_\mu P_L]_{de} + [\gamma^\mu P_L]_{ae} [\gamma_\mu P_L]_{db}) + \\
 & \left. + 2i (r_6^\ell - r_7^\ell) ([\gamma^\mu P_L]_{ab} [\gamma_\mu P_R]_{de} + [\gamma^\mu P_R]_{ab} [\gamma_\mu P_L]_{de} + [\gamma^\mu P_L]_{ae} [\gamma_\mu P_R]_{db} + [\gamma^\mu P_R]_{ae} [\gamma_\mu P_L]_{db}) \frac{1}{\Lambda^2} \right]
 \end{aligned}$$

$$\begin{array}{c}
 \begin{array}{ccc}
 \nu_a & & \nu_d \\
 & \swarrow \quad \searrow & \\
 & \text{X} & \\
 & \swarrow \quad \searrow & \\
 \nu_b & & \nu_e
 \end{array} \\
 \text{(FR.80)}
 \end{array}
 \frac{16\pi^2}{\Lambda^2} \left[4i (r_2^\ell + r_4^\ell + r_5^\ell) ([\gamma^\mu P_L]_{ab} [\gamma_\mu P_L]_{de} + [\gamma^\mu P_L]_{ae} [\gamma_\mu P_L]_{db}) \right]$$

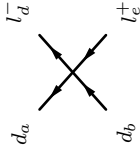
$$\begin{array}{c}
 \begin{array}{ccc}
 l_a^+ & & \nu_d \\
 & \swarrow \quad \searrow & \\
 & \text{X} & \\
 & \swarrow \quad \searrow & \\
 l_b^- & & \nu_e
 \end{array} \\
 \text{(FR.81)}
 \end{array}
 \frac{16\pi^2}{\Lambda^2} \left[2i [2(r_2^\ell - r_5^\ell) [\gamma^\mu P_L]_{ab} + (r_6^\ell + r_7^\ell) [\gamma^\mu P_R]_{ab}] [\gamma_\mu P_L]_{de} \right]$$

Two quark-two leptons

$$\begin{aligned}
 & \frac{16\pi^2}{\Lambda^2} \left[i(r_1^{\mathcal{Q}\ell} + r_3^{\mathcal{Q}\ell} - r_5^{\mathcal{Q}\ell}) ([P_L]_{ab} [P_L]_{de} + [P_R]_{ab} [P_R]_{de}) + \right. \\
 & + 2i(r_7^{\mathcal{Q}\ell} + r_9^{\mathcal{Q}\ell} - r_{11}^{\mathcal{Q}\ell} - r_{12}^{\mathcal{Q}\ell} - r_{13}^{\mathcal{Q}\ell}) [\gamma^\mu P_L]_{ab} [\gamma_\mu P_L]_{de} + 2i(r_8^{\mathcal{Q}\ell} + r_{10}^{\mathcal{Q}\ell}) [\gamma^\mu P_R]_{ab} [\gamma_\mu P_R]_{de} + \\
 & + 2i(r_{15}^{\mathcal{Q}\ell} + r_{17}^{\mathcal{Q}\ell}) [\gamma^\mu P_L]_{ab} [\gamma_\mu P_R]_{de} + 2i(r_{14}^{\mathcal{Q}\ell} - r_{16}^{\mathcal{Q}\ell} - r_{18}^{\mathcal{Q}\ell} - r_{19}^{\mathcal{Q}\ell} - r_{20}^{\mathcal{Q}\ell}) [\gamma^\mu P_R]_{ab} [\gamma_\mu P_L]_{de} + \\
 & \left. + 2ir_6^{\mathcal{Q}\ell} ([P_L]_{ae} [P_L]_{db} + [P_R]_{ae} [P_R]_{db}) + ir_{23}^{\mathcal{Q}\ell} ([\gamma^\mu P_L]_{ae} [\gamma_\mu P_R]_{db} + [\gamma^\mu P_R]_{ae} [\gamma_\mu P_L]_{db}) \right]
 \end{aligned}
 \tag{FR.82}$$



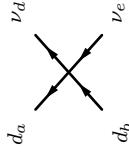
$$\begin{aligned}
 & \frac{16\pi^2}{\Lambda^2} \left[i(r_1^{\mathcal{Q}\ell} - r_3^{\mathcal{Q}\ell} + r_5^{\mathcal{Q}\ell}) ([P_L]_{ab} [P_L]_{de} + [P_R]_{ab} [P_R]_{de}) + \right. \\
 & + 2i(r_7^{\mathcal{Q}\ell} - r_9^{\mathcal{Q}\ell} - r_{11}^{\mathcal{Q}\ell} + r_{12}^{\mathcal{Q}\ell} + r_{13}^{\mathcal{Q}\ell}) [\gamma^\mu P_L]_{ab} [\gamma_\mu P_L]_{de} + 2i(r_8^{\mathcal{Q}\ell} - r_{10}^{\mathcal{Q}\ell}) [\gamma^\mu P_R]_{ab} [\gamma_\mu P_R]_{de} + \\
 & + 2i(r_{15}^{\mathcal{Q}\ell} - r_{17}^{\mathcal{Q}\ell}) [\gamma^\mu P_L]_{ab} [\gamma_\mu P_R]_{de} + 2i(r_{14}^{\mathcal{Q}\ell} - r_{16}^{\mathcal{Q}\ell} - r_{18}^{\mathcal{Q}\ell} + r_{19}^{\mathcal{Q}\ell} + r_{20}^{\mathcal{Q}\ell}) [\gamma^\mu P_R]_{ab} [\gamma_\mu P_L]_{de} + \\
 & + i(r_2^{\mathcal{Q}\ell} - r_4^{\mathcal{Q}\ell} + r_6^{\mathcal{Q}\ell}) ([P_L]_{ae} [P_L]_{db} + [P_R]_{ae} [P_R]_{db}) + \\
 & \left. + i(r_{21}^{\mathcal{Q}\ell} - r_{22}^{\mathcal{Q}\ell} + r_{23}^{\mathcal{Q}\ell}) ([\gamma^\mu P_L]_{ae} [\gamma_\mu P_R]_{db} + [\gamma^\mu P_R]_{ae} [\gamma_\mu P_L]_{db}) \right]
 \end{aligned}
 \tag{FR.83}$$



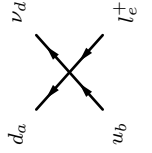
$$\frac{16\pi^2}{\Lambda^2} \left[\frac{2i}{\Lambda^2} \left[(r_7^{\mathcal{Q}\ell} + r_9^{\mathcal{Q}\ell} + r_{11}^{\mathcal{Q}\ell} + r_{12}^{\mathcal{Q}\ell} + r_{13}^{\mathcal{Q}\ell}) [\gamma^\mu P_L]_{ab} + (r_{14}^{\mathcal{Q}\ell} + r_{16}^{\mathcal{Q}\ell} + r_{18}^{\mathcal{Q}\ell} + r_{19}^{\mathcal{Q}\ell} + r_{20}^{\mathcal{Q}\ell}) [\gamma^\mu P_R]_{ab} \right] [\gamma_\mu P_L]_{de} \right]
 \tag{FR.84}$$



$$\frac{16\pi^2}{\Lambda^2} \left[\frac{2i}{\Lambda^2} \left[(r_7^{\mathcal{Q}\ell} - r_9^{\mathcal{Q}\ell} + r_{11}^{\mathcal{Q}\ell} - r_{12}^{\mathcal{Q}\ell} - r_{13}^{\mathcal{Q}\ell}) [\gamma^\mu P_L]_{ab} + (r_{14}^{\mathcal{Q}\ell} + r_{16}^{\mathcal{Q}\ell} - r_{18}^{\mathcal{Q}\ell} - r_{19}^{\mathcal{Q}\ell} - r_{20}^{\mathcal{Q}\ell}) [\gamma^\mu P_R]_{ab} \right] [\gamma_\mu P_L]_{de} \right]
 \tag{FR.85}$$



$$\begin{aligned}
 & \frac{16\pi^2}{\Lambda^2} \left[2ir_5^{\mathcal{Q}\ell} ([P_L]_{ab} [P_L]_{de} + [P_R]_{ab} [P_R]_{de}) + 4ir_{13}^{\mathcal{Q}\ell} [\gamma^\mu P_L]_{ab} [\gamma_\mu P_L]_{de} + 4ir_{20}^{\mathcal{Q}\ell} [\gamma^\mu P_R]_{ab} [\gamma_\mu P_L]_{de} + \right. \\
 & \left. + i(r_2^{\mathcal{Q}\ell} + r_4^{\mathcal{Q}\ell} - r_6^{\mathcal{Q}\ell}) [P_R]_{ae} [P_R]_{db} + i(r_{21}^{\mathcal{Q}\ell} + r_{22}^{\mathcal{Q}\ell} - r_{23}^{\mathcal{Q}\ell}) [\gamma^\mu P_R]_{ae} [\gamma_\mu P_L]_{db} \right]
 \end{aligned}
 \tag{FR.86}$$



References

- [1] **ATLAS** Collaboration, G. Aad *et. al.*, *Observation of a New Particle in the Search for the Standard Model Higgs Boson with the ATLAS Detector at the LHC*, Phys. Lett. **B716** (2012) 1–29, [[arXiv:1207.7214](#)].
- [2] **CMS** Collaboration, S. Chatrchyan *et. al.*, *Observation of a New Boson at a Mass of 125 GeV with the CMS Experiment at the LHC*, Phys. Lett. **B716** (2012) 30–61, [[arXiv:1207.7235](#)].
- [3] F. Englert and R. Brout, *Broken Symmetry and the Mass of Gauge Vector Mesons*, Phys. Rev. Lett. **13** (1964) 321–323.
- [4] P. W. Higgs, *Broken Symmetries, Massless Particles and Gauge Fields*, Phys. Lett. **12** (1964) 132–133.
- [5] P. W. Higgs, *Broken Symmetries and the Masses of Gauge Bosons*, Phys. Rev. Lett. **13** (1964) 508–509.
- [6] W. Buchmuller and D. Wyler, *Effective Lagrangian Analysis of New Interactions and Flavor Conservation*, Nucl. Phys. **B268** (1986) 621–653.
- [7] B. Grzadkowski, M. Iskrzynski, M. Misiak, and J. Rosiek, *Dimension-Six Terms in the Standard Model Lagrangian*, JHEP **10** (2010) 085, [[arXiv:1008.4884](#)].
- [8] D. B. Kaplan and H. Georgi, *$SU(2) \times U(1)$ Breaking by Vacuum Misalignment*, Phys. Lett. **B136** (1984) 183.
- [9] D. B. Kaplan, H. Georgi, and S. Dimopoulos, *Composite Higgs Scalars*, Phys. Lett. **B136** (1984) 187.
- [10] T. Banks, *Constraints on $SU(2) \times U(1)$ Breaking by Vacuum Misalignment*, Nucl. Phys. **B243** (1984) 125.
- [11] K. Agashe, R. Contino, and A. Pomarol, *The Minimal Composite Higgs Model*, Nucl. Phys. **B719** (2005) 165–187, [[hep-ph/0412089](#)].
- [12] B. Gripaios, A. Pomarol, F. Riva, and J. Serra, *Beyond the Minimal Composite Higgs Model*, JHEP **04** (2009) 070, [[arXiv:0902.1483](#)].
- [13] E. Halyo, *Technidilaton Or Higgs?*, Mod. Phys. Lett. **A8** (1993) 275–284.
- [14] W. D. Goldberger, B. Grinstein, and W. Skiba, *Distinguishing the Higgs Boson from the Dilaton at the Large Hadron Collider*, Phys. Rev. Lett. **100** (2008) 111802, [[arXiv:0708.1463](#)].
- [15] T. Appelquist and C. W. Bernard, *Strongly Interacting Higgs Bosons*, Phys. Rev. **D22** (1980) 200.

- [16] A. C. Longhitano, *Heavy Higgs Bosons in the Weinberg-Salam Model*, Phys. Rev. **D22** (1980) 1166.
- [17] A. C. Longhitano, *Low-Energy Impact of a Heavy Higgs Boson Sector*, Nucl. Phys. **B188** (1981) 118.
- [18] F. Feruglio, *The Chiral Approach to the Electroweak Interactions*, Int. J. Mod. Phys. **A8** (1993) 4937–4972, [[hep-ph/9301281](#)].
- [19] S. Weinberg, *Phenomenological Lagrangians*, Physica **A96** (1979) 327.
- [20] B. Grinstein and M. Trott, *A Higgs-Higgs Bound State Due to New Physics at a TeV*, Phys. Rev. **D76** (2007) 073002, [[arXiv:0704.1505](#)].
- [21] R. Contino, C. Grojean, M. Moretti, F. Piccinini, and R. Rattazzi, *Strong Double Higgs Production at the Lhc*, JHEP **05** (2010) 089, [[arXiv:1002.1011](#)].
- [22] R. Alonso, M. B. Gavela, L. Merlo, S. Rigolin, and J. Yepes, *The Effective Chiral Lagrangian for a Light Dynamical "Higgs Particle"*, Phys. Lett. **B722** (2013) 330–335, [[arXiv:1212.3305](#)]. [Erratum: Phys. Lett.B726,926(2013)].
- [23] R. Alonso, M. B. Gavela, L. Merlo, S. Rigolin, and J. Yepes, *Flavor with a Light Dynamical "Higgs Particle"*, Phys. Rev. **D87** (2013), no. 5 055019, [[arXiv:1212.3307](#)].
- [24] I. Brivio, T. Corbett, O. Éboli, M. Gavela, J. González-Fraile, *et. al.*, *Disentangling a Dynamical Higgs*, JHEP **1403** (2014) 024, [[arXiv:1311.1823](#)].
- [25] M. B. Gavela, J. González-Fraile, M. C. González-García, L. Merlo, S. Rigolin, and J. Yepes, *CP violation with a dynamical Higgs*, JHEP **10** (2014) 44, [[arXiv:1406.6367](#)].
- [26] G. Buchalla, O. Catà, and C. Krause, *Complete Electroweak Chiral Lagrangian with a Light Higgs at NLO*, [arXiv:1307.5017](#).
- [27] J. Yepes, *Spin-1 Resonances in a Non-Linear Left-Right Dynamical Higgs Context*, [arXiv:1507.03974](#).
- [28] J. Yepes, R. Kunming, and J. Shu, *CP Violation from Spin-1 Resonances in a Left-Right Dynamical Higgs Context*, [arXiv:1507.04745](#).
- [29] R. Alonso, I. Brivio, B. Gavela, L. Merlo, and S. Rigolin, *Sigma Decomposition*, JHEP **12** (2014) 034, [[arXiv:1409.1589](#)].
- [30] I. M. Hierro, L. Merlo, and S. Rigolin, *Sigma Decomposition: the CP-Odd Lagrangian*, [arXiv:1510.07899](#).
- [31] I. Brivio, O. J. P. Éboli, M. B. Gavela, M. C. González-García, L. Merlo, and S. Rigolin, *Higgs ultraviolet softening*, JHEP **12** (2014) 004, [[arXiv:1405.5412](#)].

- [32] R. Alonso, M. B. Gavela, L. Merlo, S. Rigolin, and J. Yepes, *Minimal Flavour Violation with Strong Higgs Dynamics*, JHEP **06** (2012) 076, [[arXiv:1201.1511](#)].
- [33] B. M. Gavela, E. E. Jenkins, A. V. Manohar, and L. Merlo, *Analysis of General Power Counting Rules in Effective Field Theory*, [arXiv:1601.07551](#).
- [34] A. Manohar and H. Georgi, *Chiral Quarks and the Nonrelativistic Quark Model*, Nucl. Phys. **B234** (1984) 189.
- [35] A. G. Cohen, D. B. Kaplan, and A. E. Nelson, *Counting 4 Pis in Strongly Coupled Supersymmetry*, Phys. Lett. **B412** (1997) 301–308, [[hep-ph/9706275](#)].
- [36] H. Georgi, D. B. Kaplan, and L. Randall, *Manifesting the Invisible Axion at Low-Energies*, Phys. Lett. **B169** (1986) 73.
- [37] L. Merlo, S. Saa, and M. Sacristan, *B and L non-Conserving Effective Lagrangian for a Dynamical Higgs*, to appear.
- [38] K. Hagiwara, S. Ishihara, R. Szalapski, and D. Zeppenfeld, *Low-Energy Effects of New Interactions in the Electroweak Boson Sector*, Phys. Rev. **D48** (1993) 2182–2203.
- [39] K. Hagiwara, T. Hatsukano, S. Ishihara, and R. Szalapski, *Probing Nonstandard Bosonic Interactions via W Boson Pair Production at Lepton Colliders*, Nucl. Phys. **B496** (1997) 66–102, [[hep-ph/9612268](#)].
- [40] T. Corbett, O. J. P. Éboli, J. González-Fraile, and M. C. González-Garcia, *Constraining anomalous Higgs interactions*, Phys. Rev. **D86** (2012) 075013, [[arXiv:1207.1344](#)].
- [41] T. Corbett, O. J. P. Éboli, J. González-Fraile, and M. C. González-Garcia, *Robust Determination of the Higgs Couplings: Power to the Data*, Phys. Rev. **D87** (2013) 015022, [[arXiv:1211.4580](#)].
- [42] T. Corbett, O. J. P. Éboli, J. González-Fraile, and M. C. González-Garcia, *Determining Triple Gauge Boson Couplings from Higgs Data*, Phys. Rev. Lett. **111** (2013) 011801, [[arXiv:1304.1151](#)].
- [43] **Particle Data Group** Collaboration, K. A. Olive *et. al.*, *Review of Particle Physics*, Chin. Phys. **C38** (2014) 090001.
- [44] **ATLAS, CMS** Collaboration, G. Aad *et. al.*, *Combined Measurement of the Higgs Boson Mass in pp Collisions at $\sqrt{s} = 7$ and 8 TeV with the ATLAS and CMS Experiments*, Phys. Rev. Lett. **114** (2015) 191803, [[arXiv:1503.07589](#)].
- [45] M. E. Peskin and T. Takeuchi, *A New constraint on a strongly interacting Higgs sector*, Phys. Rev. Lett. **65** (1990) 964–967.

- [46] M. E. Peskin and T. Takeuchi, *Estimation of oblique electroweak corrections*, Phys. Rev. **D46** (1992) 381–409.
- [47] A. Pomarol and F. Riva, *Towards the Ultimate SM Fit to Close in on Higgs Physics*, JHEP **01** (2014) 151, [[arXiv:1308.2803](#)].
- [48] M. Ciuchini, E. Franco, S. Mishima, M. Pierini, L. Reina, and L. Silvestrini, *Update of the electroweak precision fit, interplay with Higgs-boson signal strengths and model-independent constraints on new physics*, in *International Conference on High Energy Physics 2014 (ICHEP 2014) Valencia, Spain, July 2-9, 2014*, 2014. [arXiv:1410.6940](#).
- [49] **SLD Electroweak Group, DELPHI, ALEPH, SLD, SLD Heavy Flavour Group, OPAL, LEP Electroweak Working Group, L3 Collaboration**, S. Schael *et. al.*, *Precision electroweak measurements on the Z resonance*, Phys. Rept. **427** (2006) 257–454, [[hep-ex/0509008](#)].
- [50] **CDF, D0 Collaboration, T. E. W. Group**, *2012 Update of the Combination of CDF and D0 Results for the Mass of the W Boson*, [arXiv:1204.0042](#).
- [51] **Tevatron Electroweak Working Group, CDF, DELPHI, SLD Electroweak and Heavy Flavour Groups, ALEPH, LEP Electroweak Working Group, SLD, OPAL, D0, L3 Collaboration, L. E. W. Group**, *Precision Electroweak Measurements and Constraints on the Standard Model*, [arXiv:1012.2367](#).
- [52] T. Corbett, O. J. P. Éboli, D. Goncalves, J. González-Fraile, T. Plehn, and M. Rauch, *The Higgs Legacy of the LHC Run I*, JHEP **08** (2015) 156, [[arXiv:1505.05516](#)].
- [53] E. Massó and V. Sanz, *Limits on anomalous couplings of the Higgs boson to electroweak gauge bosons from LEP and the LHC*, Phys. Rev. **D87** (2013), no. 3 033001, [[arXiv:1211.1320](#)].
- [54] S. Banerjee, S. Mukhopadhyay, and B. Mukhopadhyaya, *Higher dimensional operators and the LHC Higgs data: The role of modified kinematics*, Phys. Rev. **D89** (2014), no. 5 053010, [[arXiv:1308.4860](#)].
- [55] J. Ellis, V. Sanz, and T. You, *Complete Higgs Sector Constraints on Dimension-6 Operators*, JHEP **07** (2014) 036, [[arXiv:1404.3667](#)].
- [56] J. Ellis, V. Sanz, and T. You, *The Effective Standard Model after LHC Run I*, JHEP **03** (2015) 157, [[arXiv:1410.7703](#)].
- [57] R. Edezhath, *Dimension-6 Operator Constraints from Boosted VBF Higgs*, [arXiv:1501.00992](#).
- [58] R. Lafaye, T. Plehn, M. Rauch, D. Zerwas, and M. Duhrssen, *Measuring the Higgs Sector*, JHEP **08** (2009) 009, [[arXiv:0904.3866](#)].

- [59] M. Klute, R. Lafaye, T. Plehn, M. Rauch, and D. Zerwas, *Measuring Higgs Couplings from LHC Data*, Phys. Rev. Lett. **109** (2012) 101801, [[arXiv:1205.2699](#)].
- [60] T. Plehn and M. Rauch, *Higgs Couplings after the Discovery*, Europhys. Lett. **100** (2012) 11002, [[arXiv:1207.6108](#)].
- [61] M. Klute, R. Lafaye, T. Plehn, M. Rauch, and D. Zerwas, *Measuring Higgs Couplings at a Linear Collider*, Europhys. Lett. **101** (2013) 51001, [[arXiv:1301.1322](#)].
- [62] D. Lopez-Val, T. Plehn, and M. Rauch, *Measuring extended Higgs sectors as a consistent free couplings model*, JHEP **10** (2013) 134, [[arXiv:1308.1979](#)].
- [63] T. Corbett, O. J. P. Eboli, D. Goncalves, J. Gonzalez-Fraile, T. Plehn, and M. Rauch, *The Non-Linear Higgs Legacy of the LHC Run I*, [arXiv:1511.08188](#).
- [64] O. J. P. Eboli, J. Gonzalez-Fraile, and M. C. Gonzalez-Garcia, *Scrutinizing the $ZW+W^-$ vertex at the Large Hadron Collider at 7 TeV*, Phys. Lett. **B692** (2010) 20–25, [[arXiv:1006.3562](#)].
- [65] K. Hagiwara, R. D. Peccei, D. Zeppenfeld, and K. Hikasa, *Probing the Weak Boson Sector in $e^+e^- \rightarrow W^+W^-$* , Nucl. Phys. **B282** (1987) 253.
- [66] A. Butter, O. J. P. Éboli, J. González-Fraile, M. C. González-Garcia, T. Plehn, and M. Rauch, *The Gauge-Higgs Legacy of the LHC Run I*, [arXiv:1604.03105](#).
- [67] K. Hagiwara, R. Szalapski, and D. Zeppenfeld, *Anomalous Higgs boson production and decay*, Phys. Lett. **B318** (1993) 155–162, [[hep-ph/9308347](#)].
- [68] A. Falkowski, M. Gonzalez-Alonso, A. Greljo, and D. Marzocca, *Global constraints on anomalous triple gauge couplings in effective field theory approach*, Phys. Rev. Lett. **116** (2016), no. 1 011801, [[arXiv:1508.00581](#)].
- [69] A. Drozd, J. Ellis, J. Quevillon, and T. You, *Comparing EFT and Exact One-Loop Analyses of Non-Degenerate Stops*, JHEP **06** (2015) 028, [[arXiv:1504.02409](#)].
- [70] M. Gorbahn, J. M. No, and V. Sanz, *Benchmarks for Higgs Effective Theory: Extended Higgs Sectors*, JHEP **10** (2015) 036, [[arXiv:1502.07352](#)].
- [71] A. Biekötter, A. Knochel, M. Krämer, D. Liu, and F. Riva, *Vices and virtues of Higgs effective field theories at large energy*, Phys. Rev. **D91** (2015) 055029, [[arXiv:1406.7320](#)].
- [72] J. Brehmer, A. Freitas, D. Lopez-Val, and T. Plehn, *Pushing Higgs Effective Theory to its Limits*, Phys. Rev. **D93** (2016) 075014, [[arXiv:1510.03443](#)].
- [73] A. Biekötter, J. Brehmer, and T. Plehn, *Pushing Higgs Effective Theory over the Edge*, [arXiv:1602.05202](#).
- [74] O. J. P. Eboli and M. C. Gonzalez-Garcia, *Mapping the Genuine Bosonic Quartic Couplings*, [arXiv:1604.03555](#).

- [75] G. F. Giudice, C. Grojean, A. Pomarol, and R. Rattazzi, *The Strongly-Interacting Light Higgs*, JHEP **06** (2007) 045, [[hep-ph/0703164](#)].

Summary and Conclusions

In this thesis we have focused on a specific class of scenarios beyond the Standard Model of particle physics, namely those in which the hierarchy problem is solved by adopting a symmetry principle. In these theories the Higgs field is embedded in a larger multiplet of a new symmetry, so that the four scalars of the SM appear accompanied by some new states. The presence of the latter technically helps, then, to protect the Higgs mass against large radiative corrections. We were interested, in particular, in discriminating between two main paradigms for the use of symmetries in the electroweak symmetry breaking (EWSB) sector. One possible application, implemented for example in supersymmetry, is realized in a perturbative regime and preserving, at low energy, the $SU(2)$ doublet structure of the Higgs field, which is assumed to be an elementary state. With reference to the Higgs' transformation properties under the EW group, we denoted this kind of construction as the *linear scenario*.

An alternative option is to assume that the Higgs is a pseudo-Goldstone boson of a larger symmetry breaking, so that the symmetry that protects the electroweak scale is the (approximate) shift invariance associated to the Goldstone nature of the SM scalars. This scenario is naturally realized in theories with strongly-interacting new physics, among which composite Higgs models emerge as particularly attractive realizations, being reminiscent of the successful description of QCD pions. A characteristic of this class of theories is that the Higgs boson observed at low energy does not necessarily arise as a component of an exact $SU(2)$ doublet. In contrast with the framework presented above, we referred to this second type of construction as the *non-linear scenario*.

Our main goal was to identify EW-scale signals that could distinguish between both realizations, in a way as model-independent as possible. To this aim, we have used the techniques of effective Lagrangians. On one hand we have the linear effective theory, constructed with the SM fields (in particular the Higgs doublet Φ) and organized as an expansion in canonical dimensions, where the leading corrections to the SM Lagrangian are parameterized by operators with $d = 6$. On the other, the non-linear (chiral) Lagrangian in which the physical Higgs is treated as a generic singlet of the EW group and it is independent of the three EW Goldstone bosons. The structure of the latter Lagrangian is thus more complex than that of the linear one and, in particular, it is not possible to identify a unique expansion parameter. In fact, this is rather the convolution of a momentum expansion, typical of chiral Lagrangians, with a linear expansion, in order to account for Higgs and transverse gauge bosons couplings.

8. Summary and Conclusions

We presented two complete, non-redundant sets of non-linear operators: in a first stage (Chapter 4) we restricted to the bosonic sector, where the largest effects are determined by operators with up to four derivatives. Focusing on CP-even terms, we considered the basis previously derived in Ref. [25]. Subsequently (Chapter 7) we extended the analysis and constructed the complete chiral Lagrangian at next-to-leading order, including CP-odd and fermionic terms, namely bilinears with up to two derivatives and four-fermion operators. The overall basis is composed of 148 invariants, up to flavor indices. The inclusion of fermionic terms turned out to have a particularly significant impact on the results of the global fit to electroweak precision data. For instance, we found that the presence of fermionic operators that modify independently the Fermi constant G_F (which occurs only in the chiral case) can weaken the bounds on the oblique parameters S , T , U by up to a factor 20 compared to the usual analysis, due to the larger parameter space available to the fit.

A phenomenological comparison between the chiral set of operators and its linear homologue was carried out in both setups, with and without the inclusion of fermionic invariants. As a general result, the non-linear EFT contains a much larger number of free parameters, compared to the linear basis at $d = 6$ and the two EFTs predict different patterns of signals. Two main categories of discriminators were identified:

- (a) Couplings that are expected to be correlated in the linear expansion but that are in general independent in the non-linear description.

As an example, we have shown that in a general non-linear scenario, there is *a priori* no correlation between triple gauge vertices (TGV) and couplings of the Higgs to gauge bosons pairs. This correlation is instead predicted in the linear formulation. This particular decorrelation can be tested thanks to the fact that both TGV and Higgs couplings are accessible experimentally: this was done for the first time in Fig. 2 of Chapter 4 using the Higgs data available at the end of 2013. The same plot has been updated more recently in Fig. 3 of Chapter 7: this latest result shows a striking improvement with respect to the previous analysis, which is mainly due to the inclusion of information extracted from the kinematic distributions in Higgs decays. The advancement observed is an encouraging indication, as it seems to confirm the feasibility of this kind of study for the extraction of information about the structure of the EWSB sector.

- (b) Characteristic signatures of the non-linear expansion, induced by interactions contained in four-derivative chiral operators, but that would appear only at higher orders ($d \geq 8$) of the linear Lagrangian. These effects typically concern anomalous Lorentz structures that cannot be constructed in the $d = 6$ linear expansion.

An example was identified in the triple and quartic gauge couplings contained in a chiral operator named \mathcal{P}_{14} . This operator contributes, in particular, to a TGV with a peculiar Lorentz structure, which is not generated by $d = 6$ linear operators nor it is induced at tree-level in the SM. This coupling (sometimes denoted by g_5^Z in the literature [113]) violates both C and P while preserving CP invariance. In presence of non-linearity, this particular interaction may be detected with a strength comparable to that of effects emerging at the $d = 6$ level. This event would indeed disfavor a linear scenario. It was shown that significant information about this vertex can be extracted at the LHC, which has the potential for observing g_5^Z with an accuracy up to the percent level, well below the bounds inferred from LEP data.

Another set of differentiating signatures was pointed out in Chapter 5, that contained a detailed analysis of the linear operator $\Box\Phi^\dagger\Box\Phi$ and of its non-linear counterpart $\Box h\Box h$. Both terms induce higher derivative contributions to the Higgs propagator and their impact was evaluated applying the corresponding equations of motion (or equivalently integrating out a Lee-Wick ghost). The non-linear operator was found to produce a much larger amount of anomalous couplings compared to the linear one: in the latter case, in fact, the $SU(2)$ properties of the Higgs field determine a large number of cancellations that, in general, do not occur in the non-linear scenario. This would have several physical effects, among which the most promising

signatures are represented by a subset of quartic-gauge boson, Higgs-gauge boson and fermion-gauge boson couplings, that are unique in resulting from the leading chiral corrections, while they cannot be induced neither by SM couplings at tree-level nor by $d = 6$ operators of the linear expansion.

Although our main focus was to juxtapose the phenomenological features of linear *vs.* non-linear EWSB scenarios in an effective approach, in Chapter 6 we explored a complementary aspect of the electroweak chiral Lagrangian, namely its relation to explicit BSM theories and, more precisely, to concrete composite Higgs models. Applying the CCWZ formalism, we constructed a very general “high-energy” effective Lagrangian for the bosonic sector, roughly valid at energies above the Goldstone bosons’ scale $f > v$. Interestingly, this Lagrangian turns out to contain only up to 10 CP-even operators for any symmetric coset, a number that can be further reduced upon choosing a given realization. In particular, we specialized the discussion to the context of three specific models: the original $SU(5)/SO(5)$ proposed by Georgi and Kaplan [90], the minimal custodial preserving $SO(5)/SO(4)$ [92] and the very minimal, custodial violating, $SU(3)/(SU(2) \times U(1))$. For each of these setups, we explored the connection between the high energy description and the low-energy, bosonic Lagrangian of Chapter 4. Besides representing a validation of the latter, the results of the projection uncovered strong relations existing among the low-energy Wilson coefficients in the specific models considered. This was expected given that the most general low-energy basis contains 33 free parameters, that are in correspondence with only 8 or 9 high-energy coefficients depending on the specific model. A striking result, on the other hand, is the universality in the structure of the functionals $\mathcal{F}(h)$ that encode the dependence on the Higgs boson: in fact these were found to be intriguingly identical for all models, up to a rescaling of the parameter f .

We conclude with an eye to the future, discussing the prospects for this work. The first results from the LHC Run II have already been released by the ATLAS and CMS Collaborations between December 2015 and March 2016 and important updates are expected in the next months. A very timely and reasonable question is therefore if and how the tools developed in this work and the results of our analysis can be impacted by these upcoming results.

If, once again, no direct evidence of new physics is found, the effective Lagrangians considered in this work would continue to hold and the validity of the methods proposed for disentangling the origin of EWSB would remain intact. Indeed it will be particularly important to search for the discriminating signals identified in this work, as they may assume a dominating role as probes of the EWSB, benefiting of more and more precise measurements in the EW and Higgs sectors. Nonetheless, an enhanced experimental precision would also imply that the theoretical error due to the tree-level approximation of the numerical analysis becomes more and more important. Beyond a certain threshold, for instance when a precision of a few percent is reached, it may be necessary to consider perturbative corrections to the operator coefficients discussed. At the same time, as the energy at which the relevant processes are produced increases, the impact of higher order operators is expected to become more and more important. At some point, linear operators with $d = 8$ and chiral invariants classified as NNLO terms will have to be included in our analysis. This may have a non-negligible impact on our results, as it is possible that the enlargement of the parameter space deteriorates the discriminating power of the effective approach and reduces many of the effects predicted.

In a completely different scenario, the discovery of a new exotic state would certainly revolutionize the picture outlined above. With a new resonance in our hands, the most direct way of exploring the EWSB nature would be to study the properties of the new state in depth and try to establish whether it can be linked to one of the previously proposed models. However, this program is not at all in contrast with the EFT approach. For instance, it would be useful to check the compatibility of the existing bounds on the Wilson coefficients with the expected contribution of the new particle to the corresponding couplings (see e.g. Ref. [114]); conversely, the EFT constraints may be used to set limits on unknown couplings of the new state. Another viable application of the effective approach is to extend the Lagrangians considered here by introducing an extra degree of freedom: this can be done fixing only spin and SM quantum charges for the new state. In particular, the strategy developed in this work for investigating the nature of the Higgs boson

8. Summary and Conclusions

could be applied in an almost identical way in the examination of another arbitrary scalar, or it may be adapted to the cases of a fermion or vector resonance.

The power of EFTs in this context has been recently emphasized in a long series of papers where this approach has been applied to the case of an excess around 750 GeV in the diphoton mass spectrum reported by both the ATLAS and CMS Collaborations [115, 116] in December 2015. This result sparked the interest of the HEP community, despite its yet low significance (in the spin-0 hypothesis and including the look-elsewhere effect, ATLAS and CMS currently report a significance of 2.0σ and 1.6σ respectively [117, 118]). Effective theory considerations (see for example Refs. [114, 119–124]) immediately indicate, via trivial arguments of SM gauge-invariance and using exclusively SM fields, that, would this hint become evidence, correlated excesses should be expected in other di-boson channels ($Z\gamma$, ZZ , WW). In fact, the four decay processes are described in terms of only three effective operators, in which the new boson is coupled to the structures $B_{\mu\nu}B^{\mu\nu}$, $B_{\mu\nu}W^{\mu\nu}$, $W_{\mu\nu}W^{\mu\nu}$. This simple result is a clear example of how the symmetry principle, put into effect in the formulation of gauge-invariant EFTs, will serve as a guidance for future searches, irrespective of what their outcome will be.

Resumen y Conclusiones

Esta tesis se ha centrado en una clase particular de escenarios de física de partículas más allá del Modelo Estándar, concretamente aquellos en que el problema de la jerarquía se resuelve adoptando un principio de simetría. En estas teorías, el campo de Higgs está incrustado en un multiplete más grande de una nueva simetría, de forma que los cuatro escalares del ME vienen acompañados de algunos estados nuevos. La presencia de estos últimos ayuda técnicamente a proteger la masa del Higgs de grandes correcciones radiativas. En particular, estábamos interesados en discriminar entre los dos paradigmas principales del uso de simetrías en el sector de la ruptura espontánea de la simetría electrodébil (RESE). Una posible aplicación, implementada por ejemplo en supersimetría, se realiza en un régimen perturbativo y preservando, a baja energía, la estructura de doblete de $SU(2)$ del campo de Higgs, que se asume un estado elemental. Por lo que a las propiedades de transformación del Higgs bajo el grupo electrodébil se refiere, denotamos este tipo de construcción *escenario lineal*.

Una opción alternativa es la de asumir que el Higgs es un bosón de Goldstone de la ruptura de una simetría más grande, de forma que la simetría que protege la escala electrodébil es la invariancia de translación (aproximada) asociada a la naturaleza Goldstone de los escalares del ME. Este escenario se realiza naturalmente en teorías de nueva física con interacciones fuertes, entre las cuales los modelos de Higgs compuestos constituyen realizaciones particularmente atractivas que evocan la exitosa descripción de los piones de QCD. Una característica de esta clase de teorías es que, en ellas, el Higgs físico no emerge necesariamente como una componente de un doblete exacto de $SU(2)$. En contraste con el marco presentado anteriormente, nos referimos a este segundo tipo de construcción como *escenario no-lineal*.

Nuestro objetivo principal era el de identificar señales a la escala electrodébil que puedan distinguir entre ambas realizaciones, de la manera más “independiente del modelo” posible. Con esta finalidad, hemos utilizado Lagrangianos efectivos. Por un lado tenemos la teoría efectiva lineal, construida con los campos del ME (en particular el doblete de Higgs Φ) y organizada en una expansión en dimensiones canónicas, donde las correcciones dominantes al Lagrangiano del ME están parametrizadas por operadores con $d = 6$. Por el otro, el Lagrangiano no-lineal (quiral) en que se trata el Higgs físico como un singlete genérico del grupo electrodébil y se considera a éste independiente de los tres bosones de Goldstone electrodébiles. En consecuencia, la estructura de este Lagrangiano es más compleja que la del lineal y, en particular, no es posible identificar un único parámetro de expansión. De hecho, ésta es más bien la convolución de una expansión en momentos típica de los Lagrangianos quirales con una expansión lineal para los acoplos del Higgs y de los bosones de gauge transversos.

Hemos presentado dos conjuntos completos y no-redundantes de operadores no-lineales: en una primera fase (Capítulo 4) nos restringimos al sector bosónico, donde los efectos dominantes están determinados por operadores con hasta cuatro derivadas. Centrando nuestra atención en términos pares bajo CP, consideramos la base derivada previamente en [25]. A continuación (Capítulo 7) extendimos el análisis construyendo el Lagrangiano quiral completo hasta el primer orden subdominante, incluyendo términos que violan CP y términos con fermiones, específicamente bilineales con hasta dos derivadas y operadores de cuatro fermiones. La base resultante está compuesta globalmente por 148 invariantes, sin considerar índices de sabor. La inclusión de términos fermiónicos resultó tener un impacto particularmente significativo sobre los resultados del ajuste global a los datos de precisión electrodébiles. Por ejemplo, encontramos que la presencia de operadores fermiónicos que modifican independientemente la constante de Fermi G_F (cosa que ocurre solo en el caso quiral) puede suavizar los límites sobre los parámetros oblicuos S, T, U hasta en un factor 20 comparado con el análisis habitual debido a un aumento en el espacio de parámetros disponible.

Se ha realizado una comparación fenomenológica entre el conjunto de operadores no-lineales y su homólogo lineal en ambas configuraciones: incluyendo y no los invariantes fermiónicos. Como resultado general, la TEC no-lineal contiene un número mucho más alto de parámetros libres, comparado con la base lineal a $d = 6$ y las dos TECs predicen tendencias diferentes en las señales. Se han identificado dos categorías principales de discriminantes:

8. Summary and Conclusions

- (a) Acoplos que se espera estén correlacionados en la expansión lineal, pero que son en general independientes en la descripción no-lineal.

Como ejemplo, hemos mostrado que en el escenario general no-lineal no hay *a priori* ninguna correlación entre los vértices triples de gauge (VTG) y los acoplos del Higgs con pares de bosones de gauge. Correlación que, al contrario, se predice en la formulación lineal. Esta descorrelación particular se puede poner a prueba gracias al hecho de que, tanto los VTG como los acoplos del Higgs son accesibles experimentalmente: esto se hizo por primera vez en la Figura 2 del Capítulo 4 usando los datos de Higgs disponibles a finales de 2013. La misma gráfica se ha actualizado recientemente en la Fig. 3 del Capítulo 7: este último resultado muestra una mejora notable con respecto al análisis anterior, que se debe principalmente a la inclusión de información extraída de las distribuciones cinemáticas en las desintegraciones del Higgs. Esto parece confirmar la viabilidad de este tipo de estudios para la extracción de informaciones sobre la estructura del sector de RESE, lo cual se interpreta como un hecho prometedor.

- (b) Señales características de la expansión no-lineal, inducidas por interacciones contenidas en operadores quirales de cuatro derivadas, que por otro lado aparecerían solo a ordenes más altos ($d \geq 8$) del Lagrangiano lineal. Estos efectos involucran típicamente estructuras de Lorentz anómalas que no pueden aparecer en la expansión lineal a $d = 6$.

De esto se ha identificado un ejemplo en los acoplos triples y cuárticos de gauge contenidos en un operador quiral llamado \mathcal{P}_{14} . Este operador contribuye, en particular, a un VGT con una estructura Lorentz particular, que no aparece entre los operadores lineales a $d = 6$, ni tampoco es inducida a nivel-árbol en el ME. Este acoplo (a veces referido como g_5^Z en la literatura [113]) viola tanto C como P mientras que preserva la invariancia bajo CP . En presencia de no-linealidad, esta interacción concreta se puede detectar con una fuerza comparable a la de efectos que emergen a nivel $d = 6$, lo que, de hecho, desfavorece el escenario lineal. Se mostró que es posible extraer información significativa sobre este vértice en el LHC, que tiene el potencial para observar g_5^Z con una precisión de hasta unos percentiles, bastante por debajo de los límites inferidos de los datos de LEP.

Se ha mostrado otra serie de señales distintivas en el Capítulo 5, que contenía el análisis detallado del operador lineal $\Box\Phi^\dagger\Box\Phi$ y de su homólogo no-lineal $\Box h\Box h$. Ambos términos inducen contribuciones con más de dos derivadas al propagador del Higgs. Se ha valorado su impacto aplicando las ecuaciones del movimiento asociadas (o equivalentemente eliminando un ghost “Lee-Wick” del espectro). El operador no-lineal resultó producir un número mayor de acoplos anómalos comparado con el lineal: de hecho, en este último caso, las propiedades de $SU(2)$ del campo de Higgs determinan un número mayor de cancelaciones que, en general, no ocurren en el escenario no-lineal. Esto podría tener varios efectos físicos, entre los cuales las señales más prometedoras las representan un grupo de acoplos cuárticos de gauge y acoplos de bosones de gauge a Higgs y a fermiones, que son únicos en el sentido de que aparecen al orden dominante de la expansión quiral, mientras no pueden ser inducidos ni por acoplos del ME a nivel-árbol, ni tampoco por operadores de la expansión lineal a $d = 6$.

Aunque el acento se ha puesto principalmente en contraponer las características fenomenológicas de los escenarios de RESE lineal *vs.* no-lineal con un enfoque eficaz, en el Capítulo 6 exploramos un aspecto complementario del Lagrangiano electrodébil quiral, a saber, su relación con teorías MME explícitas y, más precisamente, a modelos concretos de Higgs compuesto. Aplicando el formalismo CCWZ, construimos un Lagrangiano eficaz “de alta energía” muy general para el sector bosónico, que es aproximadamente válido para energías superiores a la escala de los bosones de Goldstone $f > v$. Un resultado interesante es que este Lagrangiano contiene un máximo de 10 operadores pares bajo CP para cualquier grupo cociente simétrico, un número que se puede incluso reducir eligiendo una realización determinada. En particular, centramos la discusión en tres modelos específicos: el original $SU(5)/SO(5)$ propuesto por Georgi y Kaplan [90], el mínimo que preserva la simetría “custodial” $SO(5)/SO(4)$ [92] y el más mínimo posible, que no respeta

la simetría “custodial”, $SU(3)/(SU(2) \times U(1))$. Para cada una de estas construcciones, exploramos la conexión entre la descripción a alta energía y el Lagrangiano bosónico a baja energía del Capítulo 4. Aparte de validar éste último, los resultados de la proyección desvelaron la existencia de fuertes relaciones entre los coeficientes de Wilson en los modelos considerados. Esto era de esperar, debido a que el Lagrangiano más general a baja energía contiene 33 parámetros libres que se corresponden con solamente 8 o 9 coeficientes a alta energía, dependiendo del modelo concreto. Un resultado llamativo, por otra parte, es la impresionante universalidad en la estructura de los funcionales $\mathcal{F}(h)$ que codifican la dependencia del bosón de Higgs: de hecho, las funciones resultaban ser intrigantemente idénticas en todos los modelos, salvo por redefiniciones de la escala f .

Concluimos con una mirada al futuro, discutiendo las previsiones de este trabajo. Las colaboraciones ATLAS y CMS estrenaron ya los primeros resultados del Run II del LHC entre diciembre de 2015 y marzo de 2016 y se esperan aún importantes actualizaciones en los próximos meses. Una pregunta oportuna y razonable es, pues, qué impacto tendrán los resultados inminentes sobre los instrumentos desarrollados en este trabajo y los resultados de nuestro análisis.

Si, de nuevo, no se encontrara evidencia directa de nueva física, los Lagrangianos eficaces considerados en este trabajo seguirían vigentes y la validez de los métodos propuestos para desanudar el origen de la RESE permanecerían intactos. De hecho se volvería particularmente importante buscar las señales discriminantes que hemos identificado en este trabajo, ya que éstas podrían asumir un papel dominante en el sondeo de la RESE, beneficiándose de medidas experimentales más y más precisas en los sectores electrodébil y del Higgs. Sin embargo, una mejora substancial en la precisión experimental implicaría también que el error teórico debido a la aproximación de nivel-árbol en el análisis numérico se volvería más importante. Mas allá de un cierto umbral, por ejemplo cuando se llegue a alcanzar una precisión de unos percentiles, podría ser necesario considerar correcciones perturbativas a los coeficientes de los operadores discutidos. Al mismo tiempo, a medida que crece la energía a la que se producen los procesos relevantes, cobra importancia el impacto de operadores de órdenes más altos. En algún momento se deberán incluir operadores lineales con $d = 8$ e invariantes quirales clasificados como términos sub-subdominantes en el análisis. Esto podría tener un impacto no-despreciable en nuestros resultados, ya que es posible que la ampliación del espacio de parámetros reduzca el poder discriminativo del método eficaz y que desaparezcan algunos de los efectos predichos.

En un escenario completamente distinto, el descubrimiento de un nuevo estado exótico revolucionaría ciertamente el panorama descrito anteriormente. Con una nueva resonancia entre manos, la manera más directa de explorar la naturaleza de la RESE sería estudiando a fondo las propiedades del nuevo estado, intentando establecer si se puede relacionar con alguno de los modelos previamente propuestos. Aún así, este programa no está completamente enfrentado con el enfoque de las TECs. Por ejemplo, sería útil averiguar la compatibilidad de los límites preexistentes sobre los coeficientes de Wilson con la contribución esperada de la nueva partícula a los acoplos correspondientes (véase por ej. Ref. [114]); e inversamente, las restricciones en la TEC podrían utilizarse para hallar límites sobre los acoplos desconocidos del nuevo estado. Otra posible aplicación del método efectivo es la de extender los Lagrangianos considerados aquí introduciendo un grado de libertad adicional: esto se puede hacer fijando simplemente un espín y unas cargas cuánticas del ME para el nuevo estado. En particular, la estrategia desarrollada en este trabajo para investigar la naturaleza del bosón de Higgs se puede aplicar de manera casi idéntica a la exploración de otro escalar arbitrario, o podría más bien ser adaptada a los casos de una resonancia fermiónica o vectorial.

El poder de las TECs en este contexto ha sido recientemente enfatizado en una larga serie de artículos que aplicaron este método al caso de un exceso alrededor de 750 GeV en el espectro de masa de dos fotones anunciado por ambos ATLAS y CMS [115, 116] en diciembre del año pasado. Este resultado ha despertado el interés de la comunidad de física de altas energías, a pesar de su aún limitada significancia (en la hipótesis de espín-0 e incluyendo el “look-elsewhere effect”, ATLAS y CMS presentan actualmente 2.0 y 1.6σ respectivamente [117, 118]). Según consideraciones de teorías efectivas (véase por ejemplo las

8. Summary and Conclusions

Refs. [114, 119–124]) mediante argumentos de invariancia gauge del ME y utilizando exclusivamente campos del ME, se apunta a que, si este indicio se llegara a convertir en señal, deberían esperarse excesos correlacionados por lo menos en otros canales di-bosón ($Z\gamma$, ZZ , WW). De hecho, los cuatro procesos de desintegración están descritos en términos de sólo tres operadores efectivos, en los que el nuevo bosón se acopla con las estructuras $B_{\mu\nu}B^{\mu\nu}$, $B_{\mu\nu}W^{\mu\nu}$ y $W_{\mu\nu}W^{\mu\nu}$. Este simple resultado es un ejemplo muy claro de cómo el principio de simetría, puesto en acción en la formulación de TEC invariantes gauge, servirá de guía en búsquedas futuras, independientemente de cuales lleguen a ser sus resultados.

Bibliography

- [1] **ATLAS** Collaboration, G. Aad *et. al.*, *Observation of a New Particle in the Search for the Standard Model Higgs Boson with the Atlas Detector at the Lhc*, Phys.Lett. **B716** (2012) 1–29, [[arXiv:1207.7214](#)].
- [2] **CMS** Collaboration, S. Chatrchyan *et. al.*, *Observation of a New Boson at a Mass of 125 GeV with the Cms Experiment at the Lhc*, Phys.Lett. **B716** (2012) 30–61, [[arXiv:1207.7235](#)].
- [3] F. Englert and R. Brout, *Broken Symmetry and the Mass of Gauge Vector Mesons*, Phys. Rev. Lett. **13** (1964) 321–323.
- [4] P. W. Higgs, *Broken symmetries, massless particles and gauge fields*, Phys. Lett. **12** (1964) 132–133.
- [5] P. W. Higgs, *Broken Symmetries and the Masses of Gauge Bosons*, Phys. Rev. Lett. **13** (1964) 508–509.
- [6] **ATLAS** and **CMS** Collaborations, *Measurements of the Higgs boson production and decay rates and constraints on its couplings from a combined ATLAS and CMS analysis of the LHC pp collision data at $\sqrt{s} = 7$ and 8 TeV*, Tech. Rep. ATLAS-CONF-2015-044, CMS-PAS-HIG-15-002.
- [7] S. L. Glashow, J. Iliopoulos, and L. Maiani, *Weak Interactions with Lepton-Hadron Symmetry*, Phys. Rev. **D2** (1970) 1285–1292.
- [8] M. K. Gaillard, B. W. Lee, and J. L. Rosner, *Search for Charm*, Rev. Mod. Phys. **47** (1975) 277–310.
- [9] G. 't Hooft, *Naturalness, chiral symmetry, and spontaneous chiral symmetry breaking*, NATO Sci. Ser. B **59** (1980) 135.
- [10] S. Weinberg, *Implications of Dynamical Symmetry Breaking*, Phys. Rev. **D13** (1976) 974–996.
- [11] L. Susskind, *Dynamics of Spontaneous Symmetry Breaking in the Weinberg-Salam Theory*, Phys. Rev. **D20** (1979) 2619–2625.
- [12] S. Dimopoulos and J. Preskill, *Massless Composites With Massive Constituents*, Nucl. Phys. **B199** (1982) 206.

BIBLIOGRAPHY

- [13] P. W. Graham, D. E. Kaplan, and S. Rajendran, *Cosmological Relaxation of the Electroweak Scale*, Phys. Rev. Lett. **115** (2015), no. 22 221801, [[arXiv:1504.07551](#)].
- [14] L. F. Abbott, *A Mechanism for Reducing the Value of the Cosmological Constant*, Phys. Lett. **B150** (1985) 427–430.
- [15] T. Appelquist and C. W. Bernard, *Strongly Interacting Higgs Bosons*, Phys. Rev. **D22** (1980) 200.
- [16] A. C. Longhitano, *Heavy Higgs Bosons in the Weinberg-Salam Model*, Phys. Rev. **D22** (1980) 1166.
- [17] A. C. Longhitano, *Low-Energy Impact of a Heavy Higgs Boson Sector*, Nucl. Phys. **B188** (1981) 118.
- [18] F. Feruglio, *The Chiral approach to the electroweak interactions*, Int. J. Mod. Phys. **A8** (1993) 4937–4972, [[hep-ph/9301281](#)].
- [19] T. Appelquist and G.-H. Wu, *The Electroweak chiral Lagrangian and new precision measurements*, Phys. Rev. **D48** (1993) 3235–3241, [[hep-ph/9304240](#)].
- [20] J. Bagger, V. D. Barger, K.-m. Cheung, J. F. Gunion, T. Han, G. A. Ladinsky, R. Rosenfeld, and C. P. Yuan, *The Strongly interacting $W W$ system: Gold plated modes*, Phys. Rev. **D49** (1994) 1246–1264, [[hep-ph/9306256](#)].
- [21] V. Koulovassilopoulos and R. S. Chivukula, *The Phenomenology of a nonstandard Higgs boson in $W(L) W(L)$ scattering*, Phys. Rev. **D50** (1994) 3218–3234, [[hep-ph/9312317](#)].
- [22] C. P. Burgess, J. Matias, and M. Pospelov, *A Higgs or not a Higgs? What to do if you discover a new scalar particle*, Int. J. Mod. Phys. **A17** (2002) 1841–1918, [[hep-ph/9912459](#)].
- [23] B. Grinstein and M. Trott, *A Higgs-Higgs bound state due to new physics at a TeV*, Phys. Rev. **D76** (2007) 073002, [[arXiv:0704.1505](#)].
- [24] R. Contino, C. Grojean, M. Moretti, F. Piccinini, and R. Rattazzi, *Strong Double Higgs Production at the LHC*, JHEP **05** (2010) 089, [[arXiv:1002.1011](#)].
- [25] R. Alonso, M. B. Gavela, L. Merlo, S. Rigolin, and J. Yepes, *The Effective Chiral Lagrangian for a Light Dynamical "Higgs Particle"*, Phys. Lett. **B722** (2013) 330–335, [[arXiv:1212.3305](#)]. [Erratum: Phys. Lett. **B726** 926 (2013)].
- [26] R. Alonso, M. B. Gavela, L. Merlo, S. Rigolin, and J. Yepes, *Flavor with a light dynamical "Higgs particle"*, Phys. Rev. **D87** (2013), no. 5 055019, [[arXiv:1212.3307](#)].
- [27] R. Alonso, M. B. Gavela, L. Merlo, S. Rigolin, and J. Yepes, *Minimal Flavour Violation with Strong Higgs Dynamics*, JHEP **06** (2012) 076, [[arXiv:1201.1511](#)].
- [28] I. Brivio, T. Corbett, O. J. P. Éboli, M. B. Gavela, J. Gonzalez-Fraile, M. C. Gonzalez-Garcia, L. Merlo, and S. Rigolin, *Disentangling a dynamical Higgs*, JHEP **03** (2014) 024, [[arXiv:1311.1823](#)].
- [29] I. Brivio, O. J. P. Éboli, M. B. Gavela, M. C. Gonzalez-Garcia, L. Merlo, and S. Rigolin, *Higgs ultraviolet softening*, JHEP **12** (2014) 004, [[arXiv:1405.5412](#)].
- [30] R. Alonso, I. Brivio, B. Gavela, L. Merlo, and S. Rigolin, *Sigma Decomposition*, JHEP **12** (2014) 034, [[arXiv:1409.1589](#)].
- [31] I. Brivio, J. Gonzalez-Fraile, M. C. Gonzalez-Garcia, and L. Merlo, *The complete HEFT Lagrangian after the LHC Run I*, submitted to EPJC. (2016) [[arXiv:1604.06801](#)].

-
- [32] I. Brivio, F. Goertz, and G. Isidori, *Probing the Charm Quark Yukawa Coupling in Higgs+Charm Production*, Phys. Rev. Lett. **115** (2015), no. 21 211801, [[arXiv:1507.02916](#)].
 - [33] I. Brivio, M. B. Gavela, L. Merlo, K. Mimasu, J. M. No, R. del Rey, and V. Sanz, *Non-linear Higgs portal to Dark Matter*, JHEP **04** (2016) 141, [[arXiv:1511.01099](#)].
 - [34] S. L. Glashow, *Partial-symmetries of weak interactions*, Nuclear Physics **22** (Feb., 1961) 579.
 - [35] S. Weinberg, *A Model of Leptons*, Physical Review Letters **19** (Nov., 1967) 1264–1266.
 - [36] Y. Nambu, *Quasiparticles and Gauge Invariance in the Theory of Superconductivity*, Phys. Rev. **117** (1960) 648–663.
 - [37] J. Goldstone, *Field Theories with Superconductor Solutions*, Nuovo Cim. **19** (1961) 154–164.
 - [38] J. Goldstone, A. Salam, and S. Weinberg, *Broken Symmetries*, Phys. Rev. **127** (1962) 965–970.
 - [39] G. S. Guralnik, C. R. Hagen, and T. W. B. Kibble, *Global Conservation Laws and Massless Particles*, Phys. Rev. Lett. **13** (1964) 585–587.
 - [40] **Particle Data Group**, K. A. Olive *et. al.*, *Review of Particle Physics*, Chin. Phys. **C38** (2014) 090001.
 - [41] P. W. Higgs, *Spontaneous Symmetry Breakdown without Massless Bosons*, Phys. Rev. **145** (1966) 1156–1163.
 - [42] N. Cabibbo, *Unitary Symmetry and Leptonic Decays*, Phys. Rev. Lett. **10** (1963) 531–533. [[648\(1963\)](#)].
 - [43] M. Kobayashi and T. Maskawa, *CP Violation in the Renormalizable Theory of Weak Interaction*, Prog. Theor. Phys. **49** (1973) 652–657.
 - [44] B. Pontecorvo, *Inverse beta processes and nonconservation of lepton charge*, Sov. Phys. JETP **7** (1958) 172–173. [[Zh. Eksp. Teor. Fiz.34,247\(1957\)](#)].
 - [45] Z. Maki, M. Nakagawa, and S. Sakata, *Remarks on the unified model of elementary particles*, Prog. Theor. Phys. **28** (1962) 870–880.
 - [46] D. Buttazzo, G. Degrossi, P. P. Giardino, G. F. Giudice, F. Sala, A. Salvio, and A. Strumia, *Investigating the near-criticality of the Higgs boson*, JHEP **12** (2013) 089, [[arXiv:1307.3536](#)].
 - [47] L. D. Landau, *On the angular momentum of a system of two photons*, Dokl. Akad. Nauk Ser. Fiz. **60** (1948), no. 2 207–209.
 - [48] C.-N. Yang, *Selection Rules for the Dematerialization of a Particle Into Two Photons*, Phys. Rev. **77** (1950) 242–245.
 - [49] **CMS Collaboration**, S. Chatrchyan *et. al.*, *Study of the Mass and Spin-Parity of the Higgs Boson Candidate Via Its Decays to Z Boson Pairs*, Phys. Rev. Lett. **110** (2013), no. 8 081803, [[arXiv:1212.6639](#)].
 - [50] **ATLAS Collaboration**, G. Aad *et. al.*, *Evidence for the spin-0 nature of the Higgs boson using ATLAS data*, Phys. Lett. **B726** (2013) 120–144, [[arXiv:1307.1432](#)].
 - [51] **ATLAS and CMS Collaborations**, G. Aad, *et. al.*, *Combined Measurement of the Higgs Boson Mass in pp Collisions at $\sqrt{s} = 7$ and 8 TeV with the ATLAS and CMS Experiments*, Phys. Rev. Lett. **114** (2015) 191803, [[arXiv:1503.07589](#)].

- [52] **CMS** Collaboration, V. Khachatryan *et. al.*, *Precise determination of the mass of the Higgs boson and tests of compatibility of its couplings with the standard model predictions using proton collisions at 7 and 8 TeV*, Eur. Phys. J. **C75** (2015), no. 5 212, [[arXiv:1412.8662](#)].
- [53] **CMS** Collaboration, V. Khachatryan *et. al.*, *Constraints on the Higgs boson width from off-shell production and decay to Z-boson pairs*, Phys. Lett. **B736** (2014) 64–85, [[arXiv:1405.3455](#)].
- [54] **ATLAS** Collaboration, G. Aad *et. al.*, *Constraints on the off-shell Higgs boson signal strength in the high-mass ZZ and WW final states with the ATLAS detector*, Eur. Phys. J. **C75** (2015), no. 7 335, [[arXiv:1503.01060](#)].
- [55] **ATLAS** Collaboration, G. Aad *et. al.*, *Constraints on new phenomena via Higgs boson couplings and invisible decays with the ATLAS detector*, JHEP **11** (2015) 206, [[arXiv:1509.00672](#)].
- [56] C. Anastasiou, C. Duhr, F. Dulat, E. Furlan, T. Gehrmann, F. Herzog, A. Lazopoulos, and B. Mistlberger, *High precision determination of the gluon fusion Higgs boson cross-section at the LHC*, [arXiv:1602.00695](#).
- [57] **CMS** Collaboration, V. Khachatryan *et. al.*, *Search for the associated production of the Higgs boson with a top-quark pair*, JHEP **09** (2014) 087, [[arXiv:1408.1682](#)]. [Erratum: JHEP10 106 (2014)].
- [58] **ATLAS** Collaboration, G. Aad *et. al.*, *Search for the Standard Model Higgs boson produced in association with top quarks and decaying into $b\bar{b}$ in pp collisions at $\sqrt{s} = 8$ TeV with the ATLAS detector*, Eur. Phys. J. **C75** (2015), no. 7 349, [[arXiv:1503.05066](#)].
- [59] **ATLAS** Collaboration, *Search for the Standard Model Higgs boson in the $H \rightarrow Z\gamma$ decay mode with pp collisions at $\sqrt{s} = 7$ and 8 TeV*, Tech. Rep. ATLAS-CONF-2013-009, CERN, Geneva, Mar, 2013.
- [60] **CMS** Collaboration, V. Khachatryan *et. al.*, *Search for a Higgs boson decaying into $\gamma^*\gamma \rightarrow \ell\ell\gamma$ with low dilepton mass in pp collisions at $\sqrt{s} = 8$ TeV*, Phys. Lett. **B753** (2016) 341–362, [[arXiv:1507.03031](#)].
- [61] **ATLAS** Collaboration, G. Aad *et. al.*, *Search for the Standard Model Higgs boson decay to $\mu^+\mu^-$ with the ATLAS detector*, Phys. Lett. **B738** (2014) 68–86, [[arXiv:1406.7663](#)].
- [62] **CMS** Collaboration, V. Khachatryan *et. al.*, *Search for a standard model-like Higgs boson in the $\mu^+\mu^-$ and e^+e^- decay channels at the LHC*, Phys. Lett. **B744** (2015) 184–207, [[arXiv:1410.6679](#)].
- [63] **LHC Higgs Cross Section Working Group**, J. R. Andersen, *et. al.*, *Handbook of LHC Higgs Cross Sections: 3. Higgs Properties*, [arXiv:1307.1347](#).
- [64] **LHC Higgs Cross Section Working Group**, A. David, A. Denner, M. Duehrssen, M. Grazzini, C. Grojean, G. Passarino, M. Schumacher, M. Spira, G. Weiglein, and M. Zanetti, *LHC HXSWG interim recommendations to explore the coupling structure of a Higgs-like particle*, [arXiv:1209.0040](#).
- [65] S. Elitzur, *Impossibility of Spontaneously Breaking Local Symmetries*, Phys. Rev. **D12** (1975) 3978–3982.
- [66] J. M. Cornwall, D. N. Levin, and G. Tiktopoulos, *Derivation of Gauge Invariance from High-Energy Unitarity Bounds on the s Matrix*, Phys. Rev. **D10** (1974) 1145. [Erratum: Phys. Rev.D11 972 (1975)].
- [67] C. E. Vayonakis, *Born Helicity Amplitudes and Cross-Sections in Nonabelian Gauge Theories*, Lett. Nuovo Cim. **17** (1976) 383.

-
- [68] M. S. Chanowitz and M. K. Gaillard, *The TeV Physics of Strongly Interacting W's and Z's*, Nucl. Phys. **B261** (1985) 379.
 - [69] G. J. Gounaris, R. Kogerler, and H. Neufeld, *Relationship Between Longitudinally Polarized Vector Bosons and their Unphysical Scalar Partners*, Phys. Rev. **D34** (1986) 3257.
 - [70] M. Gell-Mann and M. Levy, *The axial vector current in beta decay*, Nuovo Cim. **16** (1960) 705.
 - [71] P. Sikivie, L. Susskind, M. B. Voloshin, and V. I. Zakharov, *Isospin Breaking in Technicolor Models*, Nucl. Phys. **B173** (1980) 189.
 - [72] **ALEPH, CDF, D0, DELPHI, L3, OPAL and SLD** Collaborations, the LEP electroweak working group, the Tevatron electroweak working group and the SLD electroweak and heavy flavour groups, *Precision Electroweak Measurements and Constraints on the Standard Model*, [arXiv:1012.2367](#).
 - [73] M. E. Peskin and T. Takeuchi, *A New constraint on a strongly interacting Higgs sector*, Phys. Rev. Lett. **65** (1990) 964–967.
 - [74] M. Ciuchini, E. Franco, S. Mishima, M. Pierini, L. Reina, and L. Silvestrini, *Update of the electroweak precision fit, interplay with Higgs-boson signal strengths and model-independent constraints on new physics*, in *International Conference on High Energy Physics 2014 (ICHEP 2014) Valencia, Spain, July 2-9, 2014*, 2014. [arXiv:1410.6940](#).
 - [75] S. R. Coleman, J. Wess, and B. Zumino, *Structure of phenomenological Lagrangians. 1.*, Phys. Rev. **177** (1969) 2239–2247.
 - [76] C. G. Callan, Jr., S. R. Coleman, J. Wess, and B. Zumino, *Structure of phenomenological Lagrangians. 2.*, Phys. Rev. **177** (1969) 2247–2250.
 - [77] R. Haag, *Quantum field theories with composite particles and asymptotic conditions*, Phys. Rev. **112** (1958) 669–673.
 - [78] S. Weinberg, *Phenomenological Lagrangians*, Physica **A96** (1979) 327–340.
 - [79] A. Manohar and H. Georgi, *Chiral Quarks and the Nonrelativistic Quark Model*, Nucl. Phys. **B234** (1984) 189.
 - [80] M. Froissart, *Asymptotic behavior and subtractions in the Mandelstam representation*, Phys. Rev. **123** (1961) 1053–1057.
 - [81] R. Contino, *The Higgs as a Composite Nambu-Goldstone Boson*, in *Physics of the large and the small, TASI 09, proceedings of the Theoretical Advanced Study Institute in Elementary Particle Physics, Boulder, Colorado, USA, 1-26 June 2009*, pp. 235–306, 2011. [arXiv:1005.4269](#).
 - [82] M. E. Peskin and T. Takeuchi, *Estimation of oblique electroweak corrections*, Phys. Rev. **D46** (1992) 381–409.
 - [83] S. Dimopoulos and L. Susskind, *Mass Without Scalars*, Nucl. Phys. **B155** (1979) 237–252.
 - [84] E. Eichten and K. D. Lane, *Dynamical Breaking of Weak Interaction Symmetries*, Phys. Lett. **B90** (1980) 125–130.
 - [85] **UTfit** Collaboration, M. Bona *et. al.*, *Model-independent constraints on $\Delta F = 2$ operators and the scale of new physics*, JHEP **03** (2008) 049, [[arXiv:0707.0636](#)].

BIBLIOGRAPHY

- [86] D. B. Kaplan and H. Georgi, *$SU(2) \times U(1)$ Breaking by Vacuum Misalignment*, Phys. Lett. **B136** (1984) 183.
- [87] D. B. Kaplan, H. Georgi, and S. Dimopoulos, *Composite Higgs Scalars*, Phys. Lett. **B136** (1984) 187.
- [88] T. Banks, *Constraints on $SU(2) \times U(1)$ breaking by vacuum misalignment*, Nucl. Phys. **B243** (1984) 125.
- [89] H. Georgi, D. B. Kaplan, and P. Galison, *Calculation of the Composite Higgs Mass*, Phys. Lett. **B143** (1984) 152.
- [90] H. Georgi and D. B. Kaplan, *Composite Higgs and Custodial $SU(2)$* , Phys. Lett. **B145** (1984) 216.
- [91] M. J. Dugan, H. Georgi, and D. B. Kaplan, *Anatomy of a Composite Higgs Model*, Nucl. Phys. **B254** (1985) 299.
- [92] K. Agashe, R. Contino, and A. Pomarol, *The Minimal composite Higgs model*, Nucl. Phys. **B719** (2005) 165–187, [[hep-ph/0412089](#)].
- [93] R. Contino, L. Da Rold, and A. Pomarol, *Light custodians in natural composite Higgs models*, Phys. Rev. **D75** (2007) 055014, [[hep-ph/0612048](#)].
- [94] D. B. Kaplan, *Flavor at SSC energies: A New mechanism for dynamically generated fermion masses*, Nucl. Phys. **B365** (1991) 259–278.
- [95] K. Hagiwara, S. Ishihara, R. Szalapski, and D. Zeppenfeld, *Low-energy effects of new interactions in the electroweak boson sector*, Phys. Rev. **D48** (1993) 2182–2203.
- [96] K. Hagiwara, T. Hatsukano, S. Ishihara, and R. Szalapski, *Probing nonstandard bosonic interactions via W boson pair production at lepton colliders*, Nucl. Phys. **B496** (1997) 66–102, [[hep-ph/9612268](#)].
- [97] W. Buchmuller and D. Wyler, *Effective Lagrangian Analysis of New Interactions and Flavor Conservation*, Nucl. Phys. **B268** (1986) 621–653.
- [98] B. Grzadkowski, M. Iskrzynski, M. Misiak, and J. Rosiek, *Dimension-Six Terms in the Standard Model Lagrangian*, JHEP **10** (2010) 085, [[arXiv:1008.4884](#)].
- [99] A. Azatov, R. Contino, and J. Galloway, *Model-Independent Bounds on a Light Higgs*, JHEP **04** (2012) 127, [[arXiv:1202.3415](#)]. [Erratum: JHEP04 140 (2013)].
- [100] E. E. Jenkins, A. V. Manohar, and M. Trott, *Naive Dimensional Analysis Counting of Gauge Theory Amplitudes and Anomalous Dimensions*, Phys. Lett. **B726** (2013) 697–702, [[arXiv:1309.0819](#)].
- [101] G. Buchalla, O. Catá, and C. Krause, *On the Power Counting in Effective Field Theories*, Phys. Lett. **B731** (2014) 80–86, [[arXiv:1312.5624](#)].
- [102] G. Buchalla, O. Cata, and C. Krause, *A Systematic Approach to the SILH Lagrangian*, Nucl. Phys. **B894** (2015) 602–620, [[arXiv:1412.6356](#)].
- [103] B. M. Gavela, E. E. Jenkins, A. V. Manohar, and L. Merlo, *Analysis of General Power Counting Rules in Effective Field Theory*, [arXiv:1601.07551](#).
- [104] A. G. Cohen, D. B. Kaplan, and A. E. Nelson, *Counting 4 pis in strongly coupled supersymmetry*, Phys. Lett. **B412** (1997) 301–308, [[hep-ph/9706275](#)].

-
- [105] M. B. Gavela, J. Gonzalez-Fraile, M. C. Gonzalez-Garcia, L. Merlo, S. Rigolin, and J. Yepes, *CP violation with a dynamical Higgs*, JHEP **10** (2014) 44, [[arXiv:1406.6367](#)].
 - [106] R. Alonso, E. E. Jenkins, and A. V. Manohar, *A Geometric Formulation of Higgs Effective Field Theory: Measuring the Curvature of Scalar Field Space*, Phys. Lett. **B754** (2016) 335–342, [[arXiv:1511.00724](#)].
 - [107] B. Grinstein, D. O’Connell, and M. B. Wise, *The Lee-Wick standard model*, Phys. Rev. **D77** (2008) 025012, [[arXiv:0704.1845](#)].
 - [108] J. R. Espinosa and B. Grinstein, *Ultraviolet Properties of the Higgs Sector in the Lee-Wick Standard Model*, Phys. Rev. **D83** (2011) 075019, [[arXiv:1101.5538](#)].
 - [109] T. D. Lee and G. C. Wick, *Finite Theory of Quantum Electrodynamics*, Phys. Rev. **D2** (1970) 1033–1048. [[129\(1970\)](#)].
 - [110] T. D. Lee and G. C. Wick, *Negative Metric and the Unitarity of the S Matrix*, Nucl. Phys. **B9** (1969) 209–243. [[83\(1969\)](#)].
 - [111] T. Corbett, O. J. P. Eboli, J. Gonzalez-Fraile, and M. C. Gonzalez-Garcia, *Robust Determination of the Higgs Couplings: Power to the Data*, Phys. Rev. **D87** (2013) 015022, [[arXiv:1211.4580](#)].
 - [112] T. Corbett, O. J. P. Éboli, J. Gonzalez-Fraile, and M. C. Gonzalez-Garcia, *Determining Triple Gauge Boson Couplings from Higgs Data*, Phys. Rev. Lett. **111** (2013) 011801, [[arXiv:1304.1151](#)].
 - [113] K. Hagiwara, R. D. Peccei, D. Zeppenfeld, and K. Hikasa, *Probing the Weak Boson Sector in $e^+e^- \rightarrow W^+W^-$* , Nucl. Phys. **B282** (1987) 253.
 - [114] L. Berthier, J. M. Cline, W. Shepherd, and M. Trott, *Effective interpretations of a diphoton excess*, JHEP **04** (2016) 084, [[arXiv:1512.06799](#)].
 - [115] **ATLAS** Collaboration, *Search for resonances decaying to photon pairs in 3.2 fb^{-1} of pp collisions at $\sqrt{s} = 13 \text{ TeV}$ with the ATLAS detector*, Tech. Rep. ATLAS-CONF-2015-081, Dec, 2015.
 - [116] **CMS** Collaboration, *Search for new physics in high mass diphoton events in proton-proton collisions at 13 TeV* , Tech. Rep. CMS-PAS-EXO-15-004, Dec, 2015.
 - [117] **ATLAS** Collaboration, *Search for resonances in diphoton events with the ATLAS detector at $\sqrt{s} = 13 \text{ TeV}$* , Tech. Rep. ATLAS-CONF-2016-018, Mar, 2016.
 - [118] **CMS** Collaboration, *Search for new physics in high mass diphoton events in 3.3 fb^{-1} of proton-proton collisions at $\sqrt{s} = 13 \text{ TeV}$ and combined interpretation of searches at 8 TeV and 13 TeV* , Tech. Rep. CMS-PAS-EXO-16-018, Mar, 2016.
 - [119] D. Buttazzo, A. Greljo, and D. Marzocca, *Knocking on new physics’ door with a scalar resonance*, Eur. Phys. J. **C76** (2016), no. 3 116, [[arXiv:1512.04929](#)].
 - [120] R. Franceschini, G. F. Giudice, J. F. Kamenik, M. McCullough, A. Pomarol, R. Rattazzi, M. Redi, F. Riva, A. Strumia, and R. Torre, *What is the $\gamma\gamma$ resonance at 750 GeV ?*, JHEP **03** (2016) 144, [[arXiv:1512.04933](#)].
 - [121] W. Altmannshofer, J. Galloway, S. Gori, A. L. Kagan, A. Martin, and J. Zupan, *On the 750 GeV di-photon excess*, [arXiv:1512.07616](#).
 - [122] I. Low and J. Lykken, *Implications of Gauge Invariance on a Heavy Diphoton Resonance*, [arXiv:1512.09089](#).

BIBLIOGRAPHY

- [123] J. F. Kamenik, B. R. Safdi, Y. Soreq, and J. Zupan, *Comments on the diphoton excess: critical reappraisal of effective field theory interpretations*, [arXiv:1603.06566](#).
- [124] R. Franceschini, G. F. Giudice, J. F. Kamenik, M. McCullough, F. Riva, A. Strumia, and R. Torre, *Digamma, what next?*, [arXiv:1604.06446](#).